FUNDAMENTAL: 75067

THE EFFECT OF THICKNESS AND LAYING PATTERN OF PAVER ON CONCRETE BLOCK PAVEMENT

PROF. IR. DR. HASANAN BIN MD NOR

MR. CHE ROS BIN ISMAIL

RACHMAT MUDIYONO

RESEARCH VOTE NO:

75067

Department of Geotechnics and Transportation

Faculty of Civil Engineering

Universiti Teknologi Malaysia

JULY 2006

UNIVERSITI TEKNOLOGI MALAYSIA

BORANG PENGESAHAN STATUS TESIS υ

JUDUL : **PERFORMANCE OF CONCRETE BLOCK PAVEMENT ON SLOPED ROAD SECTION**

SESI PENGAJIAN: 2005/2006

Saya **RACHMAT MUDIYONO**
(HURUF BESAR)

mengaku membenarkan tesis (~~PSM/Sarjana~~/Doktor Falsafah)* ini disimpan di Perpustakaan Universiti Teknologi Malaysia dengan syarat-syarat kegunaan seperti berikut :

1. Tesis ini adalah hakmilik Universiti Teknologi Malaysia.
2. Perpustakaan Universiti Teknologi Malaysia dibenarkan membuat salinan untuk tujuan pengajian sahaja.
3. Perpustakaan dibenarkan membuat salinan tesis ini sebagai bahan pertukaran antara institusi pengajian tinggi.
4. **Sila tandakan (√)

☐	SULIT	(Megandungi maklumat yang berdarjah keselamatan atau kepentingan Malaysia seperti yang termaktub di dalam AKTA RAHSIA RASMI 1972)
☐	TERHAD	(Mengandungi maklumat TERHAD yang telah ditentukan oleh organisasi/badan di mana penyelidikan dijalankan)
☑	TIDAK TERHAD	

Disahkan oleh

.....
(TANDATANGAN PENULIS)

.....
(TANDATANGAN PENYELIA)

Alamat Tetap:
Jln. Seruni XII / 17 Tlogosari
Semarang – Indonesia

PROF. IR. DR. HASANAN BIN MD. NOR
Nama Penyelia

Tarikh: ……

Tarikh: ……

CATATAN: * Potong yang tidak berkenaan.
** Jika tesis ini SULIT atau TERHAD, sila lampirkan surat daripada pihak berkuasa/organisasi berkenaan dengan menyatakan sekali sebab dan tempoh tesis ini perlu dikelaskan sebagai SULIT dan TERHAD.
υ Tesis dimaksudkan sebagai tesis bagi Ijazah Doktor Falsafah dan Sarjana secara penyelidikan, atau disertai bagi pengajian secara kerja kursus dan peyelidikan, atau Laporan Projek Sarjana Muda (PSM)

FUNDAMENTAL: 75067

THE EFFECT OF THICKNESS AND LAYING PATTERN OF PAVER ON CONCRETE BLOCK PAVEMENT

PROF. IR. DR. HASANAN BIN MD NOR
MR. CHE ROS BIN ISMAIL
RACHMAT MUDIYONO

RESEARCH VOTE NO:
75067

Department of Geotechnics and Transportation
Faculty of Civil Engineering
Universiti Teknologi Malaysia

JULY 2006

ABSTRAK

Dalam turapan blok konkrit (CBP), blok merupakan bahan binaan untuk lapis haus, iaitu lapisan penting bagi penyebaran beban. Kajian terdahulu menunjukkan keputusan yang tidak konsisten dalam menentukan prestasi blok konkrit. Penyelidikan ini dijalankan untuk menentukan jarak rasuk penahan pada turapan blok konkrit di bahagian jalan yang cerun berdasarkan pada darjah kecerunan, corak susunan turapan, bentuk blok, tebal blok, lebar sambungan di antara blok dan ketebalan lapisan pasir penggalas. Kesan daripada pemindahan beban di atas turapan blok konkrit juga di bincangkan. Ujikaji yang dilakukan di makmal menggunakan uji tekan mendatar dan uji tekan masuk pada turapan yang dicerunkan beberapa darjah. Pemasangan alat ujikaji tekan mendatar menggunakan rangka keluli saiz 2.00 x 2.00 meter yang ditekan dari sisi hingga turapan blok konkrit mengalami kegagalan. Dalam ujikaji tekan masuk menggunakan rangka keluli saiz 1.00 x 1.00 meter dengan kedalaman 0.20 meter, beban tegak dikenakan ke atas sampel CBP kecerunan dari 0 hingga 51 kN, dimana sampel CBP di letakkan pada kecerunan 0%, 4%, 8% dan 12%. Keputusan menunjukkan susunan silang pangkah 45^{o} adalah yang terbaik jika dibandingkan susunan silang pangkah 90^{o} maupun susunan usungan untuk menahan beban mendatar, kerana peranan blok untuk menahan gesekan pada turapan, dan mengunci putaran yang disebabkan oleh tekanan mendatar. Bentuk blok uni-pave lebih kuat menahan rayapan mendatar jika dibandingkan dengan bentuk blok bersegi empat, kerana bentuk blok mempunyai gerigi (4 sisi), manakala bentuk blok bersegi empat tidak mempunyai gerigi. Pemesongan yang terjadi antara bentuk blok uni-pave dengan bentuk bersegi empat sangat kecil. Perubahan ketebalan blok dari 60 mm sampai 100 mm dapat mengurangkan pemesongan pada turapan. Semakin tebal blok semakin besar daya geserannya. Pemindahan beban akan lebih besar untuk blok yang tebal. Kekuatan turapan untuk menahan beban kenderaan sangat dipengaruhi oleh ketebalan blok.Keputusan ujikaji juga menunjukkan lebar sambungan di antara blok yang optimum adalah 3 mm. Bagi lebar sambungan kurang daripada optimum, pasir pengisi tidak dapat memasuki ruang antara blok. Hubungan antara daya tekanan dengan penurunan blok pada berbagai ketebalan pasir pengisi 30, 50, dan 70 mm menunjukkan bahawa penurunan blok semakin besar dengan peningkatan ketebalan pasir pengalas dari 30 hingga 70 mm tebal. Penurunan adalah paling kecil pada ketebalan pasir pengalas 30mm. Semakin tebal pasir pengalas, semakin tinggi penurunan yang terjadi. Kesan darjah kecerunan keatas kawasan jalan cerun adalah signifikan dengan kekuatan geseran antara blok dan kekuatan mempertahan posisi blok lebih efektif dengan peningkatan tebal blok. Penurunan semakin berkurang untuk blok yang lebih tebal dan lebih besar darjah kecerunan. Jarak rasuk penahan akan bertambah dengan berkurangnya lebar sambungan antara blok, darjah kecerunan dan tebal pasir pengalas. Untuk membandingkan hasil ujikaji di makmal dengan hasil simulasi perilaku turapan blok konkrit model struktur menggunakan 3DFEM telah dibuat.

ABSTRACT

In concrete block pavements, the blocks make up the wearing surface and are a major load-spreading component of the pavement. Earlier findings were inconsistent with respect to the deflection response of concrete blocks in the pavement. This research investigate the anchor beam spacing of concrete block pavement (CBP) on sloping road section based on the degree of slope, laying pattern, blocks shape, blocks thickness, joint width between blocks and bedding sand thickness. The effect of load transfer on the CBP behaviour is discussed. The results of a series of tests conducted in laboratory with horizontal force test and push-in test in several degrees of slopes. The horizontal force testing installation was constructed within the steel frame 2.00 x 2.00 metre and forced from the side until CBP failure (maximum horizontal creep). For the applied push-in test in a rigid steel box of 1.00 x 1.00 metre square in plan and 0.20 meter depth, the vertical load was increased from zero to 51 kN on the CBP sample in 0%, 4%, 8% and 12% degrees of slopes. The herringbone 45^{o} is the best laying pattern compared to herringbone 90^{o} and stretcher bond to restraint the horizontal force, which the blocks contribute as a whole to the friction of the pavement, the blocks being successively locked by their rotation following their horizontal creep. This reduces the incidence of creep and distributes wheel loads more evenly to the underlying pavement construction. The uni-pave block shape has more restraint of horizontal creep than rectangular block shape, because uni-pave block shape has gear (four-dents), while rectangular block shape has no gear (dents).The difference in deflections observed between uni-pave shape and rectangular shape are small. The change in block thickness from 60 to 100 mm significantly reduces the elastic deflection of pavement. Thicker blocks provide a higher frictional area. The load transfer will be high for thicker blocks. The response of the pavement is highly influenced by block thickness. The optimum joint width between blocks is 3 mm. For joint widths less than the optimum, the jointing sand was unable to enter between blocks. A large amount of sand remained outside the joint sand heaps on the block surface. The relationship between push-in force with block displacement on the varying loose thicknesses of 30, 50, and 70 mm bedding sand, shows that the deflections of pavement increase with increase in loose thickness of bedding sand. The deflection is minimum at a loose thickness of 30 mm bedding course. The higher the loose bedding sand thickness, the more the deflection will be. The effect of the degree of slope on concrete block pavements on sloping road section area is significant with friction between blocks and thrusting action between adjacent blocks at hinging points is more effective with thicker blocks. Thus, deflections are much less for thicker blocks with increasing degree of the slope. The spacing of anchor beam is increases with decreasing joint width, degree of slope and bedding sand thickness. To compare results between laboratory test with the simulated mechanical behaviour of concrete block pavements, a structural model based on a Three Dimensional Finite Element Model (3DFEM) for CBP was employed.

TABLE OF CONTENTS

LIST OF TABLES

LIST OF FIGURES

LIST OF SYMBOLS

D, d	-	Diameter
F	-	Force
W	-	Wheel Load
θ	-	Degree of Slope

LIST OF APPENDICES

CHAPTER 1

INTRODUCTION

1.1 Background

Concrete block pavement (CBP) was introduced in The Netherlands in the early 1950s as a replacement for baked clay brick roads (Van der Vlist 1980). The general worldwide were trend towards beautification of certain city pavements the rising cost of bitumen as a paving material, and the rapid increase in construction and maintenance cost have encouraged designers to consider alternative paving material such as concrete blocks. The strength, durability, and aesthetically pleasing surface of pavers have made CBP ideal for many commercial, municipal, and industrial applications.

The construction of roads on steep slopes poses particularly interesting challenges for road engineers. The horizontal (inclined) forces exerted on the road surface are severely increased due to traffic accelerating (uphill), braking (downhill) or turning. These horizontal forces cause distress in most conventional pavements, resulting in rutting and poor riding quality. Experience has shown that CBP performs well under such severe conditions. Although CBP performs well on steep slopes, there are certain considerations that must be taken into account during the design and construction of the pavement.

1.2 Statement of Problem

Due to the steepness of the slope, normally vertical traffic loading will have a surface component exerted on the blocks in a downward direction. This force is aggravated by traction of accelerating vehicles up the hill and breaking of vehicles down the hill. If uncontained, these forces will cause horizontal creep of the blocks down the slope, resulting in opening of joints at the top of the paving and weaving on the concrete block pavement.

1.3 Objectives

The objectives of the study are:

a. To study the performance of CBP deformation (horizontal creep) that is affected by horizontal force with variables; laying pattern, block thickness, block shape and joint width between blocks.
b. To test and analyse various experimental of CBP in the laboratory with push-in tests for various degrees of slopes.
c. To make a comparative study of experimental results in laboratory with three dimensional finite element model (3DFEM) simulations.
d. To define the spacing of anchor beam on sloping road section based on degree of the slope, the effect of laying pattern, block thickness, bedding sand thickness and joint width between blocks.

1.4 Scope of The Study

The scopes of this study are:

a. Factors influencing the performance of Concrete Block Pavement (CBP) such as laying pattern, bedding sand thickness, block thickness, block shape and width of jointing sand were studied.
b. A simple laboratory-scale test was carried out to design the construction model of concrete block pavements and its performance.
c. A detail study for determining the combination of bedding sand thickness, shape and thickness of block, joint width and spacing of anchor beam for sloping road section.

1.5 Significance of Research

a. Studies on CBP for sloping road section are limited. This study contributes to the understanding of CBP performance on slopes.
b. The CBP failure caused by traction of traffic for sloping road section can be alleviated by using appropriate bedding sand thickness, block thickness, laying pattern and joint width.
c. The result of the study can be used as a recommendation of utilizing CBP for sloping road section.

1.6 Thesis Organization

This thesis consists of eight chapters, and the contents of each chapter are explained as follows:

CHAPTER 1: This introductory chapter presents the background of the development of Concrete Block Pavement (CBP) used throughout world. It also explains the statement of problem, objective, and scope of the study and the significance of this research.

CHAPTER 2: This chapter reviews the component of CBP, structure of CBP and construction techniques of CBP procedure is discussed step by step. The application of CBP on sloping road section is discussed with several effects i.e. degree of the slope, laying pattern, thickness of bedding sand, joint width between blocks and thickness of pavers. It also explains the detail construction of anchor beam.

CHAPTER 3: Chapter three presents the materials and testing methodology used in this research. Two materials used in this research, which are sand material for bedding and jointing sand (from Kulai in Johor) and block paving produced by Sun-Block company in Senai of Johor Bahru branch.

CHAPTER 4: Chapter four contains the interpretation of the experimental results. The effect of laying pattern, bedding sand thickness, joint width between blocks, paver's thickness, block shape and degree of the slope considered are analyzed.

CHAPTER 5: Chapter five presents the concrete block pavement (CBP) on sloping road section area with the use of the anchor beam on the CBP especially on the sloping road section, the spacing and position of the anchor beam based on the effects of joint width, bedding sand thickness, block thickness and block shape.

CHAPTER 6: This chapter presents the Three Dimensional Finite Element Model (3DFEM) of CBP construction using SOLID WORK and COSMOS Design STAR programme package to compare with the push-in test of CBP experiment results in the laboratory.

CHAPTER 7: Chapter seven presents general discussions about spacing of anchor beam on sloping road section based on degree of the slope with variables of the laying pattern effect, shape and thickness of block, bedding sand thickness and joint width between blocks.

CHAPTER 8: This chapter summarizes the main conclusions of this research and recommendation.

CHAPTER 2

LITERATURE REVIEW

2.1 Introduction

Concrete block pavements (CBP) differ from other forms of pavement in that the wearing surface is made from small paving units bedded and jointed in sand rather than continuous paving. Beneath the bedding sand, the substructure is similar to that of a conventional flexible pavement. The material of concrete block pavement is rigid, but the construction is flexible pavement have been illustrated in the companion paper (Hasanan, 2005). In CBP, the blocks are a major load-spreading component.

The blocks are available in a variety of shapes and are installed in a number of patterns, such as stretcher bond, herringbone bond, basket weave bond, etc. A review of existing literature revealed considerable differences in findings regarding the contribution of various block parameters to the structural capacity of pavement. This chapter discusses the experimental results of research conducted by previous researcher relating to the effect on pavement performance by changing parameters such as shape and thickness of concrete block paver, thickness of bedding sand and width joint between blocks.

2.2 Structure and Component of Concrete Block Pavement

The surface of CBP comprises concrete blocks bedded and jointed in sand. It transfers the traffic loads to the substructure of the pavement. The load-spreading capacity of concrete blocks layer depends on the interaction of individual blocks with jointing sand to build up resistance against applied load. The shape, size, thickness, laying patterns, etc., are important block parameters; these influence the overall performance of the pavement. Some early plate load studies (Knapton 1976; Clark 1978) suggested that load-spreading ability of the pavement was not significantly affected by block shape. Later accelerated trafficking studies (Shackel 1980) and plate load studies (Shackel *et al.* 2000) established that shaped (dents) blocks exhibited smaller deformation than rectangular blocks of a similar thickness installed in the same laying pattern under the same applied load. Knapton (1996) found pavement performance was essentially independent of block thickness, whereas Clark (1978) reported a small improvement in pavement performance with an increase in block thickness. Shackel (1980), Miura *et. al.,* (1984) and Shackel *et al*. (1993) claimed that an increase in block thickness reduced elastic deflection and the stress transmitted to the sub-base.

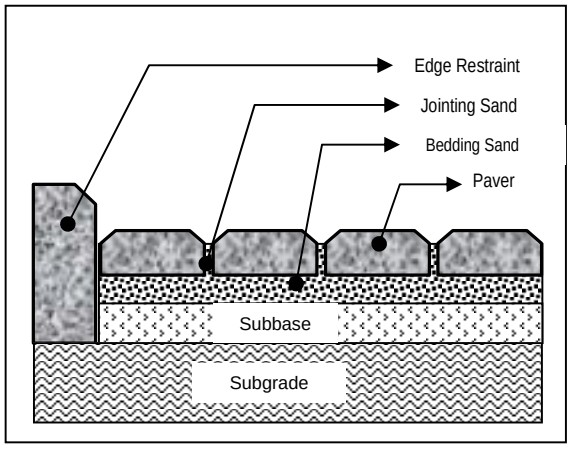

Figure 2.1 Structure of concrete block pavement

Shackel (1980) reported that the load-associated performance of block pavements was essentially independent of the size and compressive strength of the blocks. Knapton (1976) found that laying pattern did not significantly affect the static load-spreading capacity of the pavement. From plate load studies, Miura *et al*. (1984) and Shackel *et al*. (1993) have reported that, for a given shape and thickness, blocks laid in a herringbone bond exhibited higher performance than blocks laid in a stretcher bond.

The load-distributing ability of the concrete block surface course increases with increasing load (Knapton 1976; Clark 1978; Miura *et al.* 1984). This is manifested as a decrease in stress transmitted to the sub-base below the loaded area and a decrease in the rate of deformation with the increase in load. Shackel (1980), Knapton and Barber (1979), Barber and Knapton (1980), Miura *et al*. (1984), and Jacobs and Houben (1988) found that, in their early life, block pavements stiffen progressively with an increase in the number of load repetitions. This is manifested as an increase in the load-spreading ability of blocks. However, Shackel (1980) clarified that the progressive stiffening did not influence the magnitude of resilient deflections of CBP. Jacobs and Houben (1988) and Rada *et al*. (1990) reported that the elastic deflections decrease with an increase in the number of load repetitions rather than an increase, as observed in flexible and rigid pavements. It was felt that the phenomenon of block interaction under applied load needed investigation in the light of the above discussion. Such tests could then provide insights into load-spreading ability and other structural characteristics of the block pavements.

The component of concrete block pavement is shown in Table 2.1 below and has provided the necessary inputs for developing comprehensive structural design methods.

Table 2.1 Factors affecting the performance of CBP

Pavement Component	**Factors Affecting Performance under Traffic**
Concrete Block Pavers	• Paver shape • Paver thickness • Paver size • Laying pattern • Joint width
Bedding and Jointing Sands	• Sand thickness • Grading • Angularity • Moisture • Mineralogy
Base-course and Sub-base	• Material type • Grading • Plasticity • Strength and durability
Sub-grade	• Soil Type • Stiffness and strength • Moisture regime

Shackel (2003)

2.2.1 Concrete Block Paver

Concrete block paving is a unique material, exhibiting important differences to other small element paving such as stone and clay, as well as to form-less materials such as asphalt and in-situ concrete. It provides a hard surface which is good to look at, comfortable to walk on, extremely durable and easy to maintain. It adds a richness, complexity and human scale to any setting.

2.2.1.1 The Effect of Block Shape

Two shapes of blocks were selected for study. These were rectangular shape and uni-pave shape (Figure 2.2). These block types have the same thickness and nearly same plan area. Blocks were laid in stretcher bond for each test. The results obtained are compared in Figure 2.3.

Rectangular shape

Uni-pave shape

Figure 2.2 The rectangular and uni-pave shapes of block

The shape of the load deflection path is similar for two block types. The deflections are essentially the same for rectangular shape and uni-pave shape. Smaller deflections are observed for uni-pave shape than rectangular shape. In general, shaped (dents) blocks exhibited smaller deformations as compared with rectangular and square blocks (Panda and Ghosh, 2003). Complex shape (uni-pave) blocks have larger vertical surface areas than rectangular or square blocks of the same plan area.

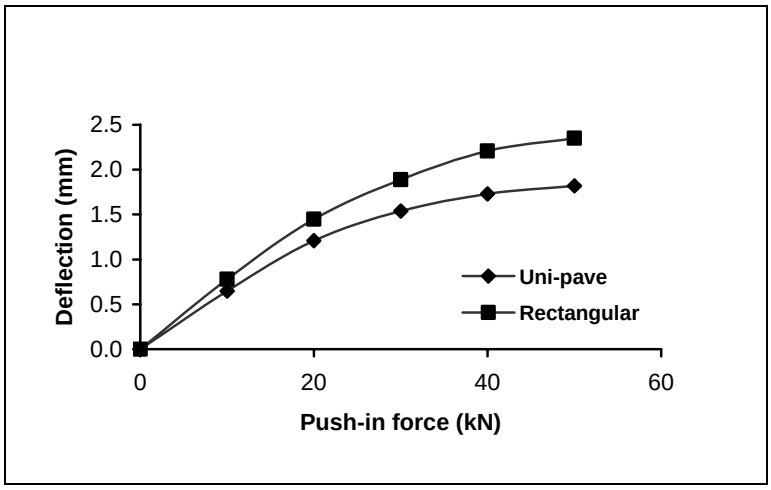

Figure 2.3 The effects of block shape on deflection
Panda and Ghosh (2003)

Consequently, shaped blocks have larger frictional areas for load transfer to adjacent blocks. It is concluded that the shape of the block influences the performance of the block pavement under load. It is postulated that the effectiveness of load transfer depends on the vertical surface area of the blocks. These results obtained are consistent with those found in earlier plate load tests by Shackel *et al*. (1993).

2.2.1.2 The Effects of Block Thickness

The rectangular shape blocks of the same plan dimension with three different thicknesses were selected for testing. The blocks thickness 60 mm, 80 mm, and 100 mm. Blocks were laid in a stretcher bond pattern for each test. The shapes of the load deflection paths are similar for all blocks thickness.

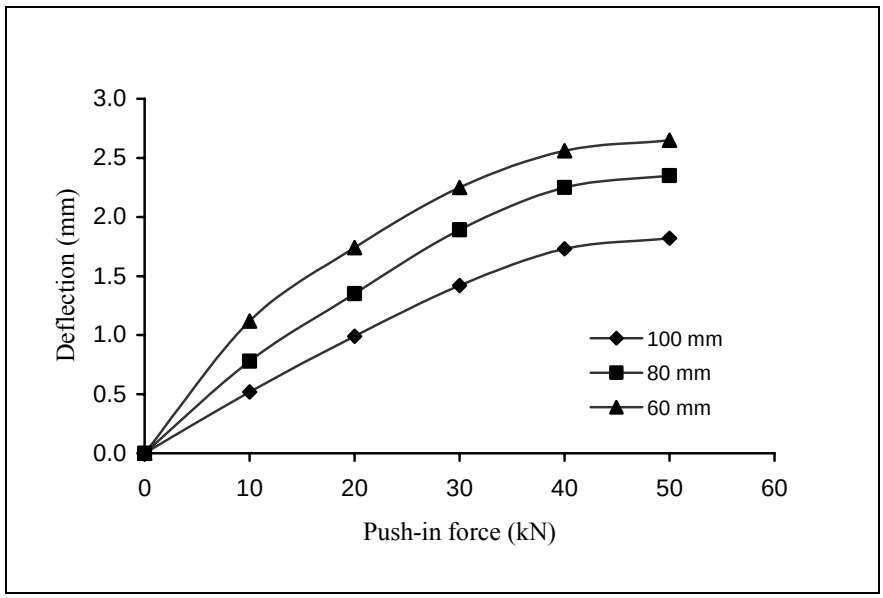

Figure 2.4 The effect of block thickness on deflection of block pavement *Panda and Ghosh (2003)*

A change in thickness from 60 to 100 mm significantly reduces the elastic deflection of pavement. The comparison is shown in Figure 2.4. Thicker blocks provide a higher frictional area. Thus, load transfer will be high for thicker blocks.

The thrusting action between adjacent blocks at hinging points (Panda and Ghosh 2001) is more effective with thicker blocks. Thus, deflections are much less for thicker blocks. The combined effect of higher friction area and higher thrusting action for thicker blocks provides more efficient load transfer. Thus, there is a significant change in deflection values from increasing the thickness of blocks. It is concluded that the response of the pavement is highly influenced by block thickness. The results obtained are similar to that found in earlier plate load tests by Shackel *et al*. (1993).

2.2.1.3 The Effect of Laying Pattern

Rectangular shape blocks were laid in the test pavement in three laying patterns: stretcher bond, herringbone 90^0 bond, and herringbone 45^0 bond (Figure 2.5).

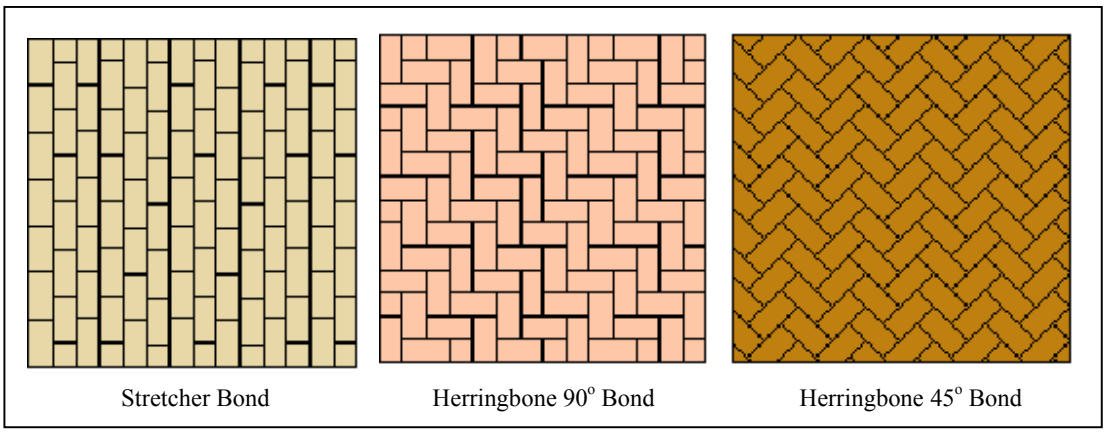

Figure 2.5 Laying patterns of CBP

The shapes of the load deflection paths are similar and the deflections are almost the same for all the laying patterns, as shown in Figure 2.6. The friction areas and thickness of blocks used for all three laying patterns are the same. Thus, the same elastic deflections are observed. It is established that deflections of block pavements are independent of the laying pattern in the pavement (Panda and Gosh, 2002). The finding is inconsistent with that reported by Shackel *et al.* (1993).

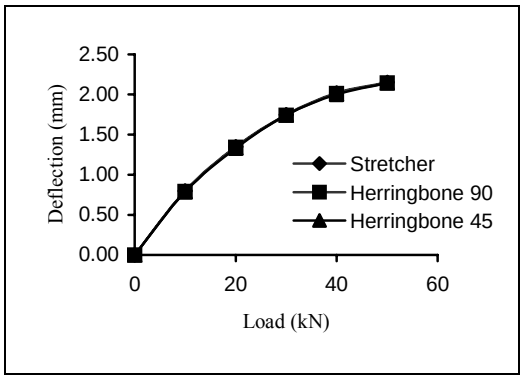

Figure 2.6a The effect of laying pattern reported by Panda (2002)

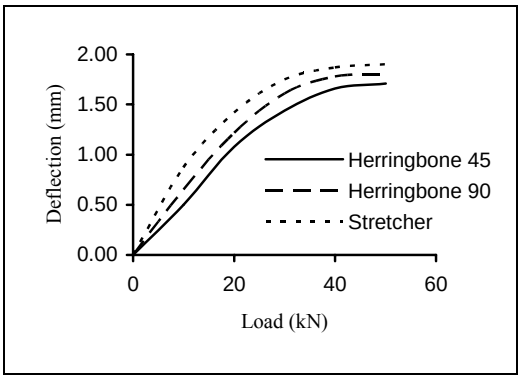

Figure 2.6b The effect of laying pattern reported by Shackel *et al.*

The test pavements were conducted with load is gradually increased from 0 to 70 kN and then released slowly to 0 kN. The deflections were measured at each load interval, and for the remaining cycles, the deflections are measured at the 0 and 70 kN load levels (Shackel, 1993).

2.2.1.4 Optimal Choice of Pavers Shape and Laying Patterns

The design guidelines direct the designer for the optimal selection of pavers shape and laying patterns was discussed. Due to the international controversy in this respect, a distinction is made between structural and functional aspects. The structural aspects for interlocking paver shapes and bi-directional laying patterns, while the functional aspects permits aesthetics considerations and self locating laying techniques. An emphasis is given to the control of optimal joint width between the blocks.

2.2.2 Bedding and Jointing Sand

The bedding sand layer in CBP is included to provide a smooth, level running surface for placing the blocks. European practices (Eisenmenn and Leykuf 1988; Lilley and Dowson 1988; Hurmann 1997) specify a bedding sand thickness after compaction of 50 mm, whereas compacted bedding sand thickness of 20 to 30 mm is used in United States (Rada *et al.* 1990) and Australia (Shackel *et al.*1993). Simmons (1979) recommended a minimum compacted sand depth of 40 mm to accommodate free movement of blocks under initial traffic. Mavin (1980) specified a compacted bedding sand depth of 30 ± 10 mm, keeping 10 mm tolerance on sub-base.

Jointing sand is the main component of CBP, and it plays a major role in promoting load transfer between blocks ultimately in spreading the load to larger areas in lower layers. Very few studies have been carried out concerning the width of joints and the quality of jointing sand for use in CBP. There are even fewer explanations of the behaviour of sand in the joints. For optimum load spreading by friction, it is necessary to provide uniform, narrow, and fully filled joints of widths between 2 and 4 mm (Shackel *at al*. 1993; Hurman 1997). Knapton and O'Grady (1983) recommended joint widths between 0.5 and 5 mm for better pavement performance. Joint widths ranging from 2 and 8 mm are often used, depending upon the shape of blocks, laying pattern, aesthetic considerations, and application areas.

In most of the pavements, the sand used for bedding course is also used in joint filling (Lilley 1980; Hurmann 1997). As reported by Shackel (1980), a finner jointing sand having a maximum particle size of 1.18 mm and less than 20 % passing the 75 μm sieve has performed well. According to Knapton and O'Grady (1983), large joints require coarser sand and tight joints require finer sand for good performance of pavement. The British Standards 1973, passing the 2.36 mm sieve as the most effective for jointing sand. Panda and Ghosh (2001) studied the dilatancy and shearing resistance of sand and recommended using coarse sand in joints of CBP. Livneh *et al.* (1988) specified a maximum particle size of 1.2 mm and 10 % passing 75 μm for jointing sand.

Regarding the grading of bedding sand, Lilley and Dowson (1988) imposed a maximum limit on the percentage passing in 75, 150, and 300 μm sieves as 5, 15, and 50, respectively. Sharp and Simons (1980) required a sand with a maximum nominal size of 5 mm, a clay/silt content of less than 3 %, and not greater than 10 % retained on the 4.75 mm sieve. Single sized grain and/or spherical shaped grain sand are not recommended. Livneh *et al.* (1988) specified a maximum particle size of 9.52 mm with a maximum limit of 10 % passing the 75 μm sieve.

Table 2.2: Grading requirements for bedding sand and jointing sand

Sieve Size	Percent Passing For Bedding Sand	Percent Passing For Jointing Sand
3/8 in. (9.5 mm)	100	-
No. 4 (4.75 mm)	95 to 100	-
No. 8 (2.36 mm)	80 to 100	100
No.16 (1.18 mm)	50 to 85	90 – 100
No. 30 (0.600 mm)	25 to 60	60 – 90
No. 50 (0.300 mm)	10 to 30	30 – 60
No. 100 (0.150 mm)	5 to 15	15 – 30
No. 200 (0.075 mm)	0 - 10	5 – 10

British Standard 882, 1201: Part 2: 1973, London

2.2.2.1 The Effect of Bedding Sand Thickness

Barber and Knapton (1980) have reported that, in a block pavement subjected to truck traffic, a significant proportion of the initial deformation occurred in the bedding sand layer which had a compacted thickness of 40 mm. similar results have been reported by Seddon (1980). These investigations tend to confirm the findings of the earlier Australian study (1989) which demonstrated that a reduction in the loose thickness of the bedding sand from 30 mm to 50 mm was beneficial to the deformation (rutting) behaviour of block pavements. Here an almost fourfold reduction in deformation was observed.

Experience gained in more than twenty-five HVS trafficking tests of prototype block pavements in South Africa has confirmed that there is no necessity to employ bedding sand thickness greater than 30 mm in the loose (initial) condition, which yields a compacted typically close to 20 mm reported by Shackel and Lim (2003).

2.2.2.2 The Effect of Sand Grading

Recently in South Africa a series of HVS accelerated trafficking tests of block pavements has been carried out with the prime objective of determining the desirable properties of the bedding and jointing sands. Here pavements utilizing block uni-pave shape laid in herringbone bond have been constructed using a loose thickness of 70 mm of sand laid over a rigid concrete base. After compacted, the sand layer thickness was reduced to between 45 and 55 mm depending on the sand and having a variety of grading have been evaluated by Shackel (1989).

It has been found that, under the action of a 40 kN single wheel load, up to 30 mm of deformation could be induced in the sand layer within 10.000 wheel traverses. This clearly demonstrates the need to select the bedding sand with care. However, it has been determined that provided the grading of the sand falls within the limits recommended by Morrish (1980), a satisfactory level of performance can be achieved under traffic. Here, rutting deformations typically between 1.5 and 4 mm have been recorded after 10.000 wheels passes where the same sand has been used for both bedding and jointing the blocks. Where, however, finer sand typically having a maximum particle size smaller than 1.0 mm has been used as jointing sand, and improvement in performance has been observed with the total deformations typically being less than 2 mm after 10.000 load repetitions. Generally, for the bedding sand, it appears that, within the limits, coarse sands tend to yield better performance than fine sands and that angular sands exhibit a marginally better performance than round sands.

Unacceptable levels of performance have been observed where the proportion of fine material smaller than 75 μm in the sand exceeds about 15 %. In sands with clay contents between 20 and 30 %, substantial deformations (up to 30 mm) have been observed especially where the sands are wet reported by Interpave (2004).

2.2.2.3 The Effect of Bedding Sand Moisture Content

Experience gained in accelerated trafficking studies in both Australia and South Africa has shown that adequate compaction of the sand bedding can be achieved at moisture contents typically lying within the range from 4 % to 8 % with a value of 6 % representing a satisfactory target value. However, Seddon (1980) has recently suggested that, for optimum compaction of the sand layer, the moisture content should be close to saturation. For sands whose grading complies with the limits set out, the effect of water content appears to have little influence under traffic. It was conducted by running HVS trafficking test whilst maintaining the sand in a soaked condition, nor has pumping been observed. However, where the bedding sand has contains a significant proportion of clay, greater than 15 %, the addition of water to the produce substantial increases in deformation accompanied by pumping. For this reason, the use of sands containing plastic fines should be avoided in the bedding layer, Shackel (1998). Limited experimental evidence suggests that such sands are nevertheless suitable for jointing sands both in respect of means of their mechanical properties and as a means of inhibiting the ingress of water into the joints.

2.2.2.4 Width of Jointing Sand

The sand was used in bedding course with a 50 mm thickness for all of these experiments. Figure 2.7 shows the response of pavement for design joint widths of 2 mm, 3 mm, 5 mm, 7 mm and 9 mm with same quality of sand reported by Mudiyono and Hasanan (2004). As the joint width decreases, the deflection of the pavement also decreases of jointing sand.

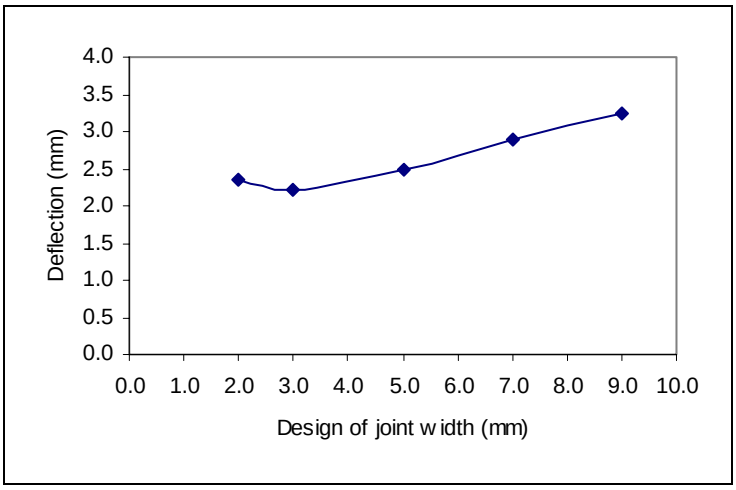

Figure 2.7 The response of pavement deflection for design joint widths

The deflection of pavement decreases up to a certain point and then slightly increases with decrease in joint width, i.e., there is an optimal joint width. The optimum joint widths for these experiments are 3 mm, respectively.

- The higher of the joint width, the normal stiffness of the joint will be lesser. This will lead to more rotations and translations of blocks. Thus, there will be more deflection under the same load for thicker joints.
- For joint widths less than the optimum, in a slight increase in deflections was observed. Some of the grains coarser than the joint width were unable to enter inside. This has been observed during filling sand in joints. A large amount of sand remained outside the joint showing sand heaps on the block surface. The coarse grains of sand choke the top surface of joints and prevent movement of other fine grains in to joint. There might be loose pockets or honeycombing inside the joint. The joint stiffness decreases and in turn reflects slightly higher deflections.

The results that decrease in joint width increases the pavement performance and the concept of optimum joint width well agree with that of a series of static load tests.

2.2.2.5 Filling of Jointing Sand

The compaction might not be fully effective for a higher thickness of bedding sand during vibration. The bedding sand rises through the joints to small heights and wedges in between the blocks. Figure 2.9 shows the rise of sand through the design joints width of 3 mm, 5 mm and 7 mm with varying thickness of bedding sand. The rise of sand increases with increase in thickness of bedding sand. The wedging of these sands absorbs the major part of applied vibration energy and transfers less to the bedding sand below. As a result, the bedding sand is not fully compacted for higher thickness reported by Shackel (2003).

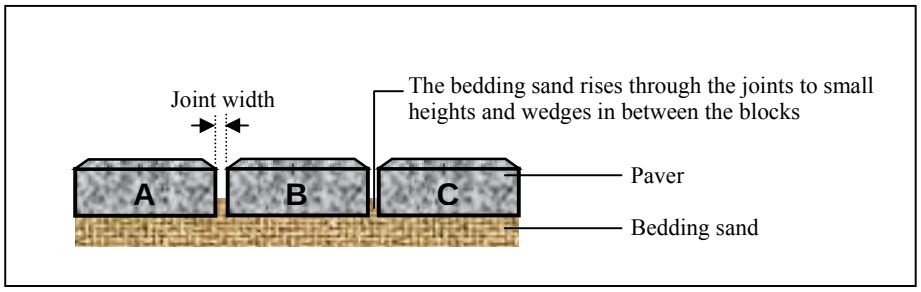

Figure 2.8 The rises of bedding sand between the blocks

Consequently, some compaction of bedding sand takes place under load and thus shows more deflection in the test pavements. The higher the bedding sand thickness, the more the deflection will be.

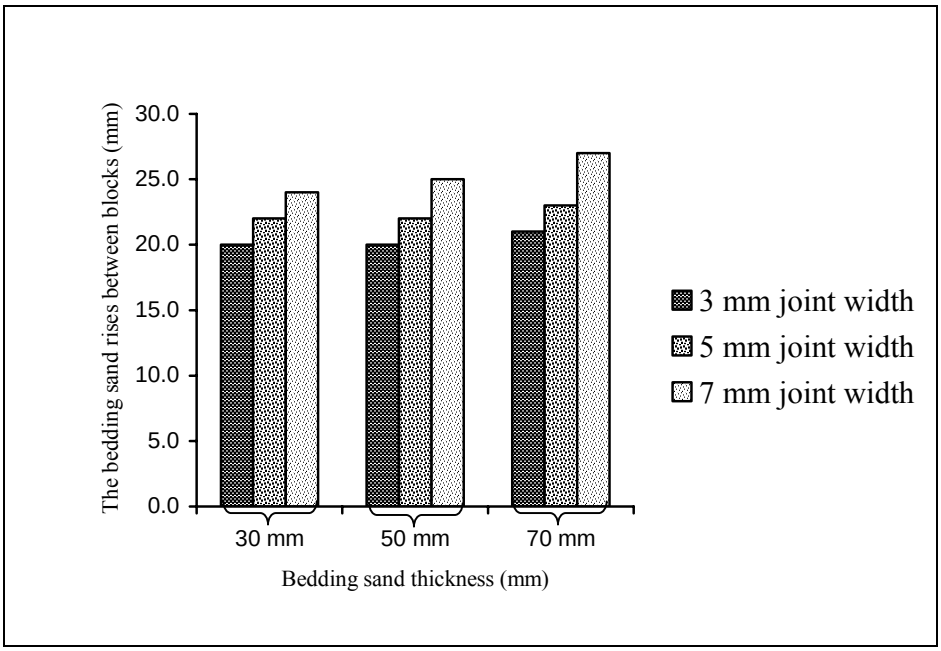

Figure 2.9 The comparison bedding sand rises in various widths joint with bedding sand thickness, *Knapton and O'Grady (1983).*

The findings of this study are contradictory to those reported by Knapton and O'Grady (1983). Knapton and O'Grady (1983) have found an increase in bedding sand thickness produced a proportionate increase in load-carrying capacity of pavement. As the pavement response is nearly for 50 mm thickness of bedding sand can be recommended to use in the field. But this depends on other factor, such as required level in sub-base tolerance and rise of bedding sand through the joints. Also, there should be a sufficient depth of bedding sand for deflection of pavements under load. Rise of bedding sand is essential to induce interlock.

2.2.3 Edge Restraints

The paved area must be restrained at its edges to prevent movement, either of the whole paved area or individual blocks. Edge restraints resist lateral movement, prevent rotation of the blocks under load and restrict loss of bedding sand material at the boundaries. Edge restraints should be laid at all boundaries of the block-paved area including where block paving abuts different flexible materials, such as bituminous bound material. They should be suitable for the relevant application and sufficiently robust to resist displacement if likely to be overrun by vehicles. It may be necessary to extend sub-layers to support the edge restraint together with any base and hunching. Compaction of pavement layers near edge restraints should be delayed until any concrete bed and hunching has gained sufficient strength to prevent movement of the edge restraint.

2.2.4 Sub-base and Base Course

Sub-Base: This is the optional layer underlying the base-course. Sub-base material will usually be lower grade than the base-course, Class 3 or better with a PI (Plasticity Index) not exceeding 10. The sub-base should be compacted to 95 per cent modified density in layers, the thickness of which must be consistent with the capabilities of the compaction equipment being used. This may require compacting equipment with a higher capacity than a standard plate compactor. The sub-base may be a cement-stabilized material, British Standard (1973).

Base-Course: The base-course should be a Class 1 material with a PI not exceeding 6. It should be compacted to 98 per cent modified density. Again this may require high capacity compaction equipment and the base-course may be cement stabilized (British Standard, 1989).

2.2.5 Sub-grade

The bearing capacity of the sub-grade (or natural ground) must be determined as a basis for the overall design. The measure used is the California Bearing Ratio (CBR) which is usually determined by indirect means such as the dynamic cone penetrometer. Laboratory-soaked CBR should be used for clay sub-grades. Clay sub-grades in particular should be drained to ensure the design CBR accurately reflects that in the field. Sub-grades should be compacted prior to the placement of road-base materials (Shackel, 1993).

2.3 Compaction

The laying course material and blocks should be compacted using a vibrating plate compactor. Some blocks may require a rubber or neoprene faced sole plate to prevent damage to the block surfaces (Interpave, 2004).

The block paved area should be fully compacted as soon as possible after the full blocks and cut blocks have been laid, to achieve finished pavement tolerances from the design level of ± 6 mm. Adjacent blocks should not differ in level by more than 2 mm and, when measured with a 3 m straight edge, there should be no surface irregularity (i.e. depression or high point) greater than 10 mm. No compaction should be carried out within 1.0 m of an unrestrained edge.

- Design level tolerance ± 6 mm
- Maximum block difference 2 mm
- Maximum under straight edge 10 mm

2.4 Load-Deflection Behaviour

The general load-deflection behaviour is irrespective of block shape, size, strength, thickness, and laying pattern that the load deflection profile has a similar shape. It is seen that the pavement deflection increased in a nonlinear manner with increasing load. An interesting observation is that the rate of deflection decreases with increasing load (within the range of magnitude of load considered in this study) rather than increases, which is the case with flexible and rigid pavements. Increase in the load was caused the rotation of individual blocks increases. This will lead to an increase in the translation of blocks and in turn an increase in the thrusting action between adjacent blocks at hinging points (Panda and Ghosh 2001). As a result, the rate of deflection of the pavement decreases. It is established that the load-distributing ability of a concrete block surface course increases with increasing load (within the range of magnitude of considered in this study). The results obtained are similar to that established in earlier plate load tests by Knapton (1976), Clark (1978), and Miura *et al*. (1984).

A type of interlock; vertical, rotational and horizontal of CBP cross section is shown in Figure 2.10 CBP is constructed of individual blocks of brick-sized units, placed in patterns with close, unmortared joints on a thin bed of sand between edge restraints overlaying a sub base. The joint spaces are then filled with sand. The blocks are available in a variety of shapes and are installed in a number of patterns, such as stretcher bond, herringbone bond, etc. The load spreading and other structural characteristics of the concrete blocks were inconsistent with different findings in respect to such factors as block shape, thickness, and laying pattern. This research presents the results of an experimental programme conducted to investigate the effects of changing parameters of bedding and jointing sand on pavement performance. A laboratory-scale model was devised to study these parameters using steel frame loading tests.

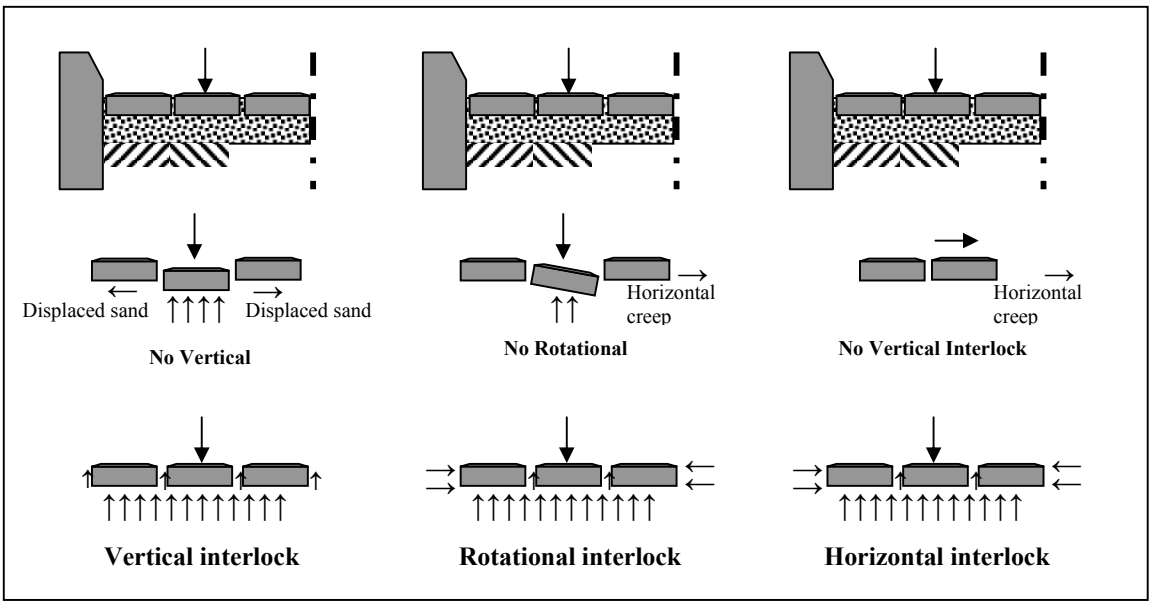

Figure 2.10 Types of interlock; vertical, rotational and horizontal of CBP *(Shackel, 1988)*

2.5 Effects of Load Repetition

(Panda and Ghosh, 2002) reported, that the rectangular blocks were laid in a herringbone pattern. The test pavements were subjected to 250 cycles of loading and unloading, and the resulting deflections were measured. In each cycle, load is gradually increased from 0 to 51 kN and then released slowly to 0 kN. The total time of loading and unloading operation for each cycle was within 30 seconds. For the first five cycles, the deflections were measured at each load interval, and for the remaining cycles, the deflections are measured at the 0 and 51 kN load levels. For each load repetition, the deflections during loading and recovery of deflections during unloading are determined. It may be seen that the response is nonlinear.

The deflection is not fully recovered. In other words, permanent residual deformations develop due to load repetition. During loading, additional compaction of sand under blocks occurs, and some part of the energy is lost in that way. As a result, the recovery is not full. It is the relationship of deflection during loading and its recovery with number of load repetitions. It may be observed that both deflection and recovery decrease with an increase in number of load repetitions. After about 150 load repetitions, the deflection and recovery are nearly the same; i.e., the recovery is full. In other words, the pavement acquires a fully elastic property. This is due to the fact that the additional compaction of bedding sand gradually increases with increase in load repetition. After a certain number of repetitions, the compaction of the underlying layers reaches its full extent and no energy is lost during additional loadings. As a result, the deflection and recovery become the same. Thus, it is established that block pavements stiffen progressively with an increase in the number of load repetitions. (Panda and Ghosh, 2002)

In accelerated trafficking tests by Shackel (1980), the range of the number of load repetitions required to achieve fully elastic property varies from 5,000 to 20,000 depending upon the magnitude of load (24 – 70 kN). The bedding sand is compacted under the wheel load. Adjacent to the loading area, the surface of the pavement bulges out. Thus, the bedding sand loosens. Areas under the wheel track are subjected to alternate bulging and compression as the wheel moves. For plate load tests, in this study, the load is applied at the same area and the bulging effect is nil, so it took only 150 kN load repetitions to achieve the fully elastic property.

2.6 Mechanism of Paver Interlock

Even block pavements which are judged to be well laid typically exhibit small rotations of the pavers relative to one another. These rotations develop both during

construction and under traffic. Such small movements are almost imperceptible to the naked eye but can be measured using profilometers to map the surface of the paving. Measurement shows the rotations are usually less than 10^{o} and are associated with surface displacements typically less than 5 mm. Accordingly, the movements may appear to be of little practical import. However, because concrete pavers are manufactured too much higher and more consistent dimensional tolerances than any other form of segmental paving they tend to be laid so that the joints between the pavers are consistently narrow and relatively uniform in width. For example, in Australia, it is customary to require paving to consistently achieve joint widths within the range 2 to 4 mm and this proves relatively easy to attain in practice provided normal tolerances are maintained during paver manufacture. With such narrow and consistent joints rotation of a paver soon results in it wedging against its neighbours as shown schematically in the cross-section, Figure 2.12 As shown in this figure, the wedging action caused by rotation of paver B around a horizontal axis leads to the development of horizontal forces within the paving.

The wedging action illustrated in Figure 2.13 explains why it is commonly observed that paver surfaces can push over inadequate edge restraints and make the reinstatement of trenches difficult or impossible unless the surrounding paving is restrained from creeping inwards (Shackel, 1990). More importantly, it also explains why pavers act as a structural surfacing rather than merely providing a wearing course (Shackel, 1979, 1980 1990, 1997, 1999, 2000 and 2001). It is therefore of interest to examine the factors and forces contributing to the development of horizontal forces between pavers within concrete segmental paving. These factors include the paver shape and the laying pattern.

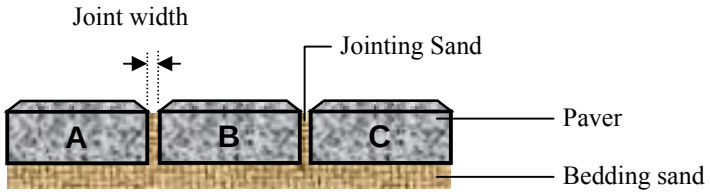

Figure 2.11 Sample of concrete block pavement

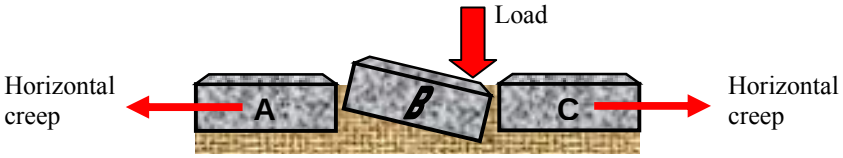

Figure 2.12 Rotation of paver B causing outward wedging of pavers A and B

The effects of paver shape can be understood by considering the effects of paver rotation upon the wedging together of the pavers. For the case of rectangular pavers this is illustrated schematically in Figure 2.12, if paver B is subject to rotation about a horizontal axis through its mid point then it is free to slide upon pavers A and C and will only push on pavers in line with the rotation such as paver D in Figure 2.13. Wedging therefore occurs only in that direction.

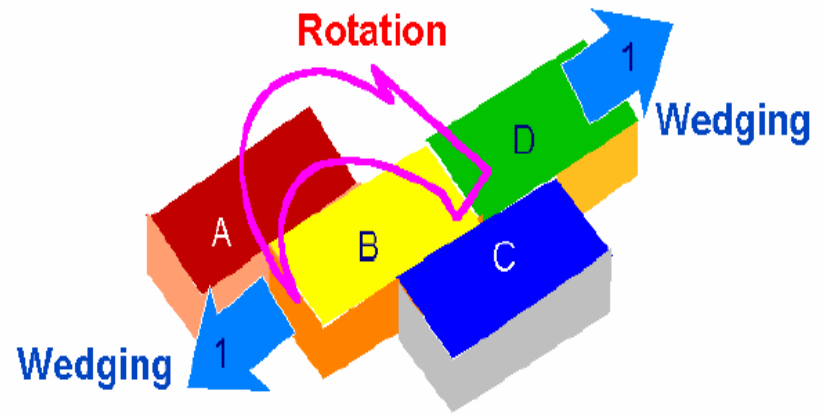

Figure 2.13 Effects of rotation on the wedging action of rectangular pavers

By contrast, if the same rotation is applied to a shaped paver, then, as shown in Figure 2.14, paver B cannot rotate without pushing pavers A and B away. Consequently wedging now develops in the two directions shown by arrows 1 and 2 even though the applied rotation remains uni-directional. This provides a simple explanation why shaped pavers have been reported to exhibit higher module and better in-service performance than rectangular pavers (Shackel, 1979, 1980, 1990 and 1997).

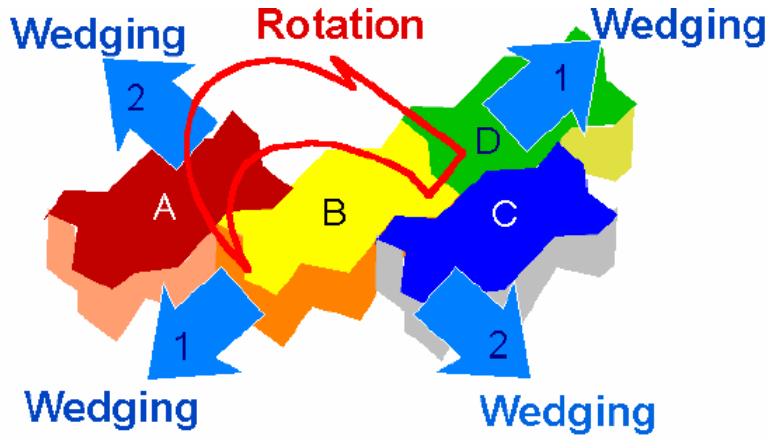

Figure 2.14 Effects of rotation on the wedging action of shaped pavers

On the basis of both tests and experience, engineers have long known that paving installed in herringbone patterns performs better than when laid in the stretcher laying pattern shown in Figure 2.13 and 2.14. Again, some explanation of this can be obtained by considering the effects of paver rotation. Figure 2.15 shows this case for rectangular pavers.

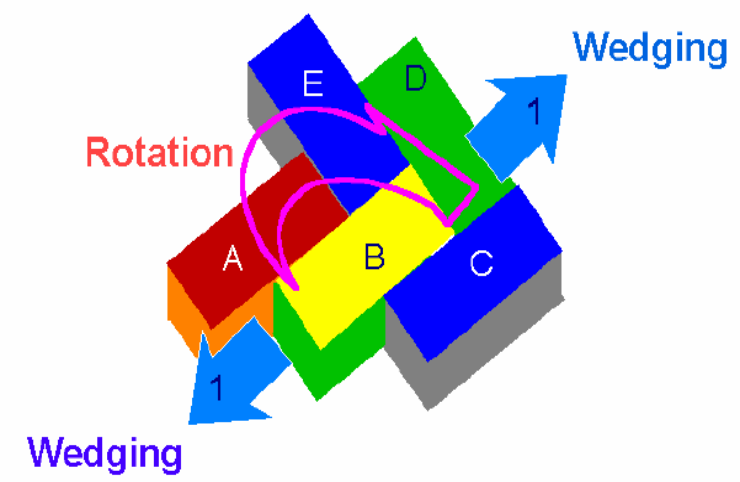

Figure 2.15 Effects of paver rotation on paving lay in herringbone bond

From Figure 2.15 it may be seen that whilst, as in the case of stretcher bond, rotation of paver B can still occur without horizontally displacing pavers A and C, the movement of paver B about a horizontal axis will now induce some rotation of paver D around a vertical axis. This is in addition to developing horizontal wedging as shown by the arrows 1. This will tend to increase the wedging action throughout the paved surface and provides some explanation why herringbone patterns perform better than stretcher bond.

Some authorities have claimed that, once rectangular pavers are installed in herringbone pattern, they perform in a manner similar to shaped pavers. This is, however, contradicted by the results of both trafficking and laboratory load tests (Shackel, 1979, 1980, 1990). The most likely explanation for this is that, as shown in Figure 2.16, wedging in directions both along and across the axis of rotation remains the inevitable consequence of paver rotation irrespective of the laying pattern. Here the choice of herringbone bond merely adds additional wedging movements to the paving surface because of the induced rotations of the pavers about vertical axes.

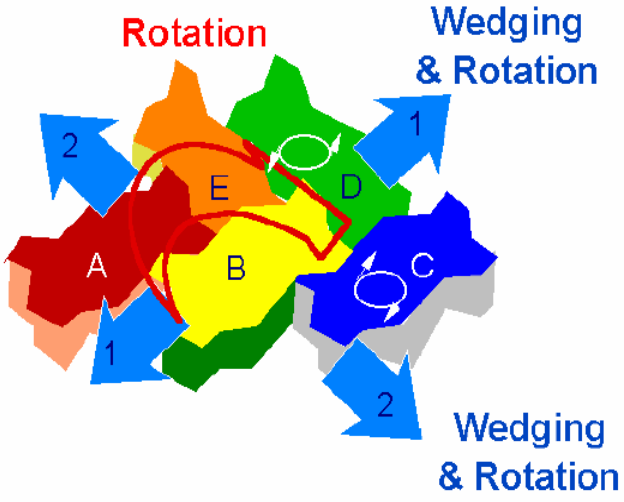

Figure 2.16 Effects of paver rotation on uni-pave shaped pavers lay in herringbone bond

The explanations of the effects of paver shape and laying pattern given above are simplistic because paver rotations are seldom confined to movements about just a single axis. Moreover, no account is taken of the joint width or the nature of the joint filling material. It might be argued that because most pavers are now fitted with spacer nibs the importance of the joint width and the joint filling material is minimal. However, it is usually found that the actual joint widths measured in pavements are bigger than the spacers. Moreover, tests of pavers fitted with spacers have shown that the pavers develop little or no structural strength when the joints are left empty (Shackel *et al,* 1996). In other words, the joints are crucial to segmental pavement performance.

2.7 The Role of the Joints in Pavement Interlock

In describing and modelling the behaviour of segmental paving many hypotheses have been advanced to explain the role of the joints. The movements that

are likely to occur at the joints in segmental paving are shown schematically in Figure 2.17. These comprise movements caused by rotations and linear displacements of the pavers. In practice the movements shown as (a) and (d) in Figure 2.17 are less likely to occur than the other movements because they imply net elongation of the pavement.

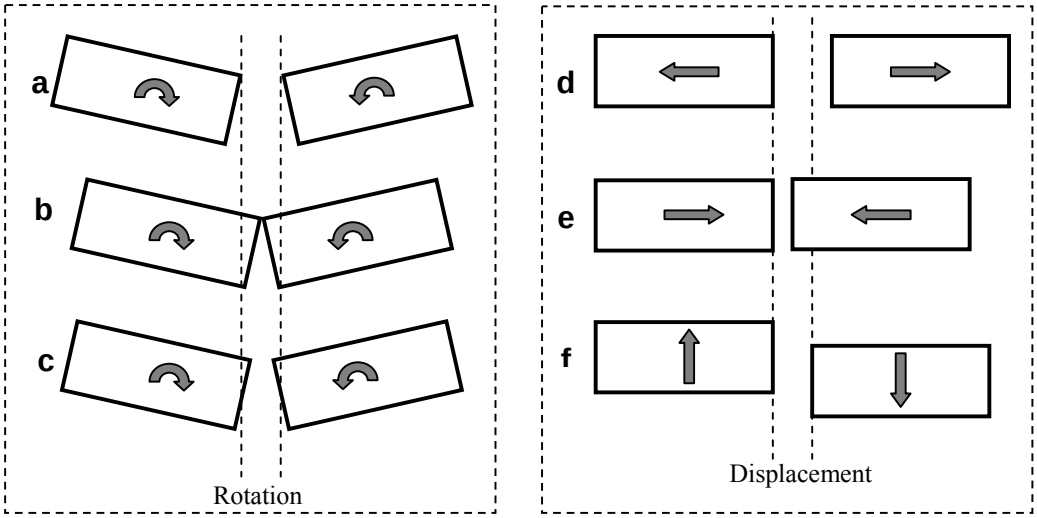

Figure 2.17 Movement of blocks at the joints

This will only occur when the pavement experiences rutting or heave i.e. some departure from the as-installed profile. In normal service the movements of pavers are likely to comprise combinations of both rotations and translations. In this it can be said, for example, that movement (c) in Figure 2.17 represents the combined effects of movements (b) and (f) or (a) and (e).

In this study, it is possible to measure rotations between adjacent pavers and to measure lipping movement such shown as Figure 2.17 (f). However, horizontal displacements such as those illustrated as Figure 2.17 (d) and (e) can only be measured directly. Nevertheless, some estimates of the strains in the jointing material can be obtained. Provided the stiffness of the jointing sand is known the strains can then be used to estimate the stresses in the material. Accordingly, to study the role of the jointing sand, measurements of typical jointing sand properties were combined and joint width of a range of concrete segmental pavements. The principal objective of this work was to estimate what magnitudes of force might be generated within the joints.

2.8 The Concrete Block Pavement on Sloping Road Section Area

Concrete Block Paving (CBP) differs from other forms of surfacing in that it comprises small segments and therefore is crisscrossed by a network of close spaced joints filled with sand. This means CBP is permeable and drainage of the surface and underlying layers is important. There is limited full scale testing world wide but from a study conducted by Shackel (1999);

a. Between 30 to 35 % of rainfall will penetrate newly laid, un-trafficked, and unsealed block pavements.
b. Increase in pavement cross-fall will increase surface runoff. (Recommended min. slope of 2 %.)
c. The permeability of the joints can be reduced by up to 50 % with an application of a water based acrylic sealer.

Similarly using 10 % of lime or 6 % bentonite to the jointing sand can inhibit infiltration. Generally no attempt is made to seal the joints hence attention should be directed towards reducing the consequences of water infiltration, particularly during the early life of the pavement. In practice care must be taken to select bedding sands not susceptible to water or seal the base if it comprises unbound granular materials or select base materials bound and waterproofed with cement, lime or bitumen. The management of water runoff and infiltration becomes therefore a critical aspect that will affect the performance and integrity of the CBP. Good, surface and subsoil drainage is essential for satisfactory pavement performance. Drainage needs to be considered during the design, specification and construction phases of a project. The following recommendations and detailing, although not new, but seldom practiced, are paramount for a trouble free and structurally sound CBP (CMA, 2000).

2.8.1 Basic Theory of Slope

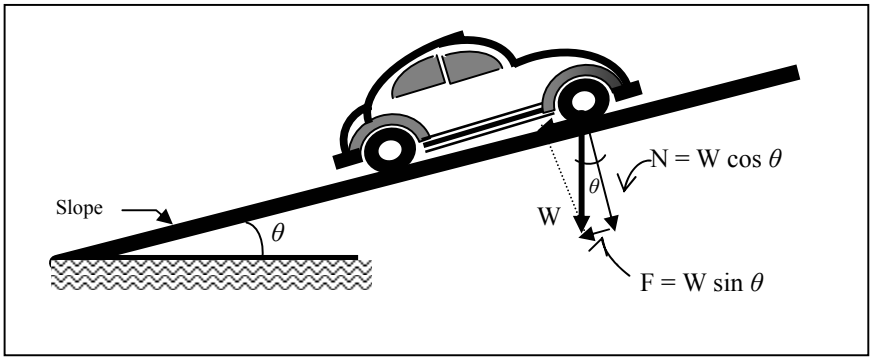

Figure 2.18 The magnitude of Force (F), Normal (N) and Load (W)

A block at rest on an adjustable inclined plane begins to move when the angle between the plane and the horizontal reaches a certain value θ, which is known as the angle repose. The weight W of the block can be resolved into a component F parallel to the plane and another component N perpendicular to the plane. Figure 2.18 the magnitudes of F and N are:

$$F = W \sin \theta \qquad (2.1)$$

$$N = W \cos \theta \qquad (2.2)$$

When the block just begins to move, the downward force along the plane F must be equal to be the maximum force μN of static friction, so that:

$$F = \mu N \qquad (2.3)$$

$$W \sin \theta = \mu W \cos \theta$$

$$\mu = \sin \theta / \cos \theta = \tan \theta$$

2.8.2 Construction of Steep Slopes

The construction of roads on steep slopes poses particularly interesting challenges for road engineers. The horizontal (inclined) forces exerted on the road surface are severely increased due to traffic accelerating (uphill), breaking (downhill) or turning. These horizontal forces cause distress in most conventional pavements, resulting in rutting and poor riding quality. Experience has shown that concrete block paving (CBP) performs well under such severe conditions.

2.8.3 Anchor Beam

It is common practice to construct edge restraints (kerbing and anchor beams) along the perimeter of all paving, to contain the paving and prevent horizontal creep and subsequent opening of joints. Due to the steepness of the slope, the normally vertical traffic loading will have a surface component exerted on the blocks in a downward direction. This force is aggravated by traction of the accelerating vehicles up the hill and breaking of vehicle down the hill. If uncontained, these forces will cause horizontal creep of the blocks down the slope, resulting in opening of joints at the top of the paving. An anchor beam at the lower end of the paving is necessary to prevent this creep. Figure 2.19 shows a typical section through an anchor beams. Anchor beams should be used on roads where the slope is greater than 12 % anchor beams should be used at the discretion of the engineer (CMA, 2000)

2.8.4 Spacing and Position of Anchor Beams

There are no fixed rules on the spacing anchor beams (if any) above the essential bottom anchor beams. The designer should determine this; however the following can be used as a guideline.

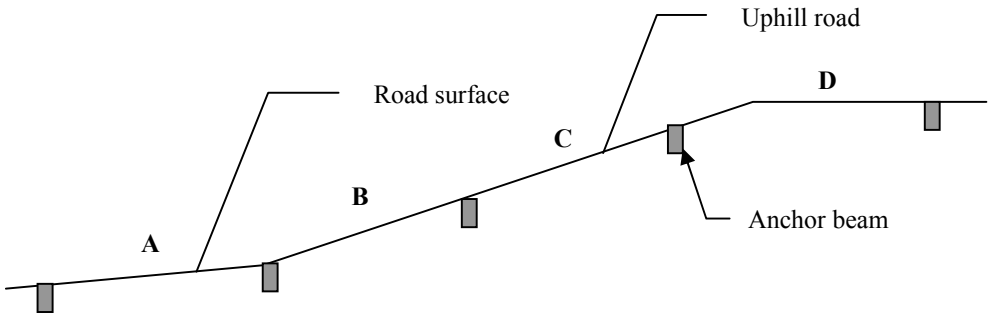

Figure 2.19 Spacing of anchor beams *(CMA, 2000)*

It is standard practice when laying pattern of concrete block paving to start at the lower and to work upwards against the slope. This practice will ensure that if there is any movement of blocks during the laying operation, it will help to consolidate the blocks against each other, rather than to open the joints.

2.8.5 Construction of Anchor Beam

For ease of construction, it is recommended that the blocks be laid continuously up the gradient. Thereafter, two rows of blocks are uplifted in the position of the beam, the sub base excavated to the required depth and width and the beam cast, such that the

top of the beam is 5 – 7 mm lower than the surrounding block work. This allows for settlement of the pavers. This method of construction will ensure that the anchor beam interlocks, with the pavers and eliminates the need to cut small pieces of block.

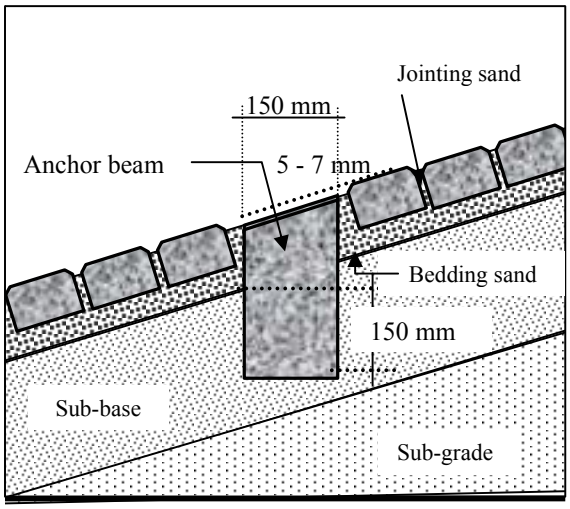

Figure 2.20 Detail construction of anchor beam *(CMA, 2000)*

2.9 Finite Element Modelling

The FE method is a numerical technique for solving problems with complicated geometries, loading, and material properties. It provides a solution for pavement problems, which are too complicated to solve by analytical approaches. The FE method has two general solution forms displacement (or stiffness method); and force (or flexible method). The former is the most popular form of the FE method. The basic FE process dictates that the complete structure is idealized as an assembly of individual 2D or 3D elements. The element stiffness matrices corresponding to the global degrees of freedom of the structural idealization are calculated and the total stiffness matrix is formed by the addition of element stiffness matrices.

The solution of the equilibrium equations of the assembly of elements yields nodes displacements, which are then used to calculate nodes stresses. Element displacements and stresses are then interpreted as an estimate of the actual structural behaviour (Bathe, 1982). The higher the number of nodes in a structure the greater the number of equations to be solved during the FE process, hence, the longer it takes to obtain a solution. Generally, the finer the mesh, the more accurate is the FE solution for a particular problem. Therefore, a compromise is needed between mesh refinement, model size, and solution time.

2.9.1 A Review of Two-Dimensional Finite Element Modelling

The enhanced computational capabilities of computers in the recent years with the availability of the FE method resulted in an innovation in the design and analysis of rigid pavements. Cheung and Zienkiewicz (1965) developed the first algorithm for the analysis of rigid pavements. They solved the problem of isotropic and orthotropic slabs on both semi-infinite elastic continuum and Winkler foundation using the FE method. Huang and Wang (1973) followed the procedure of Cheung and Zienkiewicz to develop a FE method to calculate the response of concrete slabs with load transfer at the joints. However, the developed model was incapable of handling multilayer systems.

Tabatabaie (1978) developed a computer program ILLISLAB. This program is based on the classical theory of a medium-thick plate on a Winkler foundation. Aggregate interlock and keyway joints were modelled using spring elements which transfer the load between blocks with jointing sand; while bar elements were used to model doweled joints which transfer moment as well as shear across the joint (Nasim, 1992).

Nasim developed a method to study rigid pavement damage under moving dynamic loading by combining dynamic truck tire forces with pavement response (Nasim, 1992). Computer models of trucks were used to generate truck tire forces of various trucks. Influence functions were obtained from COSMOS for different pavement designs. Truck wheel load histories were combined with those from pavement response to calculate time histories of the response of a rigid pavement to moving dynamic truck loads and therefore predict pavement damage.

Generally, 2D-FE programs demonstrate the potential capabilities of the modelling approach and represent significant improvement over traditional design methods. Most of these programs rely on plate elements to discrete concrete blocks and foundation layers (Davids, 1998), they allow the analysis of COSMOS with or without dowel bars and incorporate aggregate interlock shear transfer at the joint with linear spring elements. However, they are capable only of performing static analysis, and have limited applications. They cannot accurately model the following (Davids, 1998 and Kuo, 1994): Dynamic loading, detailed local response, such as stresses at dowel bar/concrete interfaces, realistic horizontal friction force at the interface between different pavement layers and vertical friction between the concrete blocks and jointing sand.

2.9.2 A Review of Three-Dimensional Finite Element Modelling Subjected to Traffic Loads

With the increased affordability of computer time and memory, and the need for better understanding of the reasons for some modes of pavement failure, 3D-FEM approach was adopted by many researchers. Ioannides, and Donelly (1988) examined

the effect of sub-grade support conditions on concrete block pavement. In this study, the 3D-FEM programme was used to develop a model consisting of a single concrete block and bedding sand. The study examined the effect of mesh refinement, vertical and lateral bedding sand extent, and boundary conditions on pavement response. Chatti (1992) developed the 3D-FEM called SOLIDWORK to examine the effect of load transfer mechanisms and vehicle speed on rigid pavement response to moving loads. The model is an extension of the static 2D-FE model called COSMOS. He showed that the maximum tensile stress occurs at the mid point of the block along the free edge, and observed stress reversal at the transverse joint.

Many researchers opted to use general purpose 3D-FEM software packages because of the availability of interface algorithms, thermal modules, and material models that make them most suitable for analyzing pavement structures. General purpose software such as ABAQUS, DYNA3D, and NIKE3D have been in the process of development by private and public domain organizations since the 1970s, and were used in design problems ranging from bridges to underground shelters that withstand nuclear explosions. Shoukry, *et al*. (1996 and 1997) examined the dynamic response of composite and rigid pavements to FWD impact using LS-DYNA. The results indicated the reliability of LSDYNA in predicting the dynamic surface deflections measured during FWD test. These results also demonstrated that pavement layer interface properties are very important considerations when modelling pavement structures.

Purdue University and Ohio DOT examined the effect of overloaded trucks on rigid pavements (Zaghloul, 1994). They used the FE code ABAQUS to develop a 3D-FEM of a multilayered pavement structure. An 80 kN (18-kip) Single Axle Load (SAL) was simulated by a tire print. The principal of superposition was used to model the SAL along the pavement. Results from this study showed that, when compared to interior loading, edge loading increased the vertical displacement and corresponding tensile stress by 45 and 40 percent, respectively. Increasing the load speed from 2.8 to 16 km/hr (1.75 to 10 mph) decreased the maximum surface deflection by 60 percent.

CHAPTER 3

MATERIALS AND TESTING METHODOLOGY

3.1 Introduction

This research begins by studying the interactions that can develop between adjacent blocks and between blocks (surface course) with the bedding and jointing sands especially on sloping road section. A series of tests conducted to investigate the effects of changing parameters of block shape, block thickness, laying pattern, bedding sand thickness and joint width between blocks. A laboratory-scale model to study the behaviour of concrete block pavement testing to highlight i.e. horizontal force test (to find the maximum horizontal creep) and push in test on various degree of slope (to find the maximum displacement). It can be shown that these horizontal and vertical forces can be significant to define the spacing of anchor beam that used in construction of CBP on sloping road section.

3.2 Flow Chart of Research

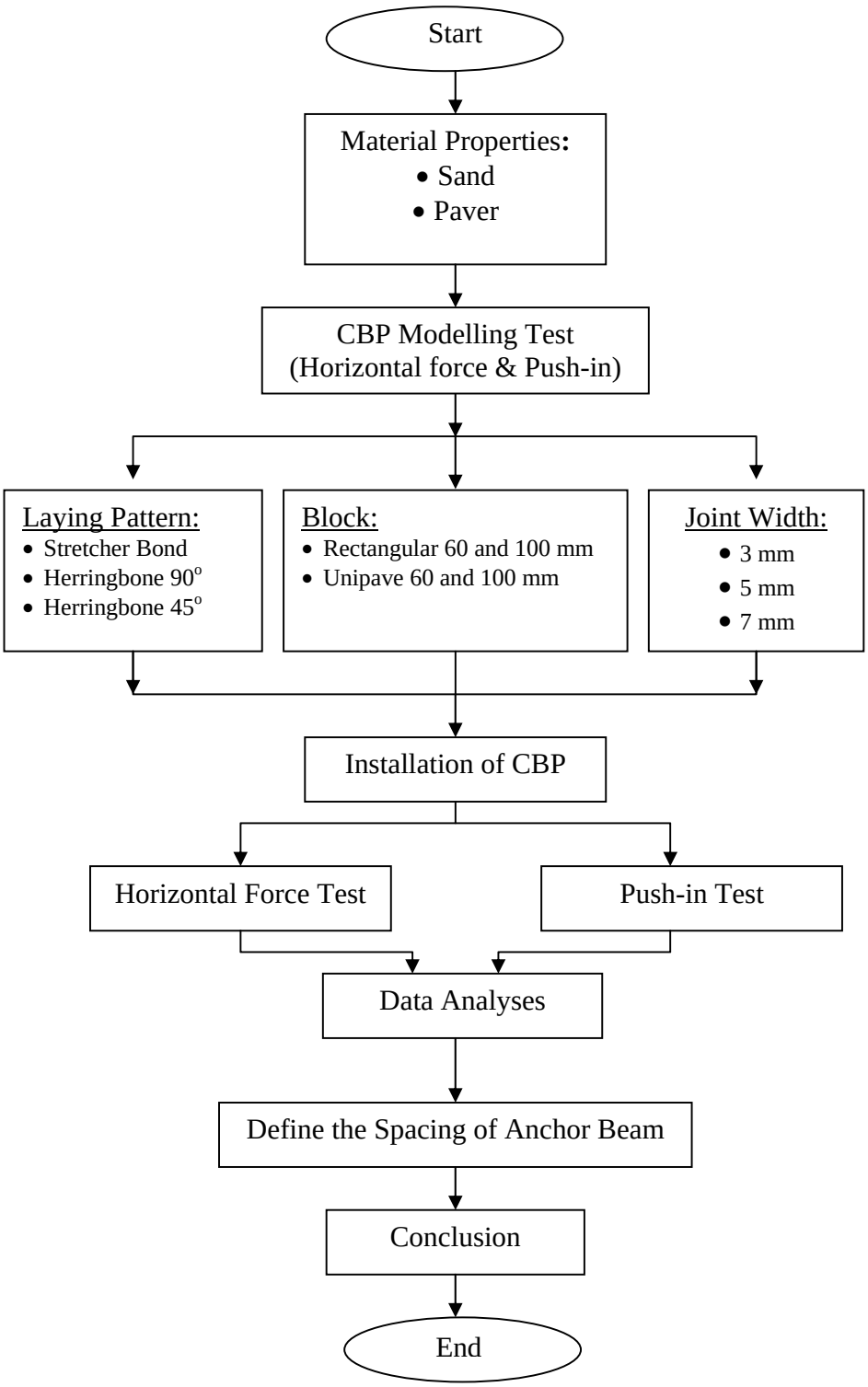

Figure 3.1 Flow chart of research

3.3 Material Properties

In this study, a series of horizontal force and push-in tests were performed to examine the interlocking concrete block pavement. Two blocks thickness (60 mm and 100 mm) were used in each experimental. Rectangular and uni-pave block shapes were used in horizontal force test.

3.3.1 Sand Material

River sand (mainly rounded quartz) from Kulai in Johor was used in this research. Sand was prepared from the coarse to fine in eight different gradations (for bedding sand) and six for jointing sand. The particle size distributions for bedding and jointing sand are described in Table 3.1. Prior to use in each experiment, the sand was oven dried at 110°C for 24 hours to maintain uniformity in test results. A maximum dry density of 17.3 kN/m^3 was obtained, corresponding to the optimum moisture content of 8.2 %.

The bedding and jointing sand material should have uniform moisture content. As a guide, after the material has been squeezed in the hand, when the hand is opened the sand should bind together without showing free moisture on its surface. Where bedding sand material is stored on site it should be covered to reduce moisture loss due to evaporation, or saturation from rainfall. If the sand becomes saturated after laying then it should be removed and replaced with bedding sand material having the correct moisture content. Alternatively the bedding sand can be left in place until it dries to the correct moisture content.

3.3.2 Paver Material

The concrete blocks were produced by Sun-Block Sdn. Bhd. in Senai Johor Bahru - Malaysia. These were made using ordinary Portland cement, siliceous fine aggregate, dolerite coarse aggregate and tap water. The portland cement conformed to the requirements of British Standard (BS). The coarse and fine aggregates complied with the requirements of BS (1983). The parameters studied in this research project include block shape and thickness. The details of block shapes studied are given in Figure 3.2 and Table 3.2.

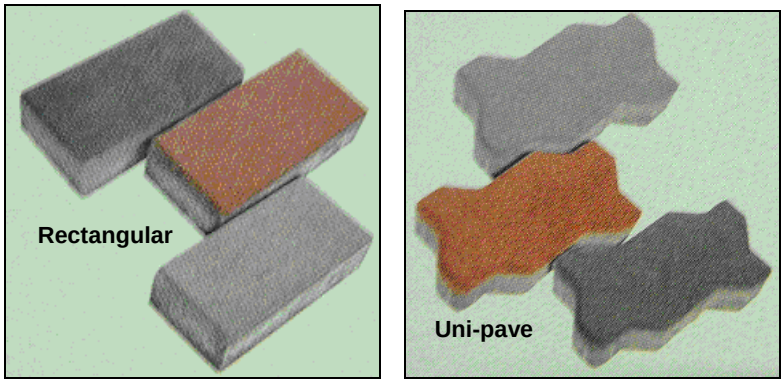

Figure 3.2 The shape of concrete block paver

The block concrete that used on experimental in laboratory is shown in Table 3.1 (for detail).

Table 3.1: Details of blocks used in study

Block type	Block shape	Length " L " (mm)	Width " B " (mm)	Area Coverage (pieces/m^2)	Thickness (mm)	Compressive strength (kg/cm^2)
1	Rectangular	198	98	49.5	60	350
2	Rectangular	198	98	49.5	100	350
3	Uni-pave	225	112.5	39.5	60	350
4	Uni-pave	225	112.5	39.5	100	350

Sun-Block Sdn. Bhd. (2004)

3.4 The Testing Installation

The horizontal force testing installation was constructed within the steel frame 2.00 x 2.00 metre. In this study, the effects of changing of laying pattern, joint width, block shape and block thickness are investigated. The steel frame as edge restraint was placed on the concrete floor and welded to the concrete floor.

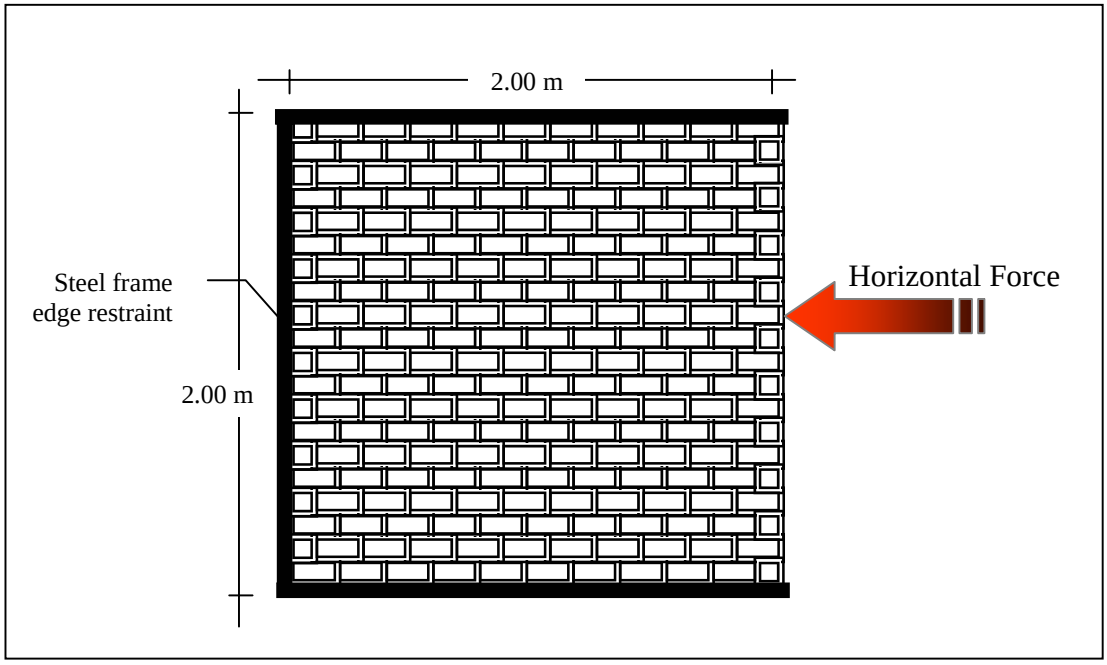

Figure 3.3 Stretcher bond laying pattern

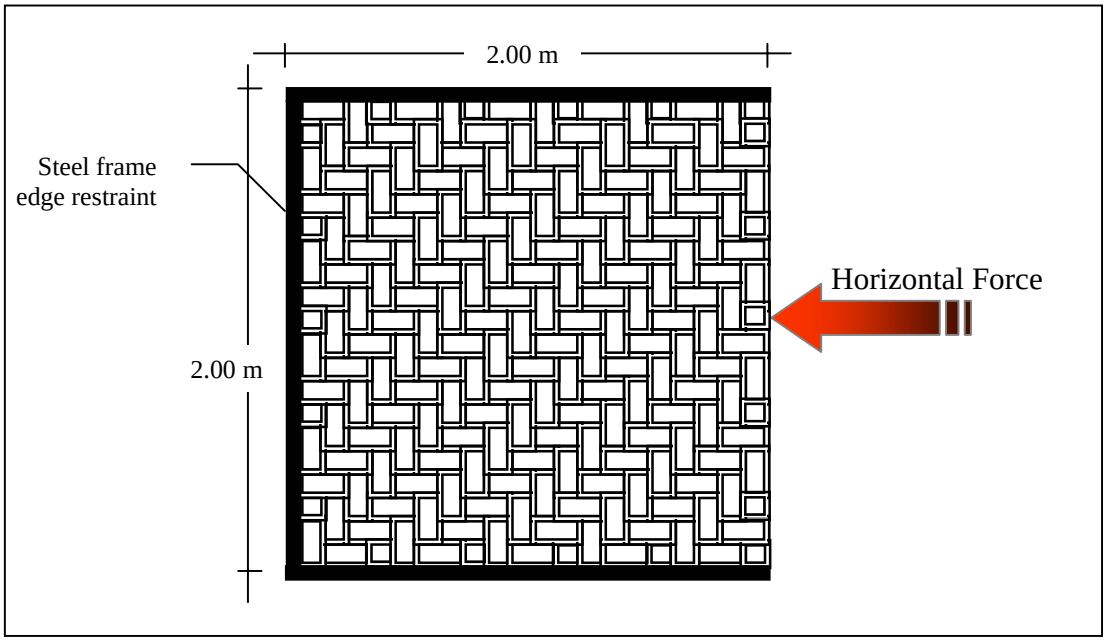

Figure 3.4 Herringbone 90^{o} bond laying pattern

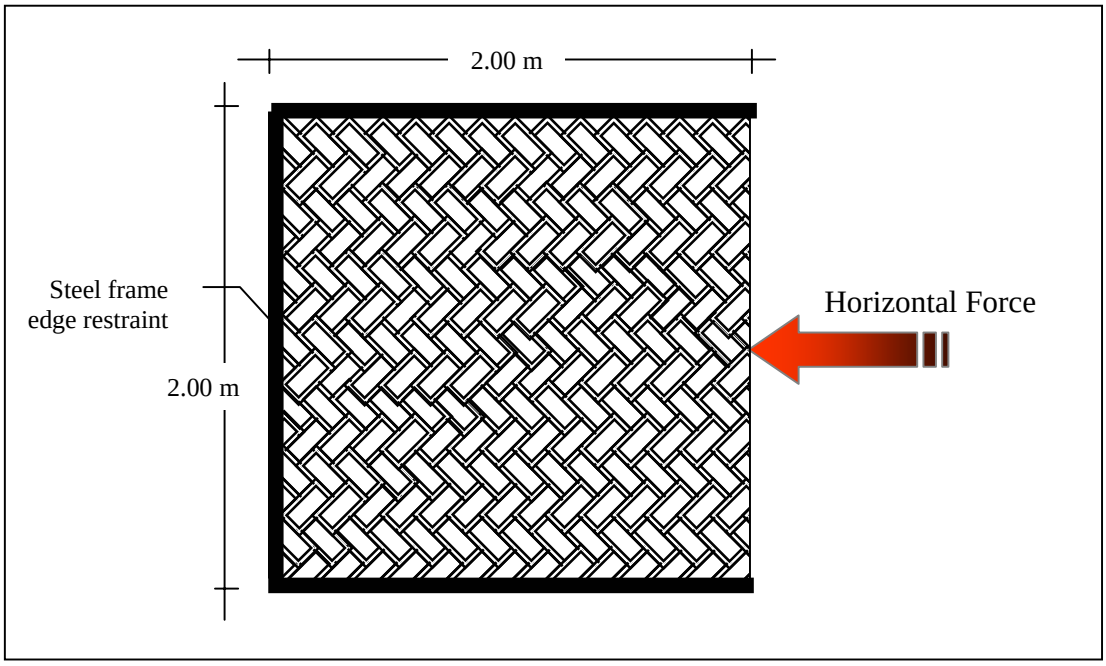

Figure 3.5 Herringbone 45^{o} bond laying pattern

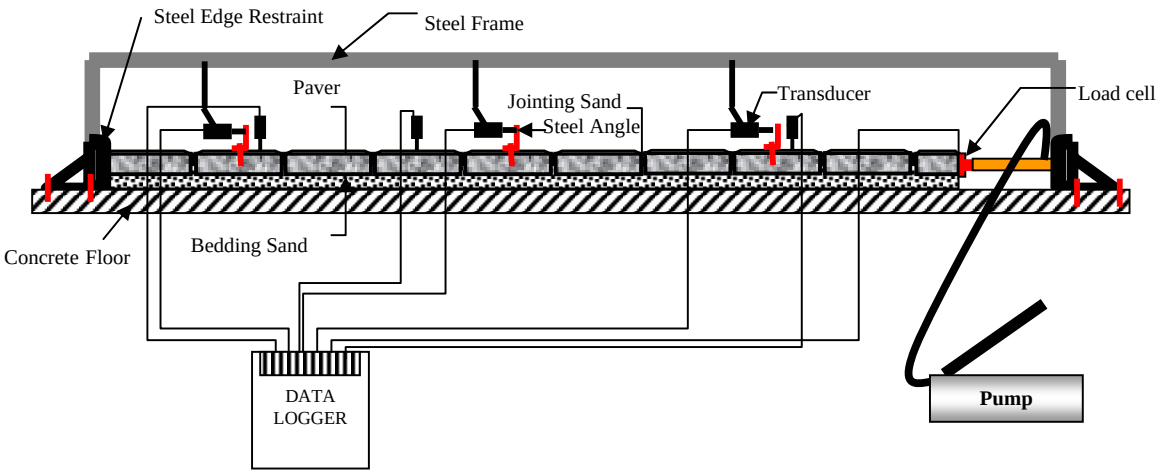

Figure 3.6 Horizontal force testing arrangement (*before testing*)

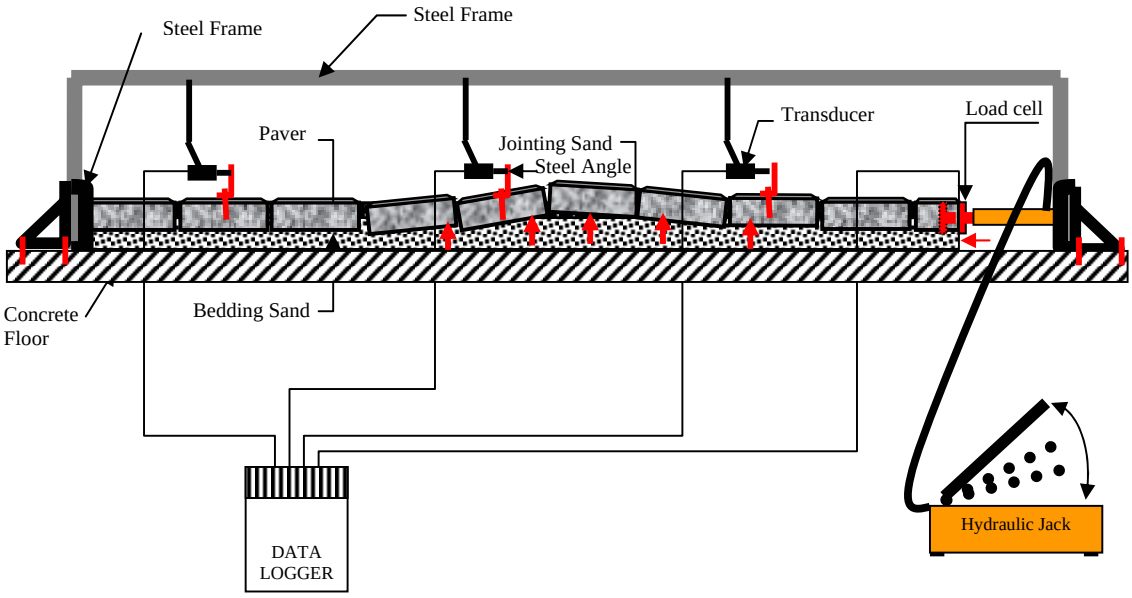

Figure 3.7 Horizontal force test condition (*after testing*)

3.5 Horizontal Force Testing Procedure

- Characterizing of the materials before testing (density, moisture content and sand grading).
- A layer of bedding sand should be spread loose and screened to a uniform thickness, it is important that the bedding sand layer remains undisturbed prior to the laying of blocks.
- Installation of the blocks and sealing of the jointing sand.
- General compaction of the block pavement with a hand-guided plate vibrator until it is firmly embedded in the bedding sand layer.
- Setting of measuring apparatus (zero settings),
- Horizontal force in successive stages tills 11 kN and measurements of horizontal creep used data logger.
- Characterizing of the CBP after experiment.

Figure 3.8 Installation of concrete block pavement (CBP)

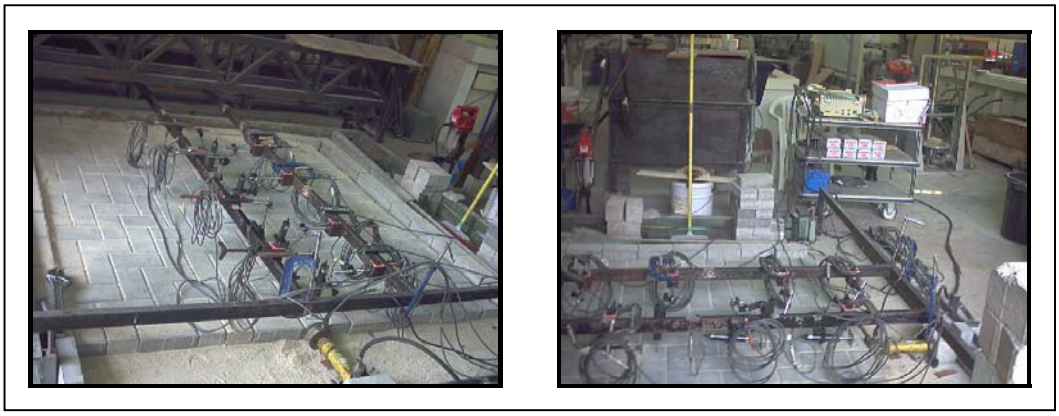

Figure 3.9 Horizontal force test installation

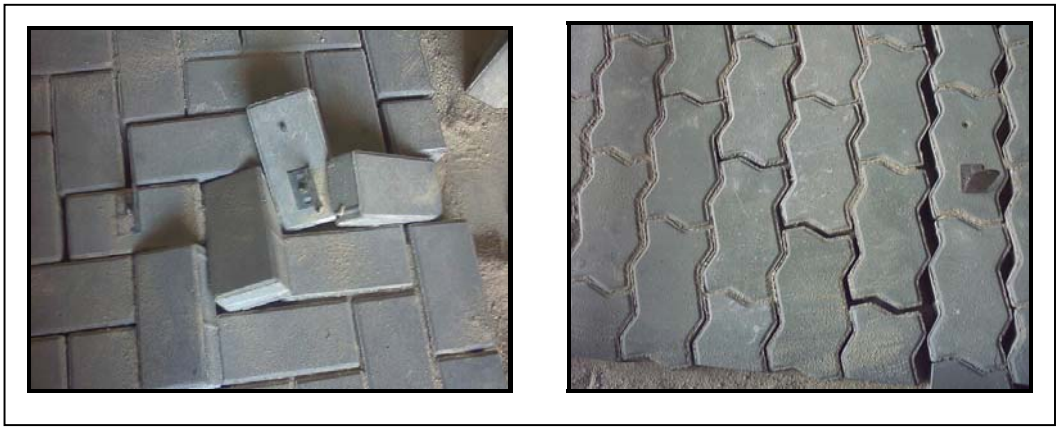

Figure 3.10 CBP failure after testing

3.6 The Variations of Testing in Laboratory

The horizontal tests of concrete block pavement (CBP) that were conducted in the laboratory were divided on several variations as shown in Table 3.2.

Table 3.2: The variation of horizontal force tests

No Test	Block				Laying Pattern	Joint Width (mm)	Bedding sand Thickness (mm)
	Shape	Length (mm)	Width (mm)	Thickness (mm)			
1	Rectangular	198	98	60	Stretcher	3	50
2	Rectangular	198	98	60	Stretcher	5	50
3	Rectangular	198	98	60	Stretcher	7	50
4	Rectangular	198	98	60	Herringbone 90^o	3	50
5	Rectangular	198	98	60	Herringbone 90^o	5	50
6	Rectangular	198	98	60	Herringbone 90^o	7	50
7	Rectangular	198	98	60	Herringbone 45^o	3	50
8	Rectangular	198	98	60	Herringbone 45^o	5	50
9	Rectangular	198	98	60	Herringbone 45^o	7	50
10	Rectangular	198	98	100	Stretcher	3	50
11	Rectangular	198	98	100	Stretcher	5	50
12	Rectangular	198	98	100	Stretcher	7	50
13	Rectangular	198	98	100	Herringbone 90^o	3	50
14	Rectangular	198	98	100	Herringbone 90^o	5	50
15	Rectangular	198	98	100	Herringbone 90^o	7	50
16	Rectangular	198	98	100	Herringbone 45^o	3	50
17	Rectangular	198	98	100	Herringbone 45^o	5	50
18	Rectangular	198	98	100	Herringbone 45^o	7	50
19	Uni-pave	225	112.5	60	Stretcher	3	50
20	Uni-pave	225	112.5	60	Stretcher	5	50
21	Uni-pave	225	112.5	60	Stretcher	7	50
22	Uni-pave	225	112.5	60	Herringbone 90^o	3	50
23	Uni-pave	225	112.5	60	Herringbone 90^o	5	50
24	Uni-pave	225	112.5	60	Herringbone 90^o	7	50
25	Uni-pave	225	112.5	60	Herringbone 45^o	3	50
26	Uni-pave	225	112.5	60	Herringbone 45^o	5	50
27	Uni-pave	225	112.5	60	Herringbone 45^o	7	50
28	Uni-pave	225	112.5	100	Stretcher	3	50
29	Uni-pave	225	112.5	100	Stretcher	5	50
30	Uni-pave	225	112.5	100	Stretcher	7	50
31	Uni-pave	225	112.5	100	Herringbone 90^o	3	50
32	Uni-pave	225	112.5	100	Herringbone 90^o	5	50
33	Uni-pave	225	112.5	100	Herringbone 90^o	7	50
34	Uni-pave	225	112.5	100	Herringbone 45^o	3	50
35	Uni-pave	225	112.5	100	Herringbone 45^o	5	50
36	Uni-pave	225	112.5	100	Herringbone 45^o	7	50

3.7 Push-in Test Arrangement

The test was conducted using steel frame tests in a laboratory-scale model assembled for this purpose (Figure 3.11). The test setup was a modified form of that used by Shackel *et al* (1993). He tested pavers laid and compacted within a steel frame in isolation from the bedding sand, sub-base course, and other elements of CBP. Here, instead of a steel frame, the tests were conducted in a box to incorporate the bedding sand, paver and jointing sand. In consists of a rigid steel box of 1000 x 1000 mm square in plan and 200 mm depth, in which pavement test sections were conducted. The box was placed on a steel frame; loads were applied to the test CBP through a rigid steel plate using a hydraulic jacking system of 100 kN capacity clamped to the reaction frame.

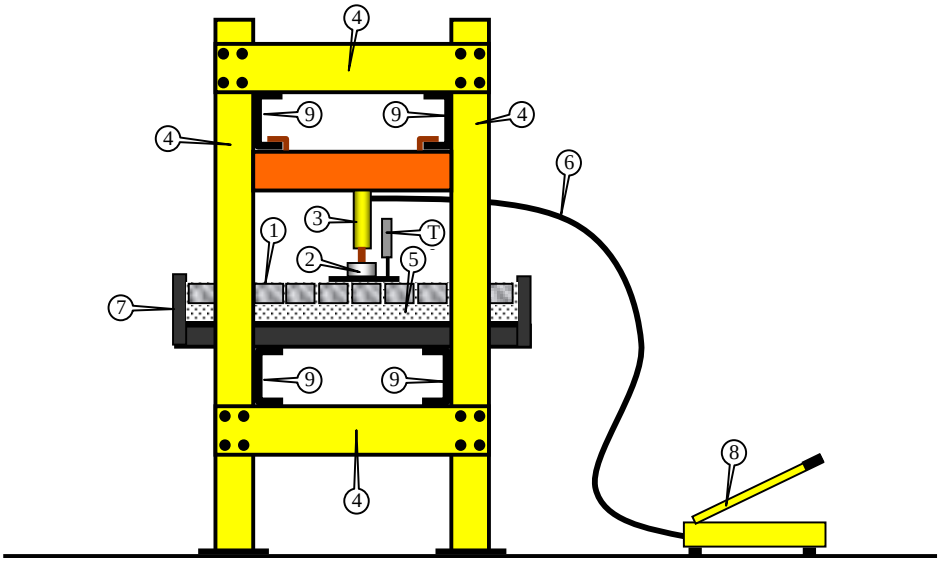

1. Block pavers
2. Load Cell
3. Hydraulic Jack
4. Steel Frame
5. Bedding sand
6. Pipe of hydraulic jack
7. Edge restraint
8. Hydraulic pump
9. Profile steel C channel
T. Transducer

Figure 3.11 Push-in test setup

3.8 Push-in Testing Procedure

A hydraulic jack fitted to the reaction frame applied a central load to the pavement through a rigid circular plate with a diameter of 250 mm. This diameter corresponds to the tyre contact area of a single wheel, normally used in pavement analysis and design. A maximum load of 51 kN was applied to the pavement. The load of 51 kN corresponds to half the single axle legal limit presently in force. Deflections of the pavements were measured using three transducers to an accuracy of 0.01 mm corresponding to a load of 51 kN. The transducers were placed on opposite sides of the plate at a distance of 100 mm from the centre of the loading plate. The average value of three deflection readings was used for comparing experimental results. The parameters, including joint width, thickness of bedding sand, and thickness of block, were varied in the experimental program. For each variation of a parameter, the test was repeated three times to check the consistency of readings. The average of the three readings is presented in the experimental results in graphical form. The range of the standard deviations (SD) of the readings for each parameter is presented in the respective figures. For each test, measurements of joint width were made at 20 randomly selected locations. The mean and standard deviation were calculated to assess the deviation from the design joint width. Design joint width as referred to herein be the desired width established in the experiment; however, the achieved joint widths always varied.

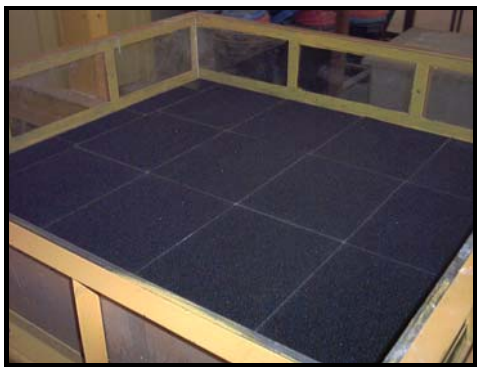

Figure 3.12 Steel frame and sand paper

Figure 3.13 Bedding sand

Figure 3.14 Installation of CBP

Figure 3.15 Compaction

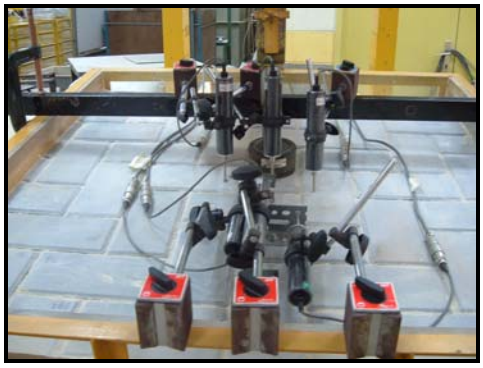

Figure 3.16 LVDT connection

Figure 3.17 Data logger in print-out

Figure 3.18 Push in test on sloping section

Table 3.3: Push-in test variations

Test No.	Degree of slope (%)	Bedding sand thickness (mm)	Block			Laying pattern
			Shape	Thickness (mm)	Joint width (mm)	
1	0	30	Rectangular	60	3	Stretcher Bond
2	0	50	Rectangular	60	3	Stretcher Bond
3	0	70	Rectangular	60	3	Stretcher Bond
4	0	30	Rectangular	60	5	Stretcher Bond
5	0	50	Rectangular	60	5	Stretcher Bond
6	0	70	Rectangular	60	5	Stretcher Bond
7	0	30	Rectangular	60	7	Stretcher Bond
8	0	50	Rectangular	60	7	Stretcher Bond
9	0	70	Rectangular	60	7	Stretcher Bond
10	0	30	Rectangular	100	3	Stretcher Bond
11	0	50	Rectangular	100	3	Stretcher Bond
12	0	70	Rectangular	100	3	Stretcher Bond
13	0	30	Rectangular	100	5	Stretcher Bond
14	0	50	Rectangular	100	5	Stretcher Bond
15	0	70	Rectangular	100	5	Stretcher Bond
16	0	30	Rectangular	100	7	Stretcher Bond
17	0	50	Rectangular	100	7	Stretcher Bond
18	0	70	Rectangular	100	7	Stretcher Bond
19	4	30	Rectangular	60	3	Stretcher Bond
20	4	50	Rectangular	60	3	Stretcher Bond
21	4	70	Rectangular	60	3	Stretcher Bond
22	4	30	Rectangular	60	5	Stretcher Bond
23	4	50	Rectangular	60	5	Stretcher Bond
24	4	70	Rectangular	60	5	Stretcher Bond
25	4	30	Rectangular	60	7	Stretcher Bond
26	4	50	Rectangular	60	7	Stretcher Bond
27	4	70	Rectangular	60	7	Stretcher Bond
28	8	30	Rectangular	100	3	Stretcher Bond
29	8	50	Rectangular	100	3	Stretcher Bond
30	8	70	Rectangular	100	3	Stretcher Bond
31	8	30	Rectangular	100	5	Stretcher Bond
32	8	50	Rectangular	100	5	Stretcher Bond
33	8	70	Rectangular	100	5	Stretcher Bond
34	8	30	Rectangular	100	7	Stretcher Bond
35	8	50	Rectangular	100	7	Stretcher Bond
36	8	70	Rectangular	100	7	Stretcher Bond
37	12	30	Uni-pave	60	3	Stretcher Bond
38	12	50	Uni-pave	100	5	Stretcher Bond
39	12	70	Uni-pave	60	7	Stretcher Bond
40	12	30	Uni-pave	100	3	Stretcher Bond
41	12	50	Uni-pave	60	5	Stretcher Bond
42	12	70	Uni-pave	100	7	Stretcher Bond
43	12	30	Uni-pave	60	3	Stretcher Bond
44	12	50	Uni-pave	100	5	Stretcher Bond
45	12	70	Uni-pave	60	7	Stretcher Bond

CHAPTER 4

INTERPRETATION OF EXPERIMENTAL RESULTS

4.1 Introduction

Results obtained from two tests conducted in laboratories which are horizontal force and push-in tests will be discussed in this chapter. First, for the horizontal test, the discussion will be about the effect of laying pattern, block shape, block thickness and joint width between blocks. Secondly, for the push-in test, the effects of bedding sand thickness, joint width and block thickness will be discussed. The rectangular block shape was used in each push-in test.

Tests data horizontal force and push-in tests were collected and presented in the table and graphical form. The maximum force of the model horizontal force and horizontal creep for each stretcher bond, herringbone 90^{o} and herringbone 45^{o} laying patterns were illustrated as shown in Appendices B1 and B2. While maximum force of the model horizontal force and horizontal creep for each rectangular and unit-pave block shape, 60 mm and 100 mm block thickness and 3 mm, 5 mm and 7 mm joints width are illustrated as shown in Appendices C1 and C2. For tests data push-in, the horizontal creep of concrete block pavement under 51 kN load for each testing are illustrated as shown in Appendices E to H.

4.2 Sieve Analysis for Bedding and Jointing Sand

The sieve analysis results from the experiment are shown in Table 4.1. From the graph plot, even though the sand distribution percentage of passing sieve 0.15 mm and 0.075 mm is small, the curve of distribution sand size still fulfil the BS requirement 882 (1201) Part 2 (1973) which is still in the state grade of curve envelope. Sieve analysis has been done separately for sand which has been used for bedding sand layer and also jointing sand. Sieve analysis for bedding sand is between 0.075 mm and 9.52 mm while for the jointing sand sieve size is between 0.075 mm and 2.36 mm.

Table 4.1: The average of sand grading distribution used for bedding and jointing sand.

Sieve Size	Bedding Sand			Jointing Sand		
	Percent Passing (%)	Lower limit (%)	Upper Limit (%)	Percent Passing (%)	Lower limit (%)	Upper limit (%)
9.52 mm	100	100	100	-	-	-
4.75 mm	95.6	95	100	-	-	-
2.36 mm	81.1	80	100	100.00	100	100
1.18 mm	50.4	50	85	91.20	90	100
600 μm	30.2	25	60	65.18	60	90
300 μm	14.0	10	30	40.08	30	60
150 μm	6.2	5	15	20.62	15	30
75 μm	2.6	0	10	6.53	5	10

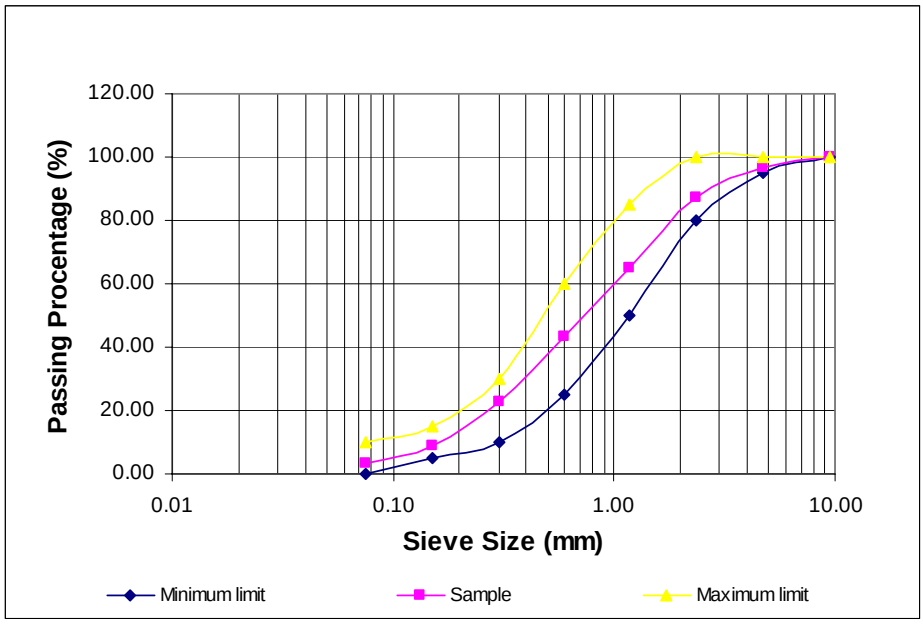

Figure 4.1 Sieve analysis graph for bedding sand

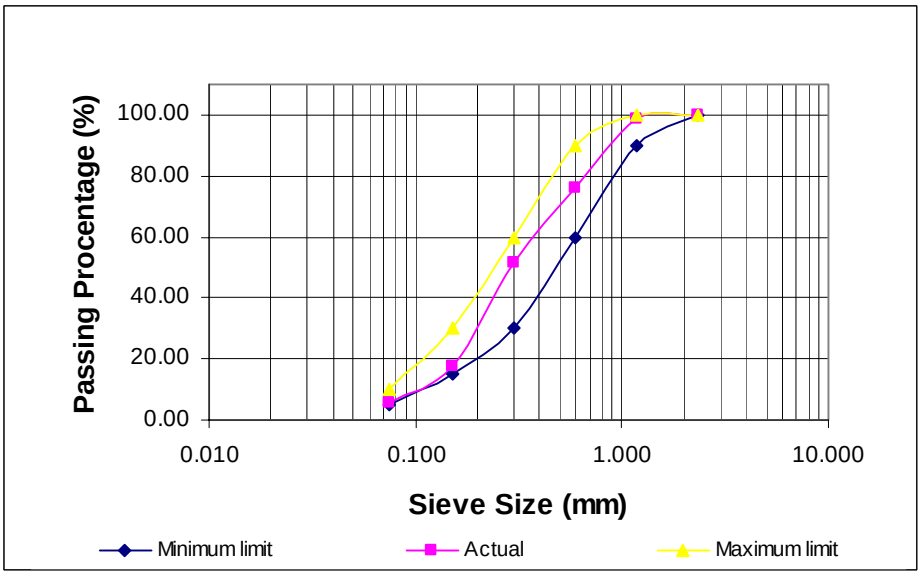

Figure 4.2 Sieve analysis graph for jointing sand

4.3 Moisture Content of Sand

The moisture content of sand required for bedding sand and jointing sand is between 4 to 8 %. From the experiment, the average of three samples is 7.4 %. Bedding sand and jointing sand moisture content should been counted because both influence the displacement and friction between blocks.

4.4 Horizontal Force Test Results

For the behaviour of block pavements under horizontal forces, the pavement may present various types of mechanical behaviour submitted to a horizontal force, depending on the laying pattern, blocks thickness, joint width between blocks and blocks shape.

4.4.1 The Effect of Laying Pattern

The effect of the laying pattern on concrete block pavements is significant with neighbour blocks movement under horizontal forces. The herringbone 45^{o} bond and herringbone 90^{o} bond have more neighbour movement effect than stretcher bond laying pattern.

4.4.1.1 Rectangular Block Shape

In the case of rectangular block shape, the experimental results from the laboratory based on joint width variable indicate that from the relationship between horizontal forces with horizontal creep, stretcher laying pattern is the highest on the horizontal creep, while herringbone 45^{o} laying pattern is the lowest. Here, the herringbone 90^{o} laying pattern has more horizontal creep than herringbone 45^{o} bond. The results are shown in Figure 4.3, Figure 4.4 and Figure 4.5. Each test was applied on CBP with 60 mm block thickness and variation of joint width (3 mm, 5 mm and 7 mm).

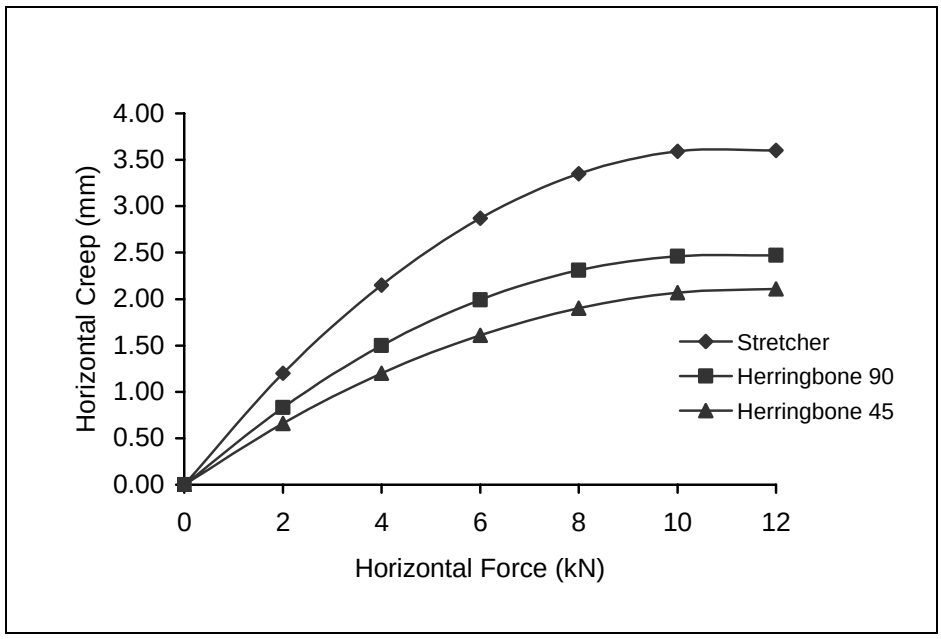

Figure 4.3 Relationship between horizontal forces with horizontal creep on CBP: rectangular block shape, 60 mm block thickness and 3 mm joint width.

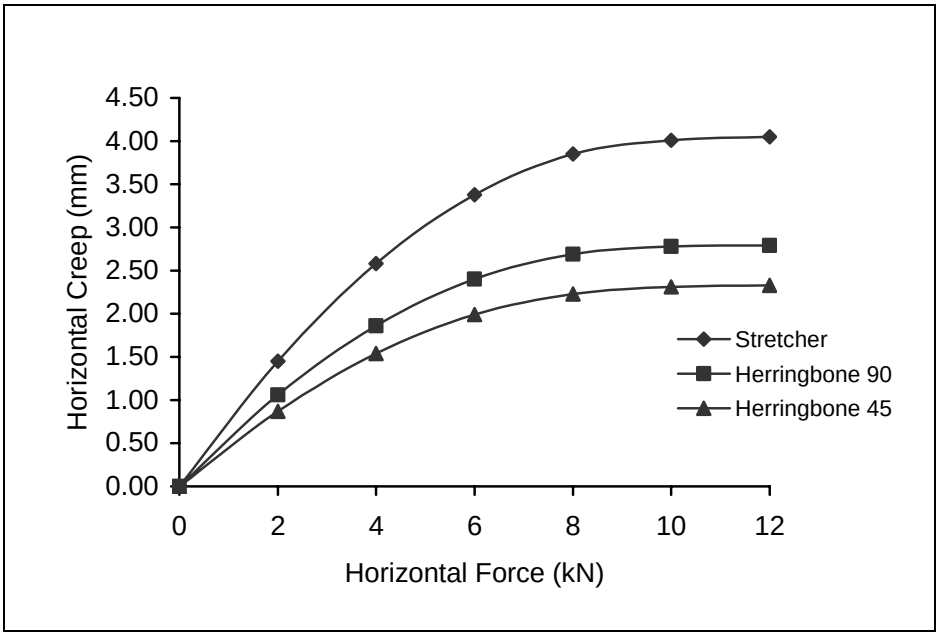

Figure 4.4 Relationship between horizontal forces with horizontal creep on CBP: rectangular block shape, 60 mm block thickness and 5 mm joint width.

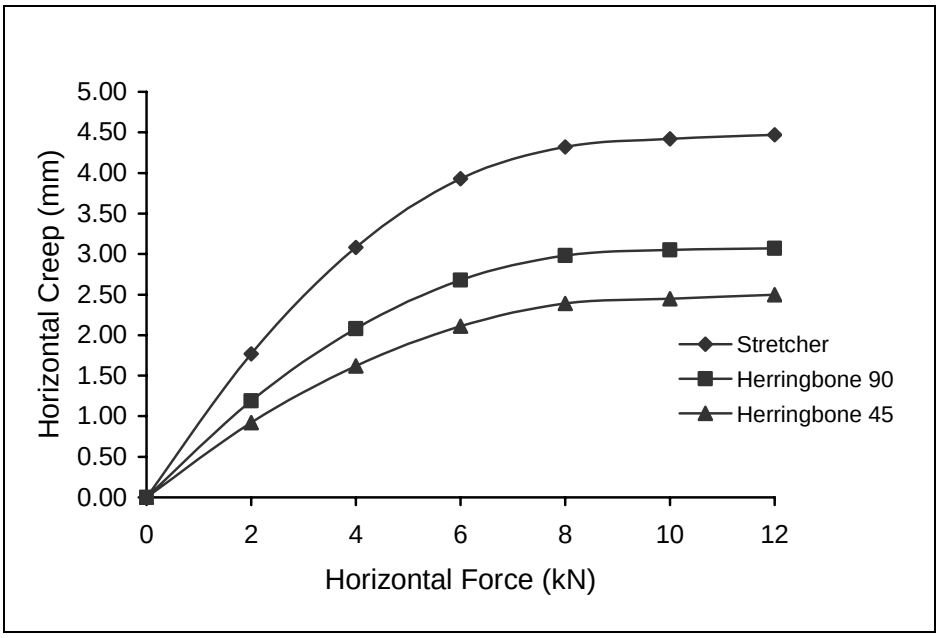

Figure 4.5 Relationship between horizontal forces with horizontal creep on CBP: rectangular block shape, 60 mm block thickness and 7 mm joint width.

4.4.1.2 Uni-pave Block Shape

In the case of uni-pave block shape, the experimental results from the laboratory based on joint width variable indicate that from the relationship between horizontal forces with horizontal creep, stretcher laying pattern is the highest the horizontal creep, while herringbone 45^o laying pattern is the lowest. Here, the herringbone 90^o laying pattern has more horizontal creep than herringbone 45^o bond. The results are shown in Figure 4.6, Figure 4.7 and Figure 4.8.

The results from Figure 4.6, Figure 4.7 and Figure 4.8, show that CBP using rectangular block shape has the lowest horizontal creep compared to uni-pave block shape, because rectangular block shape no dented while uni-pave block shape has four dents. The horizontal creep (movement) using uni-pave block shape is less than the rectangular block shape. It is illustrated in Figures 2.13 and 2.14.

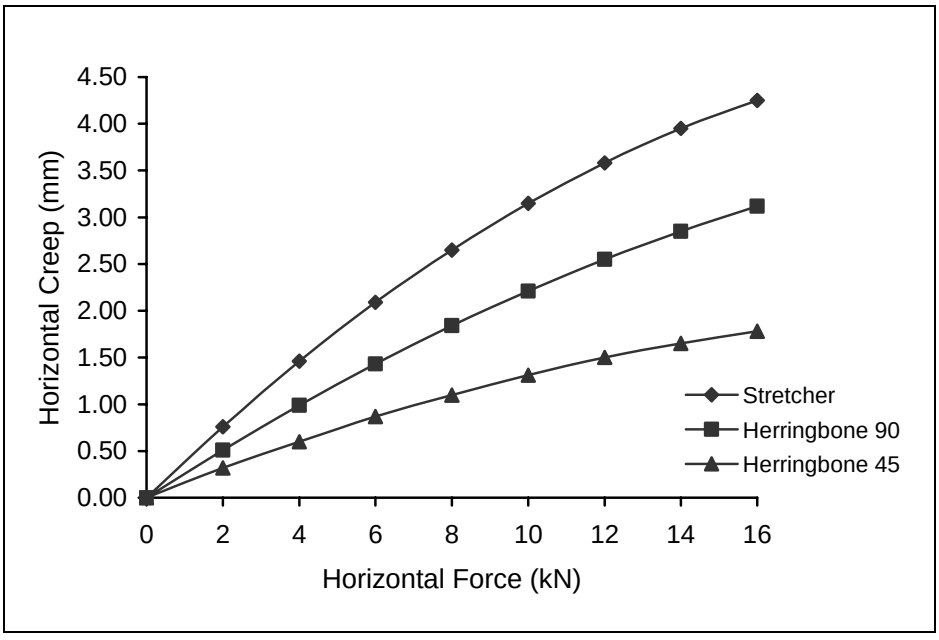

Figure 4.6 Relationship between horizontal forces with horizontal creep on CBP: uni-pave block shape, 60 mm block thickness and 3 mm joint width.

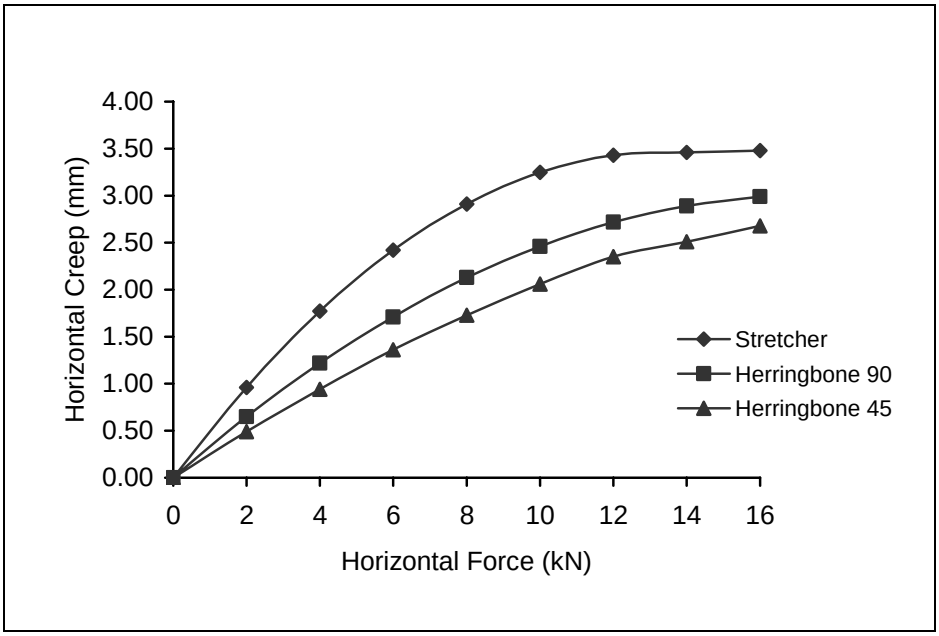

Figure 4.7 Relationship between horizontal forces with horizontal creep on CBP: unipave block shape, 60 mm block thickness and 5 mm joint width.

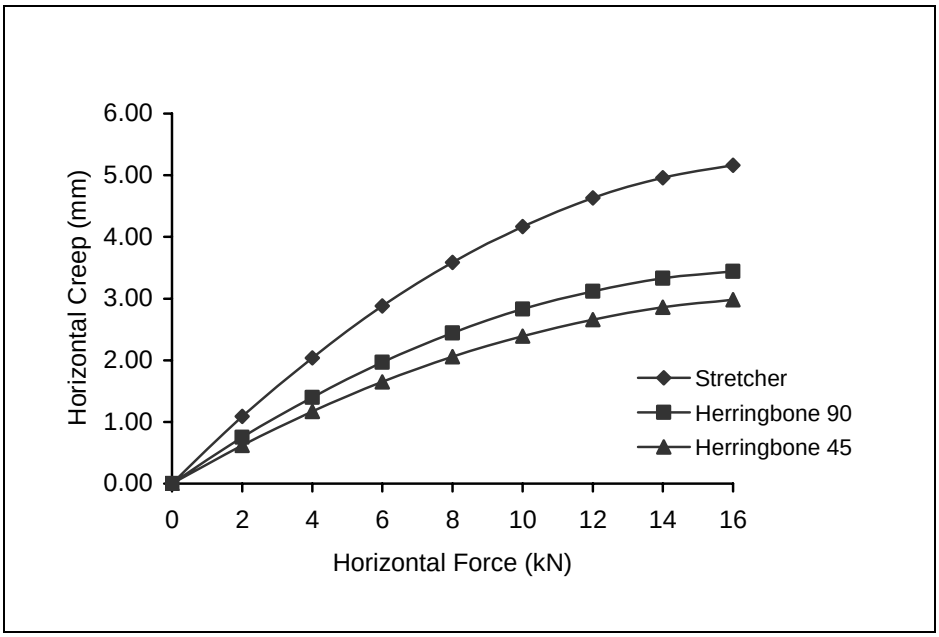

Figure 4.8 Relationship between horizontal forces with horizontal creep on CBP: unipave block shape, 60 mm block thickness and 7 mm joint width.

4.4.2 The Effect of Block Thickness

The effect of block thickness on concrete block pavements is significant with friction between blocks and the weight of block itself. The block thickness used was 60 mm and 100 mm thick. The rectangular unit weight 60 mm thickness (2.6 kg / unit) and 100 mm thickness (4.2 kg / unit).

This study includes an examination of block thickness ranging from 60 mm to 100 mm. Three parameters were used to asses the response of the pavements. There were: the surface deformations or rutting, surface elastic or resilient deflections and vertical compressive stresses transmitted to the sub-grade.

4.4.2.1 Rectangular Block Shape

The rectangular block shape has frictional area for load transfer to adjacent blocks. The friction area for rectangular shape is between blocks depending on the side surface of the block. It is concluded that the shape of the block influences the performance of the block pavement under load. It is postulated that the effectiveness of load transfer depends on the vertical surface area of the blocks.

In the case of rectangular block shape, the experimental results from the laboratory based on block thickness variable indicate that the relationship between horizontal forces with horizontal creep found that 100 mm block thickness is better than 60 mm block thick to restrain of the horizontal creep. The results are shown in Figure 4.9, Figure 4.10 and Figure 4.11. Each test was applied on CBP with stretcher bond laying pattern and variation of joint width (3 mm, 5 mm and 7 mm).

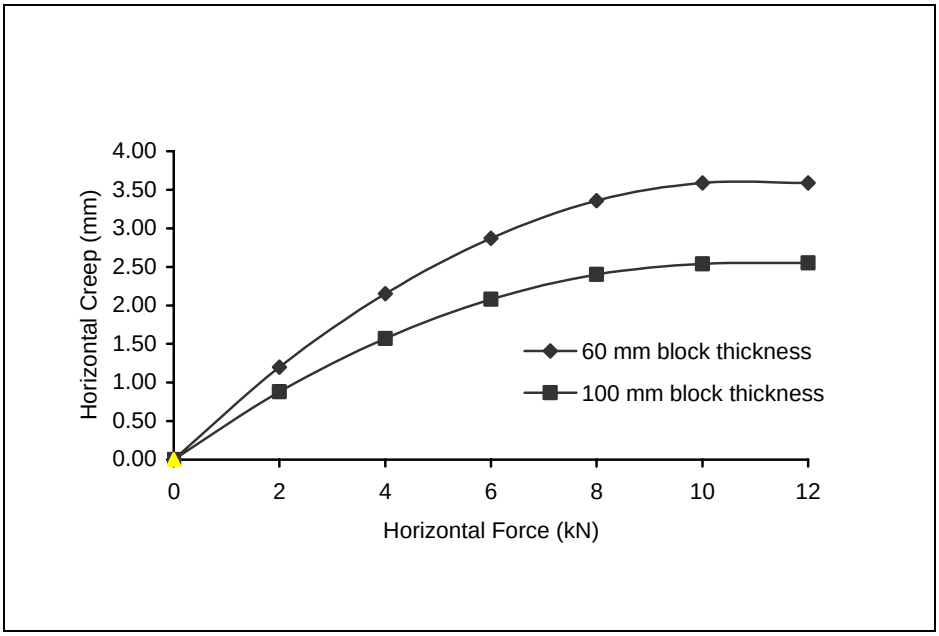

Figure 4.9 Relationship between horizontal forces with horizontal creep on CBP: rectangular block shape, stretcher bond laying pattern and 3 mm joint width.

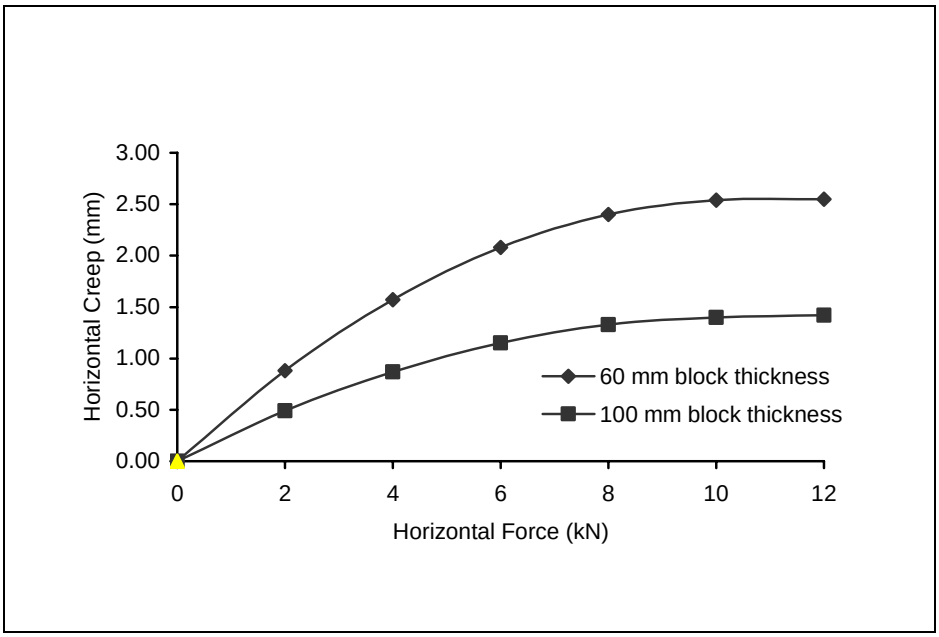

Figure 4.10 Relationship between horizontal forces with horizontal creep on CBP: rectangular block shape, 60 mm block thickness and 5 mm joint width.

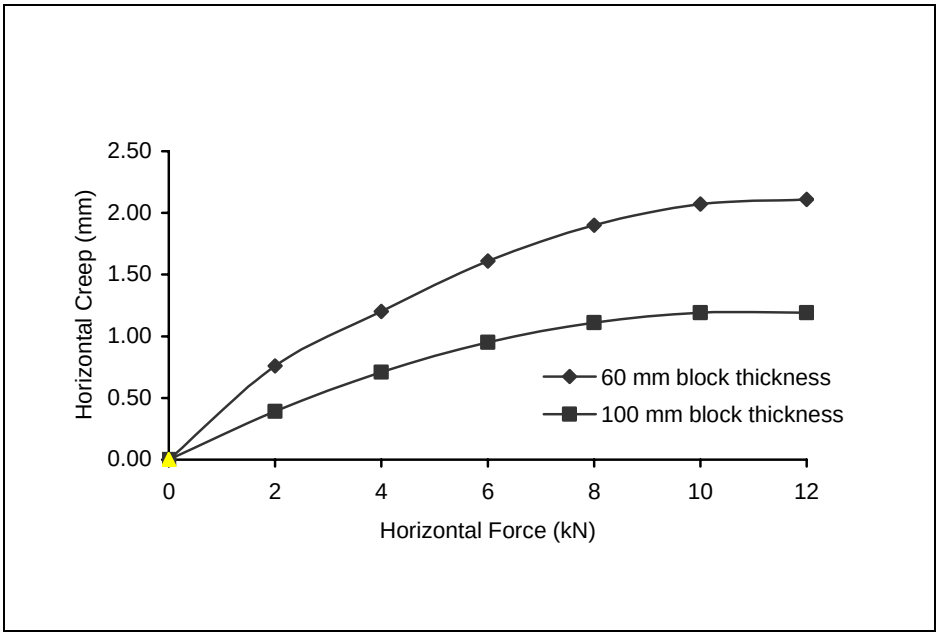

Figure 4.11 Relationship between horizontal forces with horizontal creep on CBP: rectangular block shape, 60 mm block thickness and 7 mm joint width.

4.4.2.2 Uni-pave Block Shape

The uni-pave block shape has frictional area better than rectangular shape for load transfer to adjacent blocks. It can be concluded that the blocks provided geometrical interlock along all four sides. The uni-pave block shape has better performance than rectangular (non-interlocking) block which tend to restrain horizontal creep on the pavement. It is concluded that the shape of the block influences the performance of the block pavement under load. It is postulated that the effectiveness of load transfer depends on the vertical surface area of the blocks.

In case of uni-pave block shape, the experimental results from the laboratory based on block thickness variable indicate that the relationship between horizontal forces with horizontal creep found that 100 mm block thickness is better than 60 mm block thick to restrain the horizontal creep. The results are shown in Figure 4.12, Figure 4.13 and Figure 4.14. Each test was applied on CBP with stretcher bond laying pattern and variation of joint width (3 mm, 5 mm and 7 mm).

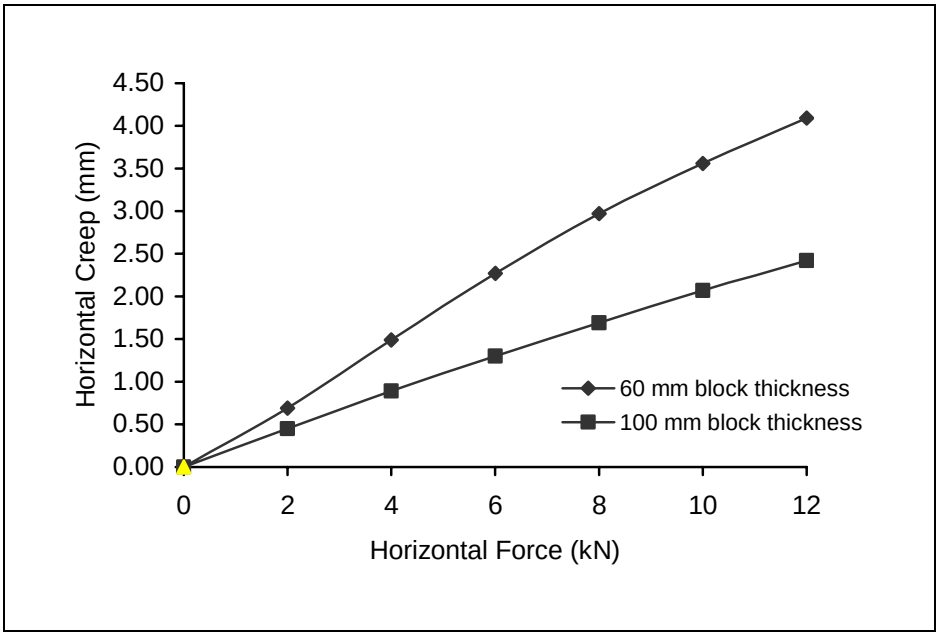

Figure 4.12 Relationship between horizontal forces with horizontal creep on CBP: uni-pave block shape, 60 mm block thickness and 3 mm joint width.

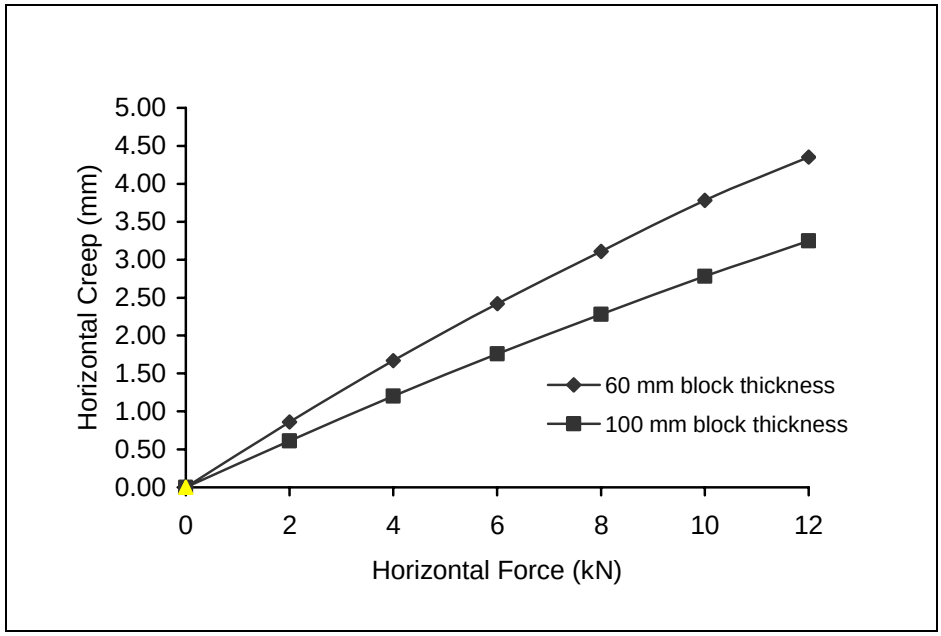

Figure 4.13 Relationship between horizontal forces with horizontal creep on CBP: uni-pave block shape, 60 mm block thickness and 5 mm joint width.

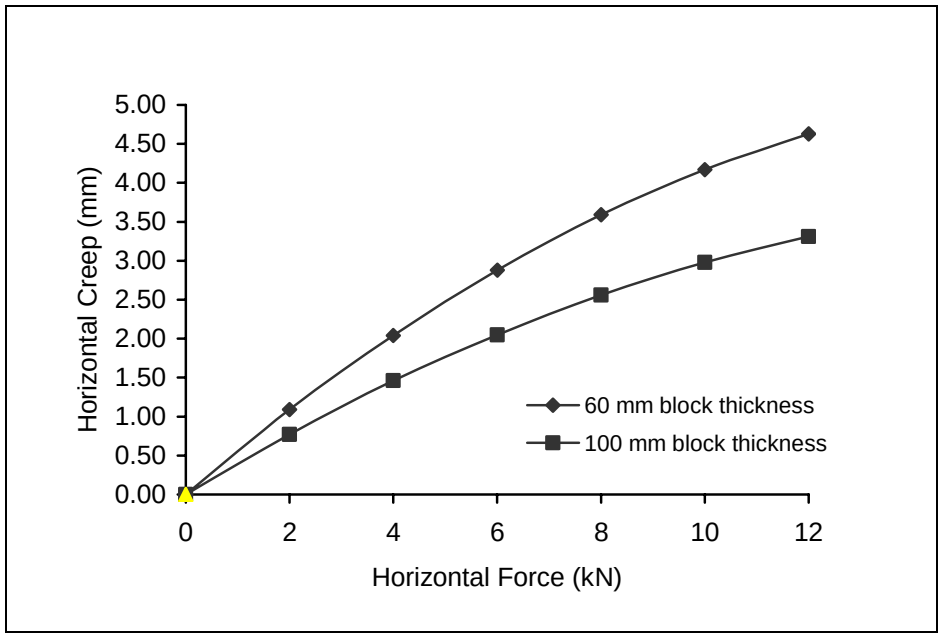

Figure 4.14 Relationship between horizontal force with horizontal creep on CBP: uni-pave block shape, 60 mm block thickness and 7 mm joint width.

4.4.3 The Effect of Joint Width

The width of joints in block paving is more important than has perhaps been realized in the past. A serious disadvantage of pavements laid in this way is that joints of less than 2 mm in width often contain little or no jointing sand. This would obviously reduce the contribution of individual blocks to the structural properties of the pavement. The individual blocks move in relation to one another which results in the breaking of the edges.

Sand filled joints are an integral part of concrete block pavement. They permit the block surface course to behave flexibly by allowing some articulation of individual blocks and they provide the structural interlock necessary for stresses to be distributed among adjacent blocks. Joints need to be sufficiently wide to allow this flexible behaviour, but not so wide as to permit excessive movement of the pavers. Joint widths should lay in the range of 2 to 7 mm with a preferred size of 3 mm. Those wider than 5 mm should not be accepted. Two mm wide spacer ribs cast integrally on the vertical surfaces of the pavers ensure minimum joint width and assist in rapid placement of the blocks.

4.4.3.1 Rectangular Block Shape

The rectangular block shape has frictional area for load transfer to adjacent blocks. The friction area for rectangular shape is between blocks depending on joint width between blocks. It is concluded that the shape of the block influences the performance of the block pavement under load. It is postulated that the effectiveness of load transfer depends on the filling of jointing sand and also joint width between blocks.

In the case of rectangular block shape, the experimental results from the laboratory based on joint width variable indicate that from the relationship between horizontal forces with horizontal creep, 100 mm block thickness is better than 60 mm block thickness for restraining of the horizontal creep. The results are shown in Figure 4.15 to Figure 4.20. Each test was applied on CBP with stretcher bond laying pattern and variation of joint width (3 mm, 5 mm and 7 mm).

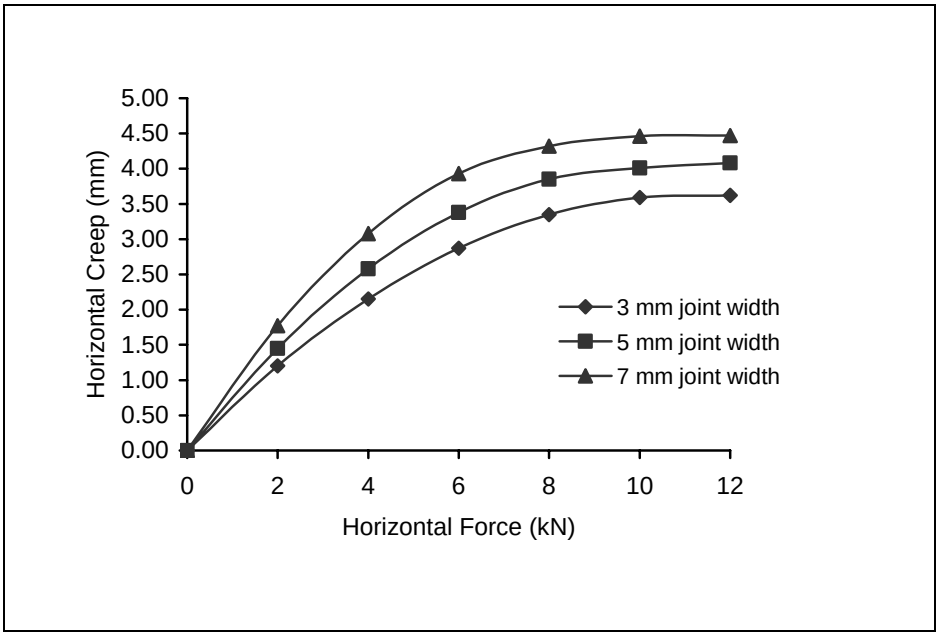

Figure 4.15 Relationship between horizontal forces with horizontal creep on CBP: rectangular block shape, stretcher bond laying pattern and 60 mm block thickness.

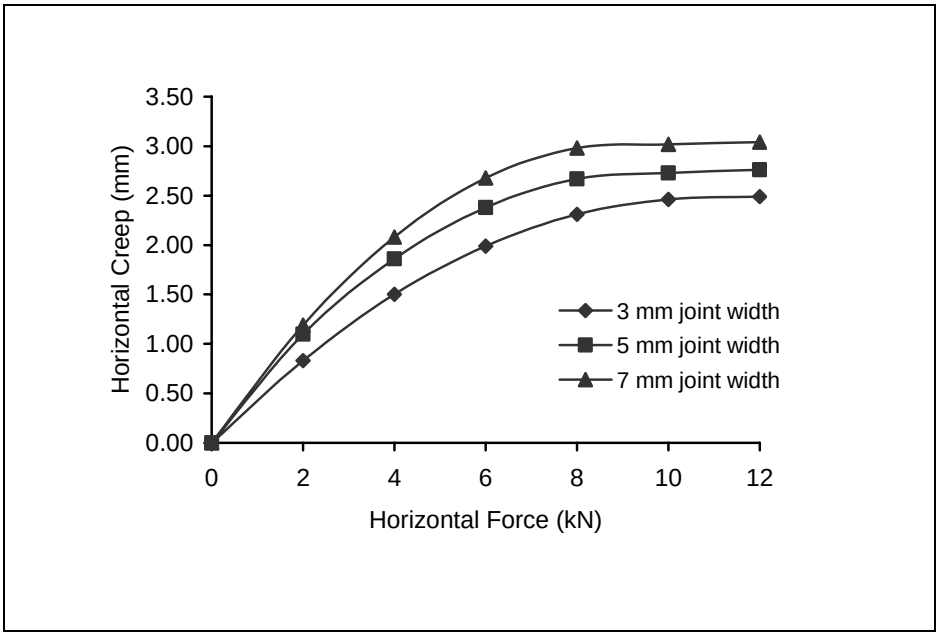

Figure 4.16 Relationship between horizontal forces with horizontal creep on CBP: rectangular block shape, Herringbone 90^{o} laying pattern and 60 mm block thickness.

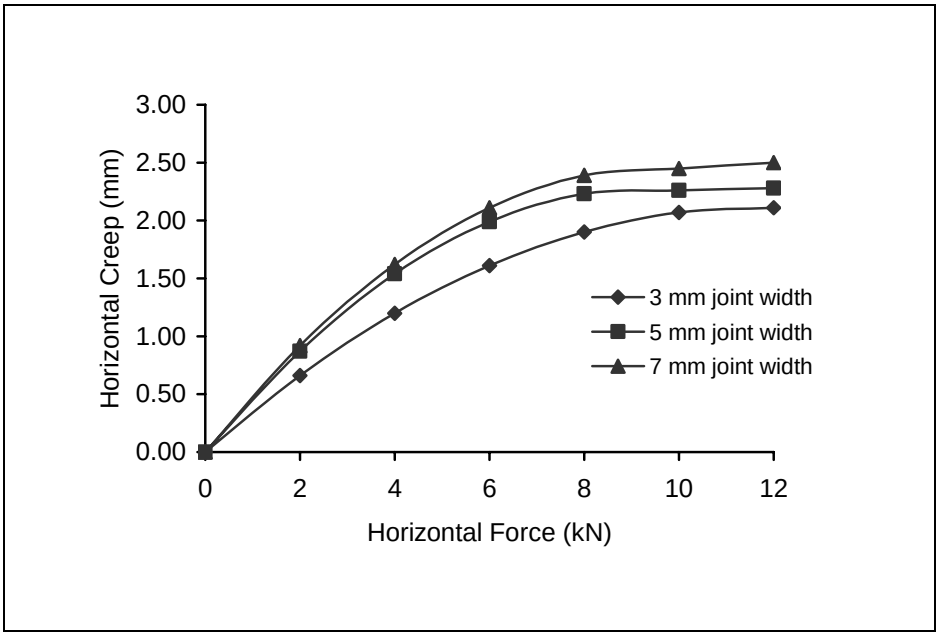

Figure 4.17 Relationship between horizontal forces with horizontal creep on CBP: rectangular block shape, Herringbone 45^{o} laying pattern and 60 mm block thickness.

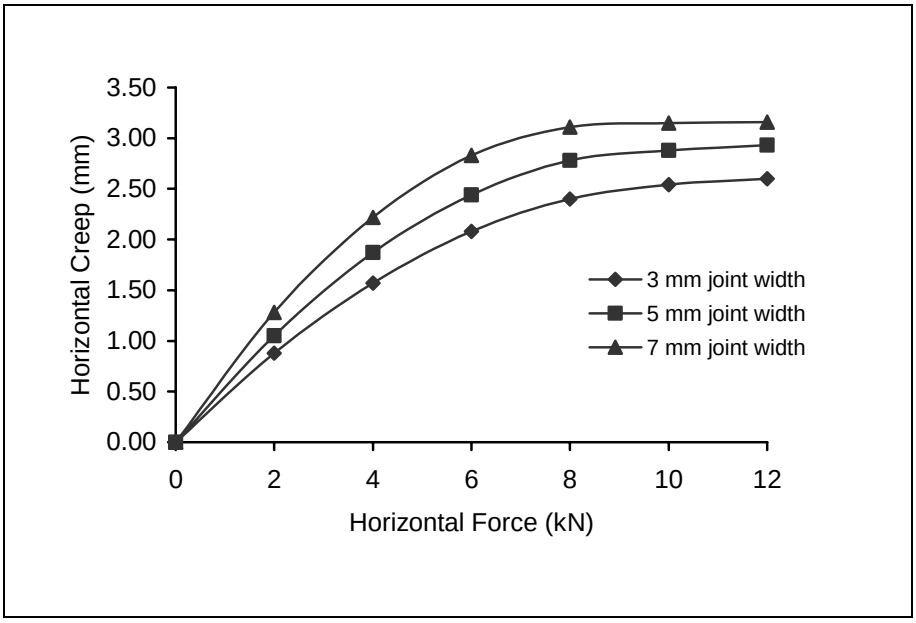

Figure 4.18 Relationship between horizontal forces with horizontal creep on CBP: rectangular block shape, stretcher laying pattern and 100 mm block thickness.

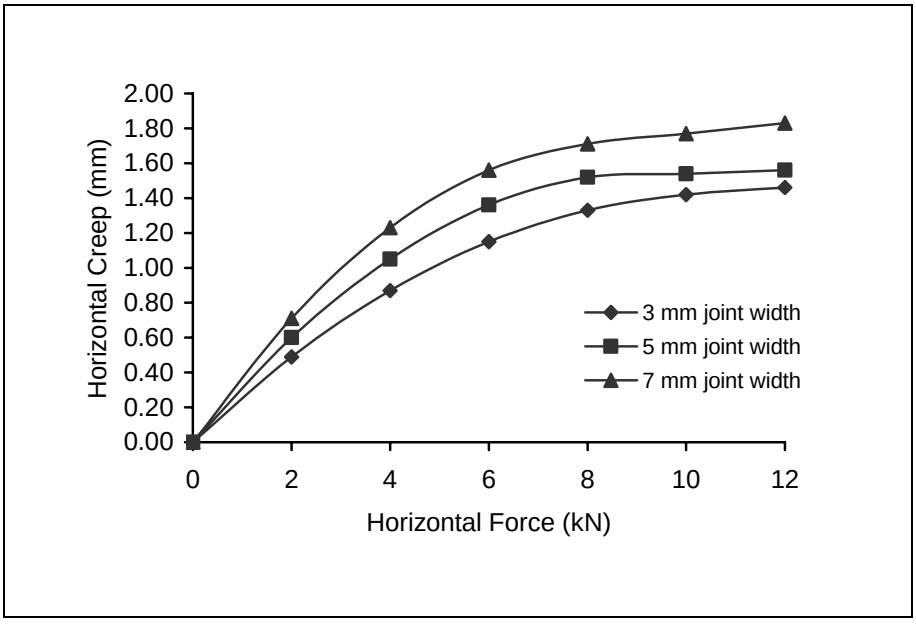

Figure 4.19 Relationship between horizontal forces with horizontal creep on CBP: rectangular block shape, herringbone 90^{o} pattern and 100 mm block thickness.

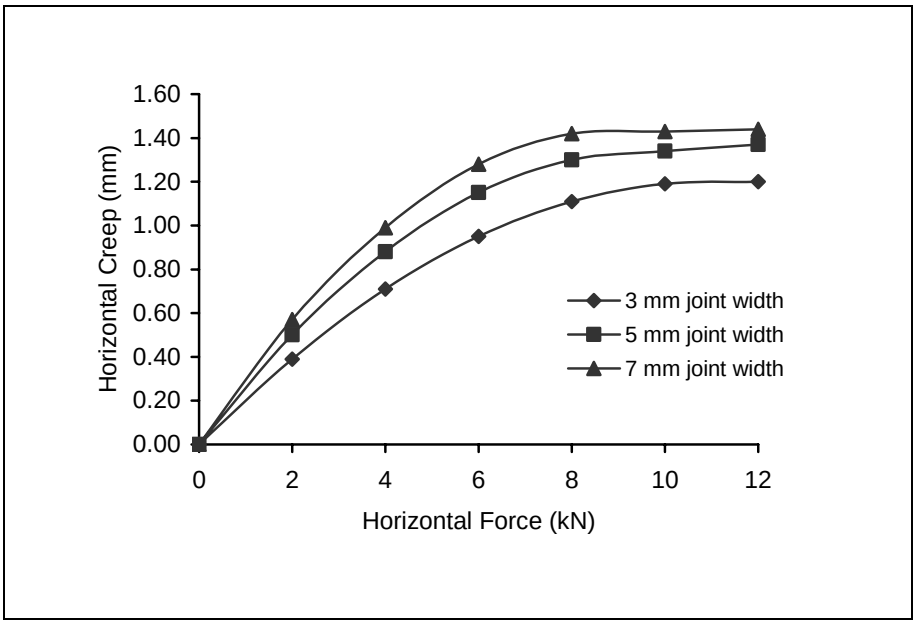

Figure 4.20 Relationship between horizontal forces with horizontal creep on CBP: rectangular block shape, herringbone 45^{o} pattern and 100 mm block thickness.

4.4.3.2 Uni-pave Block Shape

The uni-pave block shape has frictional area that is better than rectangular shape for load transfer to adjacent blocks. It can be concluded that that blocks provide geometrical interlock along all four sides. The uni-pave block shape has better performance than rectangular (non-interlocking) block which tend to restrain horizontal creep on pavement. It is concluded that the shape of the block influences the performance of the block pavement under load. It is postulated that the effectiveness of load transfer depends on the width of jointing sand between blocks.

In case of uni-pave block shape, the experimental results from the laboratory based on joint width variable indicate that from the relationship between horizontal forces with horizontal creep, 100 mm block thickness is better than 60 mm block thickness for restraining of the horizontal creep. The results are shown in Figure 4.21 to Figure 4.26. Each test was applied on CBP with stretcher bond laying pattern and variation of joint width (3 mm, 5 mm and 7 mm).

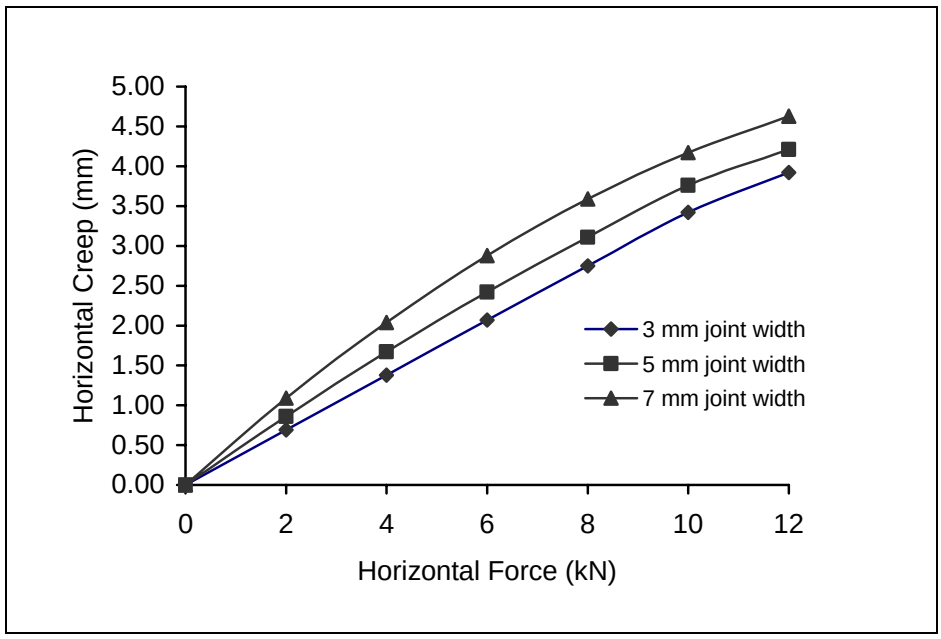

Figure 4.21 Relationship between horizontal forces with horizontal creep on CBP: uni-pave shape, 60 mm thickness, stretcher bond laying pattern

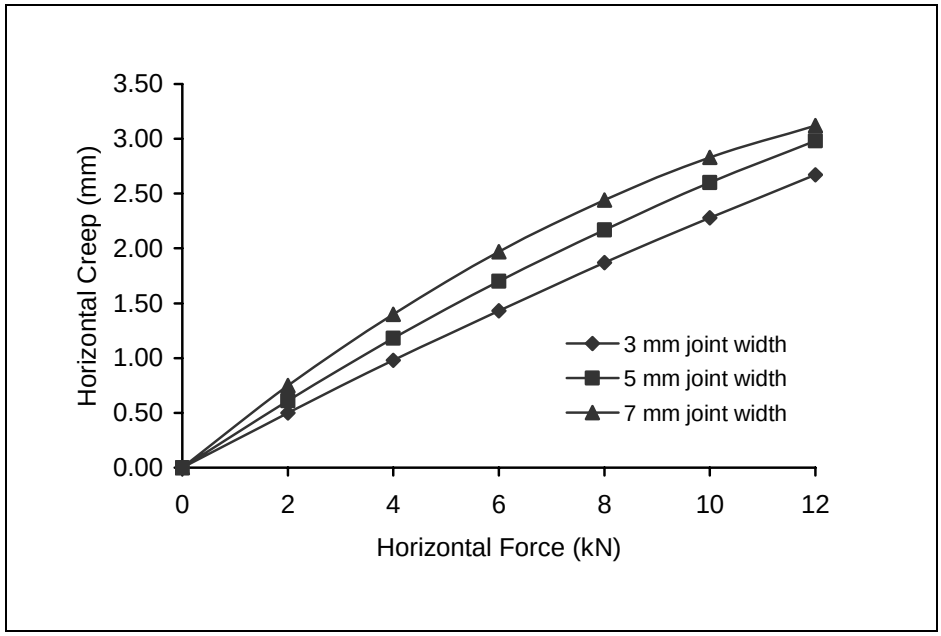

Figure 4.22 Relationship between horizontal forces with horizontal creep on CBP: uni-pave shape, 60 mm thickness, herringbone bond 90^{o} laying pattern

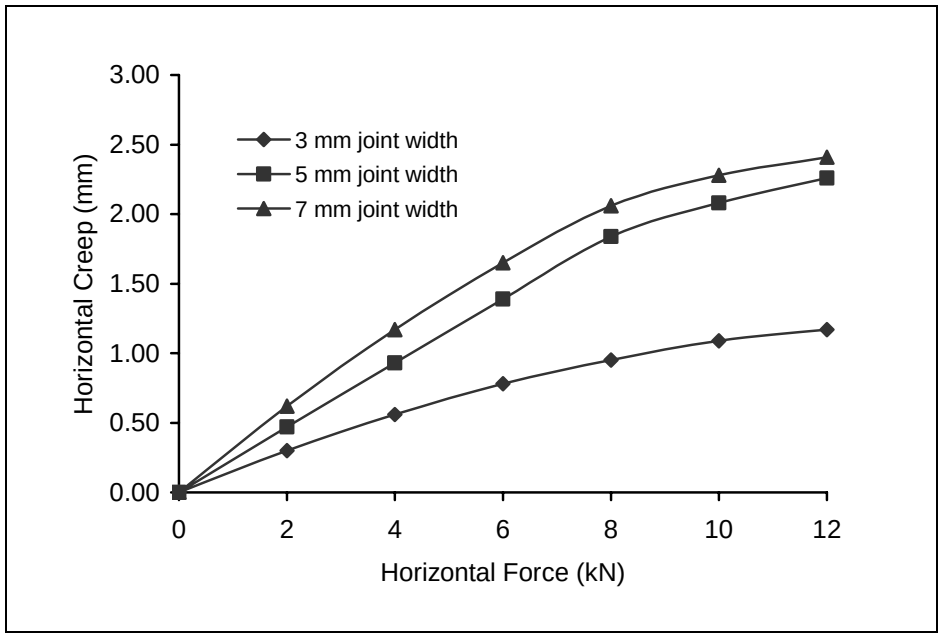

Figure 4.23 Relationship between horizontal forces with horizontal creep on CBP: uni-pave shape, 60 mm thickness, herringbone bond 45^{o} laying pattern

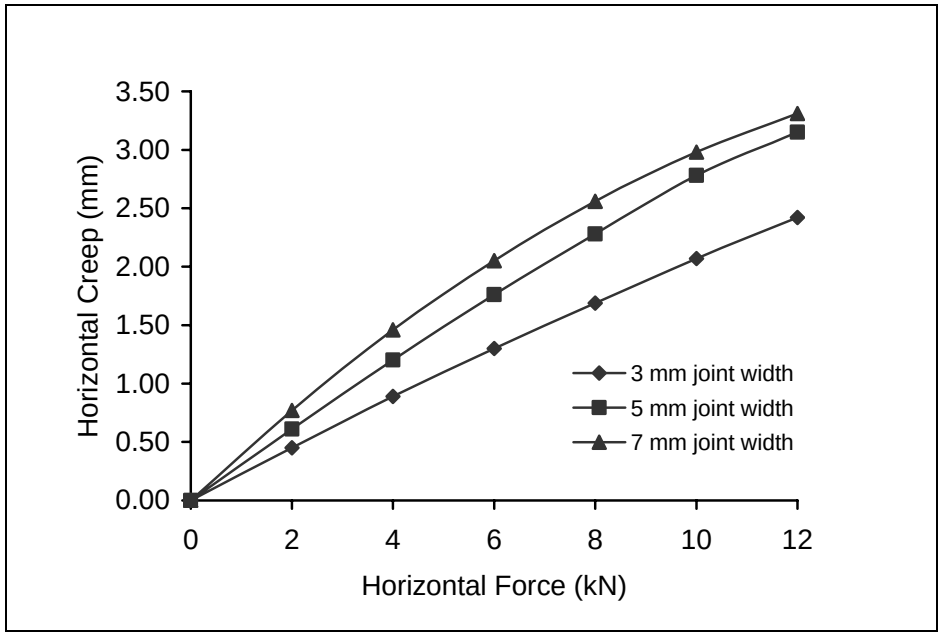

Figure 4.24 Relationship between horizontal forces with horizontal creep on CBP: uni-pave shape, 100 mm thickness, stretcher laying pattern

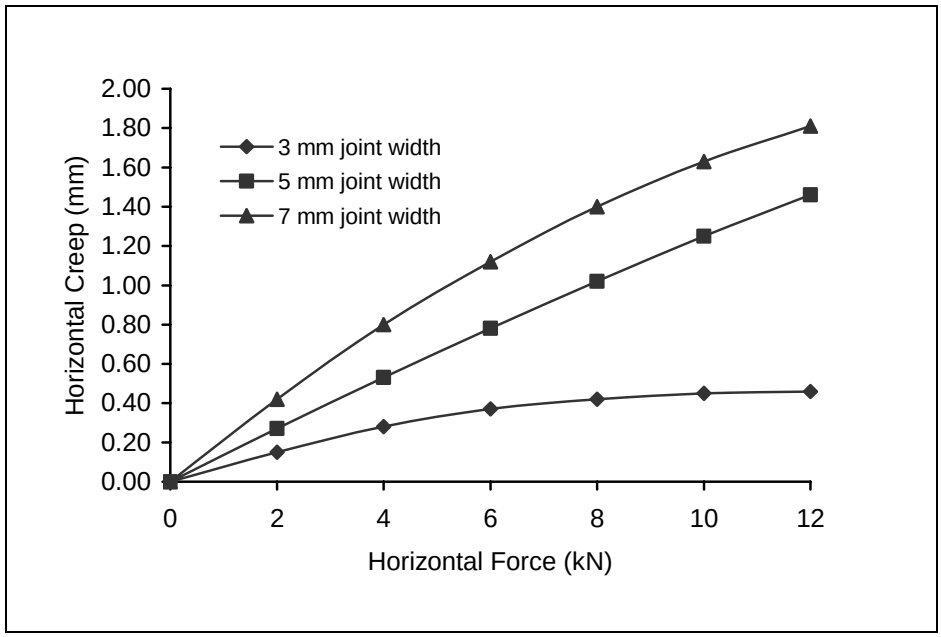

Figure 4.25 Relationship between horizontal forces with horizontal creep on CBP: uni-pave shape, 100 mm thickness, herringbone 90^{o} laying pattern

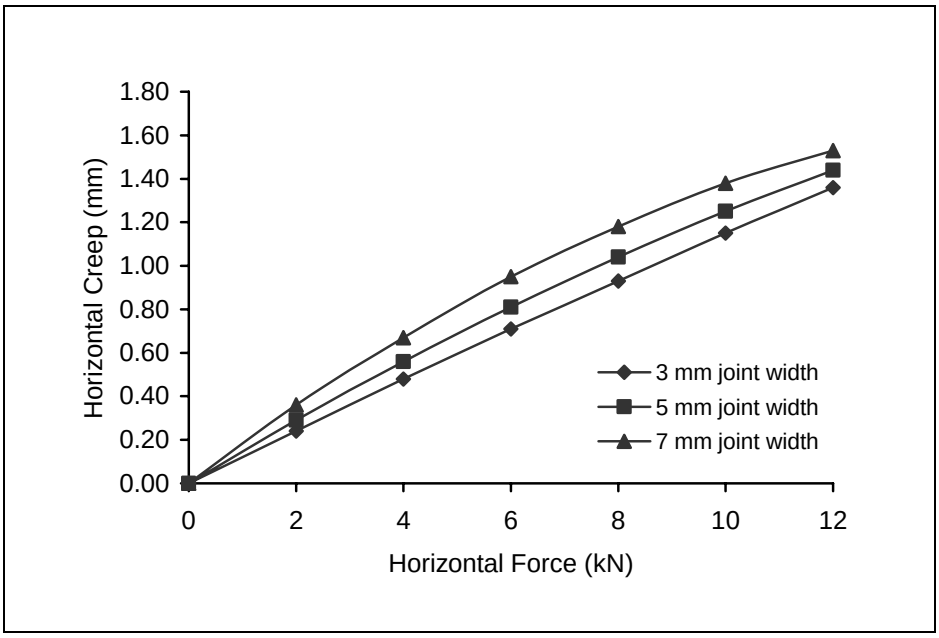

Figure 4.26 Relationship between horizontal forces with horizontal creep on CBP: uni-pave shape, 100 mm thickness, herringbone 45^{o} laying patter

4.4.4 The Effect of Block Shape

The effect of block shape has a major influence on concrete block pavement performance. In the experiment, rectangular and uni-pave block shape, 60 mm blocks thickness were laid on (30 mm, 50 mm and 70 mm) of bedding sand thickness and various joint width (3 mm, 5 mm and 7 mm).

The differences in performance between the various blocks shapes have been discussed in detail elsewhere. In general it can be concluded that blocks which provide geometrical interlock along all (uni-pave) four sides tend to yield similar levels of performance regardless of shape, and that shaped (interlocking) blocks yield much better performance than rectangular (non-interlocking) blocks.

4.5 Push-in Test Results

For the behaviour of block pavements under push-in test, the pavement may present various types of mechanical behaviour submitted to a horizontal creep, depending on the bedding sand thickness, joint width between blocks, blocks thickness and degree of slope.

4.5.1 The Effect of Bedding Sand Thickness

Figure 4.27 to Figure 4.32 show the relationship between push-in force with horizontal creep on the varying loose thicknesses of 30, 50, and 70 mm bedding sand. It is seen that the deflections of pavement decrease with the increase in loose thickness of bedding sand from 30 to 70 mm. The deflection is minimum at a loose thickness of 30 mm bedding course.

The compaction might not be fully effective for a higher thickness of bedding sand during vibration. During vibration of blocks, the bedding sand rises through the joints to small heights and wedges in between the blocks. The rise of sand increases with the increase in loose thickness of bedding sand. The wedging of these sands absorbs the major part of applied vibration energy and transfers less to the bedding sand below. As a result, the bedding sand is not fully compacted for higher thicknesses. Consequently, some compaction of bedding sand takes place under load and thus shows more deflection in the test pavements. The higher the loose bedding sand thickness, the more the deflection will be.

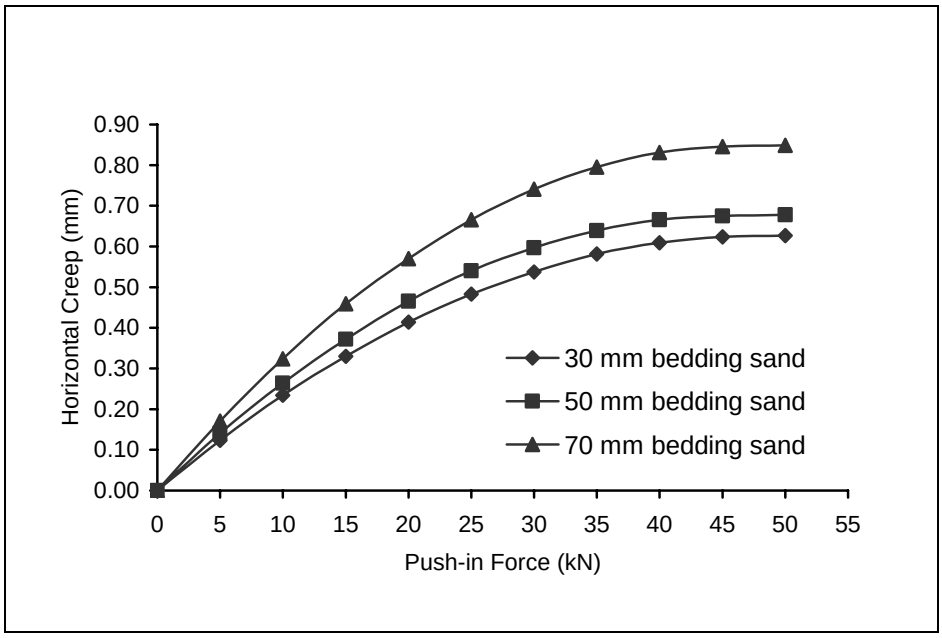

Figure 4.27 Relationship between push-in forces with horizontal creep on CBP: rectangular shape, 60 mm block thickness and 3 mm joint width

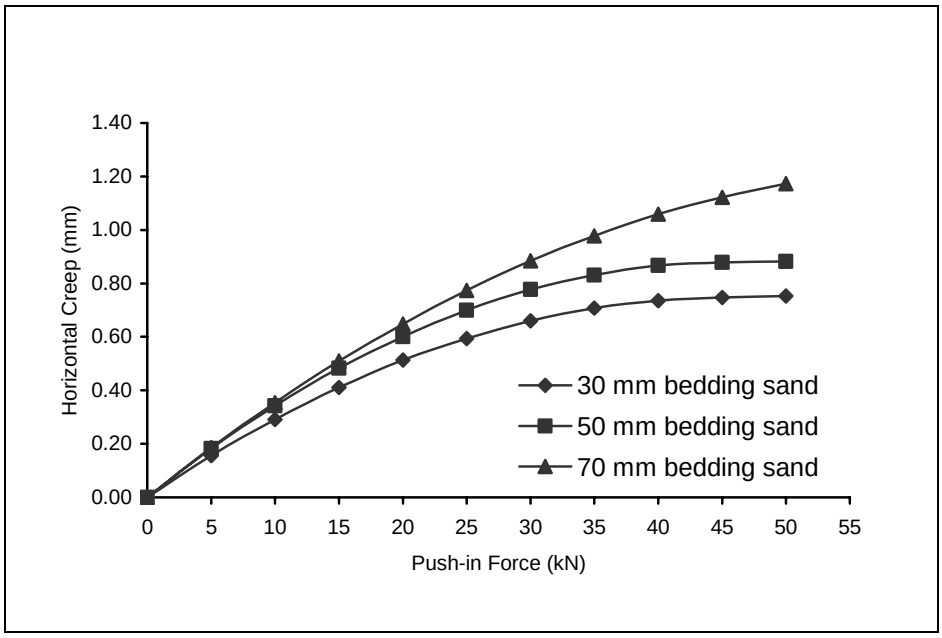

Figure 4.28 Relationship between push-in forces with horizontal creep on CBP: rectangular shape, 60 mm block thickness and 5 mm joint width

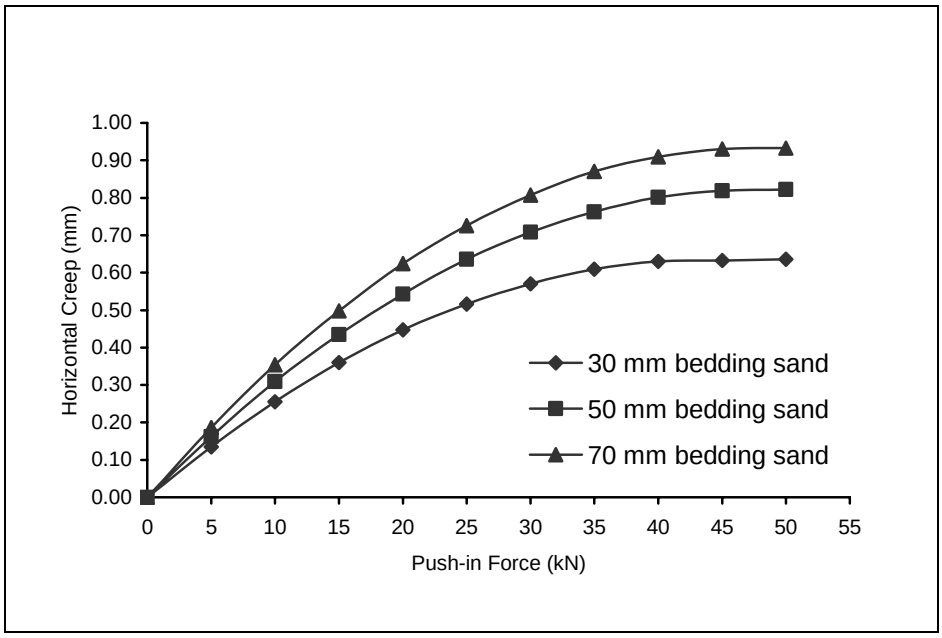

Figure 4.29 Relationship between push-in forces with horizontal creep on CBP: rectangular shape, 60 mm block thickness and 7 mm joint width

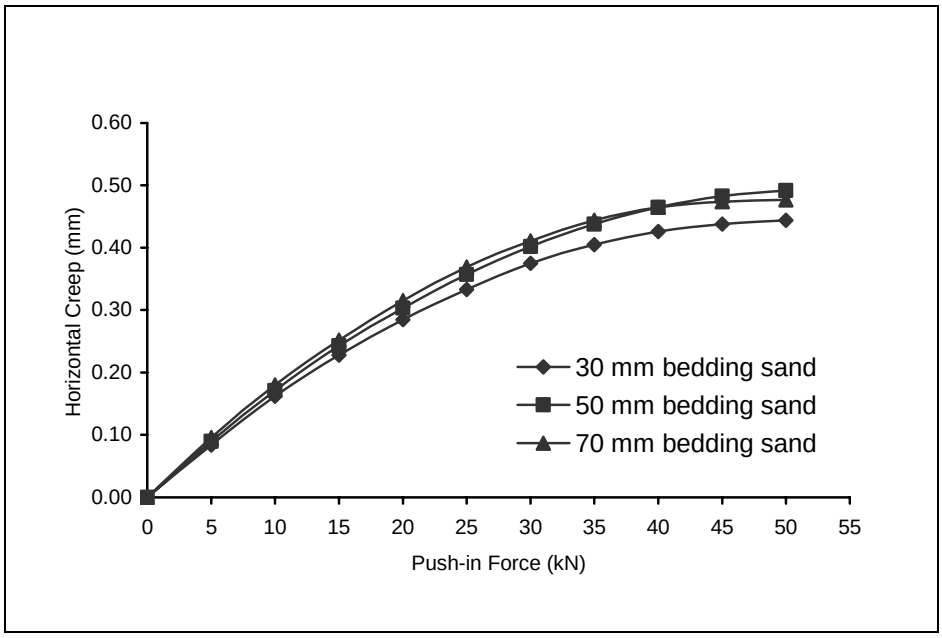

Figure 4.30 Relationship between push-in forces with horizontal creep on CBP: rectangular shape, 100 mm block thickness and 3 mm joint width

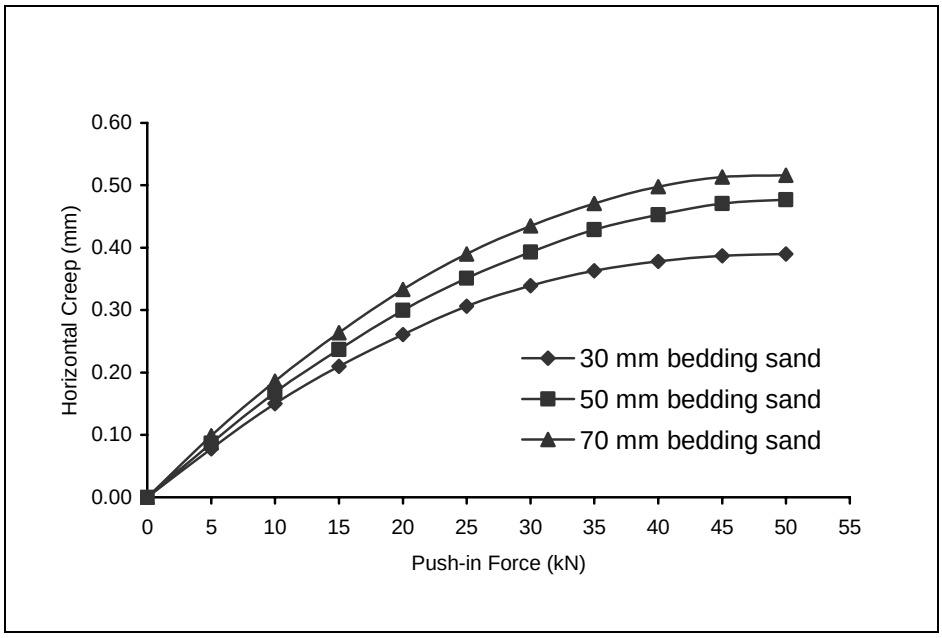

Figure 4.31 Relationship between push-in forces with horizontal creep on CBP: rectangular shape, 100 mm block thickness and 5 mm joint width

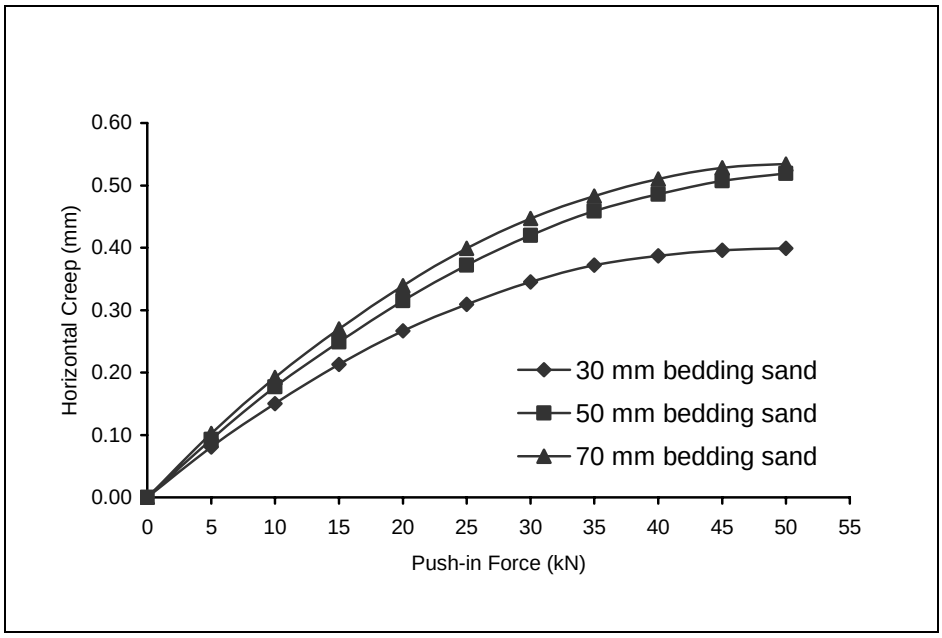

Figure 4.32 Relationship between push-in forces with horizontal creep on CBP: rectangular shape, 100 mm block thickness and 7 mm joint width

4.5.2 The Effect of Joint Width

Figure 4.33 to Figure 4.38 show the response of pavement for design joint widths of 3 mm, 5 mm and 7 mm with varying block thickness and bedding sand thickness. As the joint width decreases, the deflection of the pavement also decreases. The higher of block and bedding sand thickness, the lesser the normal stiffness of the joint will be. This will lead to more rotations and translations of blocks. Thus, there will be more deflection under the same load for thicker joints. Some of the grains coarser than the joint width were unable to enter inside. This has been observed during filling sand in joints. A large amount of sand remained outside the joint showing sand heaps on the block surface. The coarse grains of sand choke the top surface of joints and prevent movement of other fine grains into the joint. There might be loose pockets or honeycombing inside the joint. The joint stiffness decreases and in turn reflects slightly higher deflections. At the optimum joint width, there is the maximum chance that single grains of average size, close to the joint width, will be retained in the joints during joint filling.

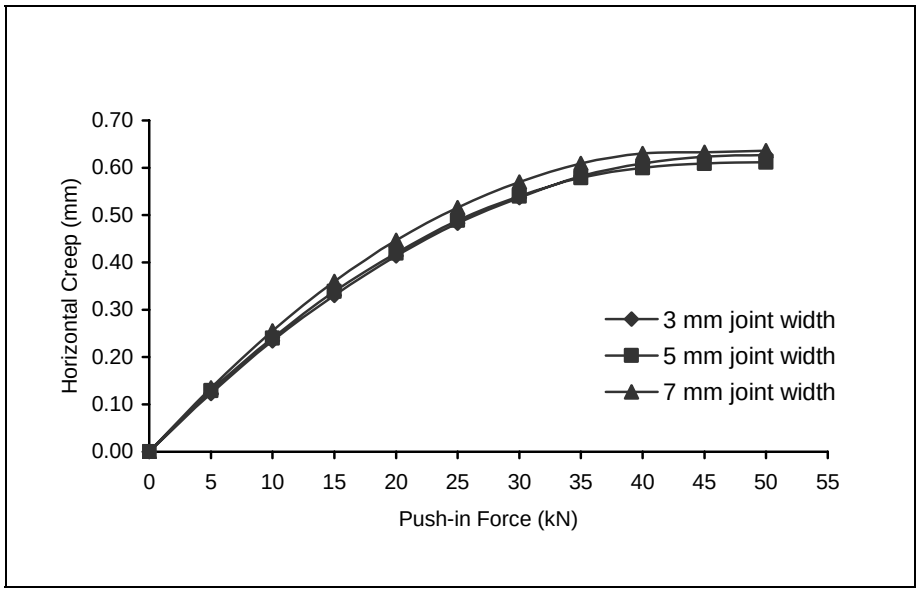

Figure 4.33 Relationship between push-in forces with horizontal creep on CBP: rectangular shape, 60 mm block thickness and 30 mm bedding sand thickness

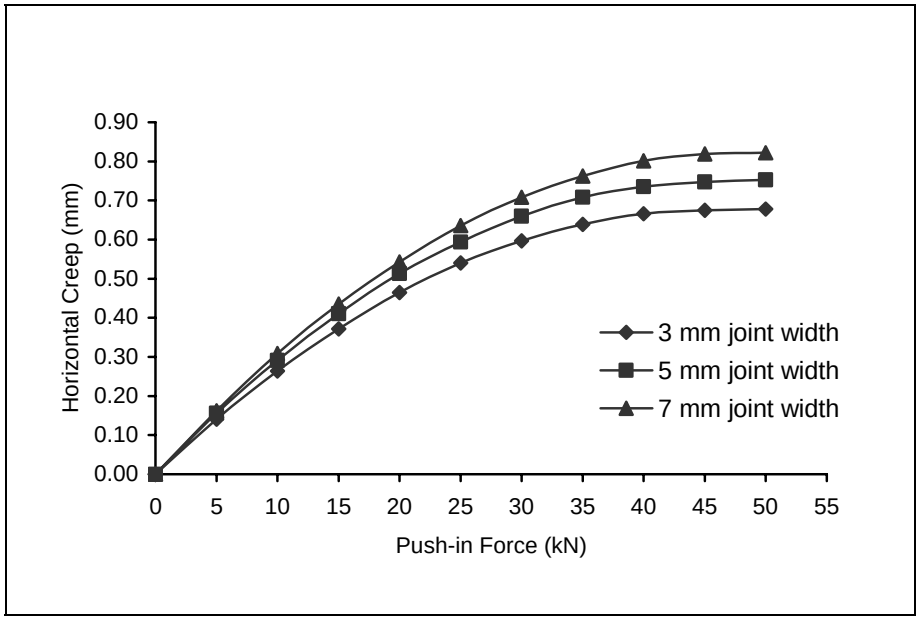

Figure 4.34 Relationship between push-in forces with horizontal creep on CBP: rectangular shape, 60 mm block thickness and 50 mm bedding sand thickness

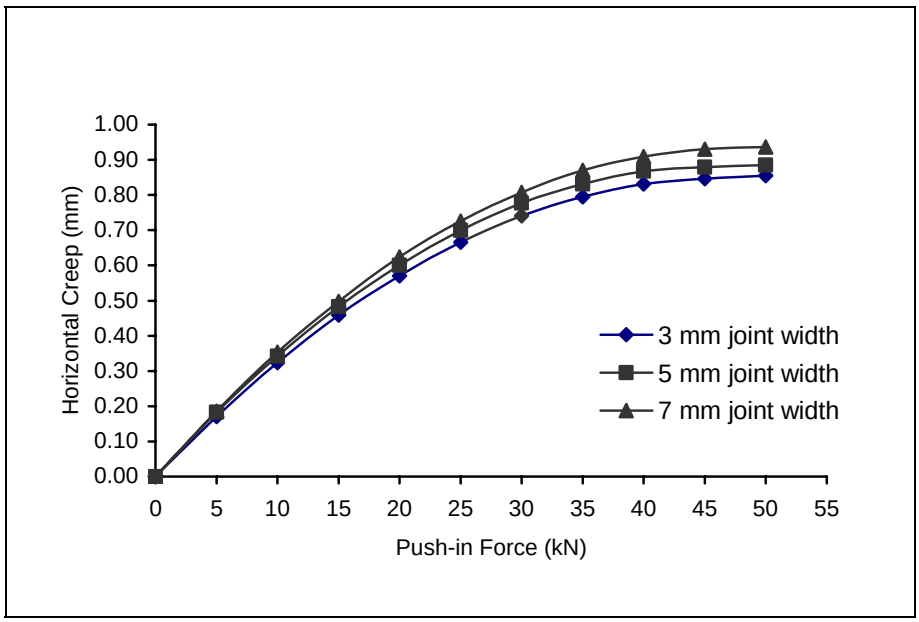

Figure 4.35 Relationship between push-in forces with horizontal creep on CBP: rectangular shape, 60 mm block thickness and 70 mm bedding sand thickness

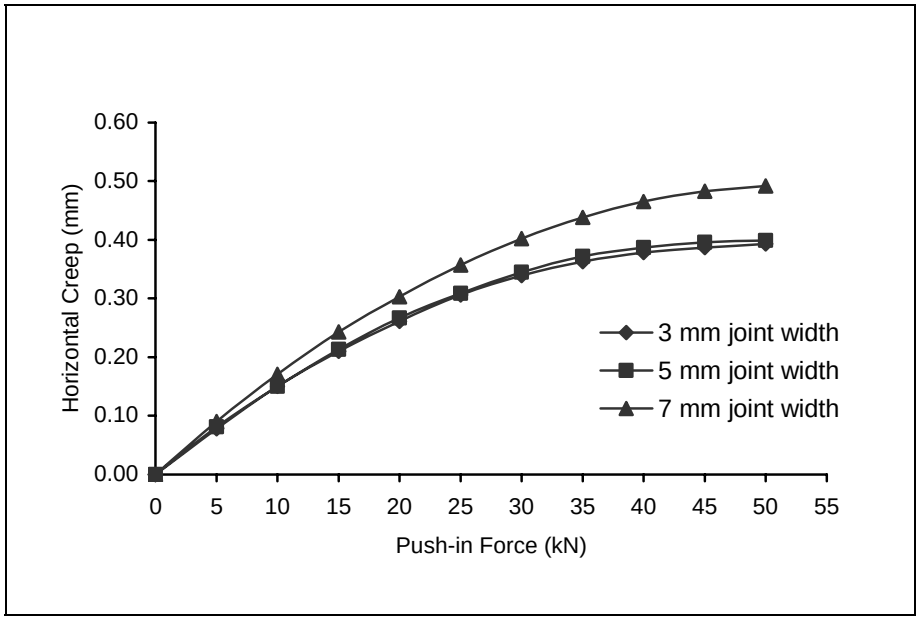

Figure 4.36 Relationship between push-in forces with horizontal creep on CBP: rectangular shape, 100 mm block thickness and 30 mm bedding sand thickness

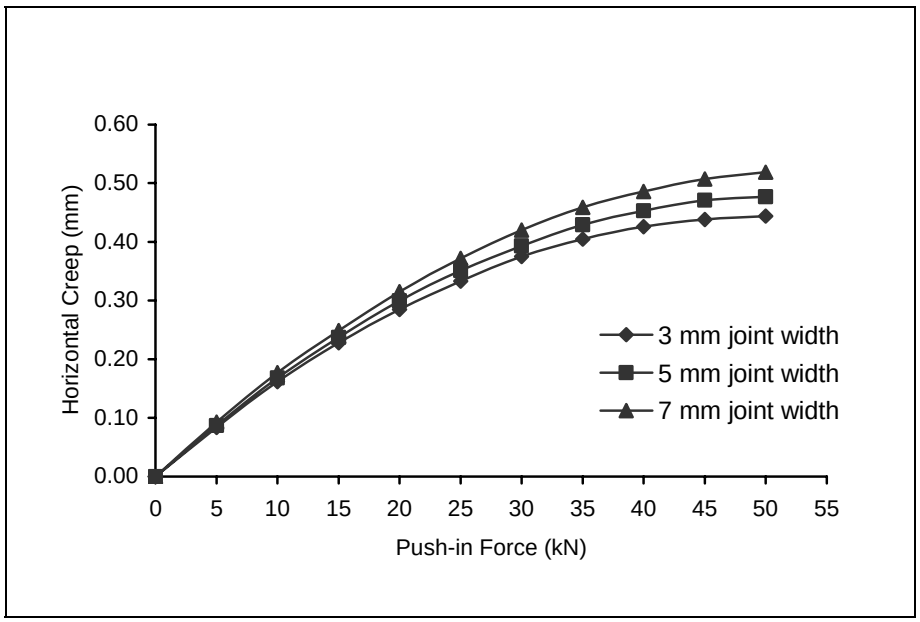

Figure 4.37 Relationship between push-in forces with horizontal creep on CBP: rectangular shape, 100 mm block thickness and 50 mm bedding sand thickness

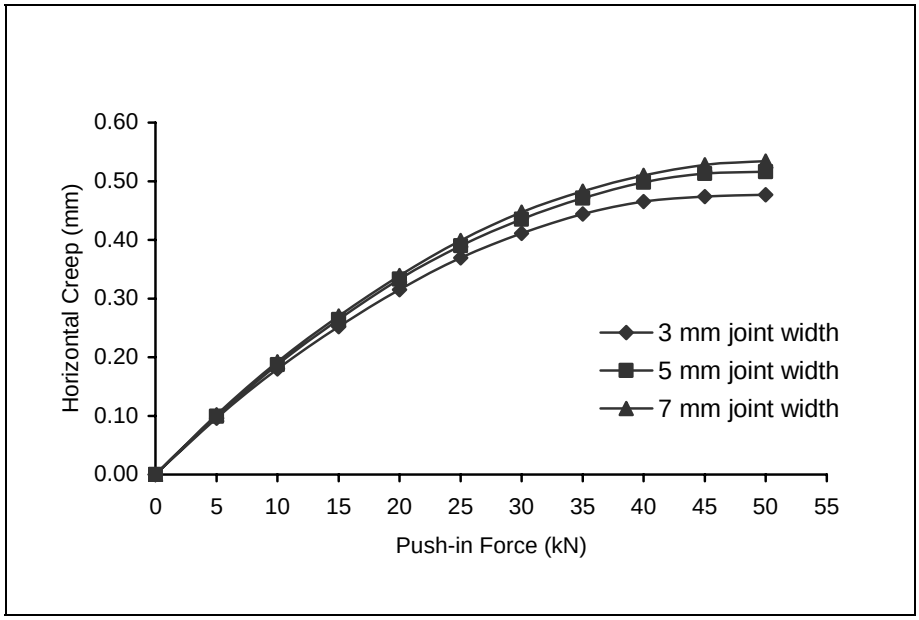

Figure 4.38 Relationship between push-in forces with horizontal creep on CBP: rectangular shape, 100 mm block thickness and 70 mm bedding sand thickness

4.5.3 The Effect of Block Thickness

Rectangular blocks shape of the same plan dimension with two different thicknesses was selected for testing. The thicknesses were 60 mm and 100 mm. Blocks were laid in a stretcher bond pattern for each test. The shapes of the load deflection paths are similar for all block thicknesses. A change in thickness from 60 to 100 mm significantly reduces the elastic deflection of pavement. The comparison is shown in Figure 4.39 to Figure 4.47. Thicker blocks provide a higher frictional area. Thus, load transfer will be high for thicker blocks. For thicker blocks, the individual block translation is more with the same amount of block rotation. As a result, the back thrust

from edge restraint will be more. The thrusting action between adjacent blocks at hinging points is more effective with thicker blocks. Thus, deflections are much less for thicker blocks.

The combined effect of higher friction area and higher thrusting action for thicker blocks provides more efficient load transfer. Thus, there is a significant change in deflection values from increasing the thickness of blocks. It is concluded that the response of the pavement is highly influenced by block thickness

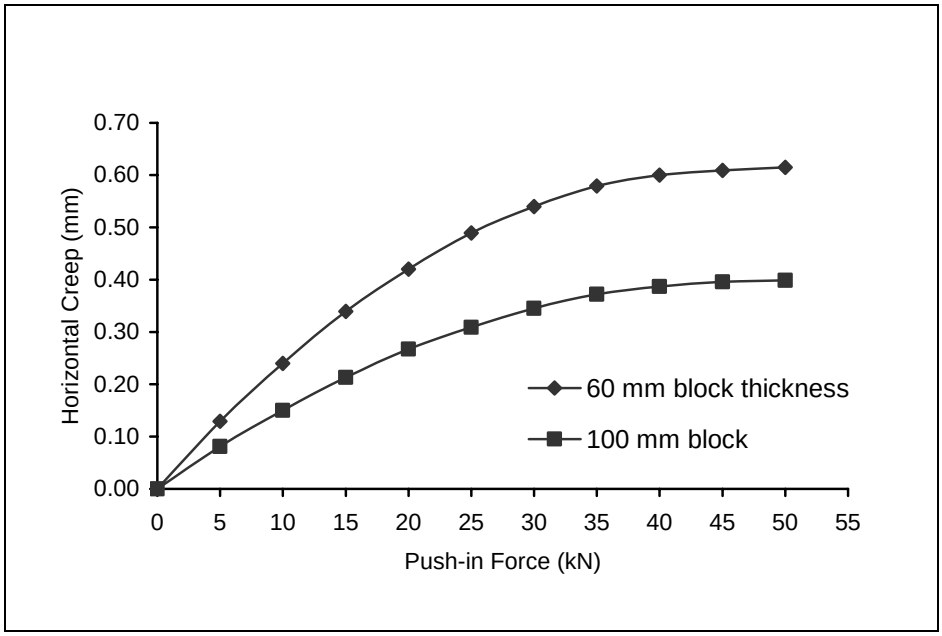

Figure 4.39 Relationship between push-in forces with horizontal creep on CBP: rectangular shape, 30 mm bedding sand thickness and 3 mm joint width

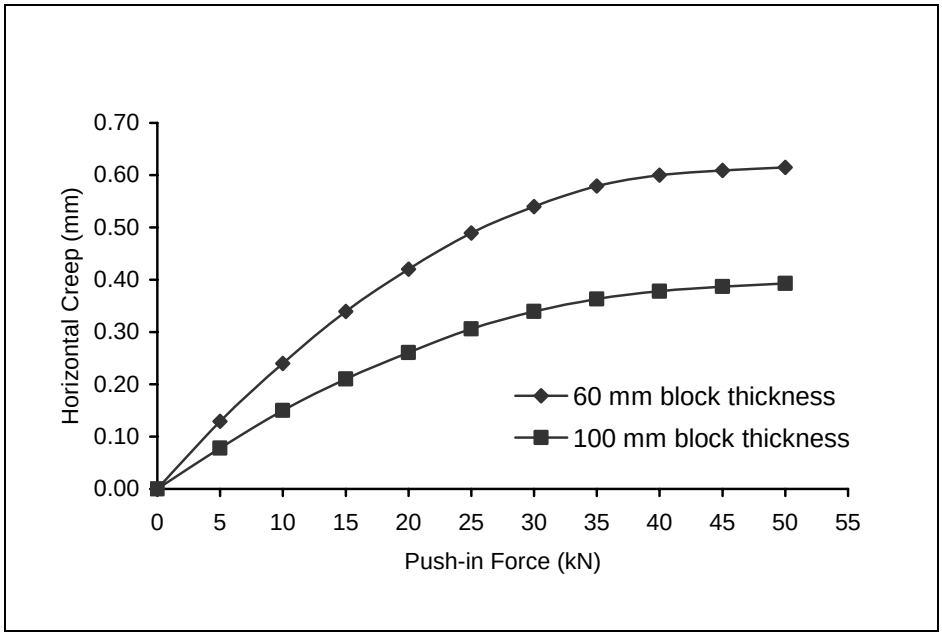

Figure 4.40 Relationship between push-in forces with horizontal creep on CBP: rectangular shape, 30 mm bedding sand thickness and 5 mm joint width

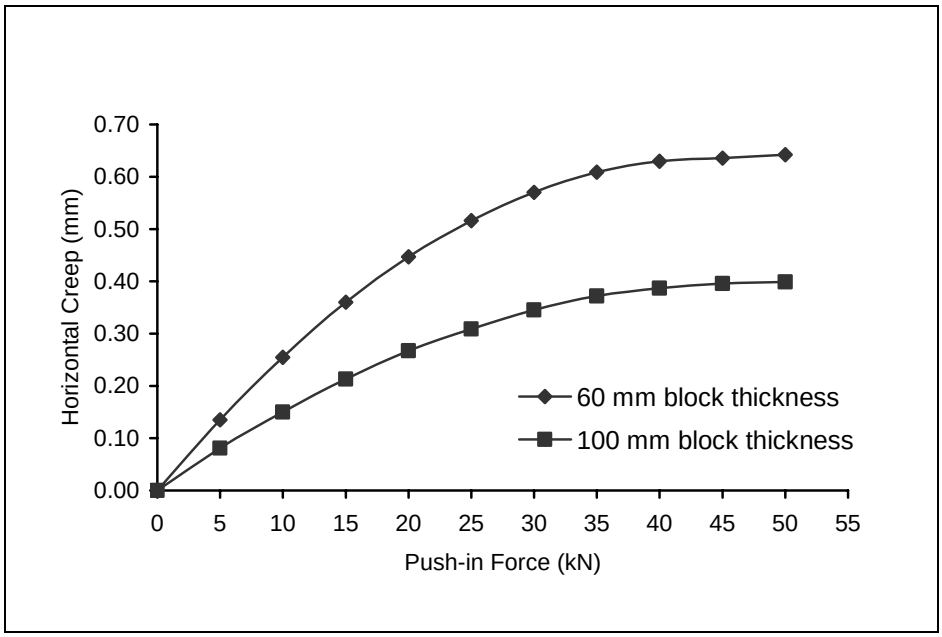

Figure 4.41 Relationship between push-in forces with horizontal creep on CBP: rectangular shape, 30 mm bedding sand thickness and 7 mm joint width

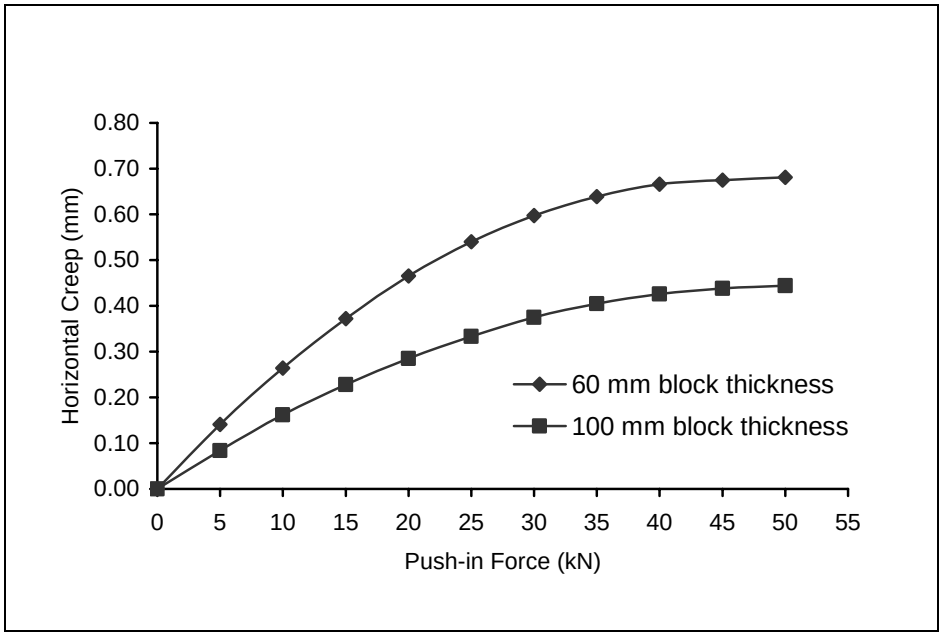

Figure 4.42 Relationship between push-in forces with horizontal creep on CBP: rectangular shape, 50 mm bedding sand thickness and 3 mm joint width

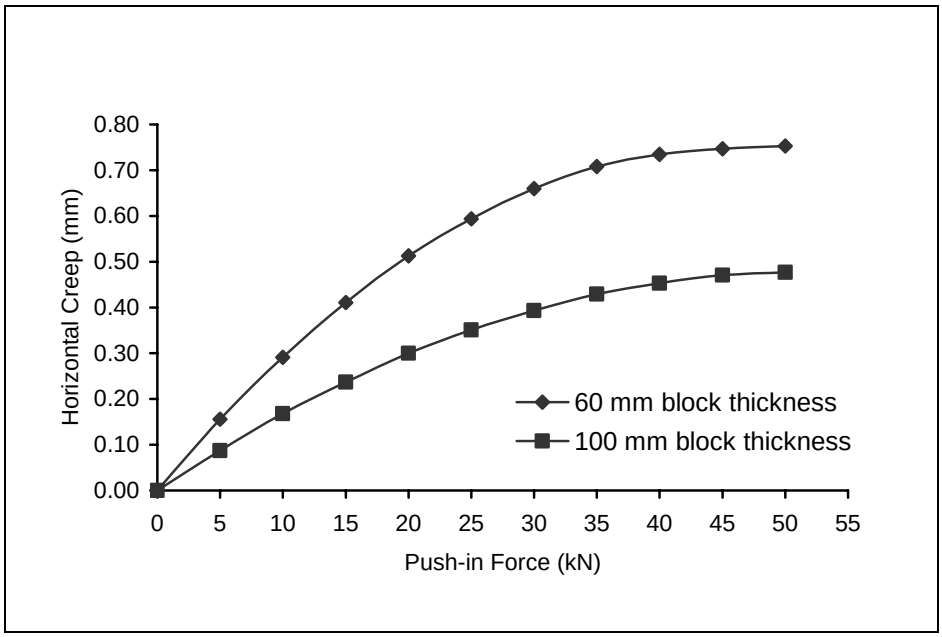

Figure 4.43 Relationship between push-in forces with horizontal creep on CBP: rectangular shape, 50 mm bedding sand thickness and 5 mm joint width

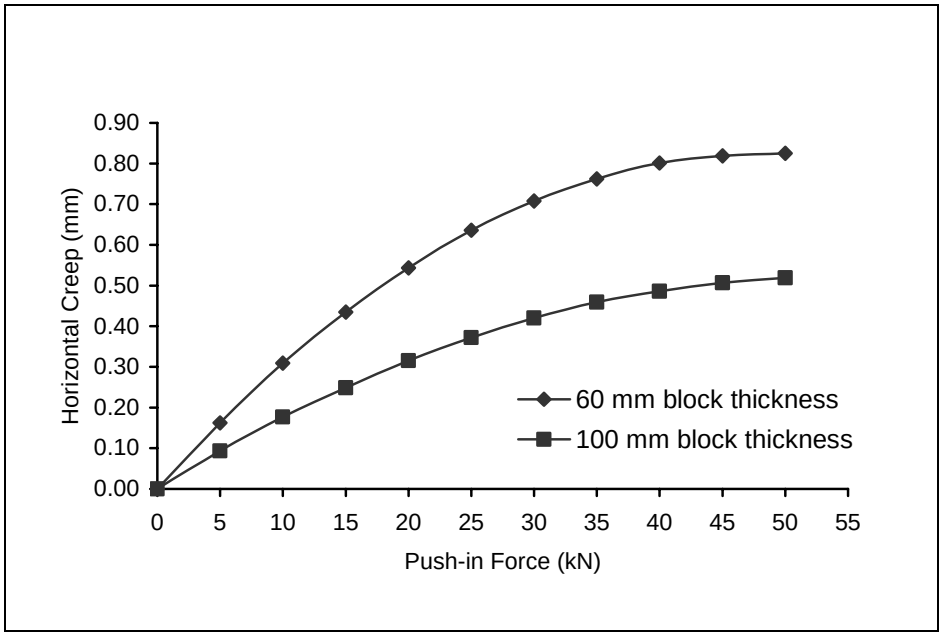

Figure 4.44 Relationship between push-in forces with horizontal creep on CBP: rectangular shape, 50 mm bedding sand thickness and 7 mm joint width

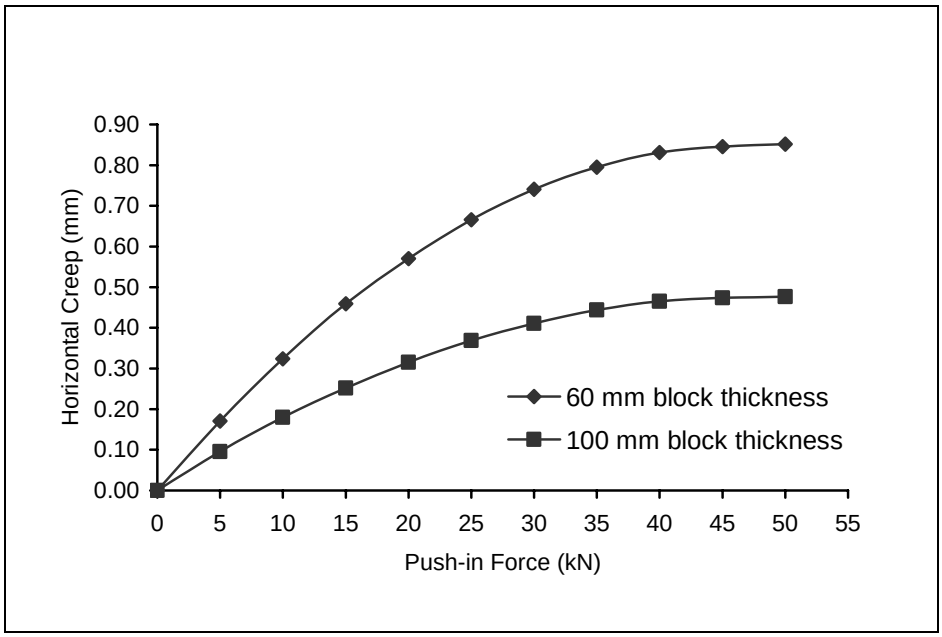

Figure 4.45 Relationship between push-in forces with horizontal creep on CBP: rectangular shape, 70 mm bedding sand thickness and 3 mm joint width

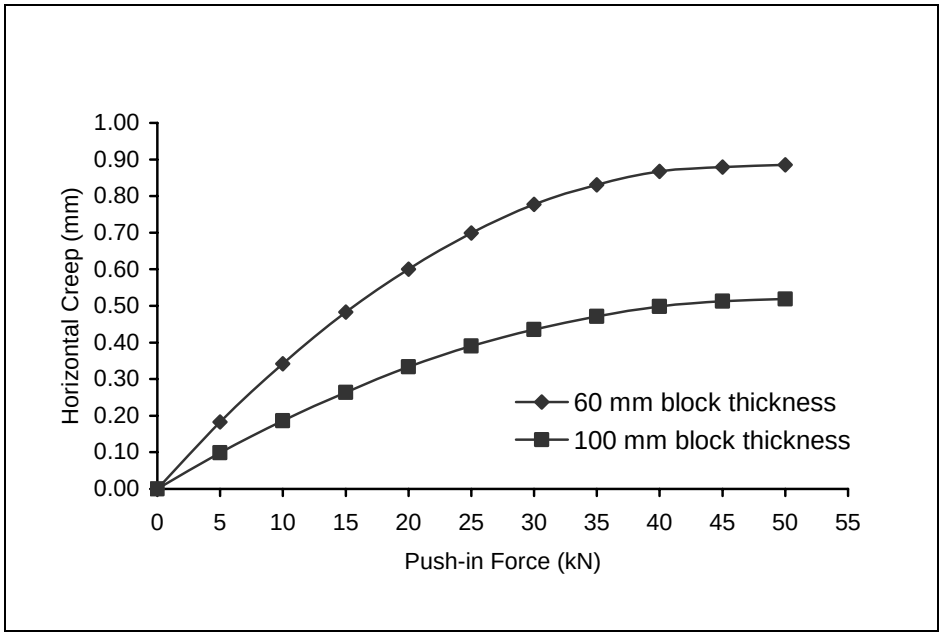

Figure 4.46 Relationship between push-in forces with horizontal creep on CBP: rectangular shape, 70 mm bedding sand thickness and 5 mm joint width

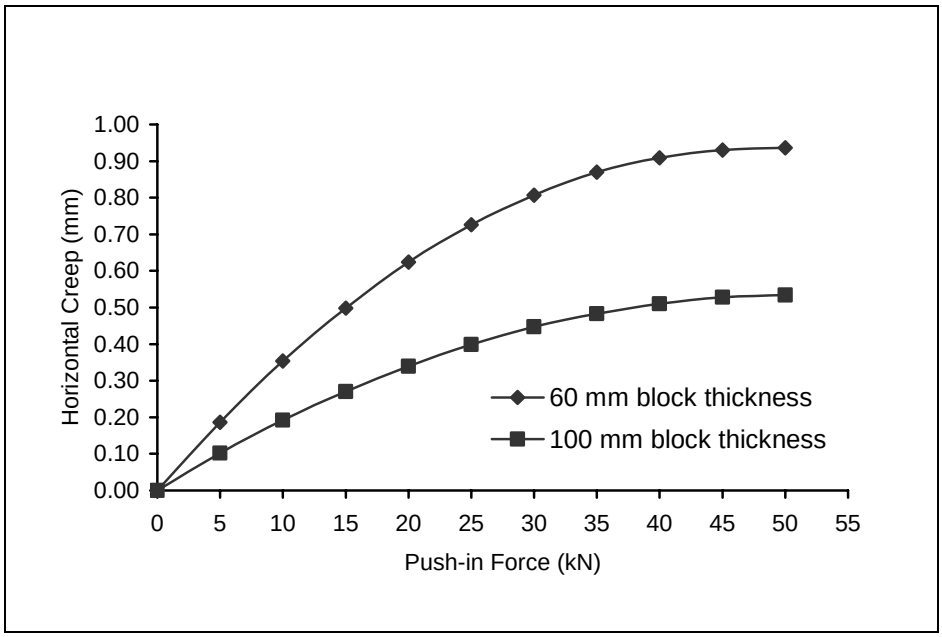

Figure 4.47 Relationship between push-in forces with horizontal creep on CBP: rectangular shape, 70 mm bedding sand thickness and 7 mm joint width

4.5.4 The Effect of Degree of Slope

The effect of degree of the slope on concrete block pavements on sloping road section area significant with friction between blocks and thrusting action between adjacent blocks at hinging points is more effective with thicker blocks. Thus, deflections are much less for thicker blocks with increasing degree of the slope. As shown in Figure 4.48 to Figure 4.65.

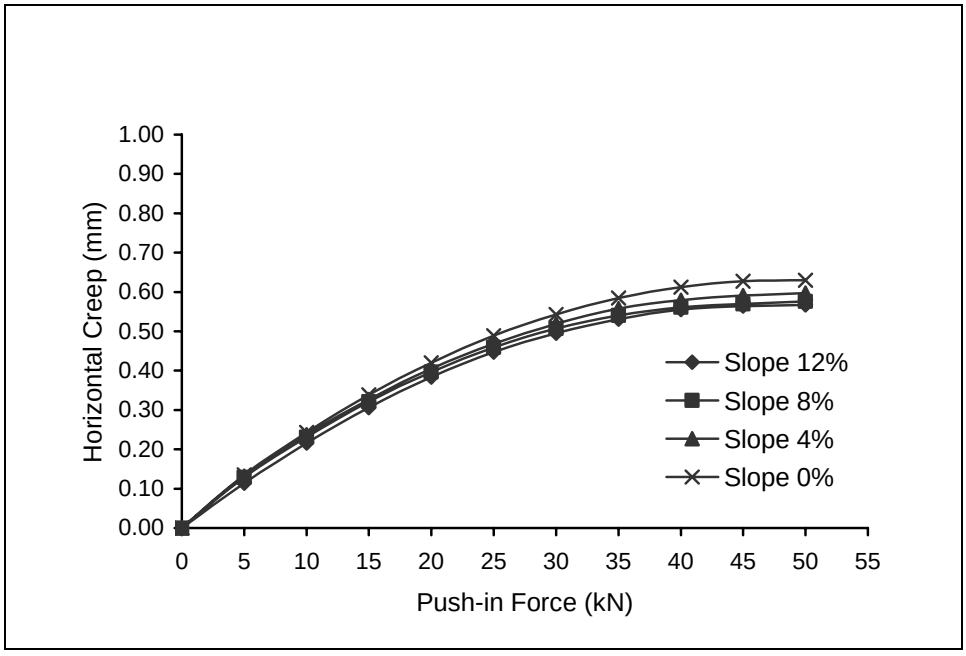

Figure 4.48 Relationship between push-in forces with horizontal creep on CBP: rectangular shape, 60 mm block thick, 30 mm bedding sand thickness and 3 mm joint width

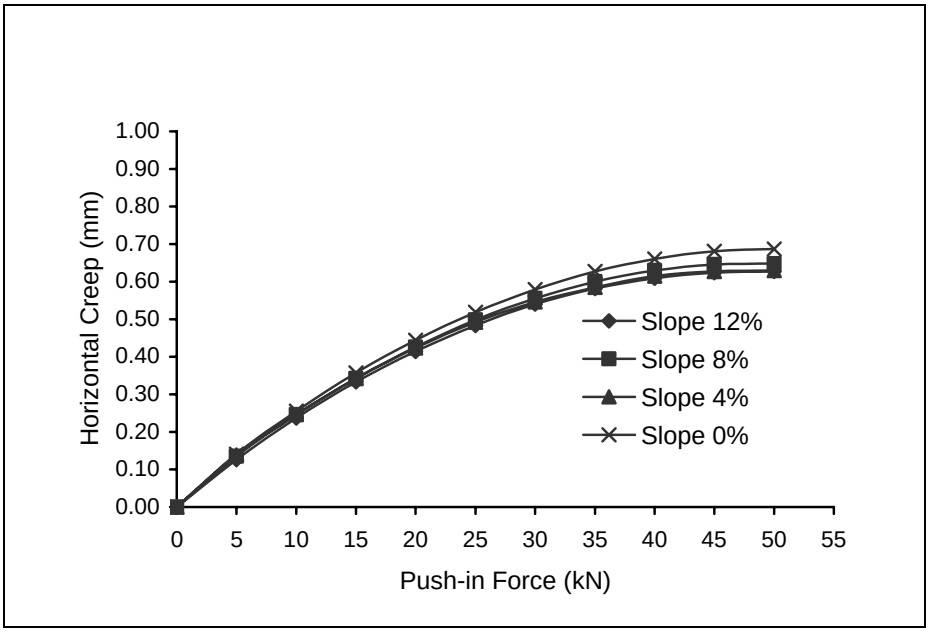

Figure 4.49 Relationship between push-in forces with horizontal creep on CBP: rectangular shape, 60 mm block thick, 50 mm bedding sand thickness and 3 mm joint width

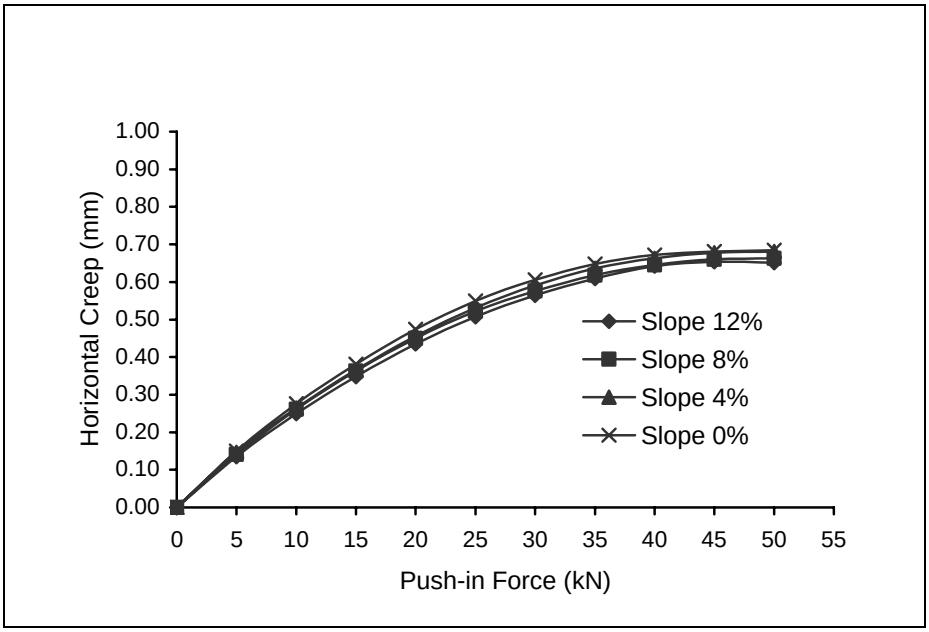

Figure 4.50 Relationship between push-in forces with horizontal creep on CBP: rectangular shape, 60 mm block thick, 70 mm bedding sand thickness and 3 mm joint width

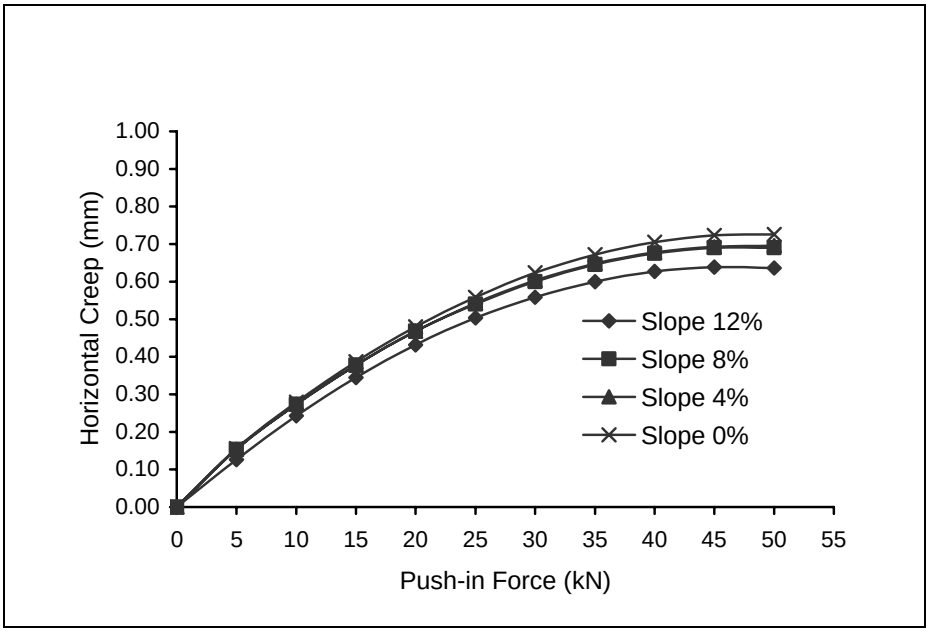

Figure 4.51 Relationship between push-in forces with horizontal creep on CBP: rectangular shape, 100 mm block thick, 30 mm bedding sand thickness and 3 mm joint width

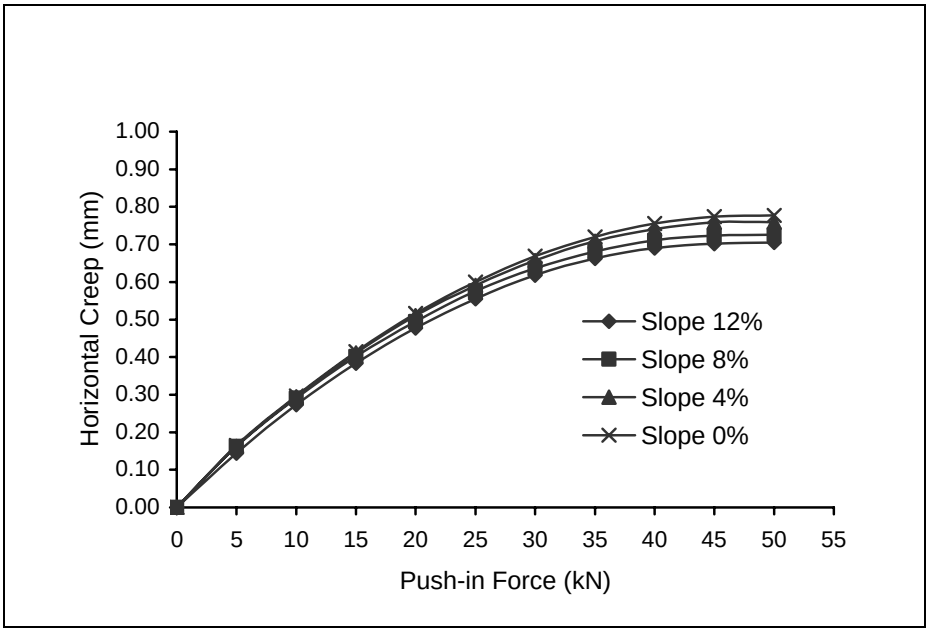

Figure 4.52 Relationship between push-in forces with horizontal creep on CBP: rectangular shape, 100 mm block thick, 50 mm bedding sand thickness and 3 mm joint width.

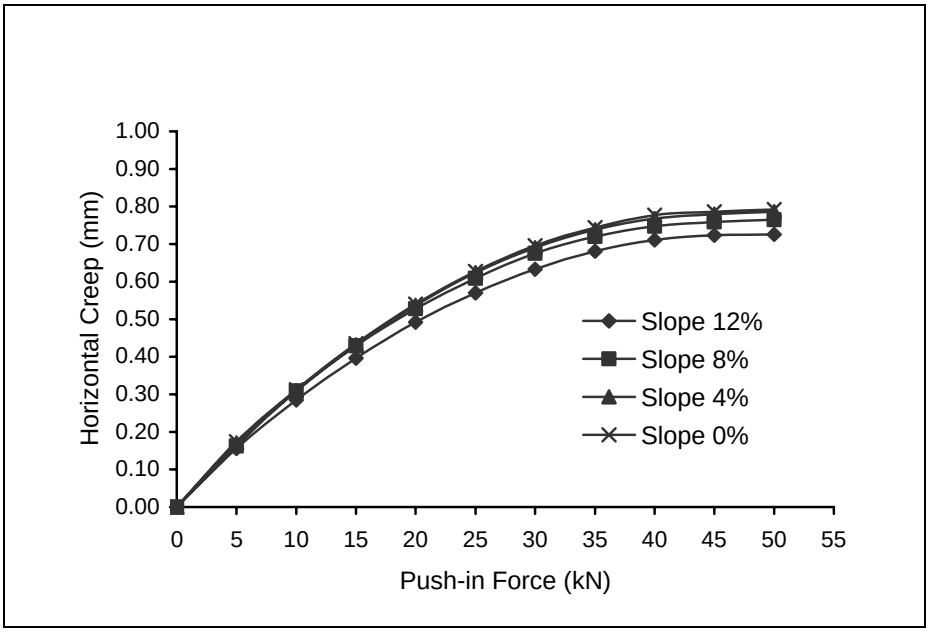

Figure 4.53 Relationship between push-in forces with horizontal creep on CBP: rectangular shape, 100 mm block thick, 70 mm bedding sand thickness and 3 mm joint width

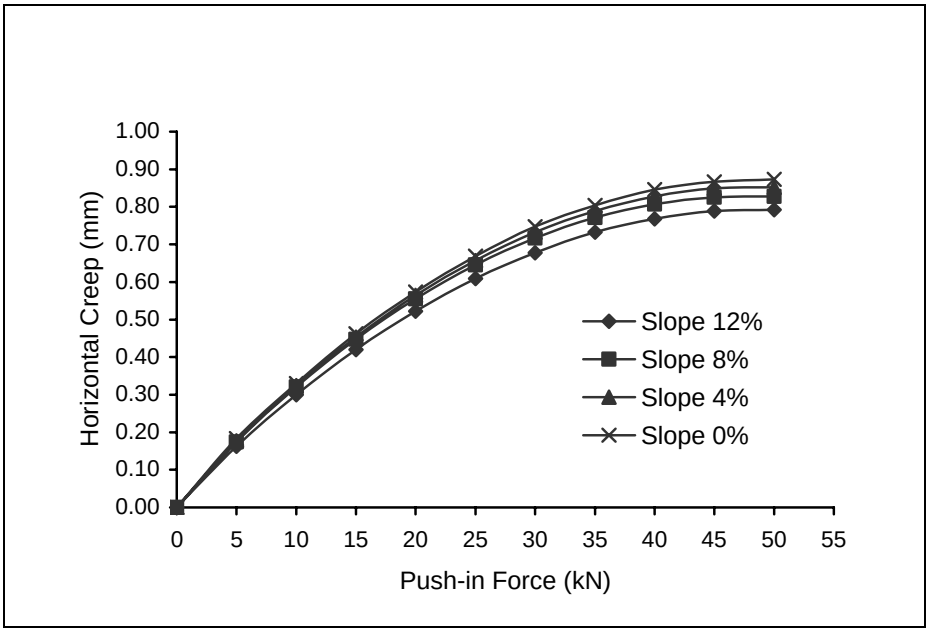

Figure 4.54 Relationship between push-in forces with horizontal creep on CBP: rectangular shape, 60 mm block thick, 30 mm bedding sand thickness and 5 mm joint width

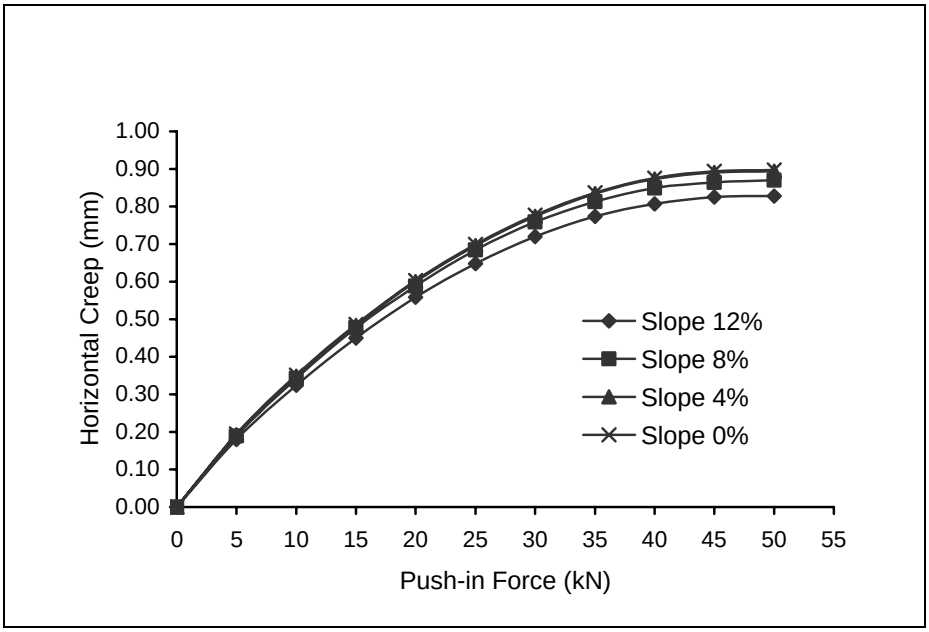

Figure 4.55 Relationship between push-in forces with horizontal creep on CBP: rectangular shape, 60 mm block thick, 50 mm bedding sand thickness and 5 mm joint width

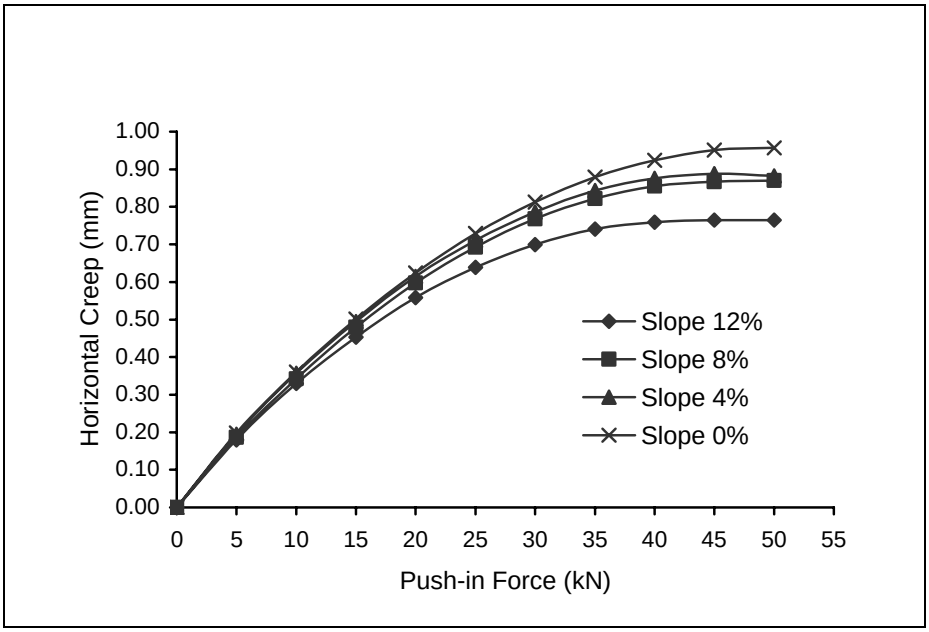

Figure 4.56 Relationship between push-in forces with horizontal creep on CBP: rectangular shape, 60 mm block thick, 70 mm bedding sand thickness and 5 mm joint width

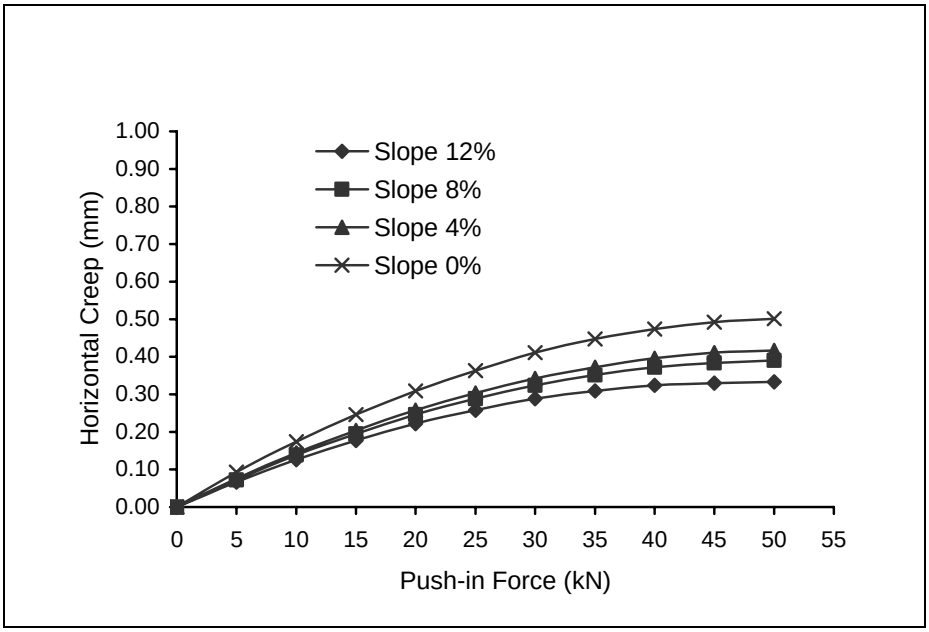

Figure 4.57 Relationship between push-in forces with horizontal creep on CBP: rectangular shape, 100 mm block thick, 30 mm bedding sand thickness and 5 mm joint width

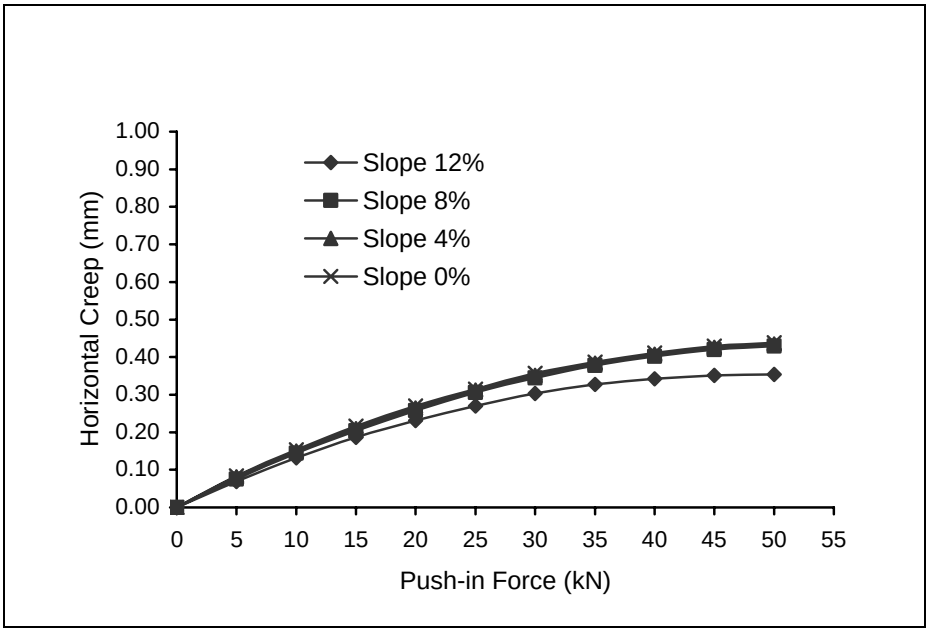

Figure 4.58 Relationship between push-in forces with horizontal creep on CBP: rectangular shape, 100 mm block thick, 50 mm bedding sand thickness and 5 mm joint width.

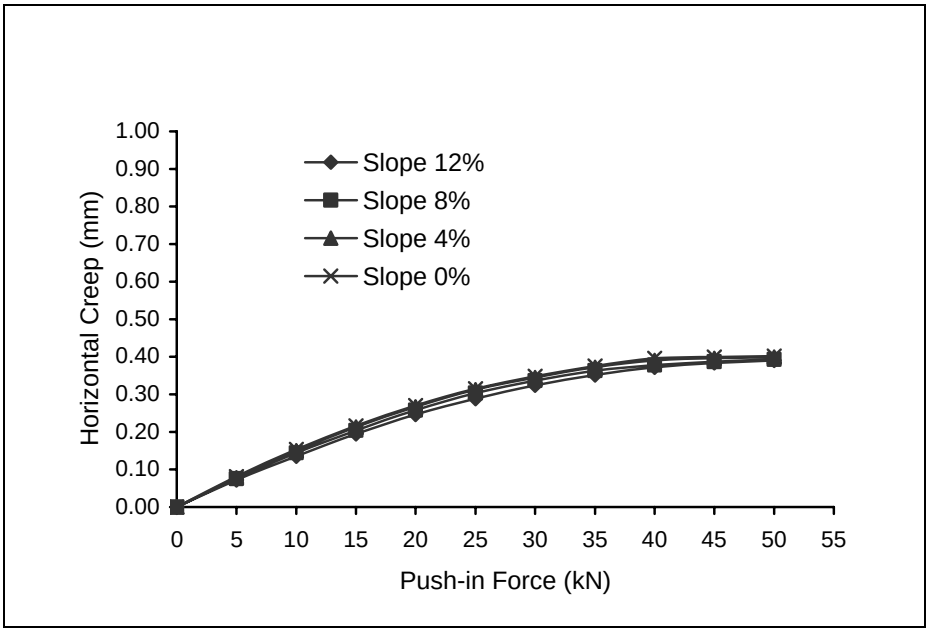

Figure 4.59 Relationship between push-in forces with horizontal creep on CBP: rectangular shape, 100 mm block thick, 70 mm bedding sand thickness and 5 mm joint width.

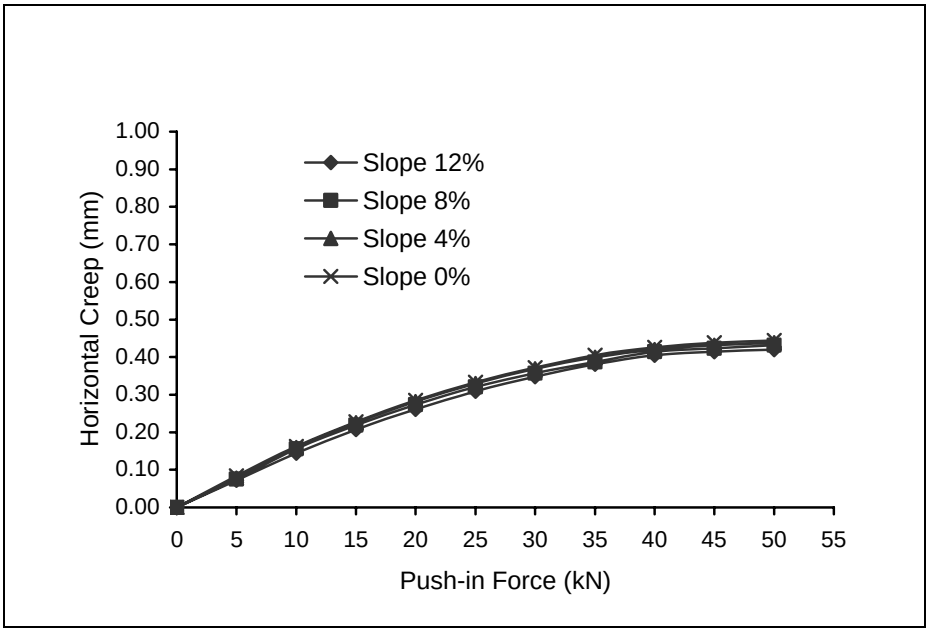

Figure 4.60 Relationship between push-in forces with horizontal creep on CBP: rectangular shape, 60 mm block thick, 30 mm bedding sand thickness and 7 mm joint width

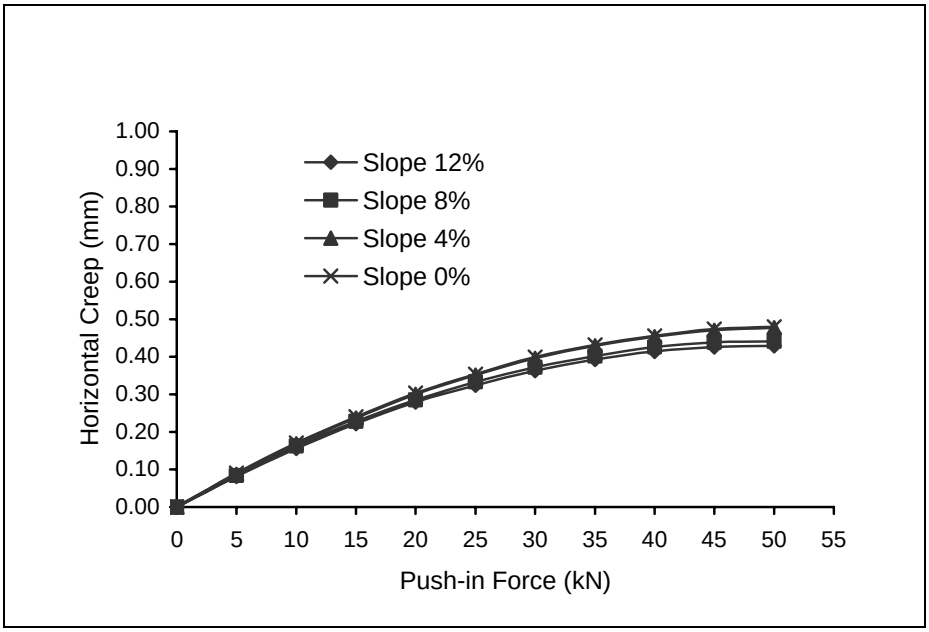

Figure 4.61 Relationship between push-in forces with horizontal creep on CBP: rectangular shape, 60 mm block thick, 50 mm bedding sand thickness and 7 mm joint width

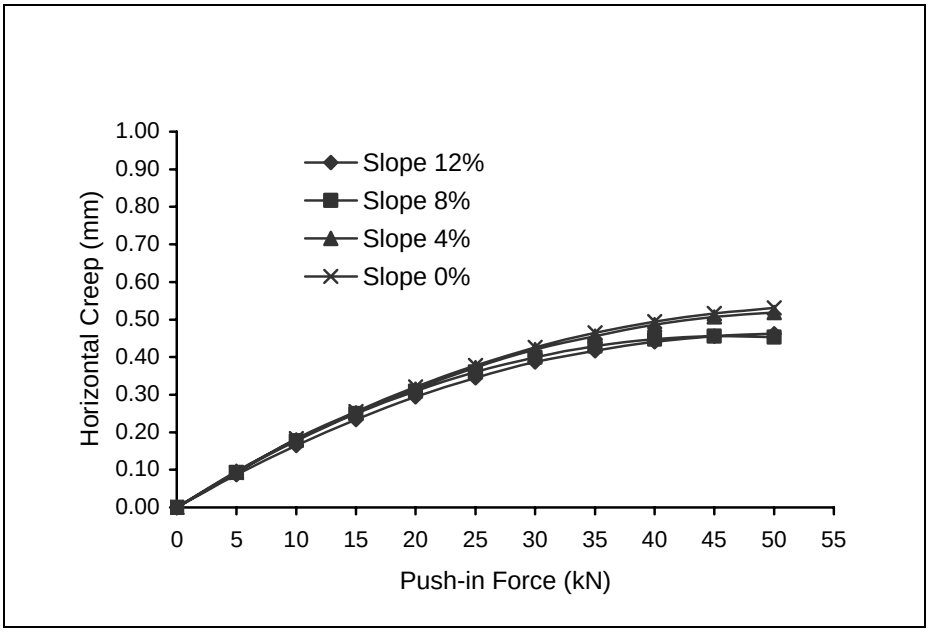

Figure 4.62 Relationship between push-in forces with horizontal creep on CBP: rectangular shape, 60 mm block thick, 70 mm bedding sand thickness and 7 mm joint width

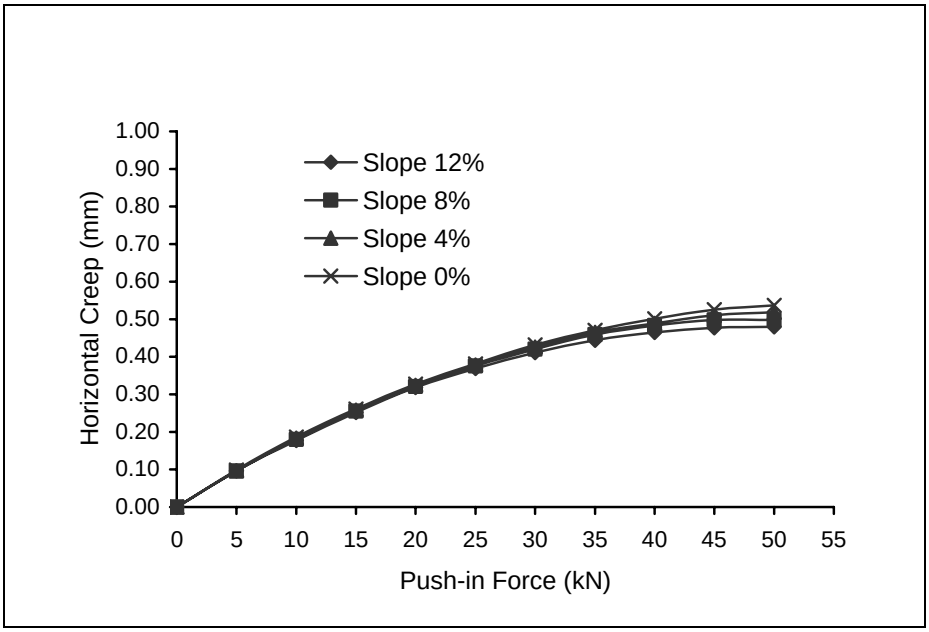

Figure 4.63 Relationship between push-in forces with horizontal creep on CBP: rectangular shape, 100 mm block thick, 30 mm bedding sand thickness and 7 mm joint width

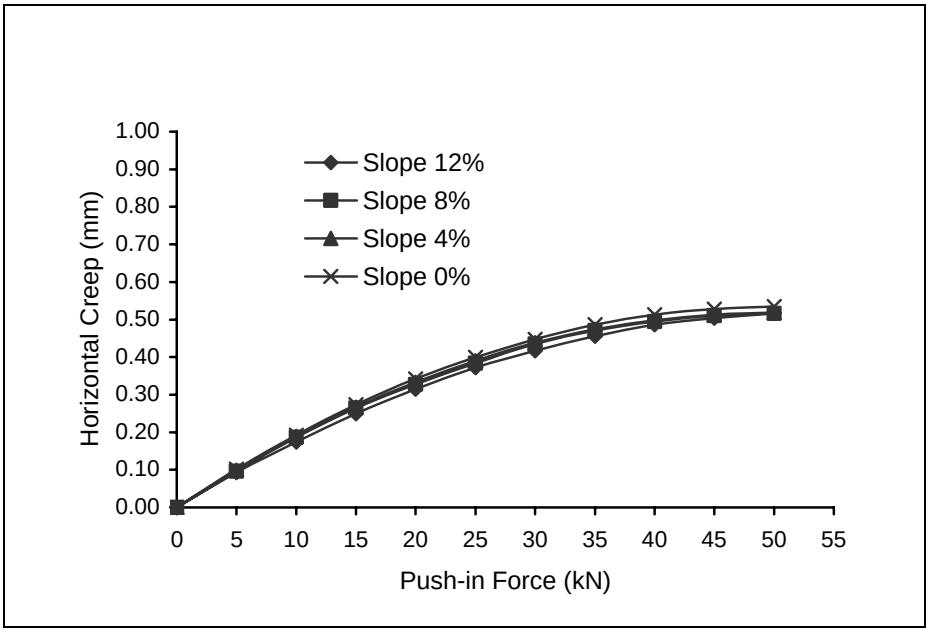

Figure 4.64 Relationship between push-in forces with horizontal creep on CBP: rectangular shape, 100 mm block thick, 50 mm bedding sand thickness and 7 mm joint width

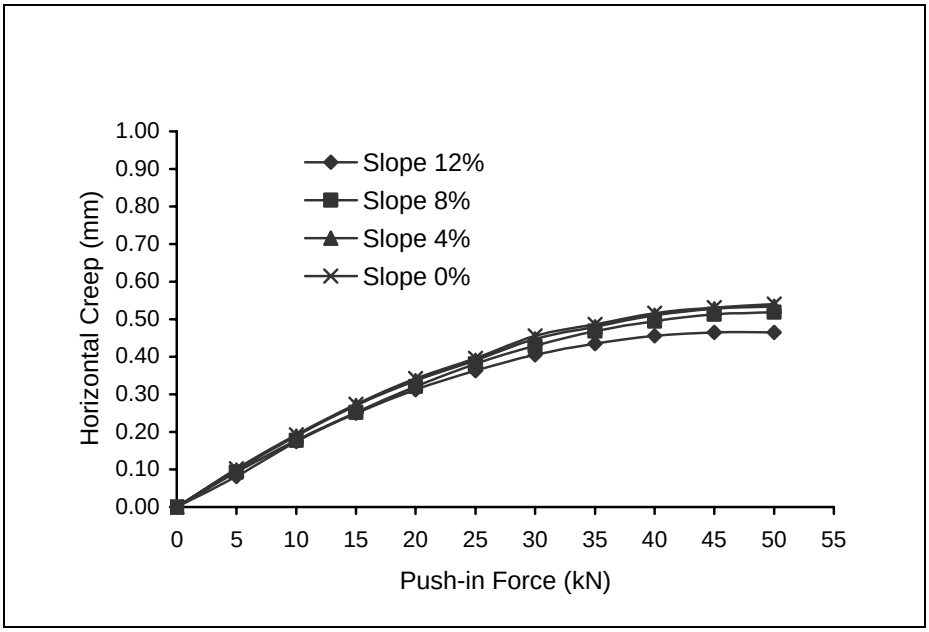

Figure 4.65 Relationship between push-in forces with horizontal creep on CBP: rectangular shape, 100 mm block thick, 70 mm bedding sand thickness and 7 mm joint width

CHAPTER 5

CONCRETE BLOCK PAVEMENT ON SLOPING ROAD SECTION USING ANCHOR BEAM

5.1 Introduction

The construction of roads on sloping road section poses particularly interesting challenges for road design. The horizontal (inclined) forces exerted on the road surface are severely increased due to traffic friction of accelerating (uphill), braking (downhill) or turning. These horizontal forces cause distress in most conventional pavements, resulting in rutting and poor riding quality. Concrete Block Pavement (CBP) performs well under such severe conditions depending on degree of slope, bedding sand thickness, block thickness, joint width between blocks, laying pattern and block shape. Each factor is used in the design of the anchor beam spacing for sloping road section area. Although CBP performs well on sloping road section area, there are certain considerations that must be taken into account during the design and construction of the pavement.

5.2 The Concept of Load Transfer on Concrete Block Pavement

Load transfer is the ability of a loaded block in a paving system to influence neighbouring blocks by causing them to deflect vertically. This load transfer reduces the vertical stress under the loaded block. The greater this spread of influence of vertical movement, the greater the degree of vertical interlock and hence the greater the load transfer.

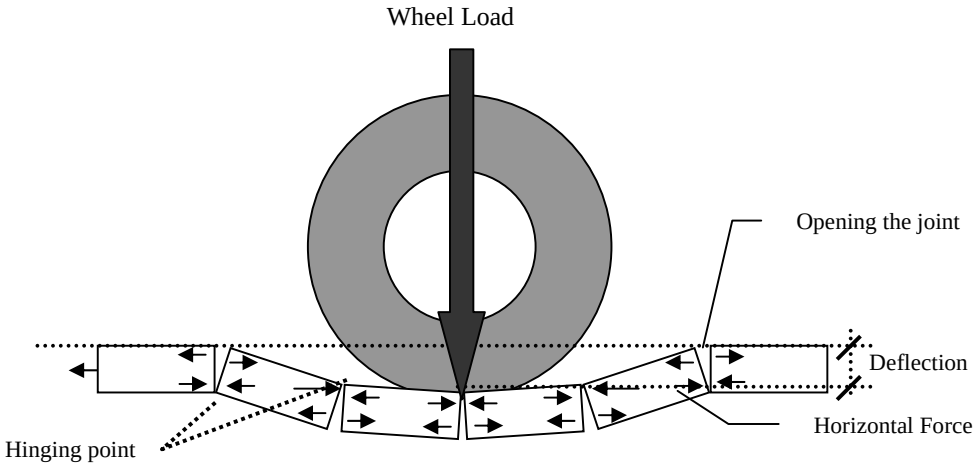

Figure 5.1 The behaviour of a concrete block pavement under load

Load transfer in the sloping road section, the factor degree of slope is influence on CBP. A block at rest on an adjustable inclined plane begins to move when the angle between the plane and the horizontal reaches a certain value θ (degree of slope), which is known as the angle repose. The weight W of the block can be resolved into a component F parallel to the plane and another component N perpendicular to the plane. For detail see Figure 5.2.

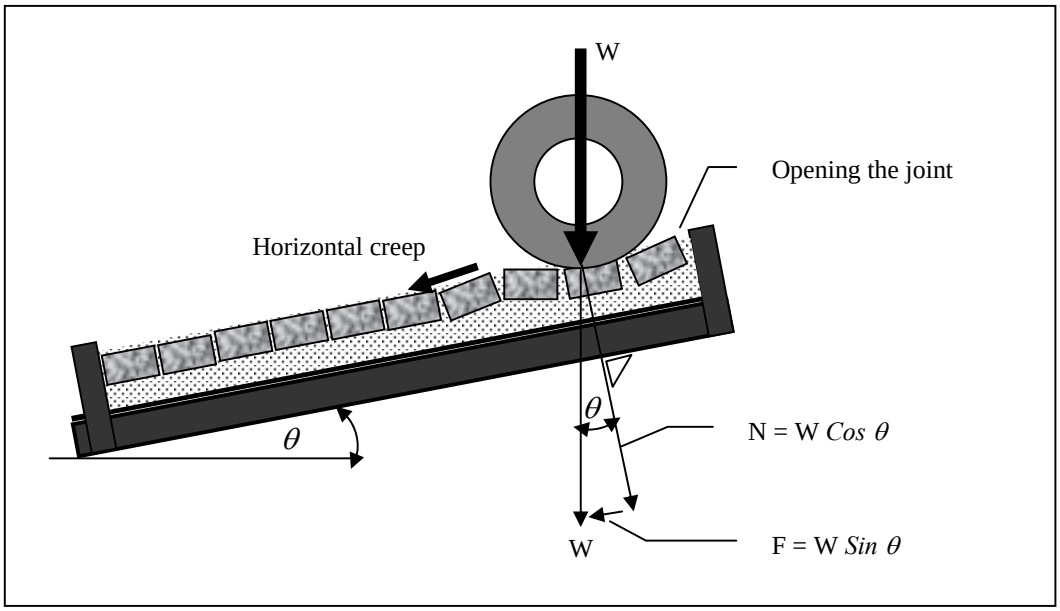

Figure 5.2 The magnitude load transfer of Force (F), Normal (N) and Wheel load (W)

5.3 CBP on Sloping Road Section Using Anchor Beam

It is common practice to construct edge restraints (kerbing and anchor beams) along the perimeter of all paving, to contain the paving and prevent horizontal creep and subsequent opening of joints. Due to the steepness of the slope, the normally vertical traffic loading will have a surface component exerted on the blocks in a downward direction. This force is aggravated by traction of accelerating vehicles up the hill and breaking of vehicles down the hill. If uncontained, these forces will cause horizontal creep of the blocks down the slope, resulting in opening of joints at the top of the paving. An anchor beam at the lower end of the paving is necessary to prevent this creep.

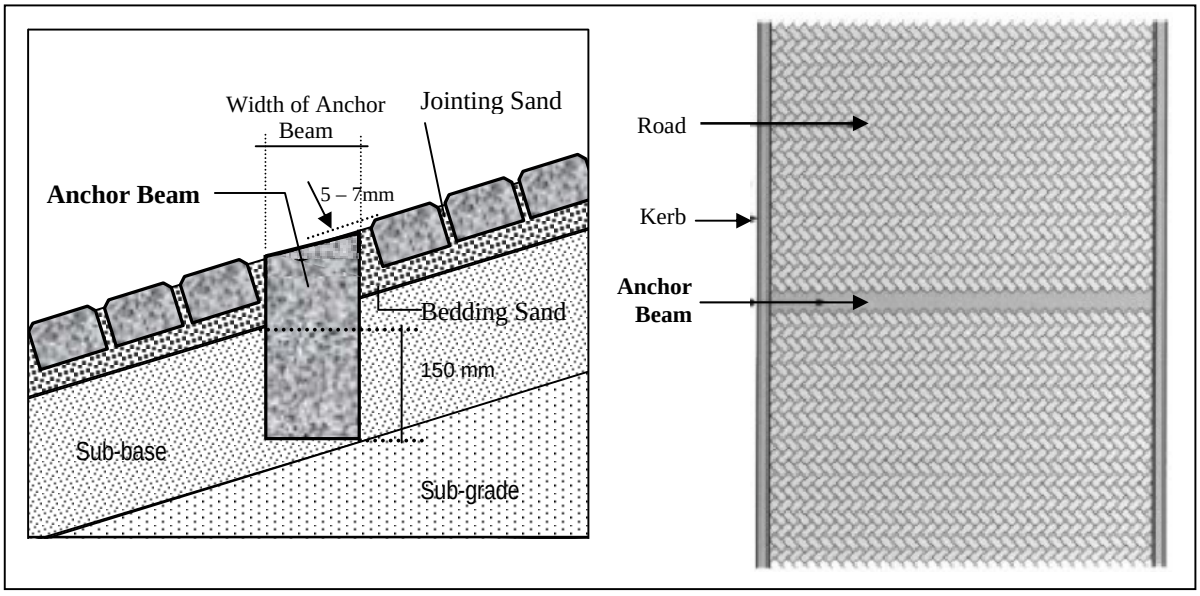

Figure 5.3 Detail construction of anchor beam.

For ease of CBP construction, the anchor beam was recommended that the blocks are laid continuously up the gradient. Thereafter, two rows of blocks are uplifted in the position of the beam, the sub-base excavated to the required depth and width and the beam cast, such that the top of the beam is 5 – 7 mm lower than the surrounding block work. This allows for settlement of the pavers. This method of construction will ensure that the anchor beam interlocks with the pavers and eliminates the need to cut small pieces of block.

5.3.1 Position of Anchor Beam

The position of the anchor beam for sloping road section area is shown in the next Figure 5.4.

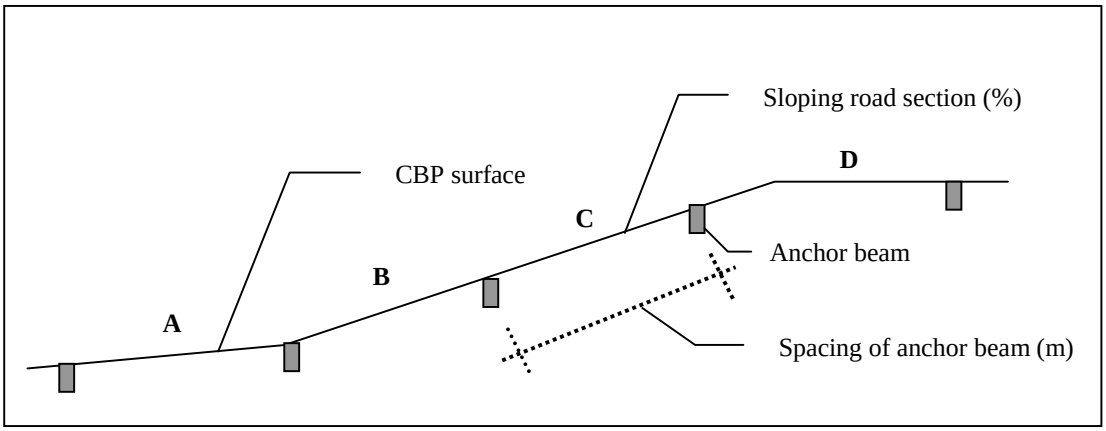

Figure 5.4 Schematic of spacing and position of anchor beam.

It is standard practice when laying CBP to start at the lower end and to work upwards against the slope. This practice will ensure that if there is any movement of blocks during the laying operation, it will help to consolidate the blocks against each other, rather than to open the joints. If one is constructing a road over undulating topography, it is suggested that one begins at the low point of the dip and work away in both directions simultaneously.

5.3.2 Spacing of Anchor Beam

The spacing of anchor beam should be determined by using horizontal force test and push-in test. The horizontal force test include changing variables of laying pattern, block thickness, block shape and joint width between blocks. While the push-in test include changing variables of bedding sand thickness, joint width between blocks, block

thickness and degree of the slope. The different changes of each variable result in the different spacing of anchor beam.

a. Horizontal Force Test

For horizontal force test, 2 m x 2 m steel frame is used in laboratory test with specification of CBP sample; rectangular block shape, 60 mm blcok thickness, stretcher bond laying pattern and 3 mm joint width (Figure 5.5). the test was conducted by push CBP sample from edge started from 0 kN until failure (block uplift). It is found the maximum horizontal creep as shown in the equation y = -0.0315x2 + 0.68x - 0.0613 in Figure 5.6. For equation of other cases are as shown in Appendix J1 to J6.

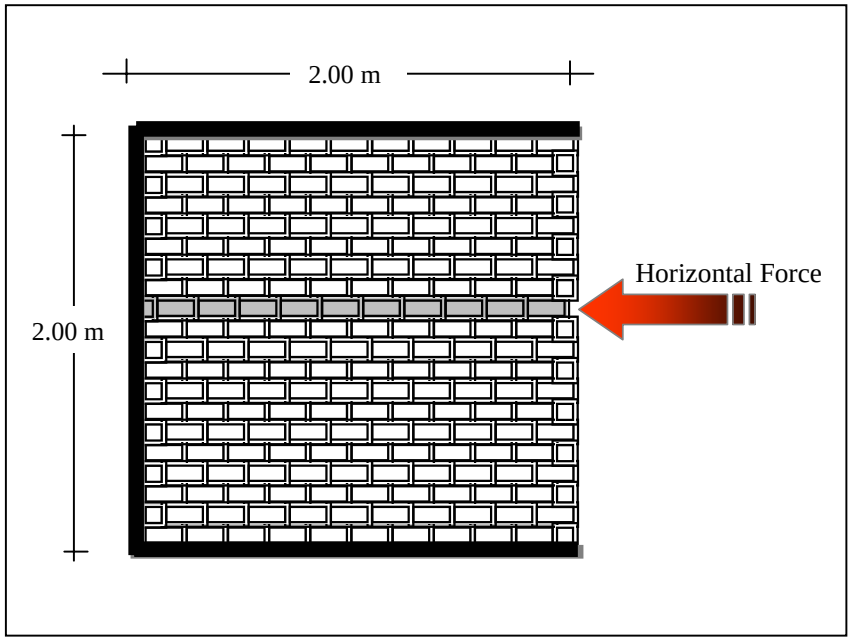

Figure 5.5 Horizontal force test

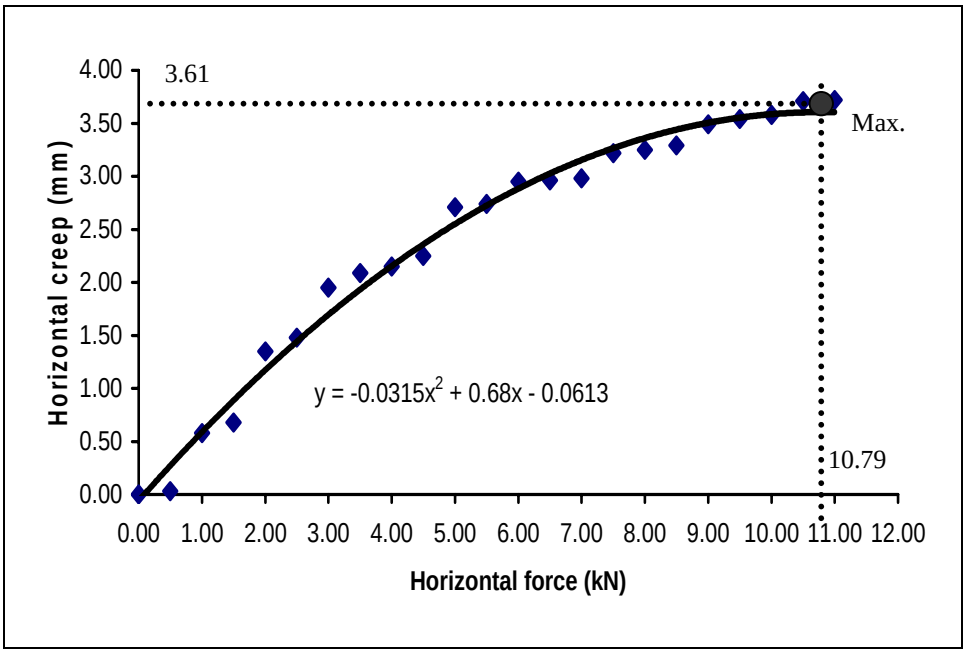

Figure 5.6 Relationship between horizontal forces with horizontal creep in horizontal force test.

In the Figure 5.6 shown, the horizontal forced was untill 10.79 kN, than the construction of CBP failure (uplift) and maximum horizontal creep is 3.61 mm.

b. Push-in Test

For case of push-in test, CBP sample laid on 1 m x 1 m steel frame. The specification of CBP sample i.e. rectangular block sahape, 60 mm block thickness, stretcher bond laying pattern, 3 mm joint width and 50 mm bedding sand thickness. The CBP sample is loaded by hydraulic jack start from 0 kN to 51 kN with 12^{o} degree of slope. The load position was set up on three points; 40 cm, 60 cm and 80 cm from edge restraint as shown in Figure 5.7. The results of experimental found the equation of maximum horizontal creep as shown in Figure 5.8.

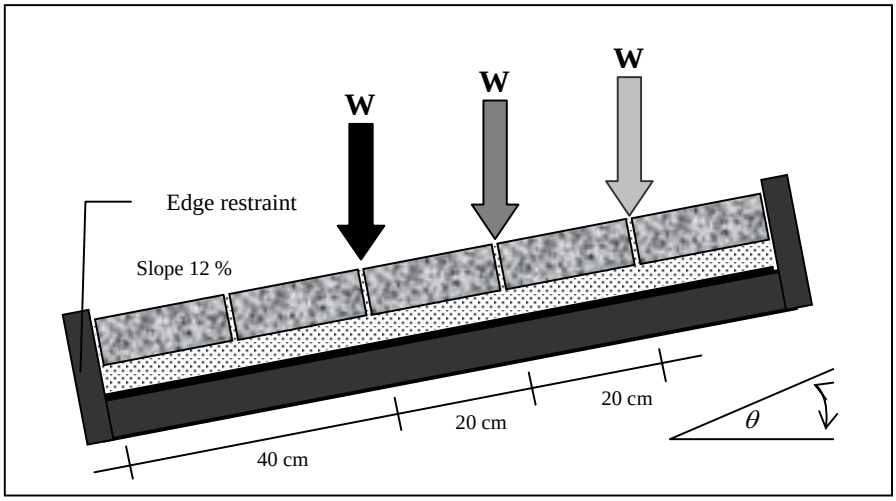

Figure 5.7 Position of load in push-in test

Horizontal force in push-in test (F) = W sin θ

Where: W = 51 kN

F = 51 sin 12

= 10.60 kN ~ 10.79 kN

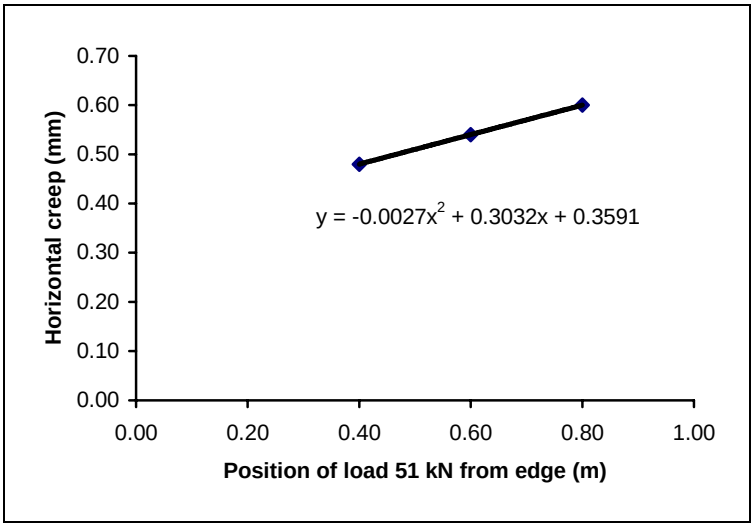

Figure 5.8 Relationship between load positions from edge restraint with horizontal creep on push-in until 51 kN.

c. Defining the spacing of anchor beam

The definition of spacing of anchor beam in this study using three steps. First, defining x maximum (horizontal force). Second, defining y maximum (horizontal creep). From the equation in Figure 5.6, $y = -0.0315x^2 + 0.68x - 0.0613$, it is found the maximum horizontal force and maximum horizontal creep.

$$y = -0.0315x^2 + 0.68x - 0.0613$$

$$\frac{dy}{dx} = 0$$

$$2(-0.0315)x + 0.68 = 0$$

$$x = \frac{-0.68}{2 * -0.0315} = 10.79kN$$

Where; x = 10.79 kN is horizontal force until construction of CBP failure (uplift). Substitute x =10.79 kN in equation $y = -0.0315x^2 + 0.68x - 0.0613$, it found y = 3.61. Where y = 3.61 mm is maximum horizontal creep.

The third step is combining x maximum and y maximum to equation $y = -0.0027x^2 + 0.3032x + 0.3591$ (Figure 5.8). Substitute y = 3.61 mm using ABC formula $X_{1,2} = \frac{-b \pm \sqrt{b^2 - 4ac}}{2a}$ and found x = 12.05 m.

Where x = 12.05 m is the spacing of anchor beam

(For calculations of other cases see Appendix L)

The next section would explain about spacing of anchor beam on various degrees of slopes, that is based on the effects of laying pattern, block thickness, block shape, joint width between blocks and thickness of bedding sand, respectively.

5.4 The Spacing of Anchor Beam Based on the Laying Pattern Effect

This section explains the estimated spacing of anchor beam based on the laying pattern effect. There are three laying patterns that used in this test i.e. stretcher bond, herringbone 90^{o} and herringbone 45^{o}. Each of these laying patterns was tested on four various degree of slope (0 %, 4 %, 8 % and 12 %). In this case, the CBP sample was used 3 mm joint width. The result of relationship between the estimation spacing of anchor beam with degree of slope is shown in Figure 5.9.

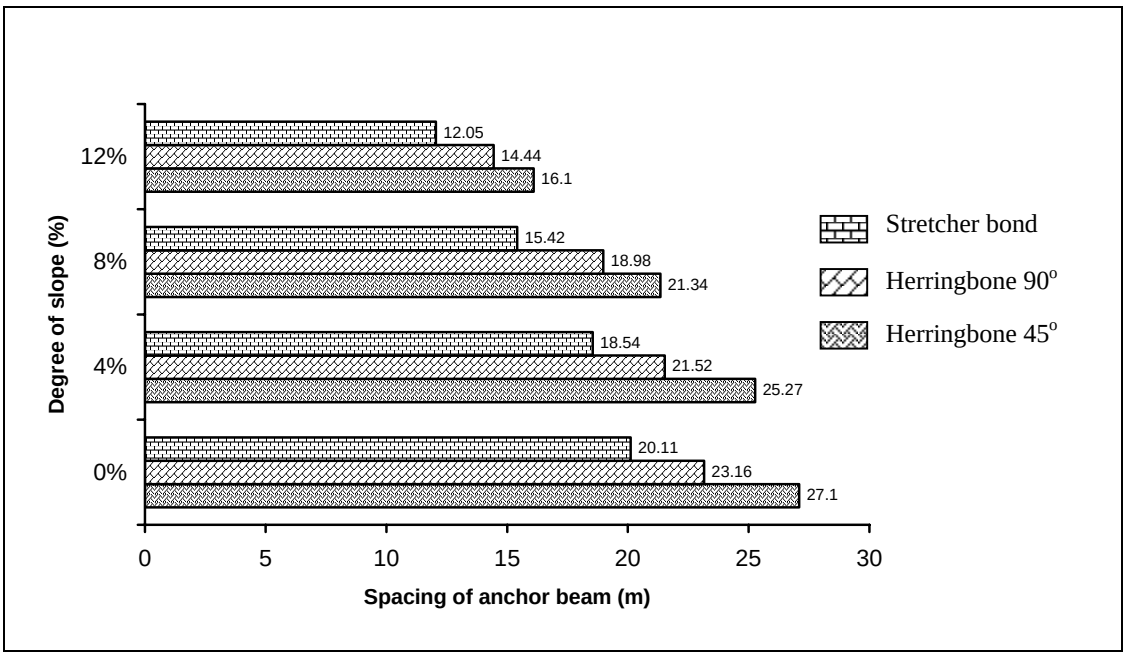

Figure 5.9 Spacing of anchor beam based on laying pattern effect with 3 mm joint width.

Figure 5.9 shows that the variation of laying pattern affecting the spacing of anchor beams in each variation degree of slope. The herringbone 45^{o} is the best laying pattern compared to herringbone 90^{o} and stretcher bond to restraint the horizontal force.

5.5 The Spacing of Anchor Beam Based on the Joint Width Effect

This section explains the estimated spacing of anchor beam based on the joint width effect. There are three joint width used in this test i.e. 3 mm, 5 mm and 7 mm. Each of these joint widths was tested on four various degree of slope (0 %, 4 %, 8 % and 12%).

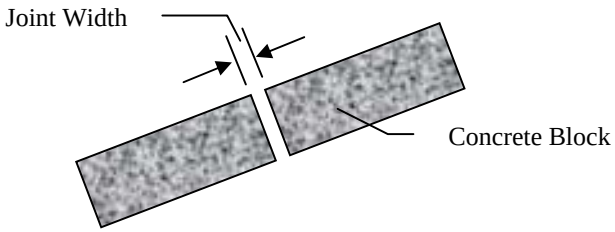

Figure 5.10 The effect of joint width in sloping road section

The relationship between spacing of anchor beam with variation of degrees of slopes is shown in Figure 5.11.

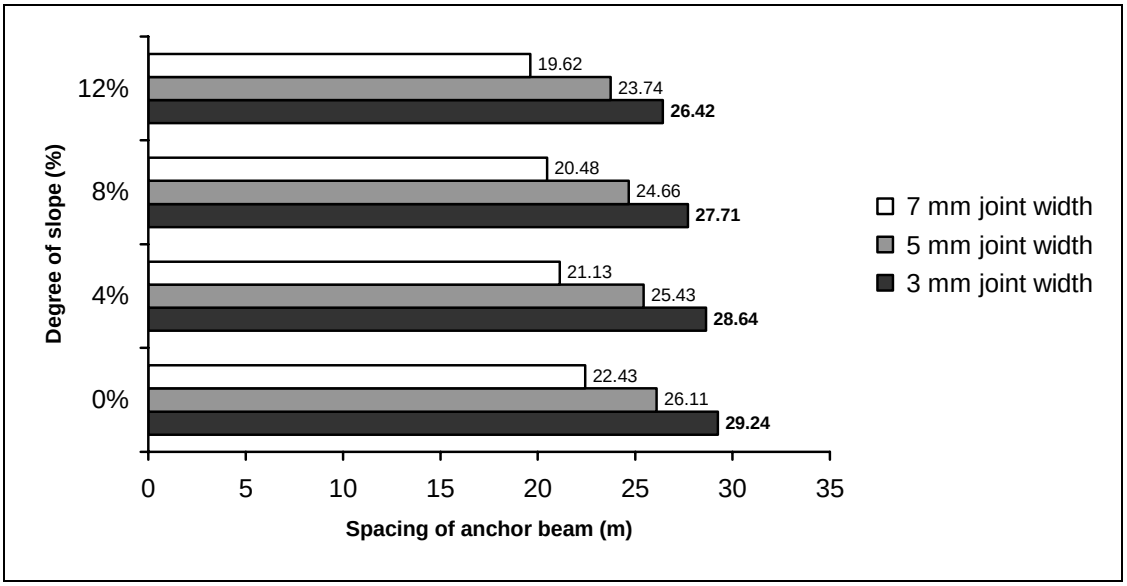

Figure 5.11 Spacing of anchor beam based on joint width effect for rectangular block shape, 60 mm block thickness and stretcher laying pattern.

Figure 5.11 shows that the variation of joint width affecting the spacing of anchor beams in each variation degree of slope. The wider the joint width, the spacing of anchor beam is shorter for each variation degree of slope. The higher degree of slope, the shorter the spacing of anchor beams for each variation degree of slope. The result also found that 3 mm joint width is the optimum model compared by 5 and 7 mm joint width.

5.6 The Spacing of Anchor Beam Based on the Block Thickness Effect

This section explains the estimated spacing of anchor beam based on the block thickness effect. There are two block thickness used in this test i.e. 60 mm and 100 mm. Each of these block thicknesses was tested on four various degree of slope (0 %, 4 %, 8% and 12 %). The result of relationship between the estimation spacing of anchor beam with degree of slope is shown in Figure 5.14.

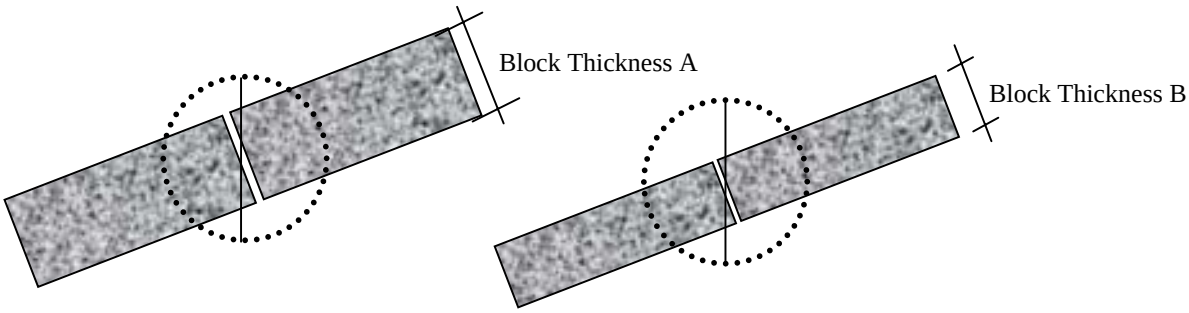

Figure 5.12 The difference of block thickness

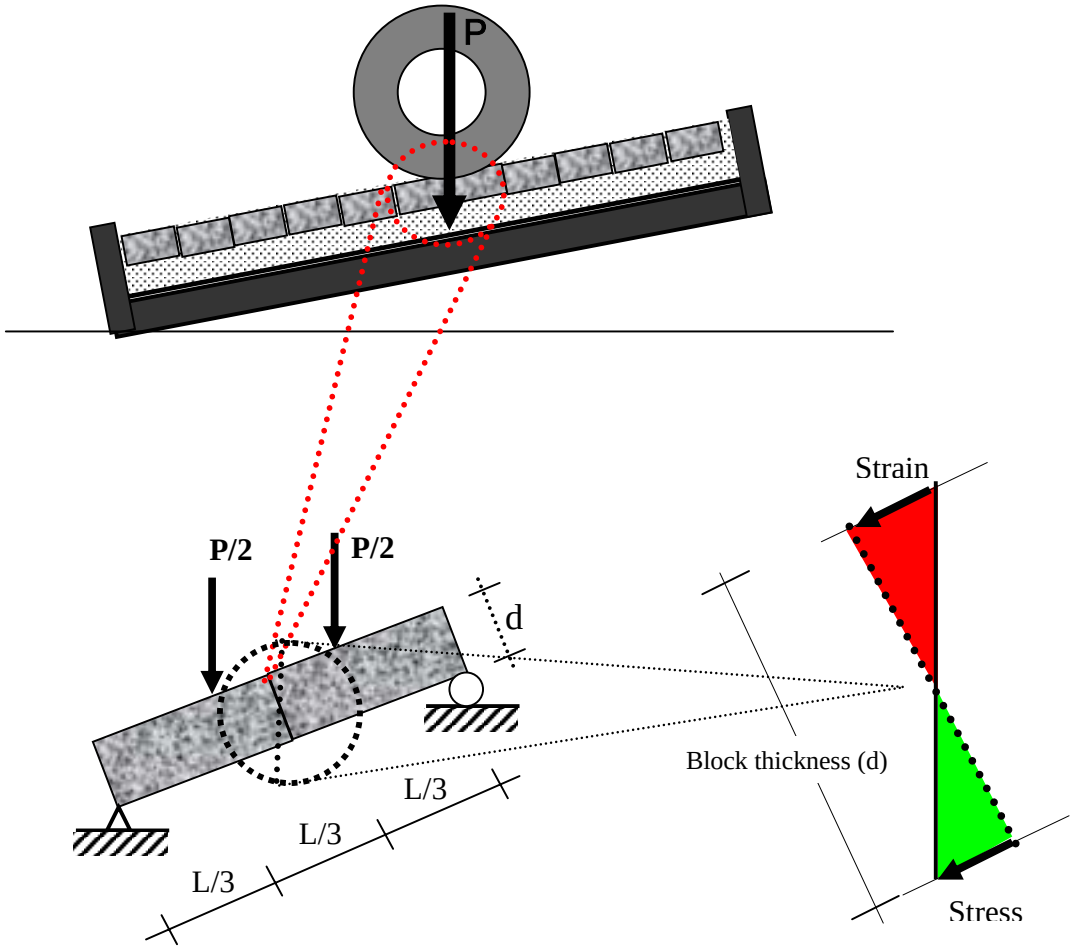

Figure 5.13 The effect of block thickness on sloping road section

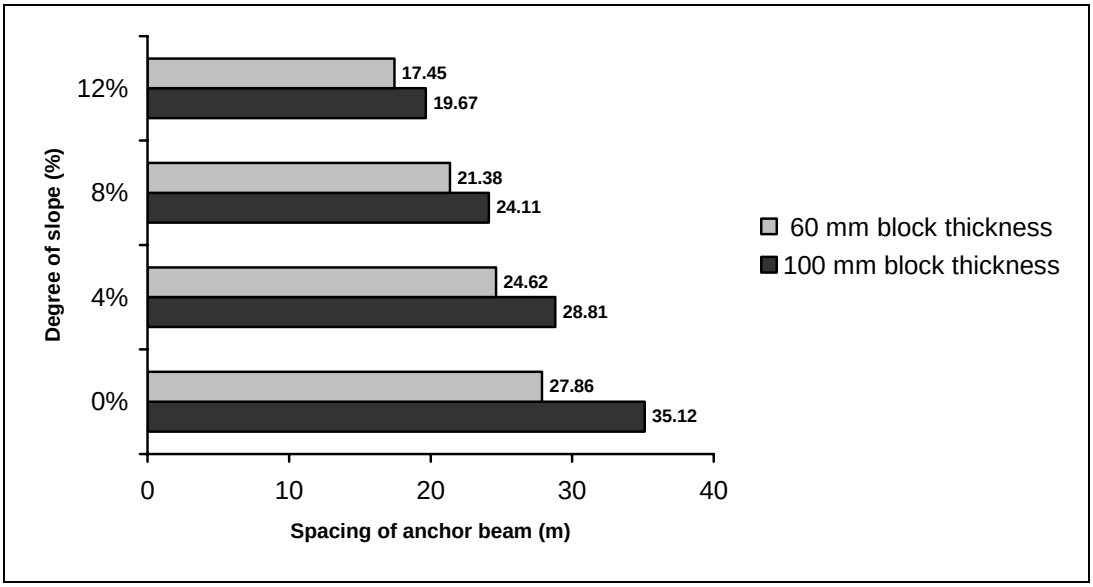

Figure 5.14 Spacing of anchor beam based on block thickness effect for 3 mm joint width and rectangular block shape.

Figure 5.14 show that for 3 mm joint width, the variation of block thickness affecting the spacing of anchor beam. The thicker of block thickness, the longer the spacing of anchor beam for each variation degree of slope. The higher degree of slope, the shorter the spacing of anchor beams for each variation of block thickness. From this test also found that 100 mm block thickness is more stable than 60 mm block thickness.

5.7 The Spacing of Anchor Beam Based on the Block Shape Effect

This section explains the estimated spacing of anchor beam based on the block shape effect. There are two block shapes that used in this test i.e. rectangular and uni-pave shape. Each of these block shapes was tested on four various degree of slope (0 %, 4 %, 8 % and 12 %). In this case, the CBP sample was used 3 mm joint width. The result

of relationship between the estimation spacing of anchor beam with degree of slope is shown in Figure 5.16.

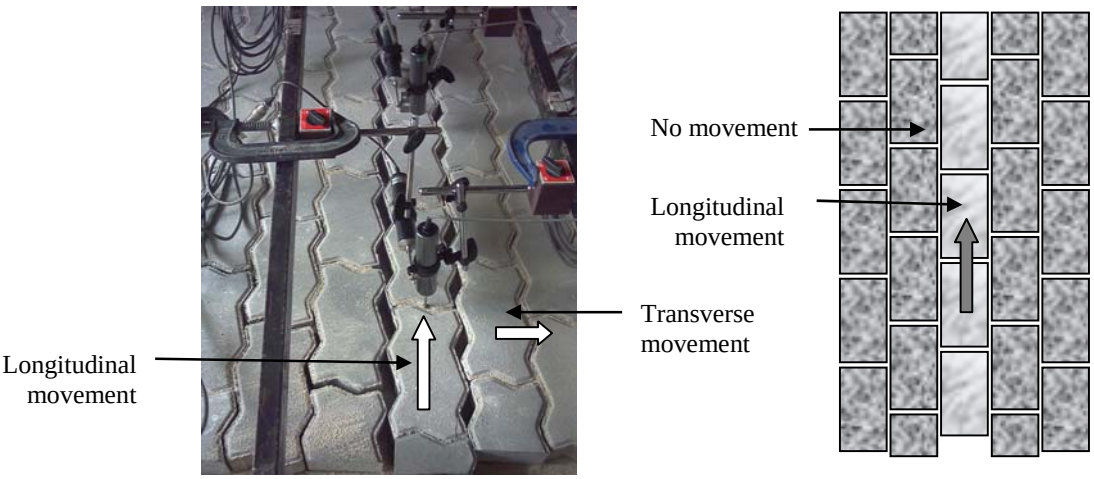

Figure 5.15 The different effect of uni-pave by rectangular blocks loaded horizontally

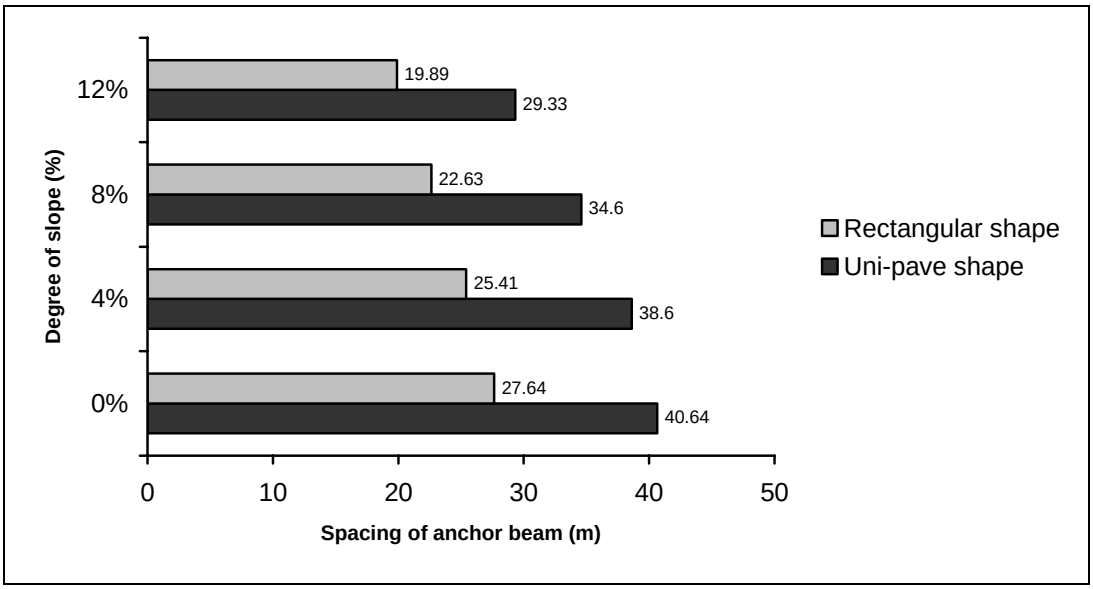

Figure 5.16 Spacing of anchor beam based on block shapes for 60 mm block thickness, 50 mm bedding sand thickness and 3 mm joint width.

Figure 5.16 shows that the variation shapes of block affecting the spacing of anchor beam for each variation degree of slope. The uni-pave block shape has more restraint of horizontal creep than rectangular block shape, because uni-pave block shape has gear (four-dents), while rectangular block shape no gear (no dents), so the spacing of anchor beam has a difference of about 10 m. The higher degree of slope, the shorter the spacing of anchor beams for each variation shape of block.

5.8 The Spacing of Anchor Beam Based on the Bedding Sand Thickness Effect

This section explains the estimated spacing of anchor beam based on the bedding sand thickness effect using 3 mm joint width. The bedding sand thickness used in this study are; 30, 50 and 70 mm. Each of these bedding sand thicknesses was tested on 0 %, 4 %, 8 % and 12 % degrees of slope. In Figure 5.17, the bedding sand thickness of 30mm has almost no difference effect if applied on sloping road section 0 to 8 %, because too small difference thickness. But, the bedding sand thickness of 50 mm and 70 mm, the difference is significant for about 1.5 mm to 8.4 mm additional thickness. The effect of bedding sand thickness on CBP slopes 0 to 12 %, the deflection in the pavement increase. The increase degree of slope will cause shorter spacing of anchor beam for each bedding sand thickness as shown in Figure 5.18.

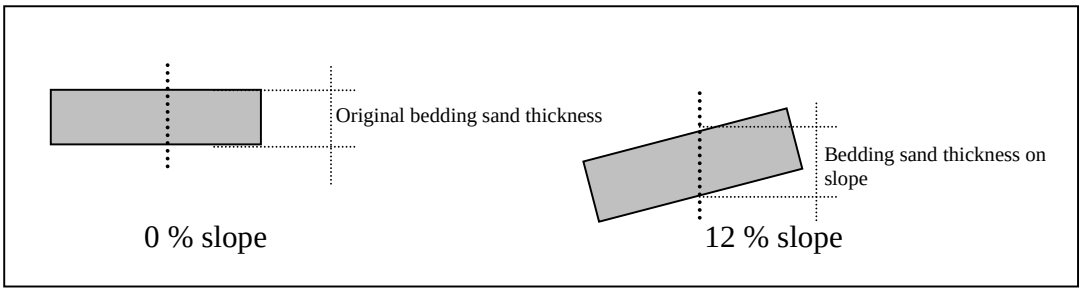

Figure 5.17 The effect of slope in bedding sand thickness

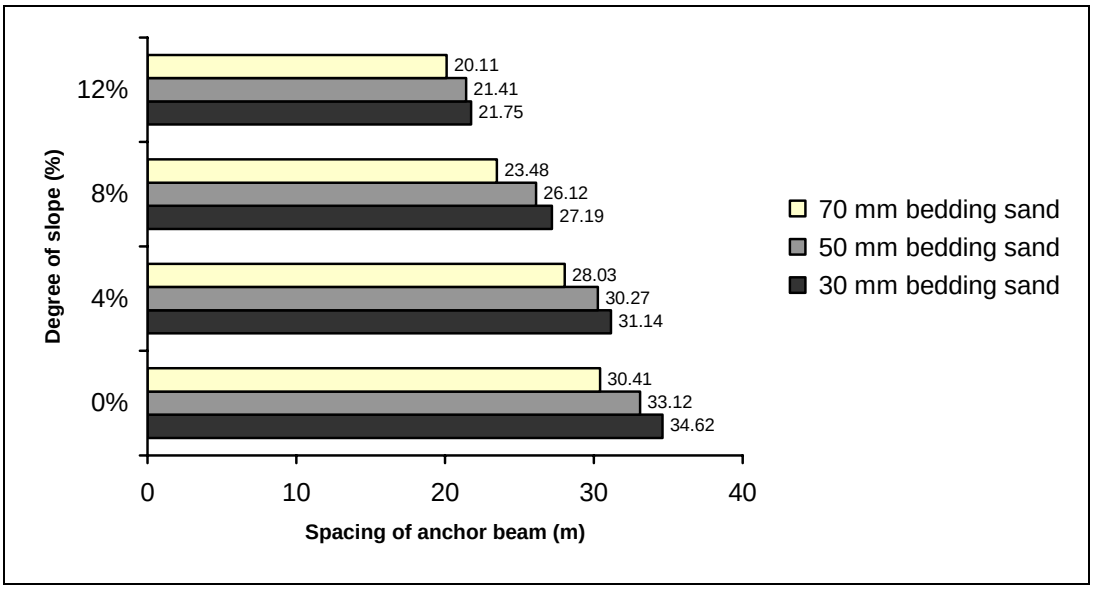

Figure 5.18 Spacing of anchor beam based on bedding sand thickness used 60 mm block thickness, rectangular block shape and stretcher laying pattern.

5.9 Summary

The spacing of anchor beam on various degrees of slopes, that is based on the effect of laying pattern, block thickness, block shape, joint width between blocks and thickness bedding sand, is summarized below:

- The herringbone 45^o is the best laying pattern compared to herringbone 90^o and stretcher bond to restraint the horizontal force.
- For the case horizontal creep, the uni-pave block shape is more restraint than rectangular, because uni-pave block shape has gear (four-dents), while rectangular block shape no gear (no dents).
- The increase of degree of slope will cause shorter spacing of anchor beam.

- The increase of joint width will cause shorter spacing of anchor beam.
- The optimum joint width is 3 mm.
- The increase of block thickness will cause longer spacing of anchor beam.
- The increase of bedding sand thickness will cause shorter spacing of anchor beam.

CHAPTER 6

FINITE ELEMENT MODEL FOR CBP

6.1 Introduction

It is difficult to model block pavements by finite elements for structural analysis, because their surface layer consists of a large number of very small blocks with complicated laying patterns. In this study, a programme package of the structural analysis for block pavements, COSMOS DESIGN STAR VERSION 4.0, has been developed based on a three dimensional finite element model for pavement structure. The SOLID WORKS version 2004 programme package can draw meshing of each element structure model pre-processor. They have to input information only on loading and pavement structural conditions including block size, joint width, laying pattern and mechanical characteristics of bedding sand layer. The solver computes displacements, stresses and strains in the blocks. In the model, the blocks are divided into solid elements and the bedding sand course and jointing sand are modelled by a general interface element. The post processor graphically displays deformations and stress contours of the entire or partial region of the pavement structure. The effects of block thickness, stiffness of joint, bedding sand course and laying pattern on deflection, also stress and strain in concrete block pavements are investigated using this tool.

6.2 Three Dimensional Finite Element Model (FEM)

In this study, in order to simulate mechanical behaviour of concrete block pavements, a structural model based on a Three Dimensional Finite Element Model (3DFEM) was developed. In this section, outline of 3DFEM model for pavement structures and its application to concrete block pavements are presented.

6.2.1 Three Dimensional FEM for Pavement

Figure 6.1 shows a pavement structure considered in SOLID WORKS. This pavement consists of elastic layers that represent concrete block, jointing sand, and bedding sand, all of which are divided into solid elements in the steel frame box. The interface between the blocks and jointing sand is modelled using a general interface element.

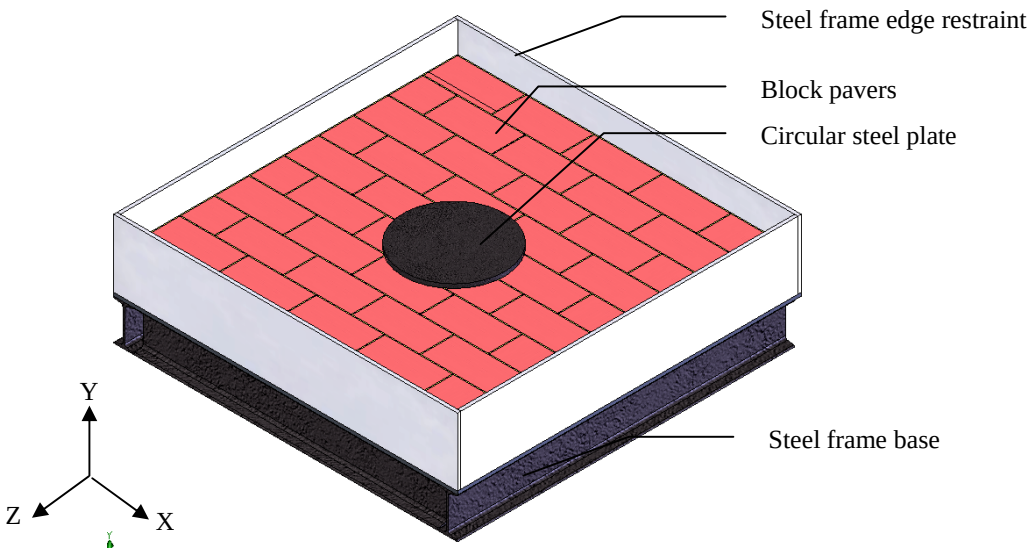

Figure 6.1 Structural model of concrete block pavement

Each layer has a finite horizontal extent and displacement in the normal direction is fixed on all side faces of the layer; other displacements are free. This boundary condition is not applied to the top layer. All displacements are fixed at nodes on the bottommost surface of the structure. Loads up to 51 kN were applied on the surface CBP vertically as uniformly distributed steel circle loads 250 mm diameter and 12 mm thickness (assumed wheel contact area on pavement).

6.2.2 Diagram Condition of Sample Tested

A block pavement consists of small blocks, joints between the blocks, a bedding sand course and steel frame as base course. The pavement structure is modelled as a combination of solid elements and tested on various slope as shown in Figure 6.2.

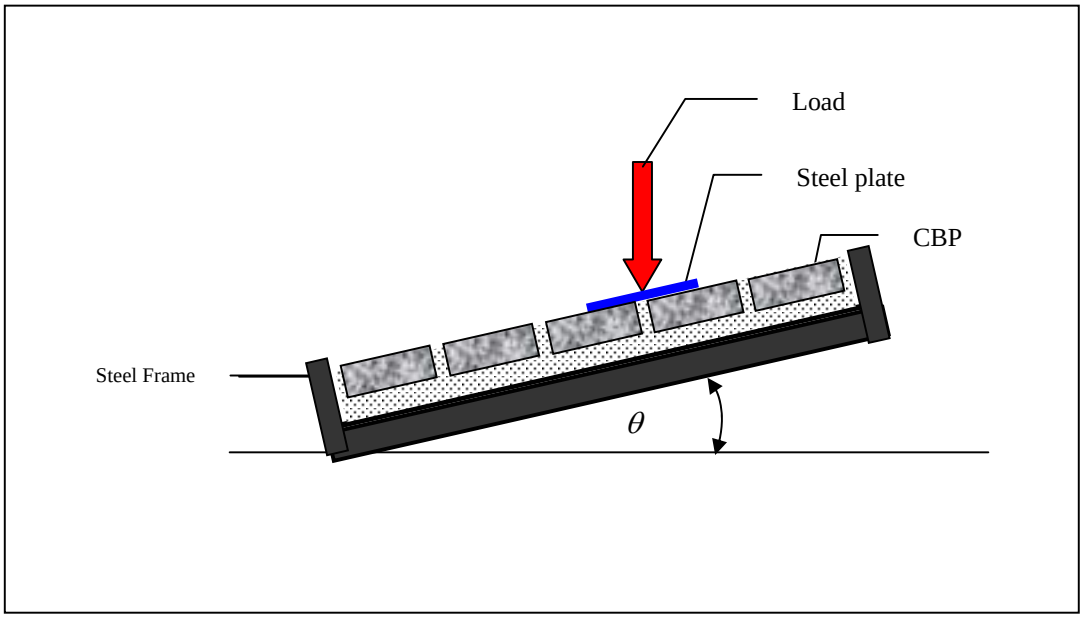

Figure 6.2 CBP tested on various slope

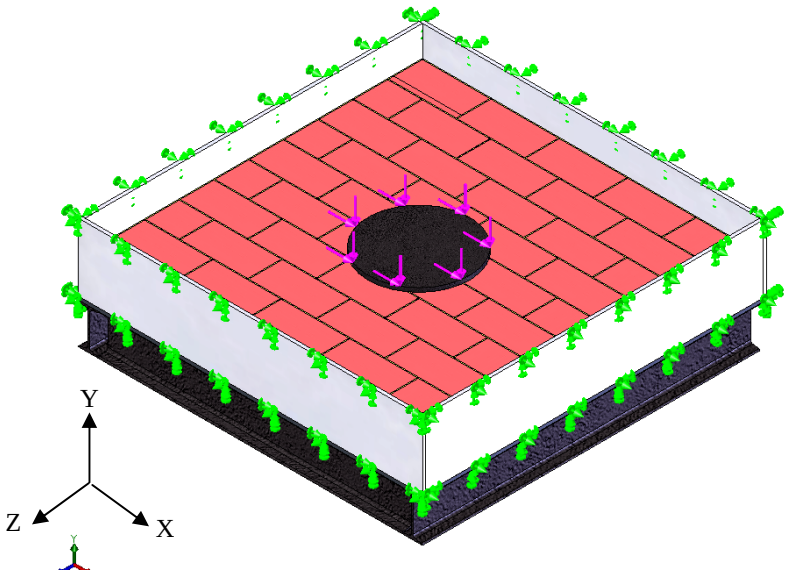

Figure 6.3 Three dimensional finite element model for a block pavement

6.3 Programme Package

6.3.1 Outline

The programme package (COSMOS DESIGN STAR) developed in this study for structural analysis of block pavements consists of a pre-processor, a solver and a post-processor. The pre-processor has a user-friendly interface, through which users input data regarding the meshing of concrete block pavement CBP and material properties of each element as well as loading condition. The solver runs the FEM programme using the input data file and stores the results in an output data file report. The post processor graphically displays the computed results and provides response data of specified nodes.

6.3.2 Pre-processor

6.3.2.1 Meshing

Meshing is a very crucial step in design analysis. The automatic mesher in COSMOS Works generates a mesh based on a global element size, tolerance, and local mesh control specifications. Mesh control could specify different sizes of elements for components, faces, edges, and vertices.

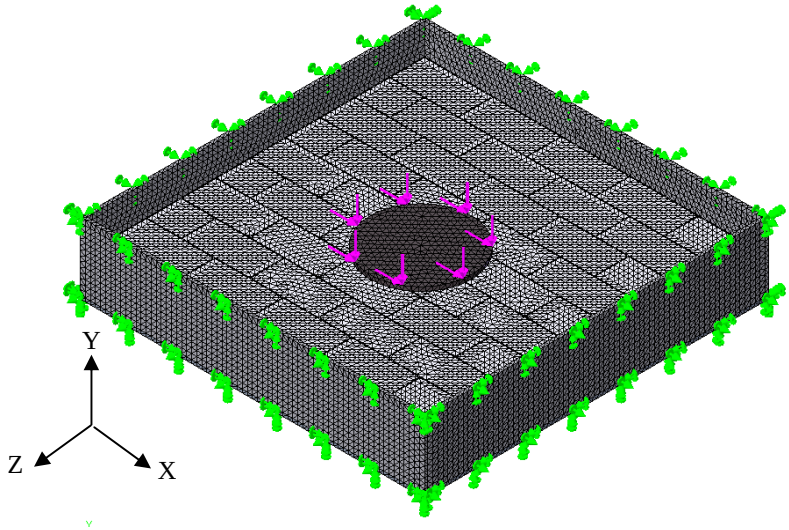

Figure 6.4 User interface of pre-processor of the package

6.3.2.2 Material Properties

In this study each material is characterized by its modulus of elasticity, density, and Poisson's ratio. The material properties used in this study are obtained from an information research and development of block company (SUN-Block Sdn. Bhd). The block thickness and the stiffness of the joint and bedding sand varied as presented in Table 6.1.

Table 6.1: Material properties used in 3DFEM

Material	Elastic Modulus (kN/m^2)	Poisson's Ratio	Mass Density (kg/m^3)
Block	3.5E+05	0.25	2,435
Bedding and jointing sand	43E+02	0.35	1,732
Steel	27E+06	0.30	4.817

For the non-linear three-dimensional analyses, concrete blocks are considered to be elastic. Bedding and jointing sand layers were assumed to have elastic perfectly plastic behaviour; it was utilized as their failure criteria. The layers were assumed to have full contact with no relative displacement between.

6.3.3 Solver

The solver, 3D FEM, computes displacements, stresses and strains using the input data file created by PRE3D. The 3D FEM opens a COSMOS Design STAR showing an iterative solution process for a nonlinear equation. The computation will take several minutes up to several hours depending on the problem size and the platform.

6.3.4 Post-processor

Clicking [Run]-[Graphics] from the COSMOS Design starts the post-processor and then open file SOLID Works. On the COSMOS, the user is able to load the report file and view displacement, stress and strain results. The Report tool helps a document user to study quickly and systematically by generating internet-ready reports. The reports are structured to describe all aspects of the study. Plots created in the COSMOS Works Manager tree can be included automatically in the report. User can also insert images, animations (AVI videos), and VRML files in the report. A printer-friendly version of the report can be generated automatically. Reports provide an excellent way to share study results with others online or in printed format. User can modify the various sections of the report by inserting text or graphics. To share a report, send all associated image files along with the html files. The receiver should place all files in the same folder for viewing.

6.4 Simulations

This section examines the effects of block thickness, friction of joint and bedding sand on deflection, stresses in block and strain at the top of each element based on the simulation results.

Pavement structures used in the simulation have a block layer with 98 mm x 198 mm block; 60 mm block thickness, 50 mm thick bedding sand. The type stretcher bond of laying pattern of blocks was employed. 3DFEM models used in the simulation are shown in Figure 6.1. The area of the pavement was 1.00 m by 1.00 m. 98 mm by 198 mm rectangular load of 51 kN was applied at the centre of the area.

6.5 Results

6.5.1 Displacement

Figure 6.5 shows the effects of the block thickness on the deflection (downward deflection is defined as negative) at the centre of the pavement. If the joint stiffness is high, the deflection decreases as the block thickness increases. On the other hand, if the joint stiffness is low, the thickness hardly affects the deflection. If the stiffness of the cushion layer is low, the deflection is large.

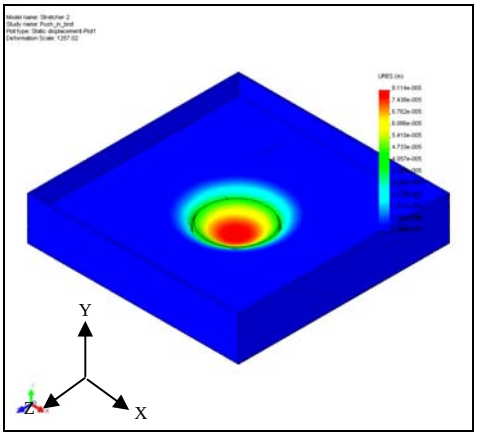

(a) Displacement of CBP on Slope 0 %

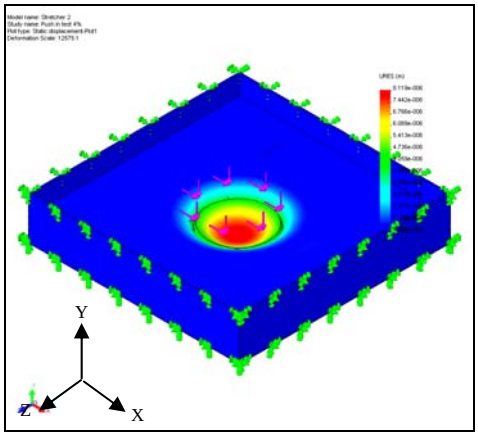

(b) Displacement of CBP on Slope 4 %

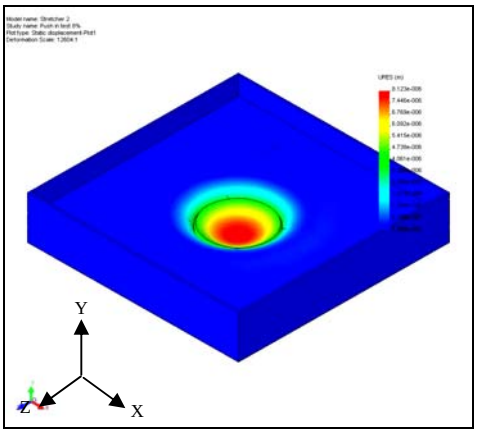

(c) Displacement of CBP on Slope 8 %

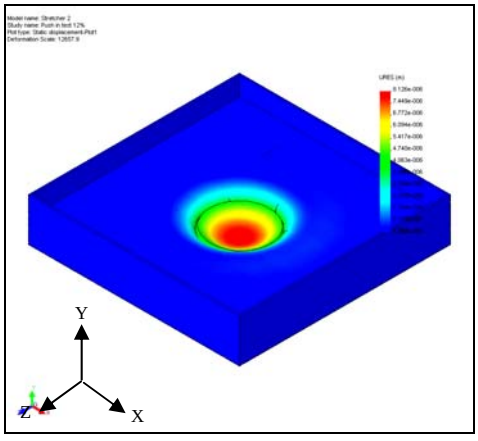

(d) Displacement of CBP on Slope 12 %

Figure 6.5 The displacement of CBP in the simulation (455277 nodes).

Table 6.2: Displacement and horizontal creep results

Slope	Type	Min	Location	Max. Displacement	Max. Horizontal Creep	Location
0 %	URES: Resultant displacement	0 m Node: 74604	(510 mm, 10 mm, 500 mm)	1.811446 mm Node: 120045	0.263242 mm Node: 120045	(-10.838 mm, 125.921 mm, 0.097129 mm)
4 %	URES: Resultant displacement	0 m Node: 74604	(510 mm, 10 mm, 500 mm)	1.811884 mm Node: 120045	0.325741 mm Node: 120045	(-10.838 mm, 125.921 mm, 0.097129 mm)
8 %	URES: Resultant displacement	0 m Node: 74604	(510 mm, 10 mm, 500 mm)	1.812273 mm Node: 120045	0.413583 mm Node: 120045	(-10.838 mm, 125.921 mm, 0.097129 mm)
12 %	URES: Resultant displacement	0 m Node: 74604	(510 mm, 10 mm, 500 mm)	1.812599 mm Node: 120045	0.582025 mm Node: 120045	(-10.838 mm, 125.921 mm, 0.097129 mm)

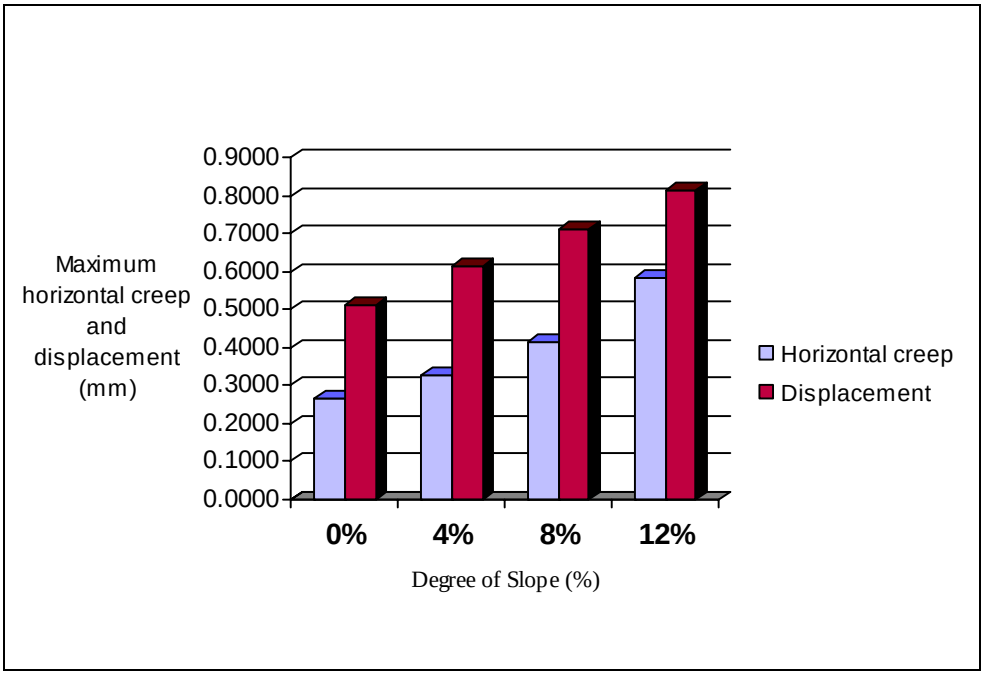

Figure 6.6 The results of displacement and horizontal creep finite element model on various slopes

6.5.2 Strain

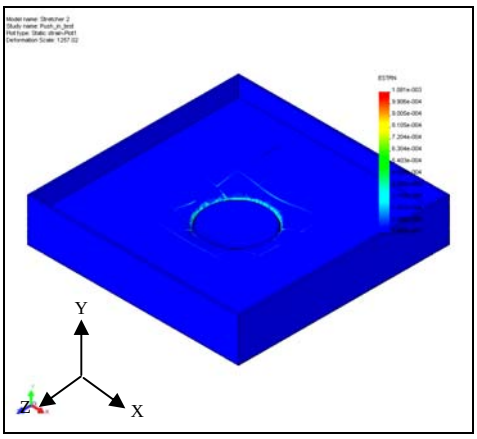

(a) Strain of CBP on Slope 0 %

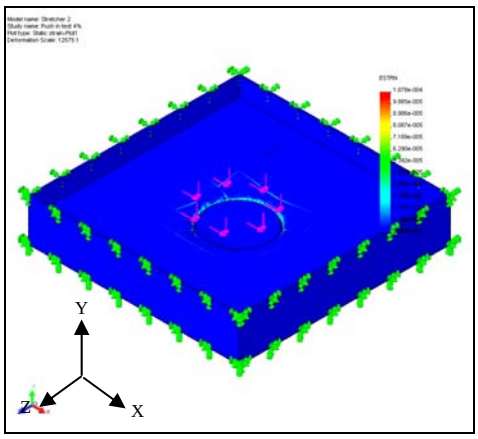

(b) Strain of CBP on Slope 4 %

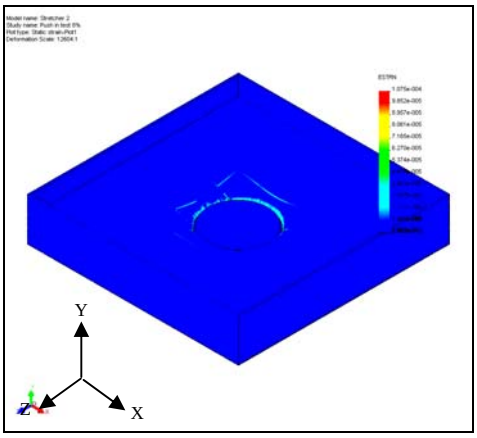

(c) Strain of CBP on Slope 8 %

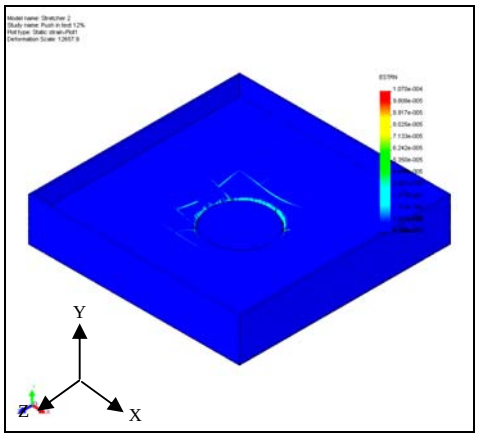

(d) Strain of CBP on Slope 12 %

Figure 6.7 Strain of CBP in the simulation (455277 nodes).

Table 6.3: Strain results

Slope	Type	Min	Location	Max	Location
0 %	ESTRN : Equivalent strain	2.68256e-012 Element: 170547	(491.287 mm, 206.25 mm, 502.5 mm)	0.000106999 Element: 234094	(19.7308 mm, 58.4109 mm, 18.9279 mm)
4 %	ESTRN : Equivalent strain	2.85803e-012 Element: 170233	(505.515 mm, 206.429 mm, 501.985 mm)	0.00010748 Element: 234094	(19.7308 mm, 58.4109 mm, 18.9279 mm)
8 %	ESTRN : Equivalent strain	2.9816e-012 Element: 171682	(508.015 mm, 206.429 mm, 504.485 mm)	0.000107831 Element: 234094	(19.7308 mm, 58.4109 mm, 18.9279 mm)
12 %	ESTRN : Equivalent strain	4.20765e-012 Element: 170547	(491.287 mm, 206.25 mm, 502.5 mm)	0.00108064 Element: 234094	(19.7308 mm, 58.4109 mm, 18.9279 mm)

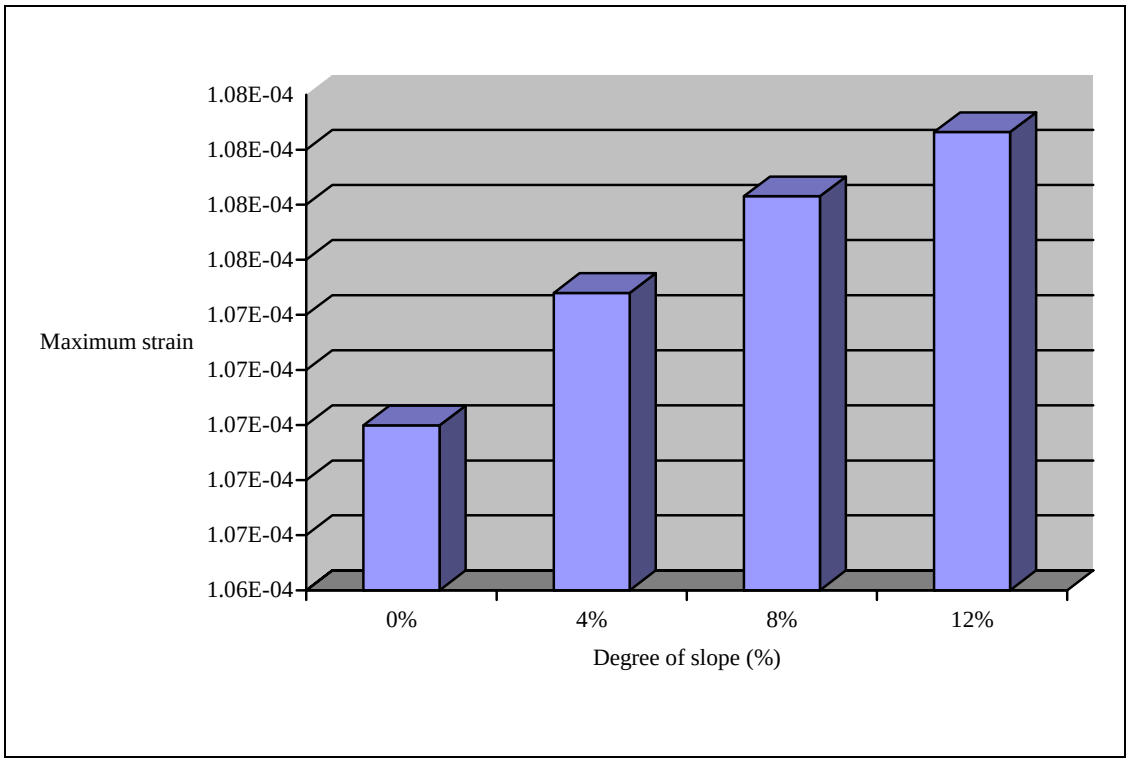

Figure 6.8 The results of strain finite element model on various slopes

6.5.3 Stress

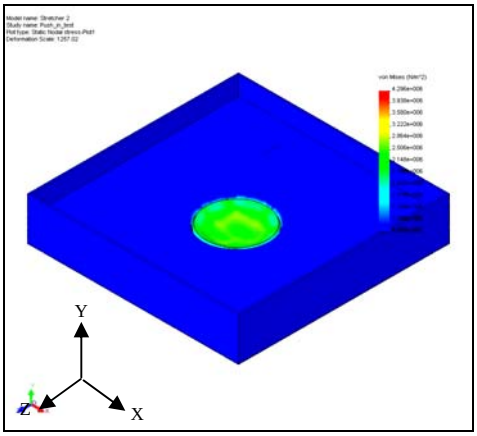

(a) Stress of CBP on Slope 0 %

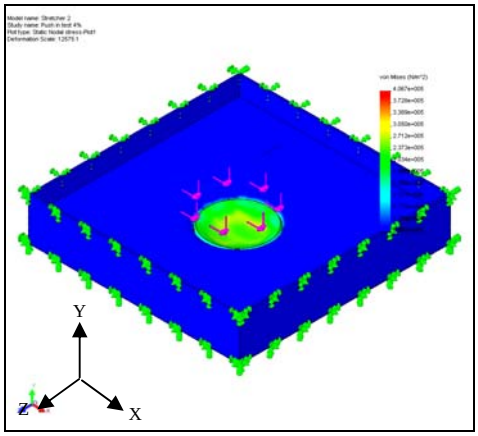

(b) Stress of CBP on Slope 4 %

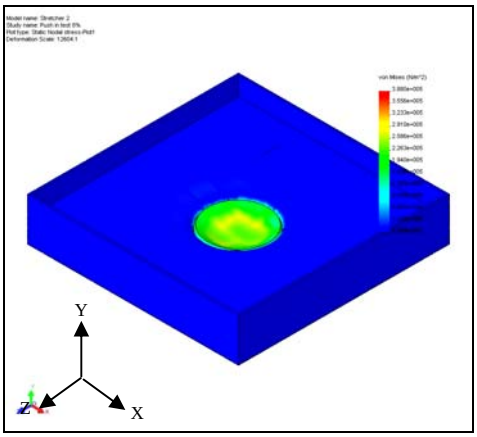

(c) Stress of CBP on Slope 8 %

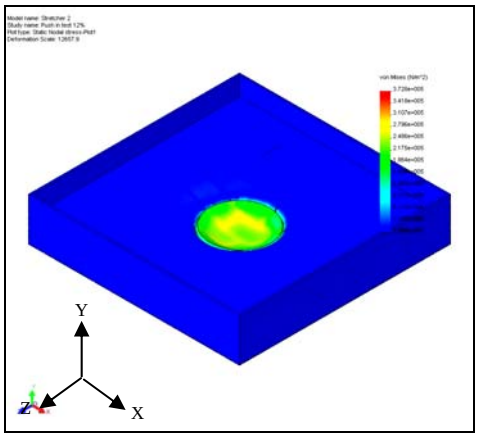

(d) Stress of CBP on Slope 12 %

Figure 6.9 Stress of CBP in the simulation (455277 nodes).

Table 6.4: Stress results

Slope	Type	Min	Location	Max	Location
0 %	VON: von Misses stress	0.00787986 N/m^2 Node: 73177	(480.545 mm, 66.6963 mm, 483.721 mm)	3.72842e+05 N/m^2 Node: 121523	(-96.6129 mm, 120 mm, 122.834 mm)
4 %	VON: von Misses stress	0.00680915 N/m^2 Node: 73177	(480.545 mm, 66.6963 mm, 483.721 mm)	3.87955e+05 N/m^2 Node: 121523	(-96.6129 mm, 120 mm, 122.834 mm)
8 %	VON: von Misses stress	0.0058612 N/m^2 Node: 73177	(480.545 mm, 66.6963 mm, 483.721 mm)	4.06725e+05 N/m^2 Node: 121523	(-96.6129 mm, 120 mm, 122.834 mm)
12 %	VON: von Misses stress	0.0495464 N/m^2 Node: 73177	(480.545 mm, 66.6963 mm, 483.721 mm)	4.29577e+05 N/m^2 Node: 121523	(-96.6129 mm, 120 mm, 122.834 mm)

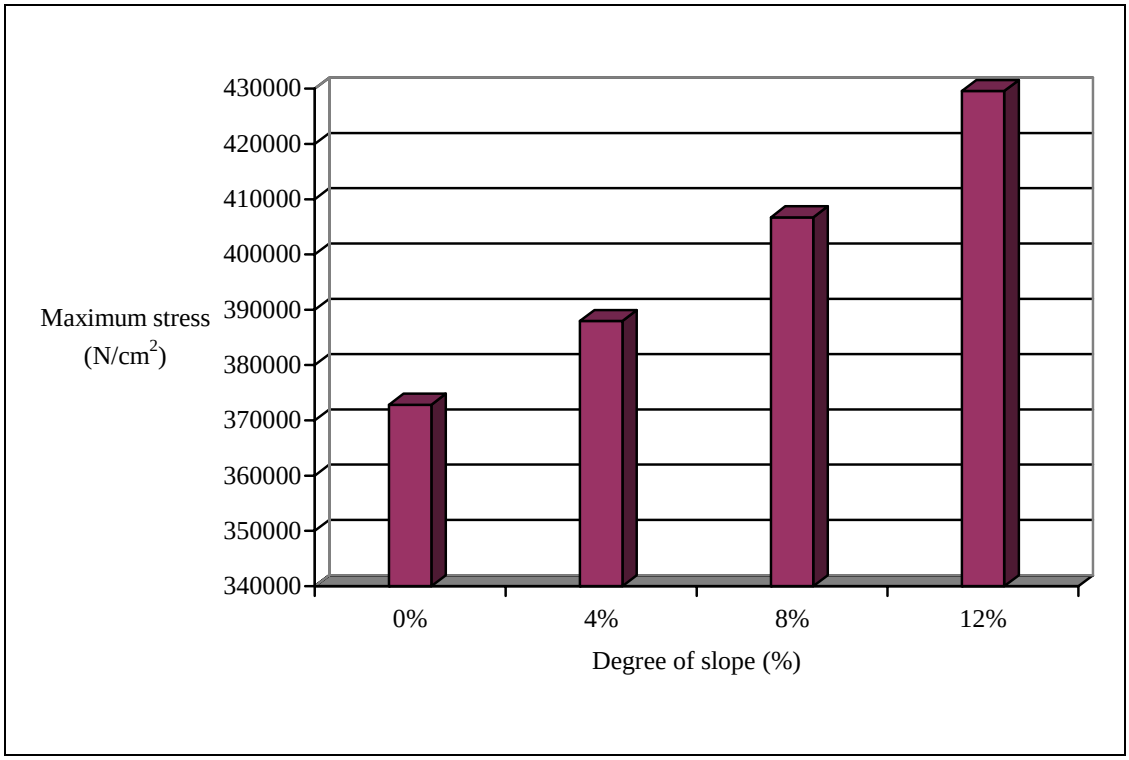

Figure 6.10 The results of strain finite element model on various slopes

6.6 Conclusions

In this study, a 3DFEM model was applied to concrete block pavements to investigate the performance behaviours of the pavements. In order to create complicated meshes in the block layer with various laying patterns, a pre-processor with a user interface was developed, which allows users to specify various features of a block pavement and generates a mesh for the pavement without time consuming data handling relating to meshing of 3DFEM. A 3DFEM solver computes deflections, stresses and strains in CBP. The results are displayed graphically on a window of a post-processor.

Using the tool, the effect of the block thickness, laying pattern, stiffness of joint and bedding sand on deflection, stress and strain in pavements were investigated. As a result, the following conclusions can be made:

a. The bending stresses in the block and base are larger in case of high joint stiffness than those of low joint stiffness. In that case, the block thickness largely affects the stresses.
b. The tensile stress in the base due to bending action is larger in the stretcher laying pattern than in the herringbone laying pattern.
c. There is very little difference in the tensile stress of the bedding sand and the compressive strain of the bedding sand between the herringbone and stretcher patterns.

CHAPTER 7

GENERAL DISUCUSSION

7.1 Introduction

Concrete block pavement (CBP) differs from other forms of pavement in that the wearing surface is made from small paving units bedded and jointed in sand rather than continuous paving. The principal components of a typical block pavement have been illustrated in the Chapter 2, as concrete block, jointing sand, bedding sand, base road, sub-base and sub-grade. In concrete block pavement (CBP), the blocks are a major load-spreading component. The blocks are available in a variety of shapes (as rectangular shape, uni-pave shape, etc). CBP is installed in a number of patterns, such as stretcher bond, herringbone 90^{o}, herringbone 45^{o}, etc. This research presented three dimensional finite element models (3DFEM) to compare the results from tests conducted in the laboratory (See Chapter 6).

7.2 The Behaviour of CBP under Horizontal Force

A block pavement may present various types of mechanical behaviour when submitted to a horizontal force, depending on the blocks shape, as well as on joint width between blocks, the laying pattern and on the direction of the horizontal force relatively to the laying pattern.

The experiments described that the horizontal force test with rectangular block shape and stretcher laying pattern, which is parallel to the continuing lines of the joints, shows that the cohesion of such a plate is near to zero whatever the restraining of the edges. Indeed, for a relatively low value of the applied force, the line of loaded blocks moves monolithically, the friction forces which are the only ones capable of reacting on the continuous lines being too weak to perform this role.

As described, the horizontal force test in herringbone 90^{o} or 45^{o} laying pattern shows that the blocks contribute as a whole to the cohesion of the pavement, the blocks being successively locked by their rotation following their horizontal creep. The herringbone 45^{o} laying pattern is the best interlock than herringbone 90^{o} and stretcher bond. The results obtained are similar to that established by (Shackel 1993, Knapton 1976; Clark 1978; Miura *et al.* 1984).

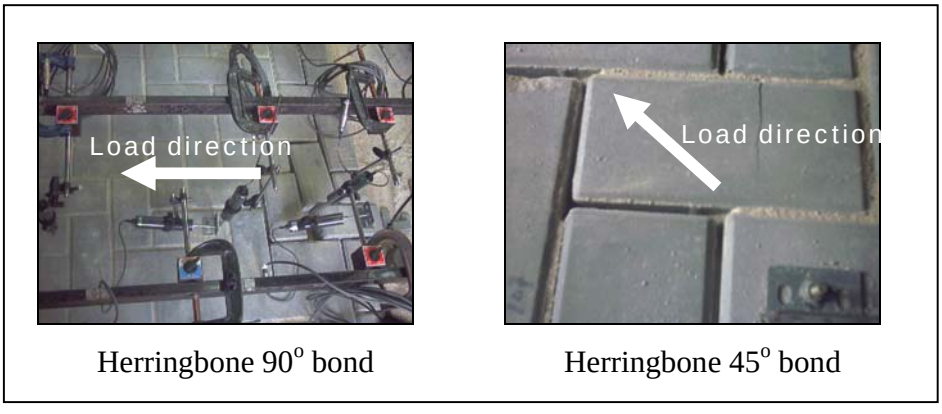

Figure 7.1 The herringbone laying pattern being successively interlock on horizontal creep.

For concrete block pavement with interlocking blocks, in which the horizontal force is parallel to the continuous joint lines, we observe that the joint lines contiguous to the loaded line contribute progressively to the load transfer through an interlocking effect. However this effect induces a lateral movement of the blocks, so that their action stops as soon as the clearance of the joints became too large. If the lateral movement is not possible because of an edge restraint, all the blocks at the plate contribute to the transfer of the horizontal force and the pavement cohesion is then assured.

.

7.3 Load Deflection Behaviour

An interesting observation is that the rate of deflection decreases with increasing load (within the range of magnitude of load considered in this study) rather than increases, which is the case with flexible and rigid pavements. Increase in the load, the rotation of individual blocks increases. This will lead to an increase in the translation of blocks and in turn an increase in the thrusting action between adjacent blocks at hinging points. As a result, the rate of deflection of the pavement decreases. It is established that the load-distributing ability of a concrete block surface course increases with increasing load. The results obtained are similar to that established in earlier plate load tests by Knapton (1996).

All the design procedures to be discussed depend upon interlock being achieved within the blocks. Interlock can be defined as the inability of a block to move in isolation from its neighbours. Three types of interlock must be achieved by adequate design and construction.

7.3.1 Vertical Interlock

If a vertical load were applied to a block without vertical interlock, that block would slide down vertically between its neighbours, placing high vertical stress into the underlying course. Vertical interlock is achieved by vibrating the blocks into a well graded sharp sand during construction. This induces the sand particles to rise 25 mm into the gaps between the blocks. These gaps are from zero to 7 mm. The well graded sand has particles from almost zero to 2.36 mm. Therefore, in any position around the perimeter of a block, particles of sand wedge between neighbouring blocks so allowing a vertically loaded block to transfer its load to its neighbour through shear. These findings are similar to those observed by Knapton and O'Grady (1983) and contradictory to those reported by Shackel (1980). Knapton and O'Grady (1983) have found coarse sand to be suitable for use in joints. Shackel (1980) had observed an improvement in pavement performance using finer sand in joints.

7.3.2 Rotational Interlock

A vertical load applied asymmetrically to a block tries to rotate that block. In order for an individual block to rotate, it must displace its neighbours laterally. Therefore, if the neighbouring blocks are prevented from moving laterally by edge restraint, an individual block is prevented from rotating and rotational interlock is achieved. Evidence also exists to support the theory that fine round sand brushed into the surface also helps to induce rotational interlock.

For the test pavement without edge restraint, block rotation and translation occurred under loading. Deflections were measured on the top face (at two of its opposite edges) of one block to assess the rotations of block. The block was situated adjacent to the edge restraint in the middle row.

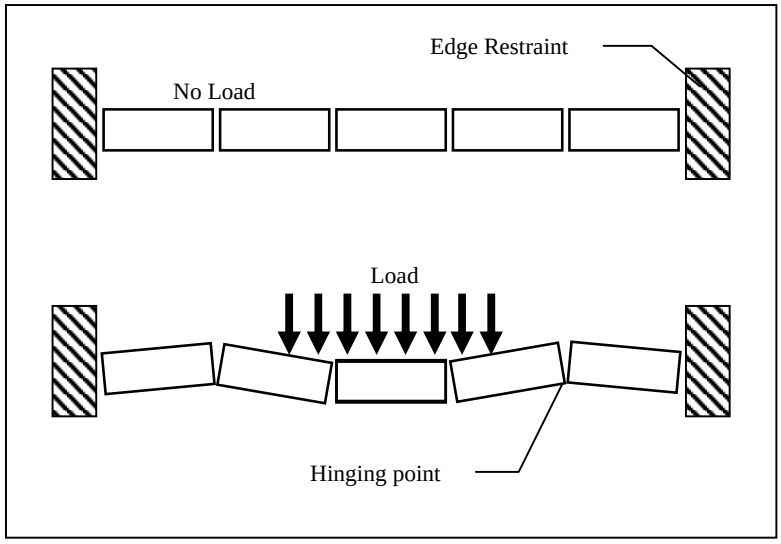

Figure 7. 2 Deflected shape of pavement with edge restraint

For the test pavement with edge restraint, rotation and translation of blocks are limited to the point that was impractical to measure. Block rotations are generally associated with following mechanisms of shear stress in the joints between loaded block and adjacent blocks causes rotation of adjacent blocks. The vertical load covering partially on a block tries to rotate that block. The blocks are rotated themselves to acquire the deflected shape of underlying layers.

7.3.3 Horizontal Interlock

The phenomenon of creep was observed in preview research, particularly when rectangular blocks were laid in stretcher bond laying pattern with their longer axis transverse to the principal direction of traffic. Horizontal braking and accelerating force

move blocks along the line of the road and eventually the blocks impart high local tensile stress into the next row. This phenomenon can be eliminated by using a shaped block or by using a rectangular block laid in a herringbone laying pattern. Although creep can not be totally eliminated at severe braking location, its effect can be reduced to a level whereby breakage is eliminated and there is no visual consequence.

The horizontal expansion is prevented by edge restraint. As a result, the block translation will lead to compression of the jointing sand and thus to buildup of the joint stresses. These joint stresses prevent the blocks from undergoing excessive relative rotations and translations and transmit part of the load to adjacent blocks. The block layer assumes a final form as shown in Figure 7.2 above. A number of blocks participate through hinging points to share the external load. Thus, the deflection of pavement is less for the pavement with edge restraint.

7.4 The Behaviour of CBP on Sloping Road Section

The construction of roads on steep slopes poses particularly interesting challenges for road engineers. The horizontal (inclined) forces exerted on the road surface are severely increased due to traffic accelerating (uphill), braking (downhill) or turning. These horizontal forces cause distress in most conventional pavements, resulting in rutting and poor riding quality. Experience has shown that concrete block pavement (CBP) performs well under such severe conditions. Although CBP performs well on steep slopes, there are certain considerations that must be taken into account during the design and construction of the pavement: The construction of concrete block pavement (CBP) on sloping road section that influences of degree of slope, laying pattern, blocks shape, blocks thickness, joint width between blocks, bedding sand thickness to define the spacing of anchor beam.

7.4.1 The Effect of Bedding Sand Thickness

The most commonly specified thickness for the bedding sand thickness has been 50 mm after compaction. A result, the bedding sand thickness was a major contributor to restraint the rutting. Thus, after compaction, the layer thickness will be 30 to 40 mm. The tolerance on the sub-base surface level is 15 ± mm. where better tolerances are achieved the thickness may be reduced to 20 mm but in no circumstances is to be less than 15 mm thick.

Knapton (1996) have reported that, in a block pavement subjected to truck traffic, a significant proportion of the initial deformation occurred in the bedding sand layer which had a compacted thickness of 40 mm. similar results have been reported by Shackel (1990). These investigations tend to confirm the findings of the earlier Australian study which demonstrated that a reduction in the loose thickness of the bedding sand from 50 mm to 30 mm was beneficial to the deformation (rutting) behaviour of block pavements. Here an almost fourfold reduction in deformation was observed. Experience gained in more than twenty five HVS trafficking tests of prototype block pavements in South Africa has confirmed that there is no necessity to employ bedding sand thickness greater than 30 mm in the loose (initial) condition which yields a compacted typically close to 20 mm.

The role of the laying course or bedding sand has been discussed, a number of main functions are: to fill the lower part of the joint spaces between adjacent blocks in order to develop interlock, to provide uniform support for the blocks and to avoid stress concentrations which could cause damage to the blocks, to provide an even surface on which to lay the blocks, to accommodate the manufacturing tolerances in block thickness and to accommodate accepted tolerances in sub-base surface level. The effect of bedding sand thickness on sloping road section is very important, as shown in Figure 7.3.

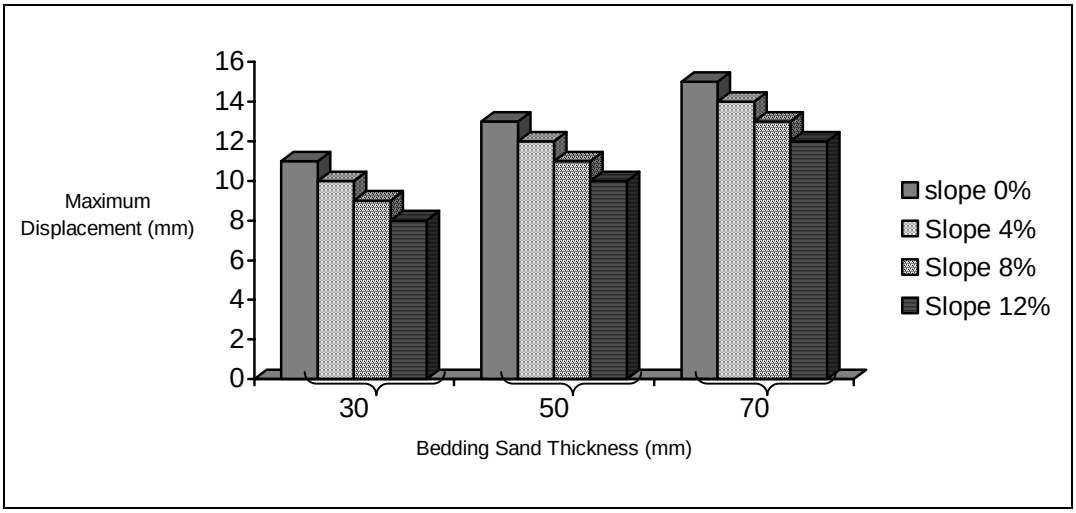

Figure 7.3 Relationship between bedding sand thickness with maximum displacement

7.4.2 The Effect of Block Thickness

Rectangular blocks of the same plan dimension with 60 mm and 100 mm different thickness were selected for testing. Blocks were laid in a stretcher bond laying pattern for each test. The shapes of the load deflection paths are similar for all block thicknesses. A change in thickness from 60 to 100 mm significantly reduces the elastic deflection of pavement. Thicker blocks provide a higher frictional area. Thus, load transfer will be high for thicker blocks. For thicker blocks, the individual block translation is more with the same amount of block rotation. As a result, the back thrust from edge restraint will be more. The thrusting action between adjacent blocks at hinging points is more effective with thicker blocks. Thus, deflections are much less for thicker blocks. The combined effect of higher friction area and higher thrusting action for thicker blocks provides more efficient load transfer. Thus, there is a significant change in deflection values from increasing the thickness of blocks. It is concluded that the response of the pavement is highly influenced by block thickness. The results obtained are similar to that found in earlier plate load tests by Shackel *et al*.(1993).

7.4.3 The Effect of Joint Width

The width of joints in block paving is more important than that perhaps been realized in the past. A serious disadvantage of pavements laid in this way is that joints of less than 2 mm in width often contain little of no jointing sand. This would obviously reduce the contribution of individual blocks to the structural properties of the pavement. Width use the individual blocks move is relation to one another which results in spelling of the edges. Although this is not structurally damaging, the overall appearance of the pavement is less desirable and the small piece of broken corners could cause problems if not swept away.

Blocks laid to a poor standard were seen where joint widths of more than 5 mm were common. The amount of sand required to fill the joints was too great to allow intimacy between blocks forming the joint to develop. The shear strength of the jointing sand would be the limiting factor in the structure of the pavement. The increase of joint width between blocks and degree of slope, decrease the friction resistant between blocks. Thus, the result is an increase of the displacement.

The optimum joint width between blocks is 3 mm. For joint widths less than the optimum, the jointing sand was unable to enter inside between blocks. A large amount of sand remained outside the joint showing sand heaps on the block surface.

7.4.4 The Effect of Block Shape

Two shapes of blocks were selected for study. These were rectangular shape and uni-pave shape. These block types have the same thickness and nearly same plan area.

Blocks were laid in stretcher bond for push-in test and laid in stretcher bond, herringbone 90^{o} and herringbone 45^{o} for horizontal force test. The smallest deflections are observed for rectangular shape and uni-pave shape, whereas the highest deflections are associated with uni-pave block shape. In general, uni-pave shaped (dents) blocks exhibited smaller deformations as compared with rectangular and square blocks. Complex shape blocks have larger vertical surface areas than rectangular or square blocks of the same plan area. Consequently, shaped blocks have larger frictional areas for load transfer to adjacent blocks. The friction area for uni-pave block shape is more than rectangular shape. It is concluded that the shape of the block influences the performance of the block pavement under load. It is postulated that the effectiveness of load transfer depends on the vertical surface area of the blocks. These results obtained are consistent with those found in earlier plate load tests by Shackel *et al.* (1993).

7.4.5 The Effect of Laying Pattern

Rectangular and uni-pave blocks shapes were tested in the horizontal force test. Each CBP sample tested in three laying patterns i.e. stretcher bond, herringbone 90^{o} bond and herringbone 45^{o} bond (Figure 2.5). The results show that horizontal creep is highest in stretcher laying pattern, almost 40 % more than laid in herringbone 90^{o} and 45 – 50 % more than laid in herringbone 45^{o}. (See Figure 7.4)

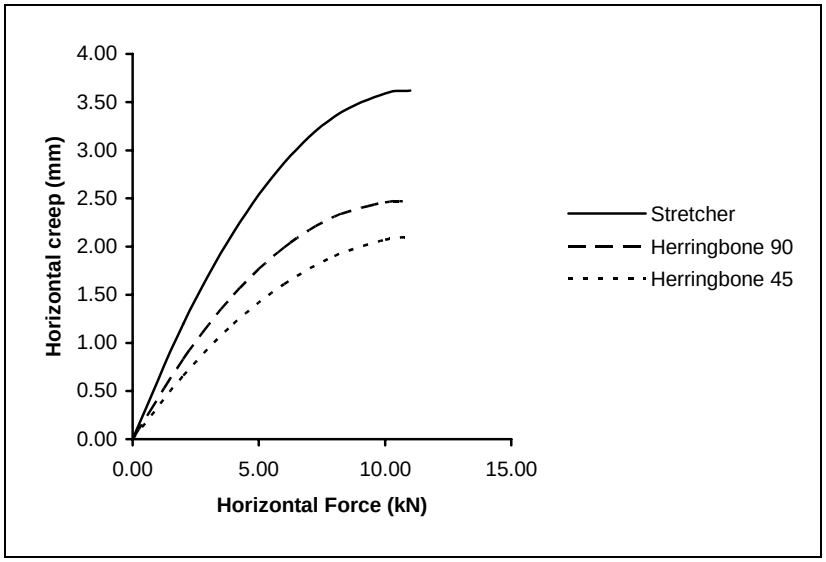

Figure 7.4 The effect of laying pattern in horizontal force test

It is established that horizontal creep of concrete block pavements is dependent on the laying pattern in the pavement. The finding is contradictive with that reported by Panda *et al*. (2002).

7.5 Comparison of Experimental Results and Finite Element Modelling

In the experimental tests reported in Chapter 4, the value of displacement and horizontal creep of CBP was measured. The measurement was conducted used transducers by connected to the data logger. While in the next work using finite element analysis, it is possible to measure the displacement and horizontal creep due to the capabilities of the software to tabulate a result on the model depending on the nodes generated. In this research, the vertical displacement and horizontal creep on several degree of slope was measured as a comparison between the COSMOS Star DESIGN and experimental result.

There are some differences between the experimental result and the COSMOS Star DESIGN result. The biggest percentage of different between the experimental data with COSMOS Star DESIGN analysis was 25.41 % for the vertical displacement reading and 14.13 % for the horizontal creep reading. The results as shown in the Table 7.1

Table 7.1 The comparison result of experimental in laboratory with FEM analysis

Slope	Experimental Max. Displacement	Experimental Max. Horizontal Creep	FEM Max. Displacement	FEM Max. Horizontal Creep	Different of Displacement Experimental with FEM	Different of Hz Creep Experimental with FEM
0 %	2.27 mm	0.28 mm	1.811446 mm	0.263242 mm	20.20 %	5.98 %
4 %	2.33 mm	0.36 mm	1.811884 mm	0.325741 mm	22.24 %	9.28 %
8 %	2.40 mm	0.47 mm	1.812273 mm	0.413583 mm	24.49 %	12.28 %
12 %	2.43 mm	0.68 mm	1.812599 mm	0.582025 mm	25.41 %	14.13 %

The difference might be due to the fact that in this research, the vertical displacement and horizontal creep in finite element model obtained using the material properties packages in software whereas the experimental results were obtained with presence material. The experimental in laboratory is not solid 100 %, for the example filling of jointing sand, width of joint, block thickness act. Otherwise, the finite element modelling obtained using the SOLID Works and COSMOS Star DESIGN software, so the optimum meshing may generate more accurate than experimental in laboratory reality.

CHAPTER 8

CONCLUSION

8.1 Introduction

This chapter discusses the conclusions on the concrete block pavement (CBP) for sloping road section in relation to performance of CBP deformation (horizontal creep and vertical displacement) that is affected by bedding sand thickness, laying pattern, block thickness, block shape and joint width between blocks.

8.2 Conclusions

The experimental work performed in this study leads to the following applicable conclusions:

- The joints in between blocks should be properly filled with sand. The optimum joint width between blocks is 3 mm. For joint widths less than the optimum, the jointing sand was unable to enter between blocks. A large amount of sand remained outside the joint showing sand heaps on the block surface.

- A block pavement may present various types of mechanical behaviour when submitted to a horizontal force, depending on the blocks shape, as well as on joint width between blocks, the laying pattern and on the direction of the horizontal force relative to the laying pattern.

- The horizontal force test with rectangular block shape and stretcher laying pattern, which is parallel to the continuing lines of the joints, shows that the cohesion of such a plate is near to zero whatever the restraining of the edges. Indeed, for a relatively low value of the applied force, the line of loaded blocks moves monolithically, the friction forces which are the only ones capable of reacting on the continuous lines being too weak to perform this role.

- To define the spacing of anchor beam of CBP on sloping road section, factors as degree of slope, joint width between blocks, laying pattern, blocks shape, blocks thickness, bedding sand thickness should be included.
  - The increase of degree of slope will cause shorter spacing of anchor beam.
  - The increase of joint width between blocks will cause shorter spacing of the anchor beam.
  - The herringbone 45^{o} is the best laying pattern compared with herringbone 90^{o} and stretcher bond to restraint the horizontal force. It was indicated that the spacing of anchor beam would be longer.
  - The uni-pave block shape has more restraint of horizontal creep than rectangular block shape, because uni-pave block shape has gear (four-dents), while rectangular block shape no gear (no dents), so the spacing of anchor beam has a difference of about 10 m.
  - A change in thickness from 60 to 100 mm significantly reduces the elastic deflection of pavement. Thicker blocks provide a higher frictional area. Thus, load transfer will be high for thicker blocks. For thicker blocks, the individual block translation is more with the same amount of block rotation. The increase of block thickness will cause longer spacing of anchor beam.

  - The role of the bedding sand is very important, a number of main functions are: to fill the lower part of the joint spaces between adjacent blocks in order to develop interlock, to provide uniform support for the blocks and to avoid stress concentrations which could cause damage to the blocks, to provide an even surface on which to lay the blocks, to accommodate the manufacturing tolerances in block thickness and to accommodate accepted tolerances in sub-base surface level. The increase of bedding sand thickness will cause shorter spacing of anchor beam.

- The biggest percentage differences between experimental data reading with finite element model analysis was 25.41 % for vertical displacement and 14.13 % for horizontal creep.

8.3 Recommendations

- Stretcher bond is suited to pedestrian areas and very lightly trafficked areas not subjected to regular turning movements or frequent braking or acceleration. Block rows should be laid at right angles to traffic flow.

- Herringbone laying patterns are suitable for all applications. Either 90° or 45° Herringbone pattern oriented to the longest straight edge should be used with vehicular areas. This reduces the incidence of creep and distributes wheel loads more evenly to the underlying pavement construction.

- The shape of the load deflection path is similar for two block types. The deflections are essentially the same for rectangular shape and uni-pave shape. The small deflections observed for uni-pave shape are less compared to the rectangular shape.

In general, shaped (dented) blocks exhibited smaller deformations as compared to rectangular and square blocks. Complex shape (uni-pave) blocks have larger vertical surface areas than rectangular or square blocks of the same plan area.

The results of horizontal creep on push-in test with load position 40 cm, 60 cm and 80 cm from edge restraint

No	Block Shape	Block thick. (mm)	Bedding sand thick.(mm)	Joint width (mm)	Slope (%)	Equation
1	Rectangular	60	30	3	0	$Y = -0.0009x^2 + 0.0868x$
2	Rectangular	60	50	3	0	$Y = -0.0011x^2 + 0.0994x$
3	Rectangular	60	70	3	0	$Y = -0.0013x^2 + 0.1212x$
4	Rectangular	60	30	5	0	$Y = -0.001x^2 + 0.09x$
5	Rectangular	60	50	5	0	$Y = -0.0012x^2 + 0.1093x$
6	Rectangular	60	70	5	0	$Y = -0.0014x^2 + 0.1282x$
7	Rectangular	60	30	7	0	$Y = -0.0011x^2 + 0.0964x$
8	Rectangular	60	50	7	0	$Y = -0.0012x^2 + 0.1147x$
9	Rectangular	60	70	7	0	$Y = -0.0014x^2 + 1318x$
10	Rectangular	100	30	3	0	$Y = -0.0006x^2 + 0.0595x$
11	Rectangular	100	50	3	0	$Y = -0.0006x^2 + 0.0627x$
12	Rectangular	100	70	3	0	$Y = -0.0007x^2 + 0.0667x$
13	Rectangular	100	30	5	0	$Y = -0.0006x^2 + 0.0556x$
14	Rectangular	100	50	5	0	$Y = -0.0006x^2 + 0.0618x$

15	Rectangular	100	70	5	0	$Y = -0.0007x^2 + 0.0694x$
16	Rectangular	100	30	7	0	$Y = -0.0006x^2 + 0.0563x$
17	Rectangular	100	50	7	0	$Y = -0.0006x^2 + 0.0646x$
18	Rectangular	100	70	7	0	$Y = -0.0007x^2 + 0.0706x$
19	Rectangular	60	30	3	4	$Y = -0.0009x^2 + 0.0816x + 0.0484$
20	Rectangular	60	50	3	4	$Y = -0.001.x^2 + 0.0948x + 0.0493$
21	Rectangular	60	70	3	4	$Y = -0.0012x^2 + 0.1161x + 0.0396$
22	Rectangular	60	30	5	4	$Y = -0.0009x^2 + 0.0859x + 0.0503$
23	Rectangular	60	50	5	4	$Y = -0.0011x^2 + 0.1046x + 0.0463$
24	Rectangular	60	70	5	4	$Y = -0.0013x^2 + 0.1234x + 0.0512$
25	Rectangular	60	30	7	4	$Y = -0.001x^2 + 0.0948x + 0.022$
26	Rectangular	60	50	7	4	$Y = -0.0012x^2 + 0.1116x + 0.0386$
27	Rectangular	60	70	7	4	$Y = -0.0013x^2 + 0.1279x + 0.0468$
28	Rectangular	100	30	3	8	$Y = -0.0005x^2 + 0.0509x - 0.0014$
29	Rectangular	100	50	3	8	$Y = -0.0006x^2 + 0.0576x - 0.0024$
30	Rectangular	100	70	3	8	$Y = -0.0007x^2 + 0.0681x - 0.0084$

31	Rectangular	100	30	5	8	$Y = -0.0005x^2 + 0.0533x - 0.0129$
32	Rectangular	100	50	5	8	$Y = -0.0006x^2 + 0.0593x - 0.0044$
33	Rectangular	100	70	5	8	$Y = -0.0007x^2 + 0.0705x - 0.0050$
34	Rectangular	100	30	7	8	$Y = -0.0005x^2 + 0.0545x - 0.0110$
35	Rectangular	100	50	7	8	$Y = -0.0006x^2 + 0653x - 0.0014$
36	Rectangular	100	70	7	8	$Y = -0.0006x^2 + 0.0709x + 0.0005$
37	Uni-pave	60	30	3	12	$Y = 0000.x^2 + 0000.x + 0000$
38	Uni-pave	100	50	5	12	$Y = 0000.x^2 + 0000.x + 0000$
39	Uni-pave	60	70	7	12	$Y = 0000.x^2 + 0000.x + 0000$
40	Uni-pave	100	30	3	12	$Y = 0000.x^2 + 0000.x + 0000$
41	Uni-pave	60	50	5	12	$Y = 0000.x^2 + 0000.x + 0000$
42	Uni-pave	100	70	7	12	$Y = 0000.x^2 + 0000.x + 0000$
43	Uni-pave	60	30	3	12	$Y = 0000.x^2 + 0000.x + 0000$
44	Uni-pave	100	50	5	12	$Y = 0000.x^2 + 0000.x + 0000$
45	Uni-pave	60	70	7	12	$Y = 0000.x^2 + 0000.x + 0000$

Appendix A1
Horizontal Force Test using Rectangular Block Shape

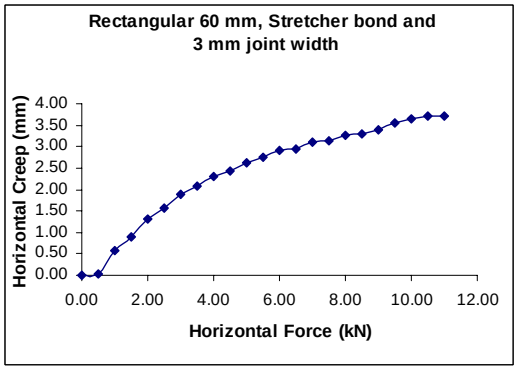

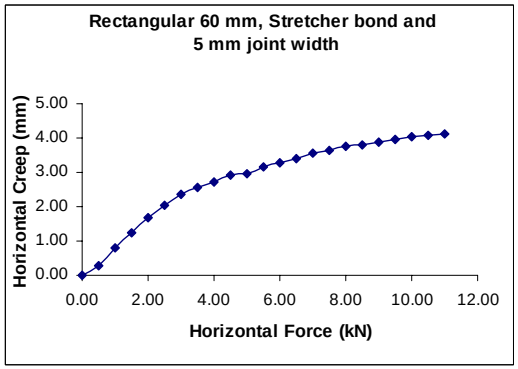

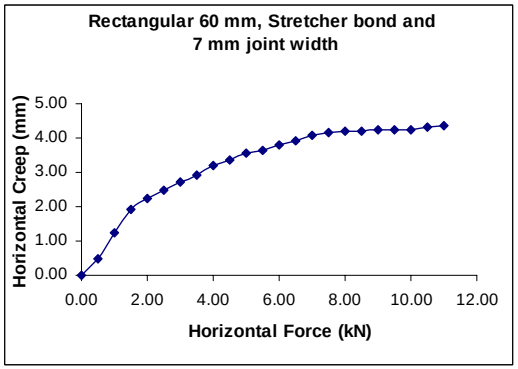

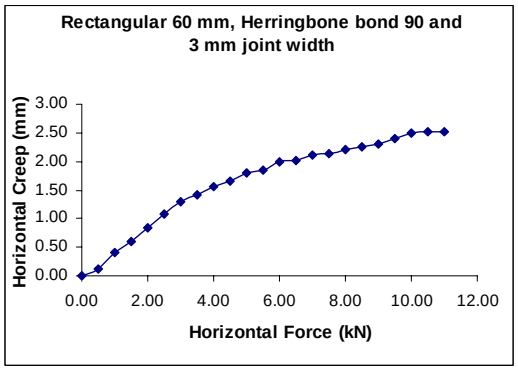

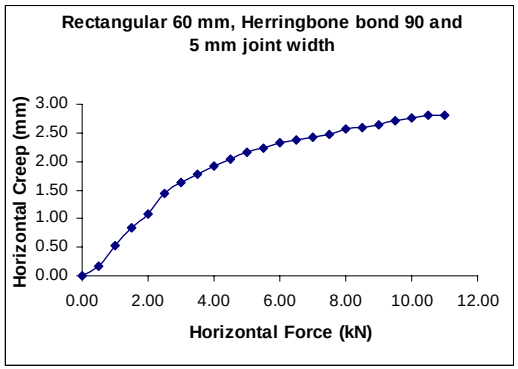

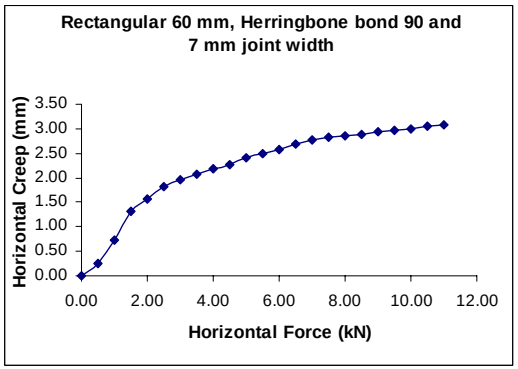

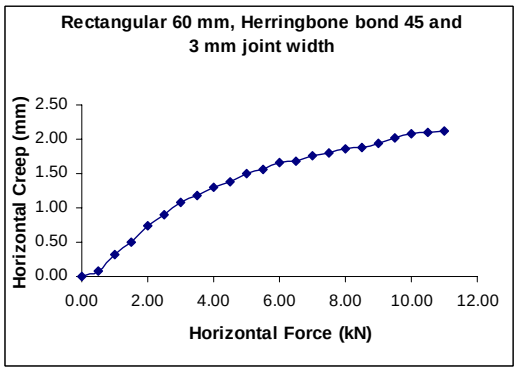

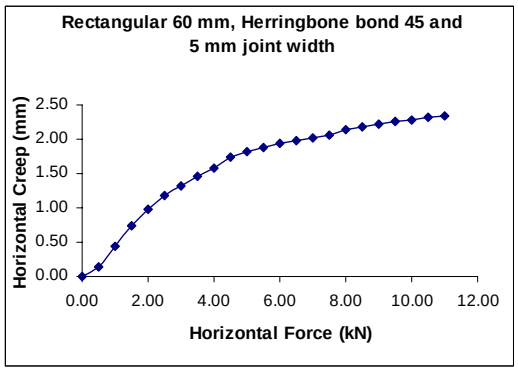

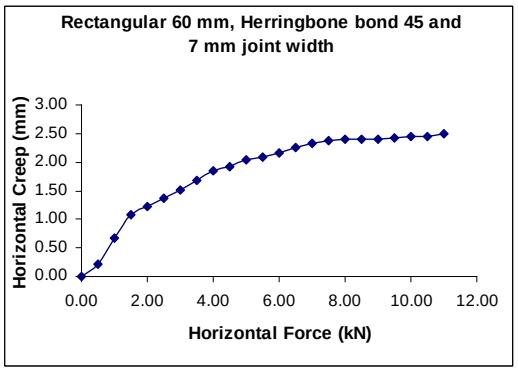

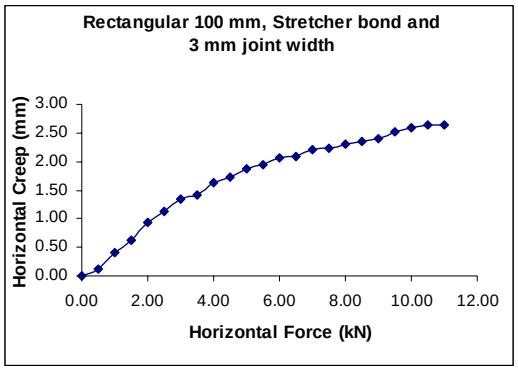
Rectangular 100 mm, Stretcher bond and 3 mm joint width
Horizontal Creep (mm)
3.00
2.50
2.00
1.50
1.00
0.50
0.00
0.00 2.00 4.00 6.00 8.00 10.00 12.00
Horizontal Force (kN)

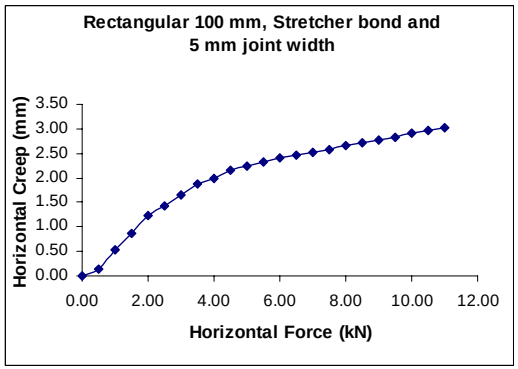
Rectangular 100 mm, Stretcher bond and 5 mm joint width
Horizontal Creep (mm)
3.50
3.00
2.50
2.00
1.50
1.00
0.50
0.00
0.00 2.00 4.00 6.00 8.00 10.00 12.00
Horizontal Force (kN)

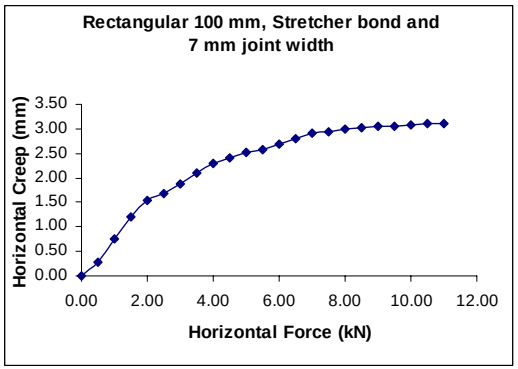
Rectangular 100 mm, Stretcher bond and 7 mm joint width
Horizontal Creep (mm)
3.50
3.00
2.50
2.00
1.50
1.00
0.50
0.00
0.00 2.00 4.00 6.00 8.00 10.00 12.00
Horizontal Force (kN)

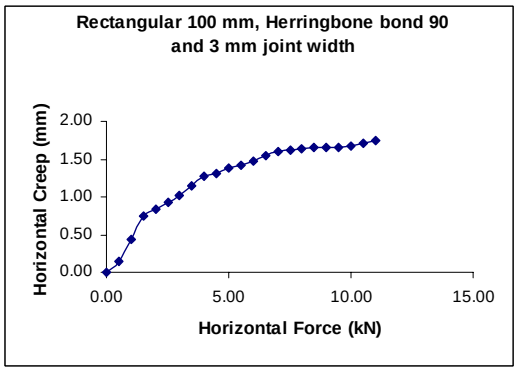
Rectangular 100 mm, Herringbone bond 90 and 3 mm joint width
Horizontal Creep (mm)
2.00
1.50
1.00
0.50
0.00
0.00 5.00 10.00 15.00
Horizontal Force (kN)

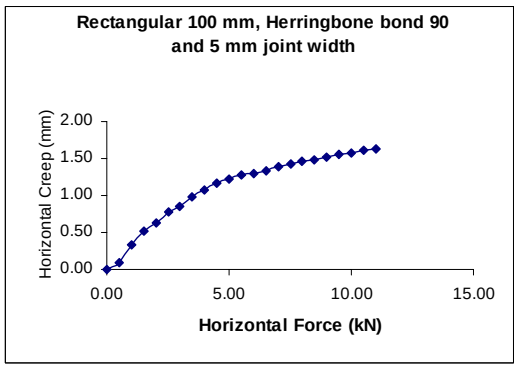
Rectangular 100 mm, Herringbone bond 90 and 5 mm joint width
Horizontal Creep (mm)
2.00
1.50
1.00
0.50
0.00
0.00 5.00 10.00 15.00
Horizontal Force (kN)

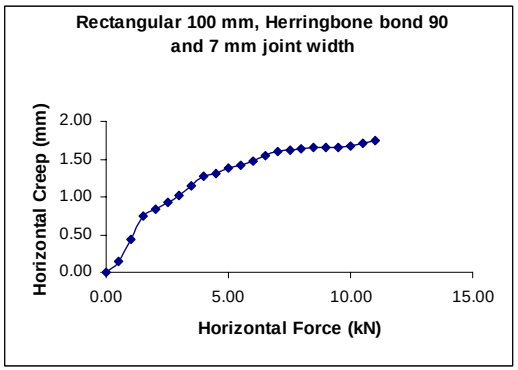
Rectangular 100 mm, Herringbone bond 90 and 7 mm joint width
Horizontal Creep (mm)
2.00
1.50
1.00
0.50
0.00
0.00 5.00 10.00 15.00
Horizontal Force (kN)

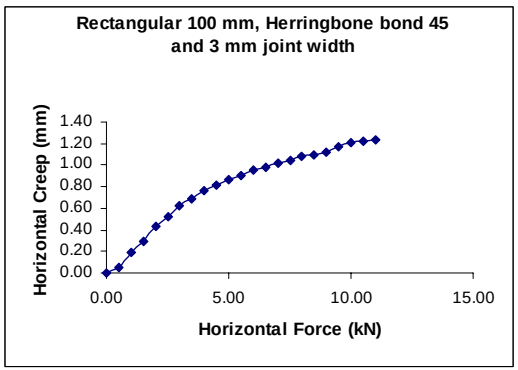
Rectangular 100 mm, Herringbone bond 45 and 3 mm joint width
Horizontal Creep (mm)
1.40
1.20
1.00
0.80
0.60
0.40
0.20
0.00
0.00 5.00 10.00 15.00
Horizontal Force (kN)

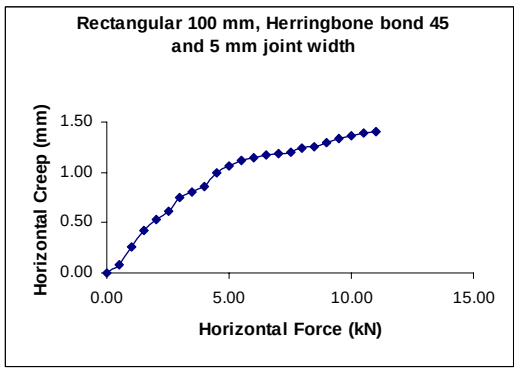
Rectangular 100 mm, Herringbone bond 45 and 5 mm joint width
Horizontal Creep (mm)
1.50
1.00
0.50
0.00
0.00 5.00 10.00 15.00
Horizontal Force (kN)

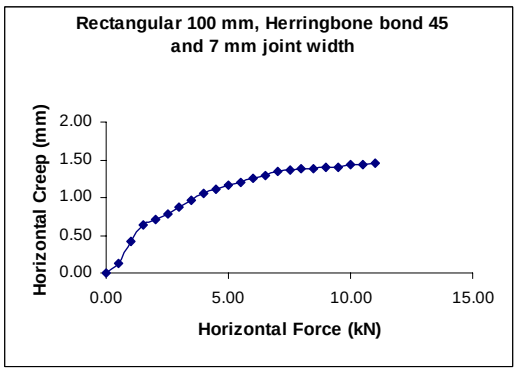
Rectangular 100 mm, Herringbone bond 45 and 7 mm joint width
Horizontal Creep (mm)
2.00
1.50
1.00
0.50
0.00
0.00 5.00 10.00 15.00
Horizontal Force (kN)

Appendix A2
Horizontal Force Test using Uni-pave Block Shape

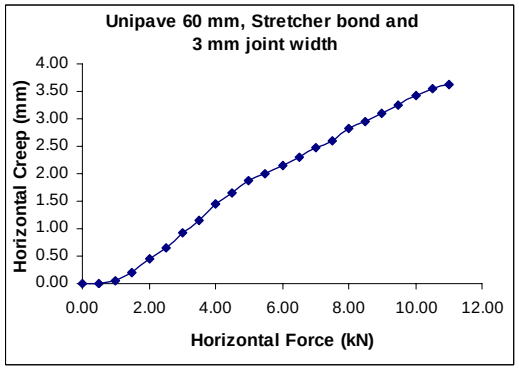

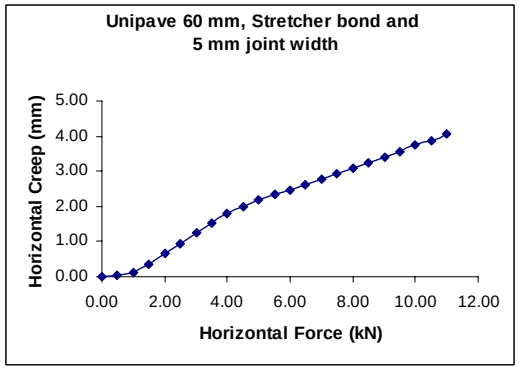

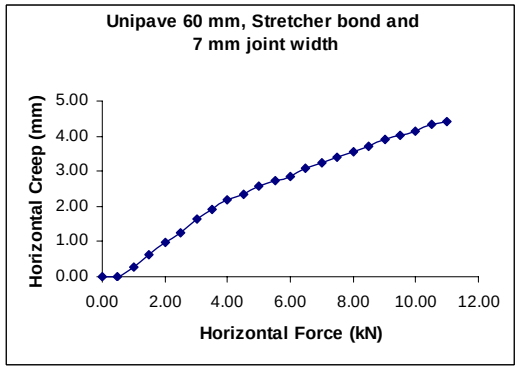

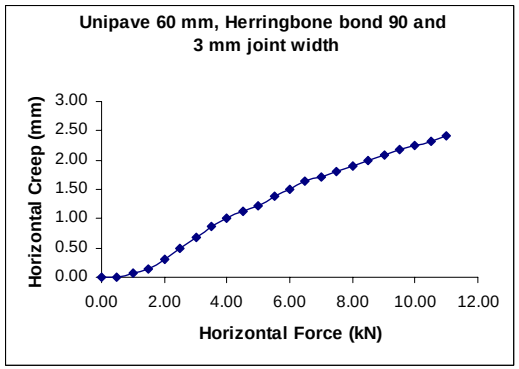

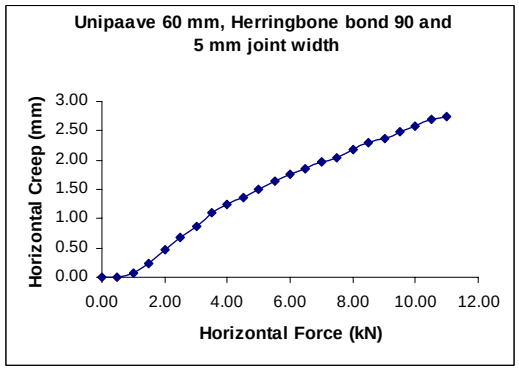

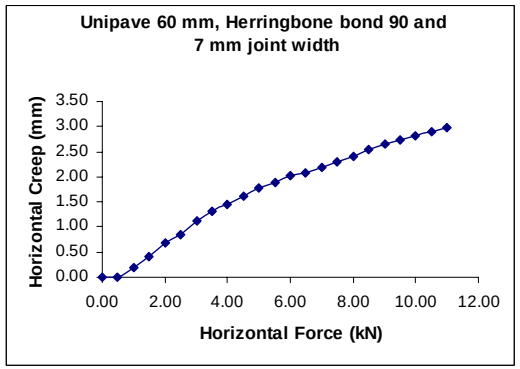

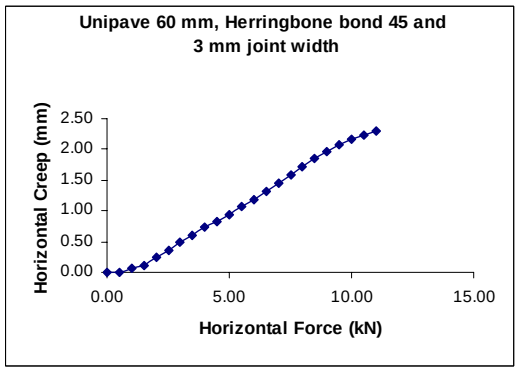

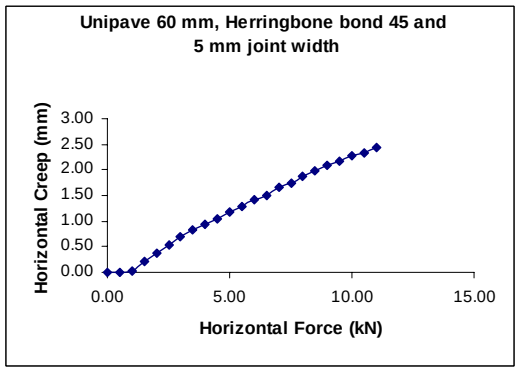

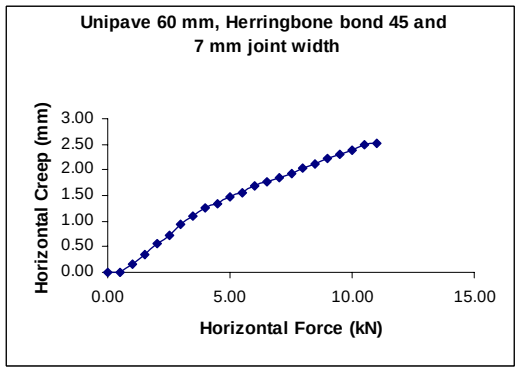

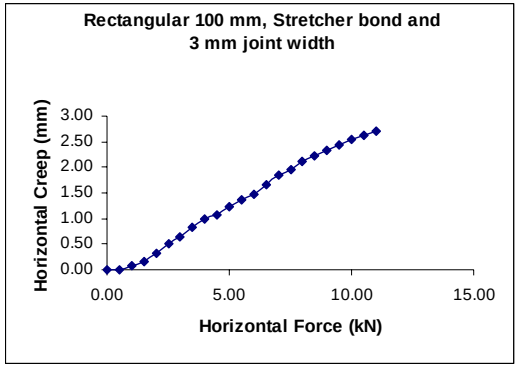
Rectangular 100 mm, Stretcher bond and 3 mm joint width
Horizontal Creep (mm)
3.00
2.50
2.00
1.50
1.00
0.50
0.00
0.00
5.00
10.00
15.00
Horizontal Force (kN)

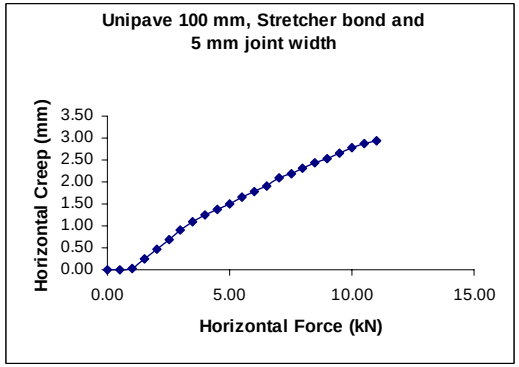
Unipave 100 mm, Stretcher bond and 5 mm joint width
Horizontal Creep (mm)
3.50
3.00
2.50
2.00
1.50
1.00
0.50
0.00
0.00
5.00
10.00
15.00
Horizontal Force (kN)

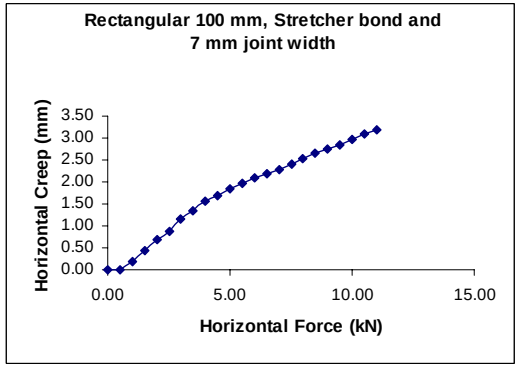
Rectangular 100 mm, Stretcher bond and 7 mm joint width
Horizontal Creep (mm)
3.50
3.00
2.50
2.00
1.50
1.00
0.50
0.00
0.00
5.00
10.00
15.00
Horizontal Force (kN)

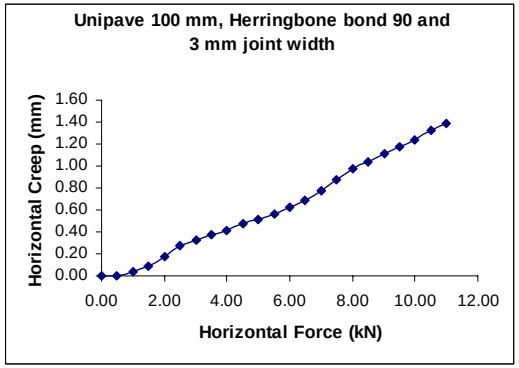
Unipave 100 mm, Herringbone bond 90 and 3 mm joint width
Horizontal Creep (mm)
1.60
1.40
1.20
1.00
0.80
0.60
0.40
0.20
0.00
0.00
2.00
4.00
6.00
8.00
10.00
12.00
Horizontal Force (kN)

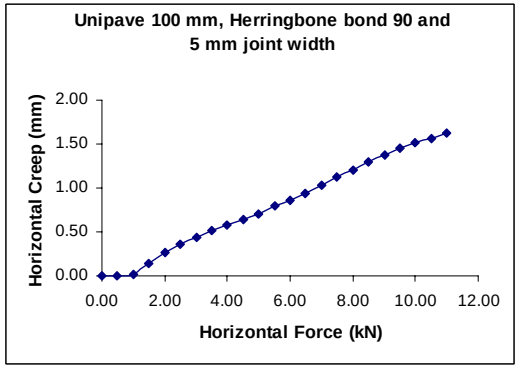
Unipave 100 mm, Herringbone bond 90 and 5 mm joint width
Horizontal Creep (mm)
2.00
1.50
1.00
0.50
0.00
0.00
2.00
4.00
6.00
8.00
10.00
12.00
Horizontal Force (kN)

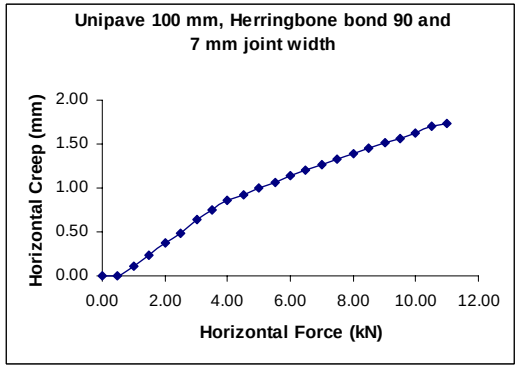
Unipave 100 mm, Herringbone bond 90 and 7 mm joint width
Horizontal Creep (mm)
2.00
1.50
1.00
0.50
0.00
0.00
2.00
4.00
6.00
8.00
10.00
12.00
Horizontal Force (kN)

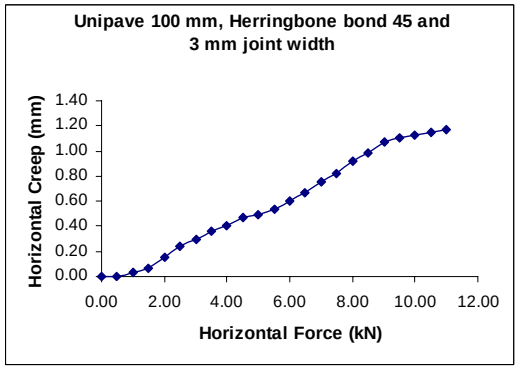
Unipave 100 mm, Herringbone bond 45 and 3 mm joint width
Horizontal Creep (mm)
1.40
1.20
1.00
0.80
0.60
0.40
0.20
0.00
0.00
2.00
4.00
6.00
8.00
10.00
12.00
Horizontal Force (kN)

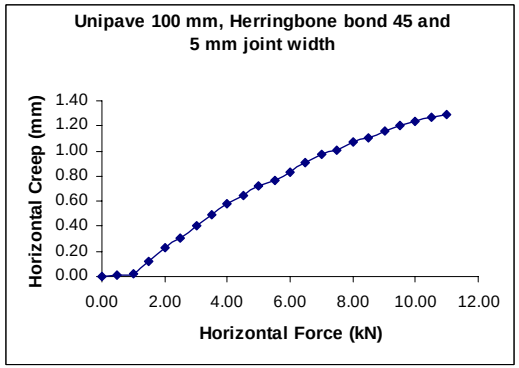
Unipave 100 mm, Herringbone bond 45 and 5 mm joint width
Horizontal Creep (mm)
1.40
1.20
1.00
0.80
0.60
0.40
0.20
0.00
0.00
2.00
4.00
6.00
8.00
10.00
12.00
Horizontal Force (kN)

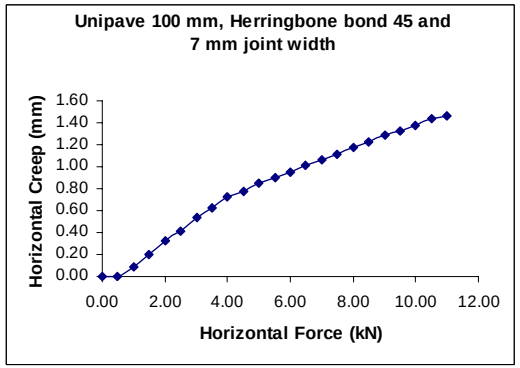
Unipave 100 mm, Herringbone bond 45 and 7 mm joint width
Horizontal Creep (mm)
1.60
1.40
1.20
1.00
0.80
0.60
0.40
0.20
0.00
0.00
2.00
4.00
6.00
8.00
10.00
12.00
Horizontal Force (kN)

APPENDIX – B1

Horizontal Force Test
(The Effect of Laying Pattern by Using Rectangular Block Shape)

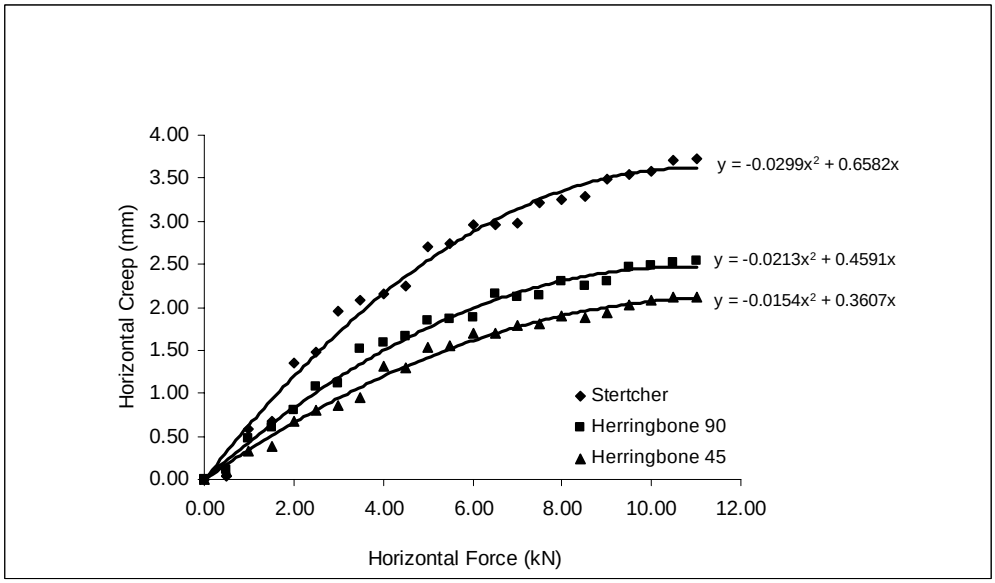

Figure B1.1 CBP specifications: Rectangular shape, 60 mm block thickness and 3 mm joint width.

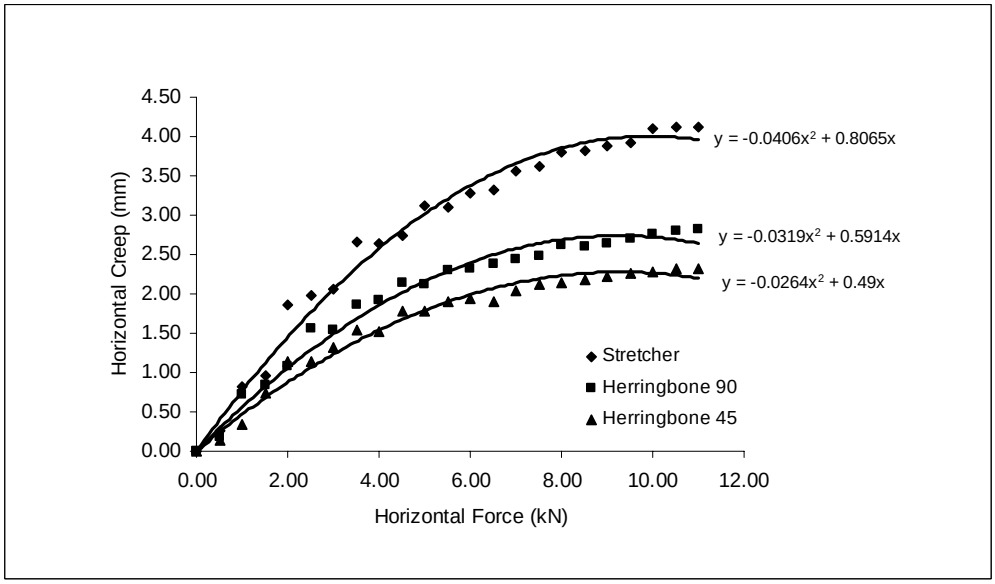

Figure B1.2 CBP specifications: Rectangular shape, 60 mm block thickness and 5 mm joint width.

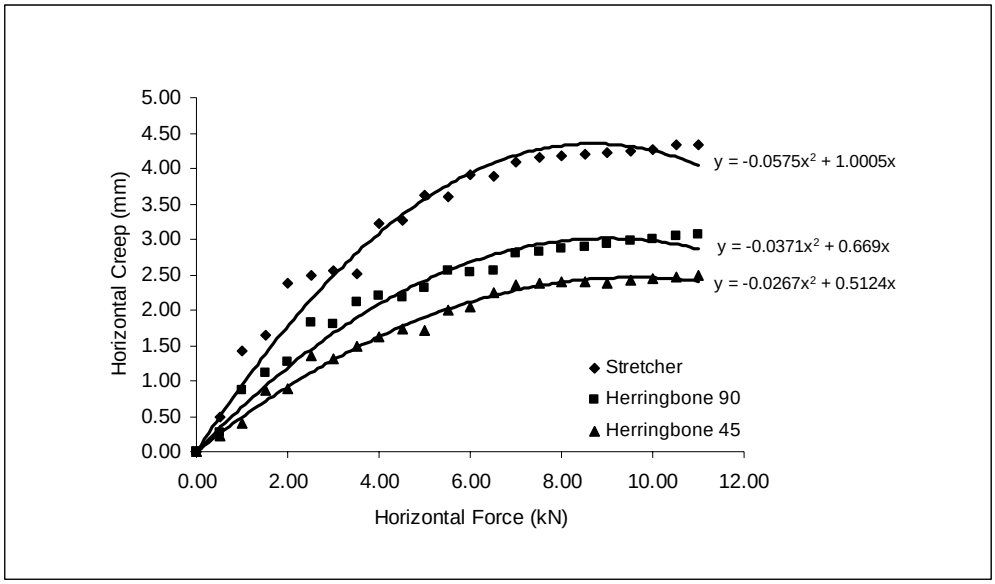

Figure B1.3 CBP specifications: Rectangular shape, 60 mm block thickness and 7 mm joint width.

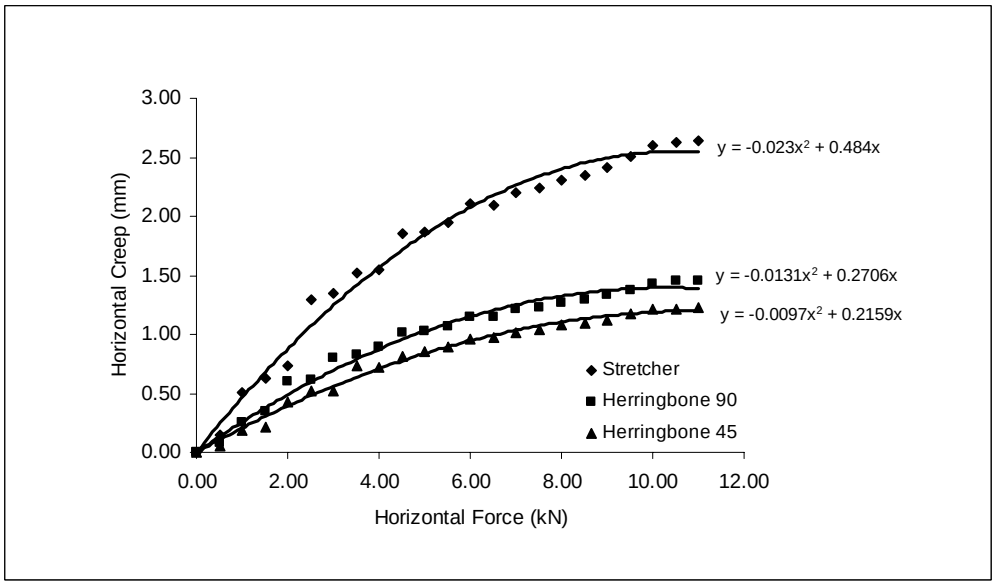

Figure B1.4 CBP specifications: Rectangular shape, 100 mm block thickness and 3 mm joint width.

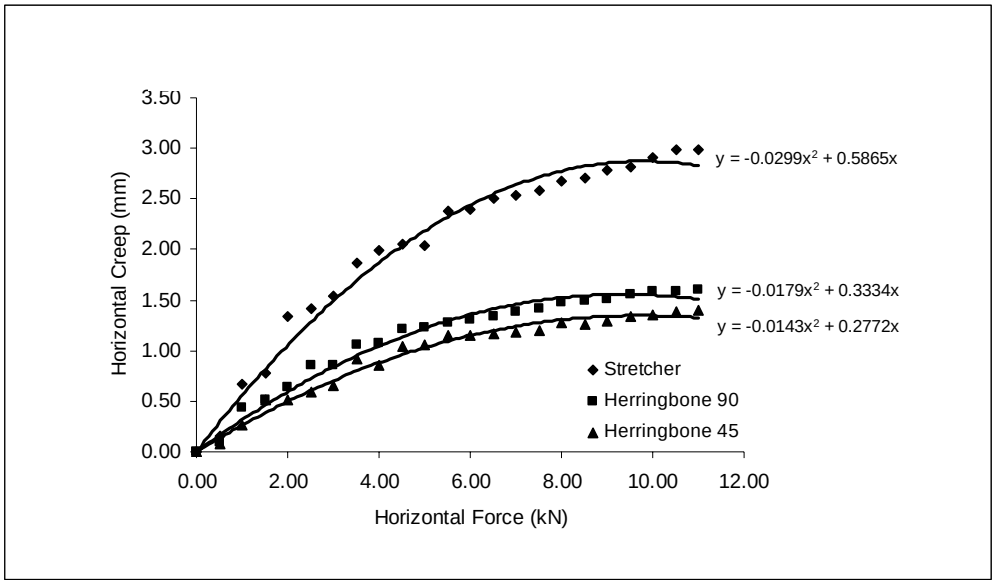

Figure B1.5 CBP specifications: Rectangular shape, 100 mm block thickness and 5 mm joint width.

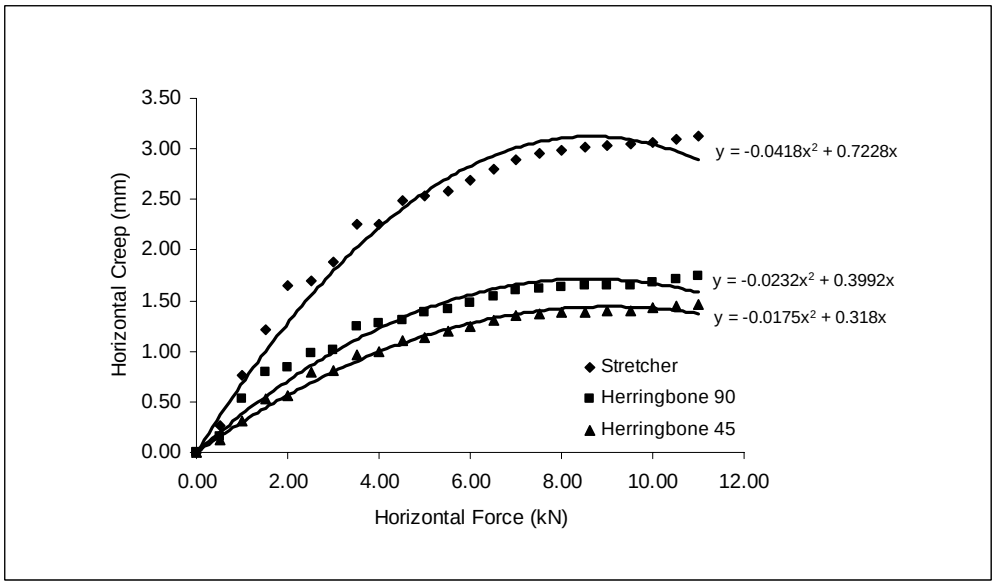

Figure B1.6 CBP specifications: Rectangular shape, 100 mm block thickness and 7 mm joint width.

APPENDIX – B2

Horizontal Force Test
(The Effect of Laying Pattern by Using Uni-pave Block Shape)

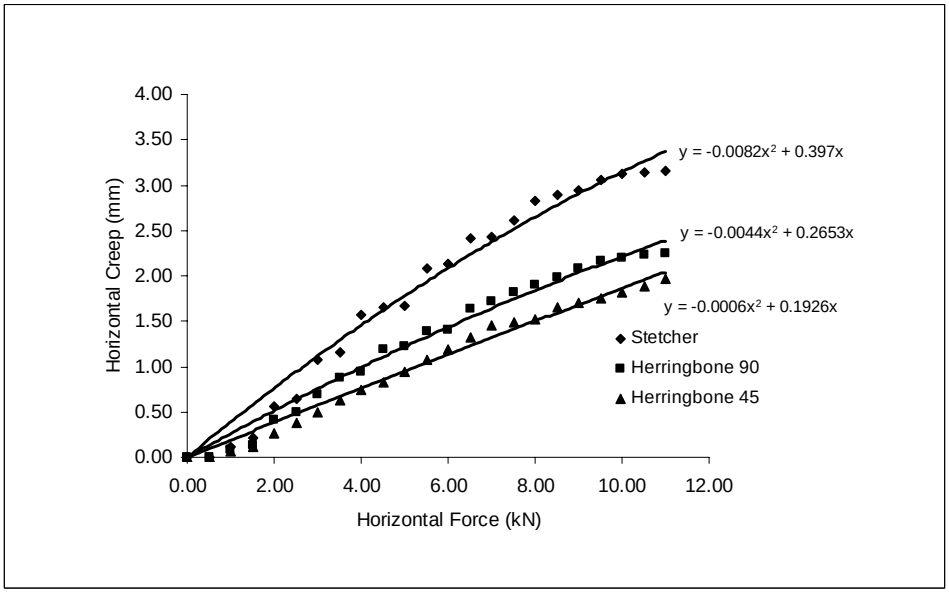

Figure B2.1 CBP specifications: Uni-pave shape, 60 mm block thickness and 3 mm joint width.

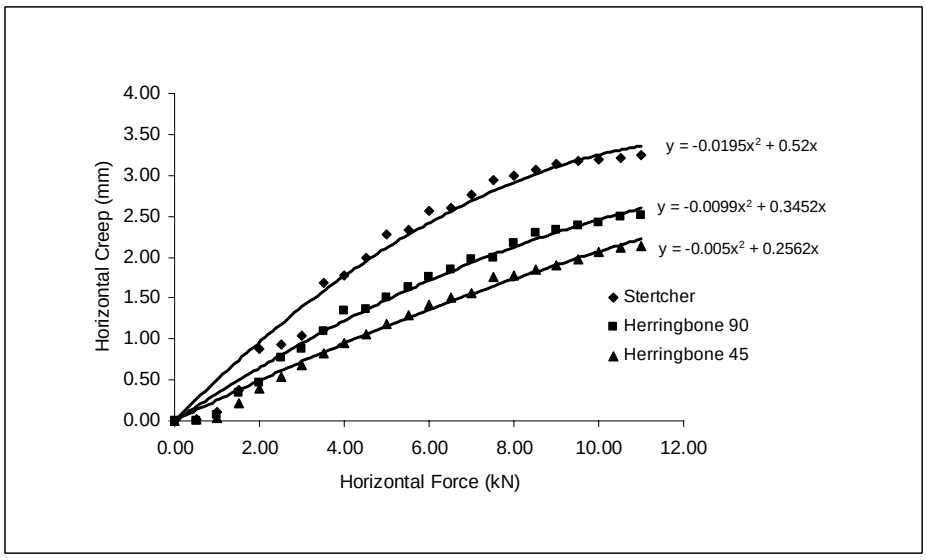

Figure B2.2 CBP specifications: Uni-pave shape, 60 mm block thickness and 5 mm joint width.

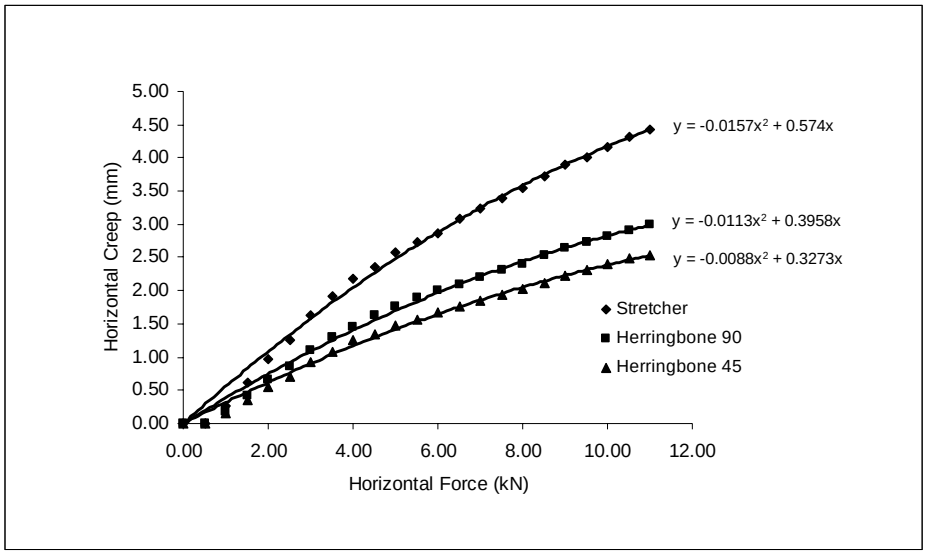

Figure B2.3 CBP specifications: Uni-pave shape, 60 mm block thickness and 7 mm joint width

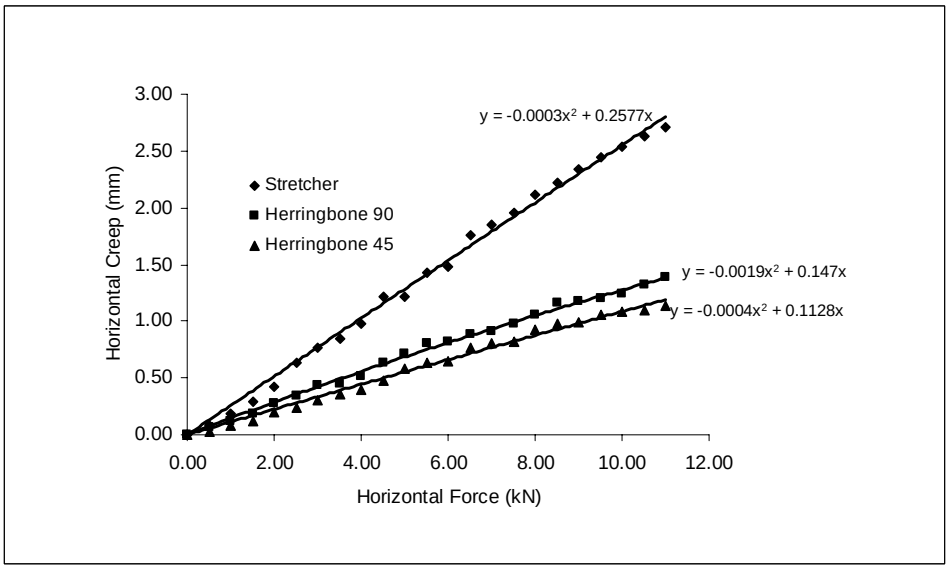

Figure B2.4 CBP specifications: Uni-pave shape, 100 mm block thickness and 3 mm joint width.

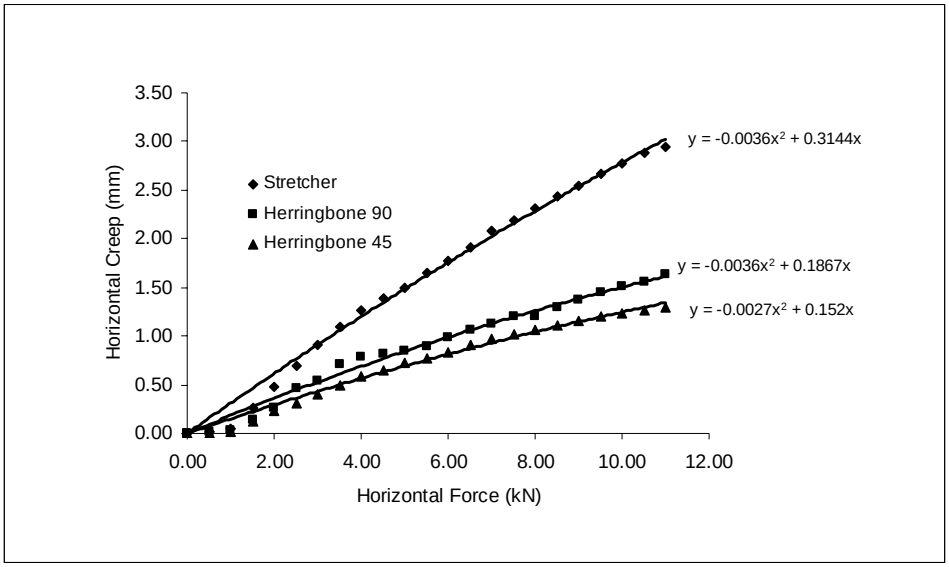

Figure B2.5 CBP specifications: Uni-pave shape, 100 mm block thickness and 5 mm joint width

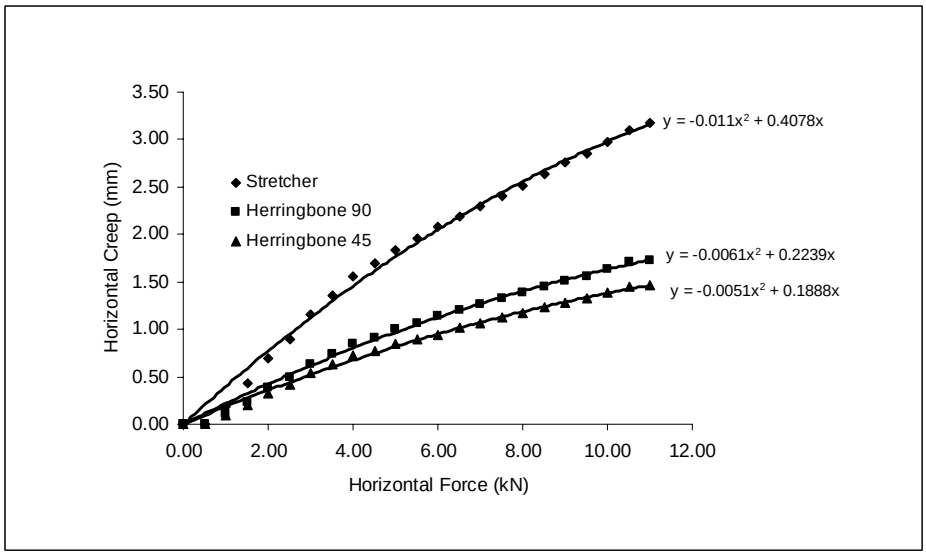

Figure B2.6 CBP specifications: Uni-pave shape, 100 mm block thickness and 7 mm joint width

APPENDIX – C1

Horizontal Force Test
(The Effect of Block Thickness by Using Rectangular Block Shape)

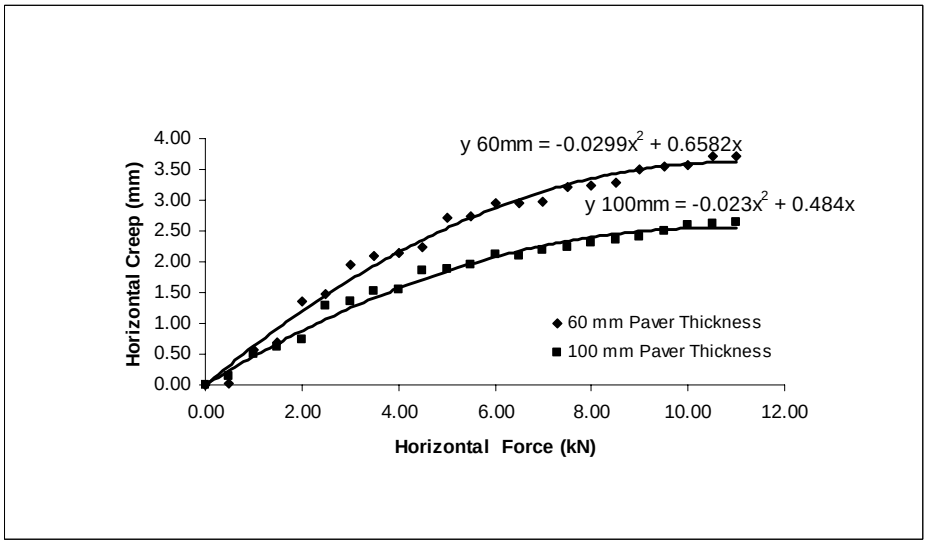

Figure C1.1 CBP specifications: rectangular shape, stretcher laying pattern and 3 mm joint width.

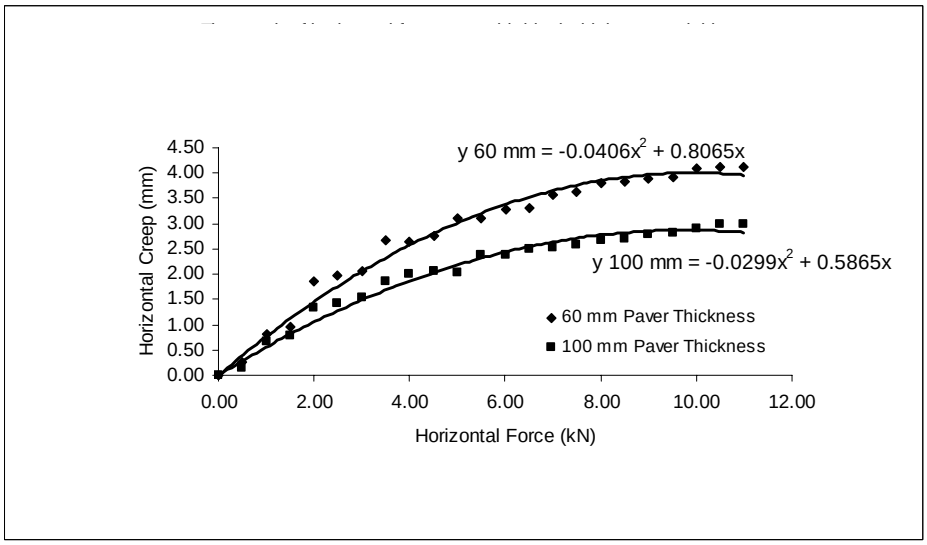

Figure C1.2 CBP specifications: rectangular shape, stretcher laying pattern and 5 mm joint width.

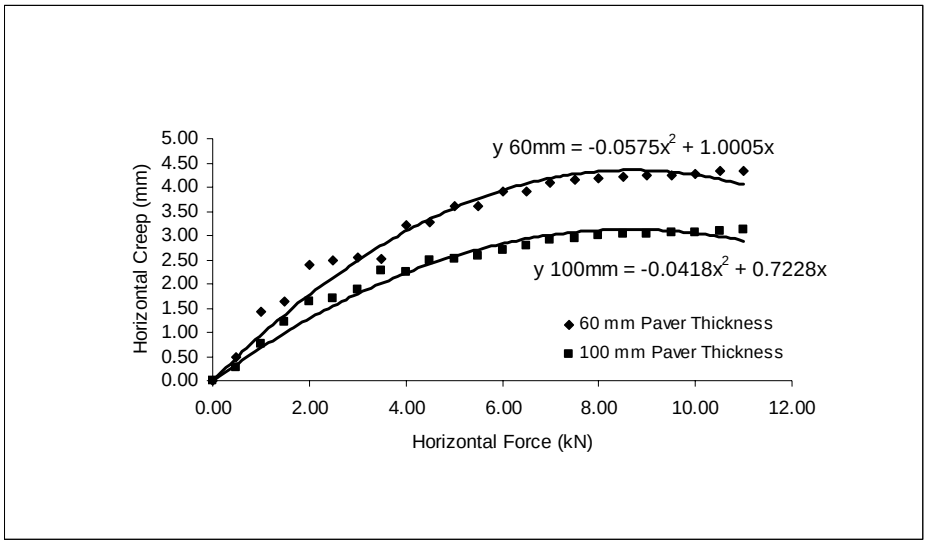

Figure C1.3 CBP specifications: rectangular shape, stretcher laying pattern and 7 mm joint width.

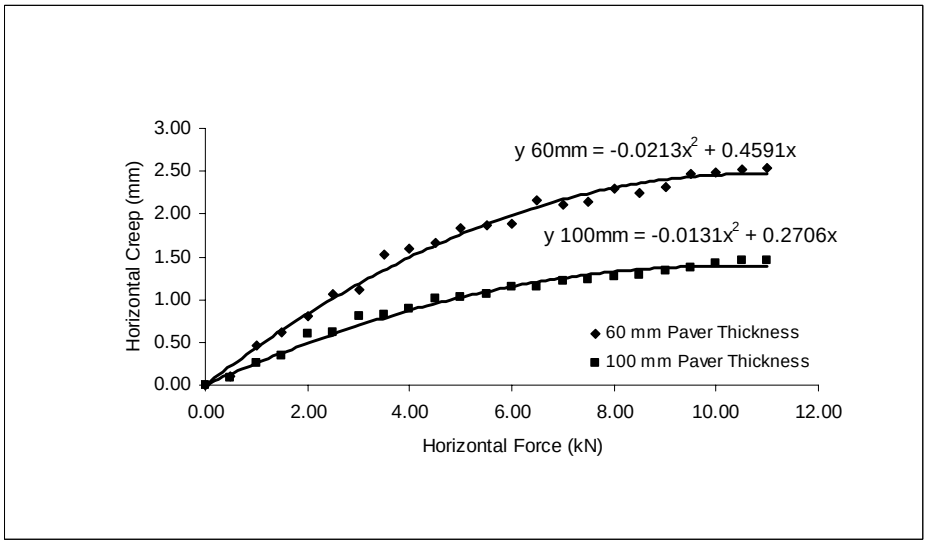

Figure C1.4 CBP specifications: rectangular shape, herringbone 90^{o} laying pattern and 3 mm joint width.

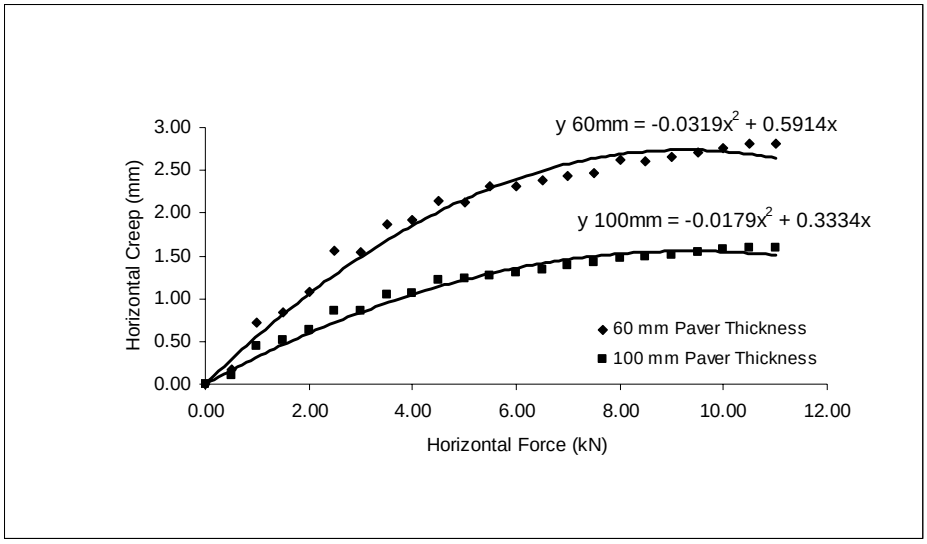

Figure C1.5 CBP specifications: rectangular shape, herringbone 90^{o} laying pattern and 5 mm joint width.

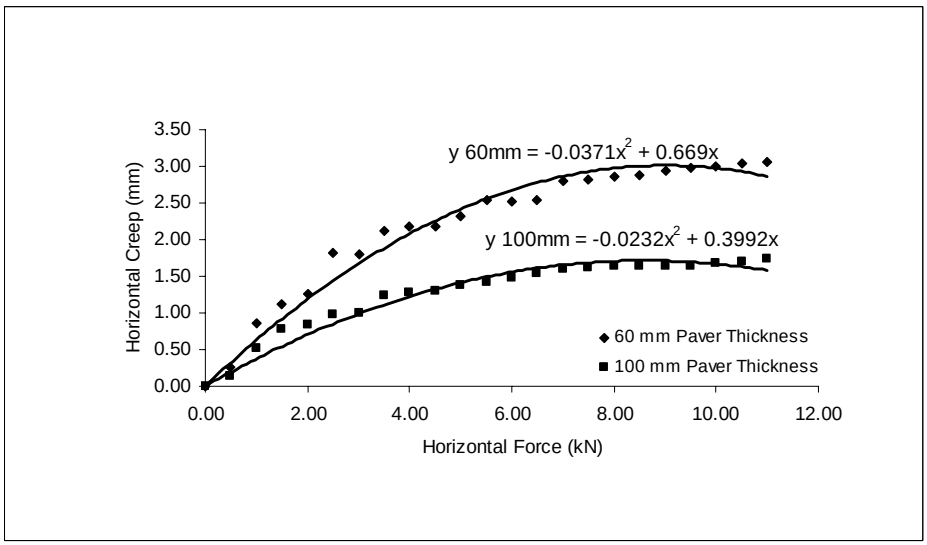

Figure C1.6 CBP specifications: rectangular shape, herringbone 90^{o} laying pattern and 7 mm joint width.

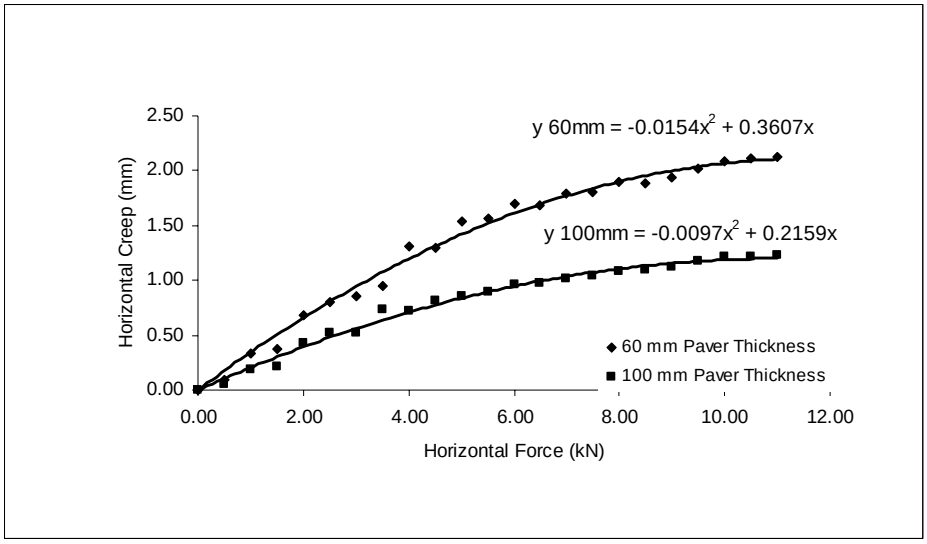

Figure C1.7 CBP specifications: rectangular shape, herringbone 45^{o} laying pattern and 3 mm joint width.

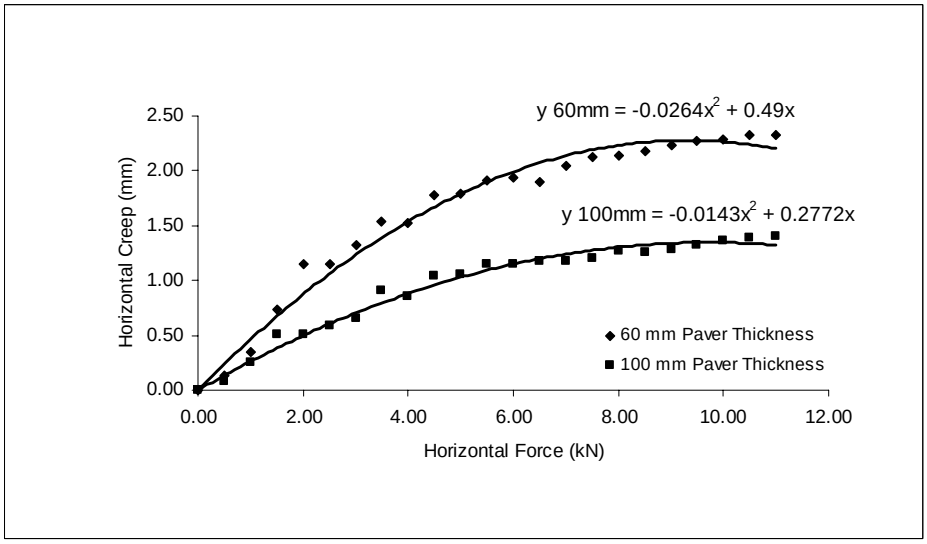

Figure C1.8 CBP specifications: rectangular shape, herringbone 45^{o} laying pattern and 5 mm joint width.

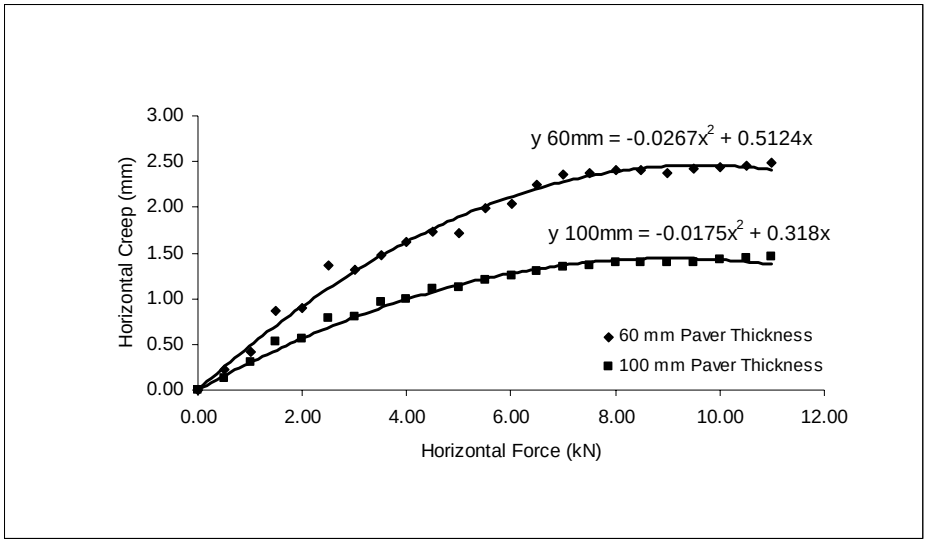

Figure C1.9 CBP specifications: rectangular shape, herringbone 45^{o} laying pattern and 7 mm joint width.

APPENDIX – C2

Horizontal Force Test
The Effect of Block Thickness by Using Uni-pave Block Shape

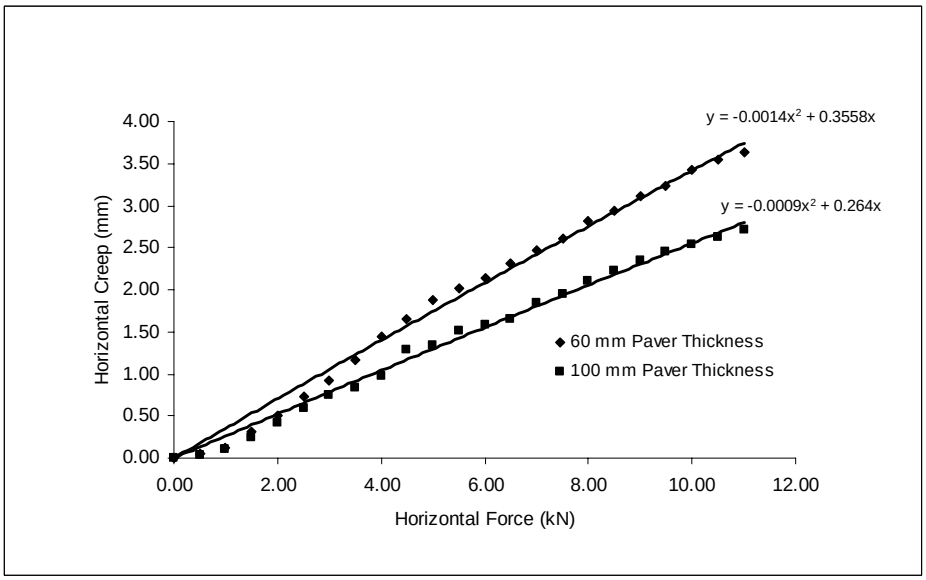

Figure C2.1 CBP specifications: Uni-pave shape, stretcher laying pattern and 3 mm joint width.

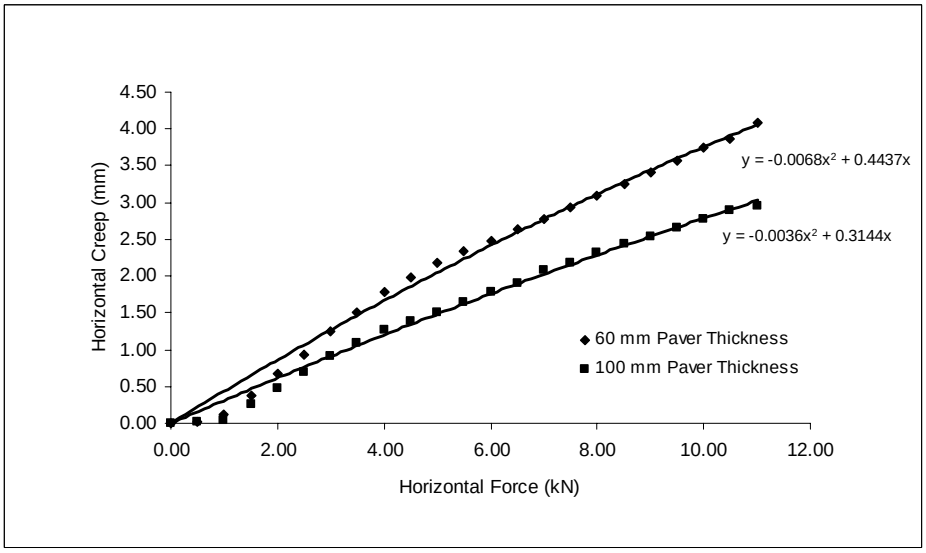

Figure C2.2 CBP specifications: Uni-pave shape, stretcher laying

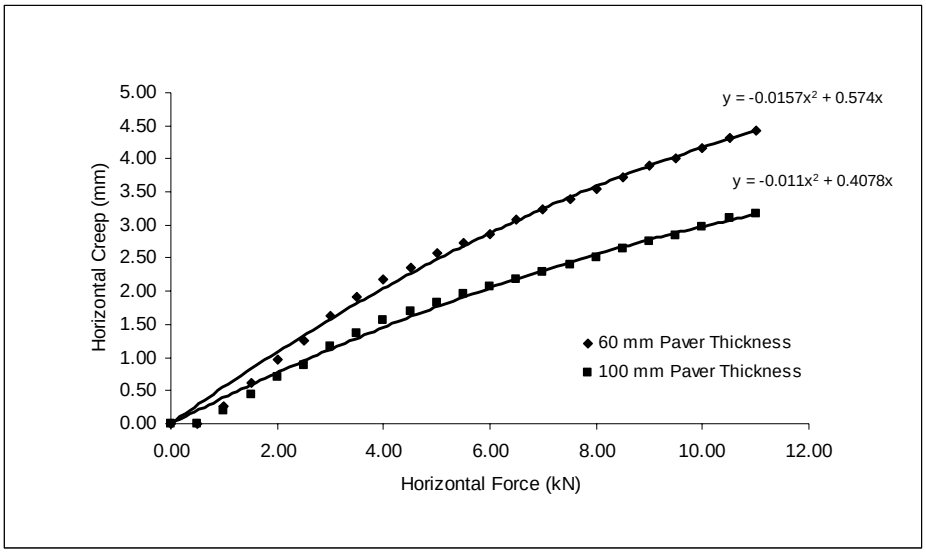

Figure C2.3 CBP specifications: Uni-pave shape, stretcher laying pattern and 7 mm joint width.

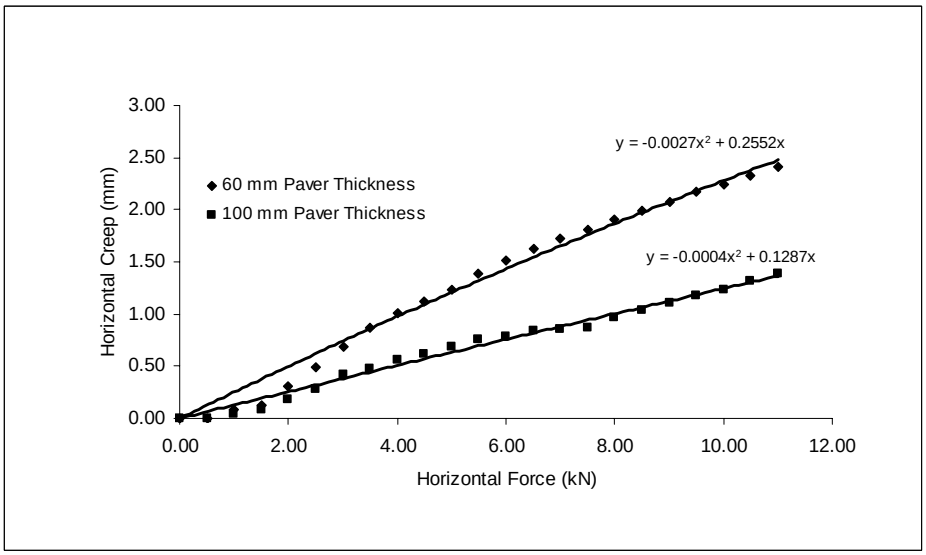

Figure C2.4 CBP specifications: Uni-pave shape, herringbone 90^{o} laying pattern and 3 mm joint width.

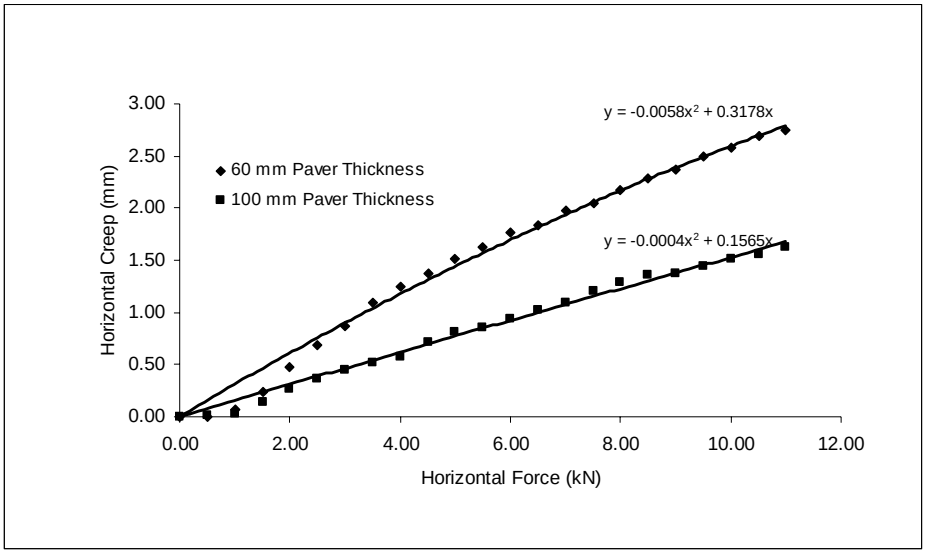

Figure C2.5 CBP specifications: Uni-pave shape, herringbone 90^{o} laying pattern and 5 mm joint width.

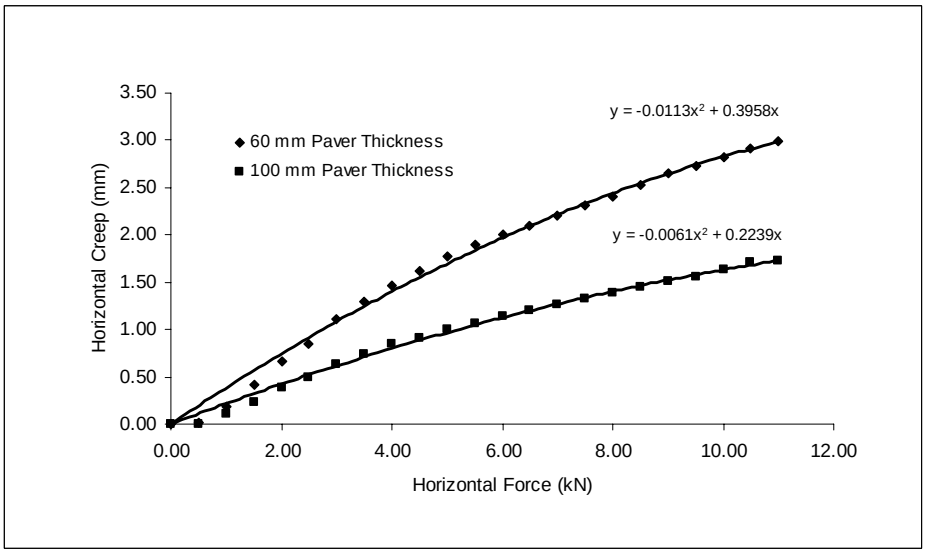

Figure C2.6 CBP specifications: Uni-pave shape, herringbone 90^{o} laying pattern and 7 mm joint width.

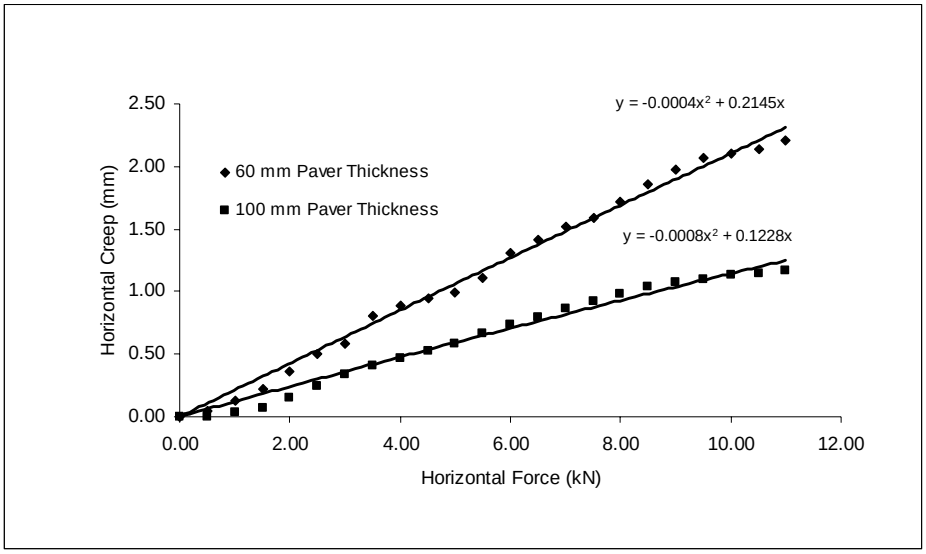

Figure C2.7 CBP specifications: Uni-pave shape, herringbone 45^{o} laying pattern and 3 mm joint width.

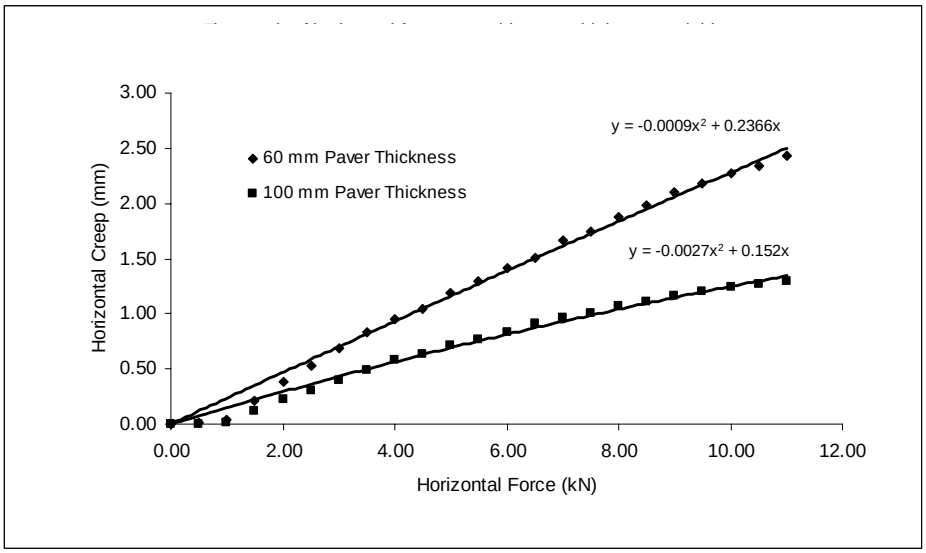

Figure C2.8 CBP specifications: Uni-pave shape, herringbone 45^{o} laying pattern and 5 mm joint width.

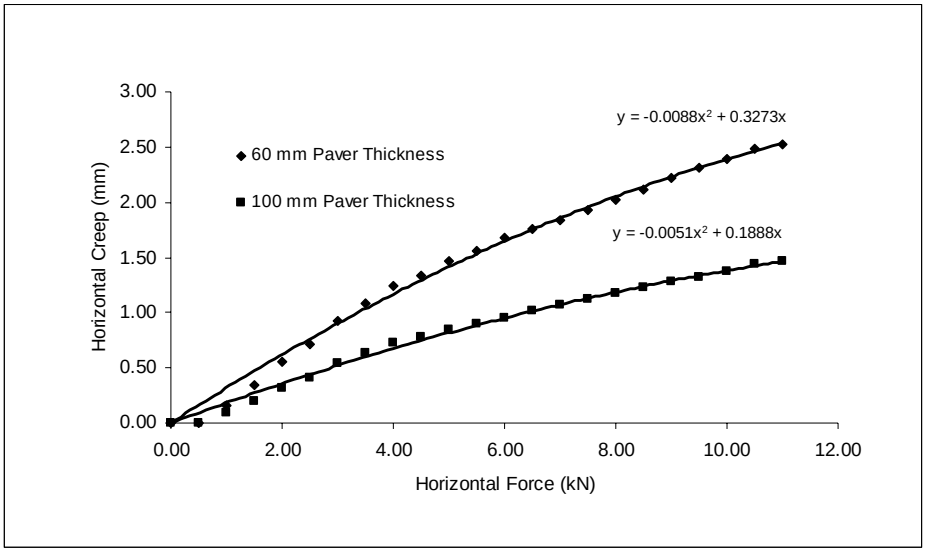

Figure C2.9 CBP specifications: Uni-pave shape, herringbone 45^{o} laying pattern and 7 mm joint width.

APPENDIX – D1

Horizontal Force Test
The Effect of Joint Width by Using Rectangular Block Shape

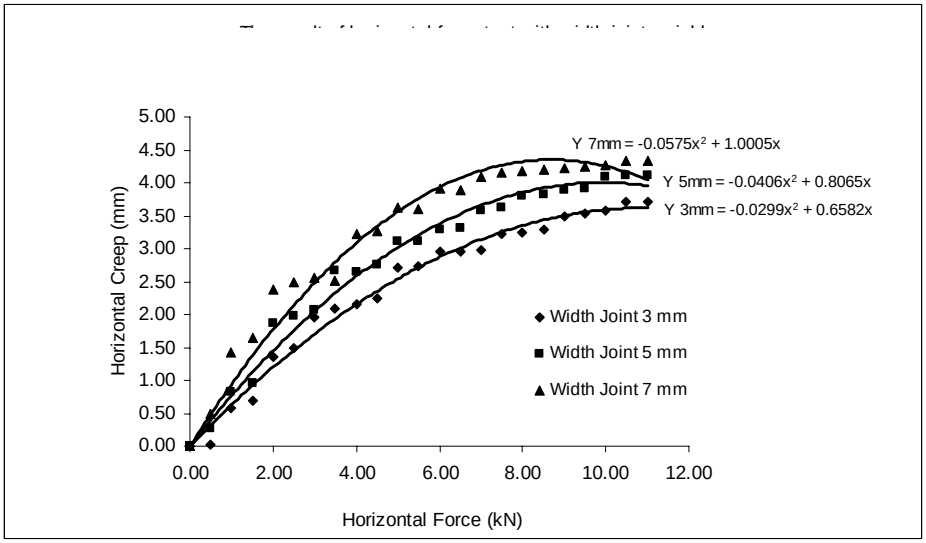

Figure D1.1 CBP specifications: rectangular shape, 60 mm block thickness and stretcher bond laying pattern

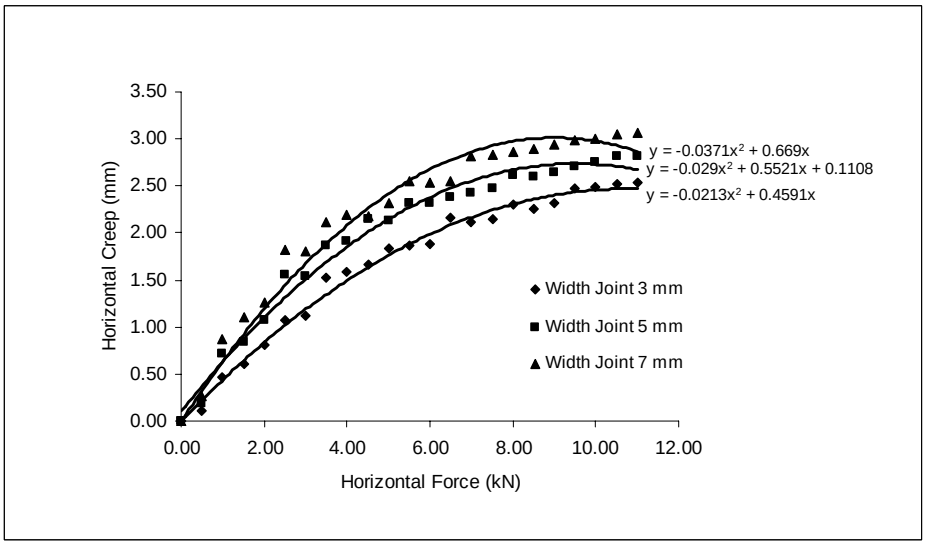

Figure D1.2 CBP specifications: rectangular shape, 60 mm block thickness and herringbone 90^{o} laying pattern

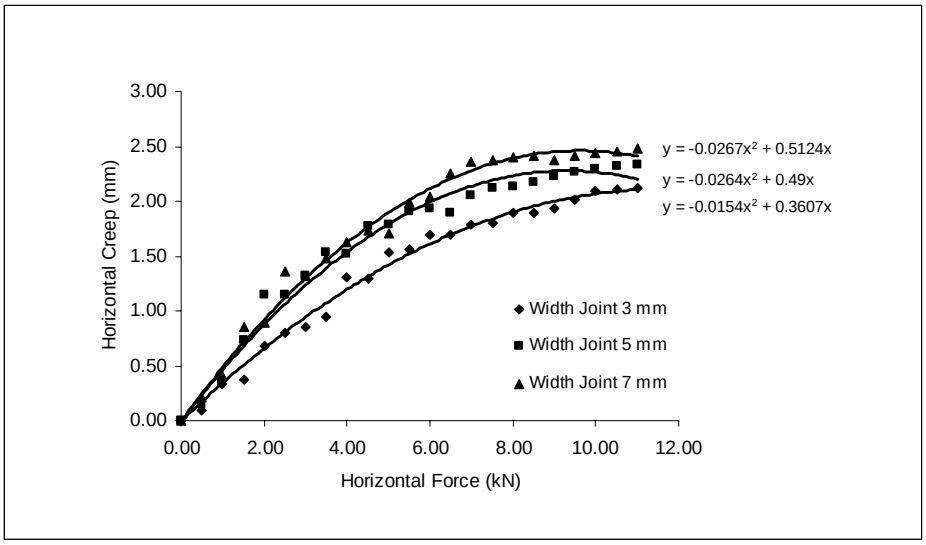

Figure D1.3 CBP specifications: rectangular shape, 60 mm block thickness and herringbone 45^{o} laying pattern

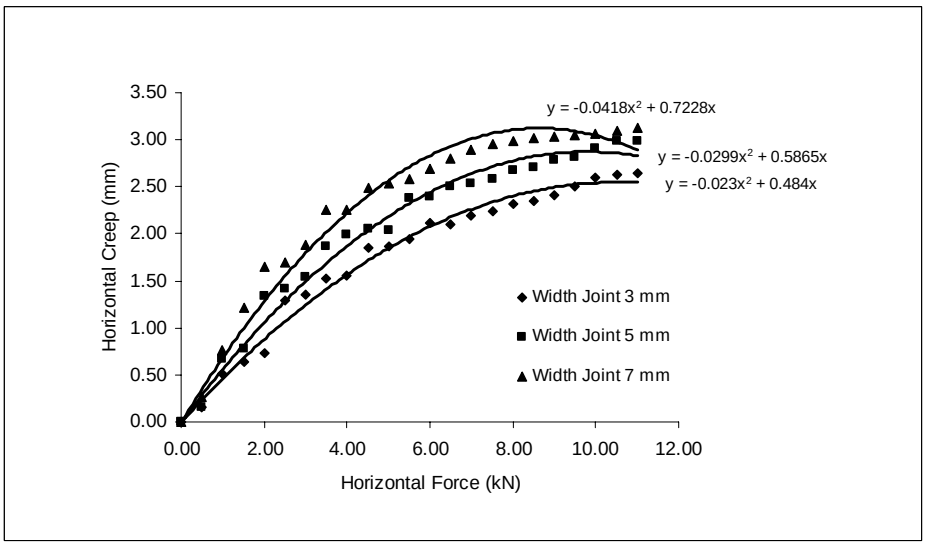

Figure D1.4 CBP specifications: rectangular shape, 100 mm block thickness and stretcher bond laying pattern

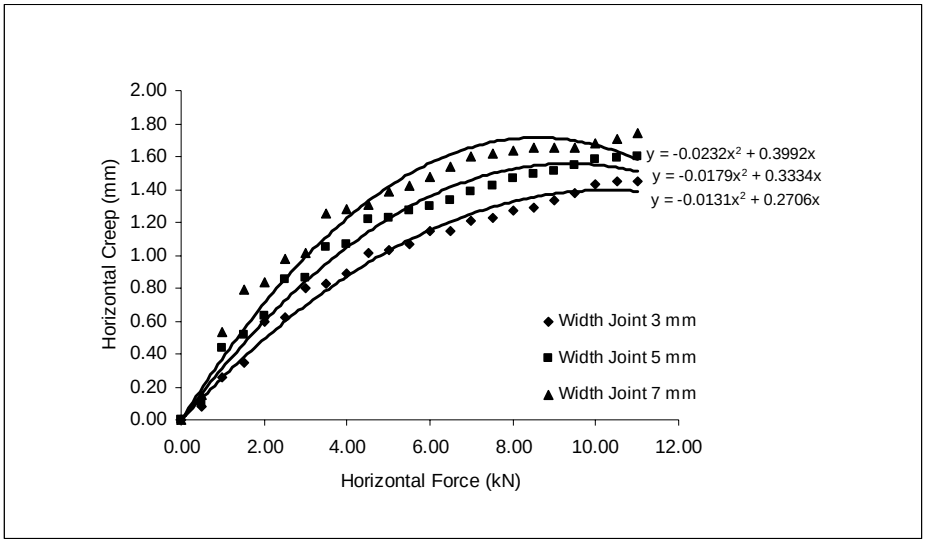

Figure D1.5 CBP specifications: rectangular shape, 100 mm block thickness and herringbone 90^{o} laying pattern

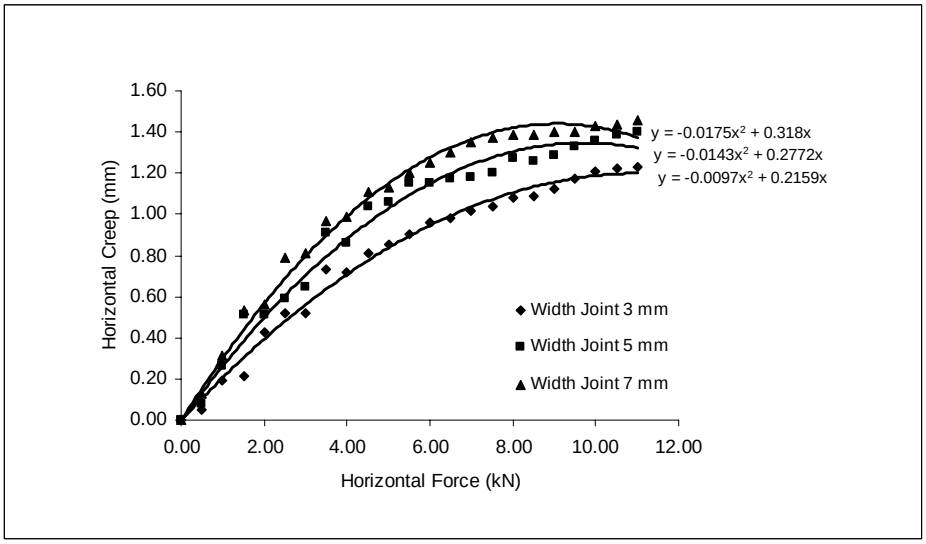

Figure D1.6 CBP specifications: rectangular shape, 100 mm block thickness and herringbone 45^{o} laying pattern

APPENDIX – D2

Horizontal Force Test
The Effect of Joint Width by Using Uni-pave Block Shape

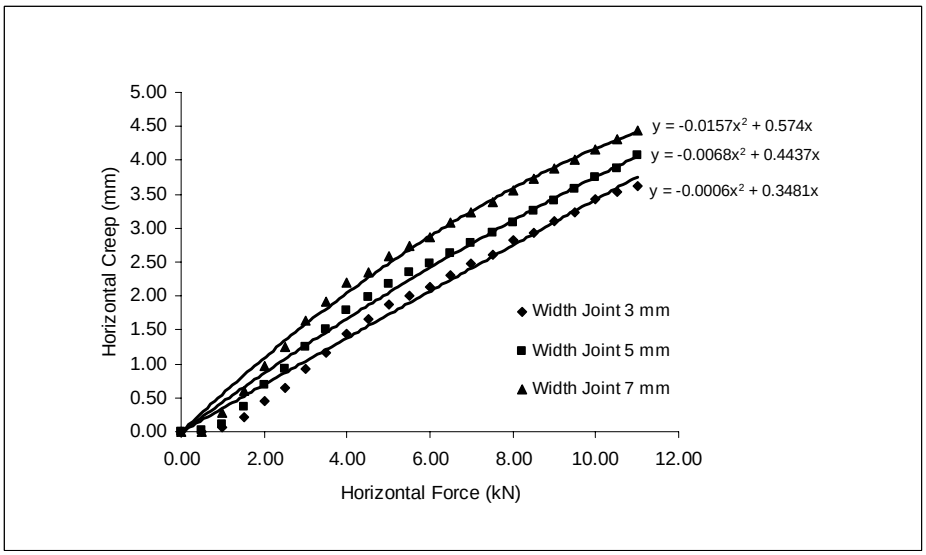

Figure D2.1 CBP specifications: uni-pave shape, 60 mm block thickness and stretcher bond laying pattern

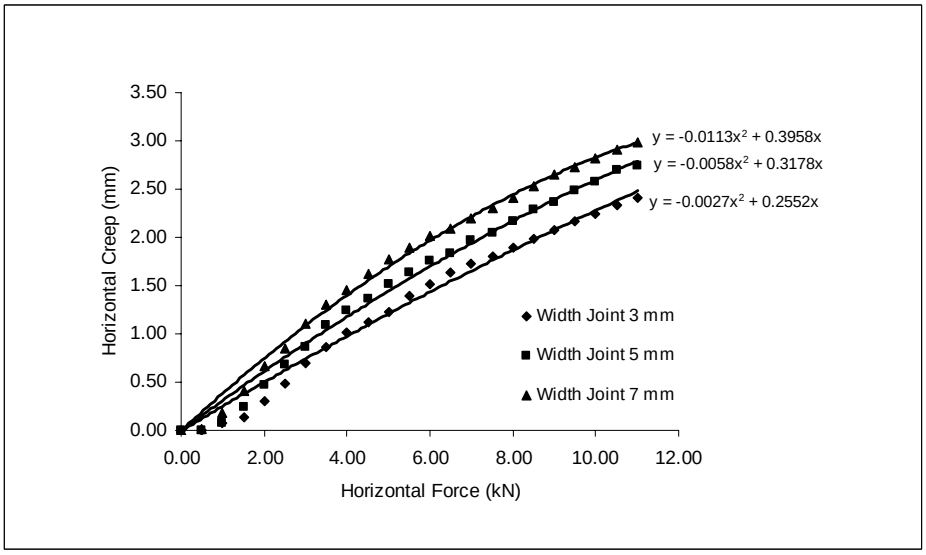

Figure D2.2 CBP specifications: uni-pave shape, 60 mm block thickness and herringbone 90^{o} laying pattern

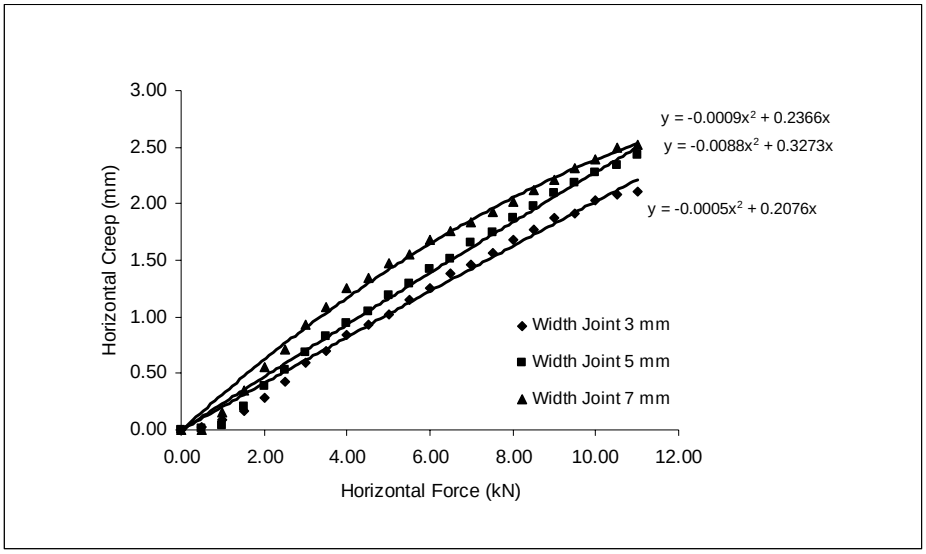

Figure D2.3 CBP specifications: uni-pave shape, 60 mm block thickness and herringbone 45^{o} laying pattern

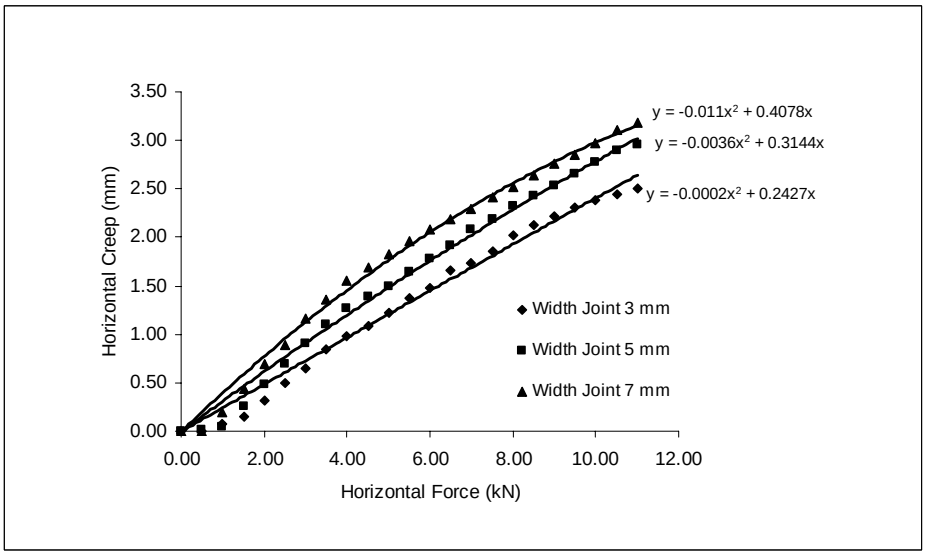

Figure D2.4 CBP specifications: uni-pave shape, 100 mm block thickness and stretcher bond laying pattern

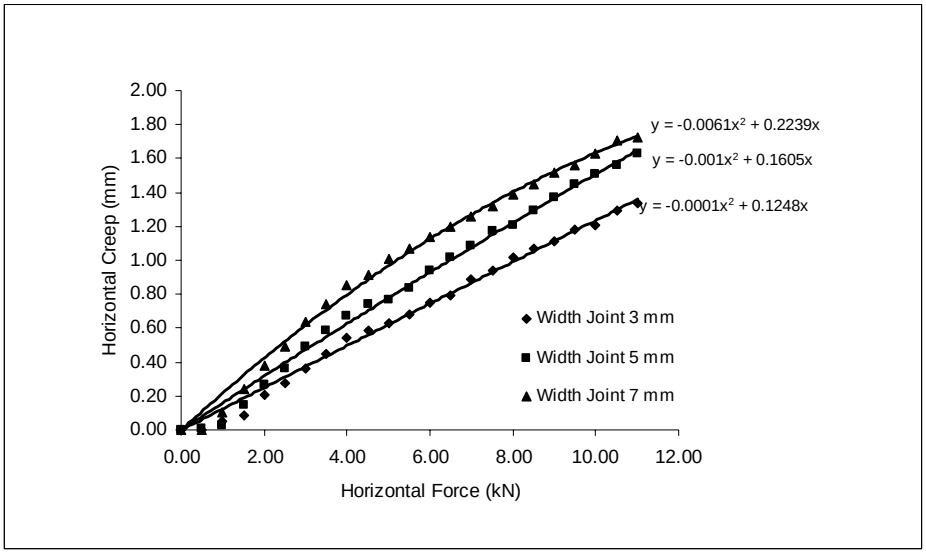

Figure D2.5 CBP specifications: uni-pave shape, 100 mm block thickness and herringbone 90^{o} laying pattern

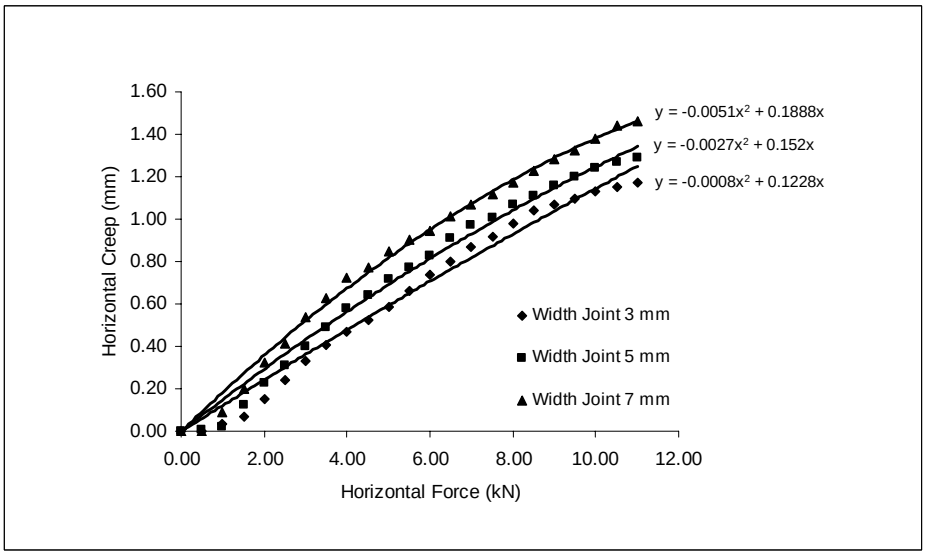

Figure D2.6 CBP specifications: uni-pave shape, 100 mm block thickness and herringbone 45^{o} laying pattern

APPENDIX – E1

Horizontal Creep on Push-in Test 0 % CBP Slope
The Effect of Bedding Sand Thickness

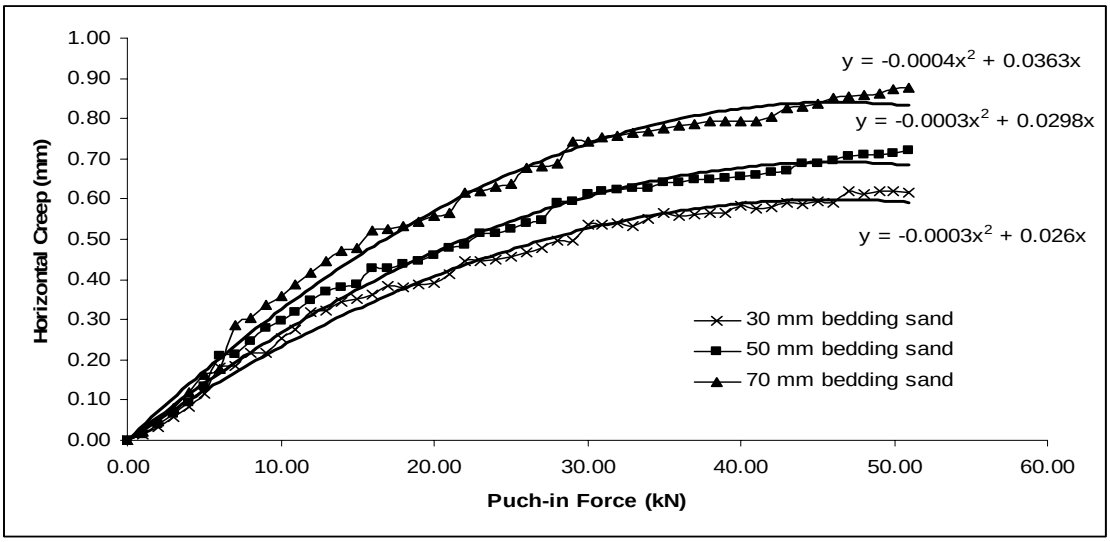

Figure E1.1 CBP specifications: rectangular block shape, 60 mm block thickness, stretcher bond laying pattern, 3 mm joint width and 0 % degree of slope.

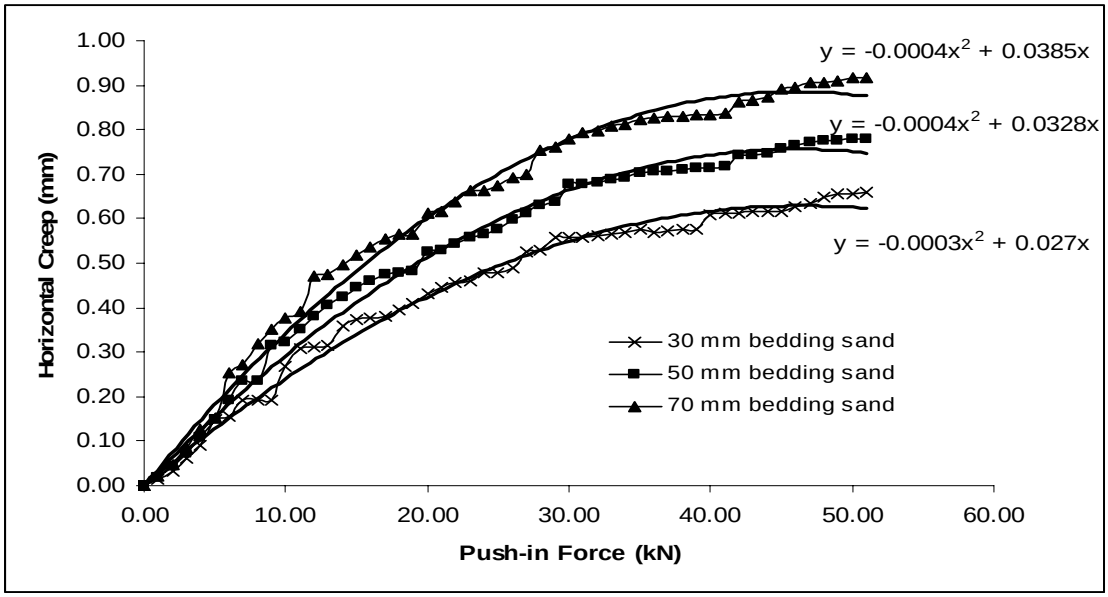

Figure E1.2 CBP specifications: rectangular block shape, 60 mm block thickness, stretcher bond laying pattern, 5 mm joint width and 0 % degree of slope.

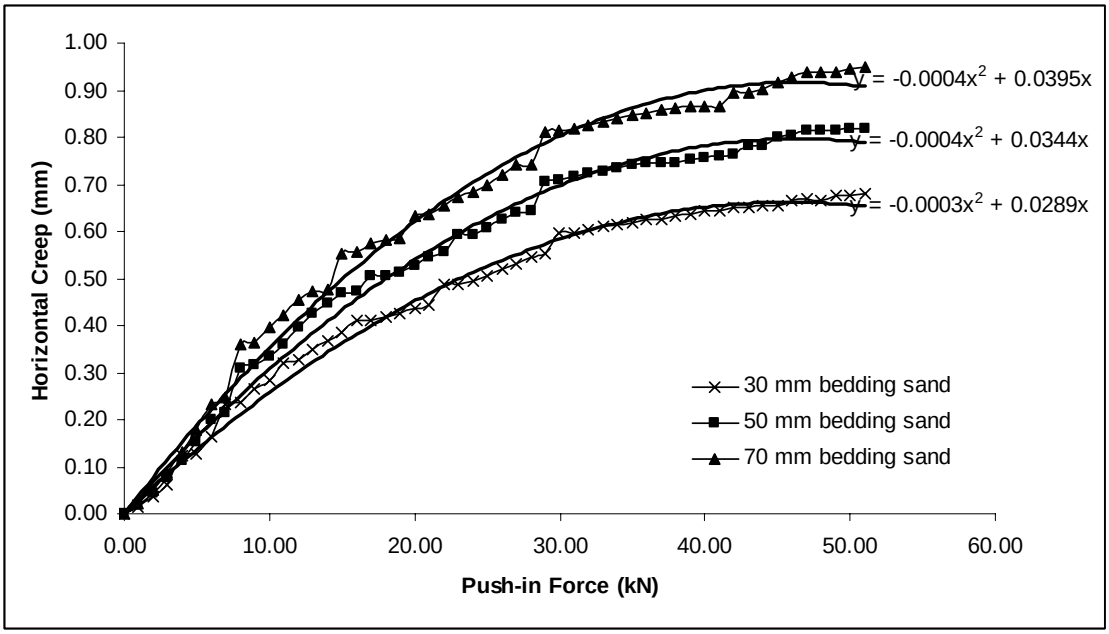

Figure E1.3 CBP specifications: rectangular block shape, 60 mm block thickness, stretcher bond laying pattern, 7 mm joint width and 0 % degree of slope.

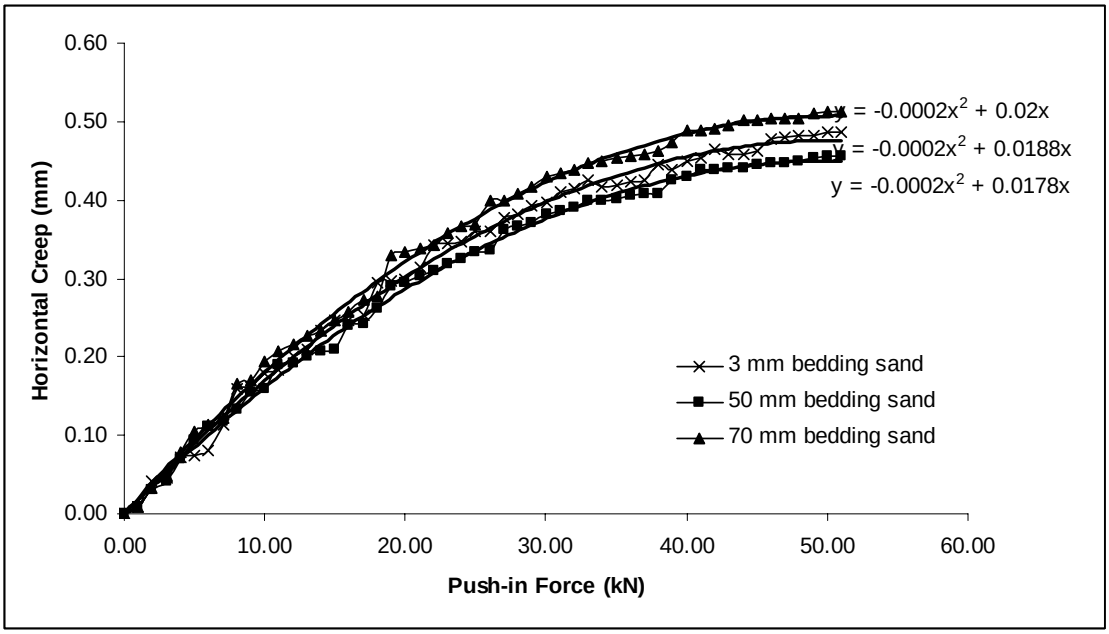

Figure E1.4 CBP specifications: rectangular block shape, 100 mm block thickness, stretcher bond laying pattern, 3 mm joint width and 0 % degree of slope.

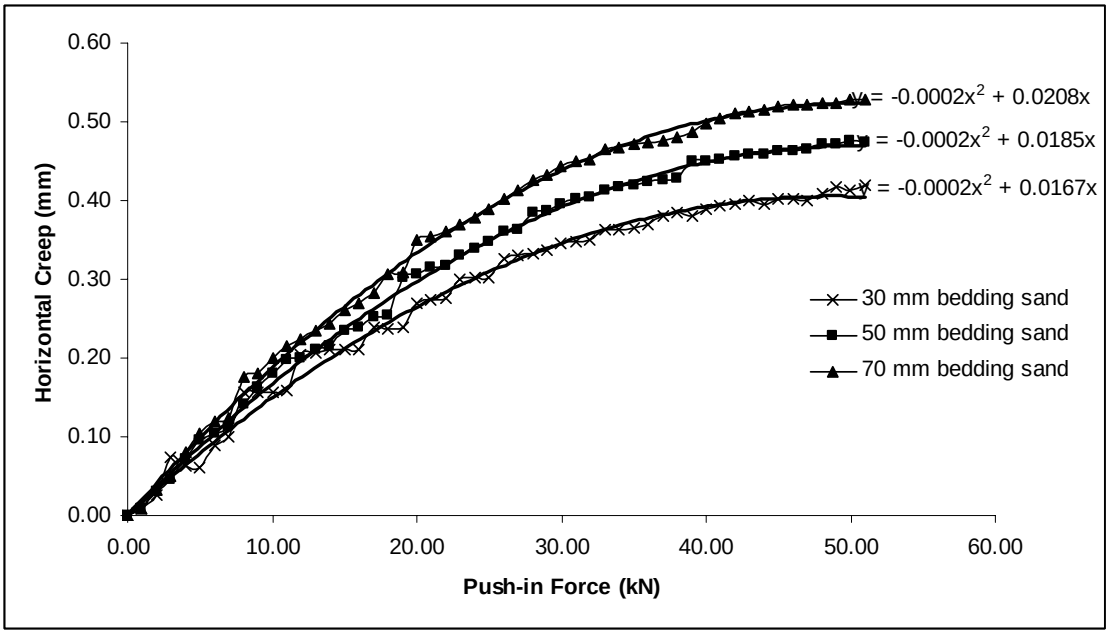

Figure E1.5 CBP specifications: rectangular block shape, 100 mm block thickness, stretcher bond laying pattern, 5 mm joint width and 0 % degree of slope.

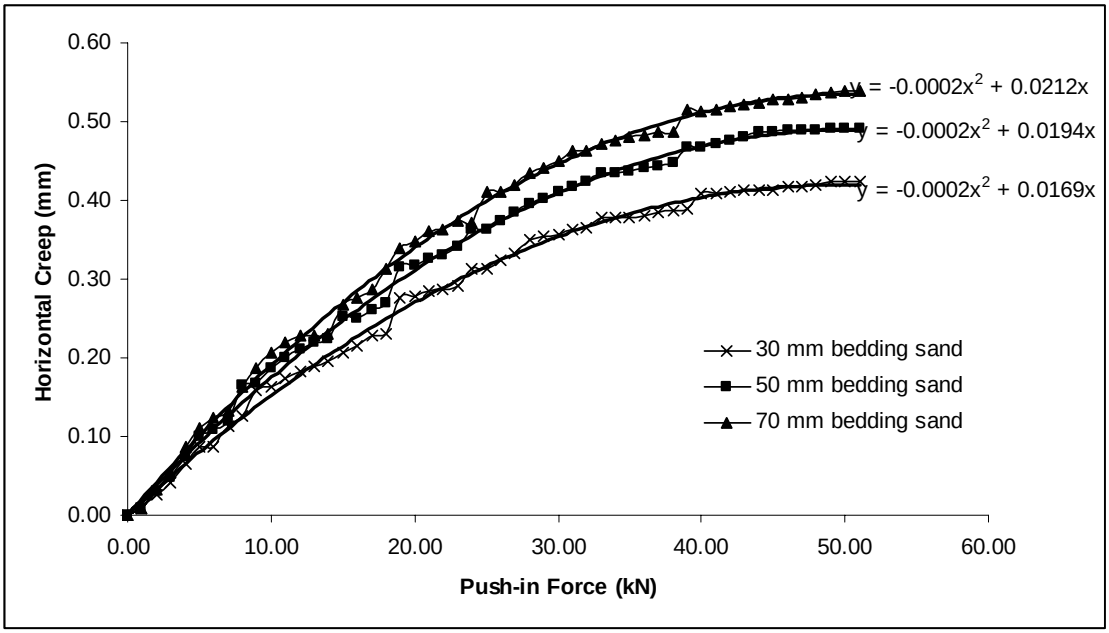

Figure E1.6 CBP specifications: rectangular block shape, 100 mm block thickness, stretcher bond laying pattern, 7 mm joint width and 0 % degree of slope.

APPENDIX – E1

Push-in Test on CBP 0 % Slope
The Effect of Bedding Sand Thickness

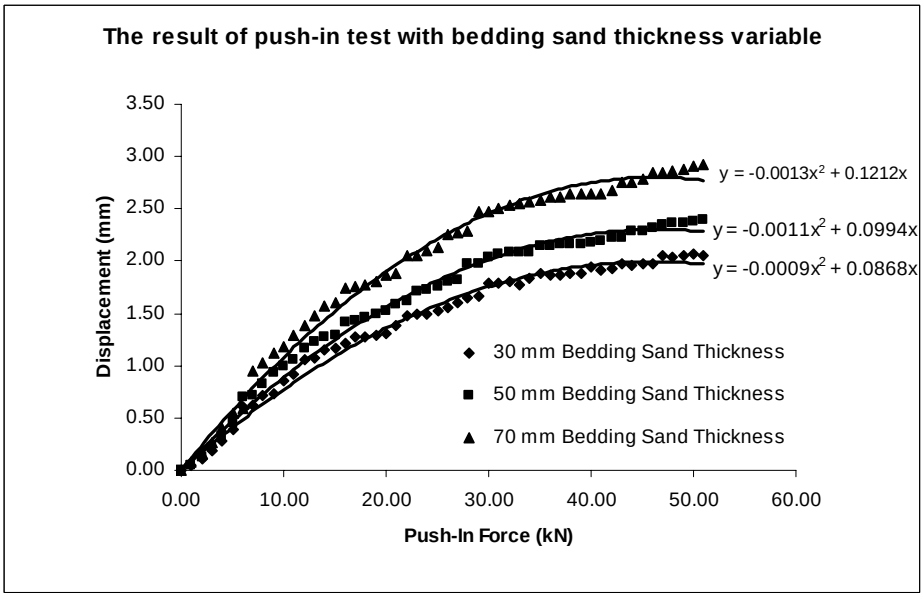

Figure E1.1 CBP specifications: rectangular block shape, 60 mm block thickness, stretcher bond laying pattern, 3 mm joint width and 0 % degree of slope.

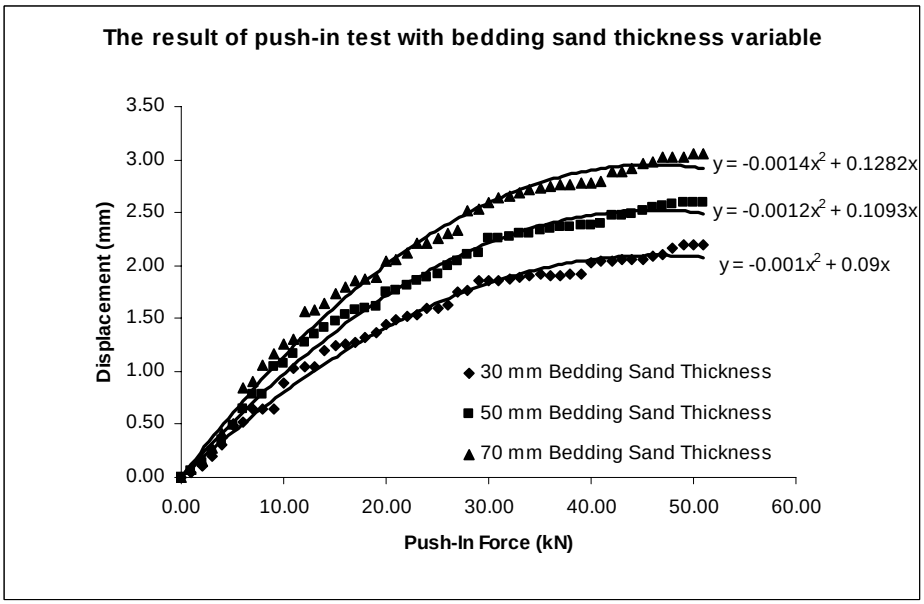

Figure E1.2 CBP specifications: rectangular block shape, 60 mm block thickness, stretcher bond laying pattern, 5 mm joint width and 0 % degree of slope.

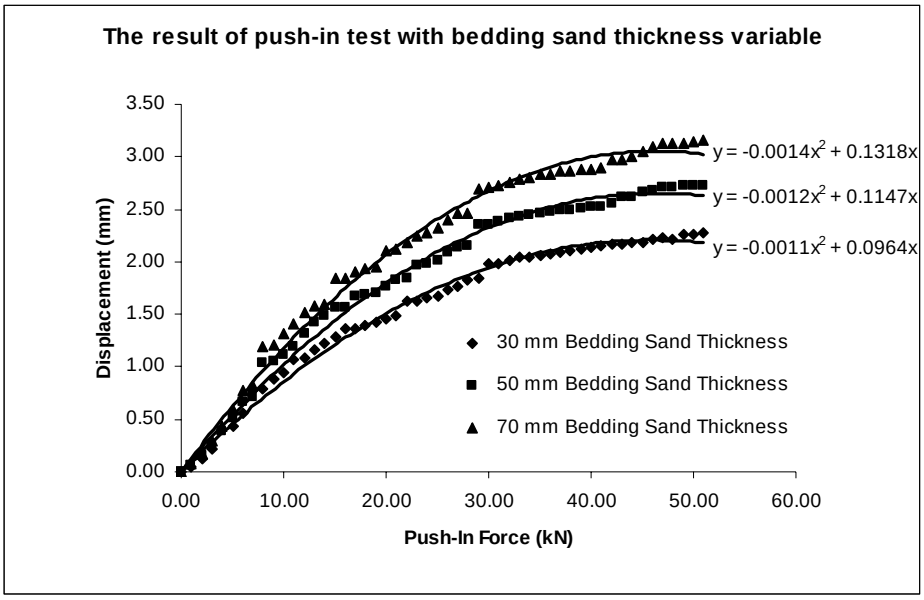

Figure E1.3 CBP specifications: rectangular block shape, 60 mm block thickness, stretcher bond laying pattern, 7 mm joint width and 0 % degree of slope.

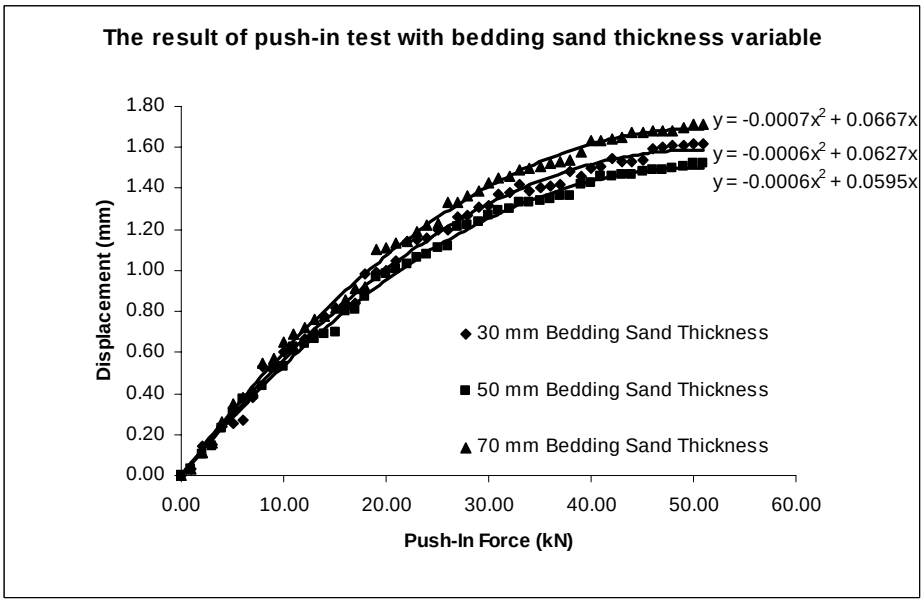

Figure E1.4 CBP specifications: rectangular block shape, 100 mm block thickness, stretcher bond laying pattern, 3 mm joint width and 0 % degree of slope.

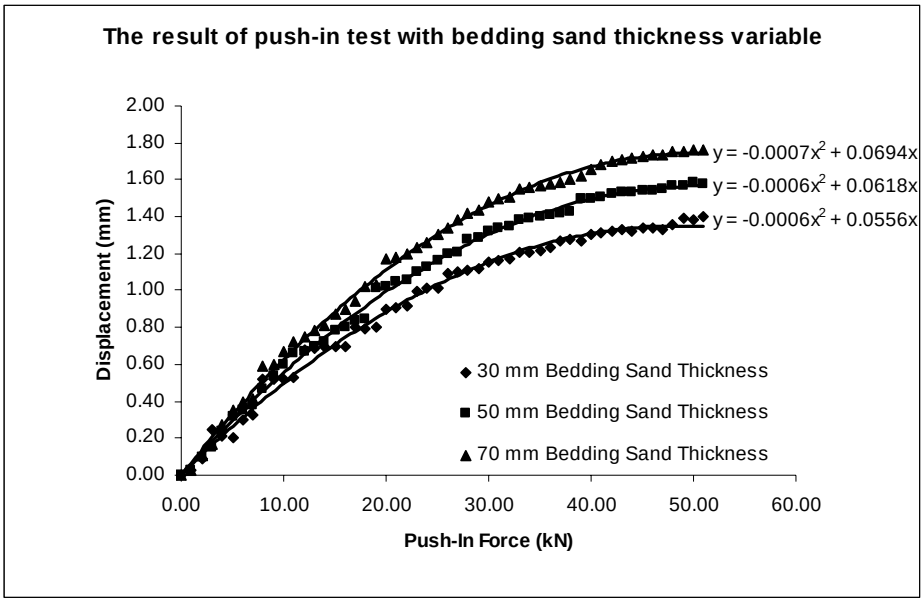

Figure E1.5 CBP specifications: rectangular block shape, 100 mm block thickness, stretcher bond laying pattern, 5 mm joint width and 0 % degree of slope.

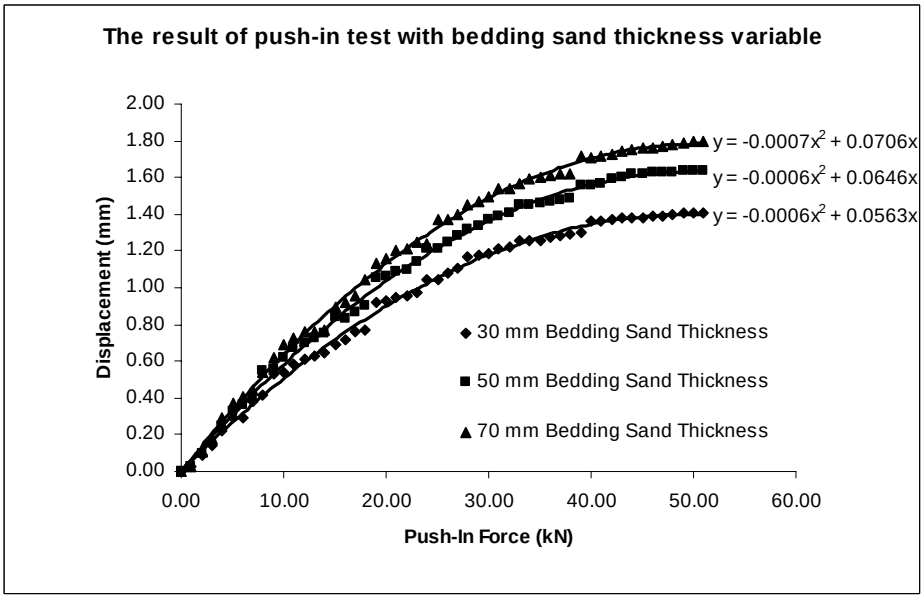

Figure E1.6 CBP specifications: rectangular block shape, 100 mm block thickness, stretcher bond laying pattern, 7 mm joint width and 0 % degree of slope.

APPENDIX – E2

Push-in Test on CBP 0 % Slope
The Effect of Block Thickness

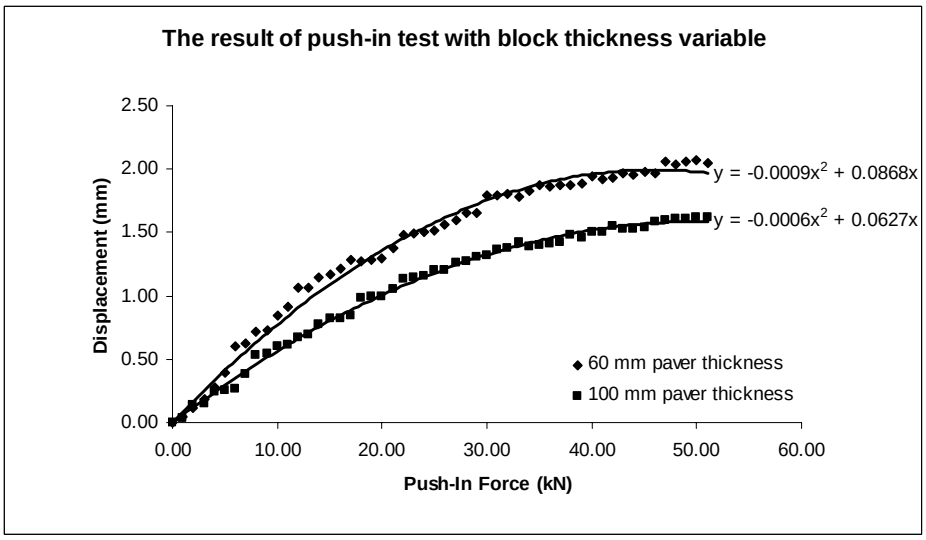

Figure E2.1 CBP specifications: rectangular block shape, 30 mm bedding sand thick, stretcher bond laying pattern, 3 mm joint width and 0 % degree of slope.

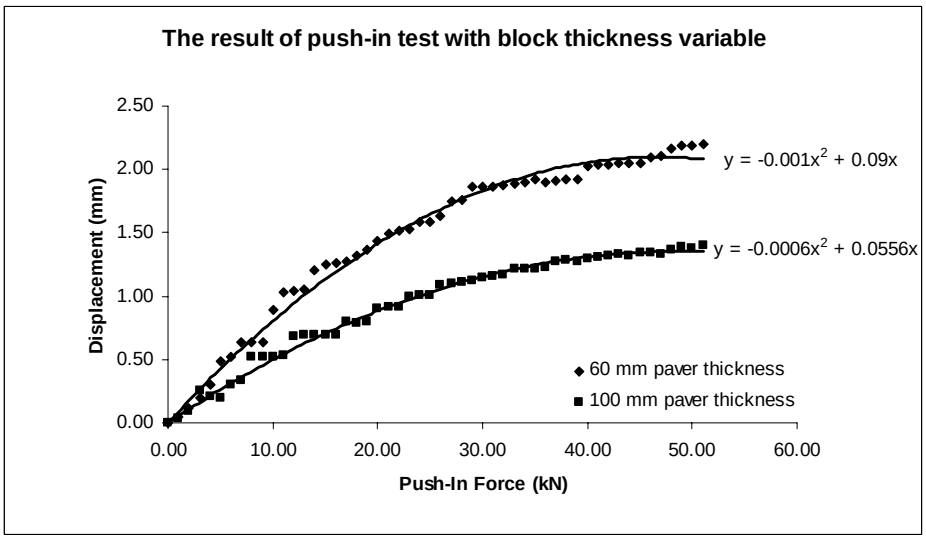

Figure E2.2 CBP specifications: rectangular block shape, 30 mm bedding sand thick, stretcher bond laying pattern, 5 mm joint width and 0 % degree of slope.

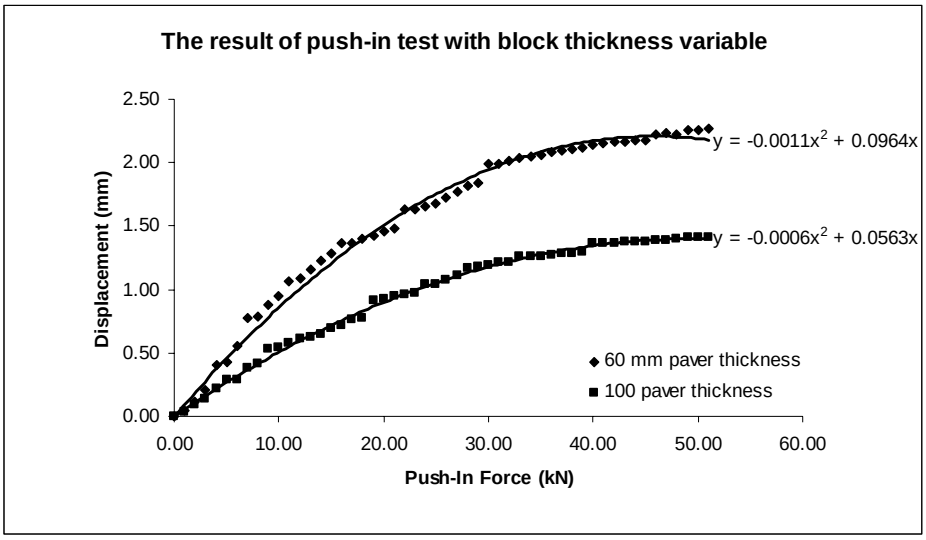

Figure E2.3 CBP specifications: rectangular block shape, 30 mm bedding sand thick, stretcher bond laying pattern, 7 mm joint width and 0 % degree of slope.

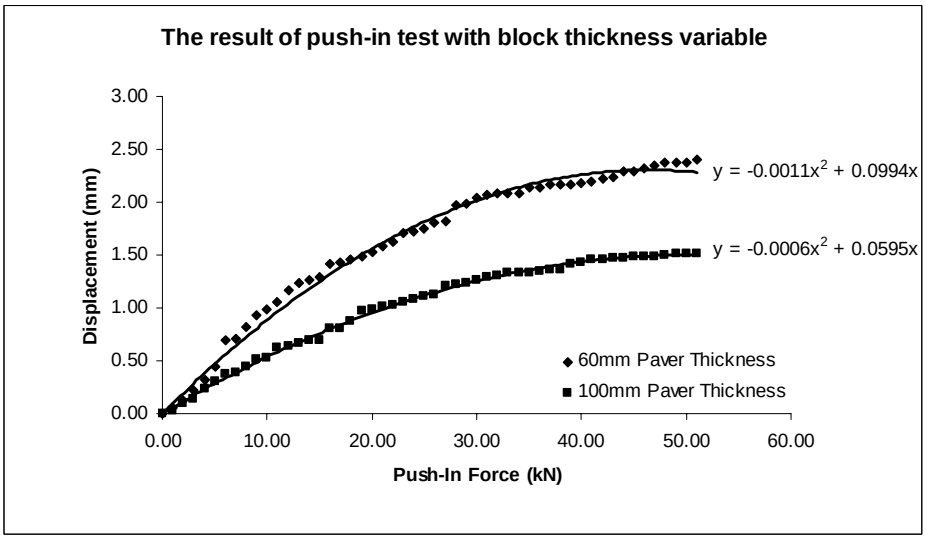

Figure E2.4 CBP specifications: rectangular block shape, 50 mm bedding sand thick, stretcher bond laying pattern, 3 mm joint width and 0 % degree of slope.

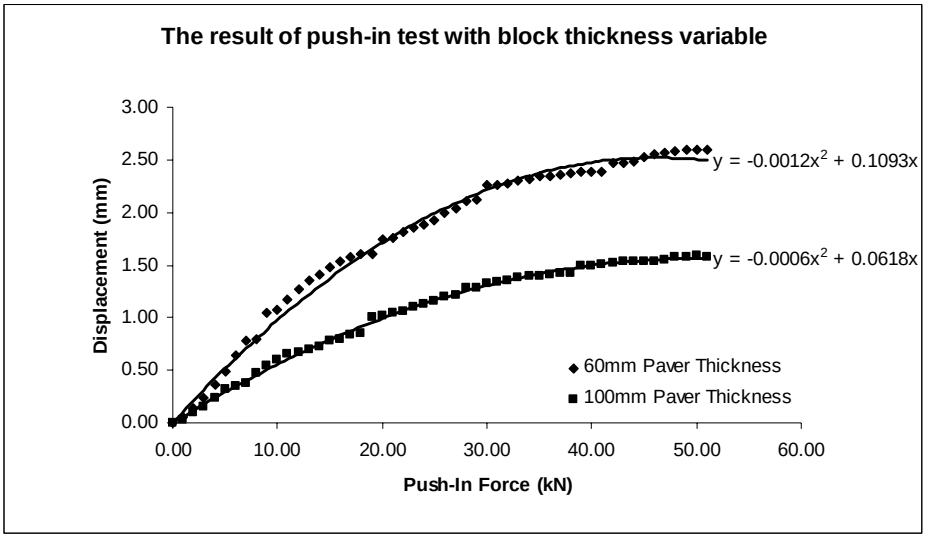

Figure E2.5 CBP specifications: rectangular block shape, 50 mm bedding sand thick, stretcher bond laying pattern, 5 mm joint width and 0 % degree of slope.

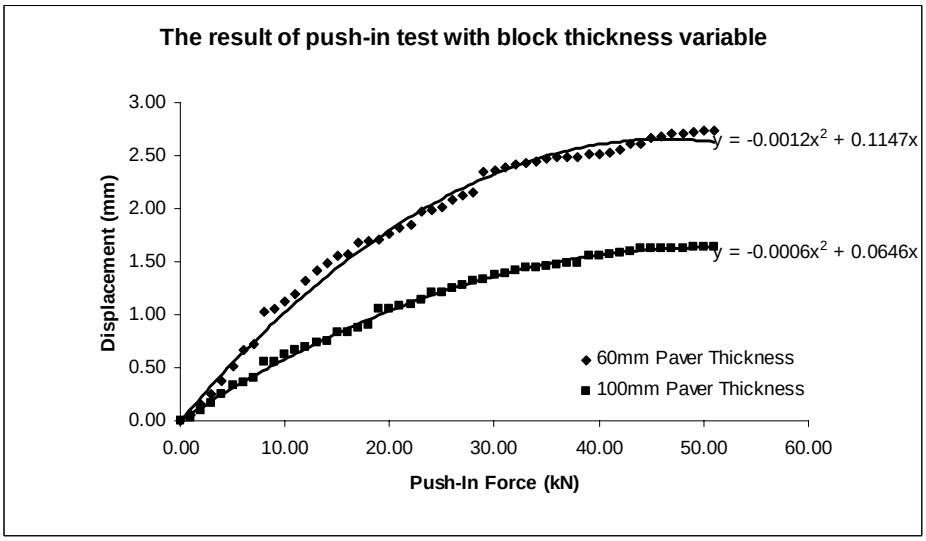

Figure E2.6 CBP specifications: rectangular block shape, 50 mm bedding sand thick, stretcher bond laying pattern, 7 mm joint width and 0 % degree of slope.

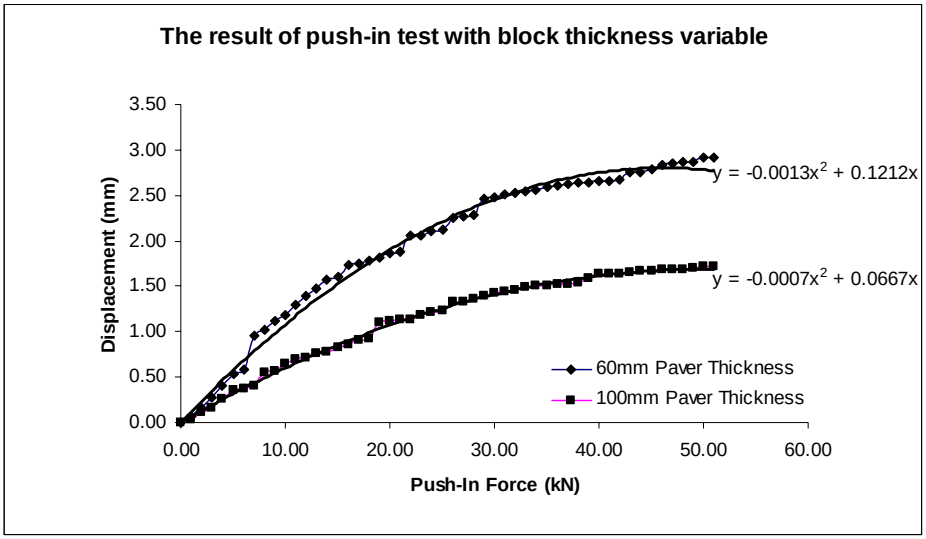

Figure E2.7 CBP specifications: rectangular block shape, 70 mm bedding sand thick, stretcher bond laying pattern, 3 mm joint width and 0 % degree of slope.

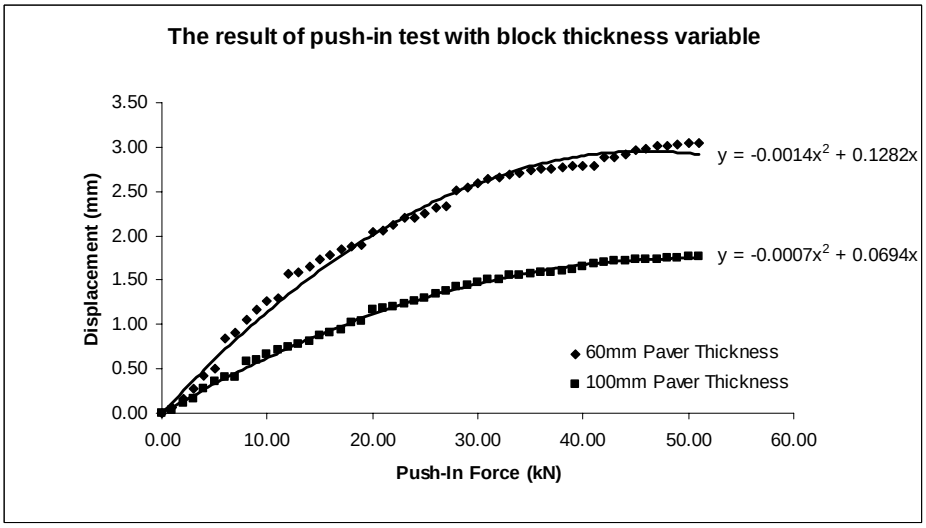

Figure E2.8 CBP specifications: rectangular block shape, 70 mm bedding sand thick, stretcher bond laying pattern, 5 mm joint width and 0 % degree of slope.

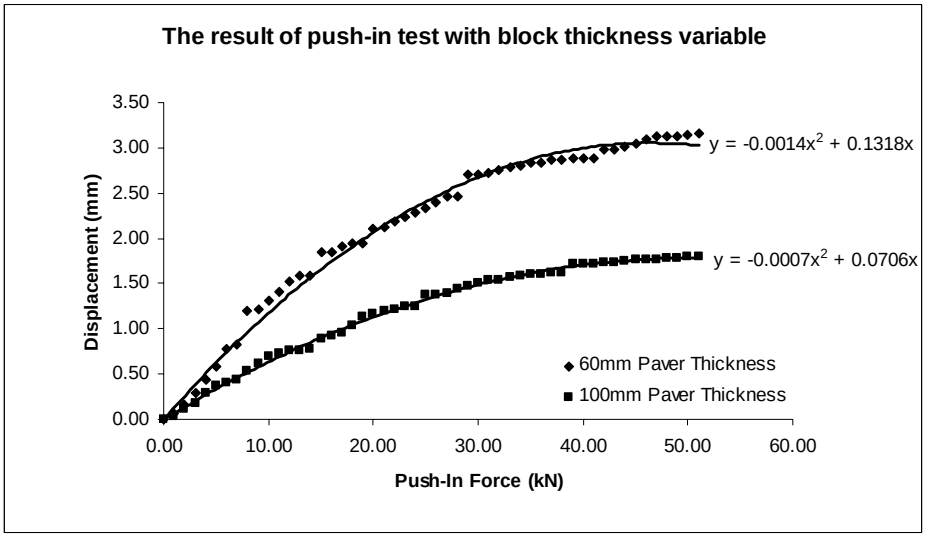

Figure E2.9 CBP specifications: rectangular block shape, 70 mm bedding sand thick, stretcher bond laying pattern, 7 mm joint width and 0 % degree of slope.

APPENDIX – E2

Horizontal Creep on Push-in Test CBP 0 % Slope
The Effect of Block Thickness

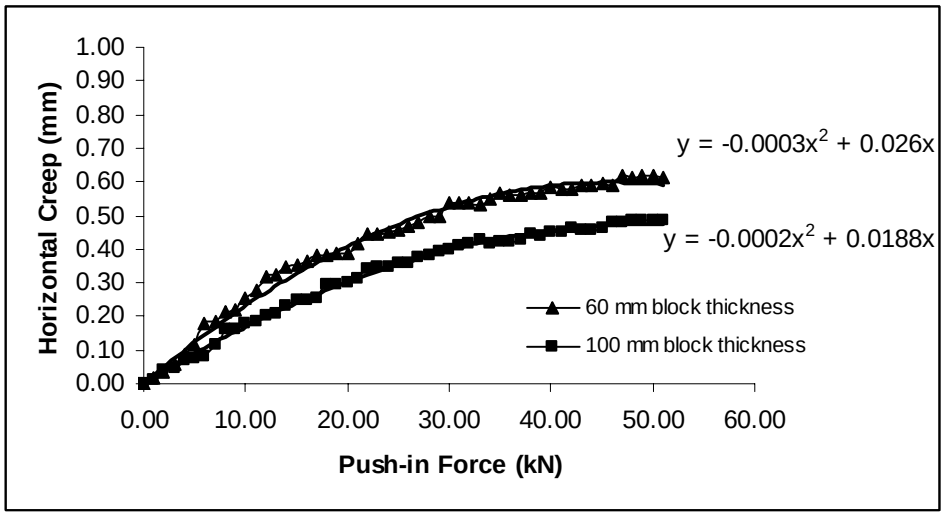

Figure E2.1 CBP specifications: rectangular block shape, 30 mm bedding sand thick, stretcher bond laying pattern, 3 mm joint width and 0 % degree of slope.

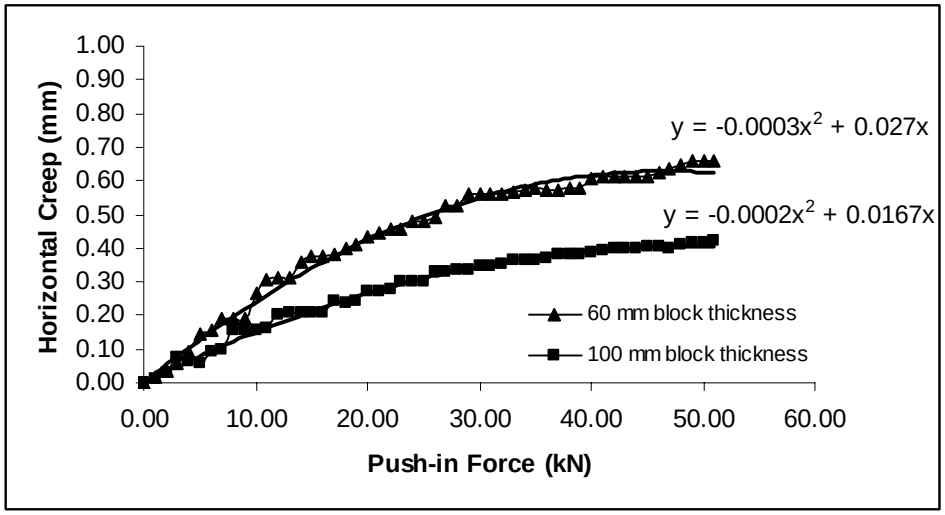

Figure E2.2 CBP specifications: rectangular block shape, 30 mm bedding sand thick, stretcher bond laying pattern, 5 mm joint width and 0 % degree of slope.

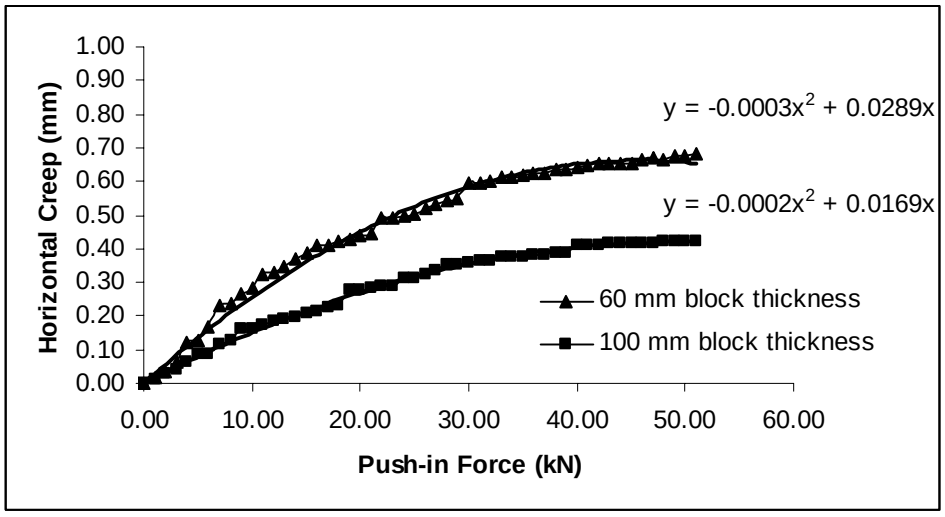

Figure E2.3 CBP specifications: rectangular block shape, 30 mm bedding sand thick, stretcher bond laying pattern, 7 mm joint width and 0 % degree of slope.

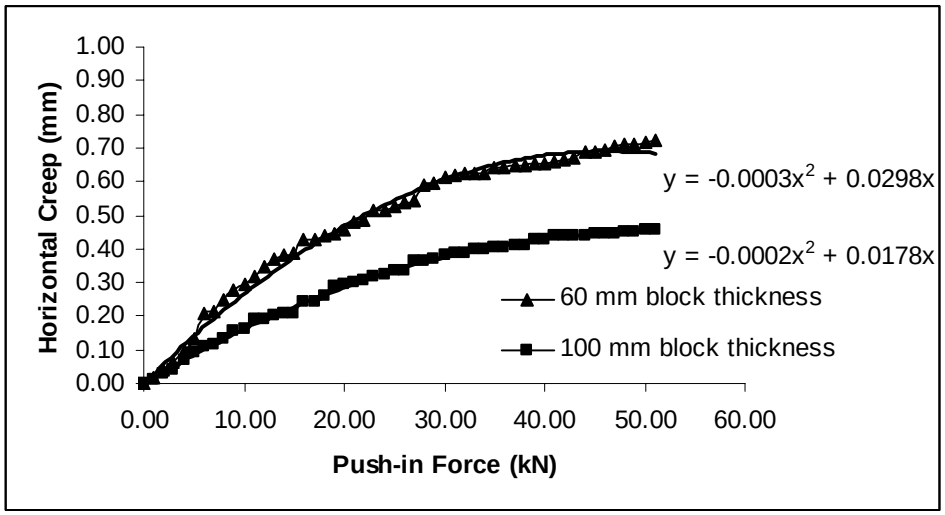

Figure E2.4 CBP specifications: rectangular block shape, 50 mm bedding sand thick, stretcher bond laying pattern, 3 mm joint width and 0 % degree of slope.

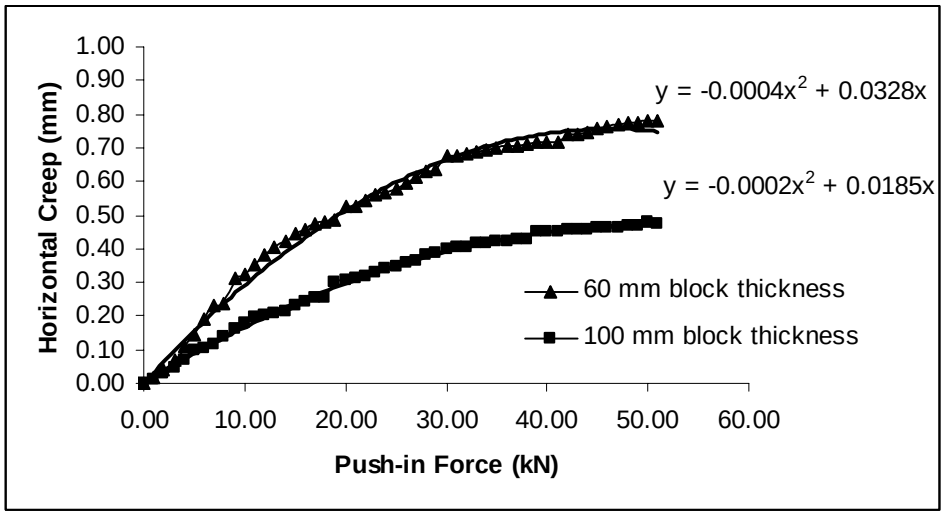

Figure E2.5 CBP specifications: rectangular block shape, 50 mm bedding sand thick, stretcher bond laying pattern, 5 mm joint width and 0 % degree of slope.

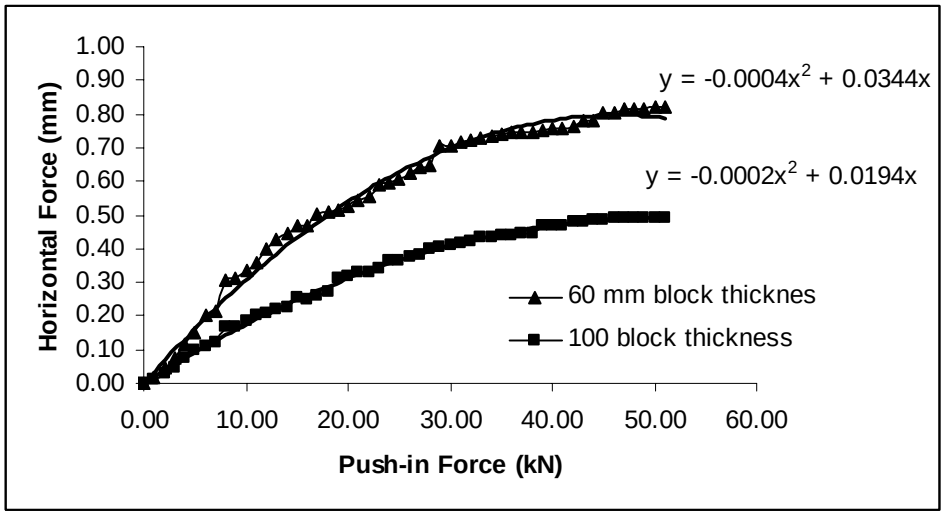

Figure E2.6 CBP specifications: rectangular block shape, 50 mm bedding sand thick, stretcher bond laying pattern, 7 mm joint width and 0 % degree of slope.

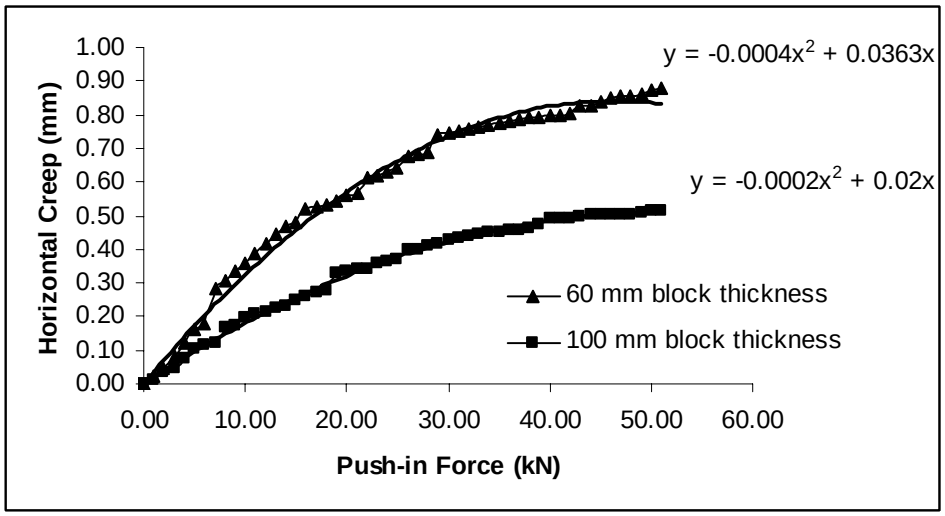

Figure E2.7 CBP specifications: rectangular block shape, 70 mm bedding sand thick, stretcher bond laying pattern, 3 mm joint width and 0 % degree of slope.

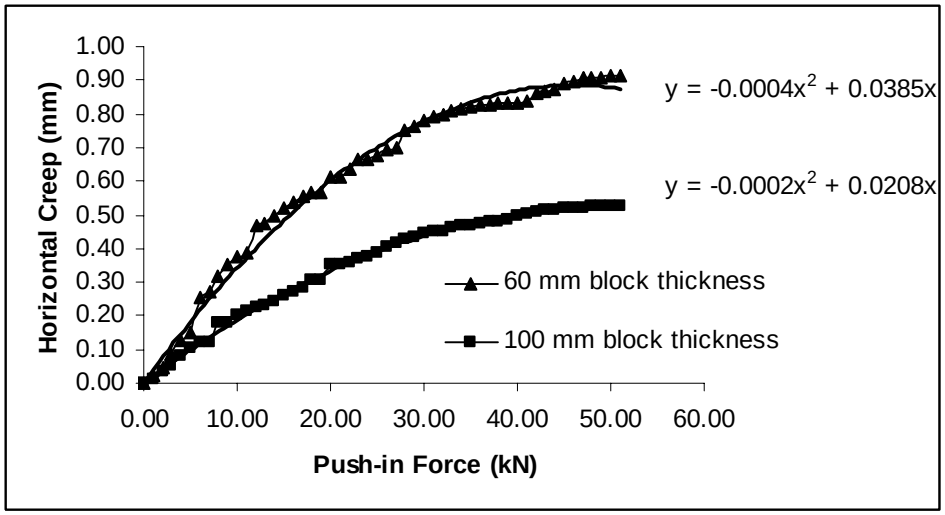

Figure E2.8 CBP specifications: rectangular block shape, 70 mm bedding sand thick, stretcher bond laying pattern, 5 mm joint width and 0 % degree of slope.

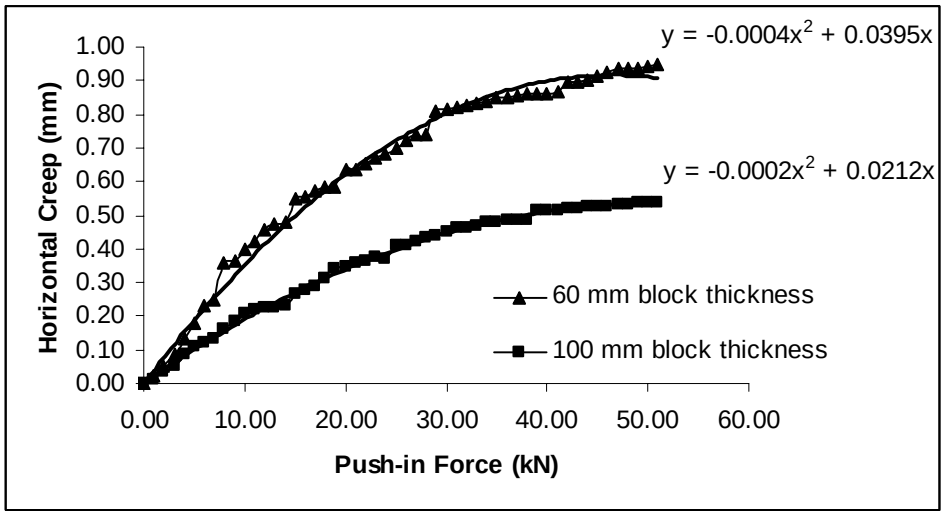

Figure E2.9 CBP specifications: rectangular block shape, 70 mm bedding sand thick, stretcher bond laying pattern, 7 mm joint width and 0 % degree of slope.

APPENDIX – E3

Push-in Test on CBP 0 % Slope
The Effect of Joint Width

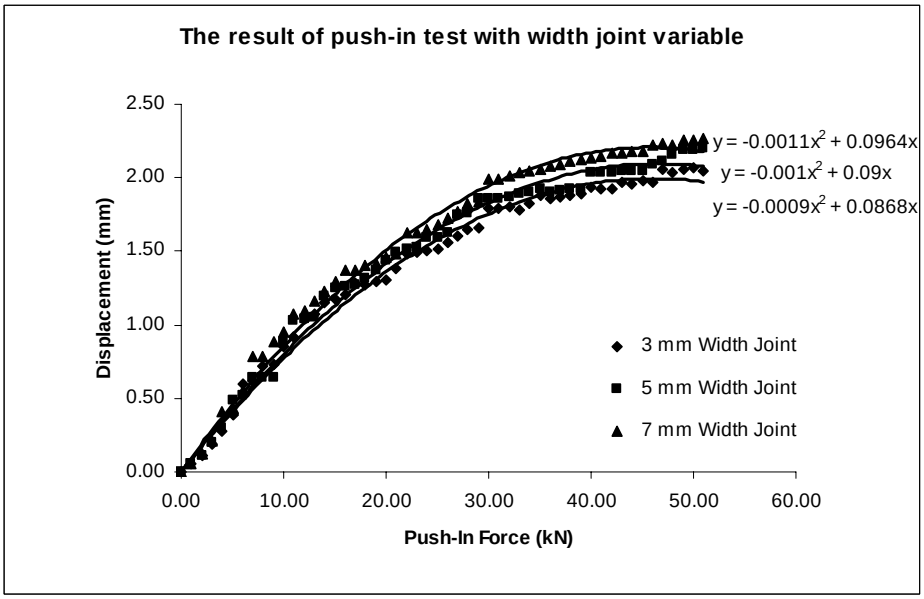

Figure E3.1 CBP specifications: rectangular block shape, 60 mm block thick, stretcher bond laying pattern, 30 mm bedding sand thick and 0 % degree of slope.

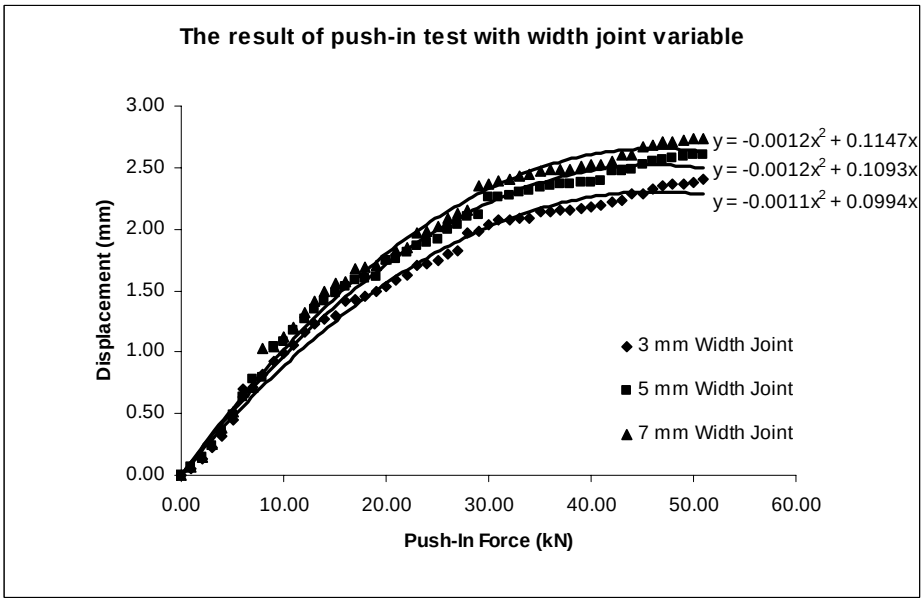

Figure E3.2 CBP specifications: rectangular block shape, 60 mm block thick, stretcher bond laying pattern, 50 mm bedding sand thick and 0 % degree of slope.

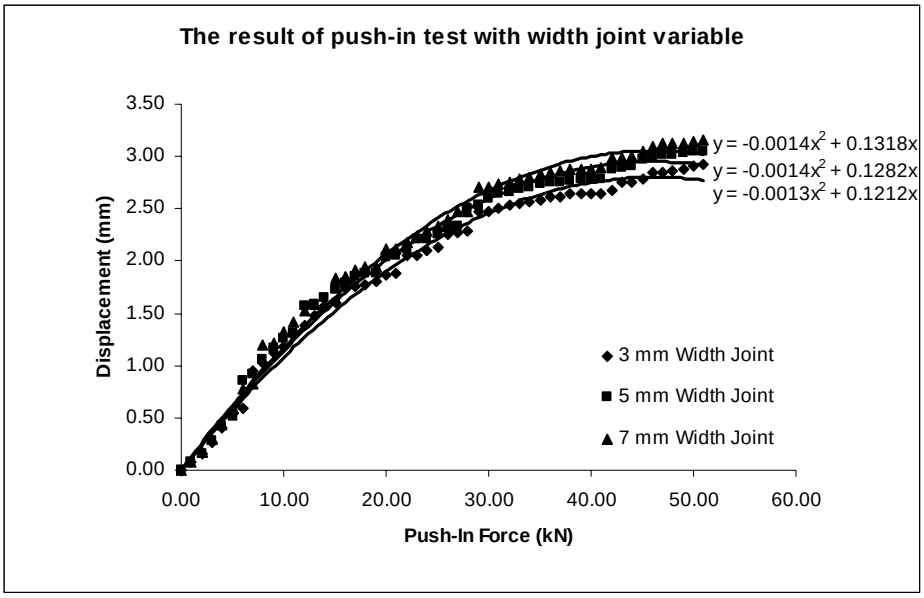

Figure E3.3 CBP specifications: rectangular block shape, 60 mm block thick, stretcher bond laying pattern, 70 mm bedding sand thick and 0 % degree of slope.

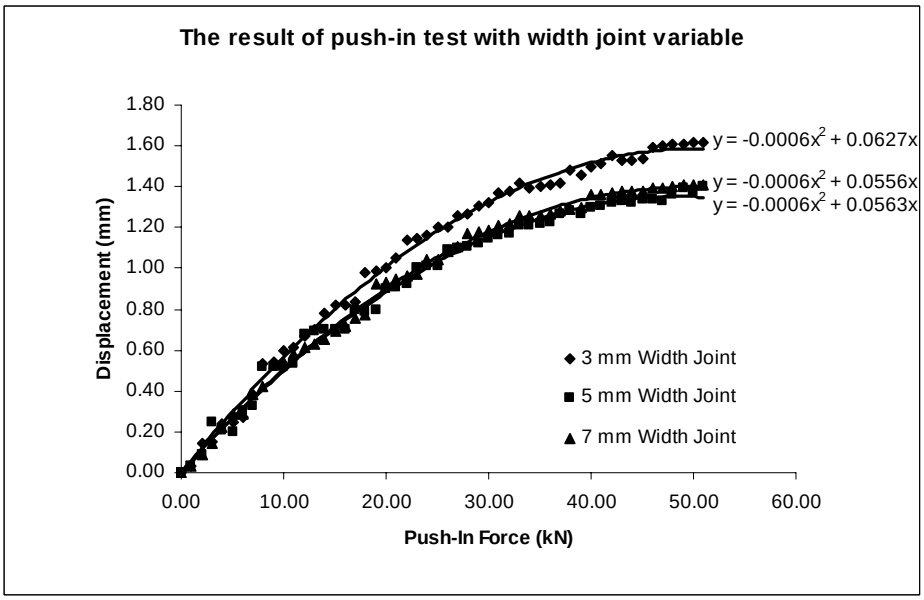

Figure E3.4 CBP specifications: rectangular shape, 100 mm block thick, stretcher bond laying pattern, 30 mm bedding sand thick and 0 % degree of slope.

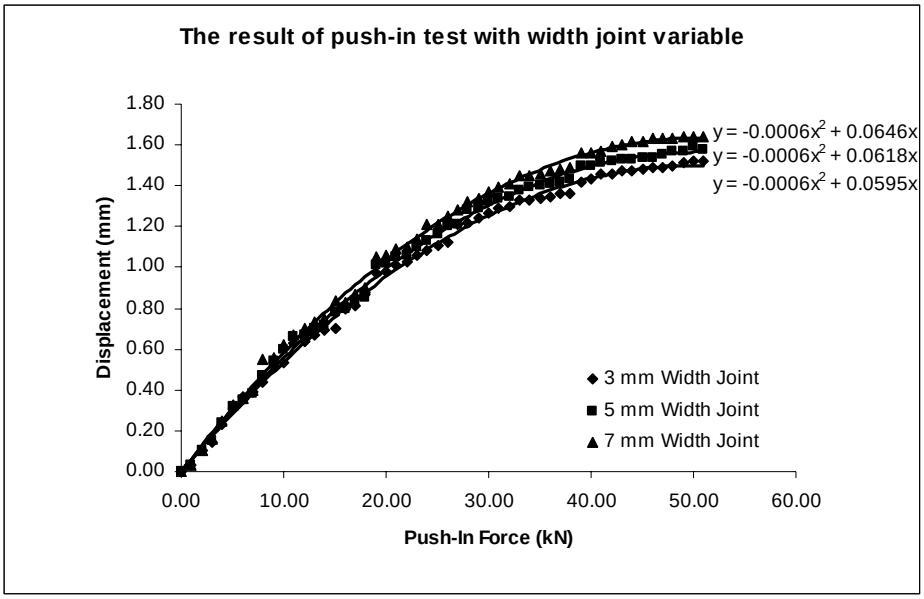

Figure E3.5 CBP specifications: rectangular shape, 100 mm block thick, stretcher bond laying pattern, 50 mm bedding sand thick and 0 % degree of slope.

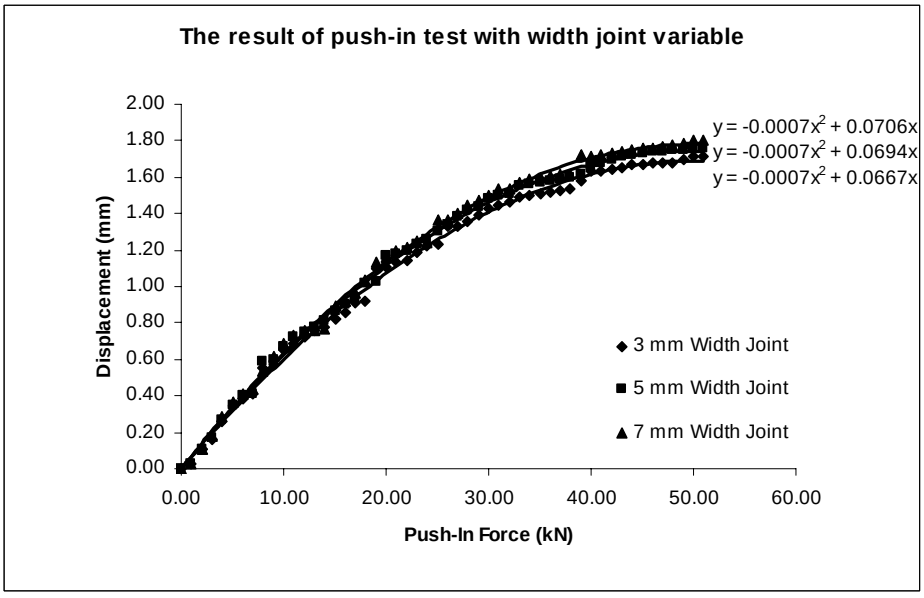

Figure E3.6 CBP specifications: rectangular shape, 100 mm block thick, stretcher bond laying pattern, 70 mm bedding sand thick and 0 % degree of slope.

APPENDIX – E3

Horizontal Creep on Push-in Test CBP 0 % Slope
The Effect of Joint Width

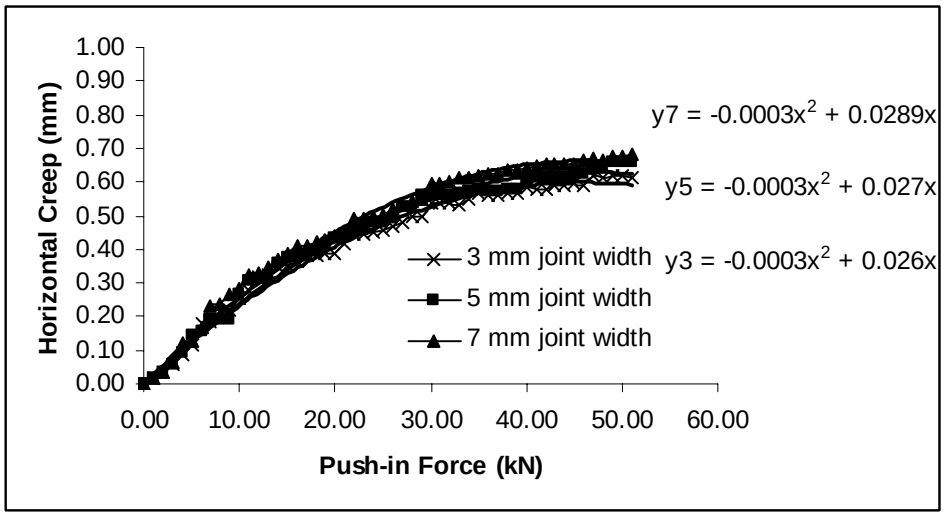

Figure E3.1 CBP specifications: rectangular block shape, 60 mm block thick, stretcher bond laying pattern, 30 mm bedding sand thick and 0 % degree of slope.

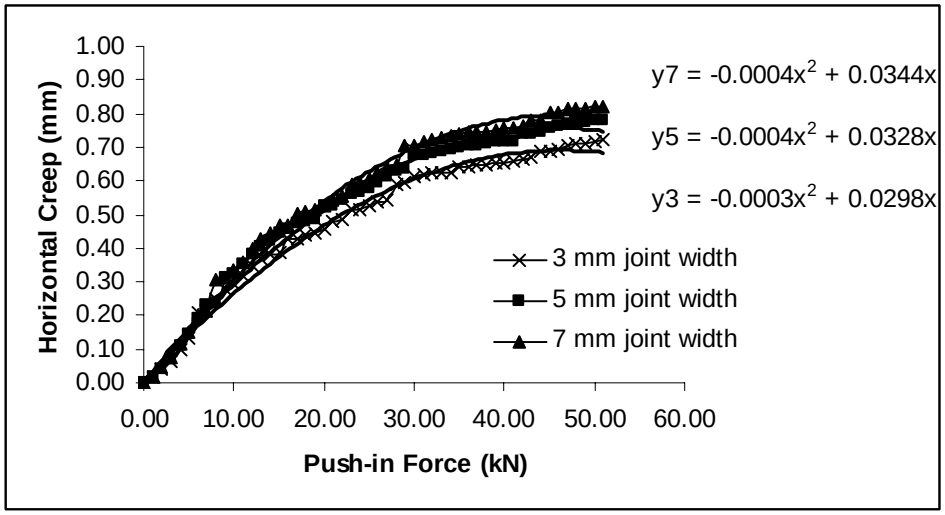

Figure E3.2 CBP specifications: rectangular block shape, 60 mm block thick, stretcher bond laying pattern, 50 mm bedding sand thick and 0 % degree of slope.

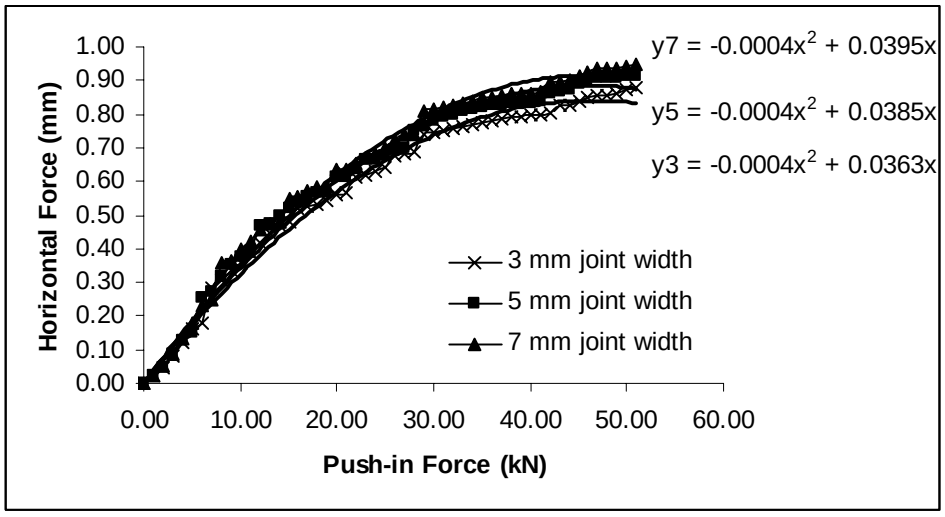

Figure E3.3 CBP specifications: rectangular block shape, 60 mm block thick, stretcher bond laying pattern, 70 mm bedding sand thick and 0 % degree of slope.

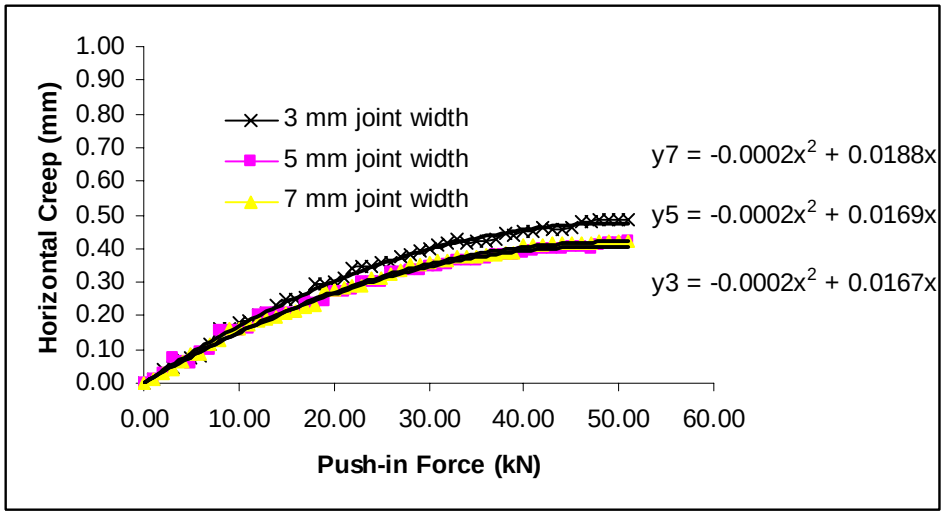

Figure E3.4 CBP specifications: rectangular shape, 100 mm block thick, stretcher bond laying pattern, 30 mm bedding sand thick and 0 % degree of slope.

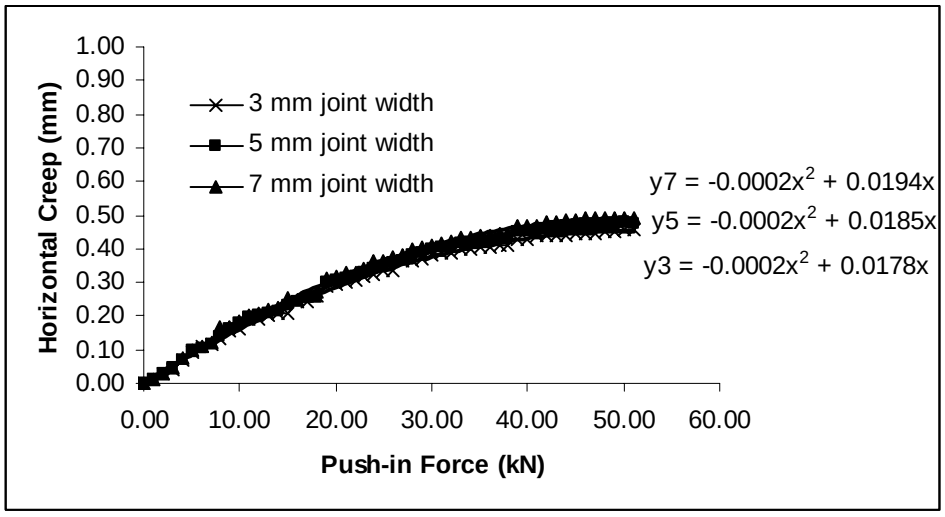

Figure E3.5 CBP specifications: rectangular shape, 100 mm block thick, stretcher bond laying pattern, 50 mm bedding sand thick and 0 % degree of slope.

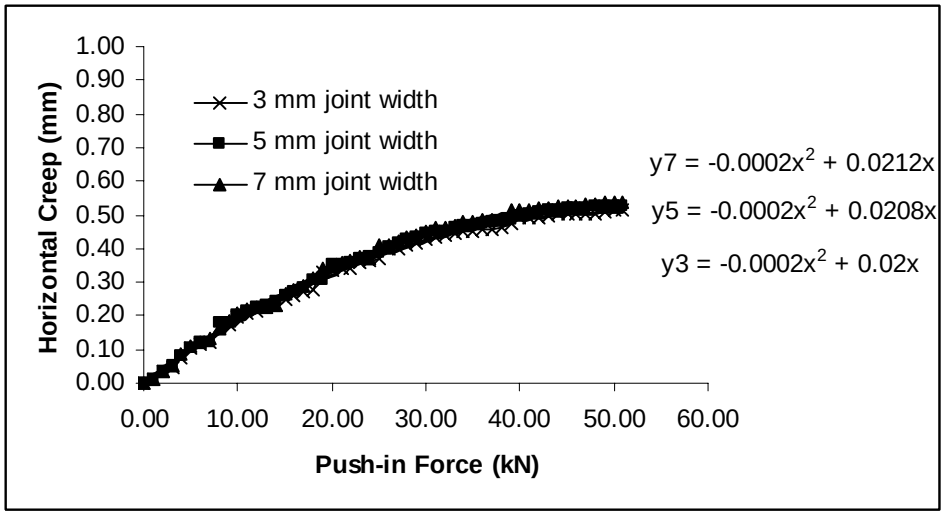

Figure E3.6 CBP specifications: rectangular shape, 100 mm block thick, stretcher bond laying pattern, 70 mm bedding sand thick and 0 % degree of slope.

APPENDIX – F1

Push-in Test on CBP 4 % Slope
The Effect of Bedding Sand Thickness

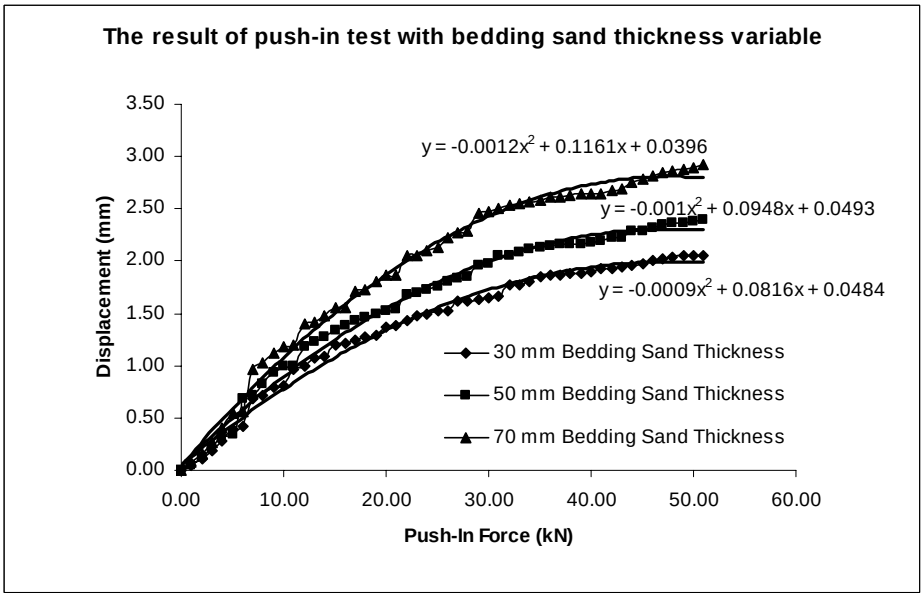

Figure F1.1 CBP specifications: rectangular block shape, 60 mm block thickness, stretcher bond laying pattern, 3 mm joint width and 4 % degree of slope.

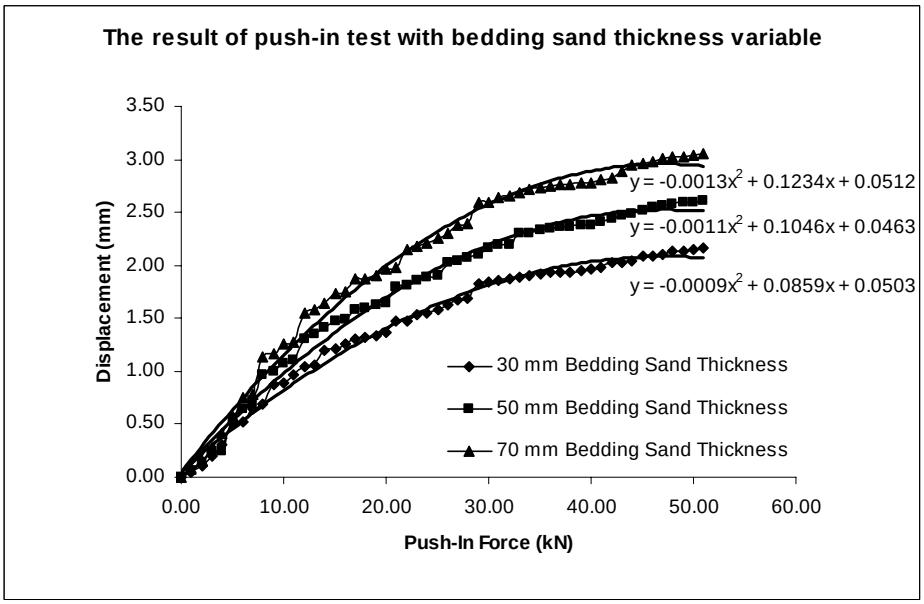

Figure F1.2 CBP specifications: rectangular block shape, 60 mm block thickness, stretcher bond laying pattern, 5 mm joint width and 4 % degree of slope.

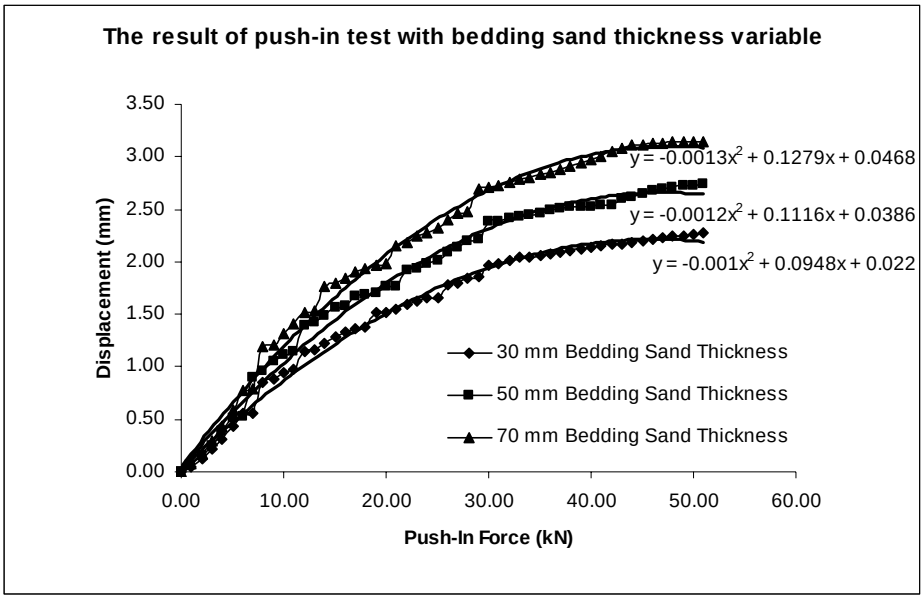

Figure F1.3 CBP specifications: rectangular block shape, 60 mm block thickness, stretcher bond laying pattern, 7 mm joint width and 4 % degree of slope.

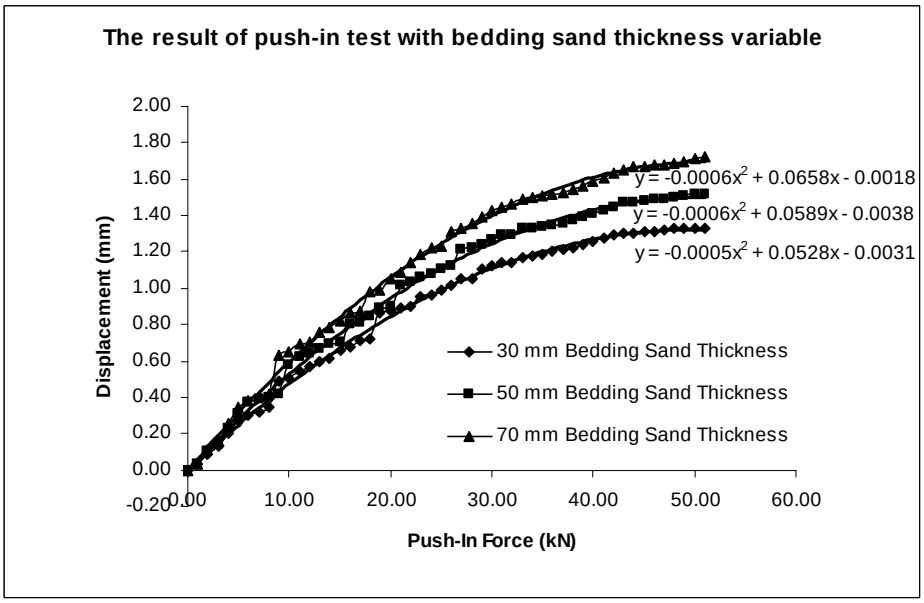

Figure F1.4 CBP specifications: rectangular block shape, 100 mm block thickness, stretcher bond laying pattern, 3 mm joint width and 4 % degree of slope.

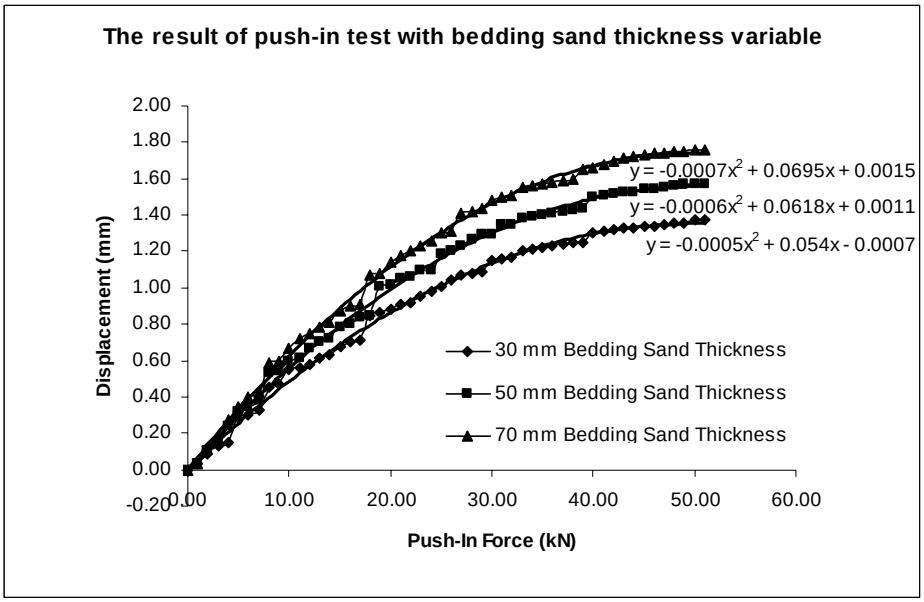

Figure F1.5 CBP specifications: rectangular block shape, 100 mm block thickness, stretcher bond laying pattern, 5 mm joint width and 4 % degree of slope.

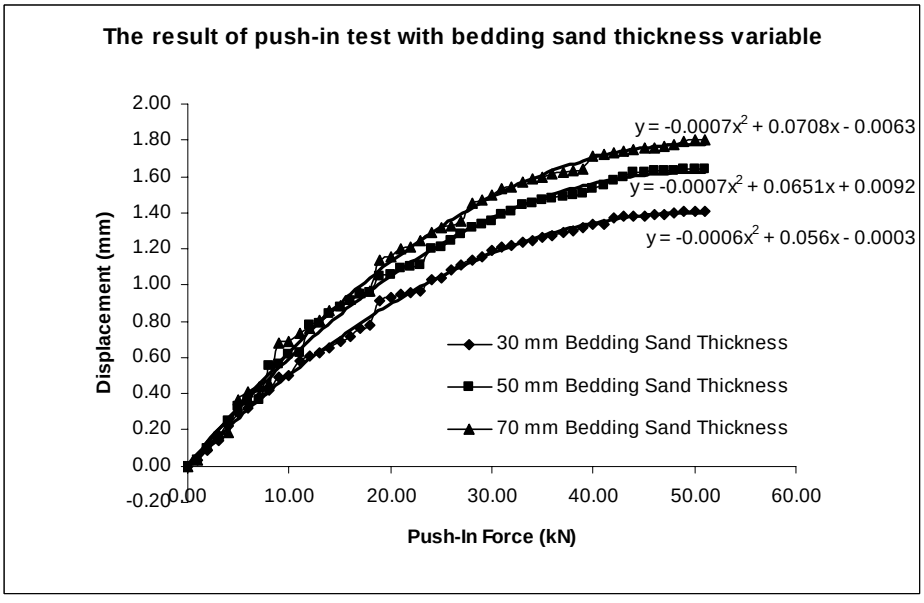

Figure F1.6 CBP specifications: rectangular block shape, 100 mm block thickness, stretcher bond laying pattern, 7 mm joint width and 4 % degree of slope.

APPENDIX – F1

Horizontal Creep on Push-in Test 4 % CBP Slope
The Effect of Bedding Sand Thickness

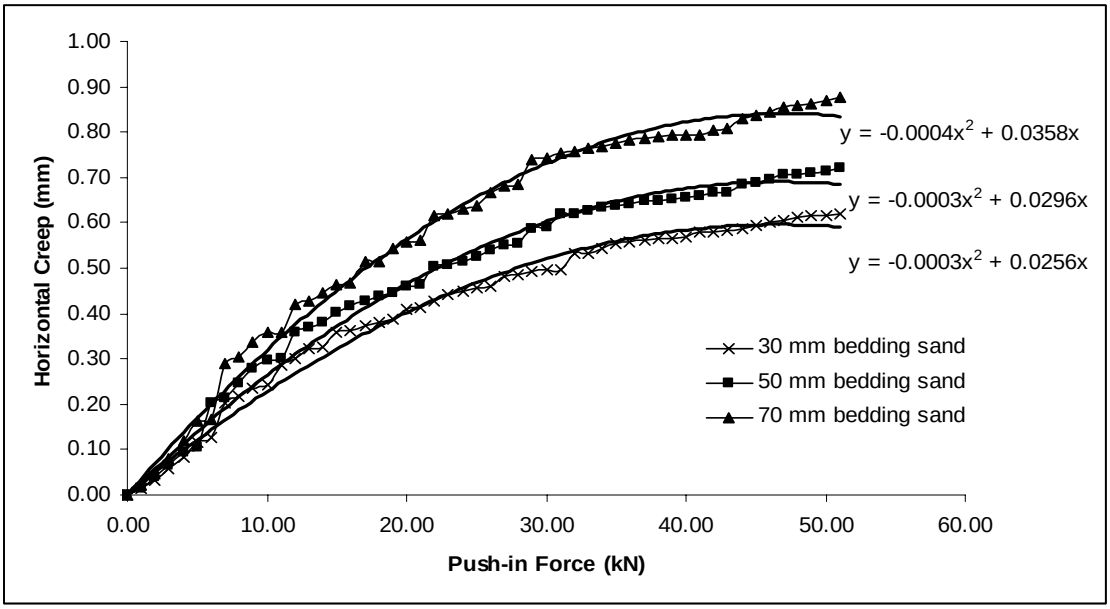

Figure F1.1 CBP specifications: rectangular block shape, 60 mm block thickness, stretcher bond laying pattern, 3 mm joint width and 4 % degree of slope.

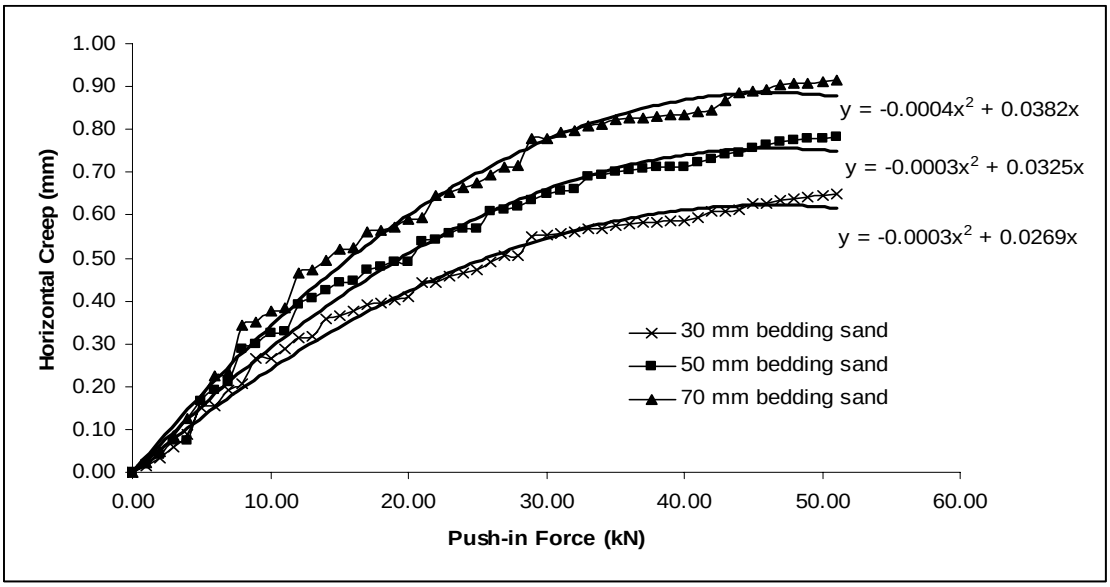

Figure F1.2 CBP specifications: rectangular block shape, 60 mm block thickness, stretcher bond laying pattern, 5 mm joint width and 4 % degree of slope.

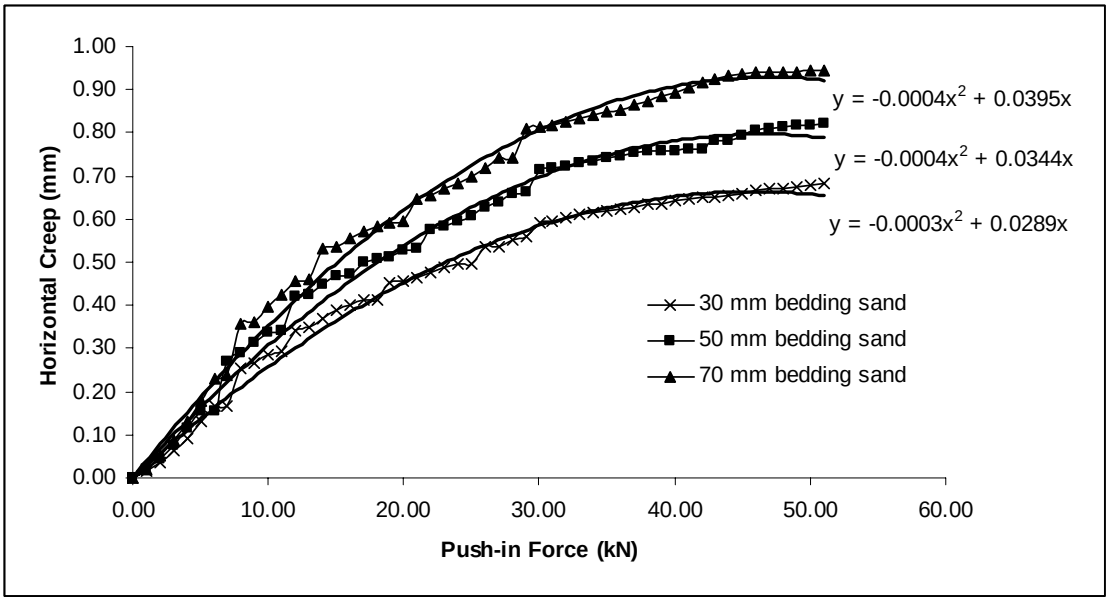

Figure F1.3 CBP specifications: rectangular block shape, 60 mm block thickness, stretcher bond laying pattern, 7 mm joint width and 4 % degree of slope.

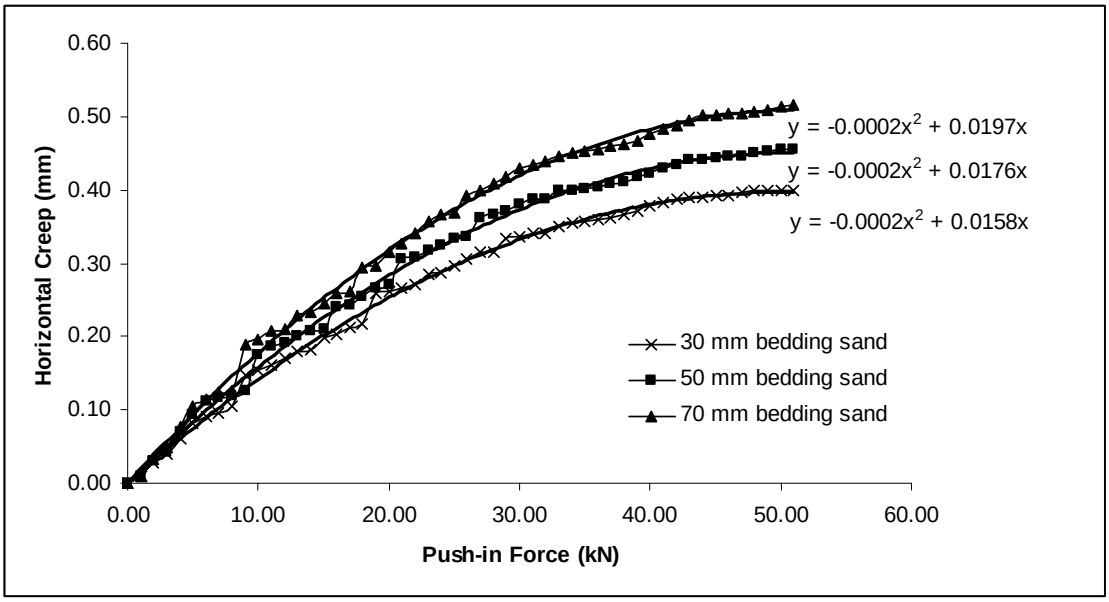

Figure F1.4 CBP specifications: rectangular block shape, 100 mm block thickness, stretcher bond laying pattern, 3 mm joint width and 4 % degree of slope.

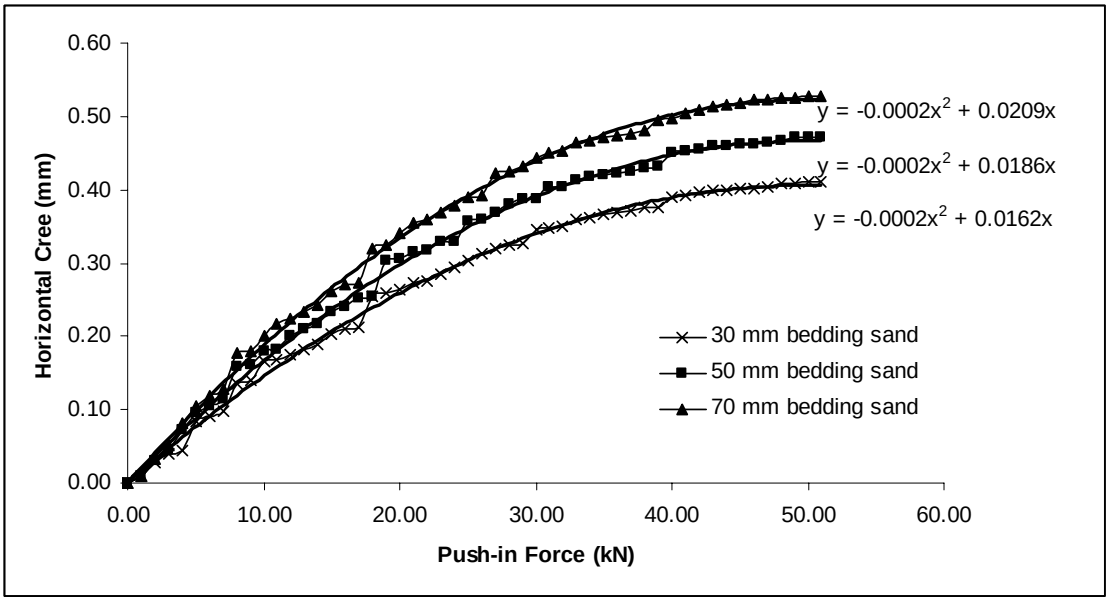

Figure F1.5 CBP specifications: rectangular block shape, 100 mm block thickness, stretcher bond laying pattern, 5 mm joint width and 4 % degree of slope.

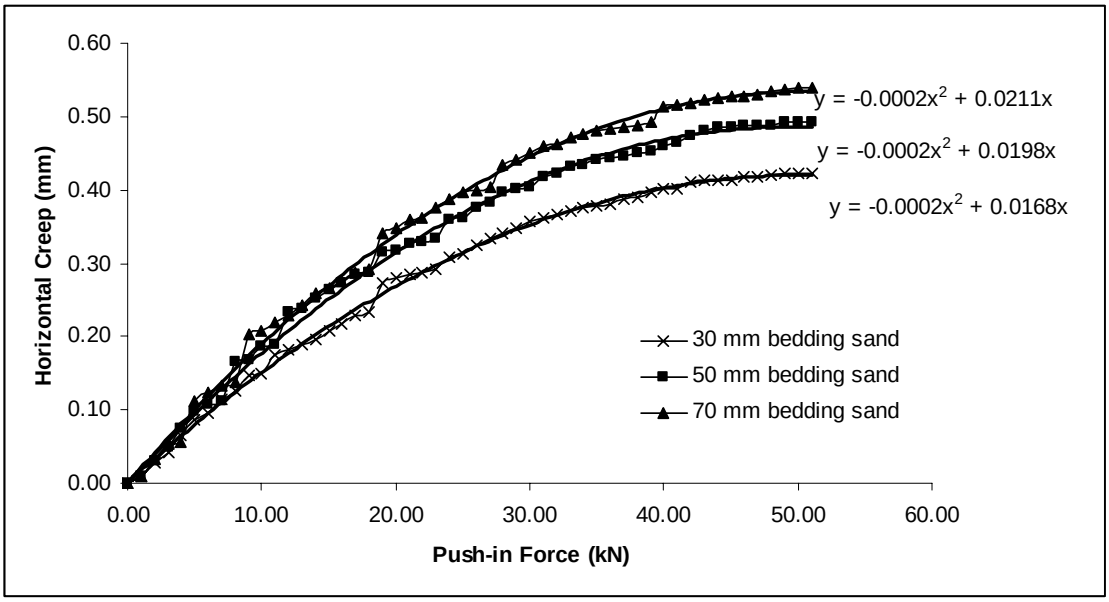

Figure F1.6 CBP specifications: rectangular block shape, 100 mm block thickness, stretcher bond laying pattern, 7 mm joint width and 4 % degree of slope.

APPENDIX – F2

Push-in Test on CBP 4 % Slope
The Effect of Block Thickness

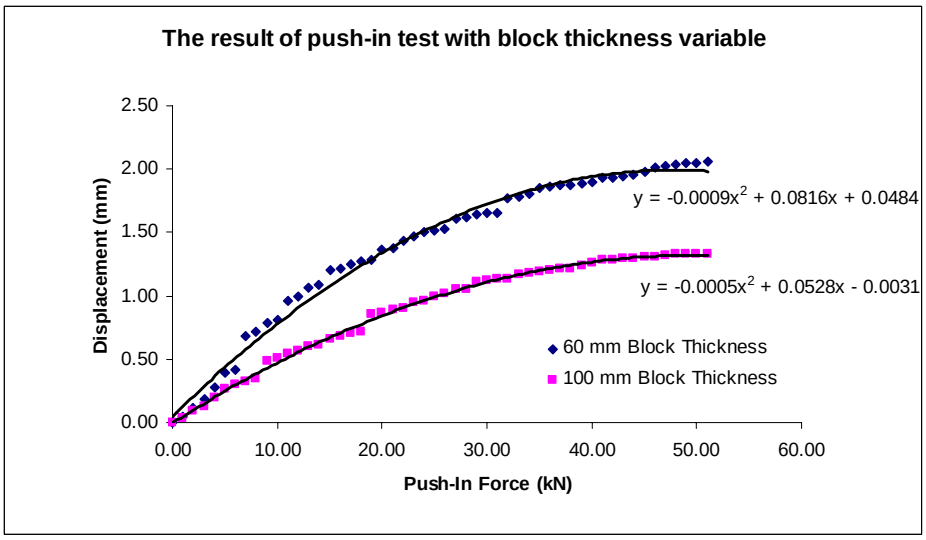

Figure F2.1 CBP specifications: rectangular block shape, 30 mm bedding sand thick, stretcher bond laying pattern, 3 mm joint width and 4 % degree of slope.

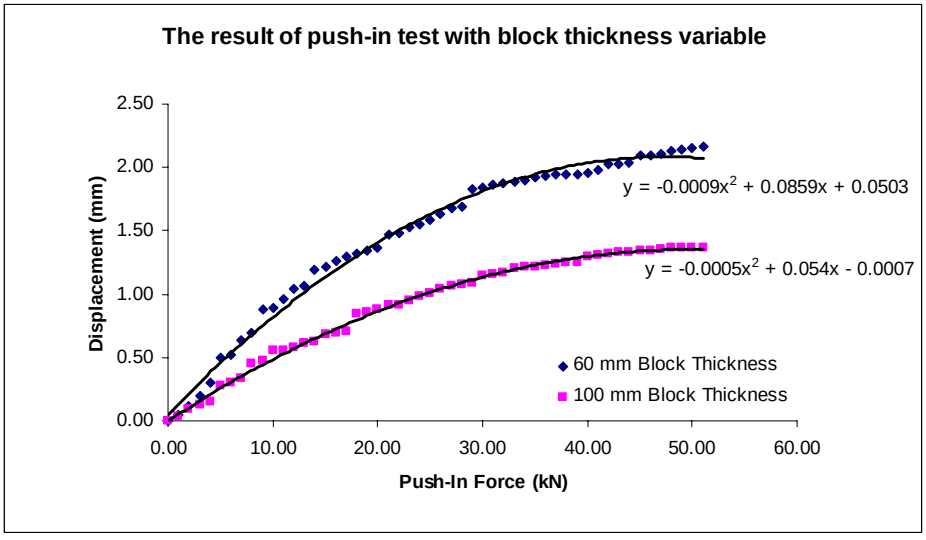

Figure F2.2 CBP specifications: rectangular block shape, 30 mm bedding sand thick, stretcher bond laying pattern, 5 mm joint width and 4 % degree of slope.

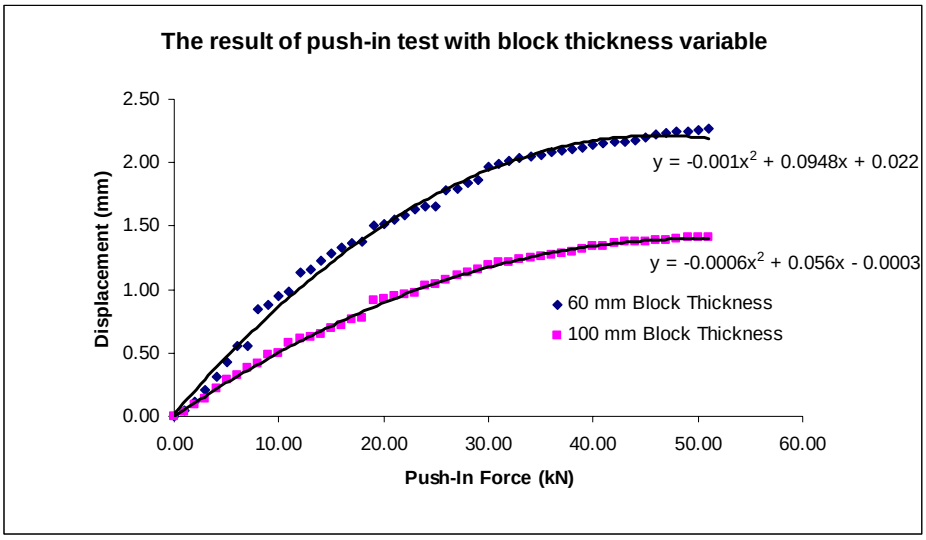

Figure E2.3 CBP specifications: rectangular block shape, 30 mm bedding sand thick, stretcher bond laying pattern, 7 mm joint width and 4 % degree of slope.

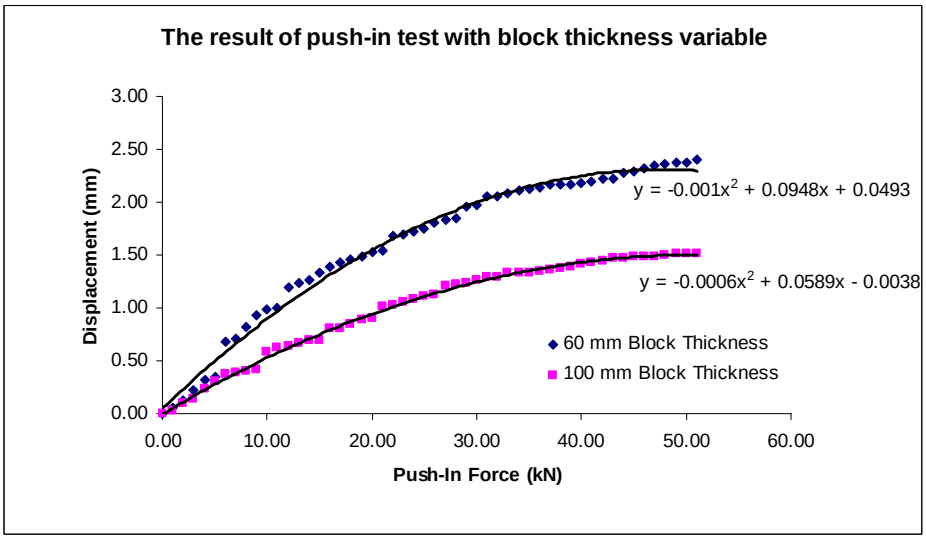

Figure F2.4 CBP specifications: rectangular block shape, 50 mm bedding sand thick, stretcher bond laying pattern, 3 mm joint width and 4 % degree of slope.

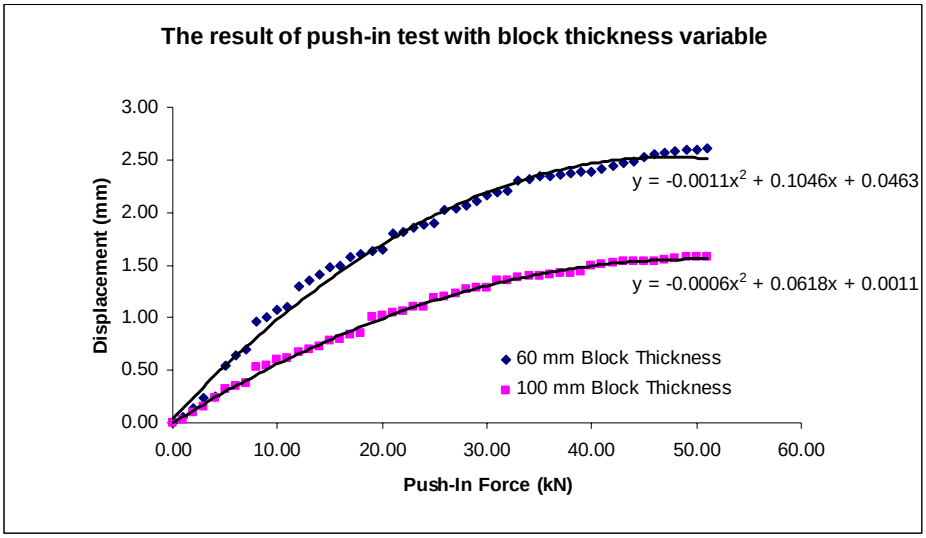

Figure F2.5 CBP specifications: rectangular block shape, 50 mm bedding sand thick, stretcher bond laying pattern, 5 mm joint width and 4 % degree of slope.

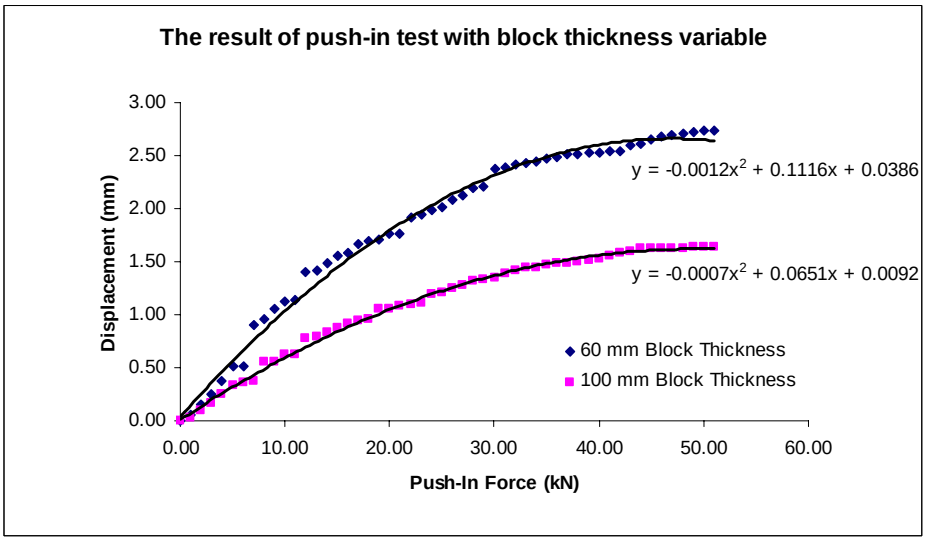

Figure F2.6 CBP specifications: rectangular block shape, 50 mm bedding sand thick, stretcher bond laying pattern, 7 mm joint width and 4 % degree of slope.

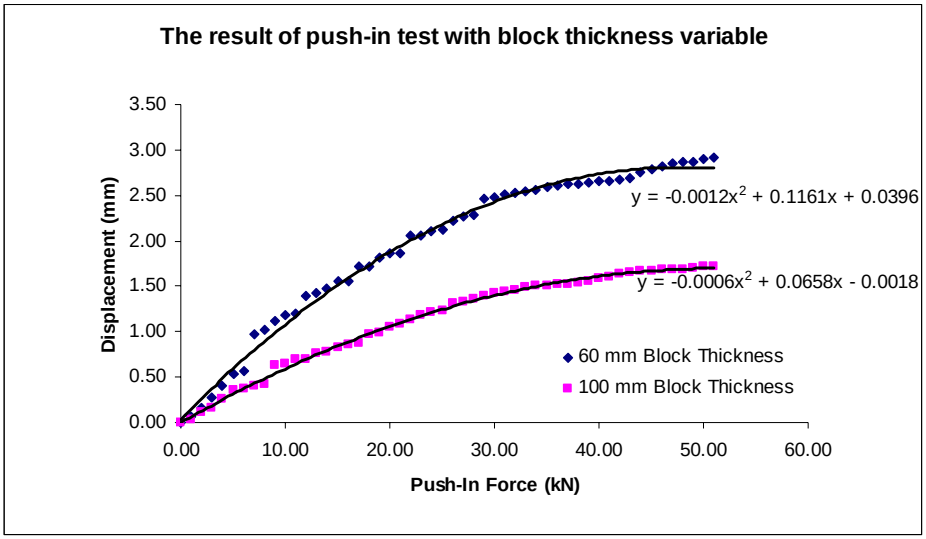

Figure F2.7 CBP specifications: rectangular block shape, 70 mm bedding sand thick, stretcher bond laying pattern, 3 mm joint width and 4 % degree of slope.

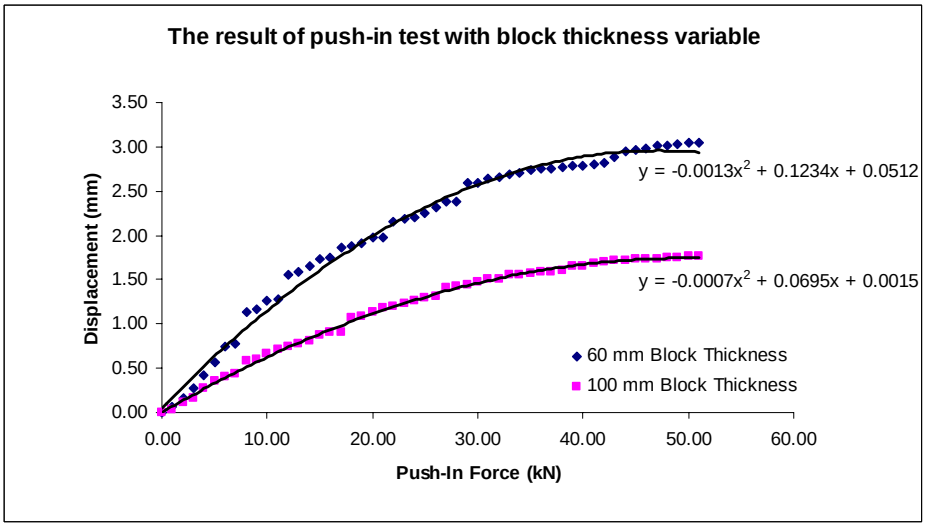

Figure F2.8 CBP specifications: rectangular block shape, 70 mm bedding sand thick, stretcher bond laying pattern, 5 mm joint width and 4 % degree of slope.

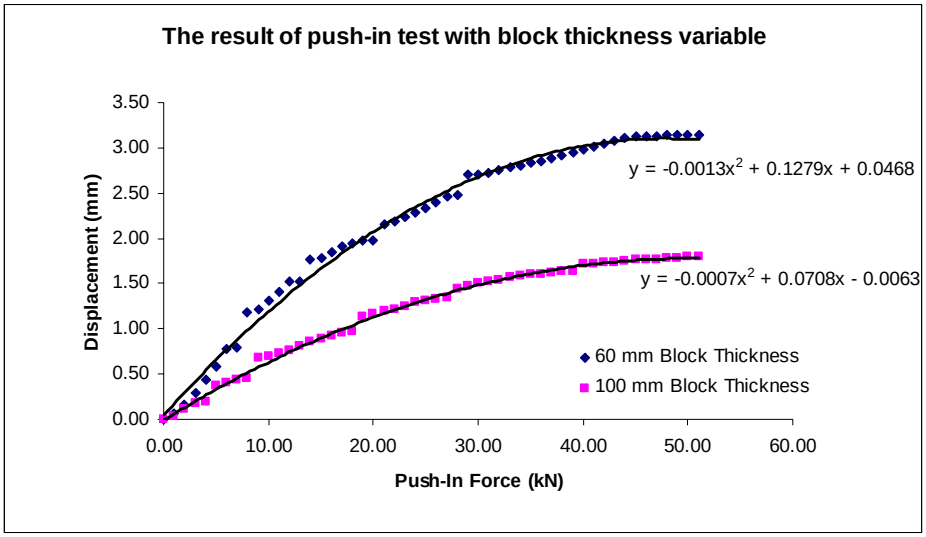

Figure F2.9 CBP specifications: rectangular block shape, 70 mm bedding sand thick, stretcher bond laying pattern, 7 mm joint width and 4 % degree of slope.

APPENDIX – F2

Horizontal Creep on Push-in Test CBP 4 % Slope
The Effect of Block Thickness

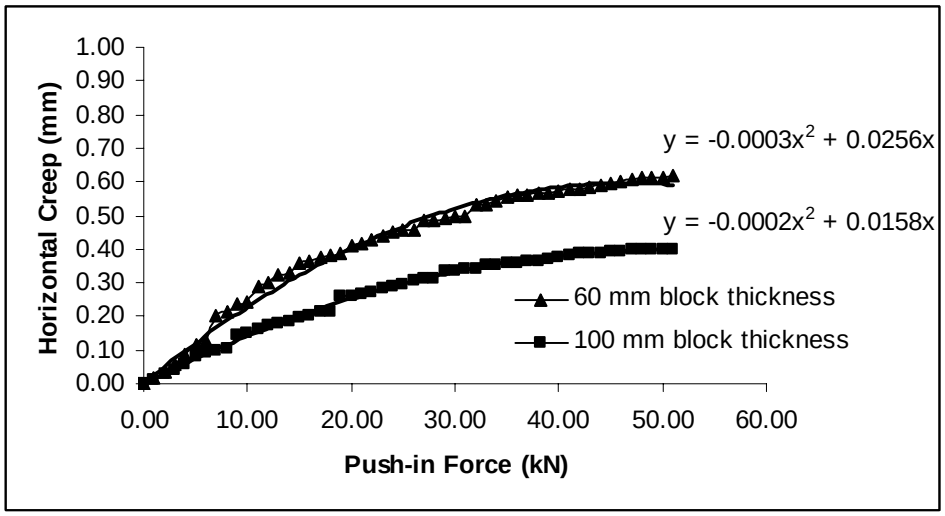

Figure F2.1 CBP specifications: rectangular block shape, 30 mm bedding sand thick, stretcher bond laying pattern, 3 mm joint width and 4 % degree of slope.

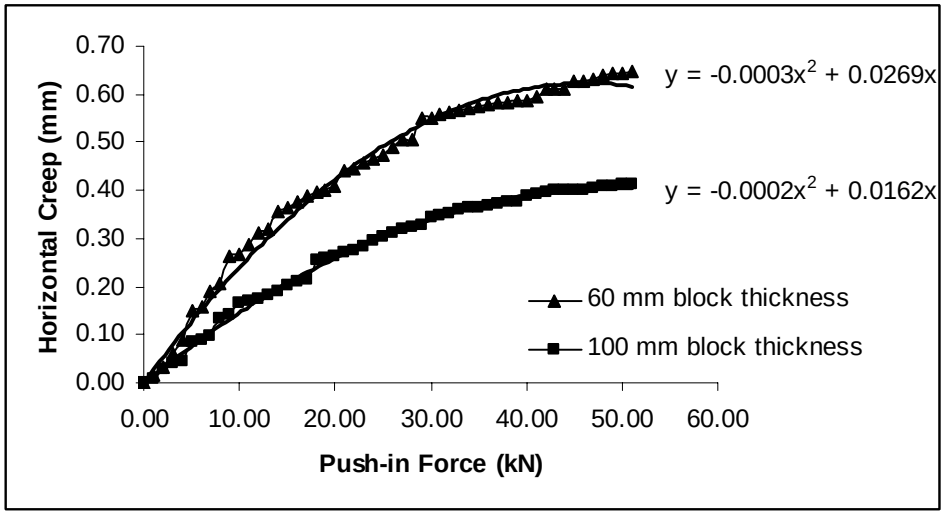

Figure F2.2 CBP specifications: rectangular block shape, 30 mm bedding sand thick, stretcher bond laying pattern, 5 mm joint width and 4 % degree of slope.

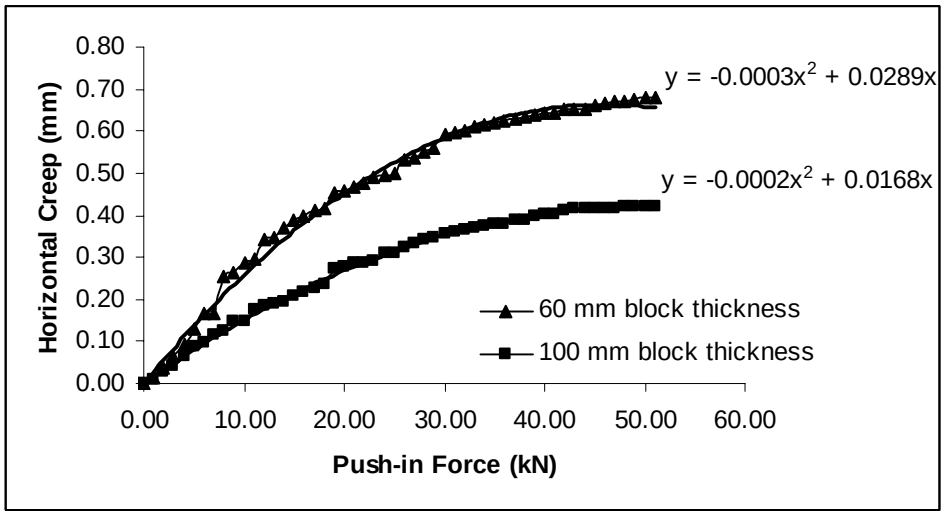

Figure E2.3 CBP specifications: rectangular block shape, 30 mm bedding sand thick, stretcher bond laying pattern, 7 mm joint width and 4 % degree of slope.

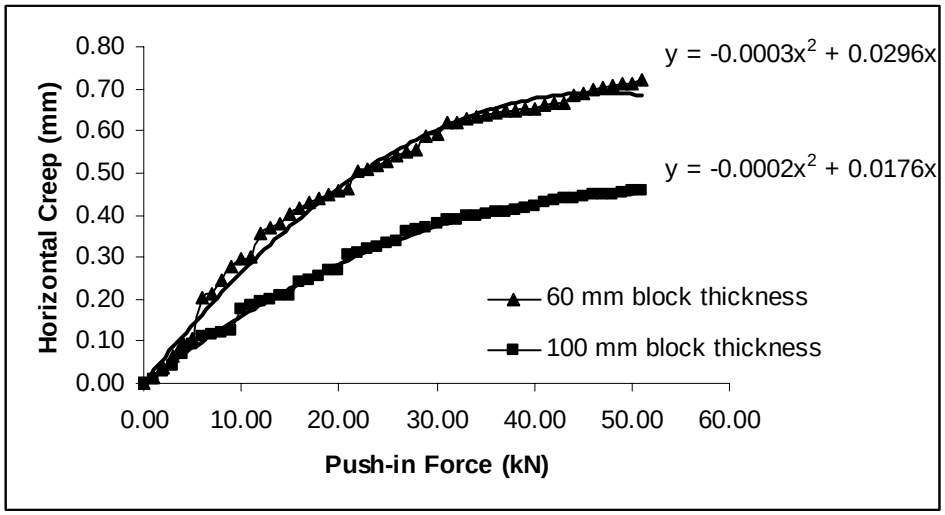

Figure F2.4 CBP specifications: rectangular block shape, 50 mm bedding sand thick, stretcher bond laying pattern, 3 mm joint width and 4 % degree of slope.

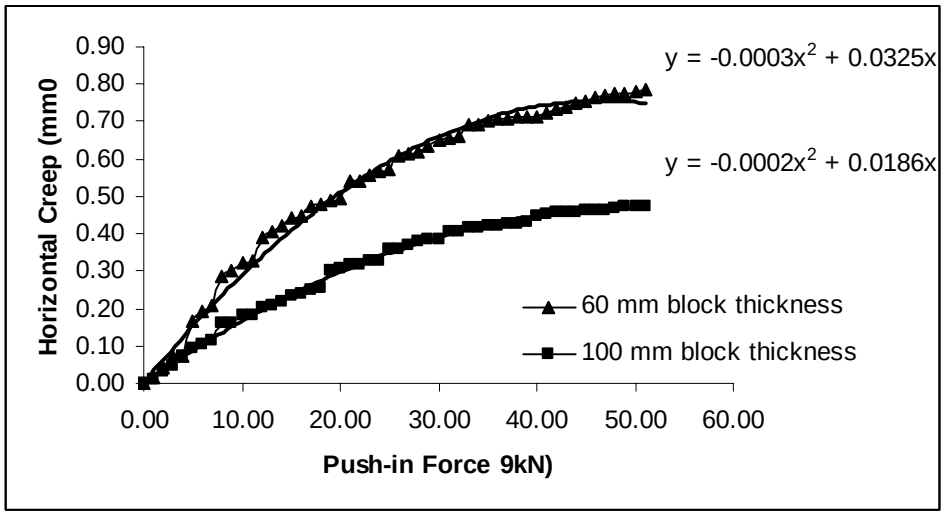

Figure F2.5 CBP specifications: rectangular block shape, 50 mm bedding sand thick, stretcher bond laying pattern, 5 mm joint width and 4 % degree of slope.

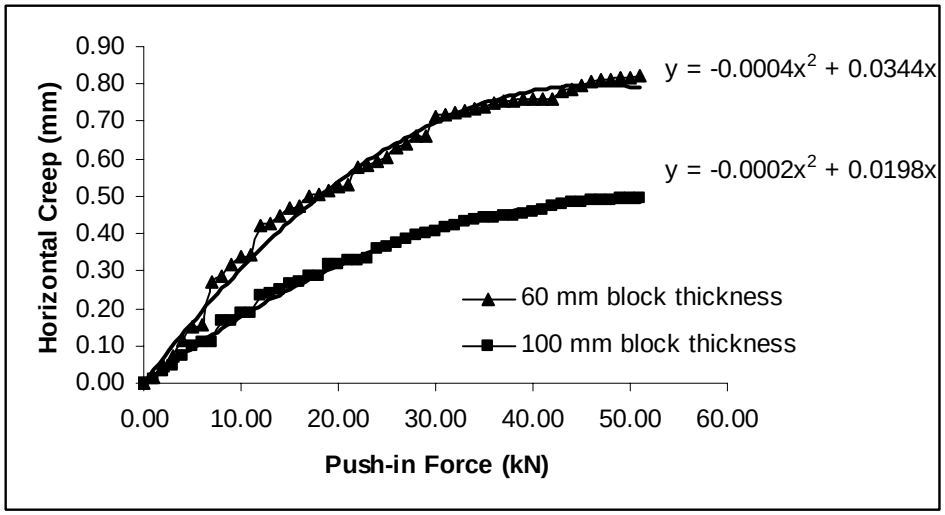

Figure F2.6 CBP specifications: rectangular block shape, 50 mm bedding sand thick, stretcher bond laying pattern, 7 mm joint width and 4 % degree of slope.

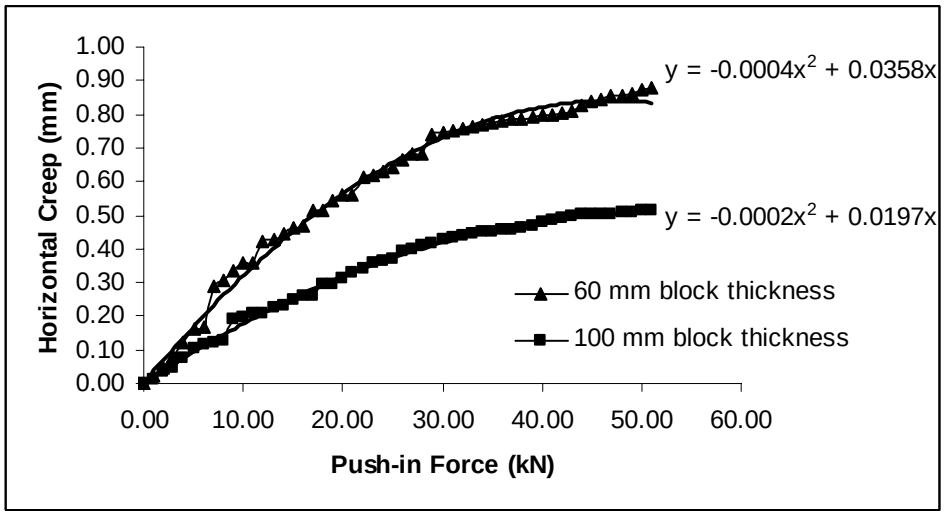

Figure F2.7 CBP specifications: rectangular block shape, 70 mm bedding sand thick, stretcher bond laying pattern, 3 mm joint width and 4 % degree of slope.

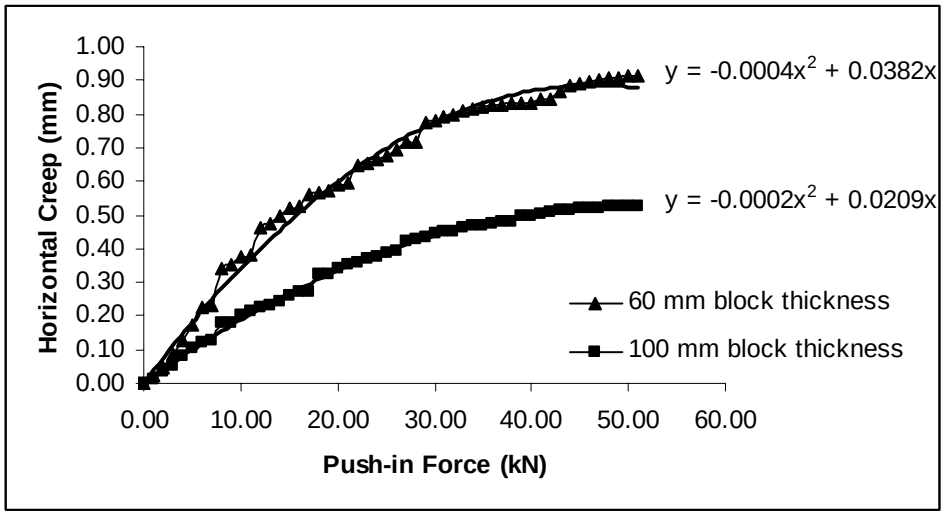

Figure F2.8 CBP specifications: rectangular block shape, 70 mm bedding sand thick, stretcher bond laying pattern, 5 mm joint width and 4 % degree of slope.

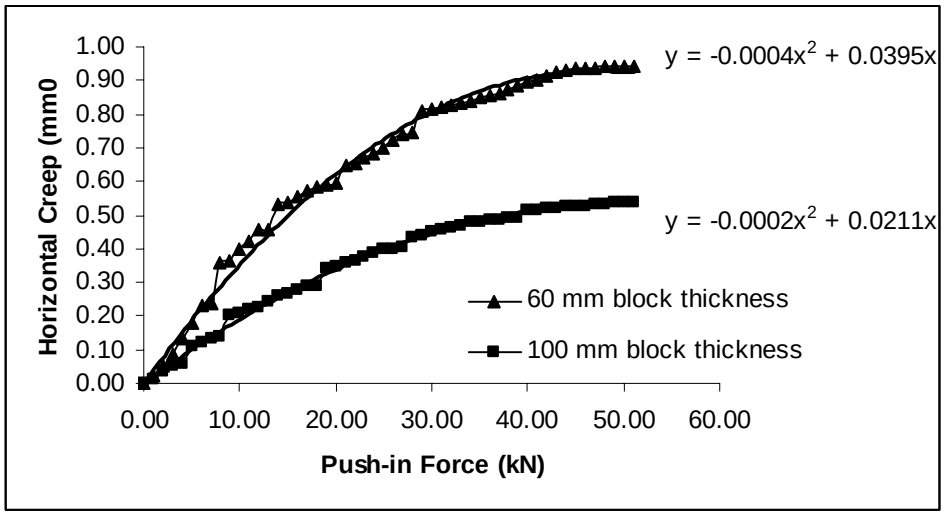

Figure F2.9 CBP specifications: rectangular block shape, 70 mm bedding sand thick, stretcher bond laying pattern, 7 mm joint width and 4 % degree of slope.

APPENDIX – F3

Push-in Test on CBP 4 % Slope
The Effect of Joint Width

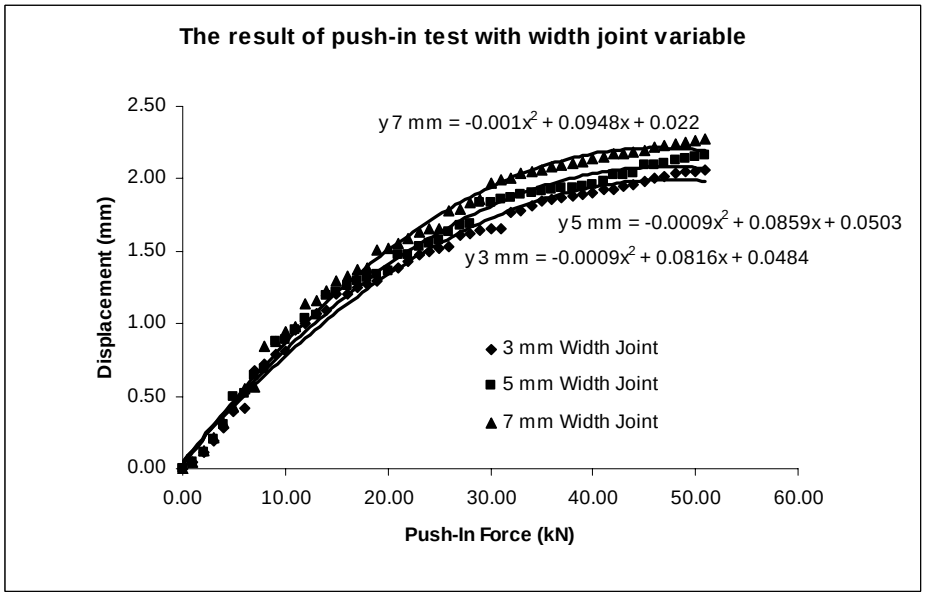

Figure F3.1 CBP specifications: rectangular block shape, 60 mm block thick, stretcher bond laying pattern, 30 mm bedding sand thick and 4 % degree of slope.

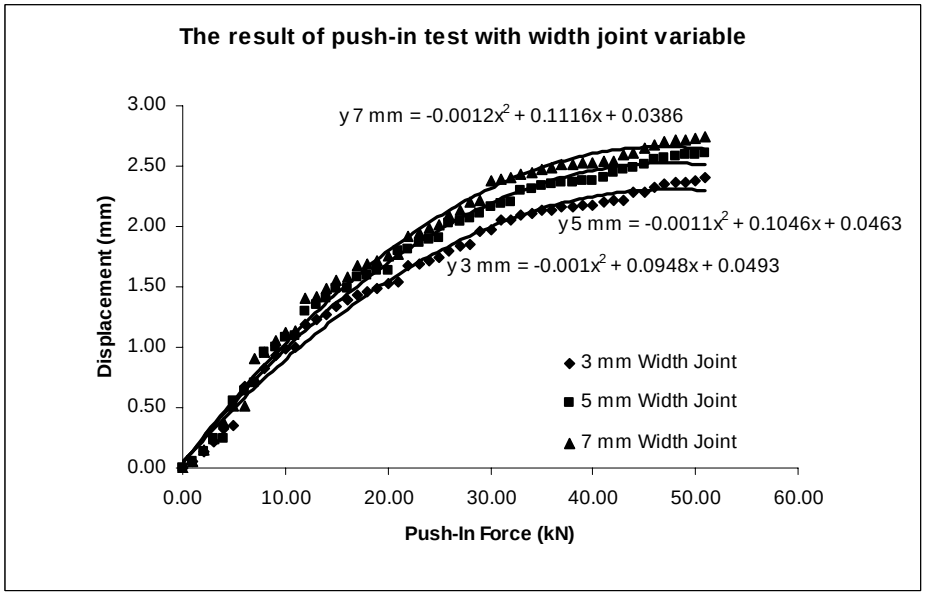

Figure F3.2 CBP specifications: rectangular block shape, 60 mm block thick, stretcher bond laying pattern, 50 mm bedding sand thick and 4 % degree of slope.

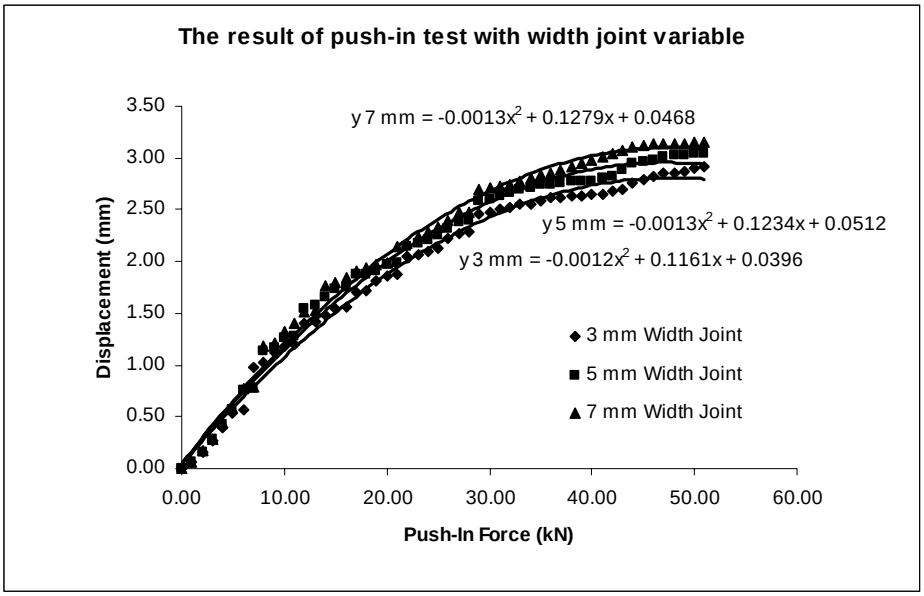

Figure F3.3 CBP specifications: rectangular block shape, 60 mm block thick, stretcher bond laying pattern, 70 mm bedding sand thick and 4 % degree of slope.

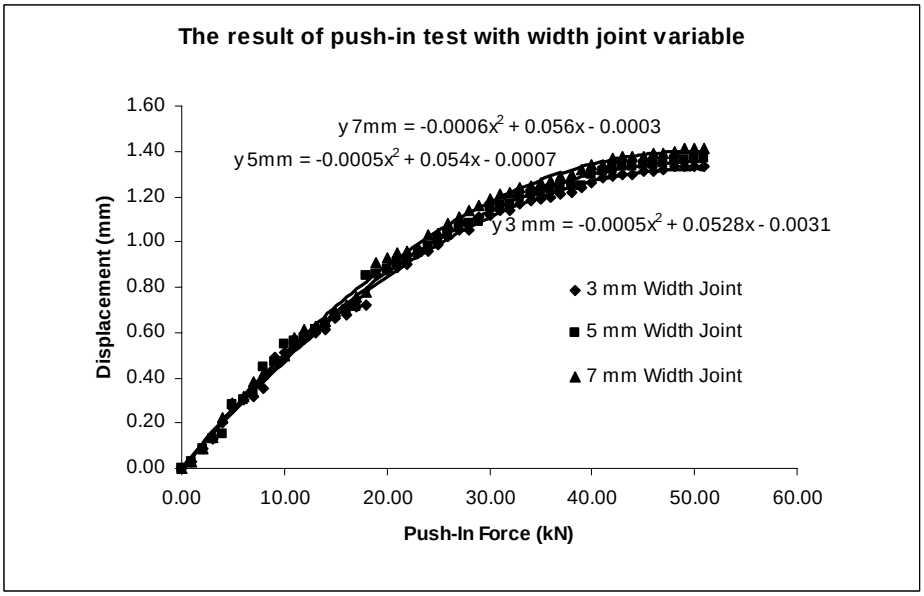

Figure F3.4 CBP specifications: rectangular shape, 100 mm block thick, stretcher bond laying pattern, 30 mm bedding sand thick and 4 % degree of slope.

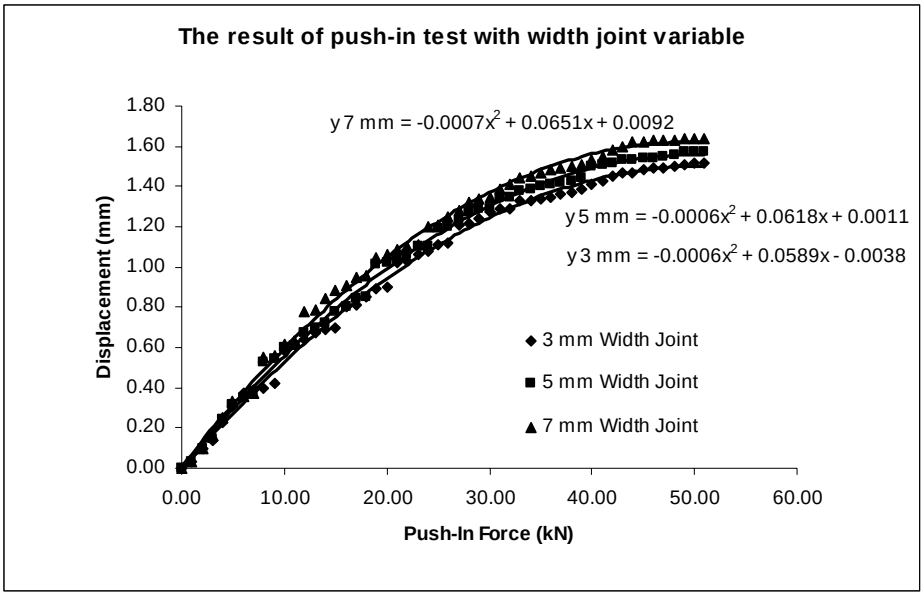

Figure F3.5 CBP specifications: rectangular shape, 100 mm block thick, stretcher bond laying pattern, 50 mm bedding sand thick and 4 % degree of slope.

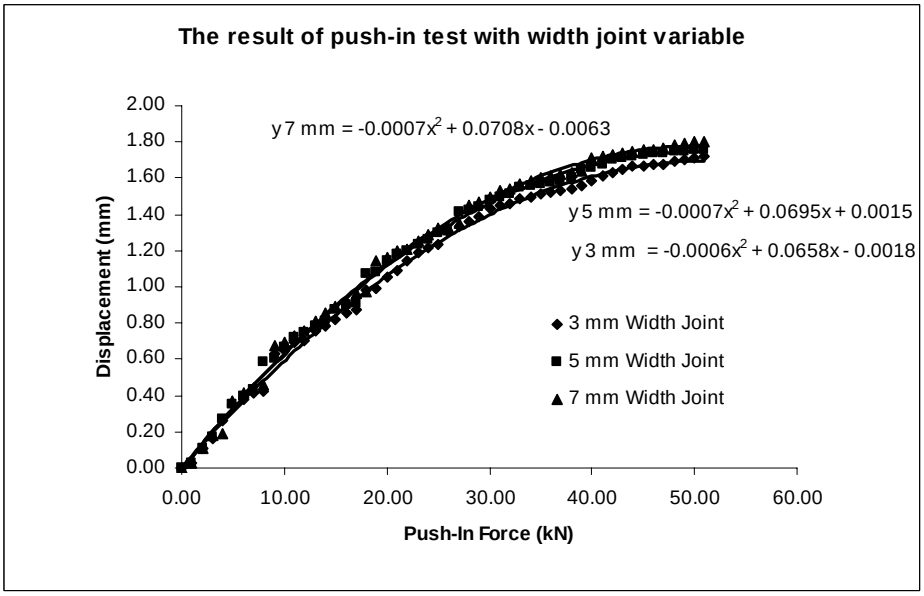

Figure F3.6 CBP specifications: rectangular shape, 100 mm block thick, stretcher bond laying pattern, 70 mm bedding sand thick and 4 % degree of slope.

APPENDIX – F3

Horizontal Creep on Push-in Test CBP 4 % Slope
The Effect of Joint Width

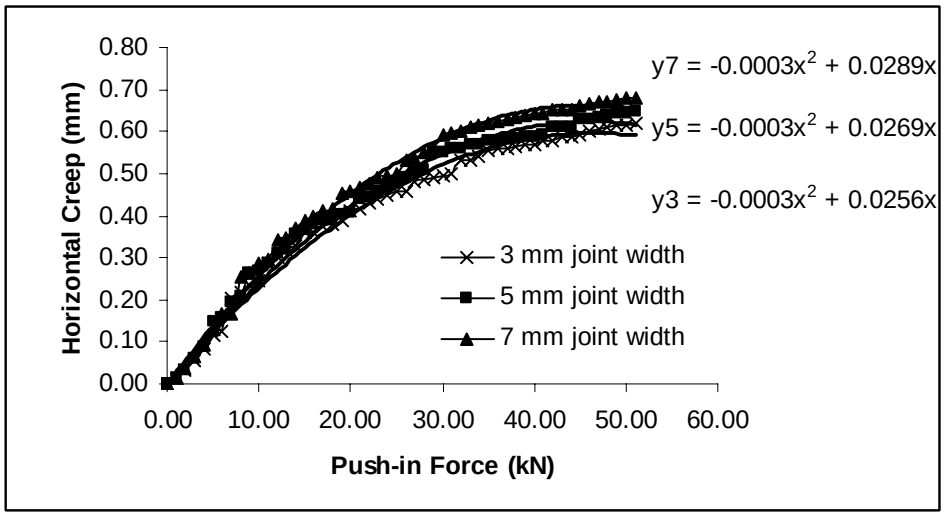

Figure F3.1 CBP specifications: rectangular block shape, 60 mm block thick, stretcher bond laying pattern, 30 mm bedding sand thick and 4 % degree of slope.

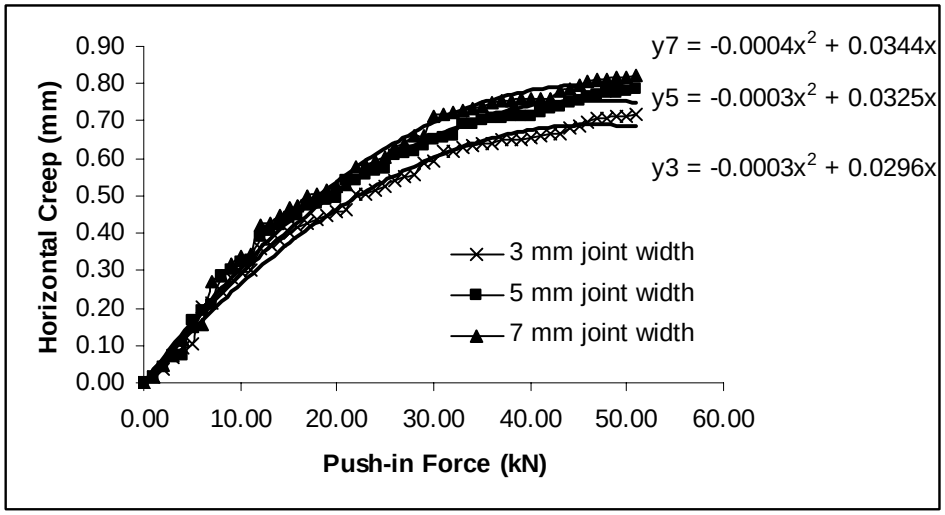

Figure F3.2 CBP specifications: rectangular block shape, 60 mm block thick, stretcher bond laying pattern, 50 mm bedding sand thick and 4 % degree of slope.

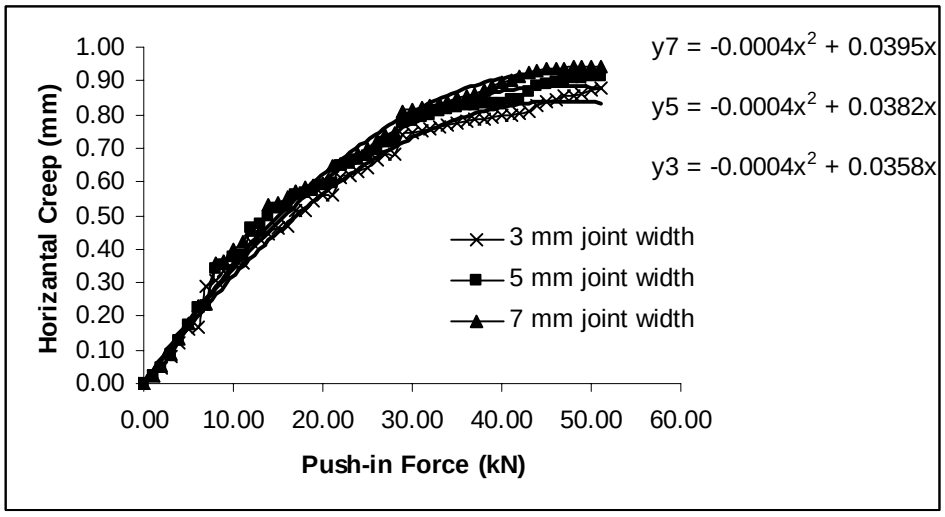

Figure F3.3 CBP specifications: rectangular block shape, 60 mm block thick, stretcher bond laying pattern, 70 mm bedding sand thick and 4 % degree of slope.

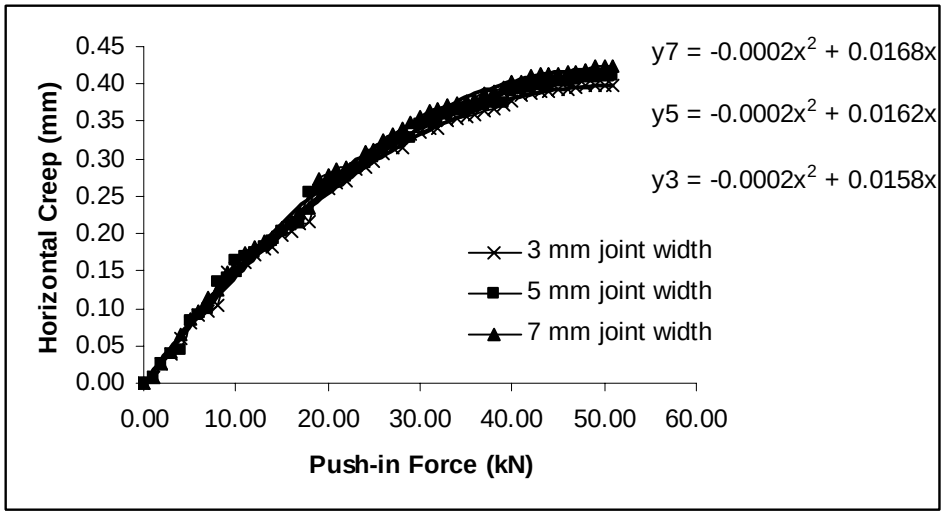

Figure F3.4 CBP specifications: rectangular shape, 100 mm block thick, stretcher bond laying pattern, 30 mm bedding sand thick and 4 % degree of slope.

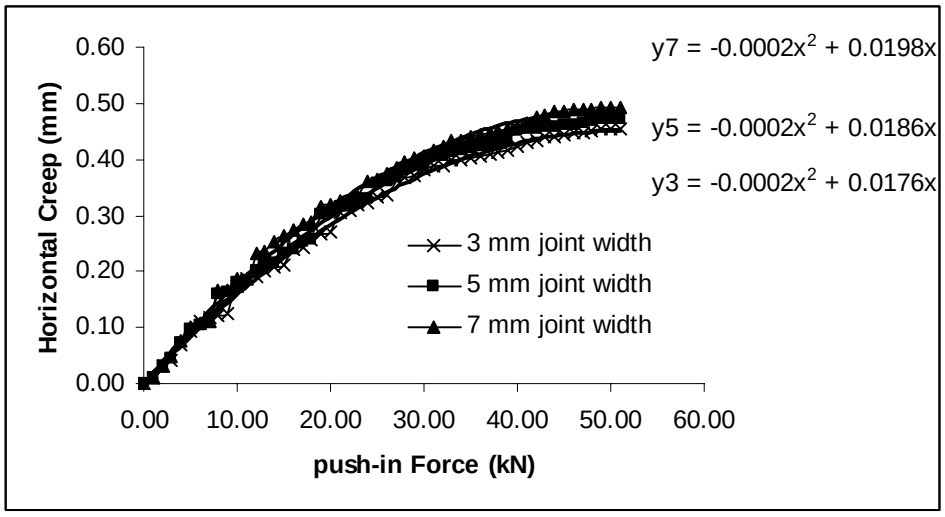

Figure F3.5 CBP specifications: rectangular shape, 100 mm block thick, stretcher bond laying pattern, 50 mm bedding sand thick and 4 % degree of slope.

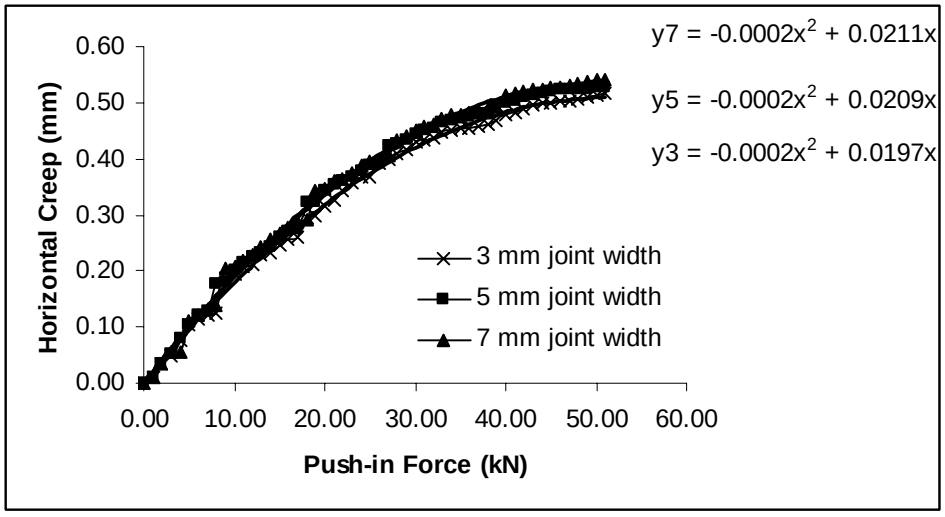

Figure F3.6 CBP specifications: rectangular shape, 100 mm block thick, stretcher bond laying pattern, 70 mm bedding sand thick and 4 % degree of slope.

APPENDIX – G1

Push-in Test on CBP 8 % Slope
The Effect of Bedding Sand Thickness

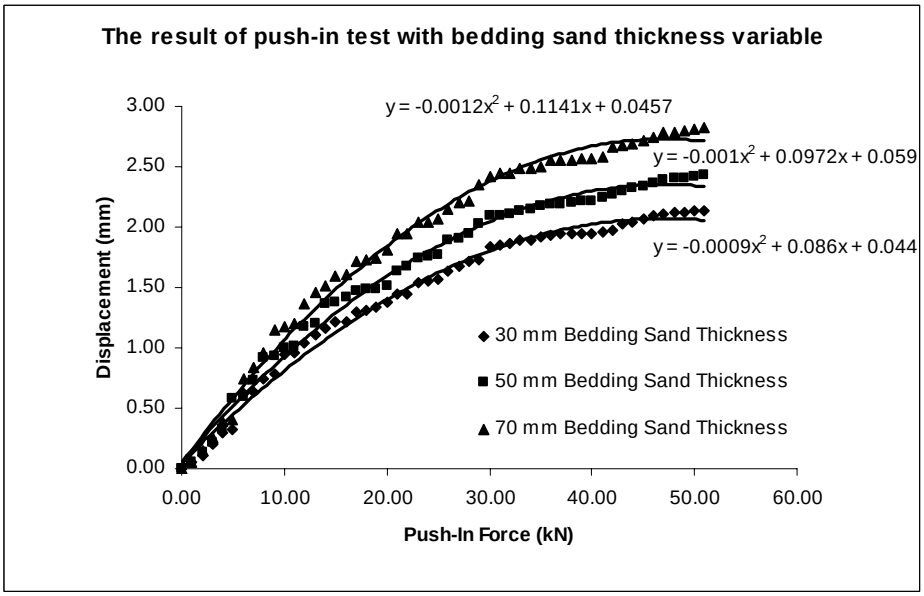

Figure G1.1 CBP specifications: rectangular block shape, 60 mm block thickness, stretcher bond laying pattern, 3 mm joint width and 8 % degree of slope.

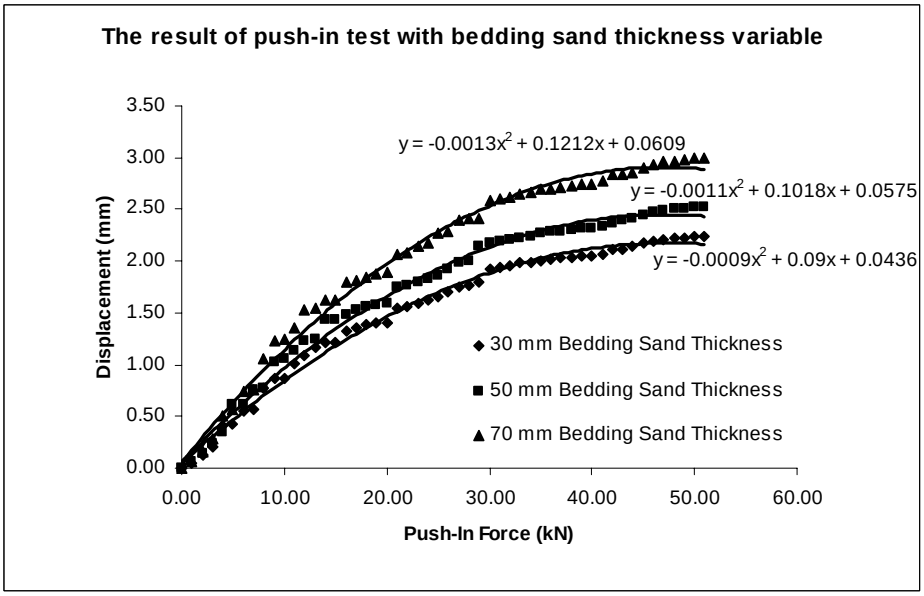

Figure G1.2 CBP specifications: rectangular block shape, 60 mm block thickness, stretcher bond laying pattern, 5 mm joint width and 8 % degree of slope.

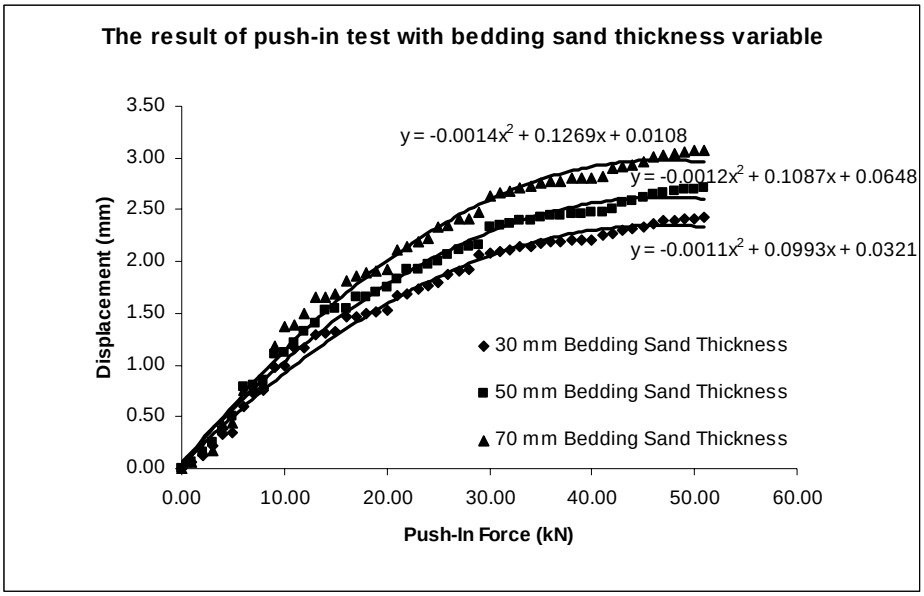

Figure G1.3 CBP specifications: rectangular block shape, 60 mm block thickness, stretcher bond laying pattern, 7 mm joint width and 8 % degree of slope.

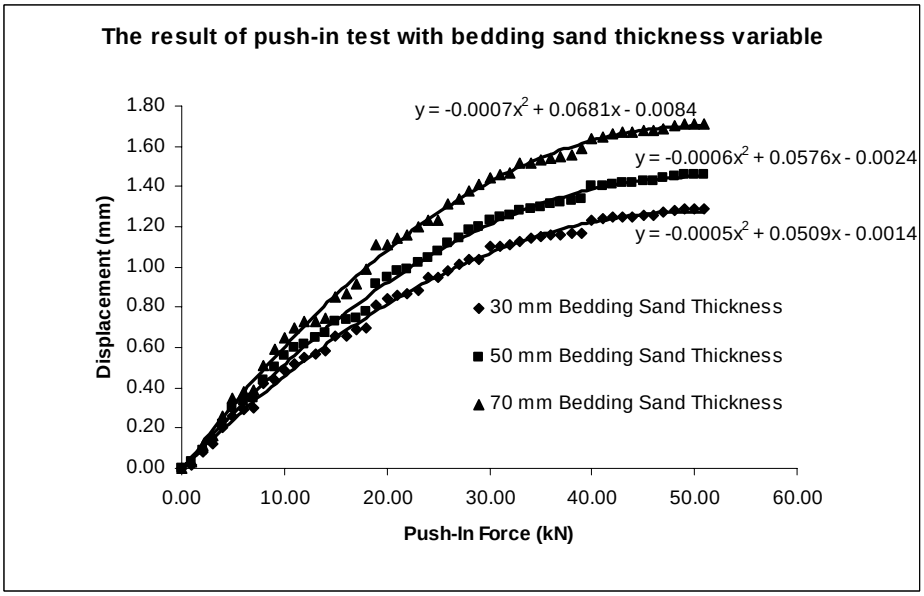

Figure G1.4 CBP specifications: rectangular block shape, 100 mm block thickness, stretcher bond laying pattern, 3 mm joint width and 8 % degree of slope.

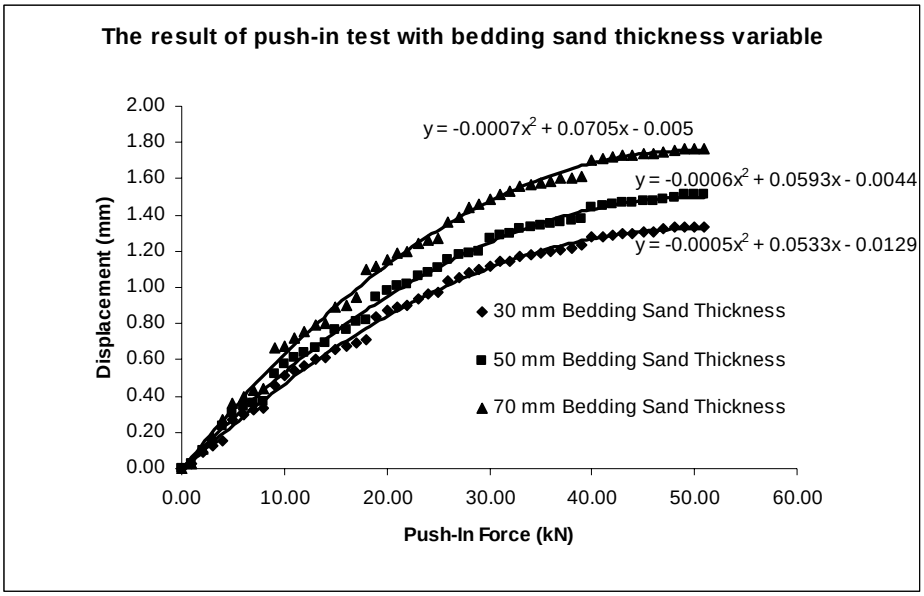

Figure G1.5 CBP specifications: rectangular block shape, 100 mm block thickness, stretcher bond laying pattern, 5 mm joint width and 8 % degree of slope.

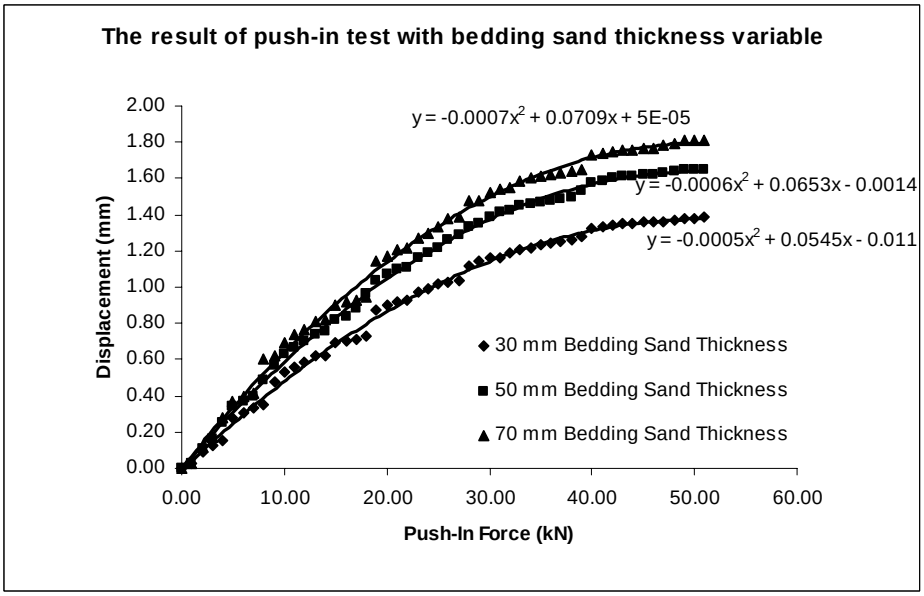

Figure G1.6 CBP specifications: rectangular block shape, 100 mm block thickness, stretcher bond laying pattern, 7 mm joint width and 8 % degree of slope.

APPENDIX – G1

Horizontal Creep on Push-in Test 8 % CBP Slope
The Effect of Bedding Sand Thickness

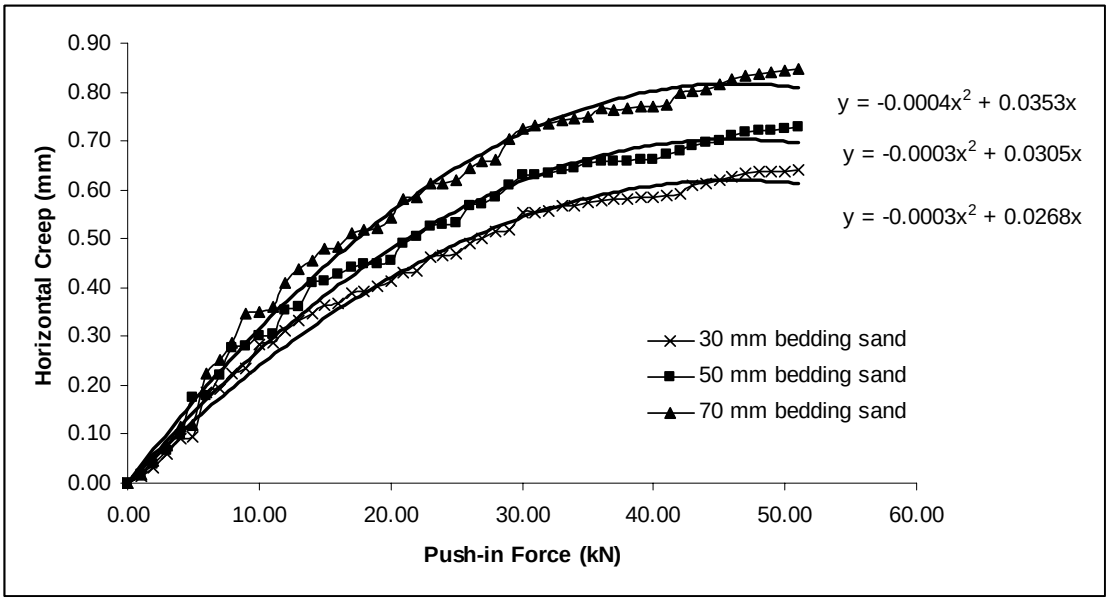

Figure G1.1 CBP specifications: rectangular block shape, 60 mm block thickness, stretcher bond laying pattern, 3 mm joint width and 8 % degree of slope.

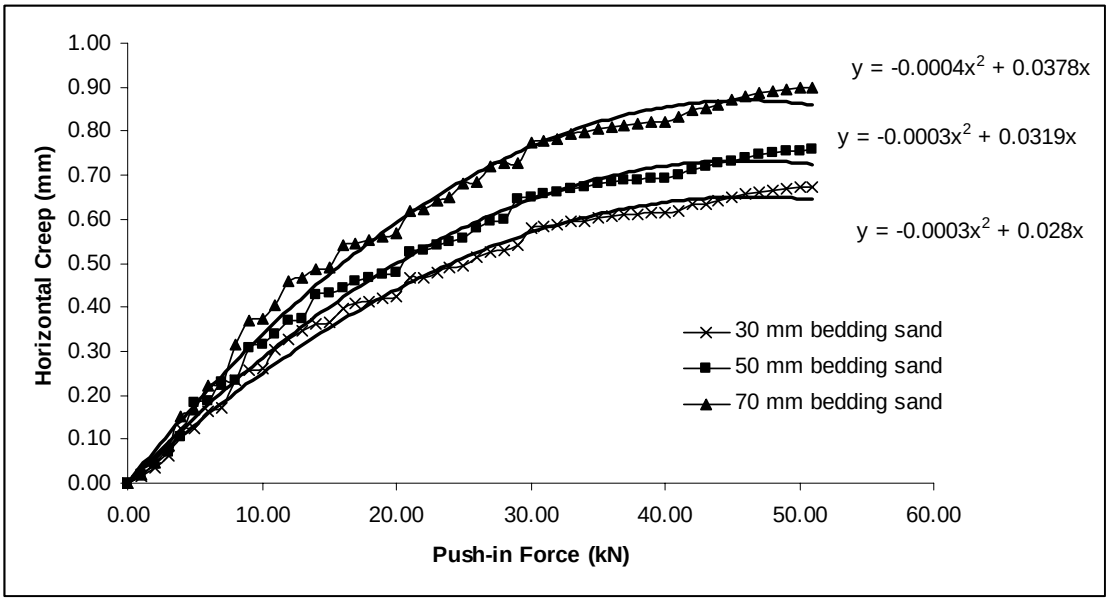

Figure G1.2 CBP specifications: rectangular block shape, 60 mm block thickness, stretcher bond laying pattern, 5 mm joint width and 8 % degree of slope.

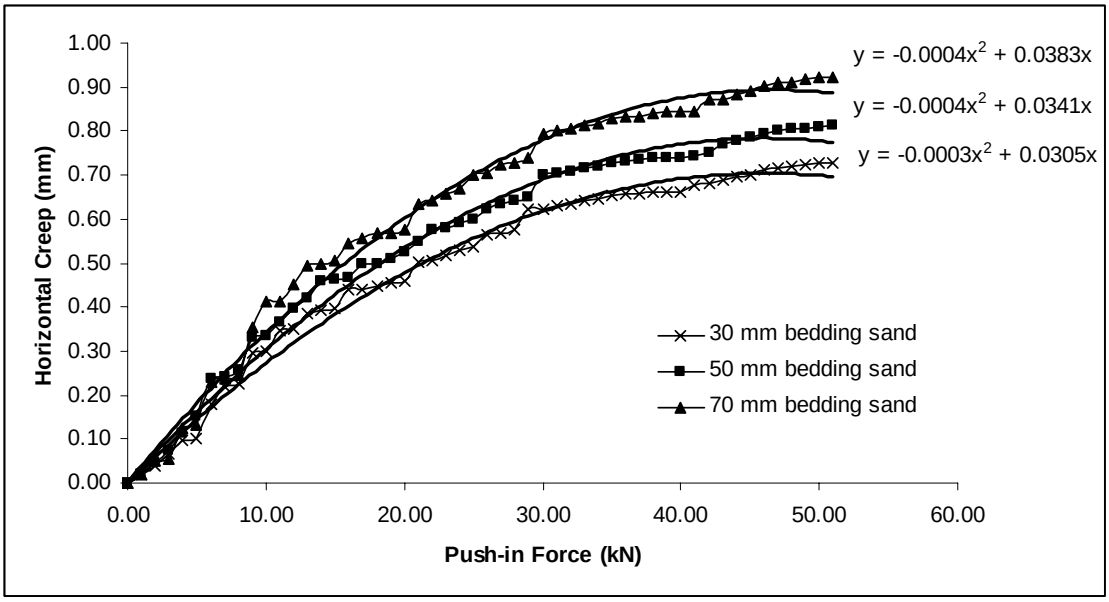

Figure G1.3 CBP specifications: rectangular block shape, 60 mm block thickness, stretcher bond laying pattern, 7 mm joint width and 8 % degree of slope.

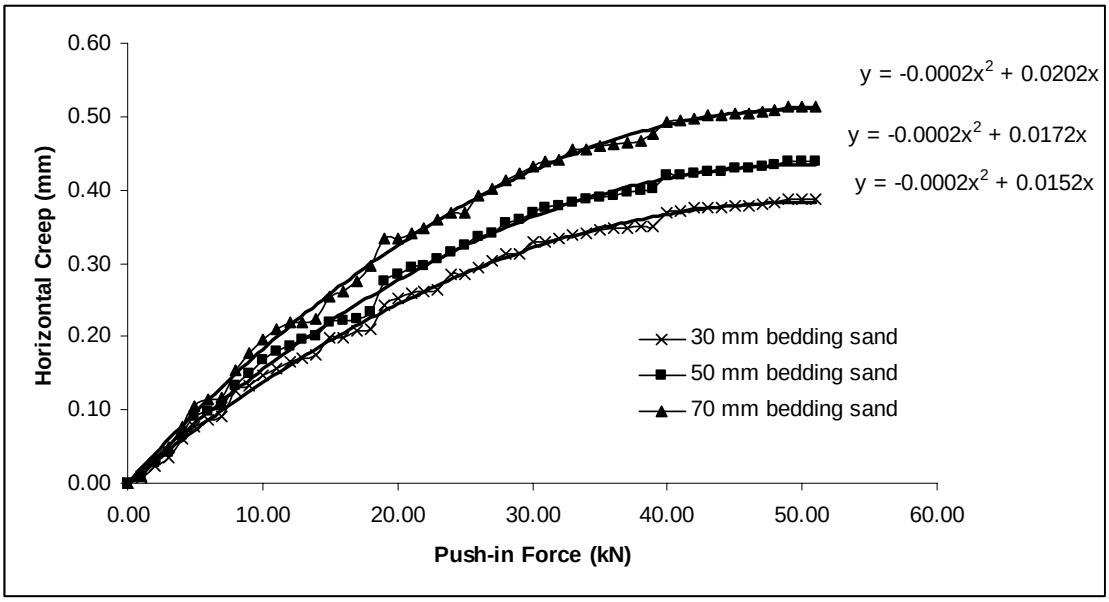

Figure G1.4 CBP specifications: rectangular block shape, 100 mm block thickness, stretcher bond laying pattern, 3 mm joint width and 8 % degree of slope.

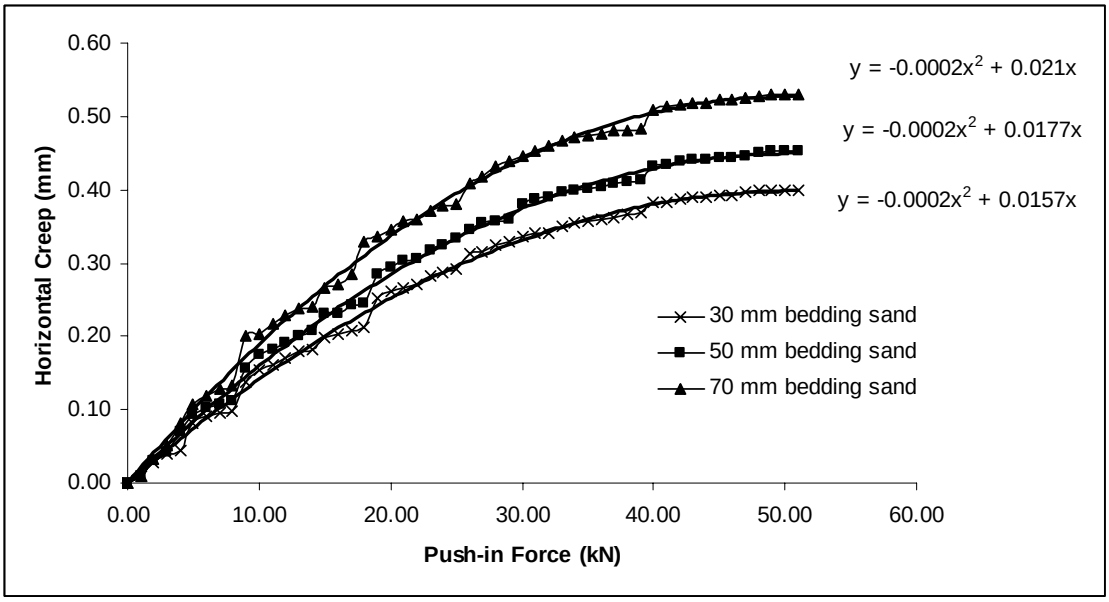

Figure G1.5 CBP specifications: rectangular block shape, 100 mm block thickness, stretcher bond laying pattern, 5 mm joint width and 8 % degree of slope.

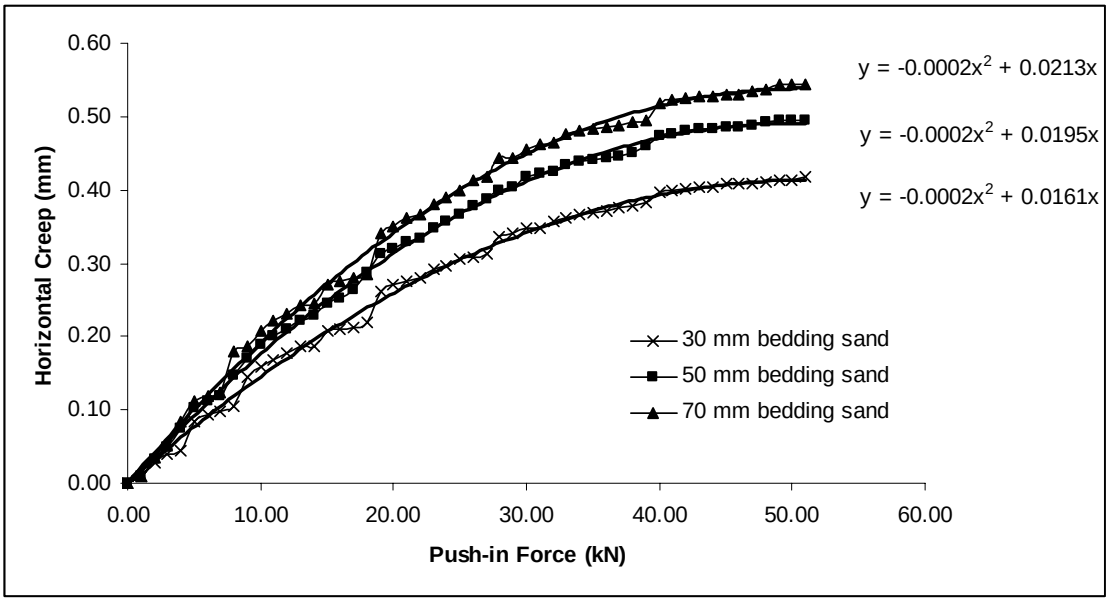

Figure G1.6 CBP specifications: rectangular block shape, 100 mm block thickness, stretcher bond laying pattern, 7 mm joint width and 8 % degree of slope.

APPENDIX – G2

Push-in Test on CBP 8 % Slope
The Effect of Block Thickness

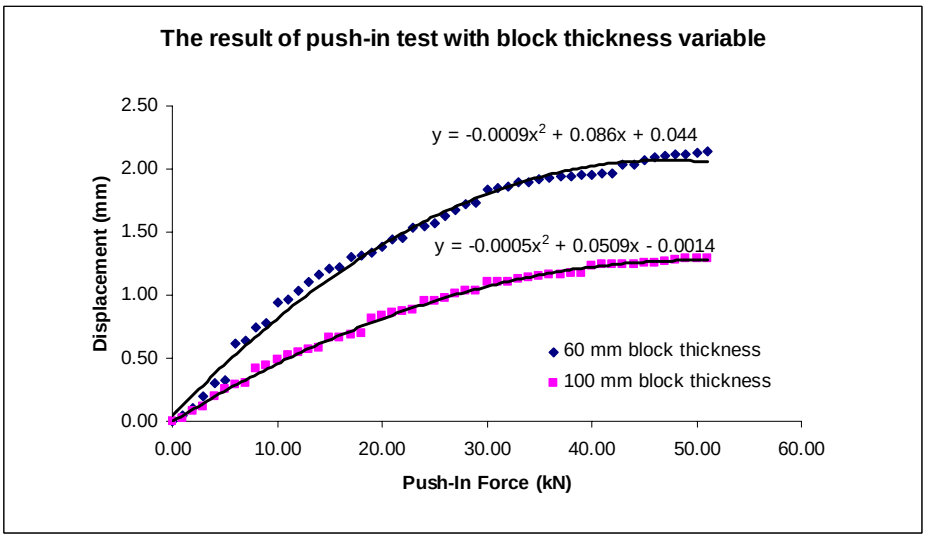

Figure G2.1 CBP specifications: rectangular block shape, 30 mm bedding sand thick, stretcher bond laying pattern, 3 mm joint width and 8 % degree of slope.

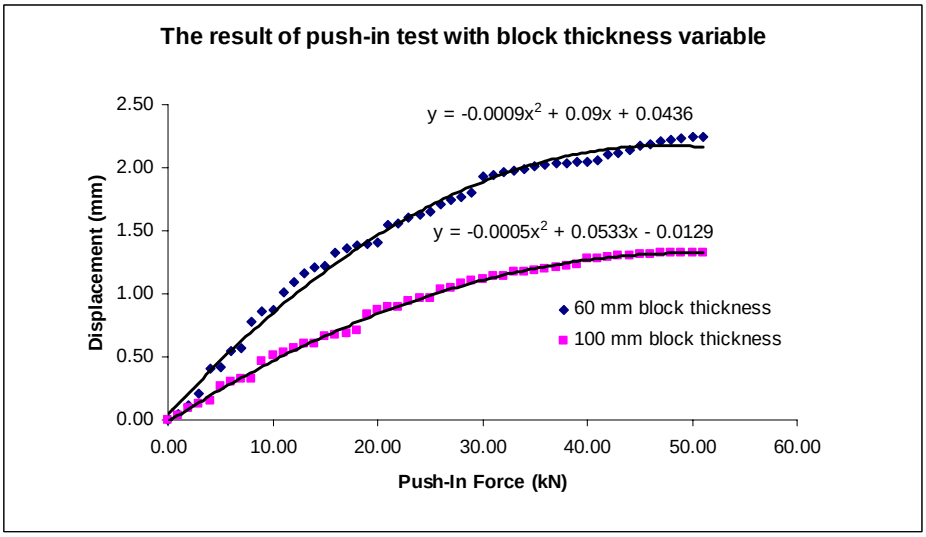

Figure G2.2 CBP specifications: rectangular block shape, 30 mm bedding sand thick, stretcher bond laying pattern, 5 mm joint width and 8 % degree of slope.

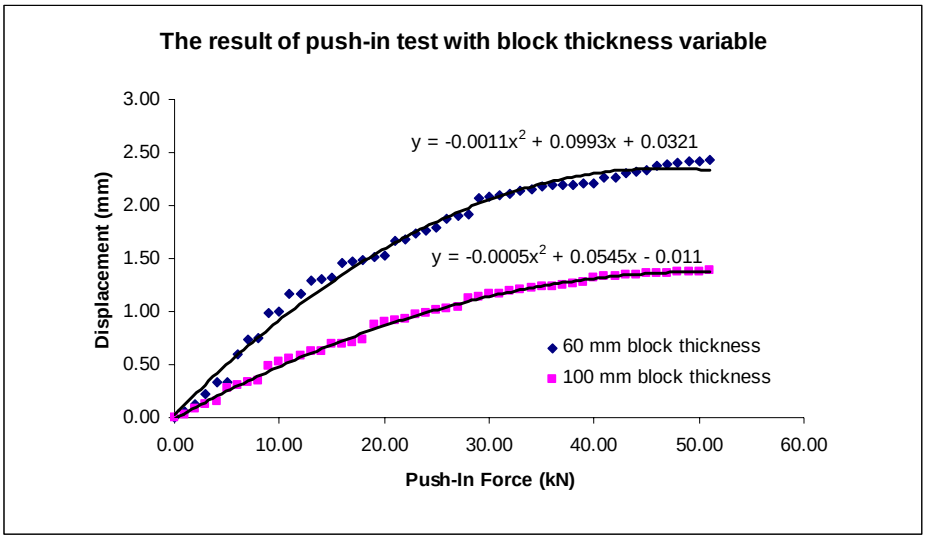

Figure G2.3 CBP specifications: rectangular block shape, 30 mm bedding sand thick, stretcher bond laying pattern, 7 mm joint width and 8 % degree of slope.

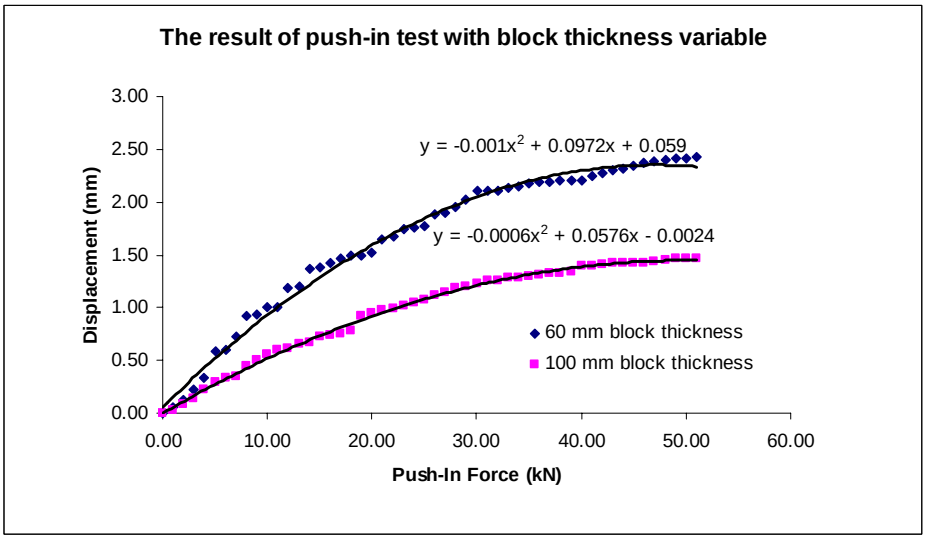

Figure G2.4 CBP specifications: rectangular block shape, 50 mm bedding sand thick, stretcher bond laying pattern, 3 mm joint width and 8 % degree of slope.

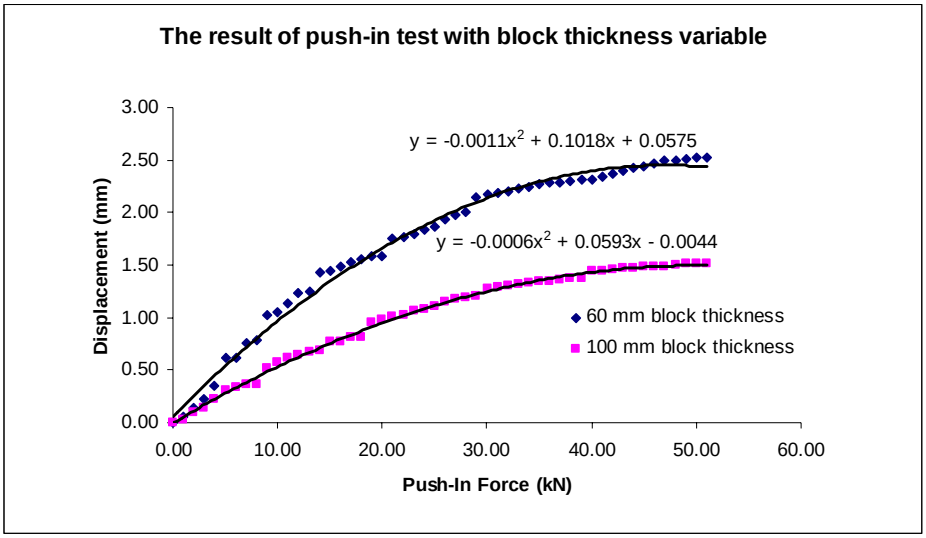

Figure G2.5 CBP specifications: rectangular block shape, 50 mm bedding sand thick, stretcher bond laying pattern, 5 mm joint width and 8 % degree of slope.

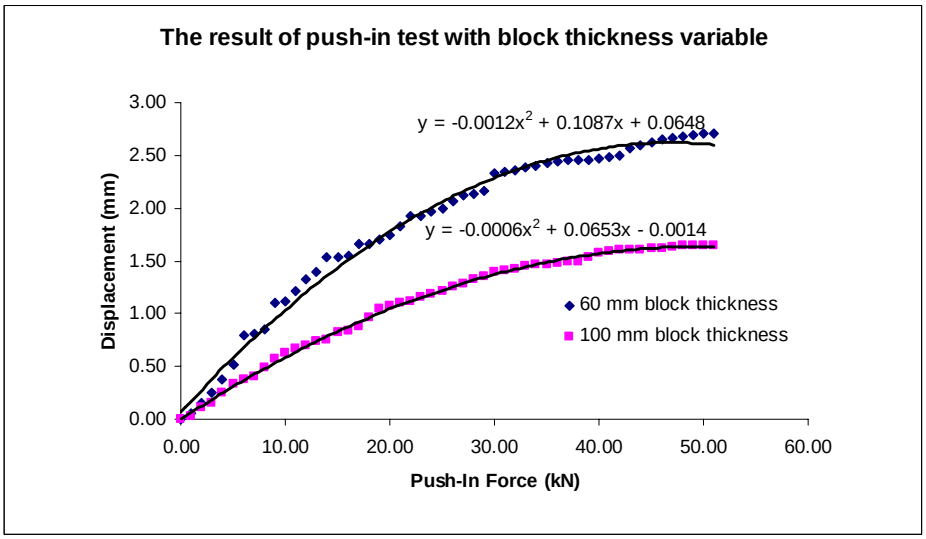

Figure G2.6 CBP specifications: rectangular block shape, 50 mm bedding sand thick, stretcher bond laying pattern, 7 mm joint width and 8 % degree of slope.

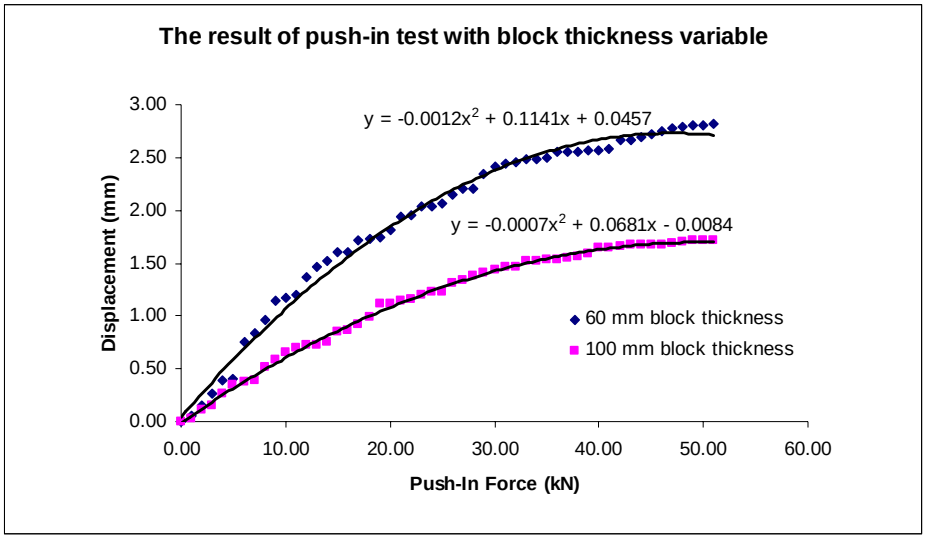

Figure G2.7 CBP specifications: rectangular block shape, 70 mm bedding sand thick, stretcher bond laying pattern, 3 mm joint width and 8 % degree of slope.

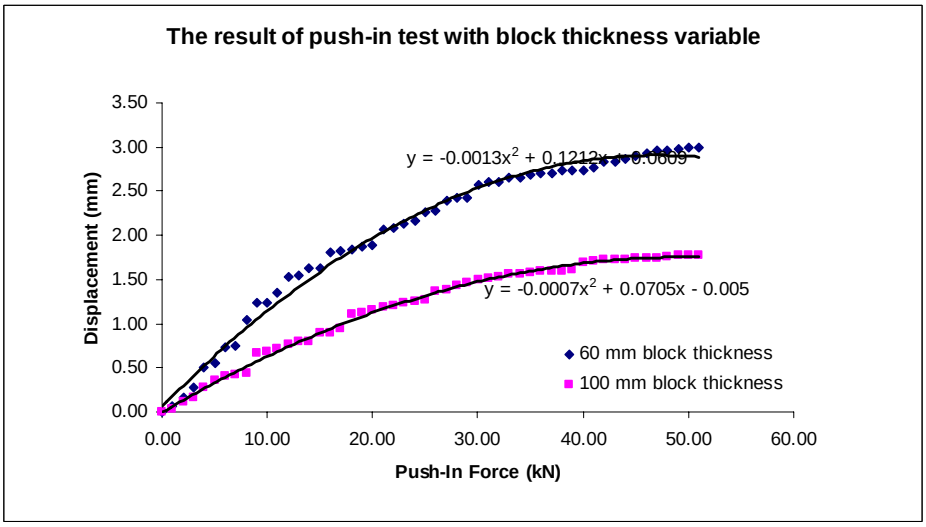

Figure G2.8 CBP specifications: rectangular block shape, 70 mm bedding sand thick, stretcher bond laying pattern, 5 mm joint width and 8 % degree of slope.

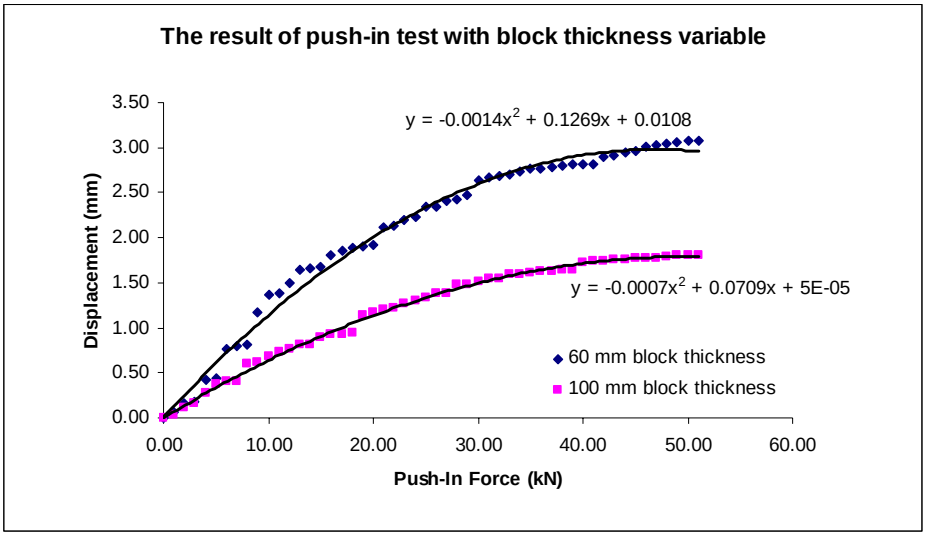

Figure G2.9 CBP specifications: rectangular block shape, 70 mm bedding sand thick, stretcher bond laying pattern, 7 mm joint width and 8 % degree of slope.

APPENDIX – G2

Horizontal Creep on Push-in Test CBP 8 % Slope
The Effect of Block Thickness

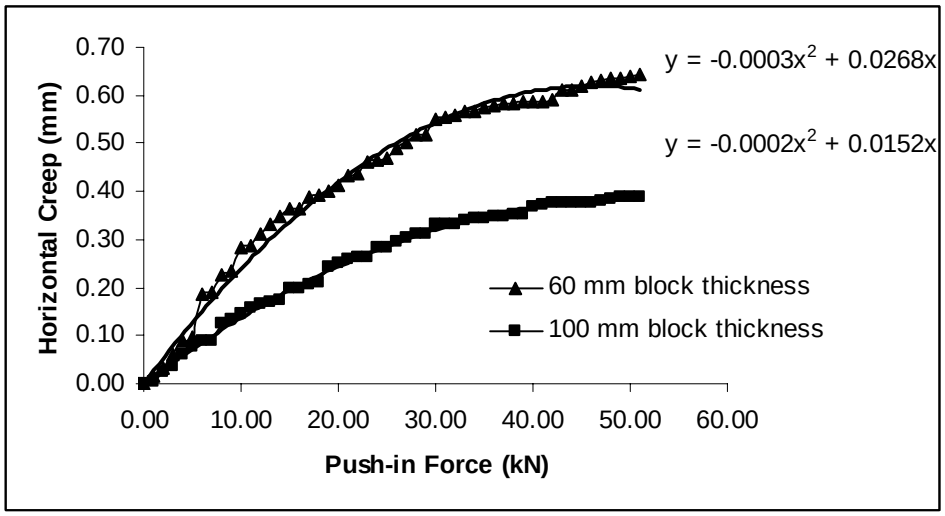

Figure G2.1 CBP specifications: rectangular block shape, 30 mm bedding sand thick, stretcher bond laying pattern, 3 mm joint width and 8 % degree of slope.

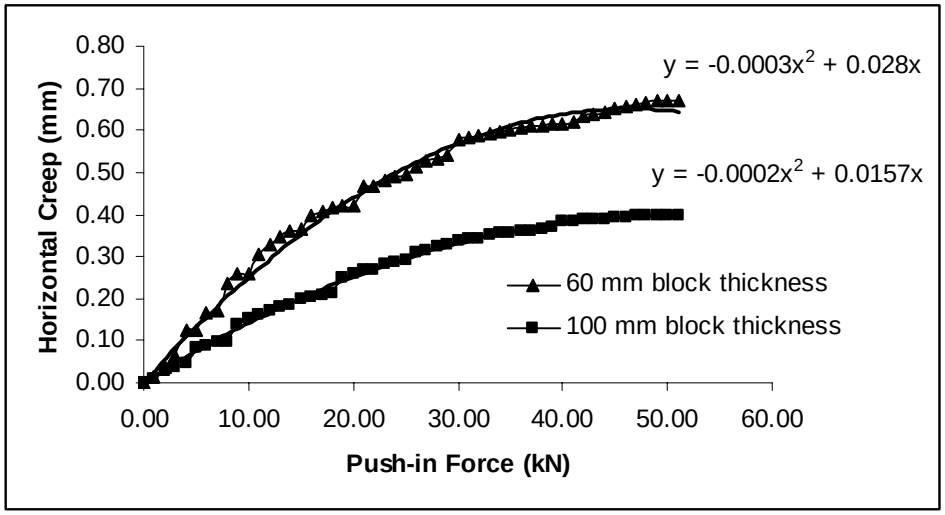

Figure G2.2 CBP specifications: rectangular block shape, 30 mm bedding sand thick, stretcher bond laying pattern, 5 mm joint width and 8 % degree of slope.

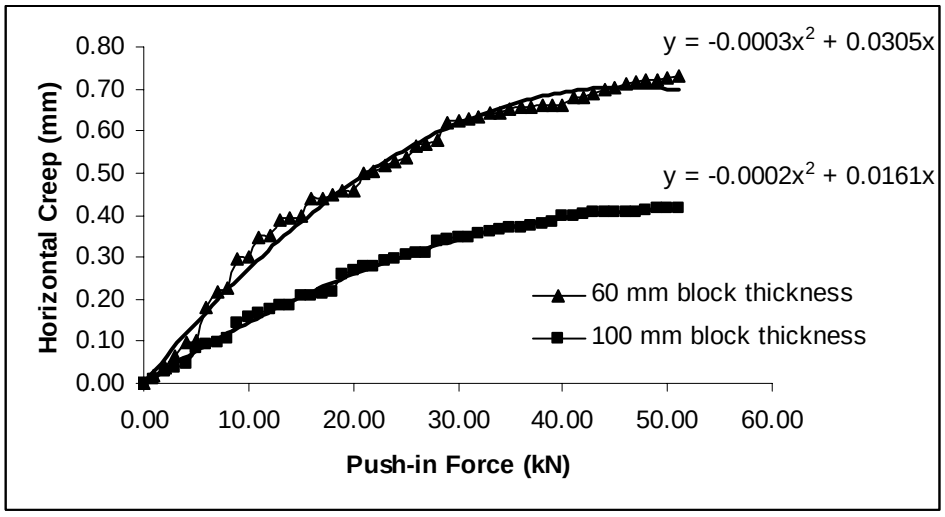

Figure G2.3 CBP specifications: rectangular block shape, 30 mm bedding sand thick, stretcher bond laying pattern, 7 mm joint width and 8 % degree of slope.

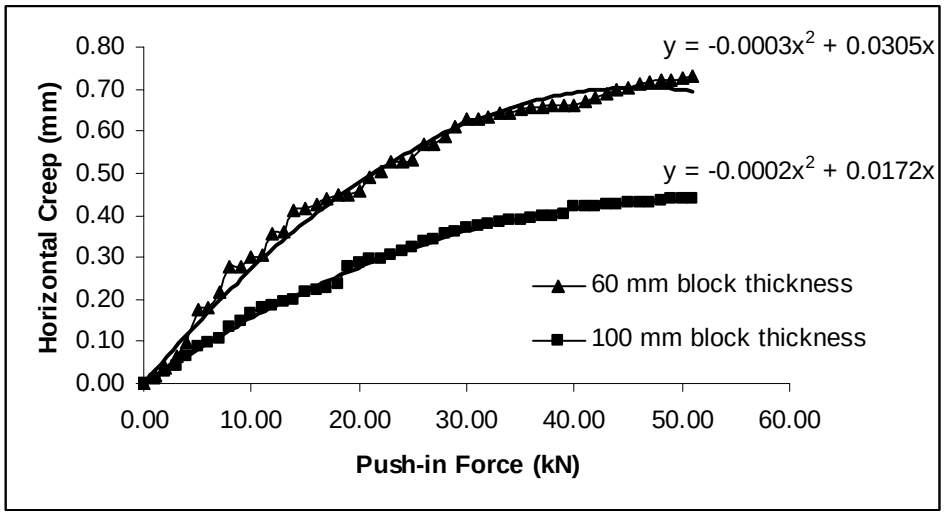

Figure G2.4 CBP specifications: rectangular block shape, 50 mm bedding sand thick, stretcher bond laying pattern, 3 mm joint width and 8 % degree of slope.

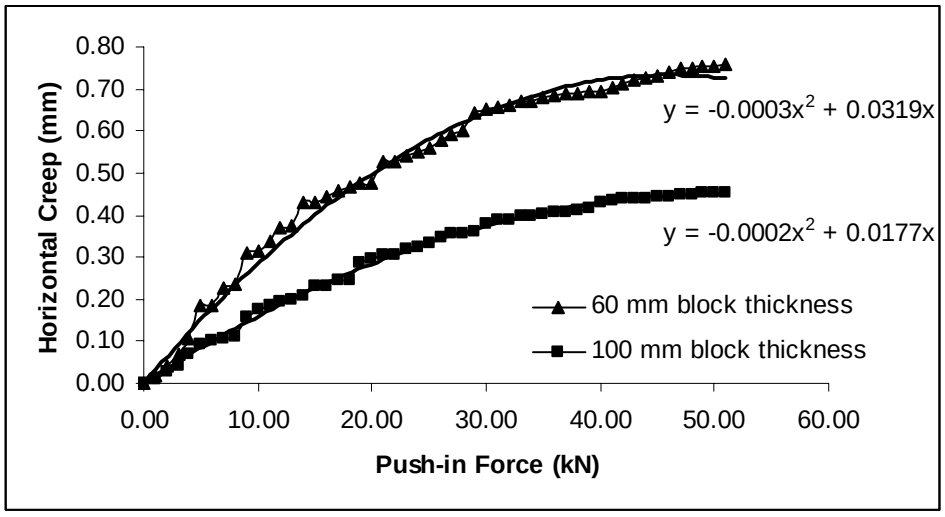

Figure G2.5 CBP specifications: rectangular block shape, 50 mm bedding sand thick, stretcher bond laying pattern, 5 mm joint width and 8 % degree of slope.

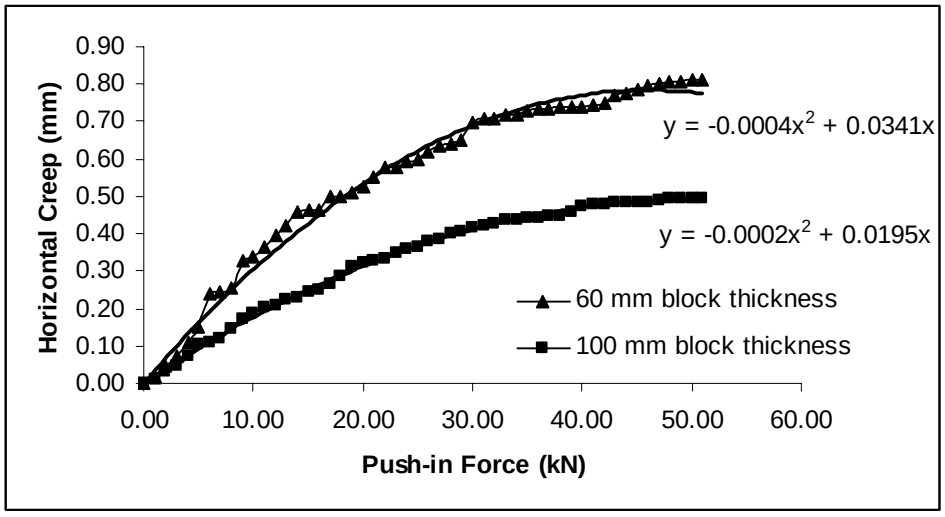

Figure G2.6 CBP specifications: rectangular block shape, 50 mm bedding sand thick, stretcher bond laying pattern, 7 mm joint width and 8 % degree of slope.

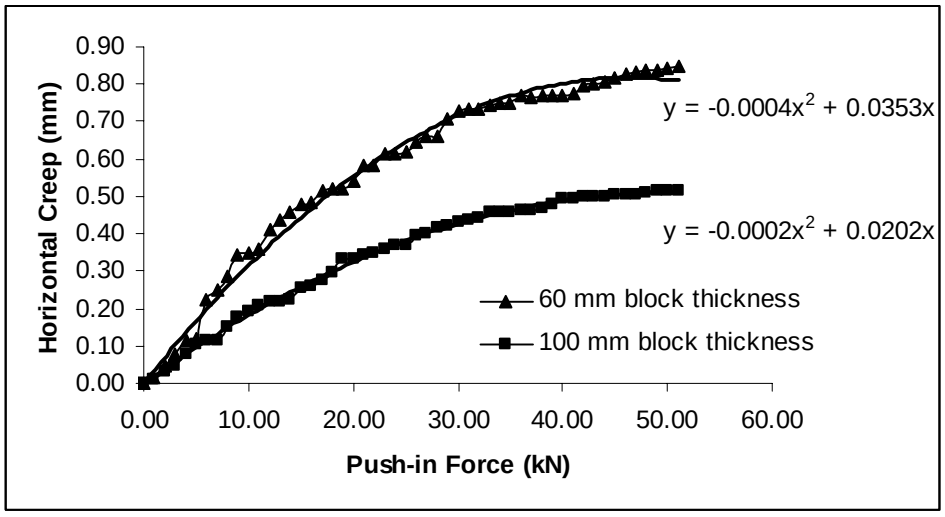

Figure G2.7 CBP specifications: rectangular block shape, 70 mm bedding sand thick, stretcher bond laying pattern, 3 mm joint width and 8 % degree of slope.

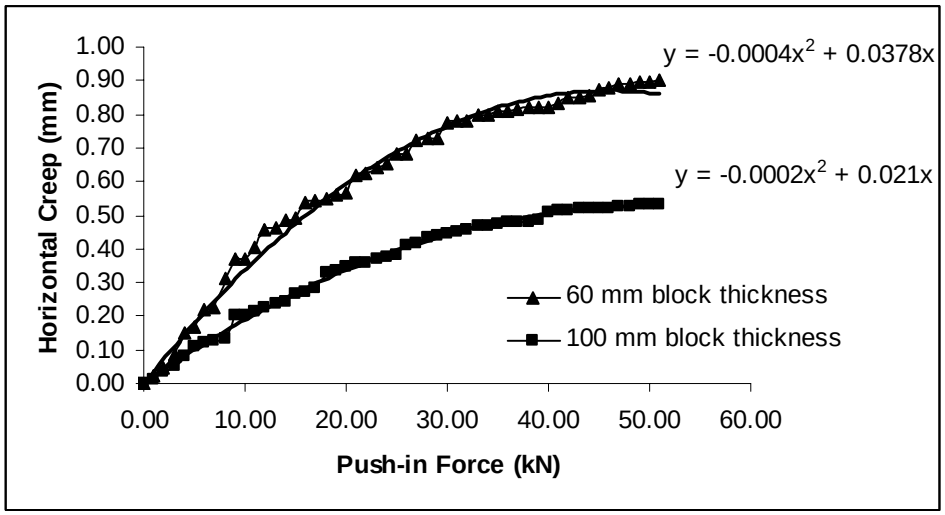

Figure G2.8 CBP specifications: rectangular block shape, 70 mm bedding sand thick, stretcher bond laying pattern, 5 mm joint width and 8 % degree of slope.

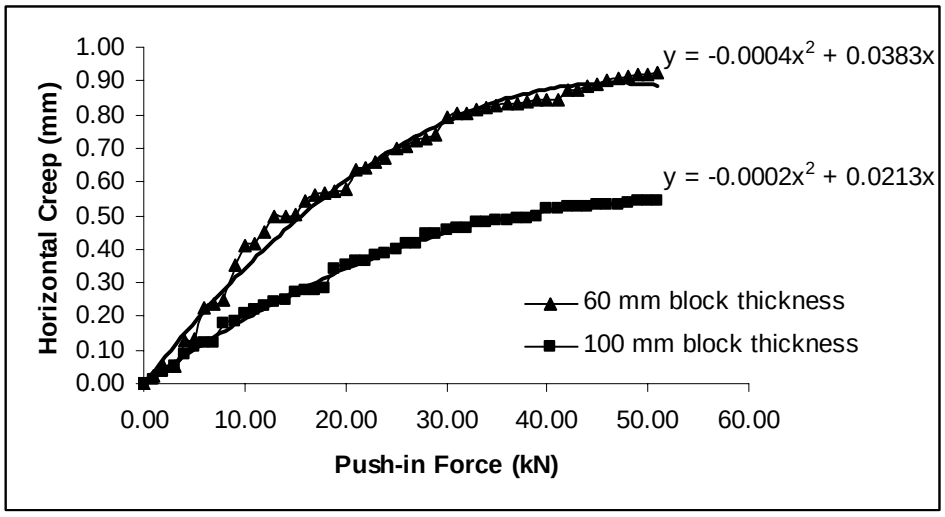

Figure G2.9 CBP specifications: rectangular block shape, 70 mm bedding sand thick, stretcher bond laying pattern, 7 mm joint width and 8 % degree of slope.

APPENDIX – G3

Push-in Test on CBP 8 % Slope
The Effect of Joint Width

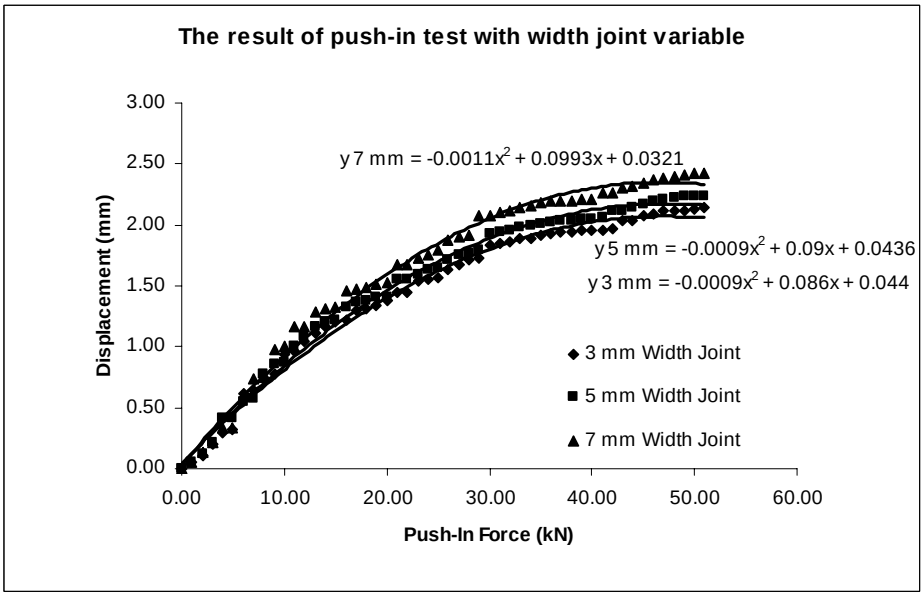

Figure G3.1 CBP specifications: rectangular block shape, 60 mm block thick, stretcher bond laying pattern, 30 mm bedding sand thick and 8 % degree of slope.

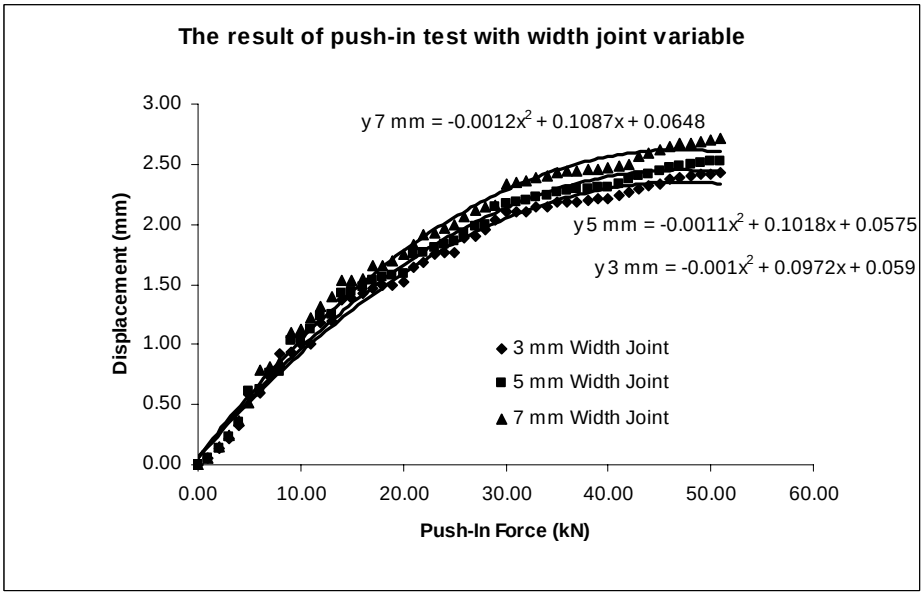

Figure G3.2 CBP specifications: rectangular block shape, 60 mm block thick, stretcher bond laying pattern, 50 mm bedding sand thick and 8 % degree of slope.

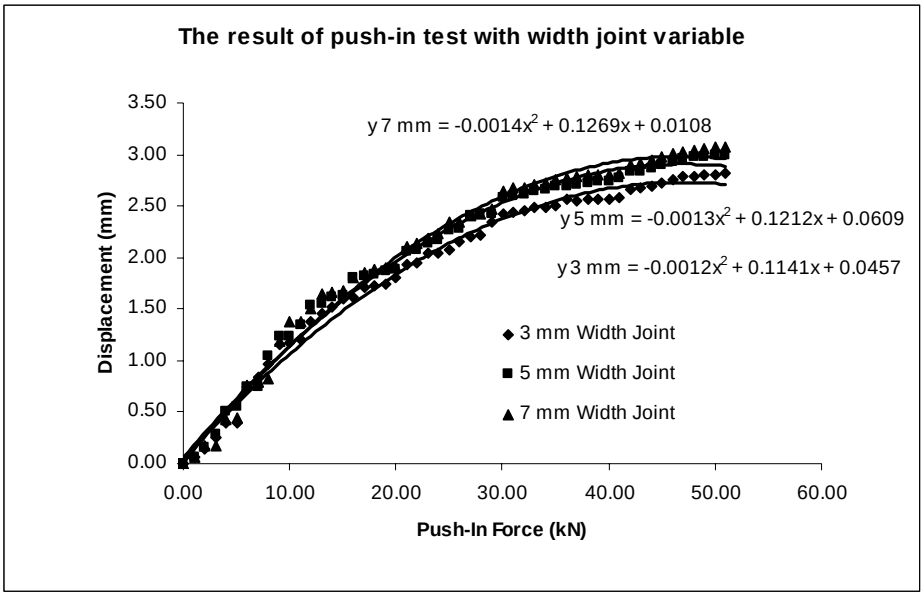

Figure G3.3 CBP specifications: rectangular block shape, 60 mm block thick, stretcher bond laying pattern, 70 mm bedding sand thick and 8 % degree of slope.

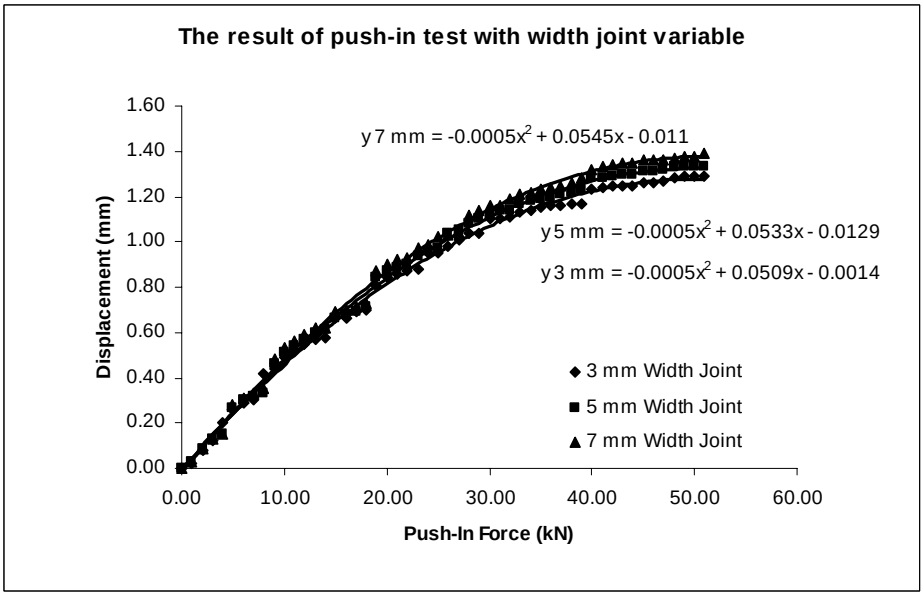

Figure G3.4 CBP specifications: rectangular shape, 100 mm block thick, stretcher bond laying pattern, 30 mm bedding sand thick and 8 % degree of slope.

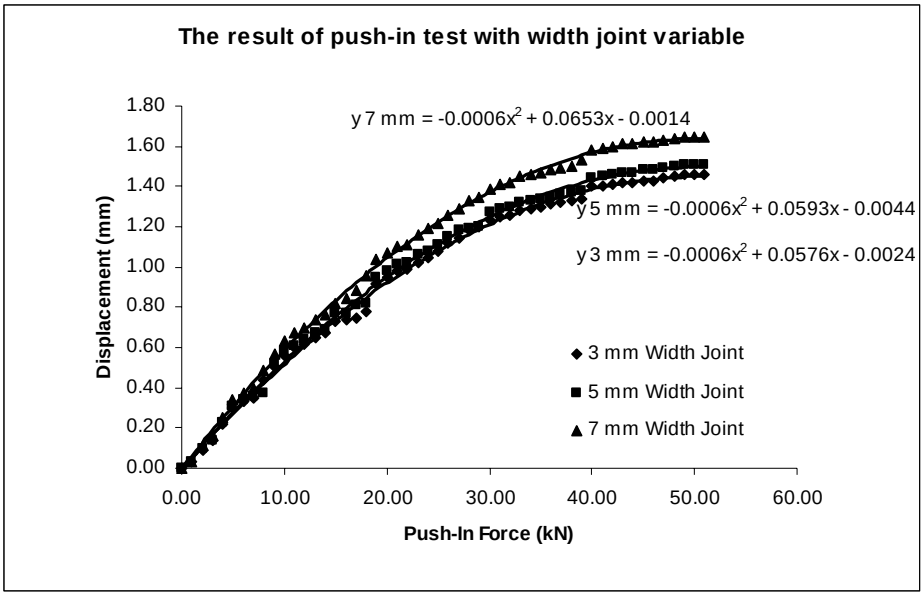

Figure G3.5 CBP specifications: rectangular shape, 100 mm block thick, stretcher bond laying pattern, 50 mm bedding sand thick and 8 % degree of slope.

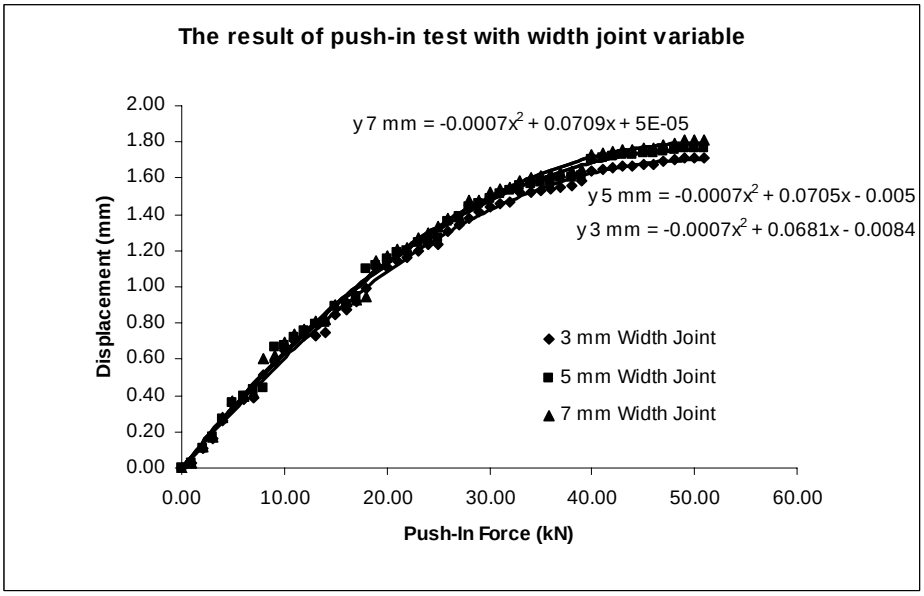

Figure G3.6 CBP specifications: rectangular shape, 100 mm block thick, stretcher bond laying pattern, 70 mm bedding sand thick and 8 % degree of slope.

APPENDIX – G3

Horizontal Creep on Push-in Test CBP 8 % Slope
The Effect of Joint Width

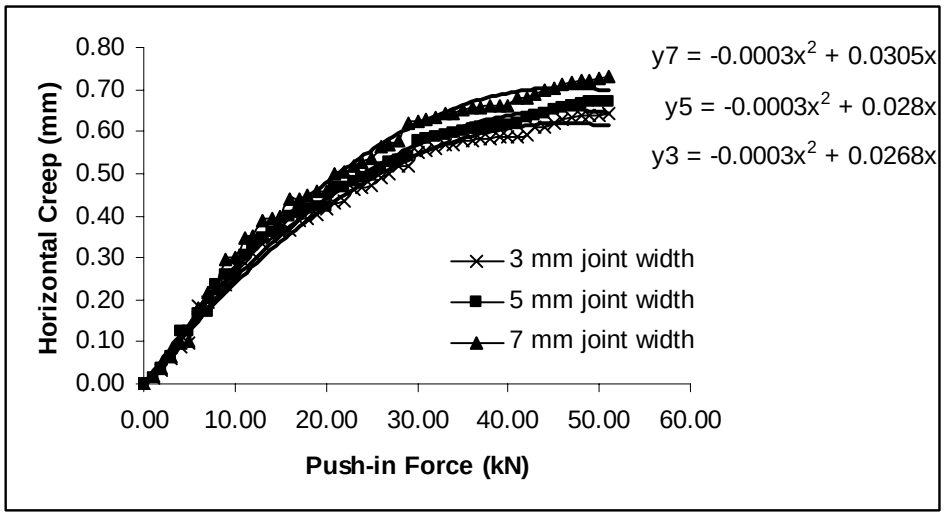

Figure G3.1 CBP specifications: rectangular block shape, 60 mm block thick, stretcher bond laying pattern, 30 mm bedding sand thick and 8 % degree of slope.

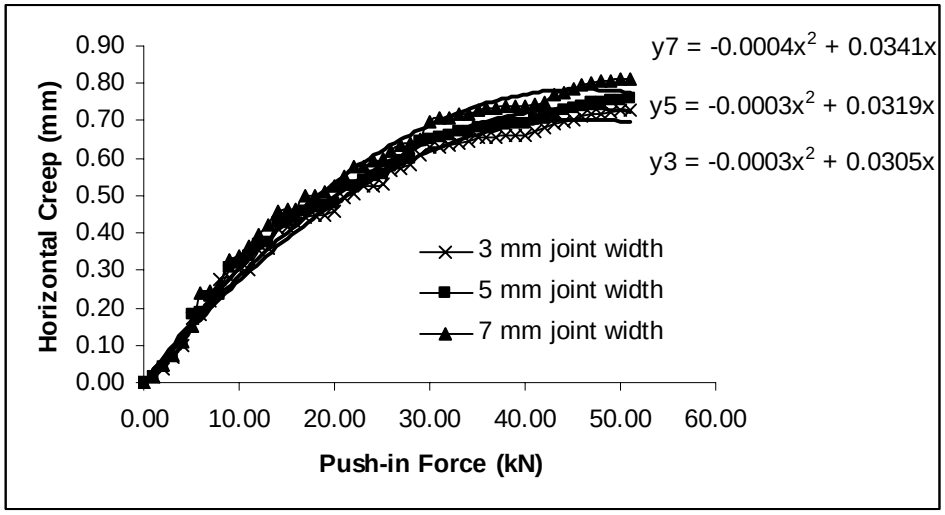

Figure G3.2 CBP specifications: rectangular block shape, 60 mm block thick, stretcher bond laying pattern, 50 mm bedding sand thick and 8 % degree of slope.

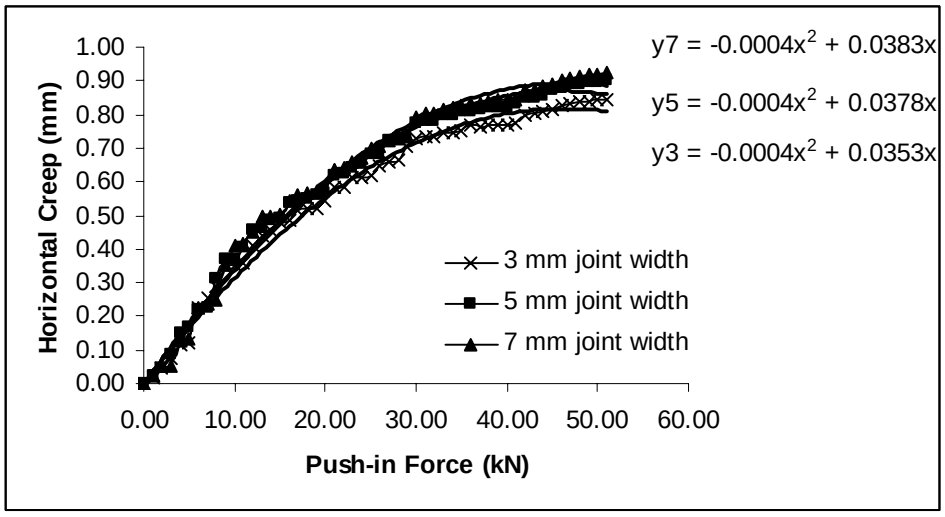

Figure G3.3 CBP specifications: rectangular block shape, 60 mm block thick, stretcher bond laying pattern, 70 mm bedding sand thick and 8 % degree of slope.

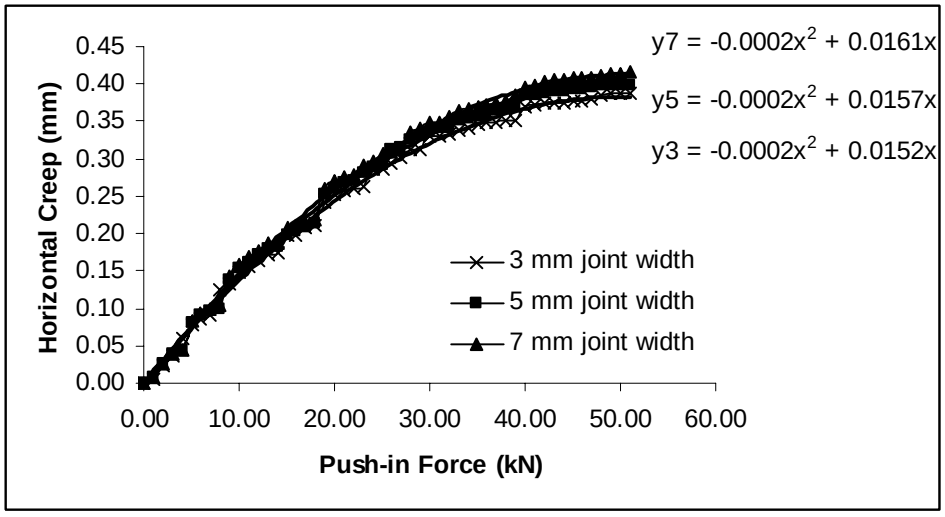

Figure G3.4 CBP specifications: rectangular shape, 100 mm block thick, stretcher bond laying pattern, 30 mm bedding sand thick and 8 % degree of slope.

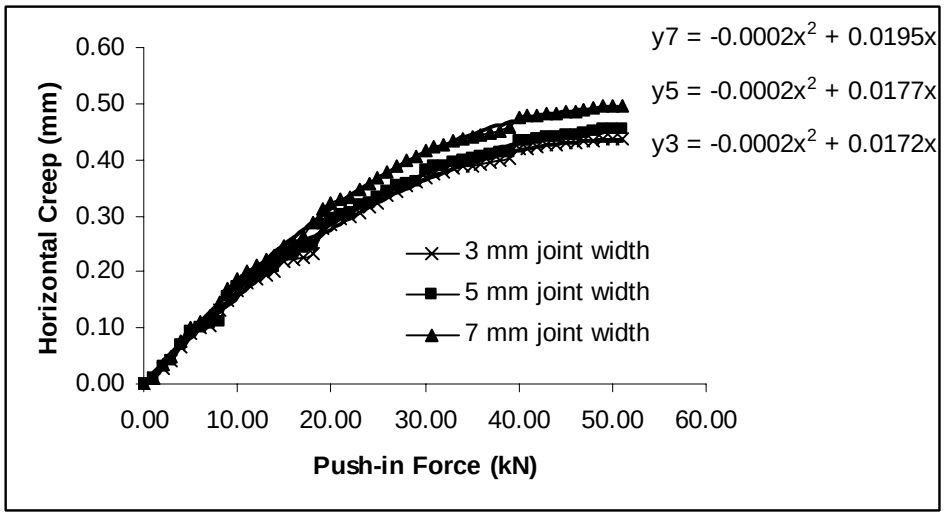

Figure G3.5 CBP specifications: rectangular shape, 100 mm block thick, stretcher bond laying pattern, 50 mm bedding sand thick and 8 % degree of slope.

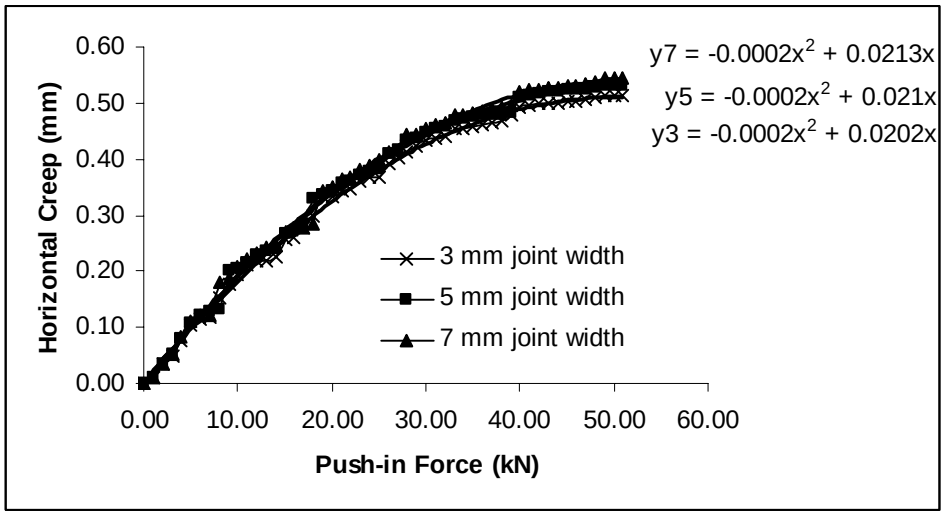

Figure G3.6 CBP specifications: rectangular shape, 100 mm block thick, stretcher bond laying pattern, 70 mm bedding sand thick and 8 % degree of slope.

APPENDIX – H1

Horizontal Creep on Push-in Test 12 % CBP Slope
The Effect of Bedding Sand Thickness

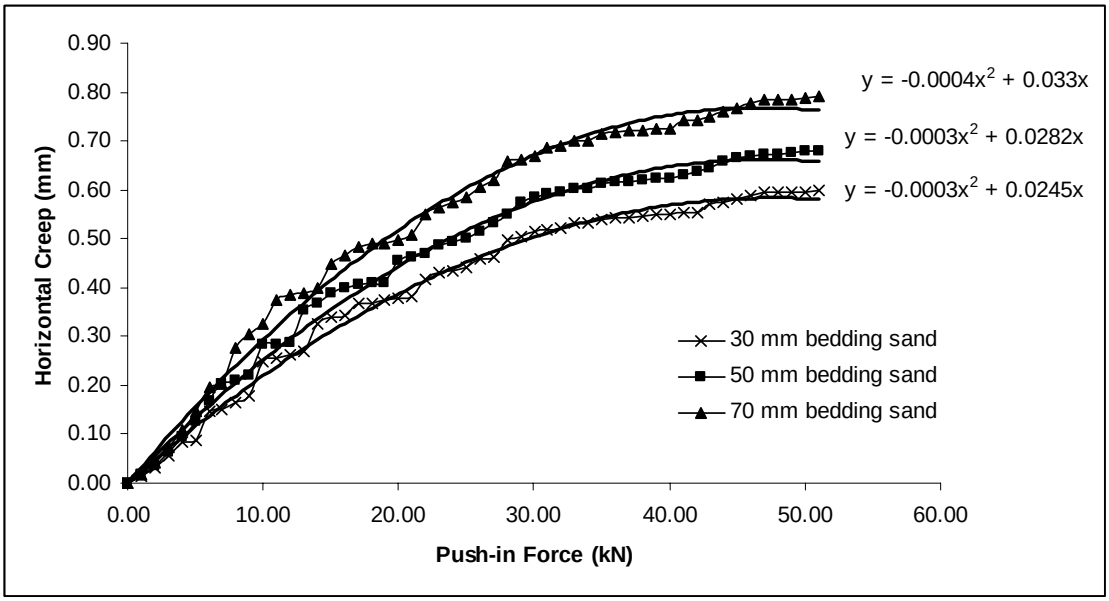

Figure H1.1 CBP specifications: rectangular block shape, 60 mm block thickness, stretcher bond laying pattern, 3 mm joint width and 12 % degree of slope.

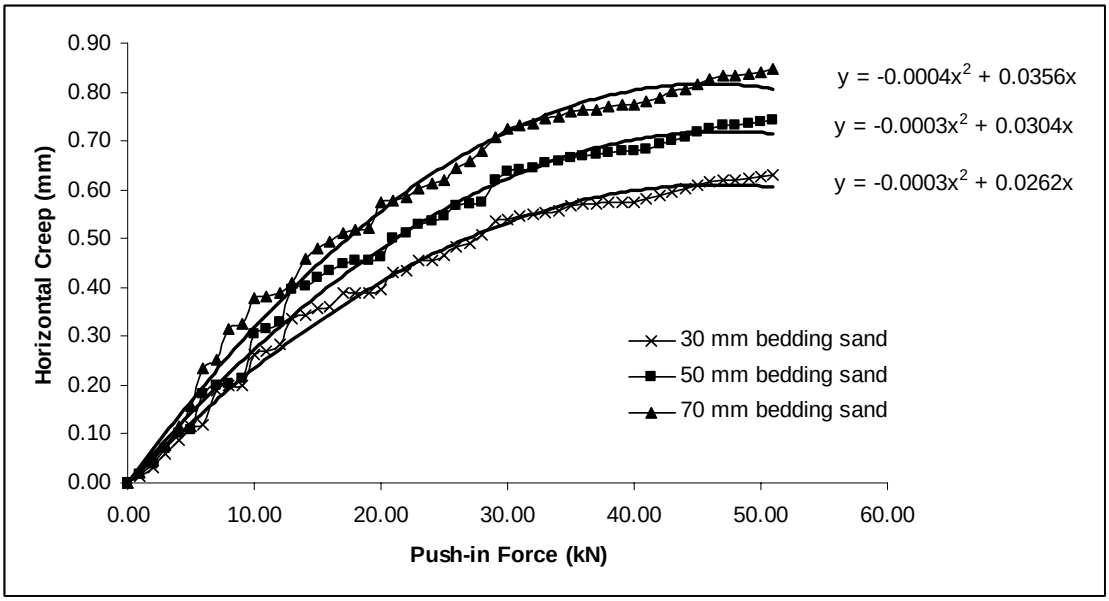

Figure H1.2 CBP specifications: rectangular block shape, 60 mm block thickness, stretcher bond laying pattern, 5 mm joint width and 12 % degree of slope.

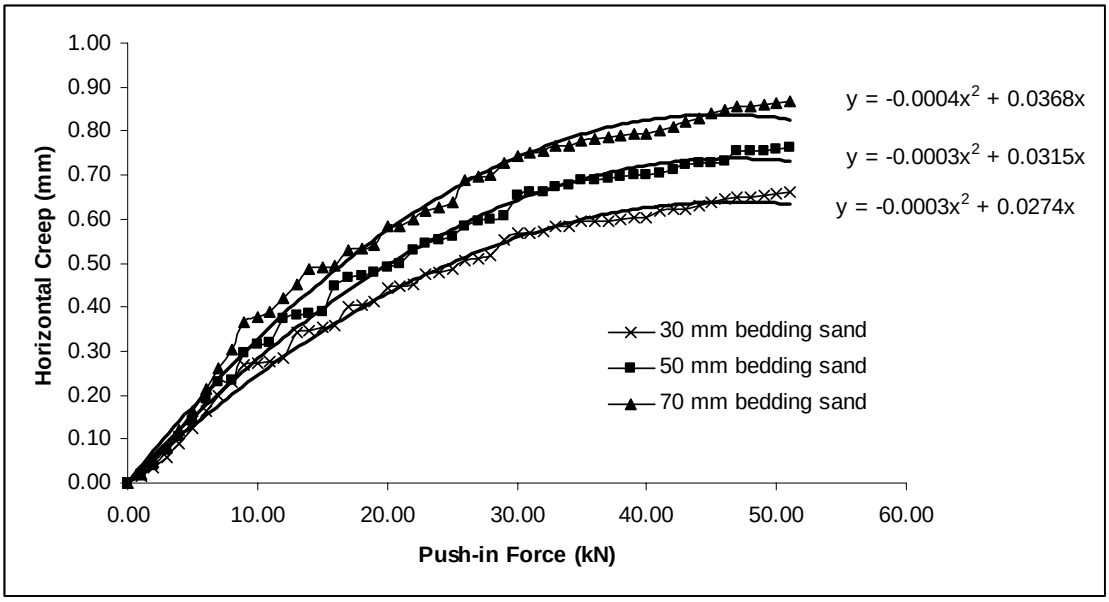

Figure H1.3 CBP specifications: rectangular block shape, 60 mm block thickness, stretcher bond laying pattern, 7 mm joint width and 12 % degree of slope.

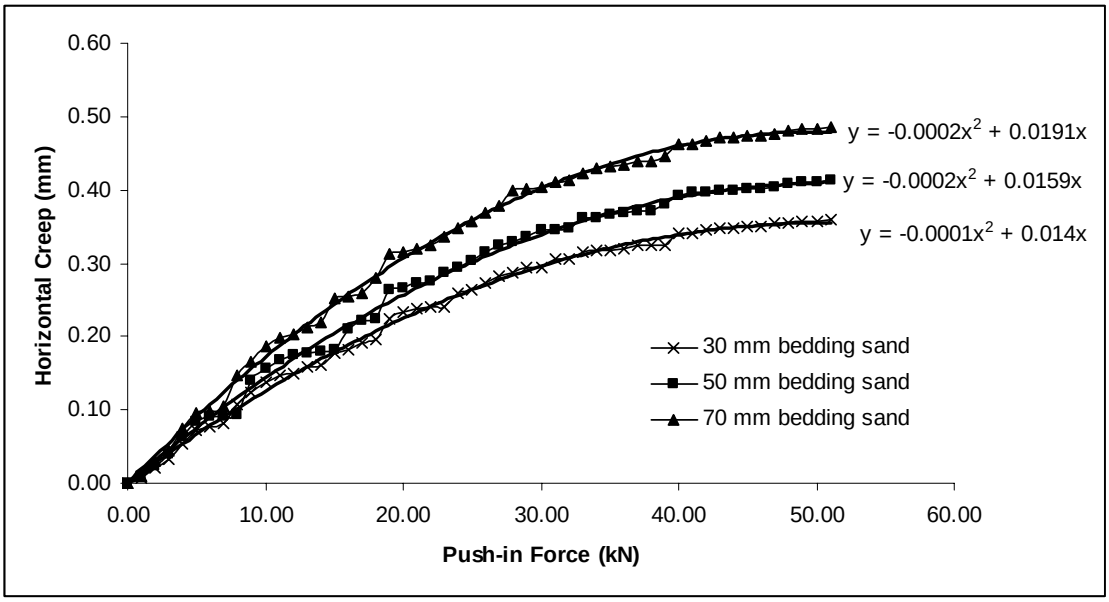

Figure H1.4 CBP specifications: rectangular block shape, 100 mm block thickness, stretcher bond laying pattern, 3 mm joint width and 12 % degree of slope.

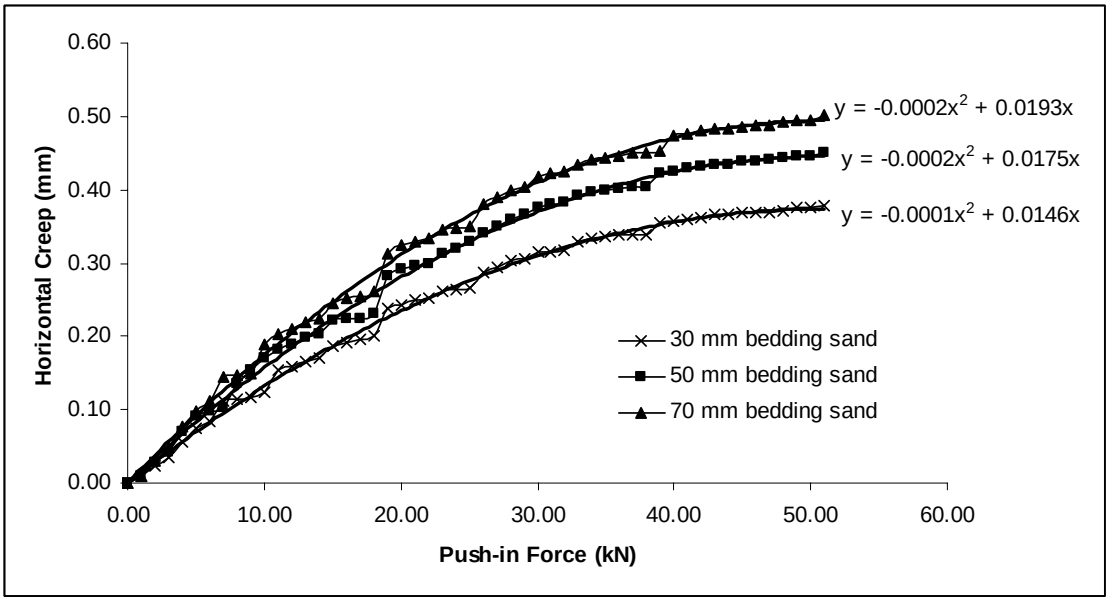

Figure H1.5 CBP specifications: rectangular block shape, 100 mm block thickness, stretcher bond laying pattern, 5 mm joint width and 12 % degree of slope.

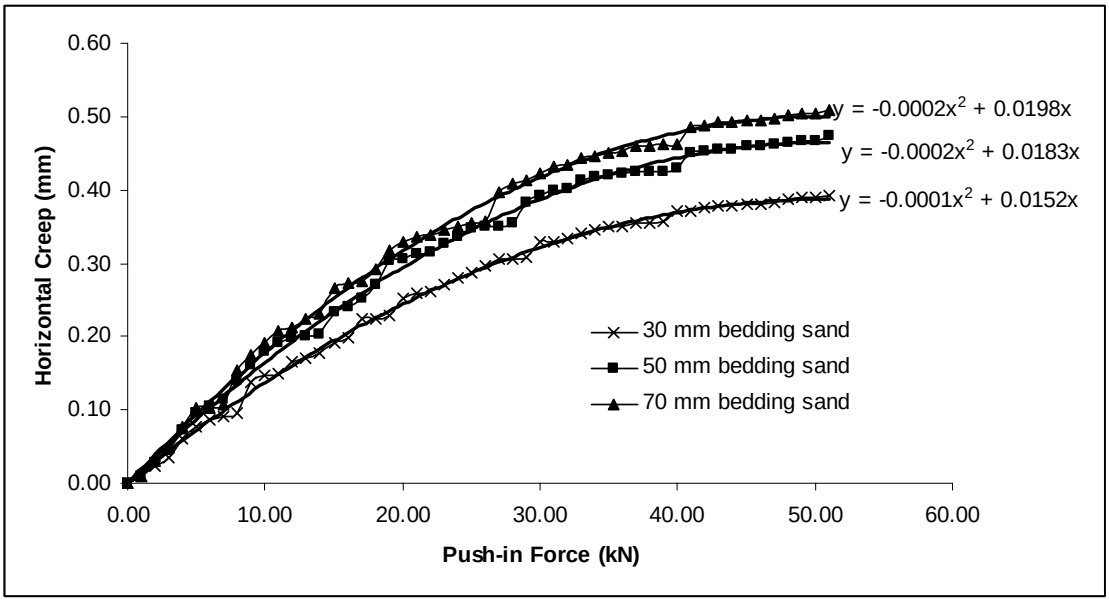

Figure H1.6 CBP specifications: rectangular block shape, 100 mm block thickness, stretcher bond laying pattern, 7 mm joint width and 12 % degree of slope.

APPENDIX – H1

Horizontal Creep on Push-in Test 12 % CBP Slope
The Effect of Bedding Sand Thickness

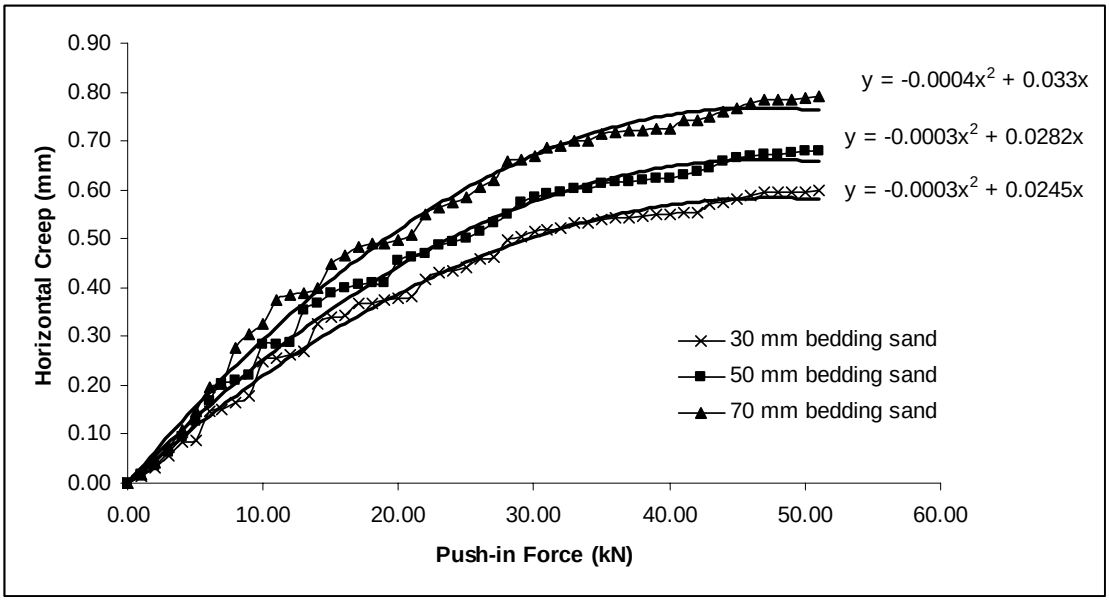

Figure H1.1 CBP specifications: rectangular block shape, 60 mm block thickness, stretcher bond laying pattern, 3 mm joint width and 12 % degree of slope.

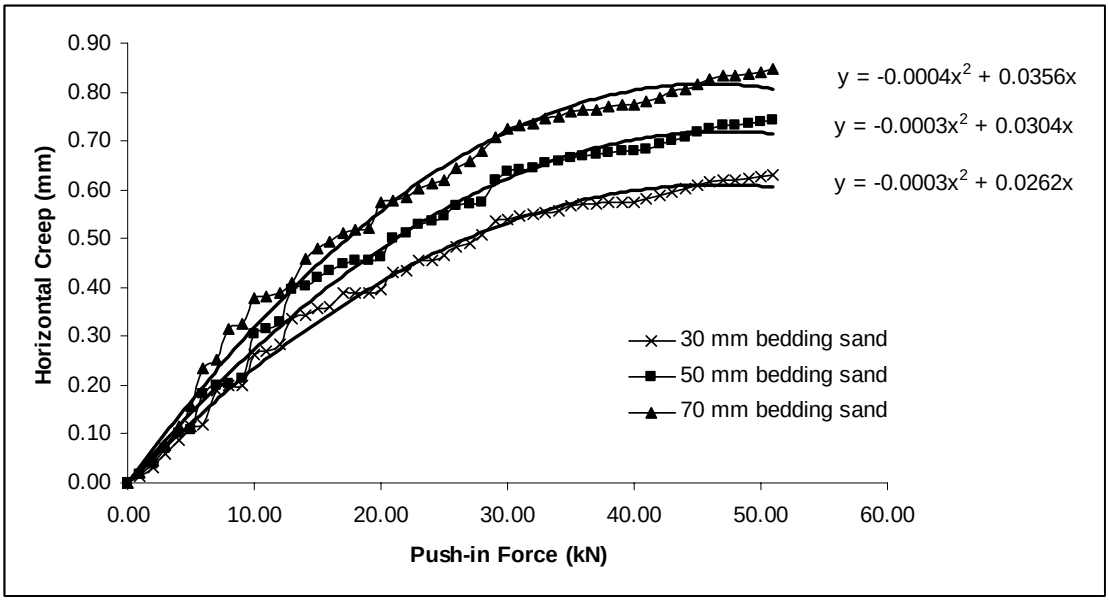

Figure H1.2 CBP specifications: rectangular block shape, 60 mm block thickness, stretcher bond laying pattern, 5 mm joint width and 12 % degree of slope.

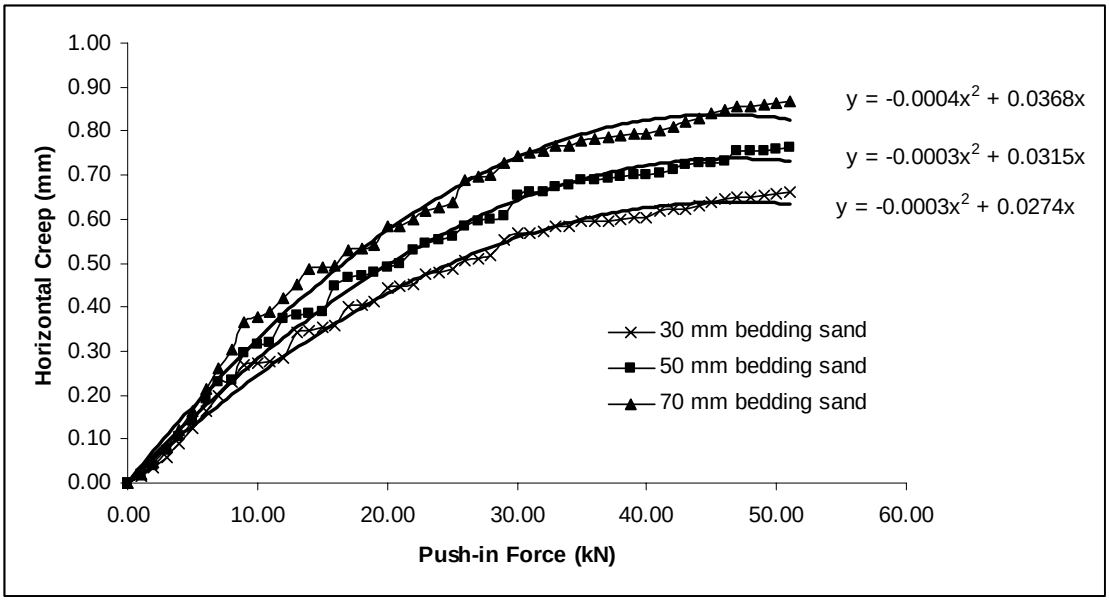

Figure H1.3 CBP specifications: rectangular block shape, 60 mm block thickness, stretcher bond laying pattern, 7 mm joint width and 12 % degree of slope.

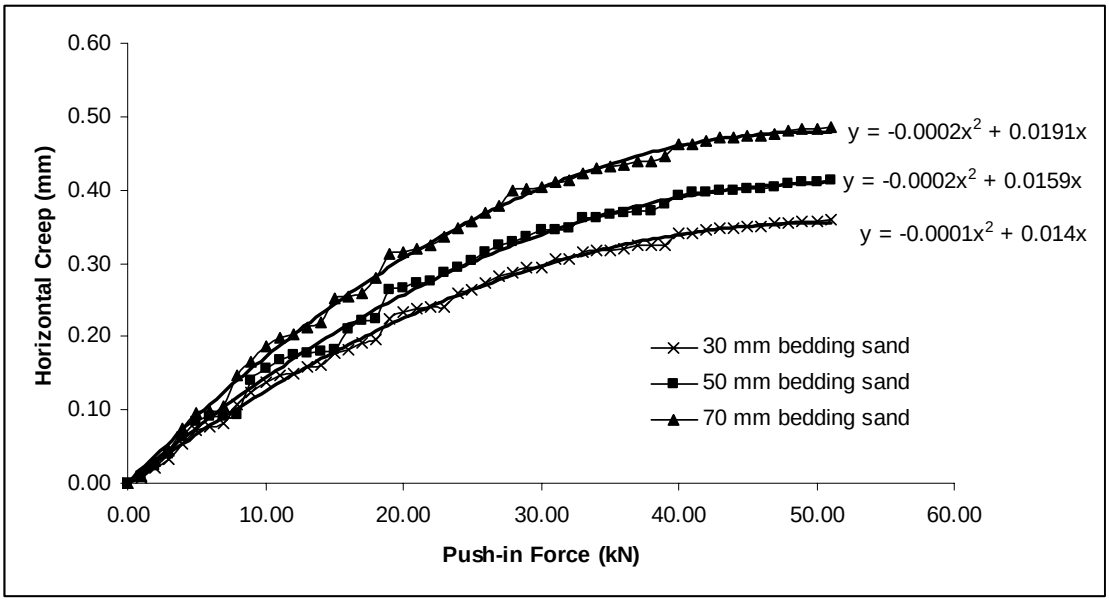

Figure H1.4 CBP specifications: rectangular block shape, 100 mm block thickness, stretcher bond laying pattern, 3 mm joint width and 12 % degree of slope.

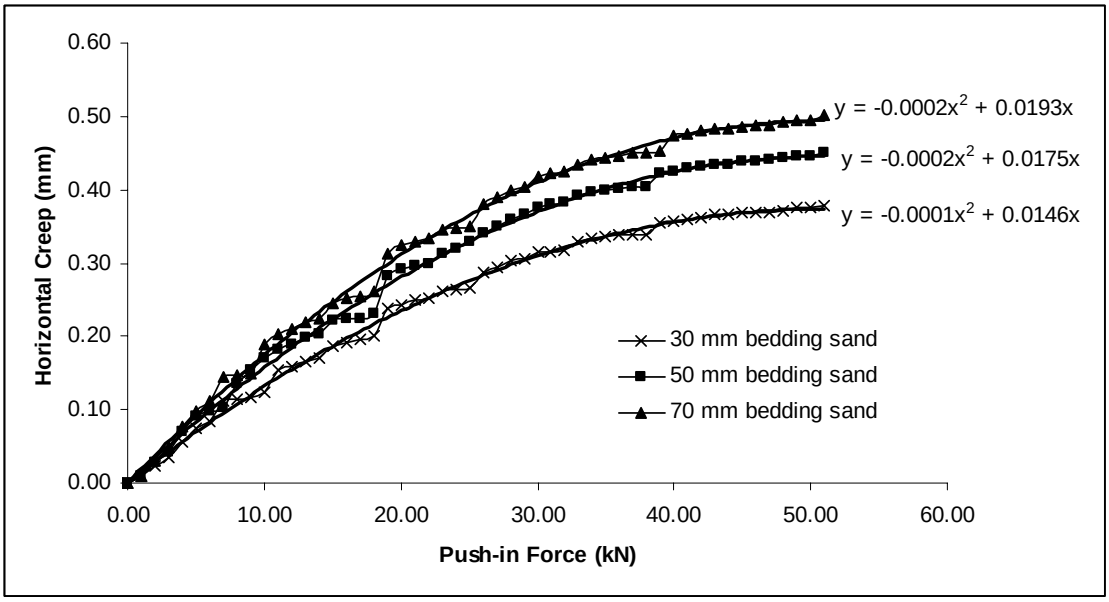

Figure H1.5 CBP specifications: rectangular block shape, 100 mm block thickness, stretcher bond laying pattern, 5 mm joint width and 12 % degree of slope.

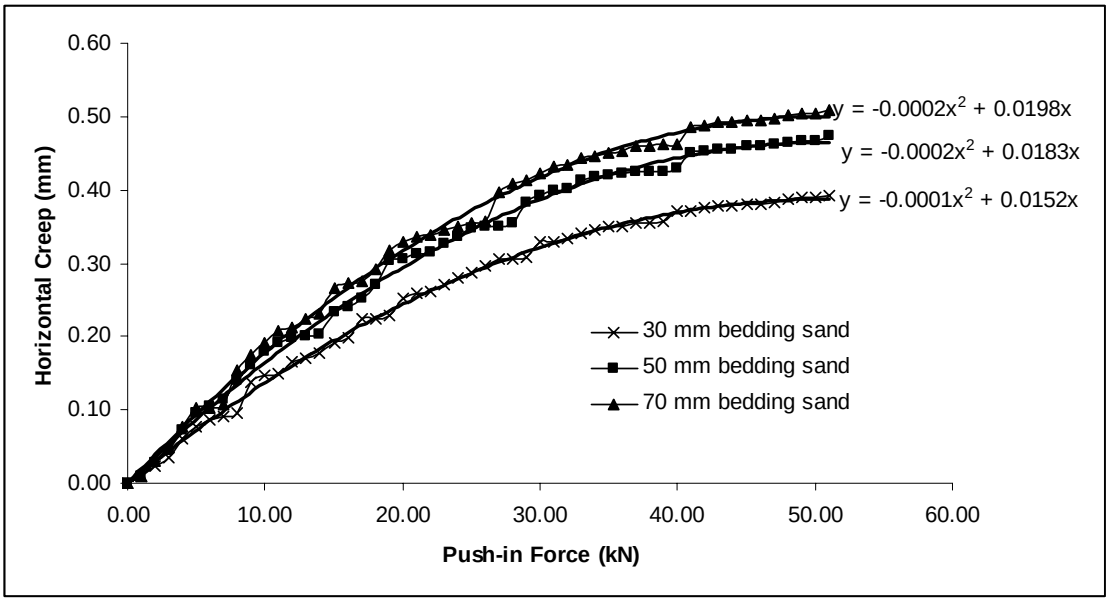

Figure H1.6 CBP specifications: rectangular block shape, 100 mm block thickness, stretcher bond laying pattern, 7 mm joint width and 12 % degree of slope.

APPENDIX – H2

Push-in Test on CBP 12 % Slope
The Effect of Block Thickness

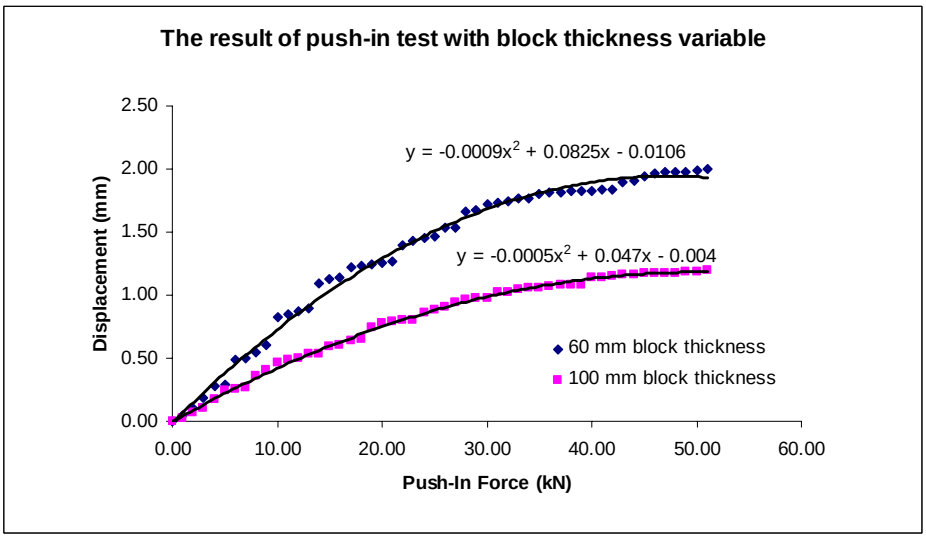

Figure H2.1 CBP specifications: rectangular block shape, 30 mm bedding sand thick, stretcher bond laying pattern, 3 mm joint width and 12 % degree of slope.

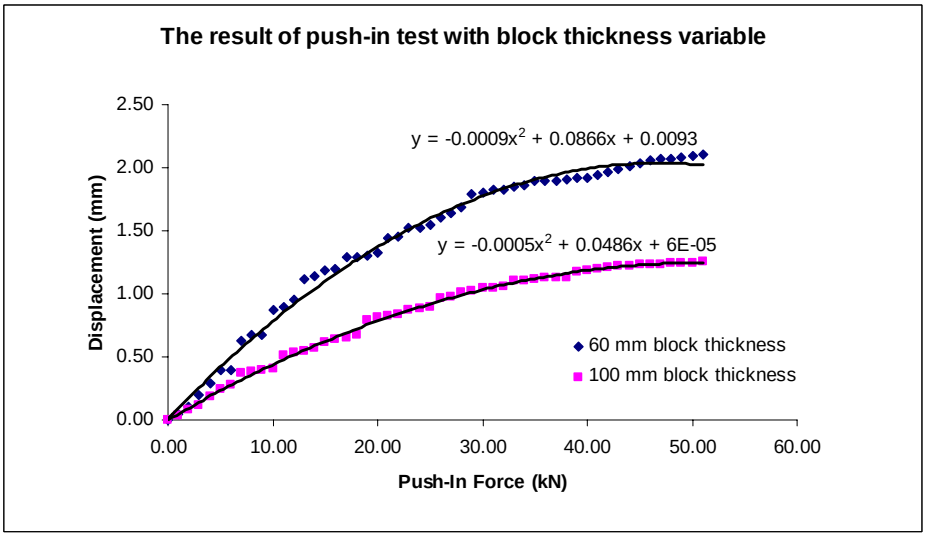

Figure H2.2 CBP specifications: rectangular block shape, 30 mm bedding sand thick, stretcher bond laying pattern, 5 mm joint width and 12 % degree of slope.

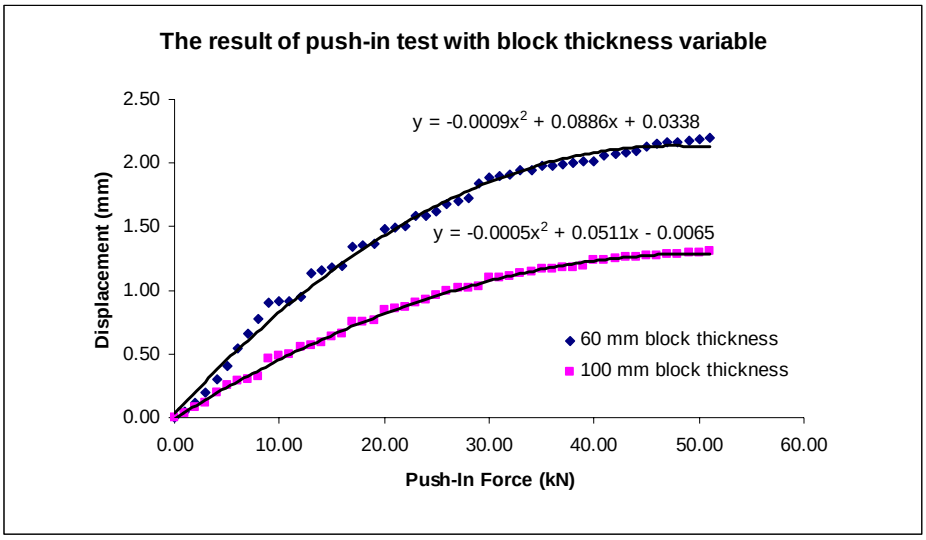

Figure H2.3 CBP specifications: rectangular block shape, 30 mm bedding sand thick, stretcher bond laying pattern, 7 mm joint width and 12 % degree of slope.

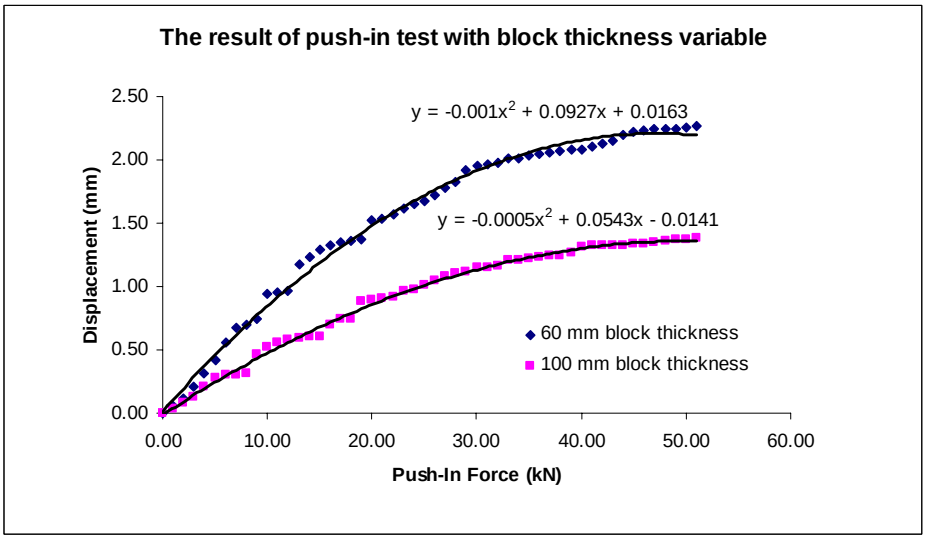

Figure H2.4 CBP specifications: rectangular block shape, 50 mm bedding sand thick, stretcher bond laying pattern, 3 mm joint width and 12 % degree of slope.

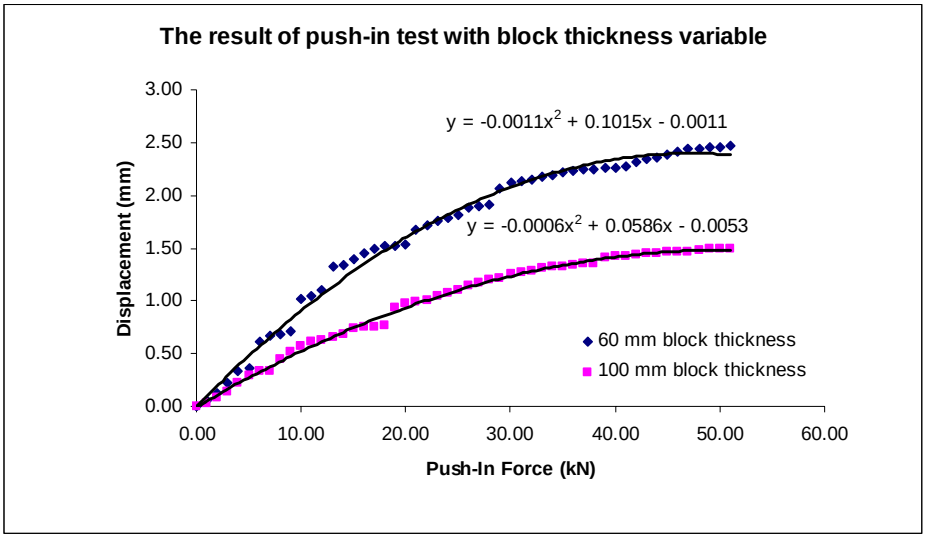

Figure H2.5 CBP specifications: rectangular block shape, 50 mm bedding sand thick, stretcher bond laying pattern, 5 mm joint width and 12 % degree of slope.

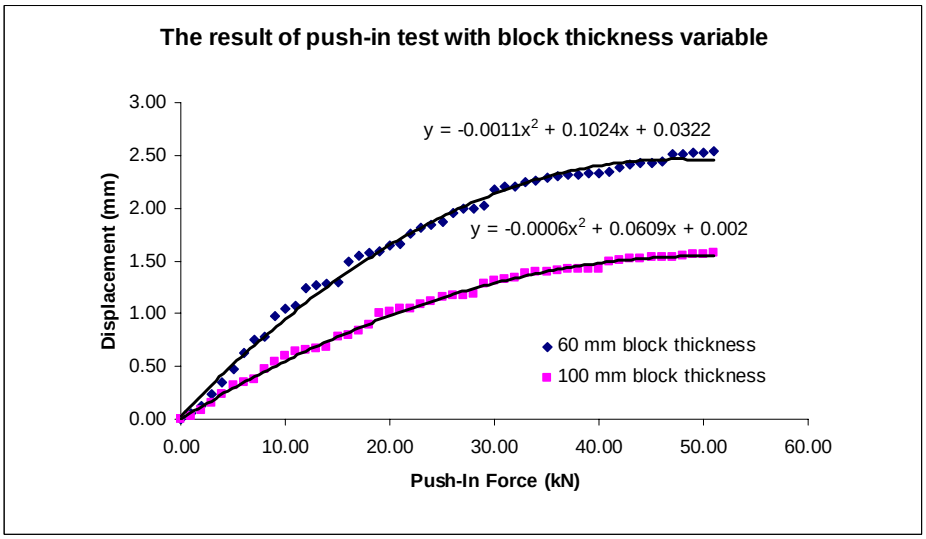

Figure H2.6 CBP specifications: rectangular block shape, 50 mm bedding sand thick, stretcher bond laying pattern, 7 mm joint width and 12 % degree of slope.

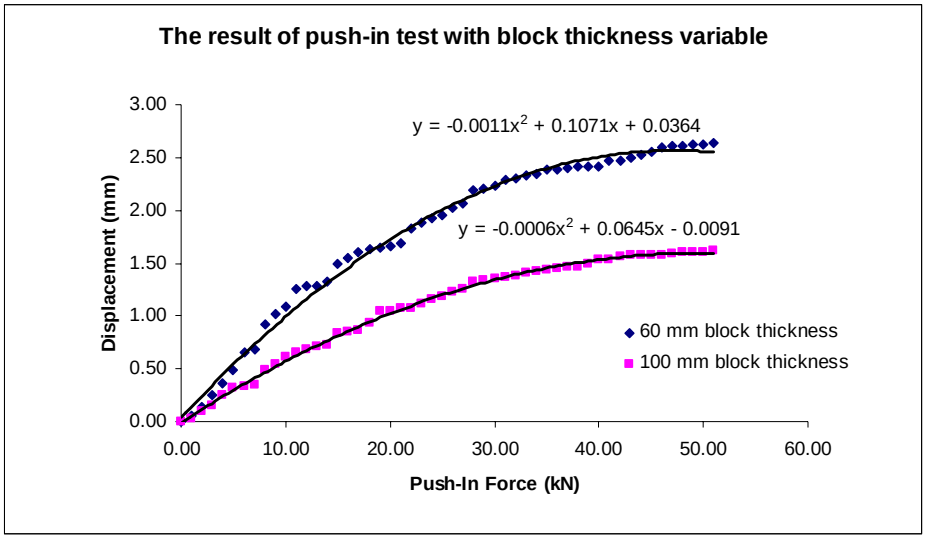

Figure H2.7 CBP specifications: rectangular block shape, 70 mm bedding sand thick, stretcher bond laying pattern, 3 mm joint width and 12 % degree of slope.

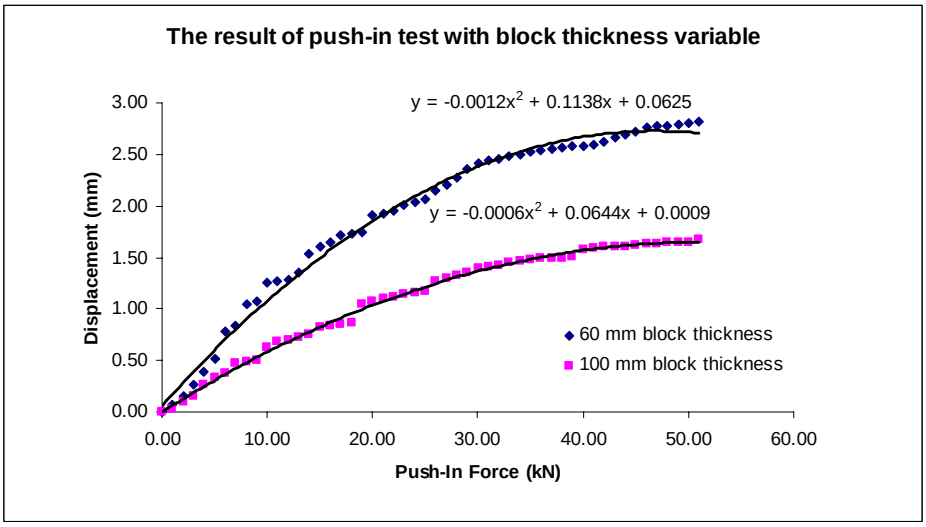

Figure H2.8 CBP specifications: rectangular block shape, 70 mm bedding sand thick, stretcher bond laying pattern, 5 mm joint width and 12 % degree of slope.

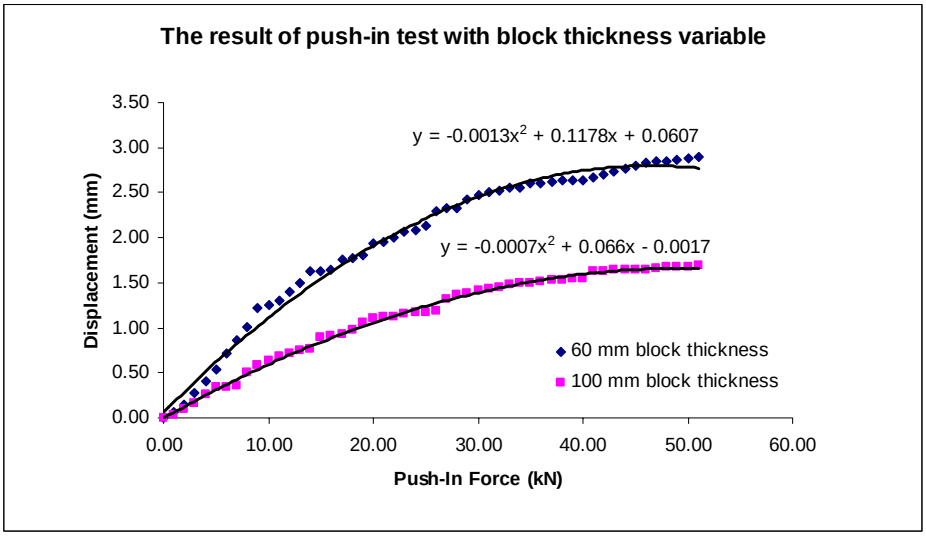

Figure H2.9 CBP specifications: rectangular block shape, 70 mm bedding sand thick, stretcher bond laying pattern, 7 mm joint width and 12 % degree of slope.

APPENDIX – H2

Horizontal Creep on Push-in Test CBP 12 % Slope
The Effect of Block Thickness

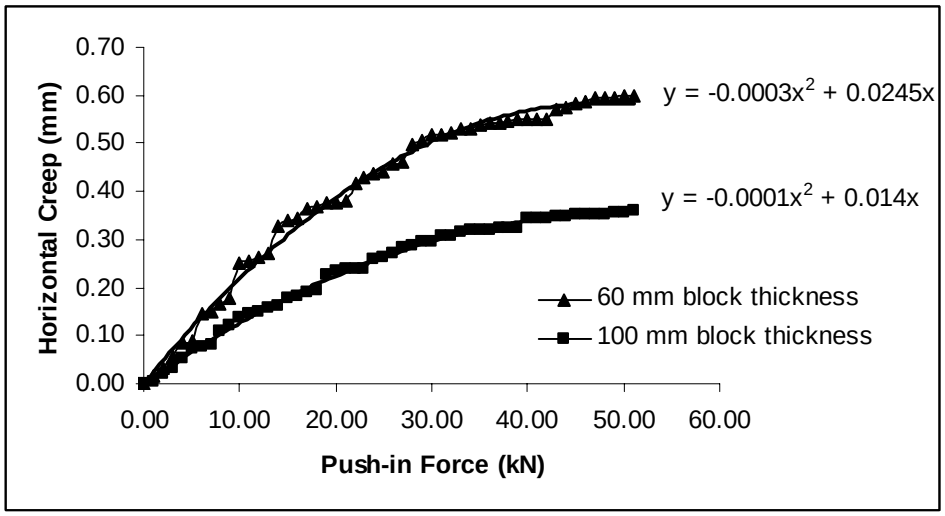

Figure H2.1 CBP specifications: rectangular block shape, 30 mm bedding sand thick, stretcher bond laying pattern, 3 mm joint width and 12 % degree of slope.

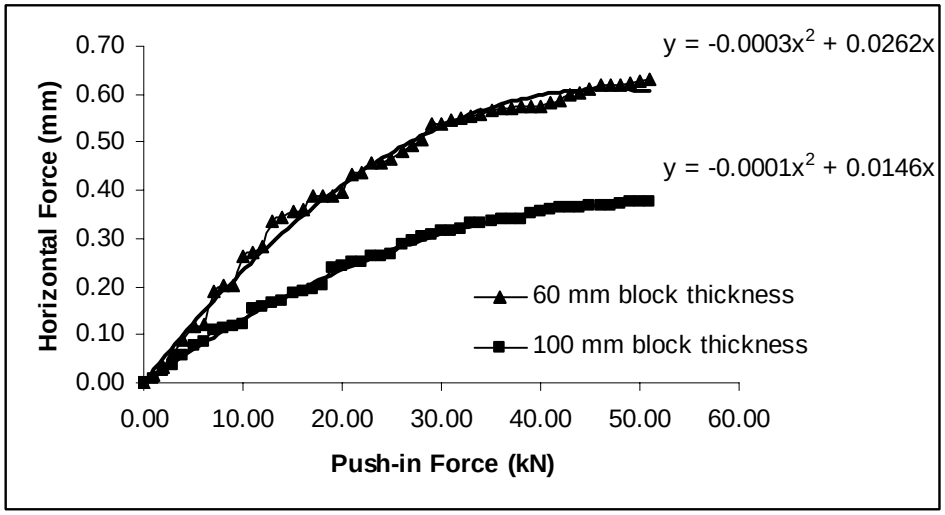

Figure H2.2 CBP specifications: rectangular block shape, 30 mm bedding sand thick, stretcher bond laying pattern, 5 mm joint width and 12 % degree of slope.

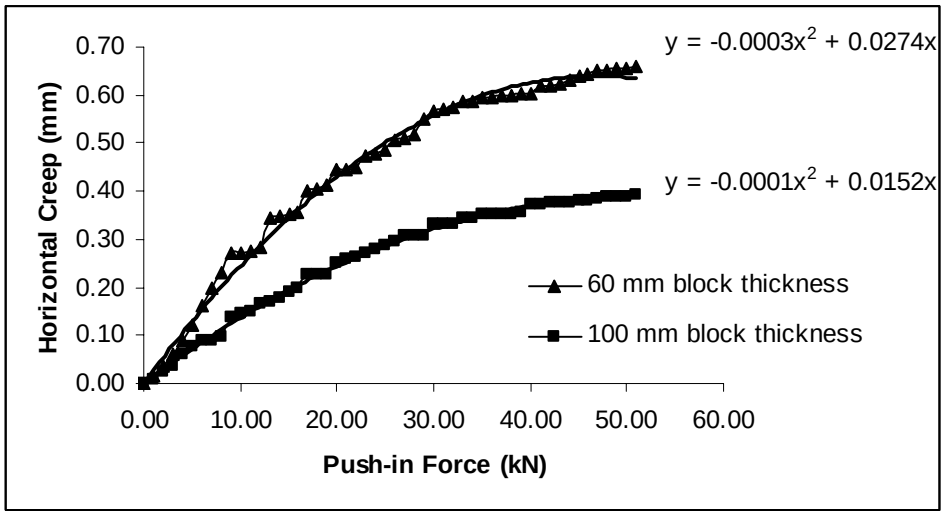

Figure H2.3 CBP specifications: rectangular block shape, 30 mm bedding sand thick, stretcher bond laying pattern, 7 mm joint width and 12 % degree of slope.

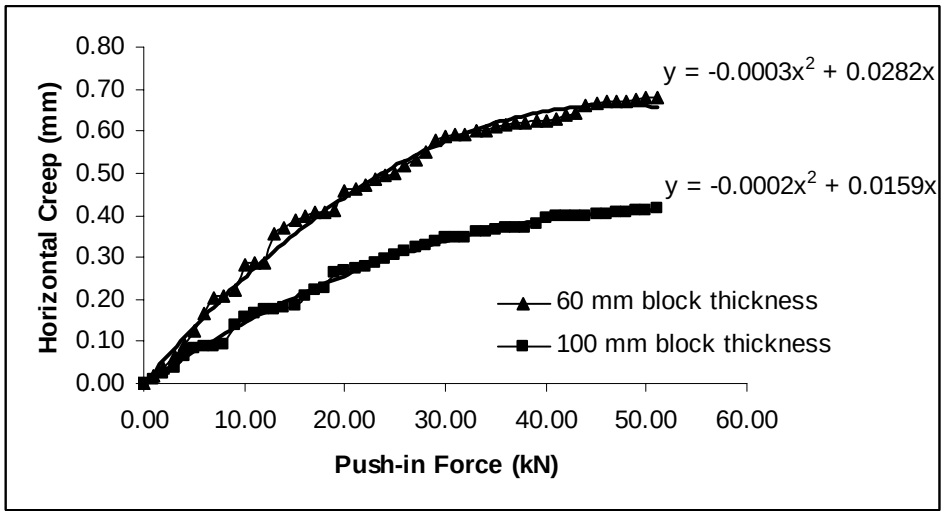

Figure H2.4 CBP specifications: rectangular block shape, 50 mm bedding sand thick, stretcher bond laying pattern, 3 mm joint width and 12 % degree of slope.

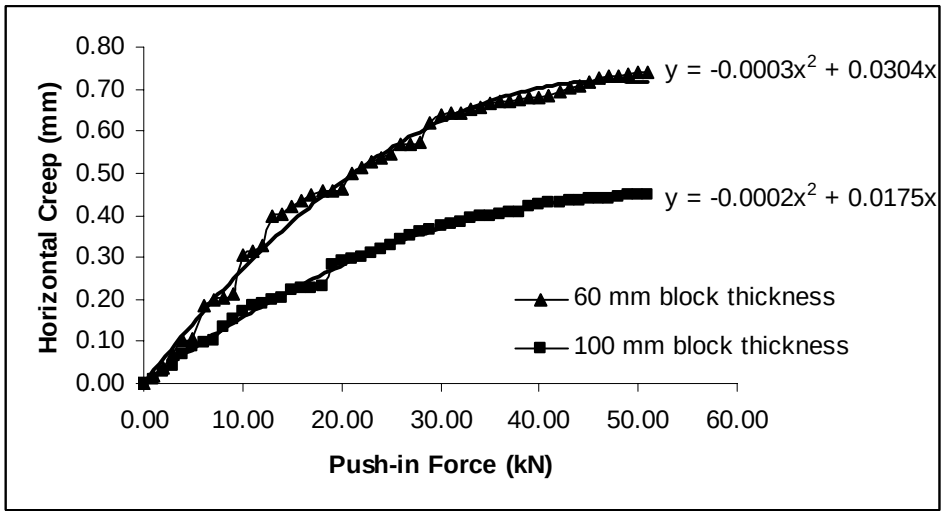

Figure H2.5 CBP specifications: rectangular block shape, 50 mm bedding sand thick, stretcher bond laying pattern, 5 mm joint width and 12 % degree of slope.

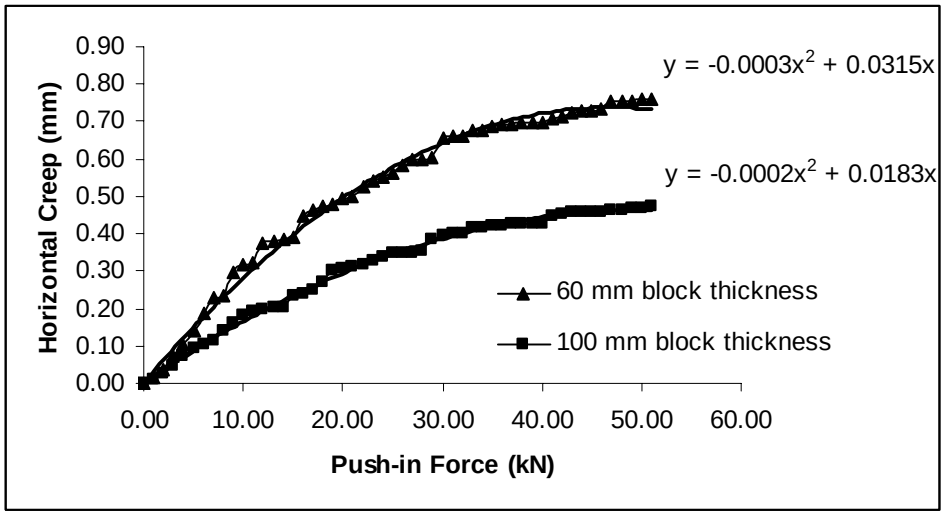

Figure H2.6 CBP specifications: rectangular block shape, 50 mm bedding sand thick, stretcher bond laying pattern, 7 mm joint width and 12 % degree of slope.

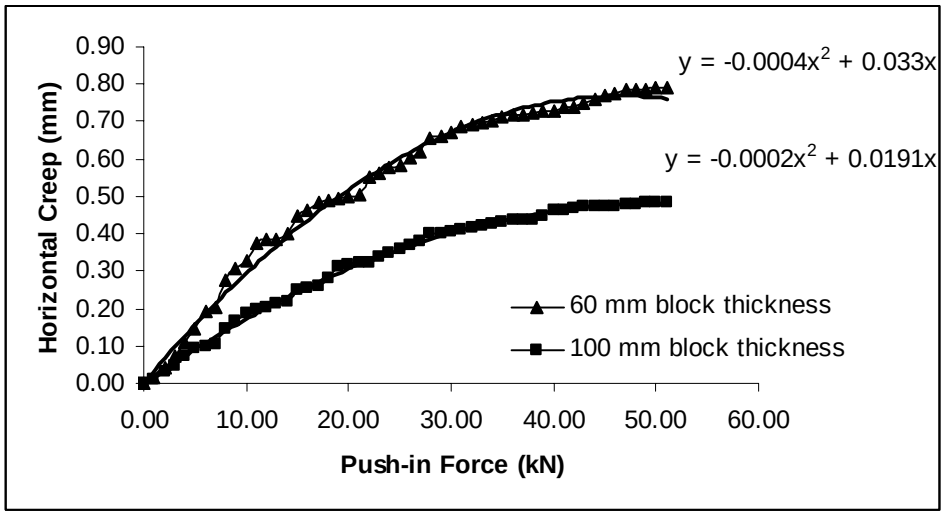

Figure H2.7 CBP specifications: rectangular block shape, 70 mm bedding sand thick, stretcher bond laying pattern, 3 mm joint width and 12 % degree of slope.

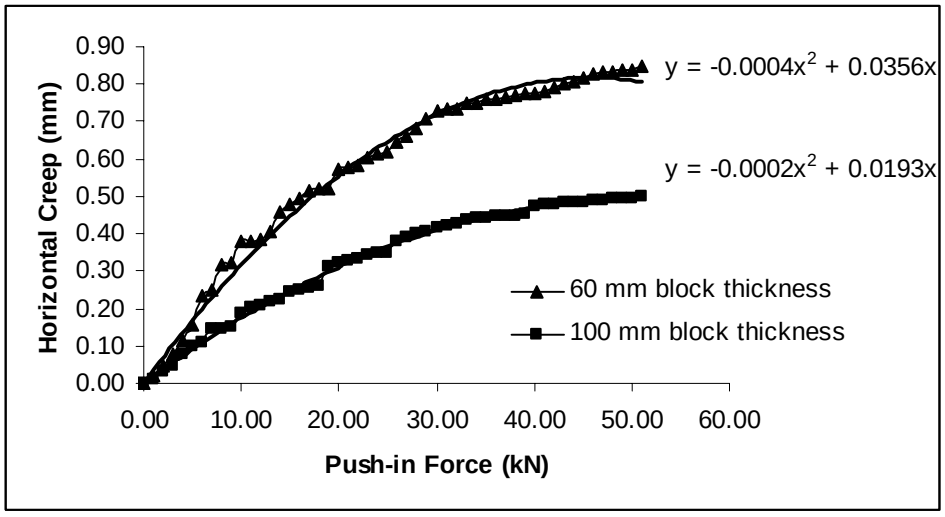

Figure H2.8 CBP specifications: rectangular block shape, 70 mm bedding sand thick, stretcher bond laying pattern, 5 mm joint width and 12 % degree of slope.

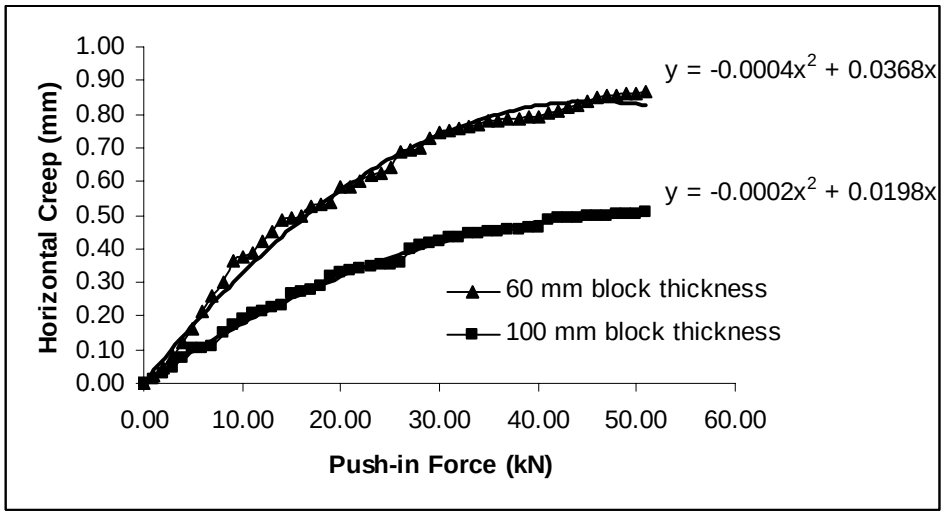

Figure H2.9 CBP specifications: rectangular block shape, 70 mm bedding sand thick, stretcher bond laying pattern, 7 mm joint width and 12 % degree of slope.

APPENDIX – H3

Push-in Test on CBP 12 % Slope
The Effect of Joint Width

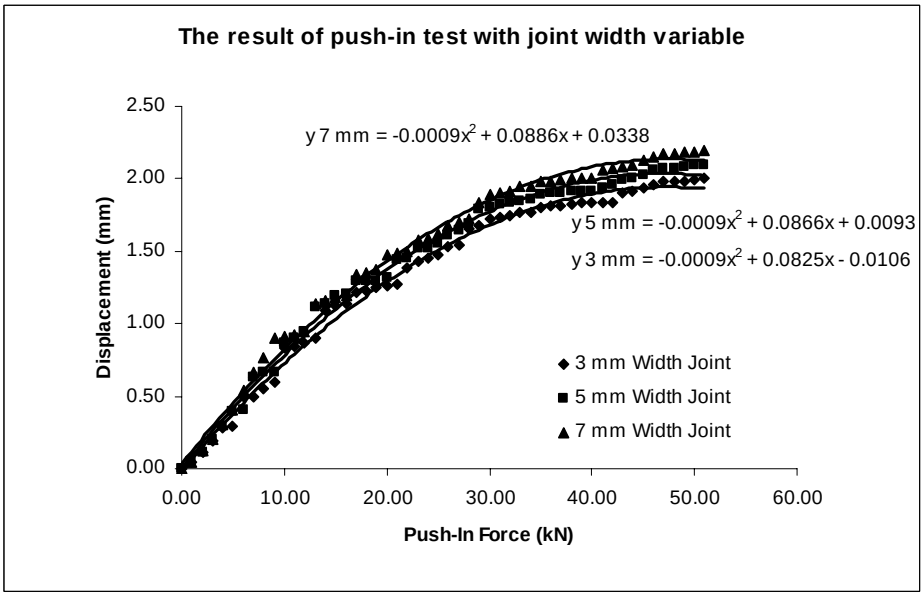

Figure H3.1 CBP specifications: rectangular block shape, 60 mm block thick, stretcher bond laying pattern, 30 mm bedding sand thick and 12 % degree of slope.

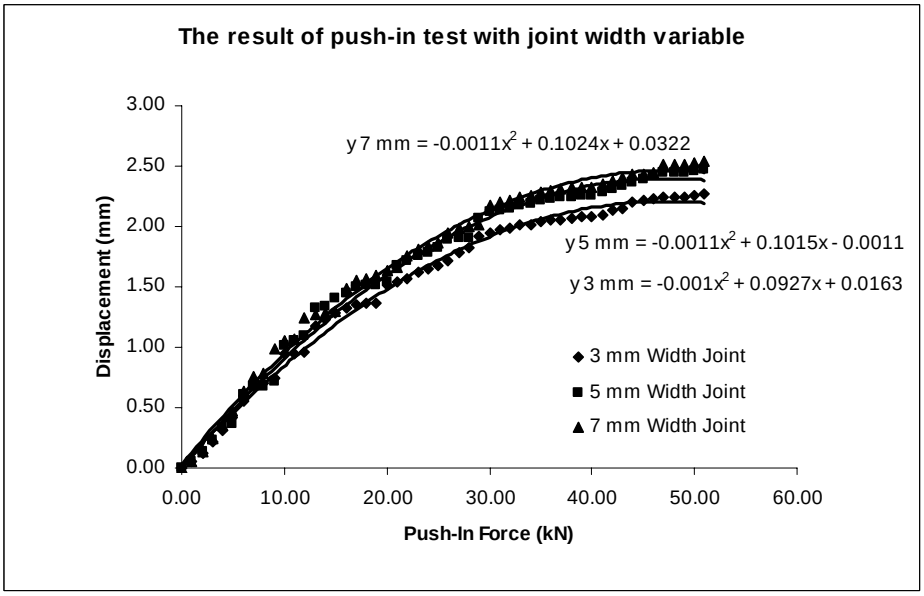

Figure H3.2 CBP specifications: rectangular block shape, 60 mm block thick, stretcher bond laying pattern, 50 mm bedding sand thick and 12 % degree of slope.

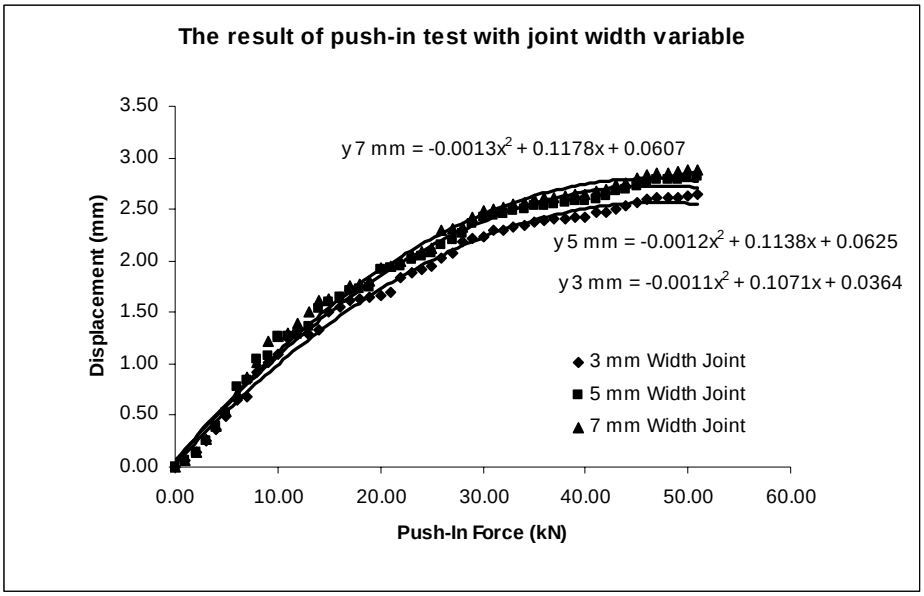

Figure H3.3 CBP specifications: rectangular block shape, 60 mm block thick, stretcher bond laying pattern, 70 mm bedding sand thick and 12 % degree of slope.

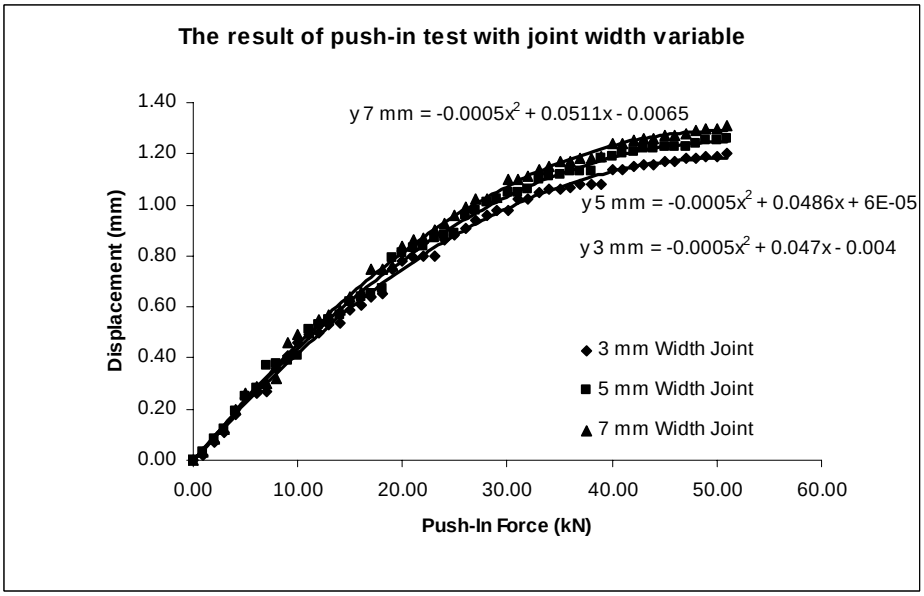

Figure H3.4 CBP specifications: rectangular shape, 100 mm block thick, stretcher bond laying pattern, 30 mm bedding sand thick and 12 % degree of slope.

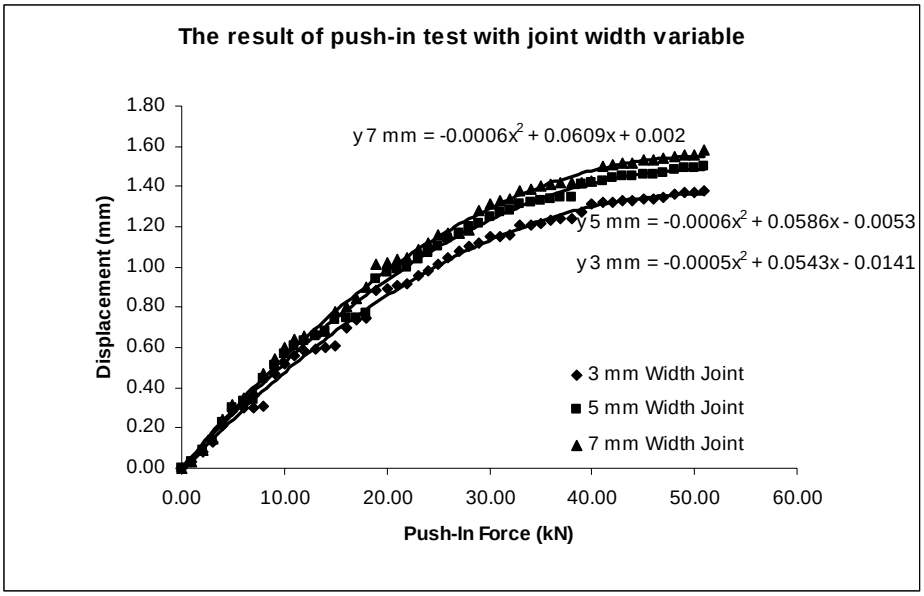

Figure H3.5 CBP specifications: rectangular shape, 100 mm block thick, stretcher bond laying pattern, 50 mm bedding sand thick and 12 % degree of slope.

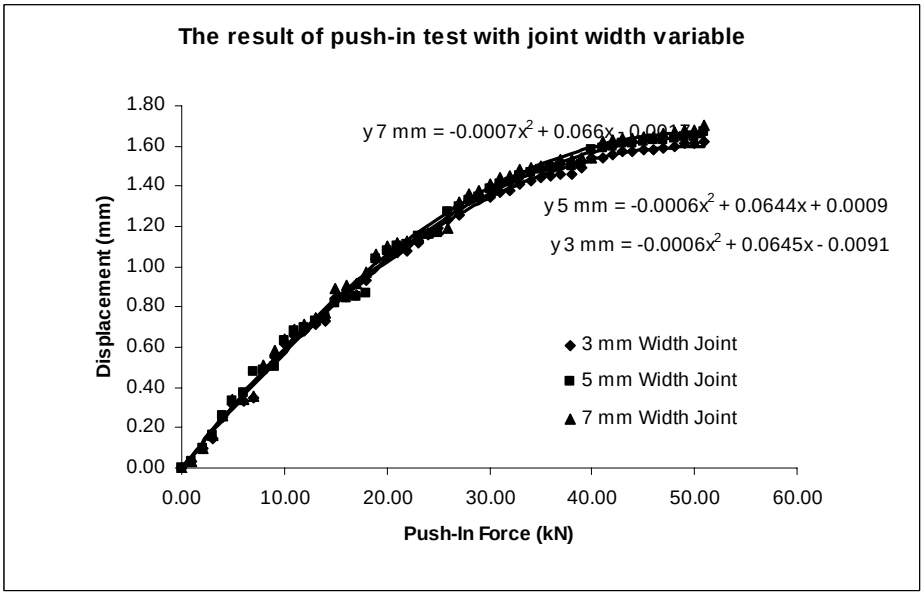

Figure H3.6 CBP specifications: rectangular shape, 100 mm block thick, stretcher bond laying pattern, 70 mm bedding sand thick and 12 % degree of slope.

APPENDIX – H3

Horizontal Creep on Push-in Test CBP 12 % Slope
The Effect of Joint Width

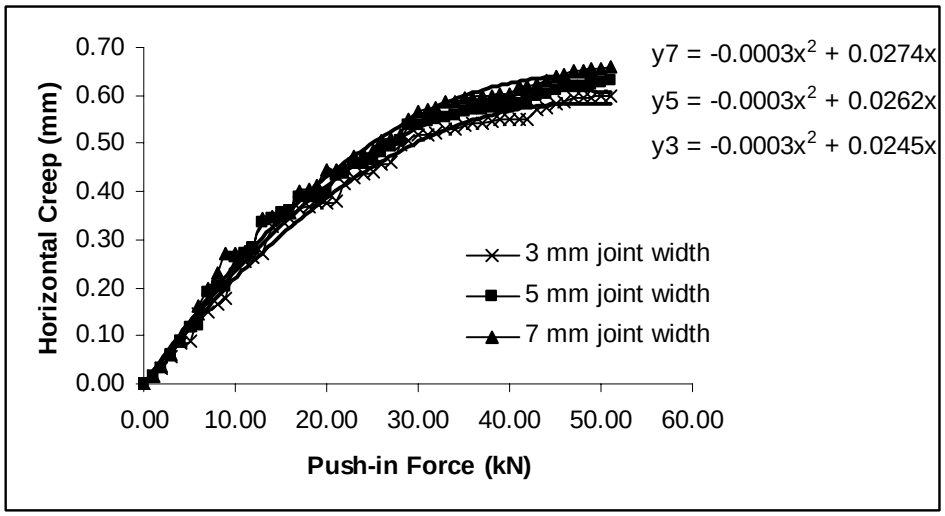

Figure H3.1 CBP specifications: rectangular block shape, 60 mm block thick, stretcher bond laying pattern, 30 mm bedding sand thick and 12 % degree of slope.

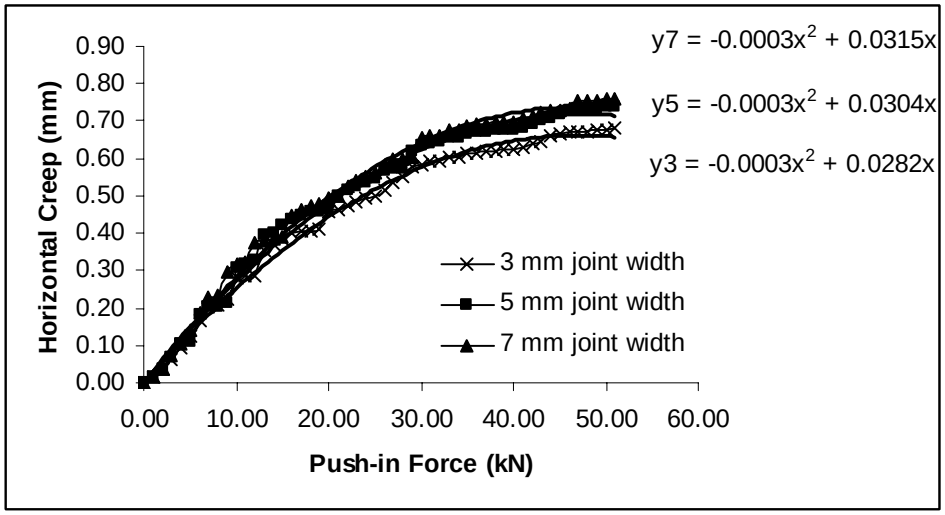

Figure H3.2 CBP specifications: rectangular block shape, 60 mm block thick, stretcher bond laying pattern, 50 mm bedding sand thick and 12 % degree of slope.

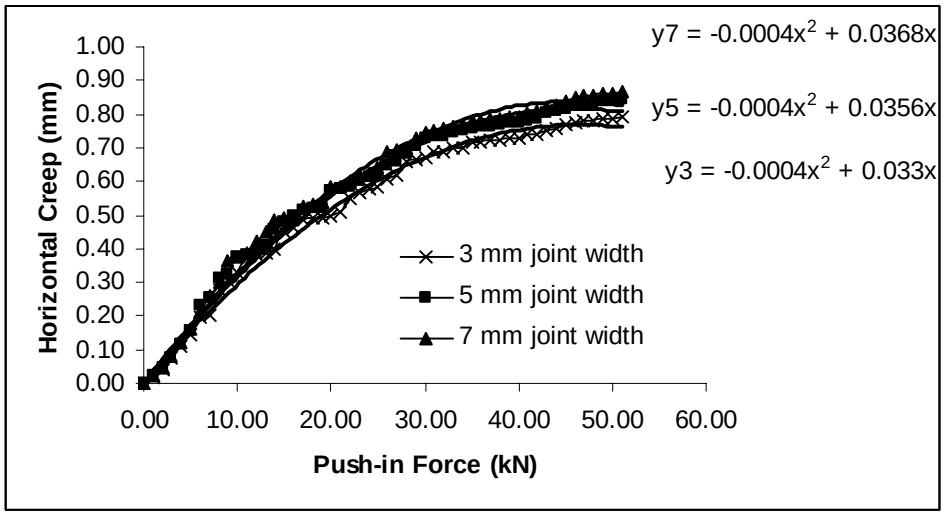

Figure H3.3 CBP specifications: rectangular block shape, 60 mm block thick, stretcher bond laying pattern, 70 mm bedding sand thick and 12 % degree of slope.

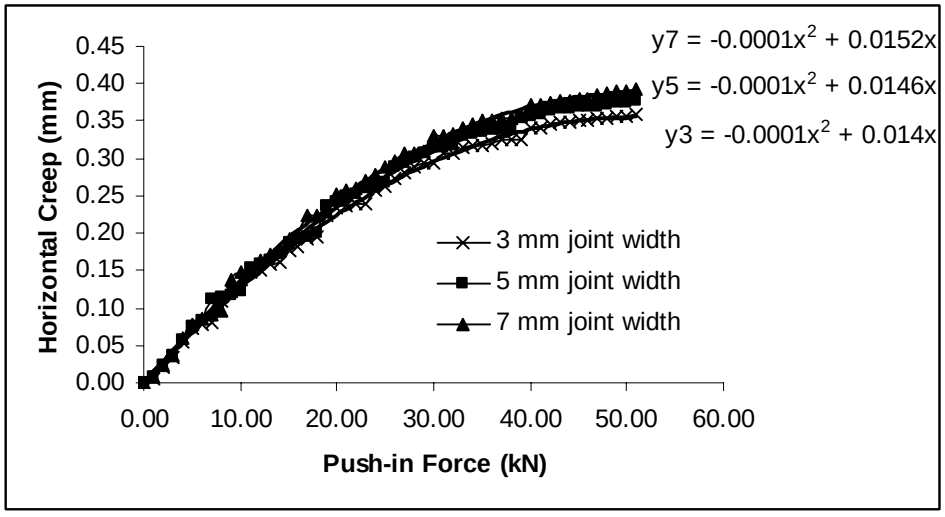

Figure H3.4 CBP specifications: rectangular shape, 100 mm block thick, stretcher bond laying pattern, 30 mm bedding sand thick and 12 % degree of slope.

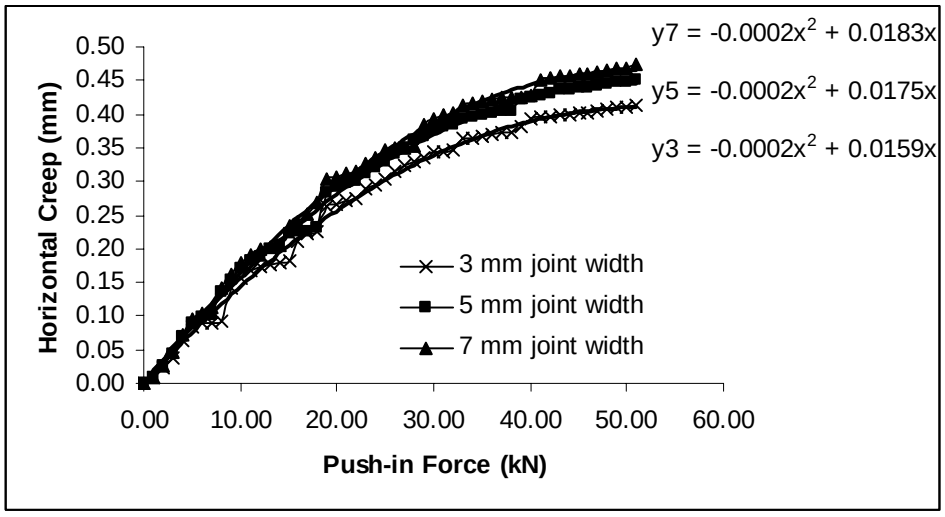

Figure H3.5 CBP specifications: rectangular shape, 100 mm block thick, stretcher bond laying pattern, 50 mm bedding sand thick and 12 % degree of slope.

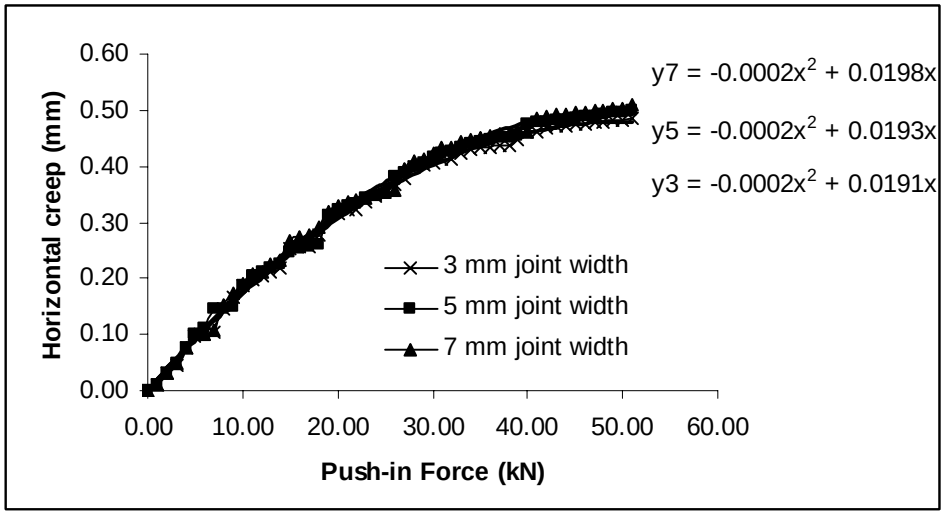

Figure H3.6 CBP specifications: rectangular shape, 100 mm block thick, stretcher bond laying pattern, 70 mm bedding sand thick and 12 % degree of slope.

Appendix - I

FINITE ELEMENT MODEL

Author: Rachmat Mudiyono

Company: FKA-UTM

Date: 17 November 2005

---

1. Introduction

Summarize the FEM analysis on Stretcher Bond

2. File Information

Model name:	Stretcher
Model location:	G:\Rachmat\Thesis\Apendix\Finite Element Folder\CBP\Stretcher.SLDASM
Results location:	C:\Program Files\COSMOS Applications\work
Study name:	Push-in Test

3. Materials

No.	Part Name	Material	Mass	Value
1	10-6-3 Joint sand-1	User Defined	0.031914 kg	1.773e-005 m^3
2	10-6-3 Joint sand-10	User Defined	0.031914 kg	1.773e-005 m^3
3	10-6-3 Joint sand-11	User Defined	0.031914 kg	1.773e-005 m^3
4	10-6-3 Joint sand-12	User Defined	0.031914 kg	1.773e-005 m^3
5	10-6-3 Joint sand-13	User Defined	0.031914 kg	1.773e-005 m^3
6	10-6-3 Joint sand-14	User Defined	0.031914 kg	1.773e-005 m^3
7	10-6-3 Joint sand-15	User Defined	0.031914 kg	1.773e-005 m^3
8	10-6-3 Joint sand-16	User Defined	0.031914 kg	1.773e-005 m^3
9	10-6-3 Joint sand-17	User Defined	0.031914 kg	1.773e-005 m^3
10	10-6-3 Joint sand-18	User Defined	0.031914 kg	1.773e-005 m^3
11	10-6-3 Joint sand-19	User Defined	0.031914 kg	1.773e-005 m^3
12	10-6-3 Joint sand-2	User Defined	0.031914 kg	1.773e-005 m^3
13	10-6-3 Joint sand-20	User Defined	0.031914 kg	1.773e-005 m^3
14	10-6-3 Joint sand-21	User Defined	0.031914 kg	1.773e-005 m^3
15	10-6-3 Joint sand-22	User Defined	0.031914 kg	1.773e-005 m^3
16	10-6-3 Joint sand-3	User Defined	0.031914 kg	1.773e-005 m^3
17	10-6-3 Joint sand-4	User Defined	0.031914 kg	1.773e-005 m^3
18	10-6-3 Joint sand-5	User Defined	0.031914 kg	1.773e-005 m^3
19	10-6-3 Joint sand-6	User Defined	0.031914 kg	1.773e-005 m^3
20	10-6-3 Joint sand-7	User Defined	0.031914 kg	1.773e-005 m^3
21	10-6-3 Joint sand-8	User Defined	0.031914 kg	1.773e-005 m^3
22	10-6-3 Joint sand-9	User Defined	0.031914 kg	1.773e-005 m^3
23	100-67-1	concrete	0.9246 kg	0.000402 m^3
24	100-79-60-1	concrete	1.0902 kg	0.000474 m^3
25	100-79-60-2	User Defined	1.0902 kg	0.000474 m^3
26	100-79-60-3	User Defined	1.0902 kg	0.000474 m^3
27	100-79-60-4	User Defined	1.0902 kg	0.000474 m^3
28	182-100-60-1	User Defined	2.5116 kg	0.001092 m^3
29	182-100-60-2	User Defined	2.5116 kg	0.001092 m^3
30	182-100-60-3	User Defined	2.5116 kg	0.001092 m^3
31	182-100-60-4	User Defined	2.5116 kg	0.001092 m^3

32	182-100-60-5	User Defined	2.5116 kg	0.001092 m^3
33	200-67-1	User Defined	1.8492 kg	0.000804 m^3
34	200-67-2	User Defined	1.8492 kg	0.000804 m^3
35	200-67-3	User Defined	1.8492 kg	0.000804 m^3
36	200-67-4	User Defined	1.8492 kg	0.000804 m^3
37	497-60-3-1	User Defined	0.322056 kg	0.00017892 m^3
38	497-60-3-2	User Defined	0.322056 kg	0.00017892 m^3
39	497-60-3-3	User Defined	0.322056 kg	0.00017892 m^3
40	497-60-3-4	User Defined	0.322056 kg	0.00017892 m^3
41	497-60-3-5	User Defined	0.322056 kg	0.00017892 m^3
42	497-60-3-6	User Defined	0.322056 kg	0.00017892 m^3
43	497-60-3-7	User Defined	0.322056 kg	0.00017892 m^3
44	67-60-3-1	User Defined	0.021708 kg	1.206e-005 m^3
45	67-60-3-2	User Defined	0.021708 kg	1.206e-005 m^3
46	67-60-3-3	User Defined	0.021708 kg	1.206e-005 m^3
47	67-60-3-4	User Defined	0.021708 kg	1.206e-005 m^3
48	67-60-3-5	User Defined	0.021708 kg	1.206e-005 m^3
49	79-67-1	[SW]concrete	0.730434 kg	0.00031758 m^3
50	Edge Rest Short-1	[SW]Acrylic (Medium-high impact)	2.4 kg	0.002 m^3
51	Edge Rest Short-2	[SW]Acrylic (Medium-high impact)	2.4 kg	0.002 m^3
52	Joint full-29	User Defined	0.324 kg	0.00018 m^3
53	Joint full-7	User Defined	0.324 kg	0.00018 m^3
54	Joint half-1	User Defined	0.0324 kg	1.8e-005 m^3
55	Joint half-10	User Defined	0.0324 kg	1.8e-005 m^3
56	Joint half-11	User Defined	0.0324 kg	1.8e-005 m^3
57	Joint half-17	User Defined	0.0324 kg	1.8e-005 m^3
58	Joint half-31	User Defined	0.0324 kg	1.8e-005 m^3
59	Joint half-36	User Defined	0.0324 kg	1.8e-005 m^3
60	Joint half-4	User Defined	0.0324 kg	1.8e-005 m^3
61	Joint half-40	User Defined	0.0324 kg	1.8e-005 m^3
62	Joint half-41	User Defined	0.0324 kg	1.8e-005 m^3
63	Joint half-47	User Defined	0.0324 kg	1.8e-005 m^3
64	Joint half-48	User Defined	0.0324 kg	1.8e-005 m^3
65	Joint half-53	User Defined	0.0324 kg	1.8e-005 m^3
66	Joint half-56	User Defined	0.0324 kg	1.8e-005 m^3

67	Joint half-6	User Defined	0.0324 kg	1.8e-005 m^3
68	Joint half-60	User Defined	0.0324 kg	1.8e-005 m^3
69	Joint half-63	User Defined	0.0324 kg	1.8e-005 m^3
70	Joint half-64	User Defined	0.0324 kg	1.8e-005 m^3
71	Joint half-9	User Defined	0.0324 kg	1.8e-005 m^3
72	Joint sand edga short-1	User Defined	0.322056 kg	0.00017892 m^3
73	Joint sand edga short-2	User Defined	0.322056 kg	0.00017892 m^3
74	Joint sand edga short-3	User Defined	0.322056 kg	0.00017892 m^3
75	Joint sand edga short-4	User Defined	0.322056 kg	0.00017892 m^3
76	Loader-1	[SW]Gray Cast Iron	6.10726 kg	0.00084823 m^3
77	Paver half-10	User Defined	1.38 kg	0.0006 m^3
78	Paver half-11	User Defined	1.38 kg	0.0006 m^3
79	Paver half-12	User Defined	1.38 kg	0.0006 m^3
80	Paver half-5	User Defined	1.38 kg	0.0006 m^3
81	Paver-10	User Defined	2.76 kg	0.0012 m^3
82	Paver-11	User Defined	2.76 kg	0.0012 m^3
83	Paver-12	User Defined	2.76 kg	0.0012 m^3
84	Paver-30	User Defined	2.76 kg	0.0012 m^3
85	Paver-32	User Defined	2.76 kg	0.0012 m^3
86	Paver-36	User Defined	2.76 kg	0.0012 m^3
87	Paver-40	User Defined	2.76 kg	0.0012 m^3
88	Paver-41	User Defined	2.76 kg	0.0012 m^3
89	Paver-43	User Defined	2.76 kg	0.0012 m^3
90	Paver-46	User Defined	2.76 kg	0.0012 m^3
91	Paver-48	User Defined	2.76 kg	0.0012 m^3
92	Paver-50	User Defined	2.76 kg	0.0012 m^3
93	Paver-51	User Defined	2.76 kg	0.0012 m^3
94	Paver-53	User Defined	2.76 kg	0.0012 m^3
95	Paver-54	User Defined	2.76 kg	0.0012 m^3
96	Paver-55	User Defined	2.76 kg	0.0012 m^3
97	Paver-56	User Defined	2.76 kg	0.0012 m^3
98	Paver-57	User Defined	2.76 kg	0.0012 m^3
99	Paver-58	User Defined	2.76 kg	0.0012 m^3
100	Paver-59	User Defined	2.76 kg	0.0012 m^3
101	Paver-60	User Defined	2.76 kg	0.0012 m^3

102	Paver-61	User Defined	2.76 kg	0.0012 m^3
103	Paver-62	User Defined	2.76 kg	0.0012 m^3
104	Paver-63	User Defined	2.76 kg	0.0012 m^3
105	Paver-64	User Defined	2.76 kg	0.0012 m^3
106	Paver-65	User Defined	2.76 kg	0.0012 m^3
107	Paver-66	User Defined	2.76 kg	0.0012 m^3
108	Paver-67	User Defined	2.76 kg	0.0012 m^3
109	Paver-68	User Defined	2.76 kg	0.0012 m^3
110	Paver-69	User Defined	2.76 kg	0.0012 m^3
111	Paver-7	User Defined	2.76 kg	0.0012 m^3
112	Paver-70	User Defined	2.76 kg	0.0012 m^3
113	Paver-71	User Defined	2.76 kg	0.0012 m^3
114	Paver-72	User Defined	2.76 kg	0.0012 m^3
115	Paver-73	User Defined	2.76 kg	0.0012 m^3
116	Paver-74	User Defined	2.76 kg	0.0012 m^3
117	Rect 1-1	[SW]Acrylic (Medium-high impact)	2.448 kg	0.00204 m^3
118	Rect 1-2	[SW]Acrylic (Medium-high impact)	2.448 kg	0.00204 m^3
119	Rect 2-1	[SW]AISI 304	83.232 kg	0.010404 m^3
120	Sand-1	sand	90 kg	0.05 m^3

4. Load & Restraint Information

Restraint	
Restraint-3 <Rect 1-1, Edge Rest Short-1, Rect 1-2, Edge Rest Short-2>	on **4 Face(s)** fixed.
Description:	
Restraint-4 <Rect 2-1>	on **1 Face(s)** fixed.
Description:	
Restraint-2 <>	on **12 Component(s)** fixed.
Description:	

Load		Slope (%)
Force-1 <Loader-1>	on **1 Face(s)** apply force **-51000 N** along plane Dir 2**Front Plane** using uniform distribution	0 %
Force-1 <Loader-1> **Force-2 <Loader-1>**	on **1 Face(s)** apply force **-5095.9 N** along plane Dir 2**Front Plane** using uniform distribution on **1 Face(s)** apply force **203.78 N** along plane Dir 1 **Front Plane** using uniform distribution	4 %
Force-1 <Loader-1> **Force-2 <Loader-1>**	on **1 Face(s)** apply force **-5083.8 N** along plane Dir 2**Front Plane** using uniform distribution on **1 Face(s)** apply force **406.35 N** along plane Dir 1 **Front Plane** using uniform distribution	8 %
Force-1 <Loader-1> **Force-2 <Loader-1>**	on **1 Face(s)** apply force **-5063.7 N** along plane Dir 2**Front Plane** using uniform distribution on **1 Face(s)** apply force **607.4 N** along plane Dir 1 **Front Plane** using uniform distribution	12 %

5. Study Property

Mesh Information	
Mesh Type:	Solid mesh
Mesher Used:	Standard
Automatic Transition:	Off
Smooth Surface:	On
Jacobian Check:	4 Points
Element Size:	15 mm
Tolerance:	0.75 mm
Quality:	High
Number of elements:	316936
Number of nodes:	455277

6. Contact

Contact state: Touching faces - Bonded

7. Stress Results

Slope	Type	Min	Location	Max	Location
0 %	VON: von Mises stress	0.0495464 N/m^2 Node: 73177	(480.545 mm, 66.6963 mm, 483.721 mm)	4.29577e+006 N/m^2 Node: 121523	(-96.6129 mm, 120 mm, 122.834 mm)
4 %	VON: von Mises stress	0.0058612 N/m^2 Node: 73177	(480.545 mm, 66.6963 mm, 483.721 mm)	406725 N/m^2 Node: 121523	(-96.6129 mm, 120 mm, 122.834 mm)
8 %	VON: von Mises stress	0.00680915 N/m^2 Node: 73177	(480.545 mm, 66.6963 mm, 483.721 mm)	387955 N/m^2 Node: 121523	(-96.6129 mm, 120 mm, 122.834 mm)
12 %	VON: von Mises stress	0.00787986 N/m^2 Node: 73177	(480.545 mm, 66.6963 mm, 483.721 mm)	372842 N/m^2 Node: 121523	(-96.6129 mm, 120 mm, 122.834 mm)

Push-in Test-Stress : 0 % Slope

Model name: Stretcher 2
Study name: Push_in_test
Plot type: Static Nodal stress-Plot1
Deformation Scale: 1257.02

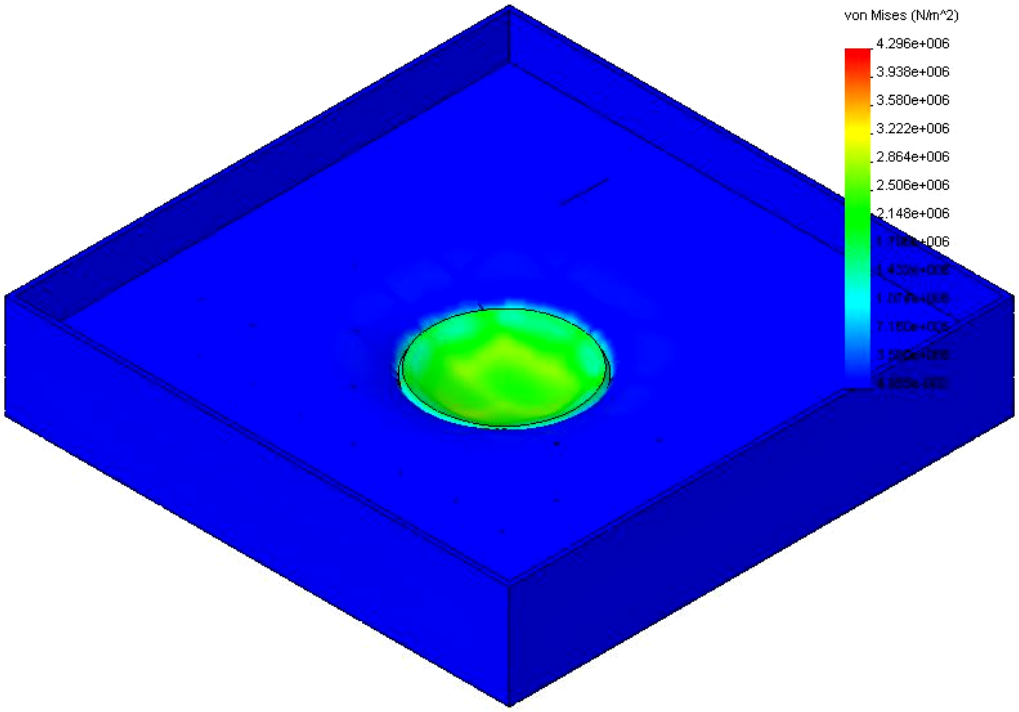

Push-in Test-Stress : 4 % Slope

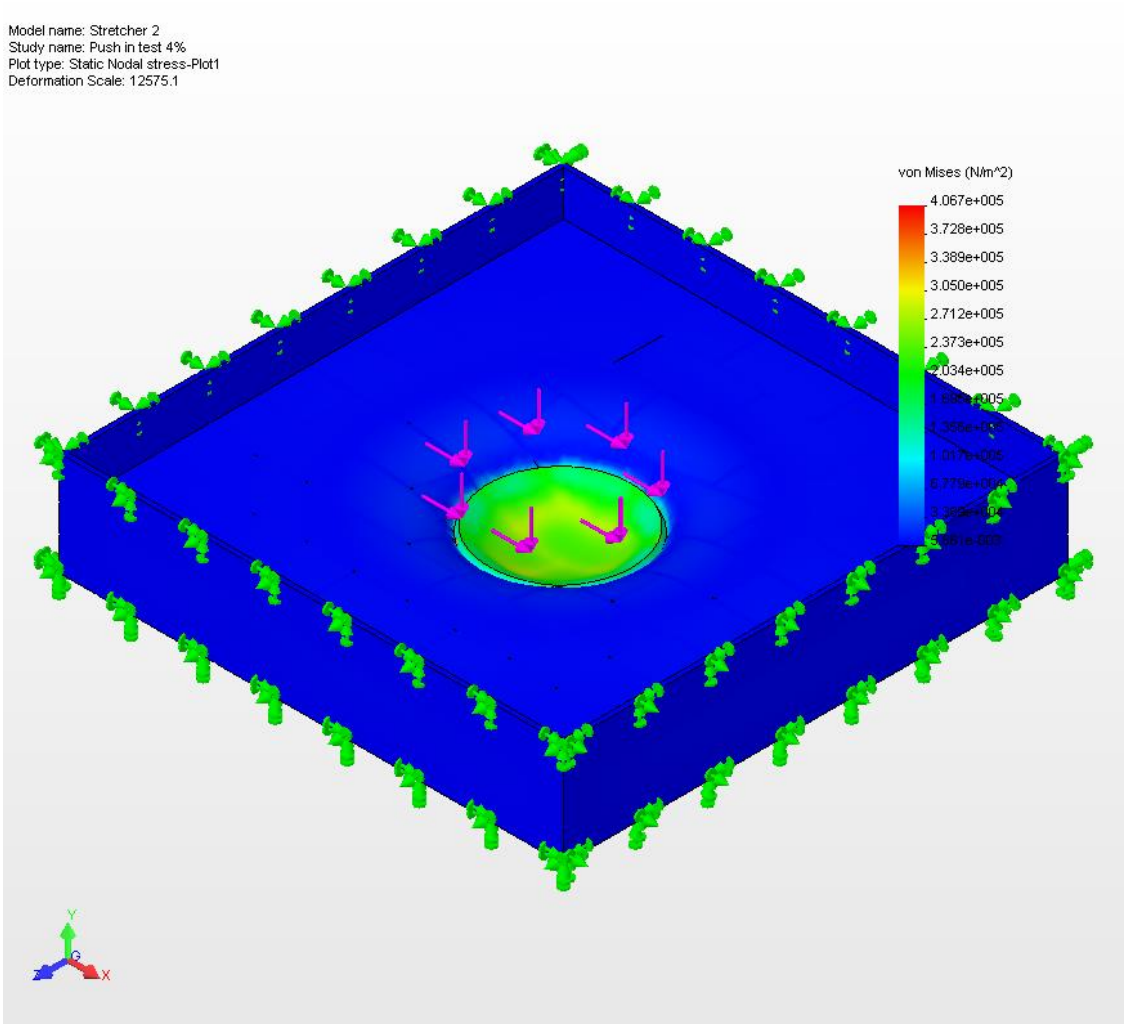

Push-in Test-Stress : 8 % Slope

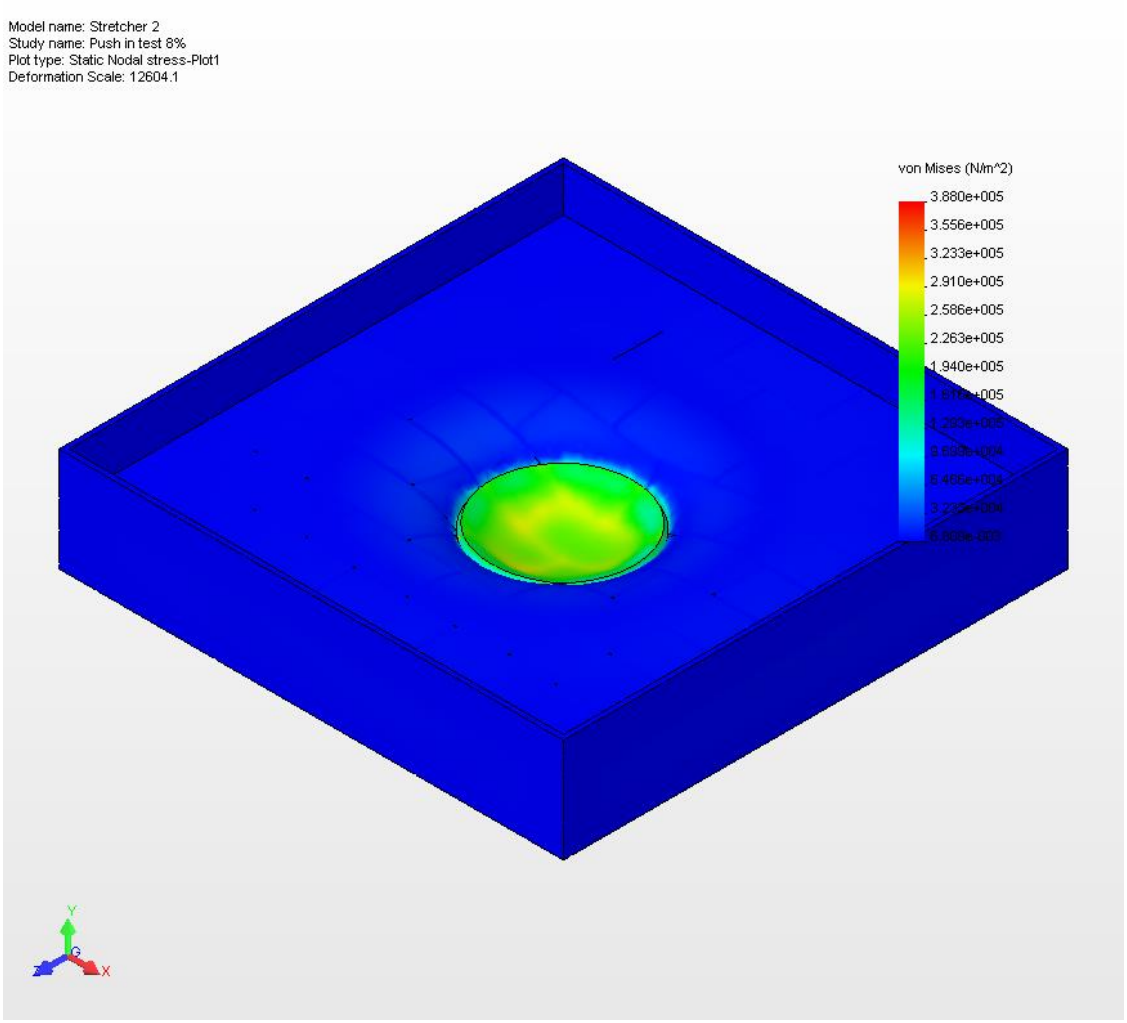

Push-in Test-Stress : 12 % Slope

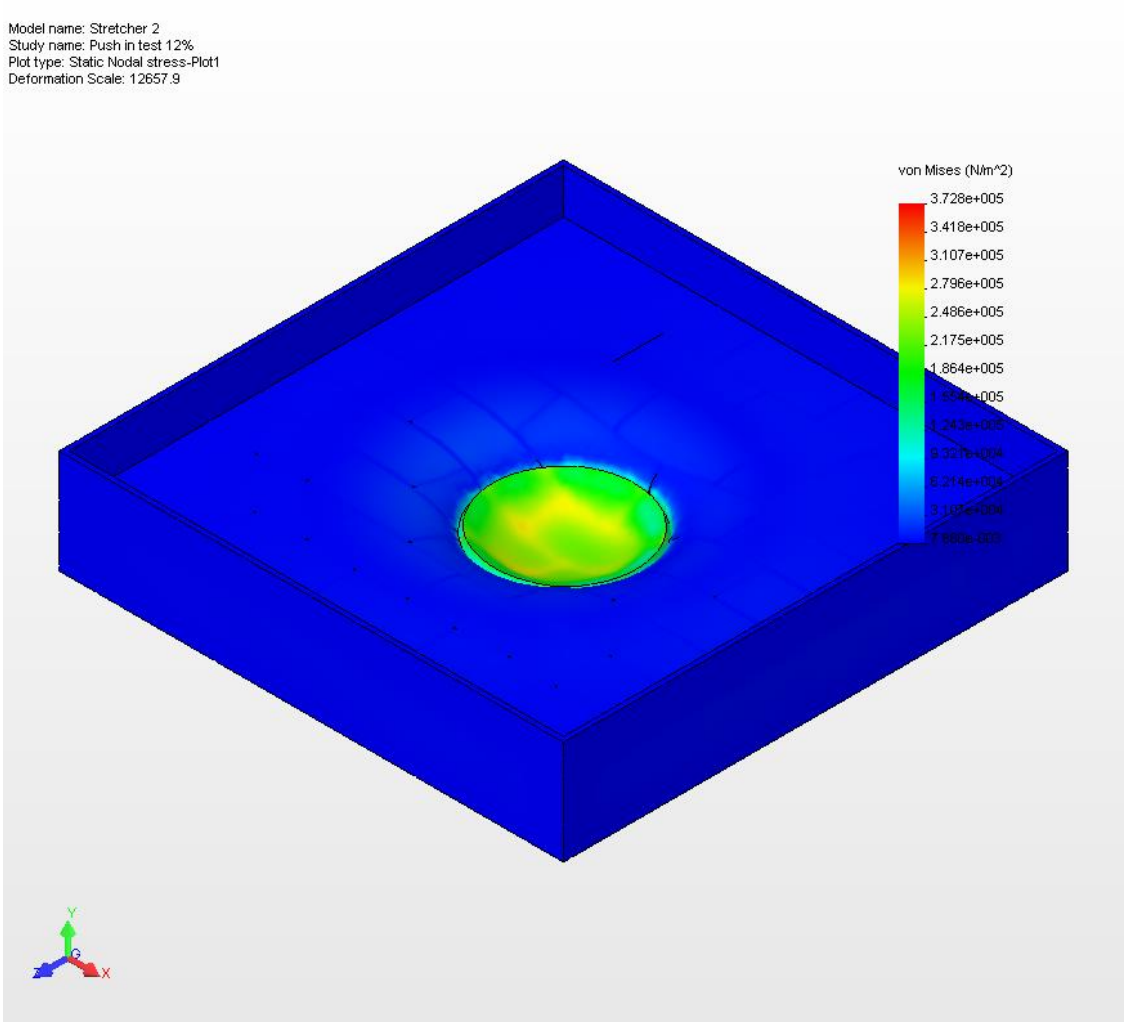

8. Strain Results

Slope	Type	Min	Location	Max	Location
0 %	ESTRN : Equivalent strain	2.68256e-011 Element: 170547	(491.287 mm, 206.25 mm, 502.5 mm)	0.00108064 Element: 234094	(19.7308 mm, 58.4109 mm, 18.9279 mm)
4 %	ESTRN : Equivalent strain	2.85803e-012 Element: 170233	(505.515 mm, 206.429 mm, 501.985 mm)	0.000107831 Element: 234094	(19.7308 mm, 58.4109 mm, 18.9279 mm)
8 %	ESTRN : Equivalent strain	2.9816e-012 Element: 171682	(508.015 mm, 206.429 mm, 504.485 mm)	0.00010748 Element: 234094	(19.7308 mm, 58.4109 mm, 18.9279 mm)
12 %	ESTRN : Equivalent strain	4.20765e-012 Element: 170547	(491.287 mm, 206.25 mm, 502.5 mm)	0.000106999 Element: 234094	(19.7308 mm, 58.4109 mm, 18.9279 mm)

Push-in Test-Strain : 0 % Slope

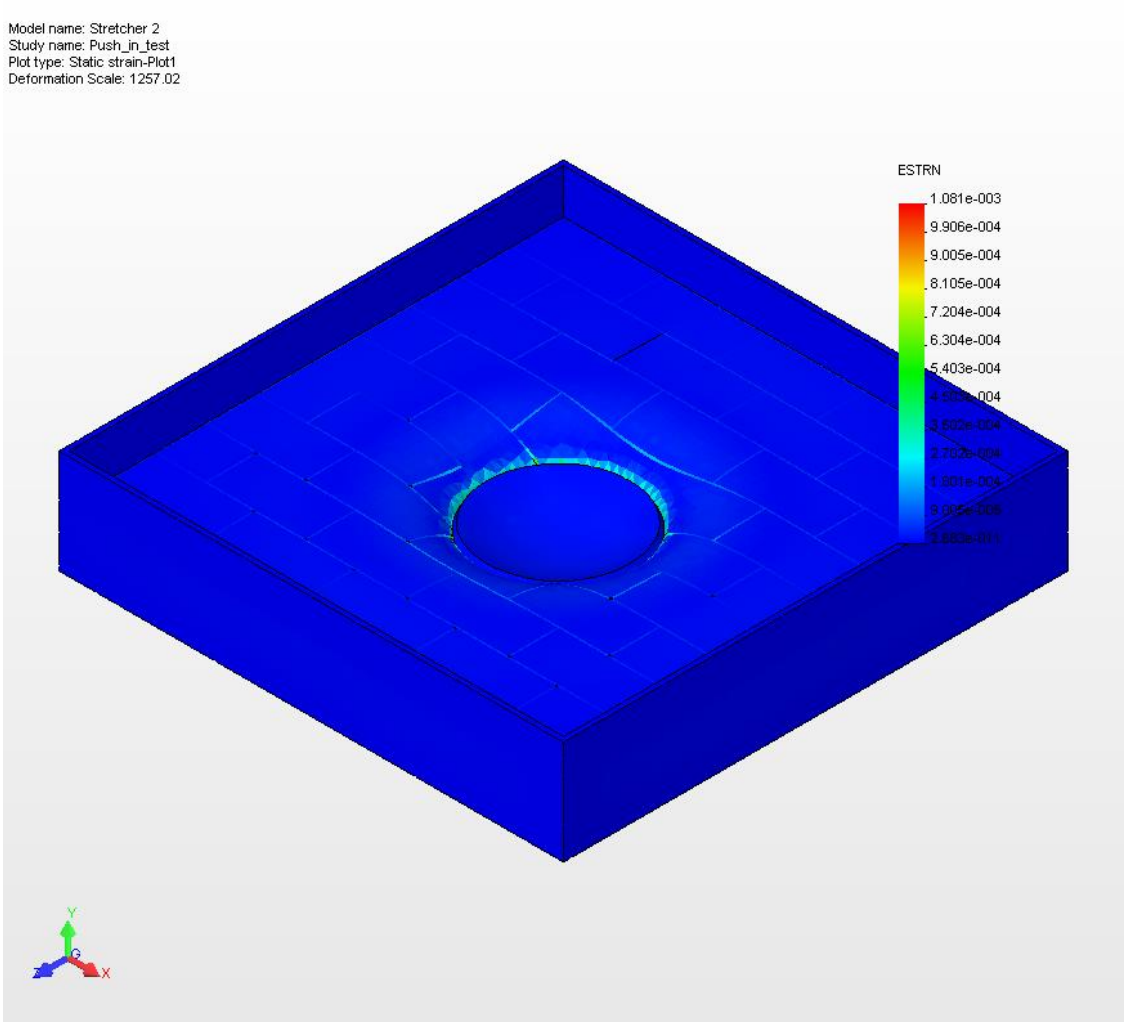

Push-in Test-Strain : 4 % Slope

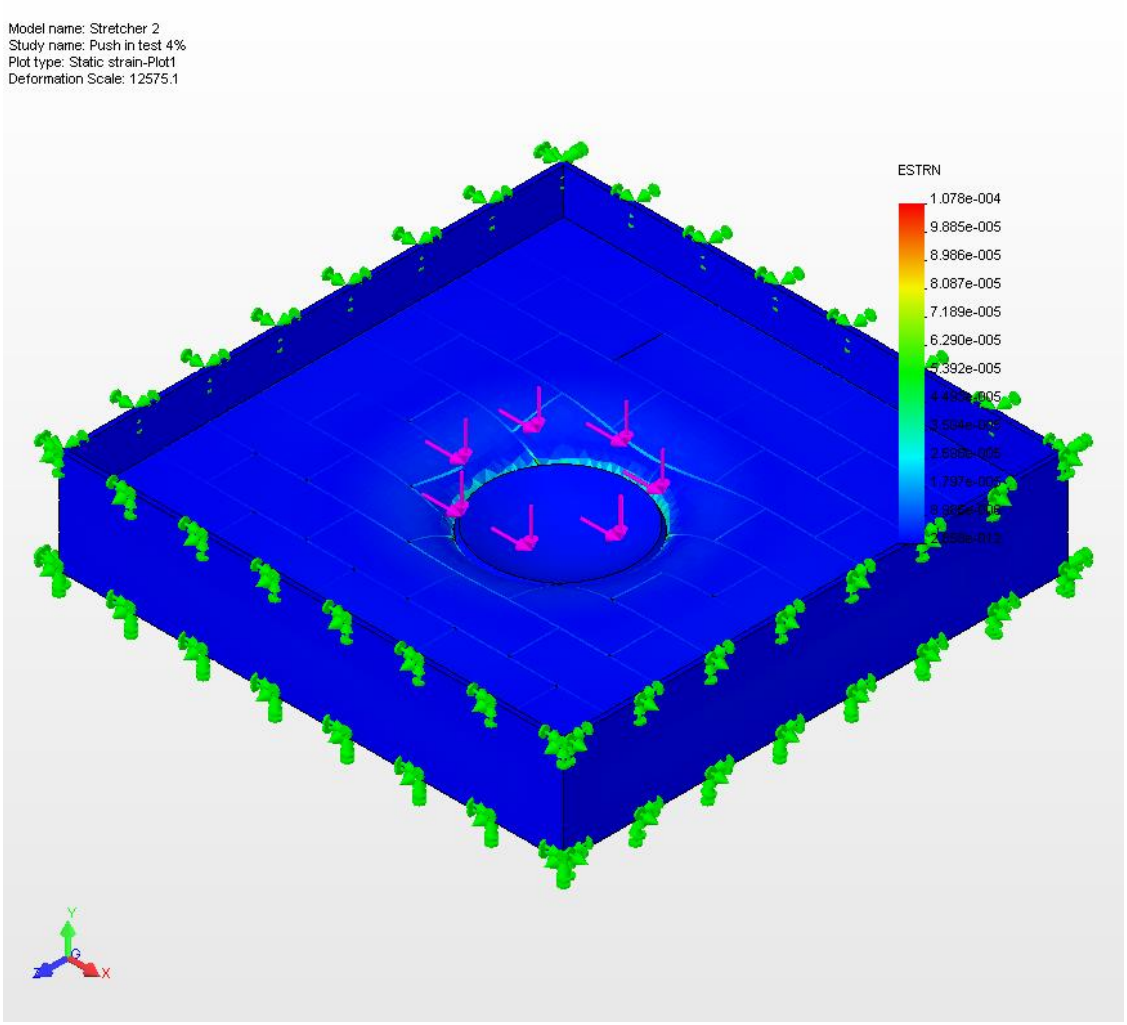

Push-in Test-Strain : 8 % Slope

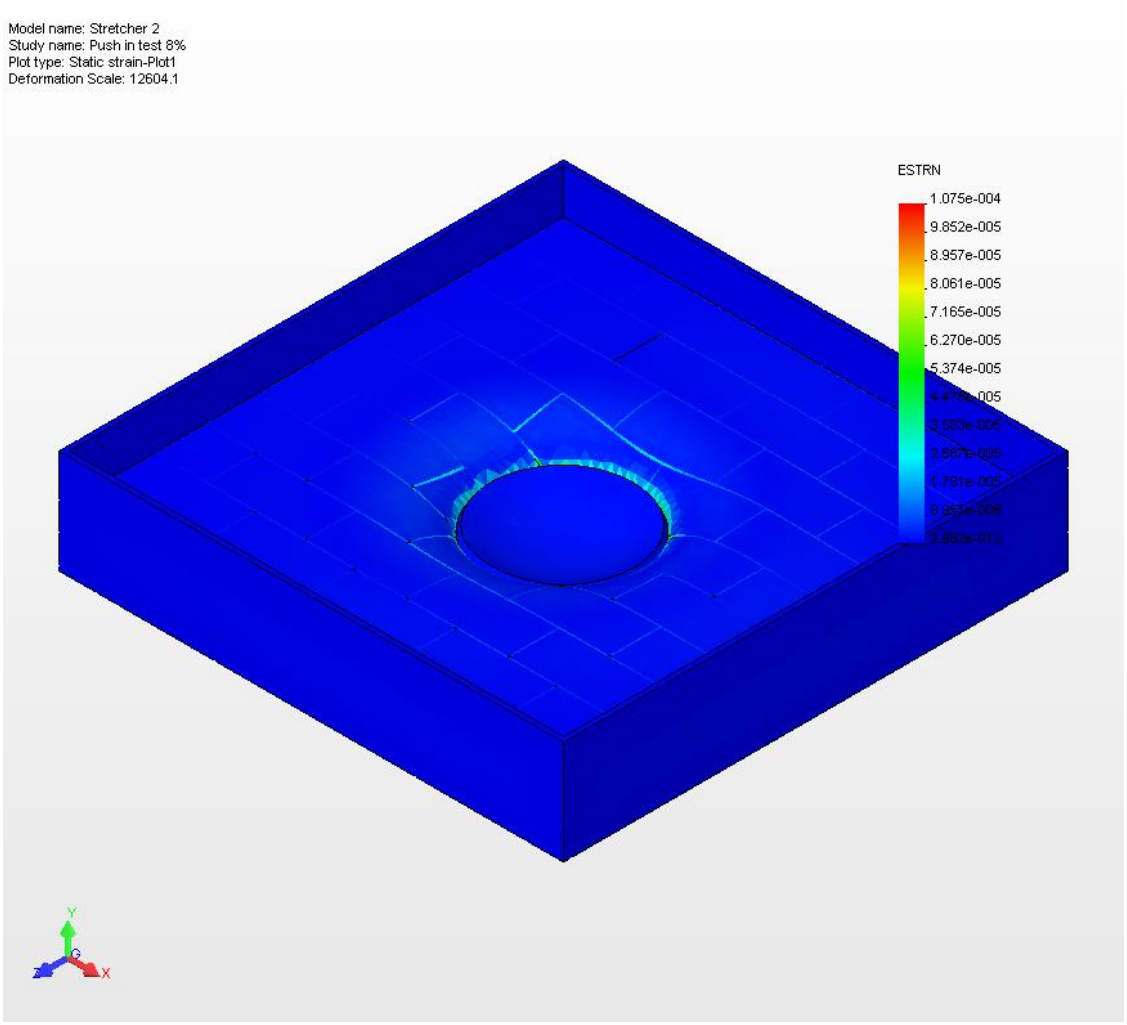

Push-in Test-Strain : 12 % Slope

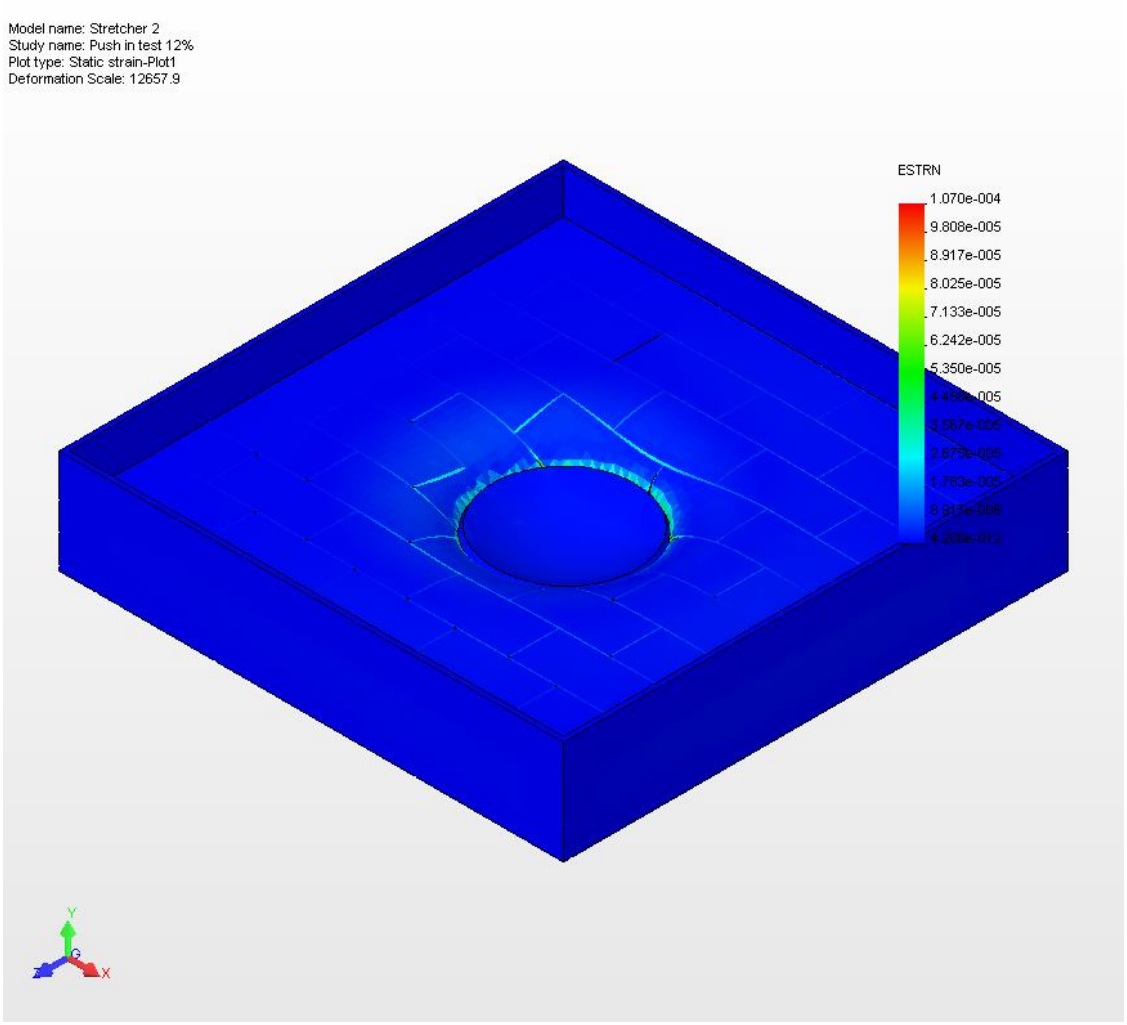

9. Displacement Results

Slope	Type	Min	Location	Max	Location
0 %	URES: Resultant displacement	0 m Node: 74604	(510 mm, 10 mm, 500 mm)	8.11446e-005 m Node: 120045	(-10.838 mm, 125.921 mm, 0.097129 mm)
4 %	URES: Resultant displacement	0 m Node: 74604	(510 mm, 10 mm, 500 mm)	8.11884e-006 m Node: 120045	(-10.838 mm, 125.921 mm, 0.097129 mm)
8 %	URES: Resultant displacement	0 m Node: 74604	(510 mm, 10 mm, 500 mm)	8.12273e-006 m Node: 120045	(-10.838 mm, 125.921 mm, 0.097129 mm)
12 %	URES: Resultant displacement	0 m Node: 74604	(510 mm, 10 mm, 500 mm)	8.12599e-006 m Node: 120045	(-10.838 mm, 125.921 mm, 0.097129 mm)

Push-in Test-Displacement : 0 % Slope

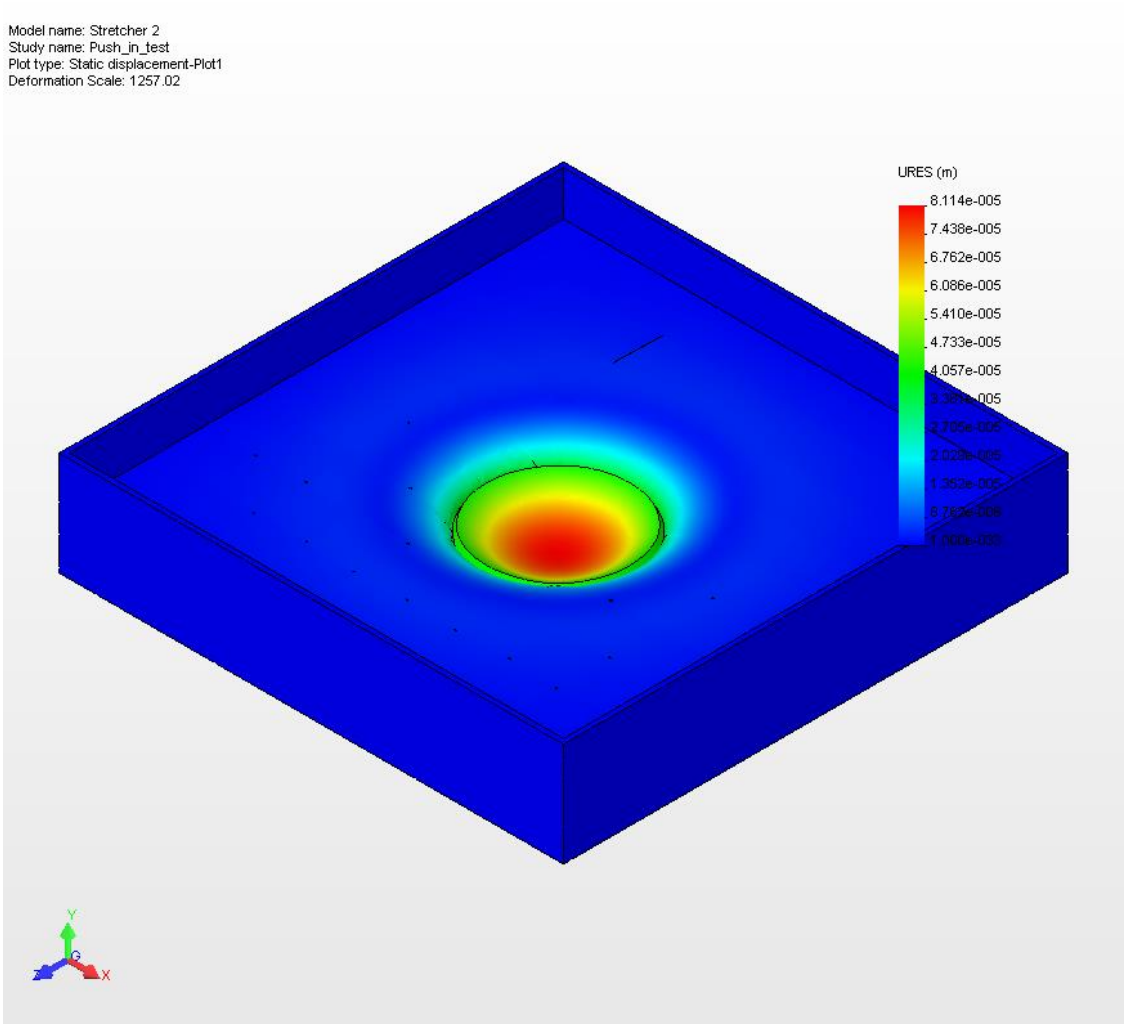

Push-in Test-Displacement : 4 % Slope

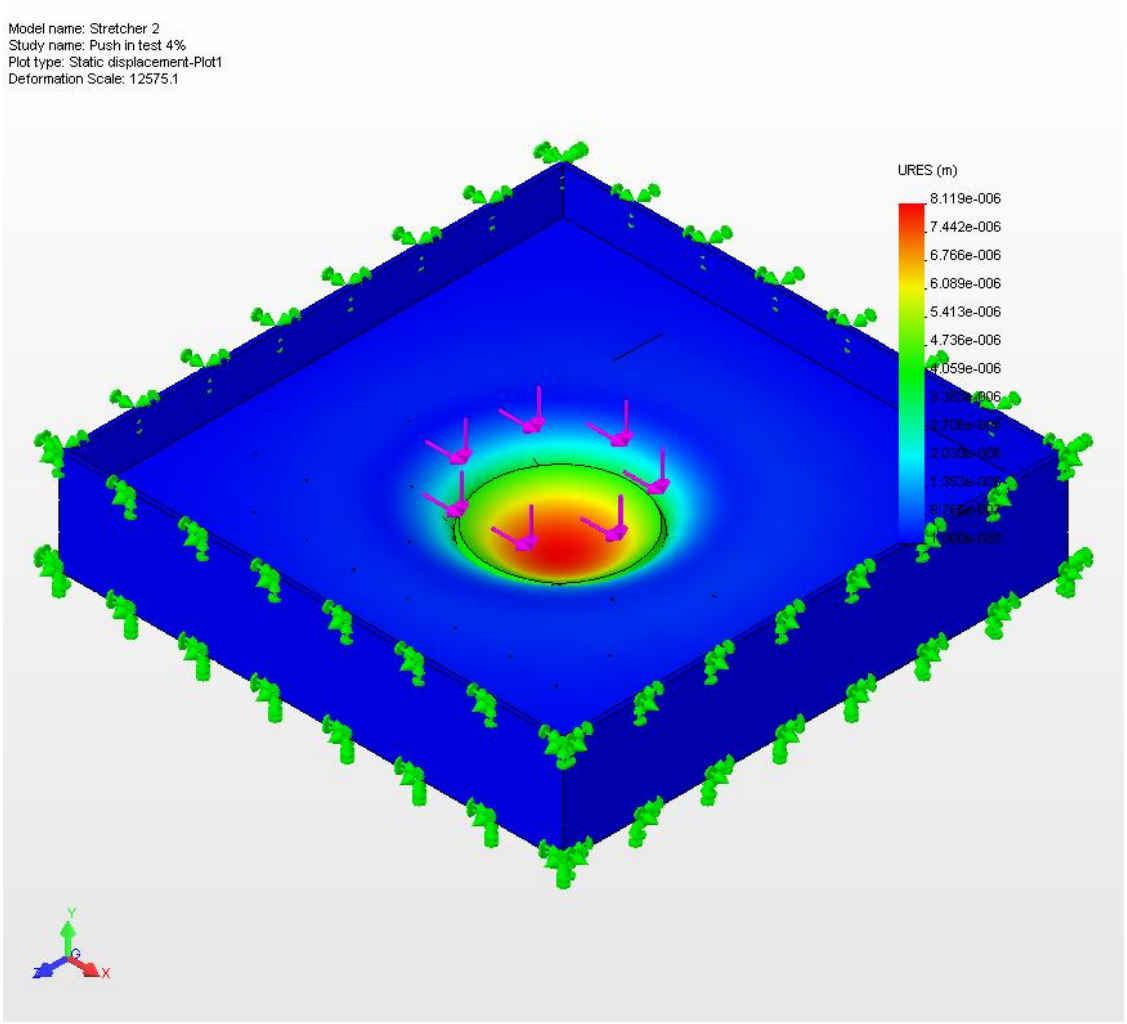

Push-in Test-Displacement : 8 % Slope

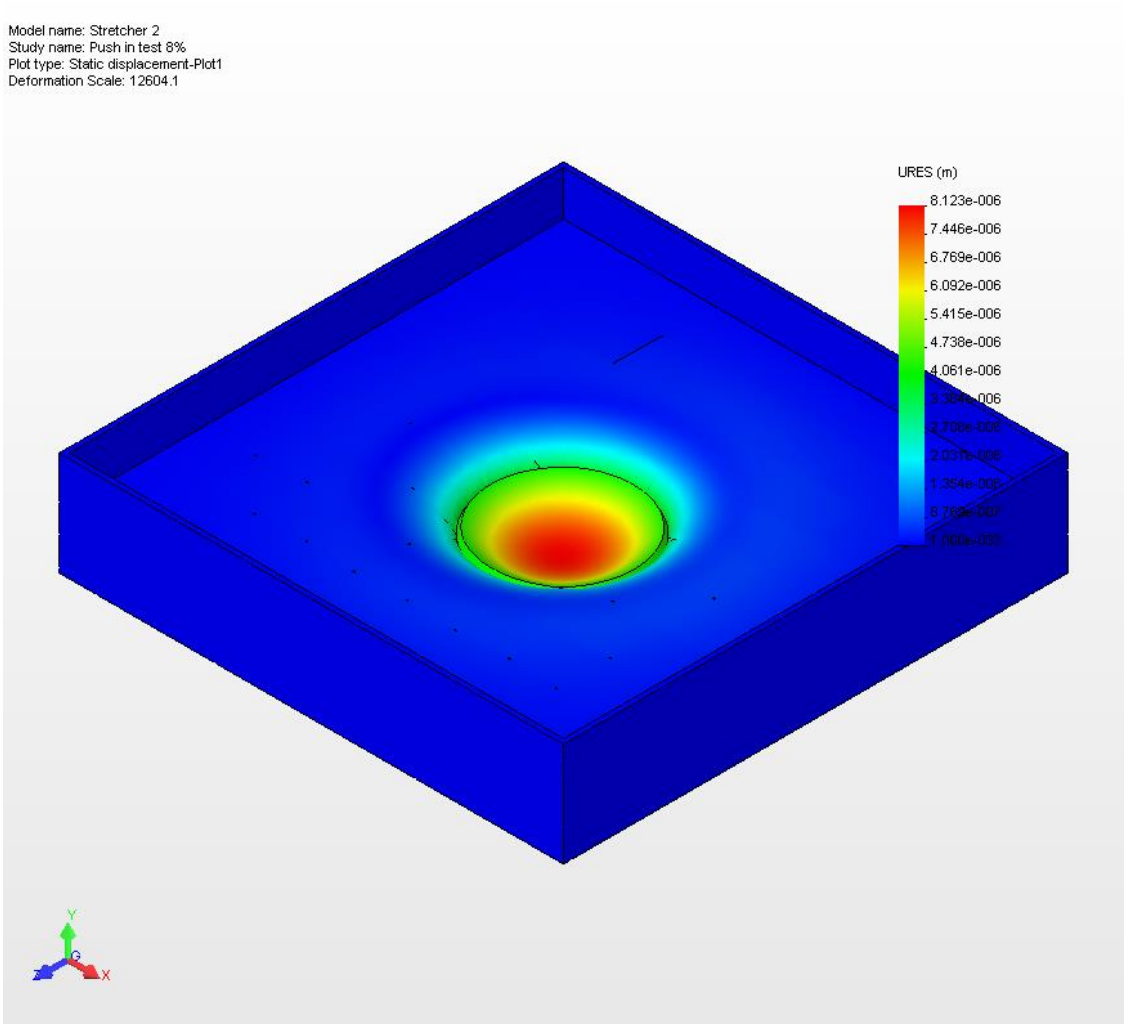

Push-in Test-Displacement : 12 % Slope

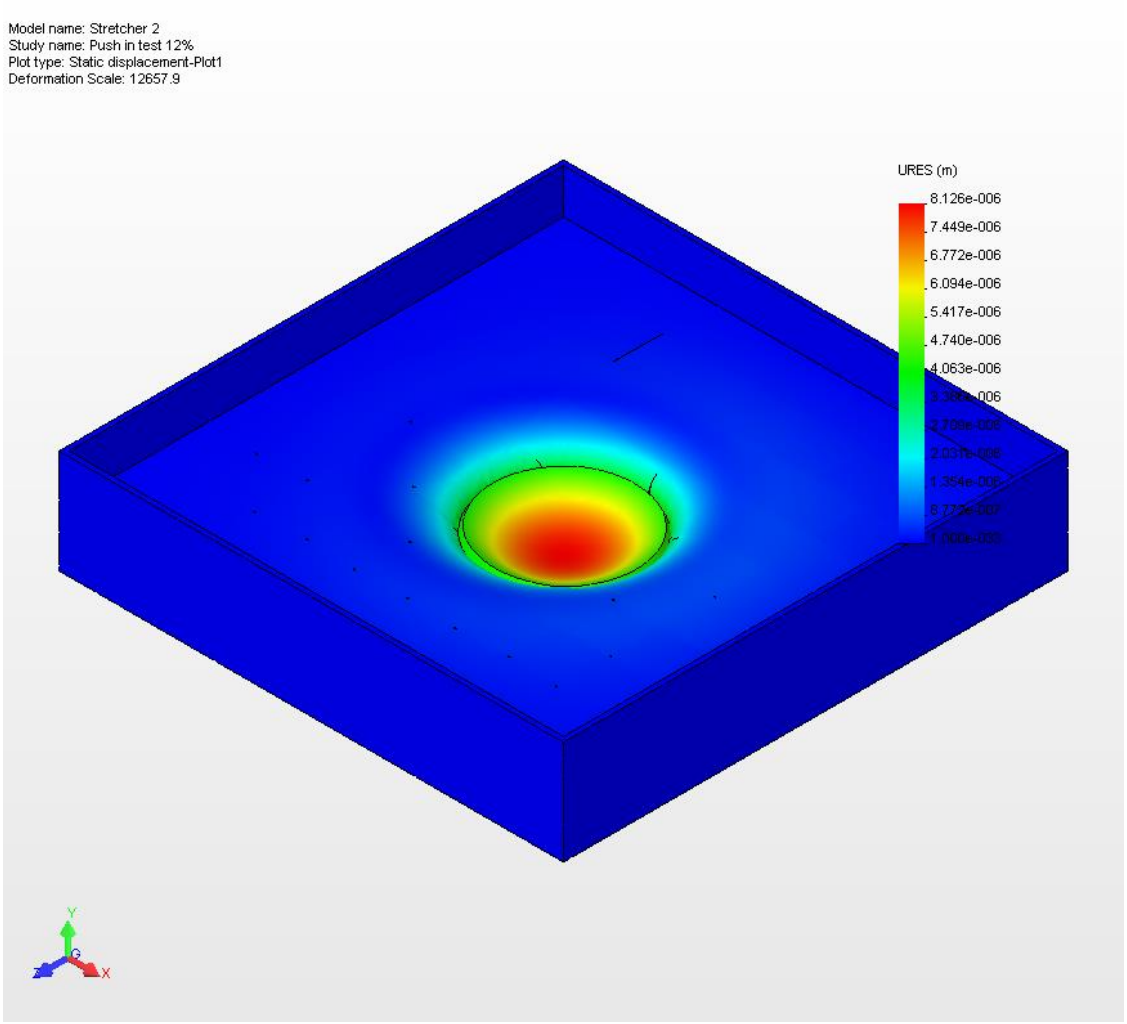

10. Deformation Results

Plot No.	Scale Factor
1	1257

Push-in Test-Deformation : 0 % Slope

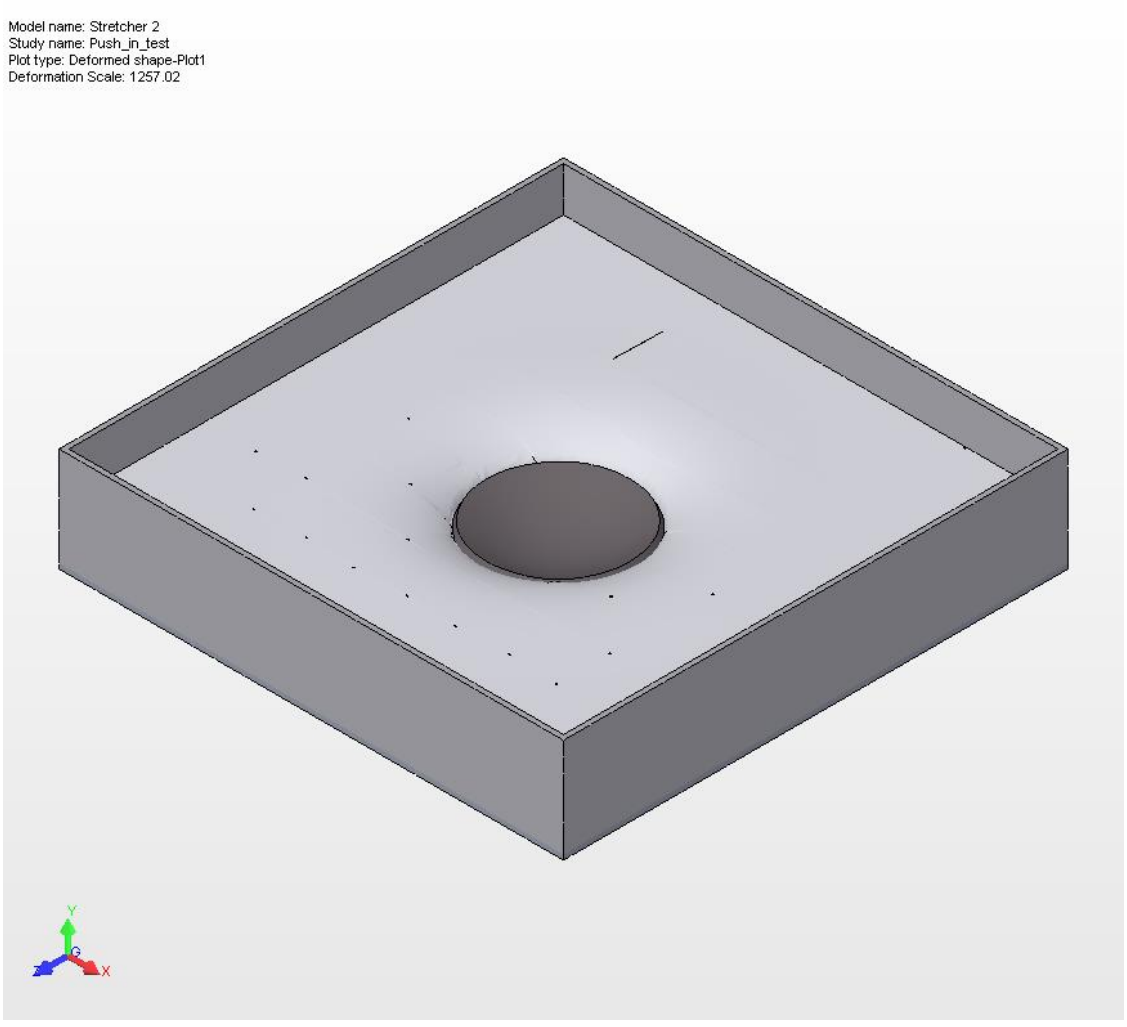

Push-in Test-Deformation : 4 % Slope

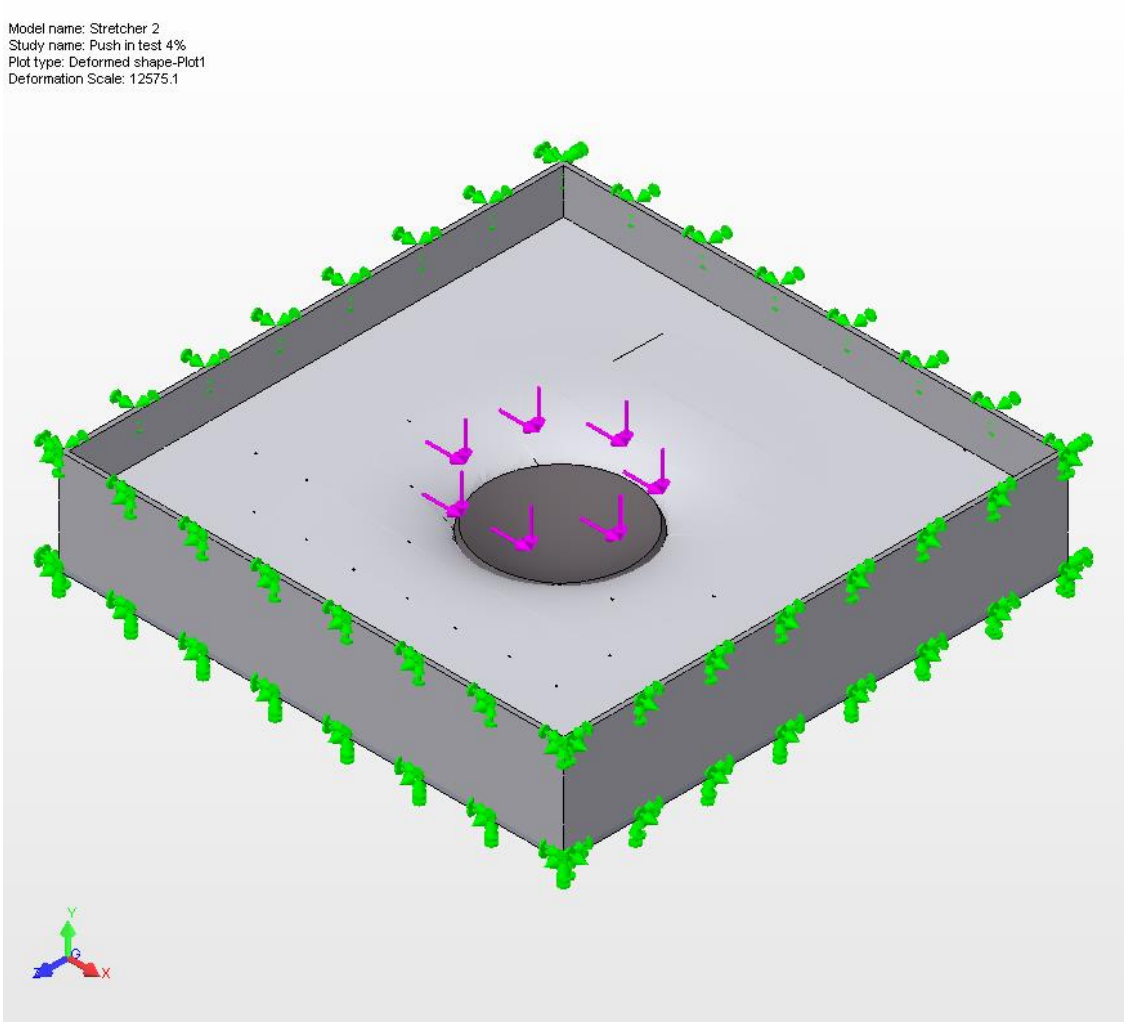

Push-in Test-Deformation : 8 % Slope

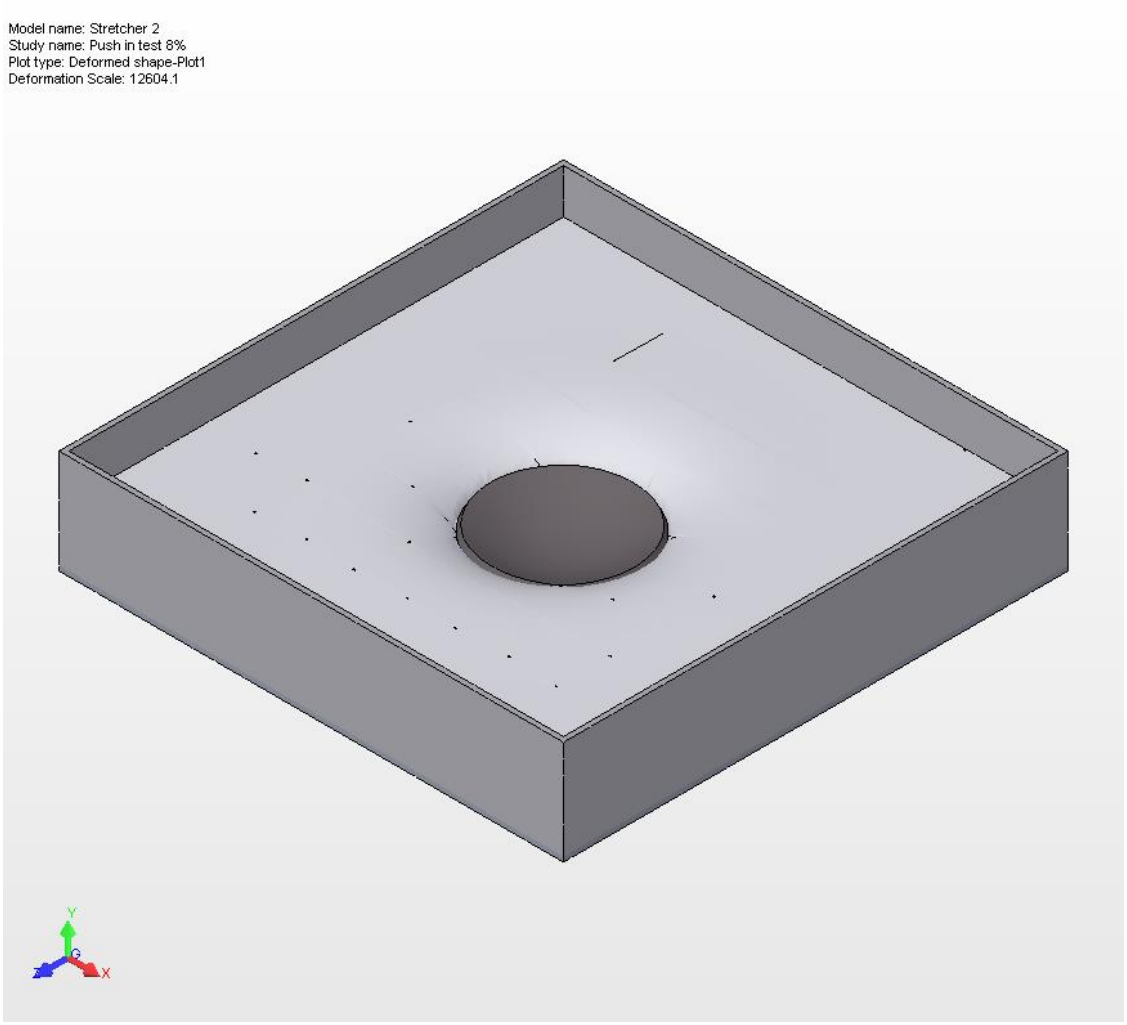

Push-in Test-Deformation : 12 % Slope

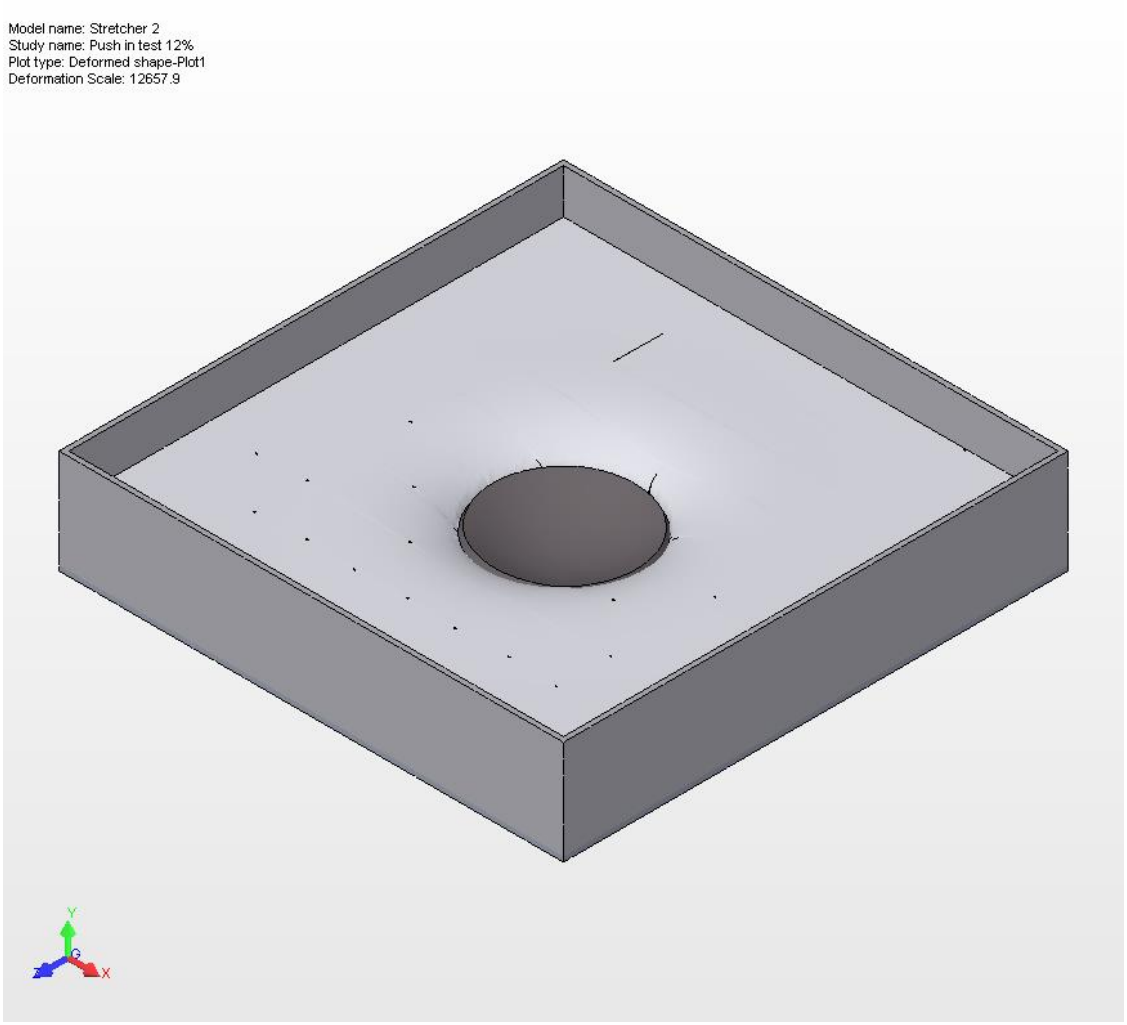

APPENDIX – J1

Equations of Maximum Horizontal Creep (Y max) on Horizontal Force Test

(Laying Pattern Effect on Rectangular Block Shape)

Figure	Laying Pattern	Equation	x = -b/(2a)	Y max
Fig B1.1	Stretcher	y = -0.0299x2 + 0.6582x	11.01	3.62
	Herringbone 90	y = -0.0213x2 + 0.4591x	10.78	2.47
	Herringbone 45	y = -0.0154x2 + 0.3607x	11.71	2.11
Fig B1.2	Stretcher	y = -0.0406x2 + 0.8065x	9.93	4.01
	Herringbone 90	y = -0.0319x2 + 0.5914x	9.27	2.74
	Herringbone 45	y = -0.0264x2 + 0.49x	9.28	2.27
Fig B1.3	Stretcher	y = -0.0575x2 + 1.0005x	8.70	4.35
	Herringbone 90	y = -0.0371x2 + 0.669x	9.02	3.02
	Herringbone 45	y = -0.0267x2 + 0.5124x	9.60	2.46
Fig B1.4	Stretcher	y = -0.023x2 + 0.484x	10.52	2.52
	Herringbone 90	y = -0.0131x2 + 0.2706x	10.33	1.40
	Herringbone 45	y = -0.0097x2 + 0.2159x	11.13	1.20
Fig B1.5	Stretcher	y = -0.0299x2 + 0.5865x	9.01	2.88
	Herringbone 90	y = -0.0179x2 + 0.3334x	9.31	1.55
	Herringbone 45	y = -0.0143x2 + 0.2772x	9.69	1.34
Fig B1.6	Stretcher	y = -0.0418x2 + 0.7228x	8.35	3.12
	Herringbone 90	y = -0.0232x2 + 0.3992x	8.60	1.72
	Herringbone 45	y = -0.0175x2 + 0.318x	9.09	1.44

APPENDIX – J2

Equations of Maximum Horizontal Creep (Y max) on Horizontal Force Test

(Laying Pattern Effect on Uni-pave Block Shape)

Figure	Laying Pattern	Equation	x = -b/(2a)	Y max
Fig B2.1	Stretcher	y = -0.0082x2 + 0.397x	24.21	4.81
	Herringbone 90	y = -0.0044x2 + 0.2653x	30.15	4.00
	Herringbone 45	y = -0.0006x2 + 0.1926x	36.50	3.46
Fig B2.2	Stretcher	y = -0.0195x2 + 0.52x	13.33	3.47
	Herringbone 90	y = -0.0099x2 + 0.3452x	17.43	3.35
	Herringbone 45	y = -0.005x2 + 0.2562x	25.62	3.28
Fig B2.3	Stretcher	y = -0.0157x2 + 0.574x	16.28	5.25
	Herringbone 90	y = -0.0113x2 + 0.3958x	17.51	3.47
	Herringbone 45	y = -0.0088x2 + 0.3273x	18.60	3.04
Fig B2.4	Stretcher	y = -0.0003x2 + 0.2577x	29.50	5.34
	Herringbone 90	y = -0.0019x2 + 0.147x	38.68	4.84
	Herringbone 45	y = -0.0004x2 + 0.1128x	41.00	3.95
Fig B2.5	Stretcher	y = -0.0036x2 + 0.3144x	23.67	6.86
	Herringbone 90	y = -0.0036x2 + 0.1867x	25.93	4.42
	Herringbone 45	y = -0.0027x2 + 0.152x	28.15	2.14
Fig B2.6	Stretcher	y = -0.011x2 + 0.4078x	18.24	3.78
	Herringbone 90	y = -0.0061x2 + 0.2239x	18.35	2.05
	Herringbone 45	y = -0.0051x2 + 0.1888x	18.51	1.75

APPENDIX – J3

Equations of Maximum Horizontal Creep (Y max) on Horizontal Force Test

(Block Thickness Effect on Rectangular Block Shape)

Figure	Block Thickness	Equation	x = -b/(2a)	Y max
Fig C1.1	60 mm block thick	y 60mm = -0.0299x2 + 0.6582x	11.01	3.62
	100 mm block thick	y 100mm = -0.023x2 + 0.484x	10.52	2.55
Fig C1.2	60 mm block thick	y 60 mm = -0.0406x2 + 0.8065x	9.93	4.01
	100 mm block thick	y 100 mm = -0.0299x2 + 0.5865x	9.81	2.88
Fig C1.3	60 mm block thick	y 60mm = -0.0575x2 + 1.0005x	8.70	4.35
	100 mm block thick	y 100mm = -0.0418x2 + 0.7228x	8.65	3.12
Fig C1.4	60 mm block thick	y 60mm = -0.0213x2 + 0.4591x	10.78	2.47
	100 mm block thick	y 100mm = -0.0131x2 + 0.2706x	10.33	1.40
Fig C1.5	60 mm block thick	y 60mm = -0.0319x2 + 0.5914x	9.27	2.74
	100 mm block thick	y 100mm = -0.0179x2 + 0.3334x	9.31	1.55
Fig C1.6	60 mm block thick	y 60mm = -0.0371x2 + 0.669x	9.02	3.02
	100 mm block thick	y 100mm = -0.0232x2 + 0.3992x	8.60	1.72
Fig C1.7	60 mm block thick	y 60mm = -0.0154x2 + 0.3607x	11.71	2.11
	100 mm block thick	y 100mm = -0.0097x2 + 0.2159x	11.13	1.20
Fig C1.8	60 mm block thick	y 60mm = -0.0264x2 + 0.49x	9.28	2.27
	100 mm block thick	y 100mm = -0.0143x2 + 0.2772x	9.69	1.34
Fig C1.9	60 mm block thick	y 60mm = -0.0267x2 + 0.5124x	9.60	2.46
	100 mm block thick	y 100mm = -0.0175x2 + 0.318x	9.09	1.44

APPENDIX – J4

Equations of Maximum Horizontal Creep (Y max) on Horizontal Force Test

(Block Thickness Effect on Uni-pave Block Shape)

Figure	Block Thickness	Equation	x = -b/(2a)	Y max
Fig C2.1	60 mm block thick	y = -0.0014x2 + 0.3558x	27.07	12.61
	100 mm block thick	y = -0.0009x2 + 0.264x	26.67	9.36
Fig C2.2	60 mm block thick	y = -0.0068x2 + 0.4437x	22.63	6.48
	100 mm block thick	y = -0.0036x2 + 0.3144x	23.67	5.86
Fig C2.3	60 mm block thick	y = -0.0157x2 + 0.574x	18.28	5.17
	100 mm block thick	y = -0.011x2 + 0.4078x	18.54	3.78
Fig C2.4	60 mm block thick	y = -0.0027x2 + 0.2552x	17.26	6.03
	100 mm block thick	y = -0.0004x2 + 0.1287x	16.88	5.35
Fig C2.5	60 mm block thick	y = -0.0058x2 + 0.3178x	27.40	4.35
	100 mm block thick	y = -0.0004x2 + 0.1565x	25.63	5.31
Fig C2.6	60 mm block thick	y = -0.0113x2 + 0.3958x	32.44	0.95
	100 mm block thick	y = -0.0061x2 + 0.2239x	18.35	2.05
Fig C2.7	60 mm block thick	y = -0.0004x2 + 0.2145x	68.13	8.78
	100 mm block thick	y = -0.0008x2 + 0.1228x	76.75	4.71
Fig C2.8	60 mm block thick	y = -0.0009x2 + 0.2366x	31.44	5.55
	100 mm block thick	y = -0.0027x2 + 0.152x	28.15	2.14
Fig C2.9	60 mm block thick	y = -0.0088x2 + 0.3273x	18.60	3.04
	100 mm block thick	y = -0.0051x2 + 0.1888x	18.51	1.75

APPENDIX – J5

Equations of Maximum Horizontal Creep (Y max) on Horizontal Force Test

(Joint Width Effect on Rectangular Block Shape)

Figure	Joint Width	Equation	x = -b/(2a)	Y max
Fig D1.1	3 mm joint width	Y = -0.0299x2 + 0.6582x	11.01	3.62
	5 mm joint width	Y = -0.0406x2 + 0.8065x	9.93	4.01
	7 mm joint width	Y = -0.0575x2 + 1.0005x	8.70	4.35
Fig D1.2	3 mm joint width	y = -0.0213x2 + 0.4591x	10.78	2.47
	5 mm joint width	y = -0.029x2 + 0.5521x + 0.1108	9.52	2.72
	7 mm joint width	y = -0.0371x2 + 0.669x	9.02	3.29
Fig D1.3	3 mm joint width	y = -0.0154x2 + 0.3607x	11.71	2.11
	5 mm joint width	y = -0.0264x2 + 0.49x	9.28	2.27
	7 mm joint width	y = -0.0267x2 + 0.5124x	9.60	2.46
Fig D1.4	3 mm joint width	y = -0.023x2 + 0.484x	10.52	2.55
	5 mm joint width	y = -0.0299x2 + 0.5865x	9.81	2.88
	7 mm joint width	y = -0.0418x2 + 0.7228x	8.65	3.12
Fig D1.5	3 mm joint width	y = -0.0131x2 + 0.2706x	10.33	1.40
	5 mm joint width	y = -0.0179x2 + 0.3334x	9.31	1.55
	7 mm joint width	y = -0.0232x2 + 0.3992x	8.60	1.72
Fig D1.6	3 mm joint width	y = -0.0097x2 + 0.2159x	11.13	1.20
	5 mm joint width	y = -0.0143x2 + 0.2772x	9.69	1.34
	7 mm joint width	y = -0.0175x2 + 0.318x	9.09	1.44

APPENDIX – J6

Equations of Maximum Horizontal Creep (Y max) on Horizontal Force Test

(Joint Width Effect on Uni-pave Block Shape)

Figure	Joint Width	Equation	x = -b/(2a)	Y max
Fig D2.1	3 mm joint width	y = -0.0006x2 + 0.3481x	29.08	5.49
	5 mm joint width	y = -0.0068x2 + 0.4437x	32.63	6.24
	7 mm joint width	y = -0.0157x2 + 0.574x	28.28	7.25
Fig D2.2	3 mm joint width	y = -0.0027x2 + 0.2552x	27.26	6.03
	5 mm joint width	y = -0.0058x2 + 0.3178x	27.40	4.35
	7 mm joint width	y = -0.0113x2 + 0.3958x	27.51	3.47
Fig D2.3	3 mm joint width	y = -0.0005x2 + 0.2076x	27.60	2.55
	5 mm joint width	y = -0.0088x2 + 0.3273x	28.60	3.04
	7 mm joint width	y = -0.0009x2 + 0.2366x	31.44	5.55
Fig D2.4	3 mm joint width	y = -0.0002x2 + 0.2427x	36.75	3.63
	5 mm joint width	y = -0.0036x2 + 0.3144x	43.67	3.86
	7 mm joint width	y = -0.011x2 + 0.4078x	38.54	3.78
Fig D2.5	3 mm joint width	y = -0.0001x2 + 0.1248x	24.00	8.94
	5 mm joint width	y = -0.001x2 + 0.1605x	20.25	6.44
	7 mm joint width	y = -0.0061x2 + 0.2239x	18.35	4.05
Fig D2.6	3 mm joint width	y = -0.0008x2 + 0.1228x	26.75	4.71
	5 mm joint width	y = -0.0027x2 + 0.152x	28.15	2.14
	7 mm joint width	y = -0.0051x2 + 0.1888x	28.51	1.75

Appendix - K

No	Block shape	Block Thickness (mm)	Joint width (mm)	Bedding sand thickness (mm)	Laying pattern	Degree of slope (%)	Equation Hz. Creep on Hz. Force test	Equation Hz. Creep on push-in test	Max. Hz Creep (mm)	Spacing of anchor beam (m)
5.9	Rectangular	60	3	50	Stretcher bond	0	$Y = -0.0299x^2 + 0.6582x$	$Y = -0.0004x^2 + 0.0363x$	3.62	20.11
	Rectangular	60	3	50	Herringbone 90	0	$Y = -0.0213x^2 + 0.4591x$	$Y = -0.0003x^2 + 0.0298x$	2.47	23.16
	Rectangular	60	3	50	Herringbone 45	0	$Y = -0.0154x^2 + 0.3607x$	$Y = -0.0003x^2 + 0.0260x$	2.11	27.10
	Rectangular	60	3	50	Stretcher bond	4	$Y = -0.0299x^2 + 0.6582x$	$Y = -0.0003x^2 + 0.0358x$	3.62	18.54
	Rectangular	60	3	50	Herringbone 90	4	$Y = -0.0213x^2 + 0.4591x$	$Y = -0.0003x^2 + 0.0296x$	2.47	21.52
	Rectangular	60	3	50	Herringbone 45	4	$Y = -0.0154x^2 + 0.3607x$	$Y = -0.0003x^2 + 0.0256x$	2.11	25.27
	Rectangular	60	3	50	Stretcher bond	8	$Y = -0.0299x^2 + 0.6582x$	$Y = -0.0003x^2 + 0.0311x$	3.62	15.42
	Rectangular	60	3	50	Herringbone 90	8	$Y = -0.0213x^2 + 0.4591x$	$Y = -0.0003x^2 + 0.0305x$	2.47	18.98
	Rectangular	60	3	50	Herringbone 45	8	$Y = -0.0154x^2 + 0.3607x$	$Y = -0.0003x^2 + 0.0268x$	2.11	21.34
	Rectangular	60	3	50	Stretcher bond	12	$Y = -0.0299x^2 + 0.6582x$	$Y = -0.0027x^2 + 0.3032x$	3.62	12.05
	Rectangular	60	3	50	Herringbone 90	12	$Y = -0.0213x^2 + 0.4591x$	$Y = -0.0003x^2 + 0.0282x$	2.47	14.44
	Rectangular	60	3	50	Herringbone 45	12	$Y = -0.0154x^2 + 0.3607x$	$Y = -0.0003x^2 + 0.0245x$	2.11	16.10
5.11	Rectangular	60	3	50	Stretcher bond	0	$Y = -0.0299x^2 + 0.6582x$	$Y = -0.0003x^2 + 0.0298x$	3.62	29.24
	Rectangular	60	5	50	Stretcher bond	0	$Y = -0.0406x^2 + 0.8065x$	$Y = -0.0004x^2 + 0.0385x$	4.01	26.11
	Rectangular	60	7	50	Stretcher bond	0	$Y = -0.0575x^2 + 1.0005x$	$Y = -0.0003x^2 + 0.0270x$	4.35	22.43
	Rectangular	60	3	50	Stretcher bond	4	$Y = -0.0299x^2 + 0.6582x$	$Y = -0.0004x^2 + 0.0382x$	3.62	28.64
	Rectangular	60	5	50	Stretcher bond	4	$Y = -0.0406x^2 + 0.8065x$	$Y = -0.0003x^2 + 0.0325x$	4.01	25.43
	Rectangular	60	7	50	Stretcher bond	4	$Y = -0.0575x^2 + 1.0005x$	$Y = -0.0003x^2 + 0.0268x$	4.35	21.13
	Rectangular	60	3	50	Stretcher bond	8	$Y = -0.0299x^2 + 0.6582x$	$Y = -0.0004x^2 + 0.0378x$	3.62	27.71
	Rectangular	60	5	50	Stretcher bond	8	$Y = -0.0406x^2 + 0.8065x$	$Y = -0.0003x^2 + 0.0319x$	4.01	24.66
	Rectangular	60	7	50	Stretcher bond	8	$Y = -0.0575x^2 + 1.0005x$	$Y = -0.0003x^2 + 0.0280x$	4.35	20.48
	Rectangular	60	3	50	Stretcher bond	12	$Y = -0.0299x^2 + 0.6582x$	$Y = -0.0003x^2 + 0.0356x$	3.62	26.42
	Rectangular	60	5	50	Stretcher bond	12	$Y = -0.0406x^2 + 0.8065x$	$Y = -0.0003x^2 + 0.0304x$	4.01	23.74
	Rectangular	60	7	50	Stretcher bond	12	$Y = -0.0575x^2 + 1.0005x$	$Y = -0.0003x^2 + 0.0262x$	4.35	19.62
5.14	Rectangular	60	3	50	Stretcher bond	0	$Y = -0.0299x^2 + 0.6582x$	$Y = -0.0002x^2 + 0.0178x$	3.62	27.86
	Rectangular	100	3	50	Stretcher bond	0	$Y = -0.0230x^2 + 0.4840x$	$Y = -0.0002x^2 + 0.0188x$	2.52	35.12
	Rectangular	60	3	50	Stretcher bond	4	$Y = -0.0299x^2 + 0.6582x$	$Y = -0.0003x^2 + 0.0344x$	3.62	24.62
	Rectangular	100	3	50	Stretcher bond	4	$Y = -0.0230x^2 + 0.4840x$	$Y = -0.0003x^2 + 0.0289x$	2.52	28.81
	Rectangular	60	3	50	Stretcher bond	8	$Y = -0.0299x^2 + 0.6582x$	$Y = -0.0003x^2 + 0.0341x$	3.62	21.38
	Rectangular	100	3	50	Stretcher bond	8	$Y = -0.0230x^2 + 0.4840x$	$Y = -0.0003x^2 + 0.0305x$	2.52	24.11
	Rectangular	60	3	50	Stretcher bond	12	$Y = -0.0299x^2 + 0.6582x$	$Y = -0.0003x^2 + 0.0315x$	3.62	17.45
	Rectangular	100	3	50	Stretcher bond	12	$Y = -0.0230x^2 + 0.4840x$	$Y = -0.0003x^2 + 0.0274x$	2.52	19.67

Appendix - K

5.16	Rectangular	60	3	50	Stretcher bond	0	$Y = -0.0299x^2 + 0.6582x$	$Y = -0.0004x^2 + 0.0344x$	3.62	27.64
	Uni-pave	60	3	50	Stretcher bond	0	$Y = -0.0082x^2 + 0.3970x$	$Y = -0.0002x^2 + 0.0176x$	4.81	40.64
	Rectangular	60	3	50	Stretcher bond	4	$Y = -0.0299x^2 + 0.6582x$	$Y = -0.0002x^2 + 0.0186x$	3.62	25.41
	Uni-pave	60	3	50	Stretcher bond	4	$Y = -0.0082x^2 + 0.3970x$	$Y = -0.0002x^2 + 0.0198x$	4.81	38.60
	Rectangular	60	3	50	Stretcher bond	8	$Y = -0.0299x^2 + 0.6582x$	$Y = -0.0002x^2 + 0.0177x$	3.62	22.63
	Uni-pave	60	3	50	Stretcher bond	8	$Y = -0.0082x^2 + 0.3970x$	$Y = -0.0002x^2 + 0.0195x$	4.81	34.80
	Rectangular	60	3	50	Stretcher bond	12	$Y = -0.0299x^2 + 0.6582x$	$Y = -0.0002x^2 + 0.0175x$	3.62	19.89
	Uni-pave	60	3	50	Stretcher bond	12	$Y = -0.0082x^2 + 0.3970x$	$Y = -0.0002x^2 + 0.0183x$	4.81	29.33
5.18	Rectangular	60	3	30	Stretcher bond	0	$Y = -0.0299x^2 + 0.6582x$	$Y = -0.0003x^2 + 0.0260x$	3.62	34.62
	Rectangular	60	3	50	Stretcher bond	0	$Y = -0.0299x^2 + 0.6582x$	$Y = -0.0003x^2 + 0.0298x$	3.62	33.12
	Rectangular	60	3	70	Stretcher bond	0	$Y = -0.0299x^2 + 0.6582x$	$Y = -0.0004x^2 + 0.0363x$	3.62	30.41
	Rectangular	60	3	30	Stretcher bond	4	$Y = -0.0299x^2 + 0.6582x$	$Y = -0.0003x^2 + 0.0256x$	3.62	31.14
	Rectangular	60	3	50	Stretcher bond	4	$Y = -0.0299x^2 + 0.6582x$	$Y = -0.0003x^2 + 0.0296x$	3.62	30.27
	Rectangular	60	3	70	Stretcher bond	4	$Y = -0.0299x^2 + 0.6582x$	$Y = -0.0004x^2 + 0.0358x$	3.62	28.03
	Rectangular	60	3	30	Stretcher bond	8	$Y = -0.0299x^2 + 0.6582x$	$Y = -0.0003x^2 + 0.0268x$	3.62	27.19
	Rectangular	60	3	50	Stretcher bond	8	$Y = -0.0299x^2 + 0.6582x$	$Y = -0.0003x^2 + 0.0305x$	3.62	26.12
	Rectangular	60	3	70	Stretcher bond	8	$Y = -0.0299x^2 + 0.6582x$	$Y = -0.0004x^2 + 0.0353x$	3.62	23.48
	Rectangular	60	3	30	Stretcher bond	12	$Y = -0.0299x^2 + 0.6582x$	$Y = -0.0003x^2 + 0.0245x$	3.62	21.75
	Rectangular	60	3	50	Stretcher bond	12	$Y = -0.0299x^2 + 0.6582x$	$Y = -0.0003x^2 + 0.0282x$	3.62	21.41
	Rectangular	60	3	70	Stretcher bond	12	$Y = -0.0299x^2 + 0.6582x$	$Y = -0.0004x^2 + 0.0330x$	3.62	20.11

Appendix – L

PUBLICATIONS

1. Hasanan Md Nor and Rachmat Mudiyono (2002). "Construction of Concrete Block Pavement for Uphill Area in Campus" *Proceedings Seminar Kejuruteraan Awam (SPKA) 200*2, FAB-UTM, Skudai – Johor Bahru.

2. Rachmat Mudiyono and Hasanan Md Nor (2004). "The Effect of Changing Parameters of Bedding and Jointing Sand on Concrete Block Pavement." *Proceedings Seminar Kejuruteraan Awam (SPKA) 200*4, FKA-UTM, Skudai – Johor Bahru.

3. Hasanan Md Nor and Rachmat Mudiyono (2005). "The Construction of Concrete Block Pavement on Sloping Road Section Using Anchor Beam." *Proceedings Seminar Kejuruteraan Awam (SPKA) 200*4, Sofitel Palm Resort Hotel, Senai – Johor Bahru.

4. Rachmat Mudiyono and Hasanan Md Nor (2005).. "The Development and Application of Concrete Blocks Pavement. *"Proceeding of the International Seminar and Exihibition on Road Constructions.*
   May 26th, 2005, Semarang – Indonesia, pg: 1 – 12

5. Rachmat Mudiyono and Hasanan Md Nor (2005). "Improving CBP on Performance on sloping Road Section" *Proceeding of the International Seminar and Exihibition on Road Constructions.*
   May 26th, 2005, Semarang – Indonesia pg: 29 – 42

6. Rachmat Mudiyono and Hasanan Md Nor (2006). "The Effect of Joint Width on Concrete Block Pavement" *1st Proceeding of the Regional Postgraduate Conference on Engineering and Science* July 2006, School of Graduate Studies UTM and Indonesian Students Association.

Spacing of anchor beam based on laying pattern effect

Model	Laying pattern	joint width	Block thickness	Block shape	bedding sand thickness	The equation of Hz creep on Hz Force Test	Y max	The equation of Hz creep on Push-in Test	Spacing of Anchor Beam
1	Stretcher bond	3 mm	60 mm	Rectangular	50 mm	$Y = -0.0299x^2 + 0.6582x$	3.62	$Y = -0.0027x^2 + 0.3032x + 0.3591$	12.06
2	Herringbone 90^o	3 mm	60 mm	Rectangular	50 mm	$Y = -0.0213x^2 + 0.5914x$	4.11		
3	Herringbone 45^o	3 mm	60 mm	Rectangular	50 mm	$Y = -0.0154x^2 + 0.3607x$	2.11		

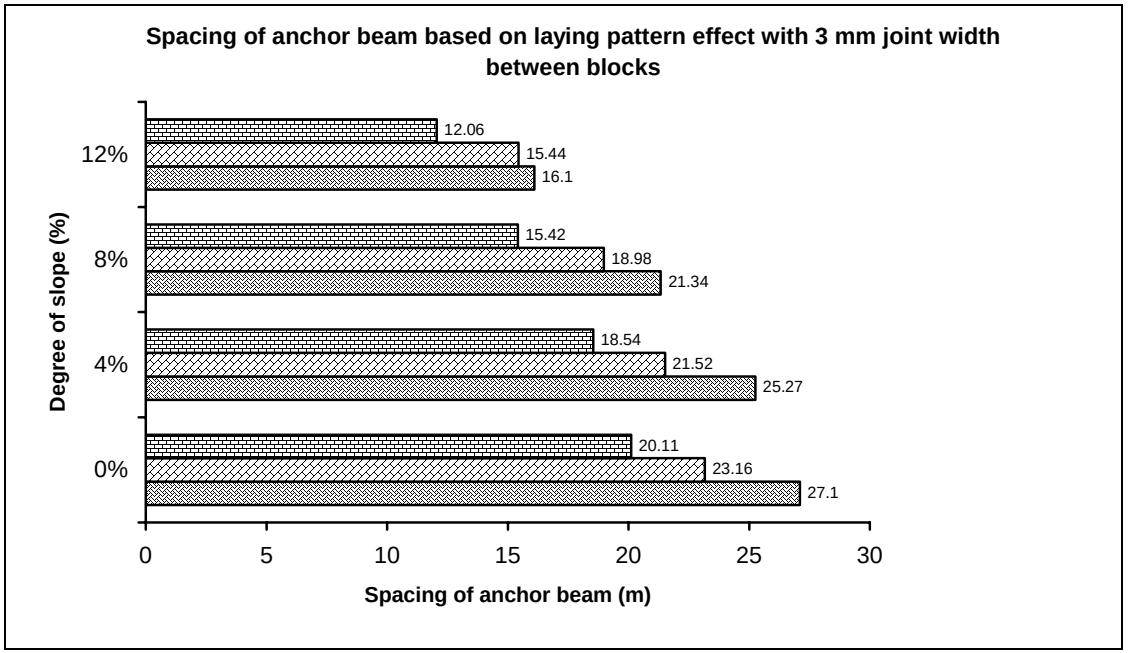

Spacing of anchor beam based on joint width effect

Model	Joint width	Laying pattern	Block thickness	Block shape	bedding sand thickness	The equation of Hz creep on Hz Force Test	Y max	The equation of Hz creep on Push-in Test
1	3 mm	Stretcher	60 mm	Rectangular	50 mm	$Y = -0.0299x^2 + 0.6582x$	3.62	
2	5 mm	Stretcher	60 mm	Rectangular	50 mm	$Y = -0.0406x^2 + 0.8065x$	4.01	
3	7 mm	Stretcher	60 mm	Rectangular	50 mm	$Y = -0.0575x^2 + 1.0001x$	4.35	

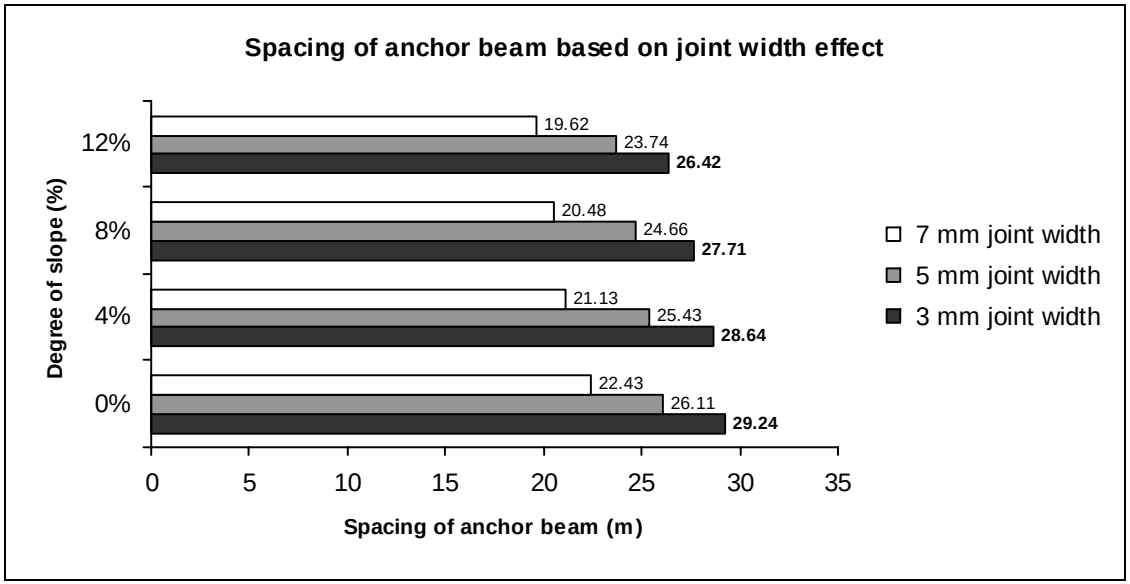

Spacing of anchor beam based on block thickness effect

Model	Block thickness	Joint width	Laying pattern	block shape	bedding sand thickness	The equation of Hz creep on Hz Force Test	Y max	The equation of Hz creep on Push-in Test
1	60 mm	3 mm	Stretcher	Rectangular	50 mm	$Y = -0.0299x^2 + 0.6582x$	3.62	
2	100 mm	3 mm	Stretcher	Rectangular	50 mm	$Y = -0.023x^2 + 0.484x$	2.55	

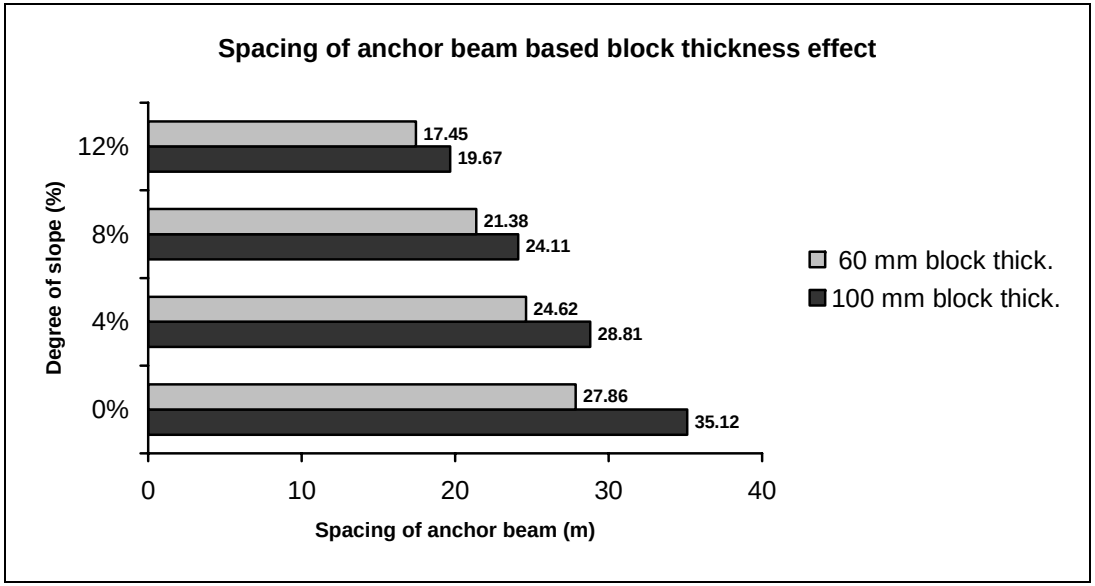

Spacing of anchor beam based on block shape effect

Model	Block shape	Block thickness	Joint width	Laying pattern	bedding sand thickness	The equation of Hz creep on Hz Force Test	Y max	The equation of Hz creep on Push-in Test
1	Rectangular	60 mm	3 mm	Stretcher	50 mm	$Y = -0.0299x^2 + 0.6582x$	3.62	
2	Uni-pave	60 mm	3 mm	Stretcher	50 mm	$Y = -0.0082x^2 + 0.397x$	4.81	

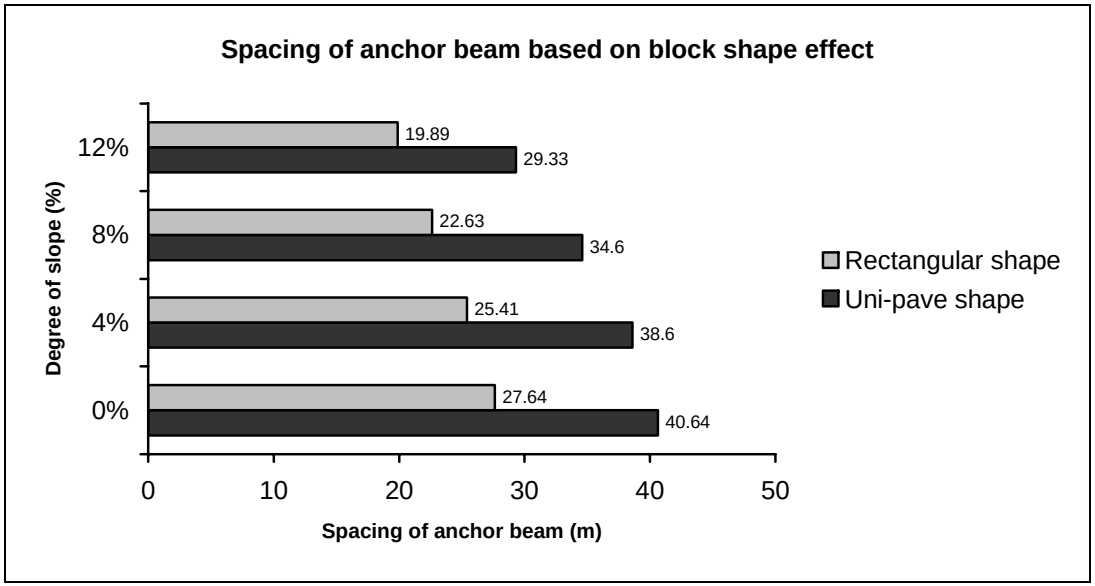

Spacing of anchor beam based on bedding sand thickness effect

Model	Bedding sand thick	Block shape	Block thickness	joint width	Laying pattern	The equation of Hz creep on Hz Force Test	Y max	The equation of Hz creep on Push-in Test
1	30 mm	Rectangular	60 mm	3 mm	Stretcher			
2	50 mm	Rectangular	60 mm	3 mm	Stretcher	$Y = -0.0299x^2 + 0.6582x$	3.62	
3	70 mm	Rectangular	60 mm	3 mm	Stretcher			

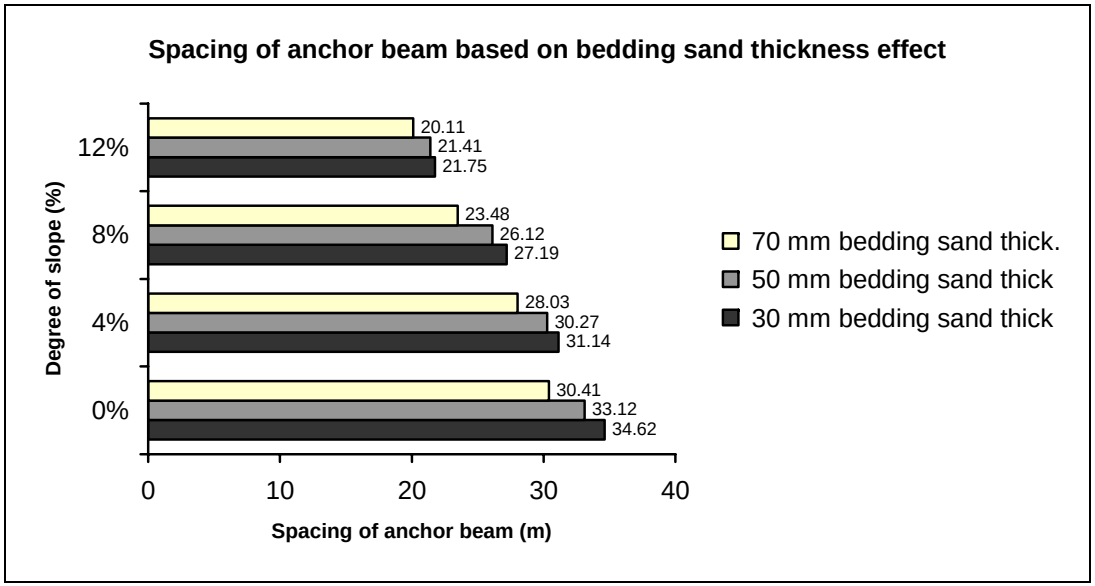

Spacing of anchor beam based on degree of slope effect

Model	Degree of slope	Bedding sand thick	Block shape	Block thickness	joint width	Laying pattern	The equation of Hz creep on Hz Force Test	Y max	The equation of Hz creep on Push-in Test
1	0%	50 mm	Rectangular	60	3 mm	Stretcher	$Y = -0.0299x^2 + 0.6582x$	3.62	$Y = -0.0002x^2 + 0.0211x + 0.0113$
2	4%	50 mm	Rectangular	60	3 mm	Stretcher	$Y = -0.0299x^2 + 0.6582x$	3.62	$Y = -0.0003x^2 + 0.0249x + 0.0109$
3	8%	50 mm	Rectangular	60	3 mm	Stretcher	$Y = -0.0299x^2 + 0.6582x$	3.62	$Y = -0.0003x^2 + 0.0311x + 0.0188$
4	12%	50 mm	Rectangular	60	3 mm	Stretcher	$Y = -0.0299x^2 + 0.6582x$	3.62	$Y = -0.0004x^2 + 0.0333x + 0.0054$

The results of horizontal creep on horizontal force test with on 2 x 2 metre (From Appendix B1& B2)

No.	Block shape	Block thick. (mm)	Joint width (mm)	Laying pattern	Bedding sand thick. (mm)	Equation (Ref. App. B1 & B2)	X max	Y max
1	Rectangular	60	3	Stretcher	50	$Y= -0.0299x^2 + 0.6582x$	11.01	3.62
2	Rectangular	60	5	Stretcher	50	$Y= -0.0406x^2 + 0.8065x$	9.93	4.01
3	Rectangular	60	7	Stretcher	50	$Y= -0.0575x^2 + 1.00005x$	8.70	4.35
4	Rectangular	60	3	Herringbone 90^o	50	$Y= -0.0213x^2 + 0.5914.x$	10.78	2.47
5	Rectangular	60	5	Herringbone 90^o	50	$Y= -0.0319x^2 + 0.5914x$	9.27	2.74
6	Rectangular	60	7	Herringbone 90^o	50	$Y= -0.0371x^2 + 0.6690x$	9.02	3.04
7	Rectangular	60	3	Herringbone 45^o	50	$Y= -0.0154x^2 + 03607x$	11.71	2.11
8	Rectangular	60	5	Herringbone 45^o	50	$Y= -0.0264x^2 + 0.4900x$	9.28	2.27
9	Rectangular	60	7	Herringbone 45^o	50	$Y= -0.0267x^2 + 0.5124x$	9.60	2.46
10	Rectangular	100	3	Stretcher	50	$Y= -0.023x^2 + 0.484x$	10.52	2.52
11	Rectangular	100	5	Stretcher	50	$Y= -0.0299x^2 + 0.5865x$	9.81	2.88
12	Rectangular	100	7	Stretcher	50	$Y= -0.0418x^2 + 0.7228x$	8.65	3.12
13	Rectangular	100	3	Herringbone 90^o	50	$Y= -0.0131x^2 + 0.2706x$	10.33	1.40
14	Rectangular	100	5	Herringbone 90^o	50	$Y= -0.0179x^2 + 0.3334x$	9.31	1.55
15	Rectangular	100	7	Herringbone 90^o	50	$Y= -0.0232x^2 + 0.3992x$	8.60	1.72
16	Rectangular	100	3	Herringbone 45^o	50	$Y= -0.0097x^2 + 0.2159x$	11.13	1.20
17	Rectangular	100	5	Herringbone 45^o	50	$Y= -0.0143x^2 + 0.2772x$	9.69	1.34

18	Rectangular	100	7	Herringbone 45^{o}	50	$Y= -0.0175x^2 + 318x$	9.09	1.44
19	Uni-pave	60	3	Stretcher	50	$Y= -0.0082x^2 + 0.397x$	24.21	4.81
20	Uni-pave	60	5	Stretcher	50	$Y= -0.0195x^2 + 0.52x$	13.33	3.47
21	Uni-pave	60	7	Stretcher	50	$Y= -0.0157x^2 + 0.574x$	18.28	5.25
22	Uni-pave	60	3	Herringbone 90^{o}	50	$Y= 0.0044x^2 + 0.2653x$	30.15	4.00
23	Uni-pave	60	5	Herringbone 90^{o}	50	$Y= -0.0099x^2 + 0.3452x$	17.43	3.01
24	Uni-pave	60	7	Herringbone 90^{o}	50	$Y= -0.0113x^2 + 0.3958x$	17.51	3.47
25	Uni-pave	60	3	Herringbone 45^{o}	50	$Y= -0.0006x^2 + 0.1926x$	26.05	5.46
26	Uni-pave	60	5	Herringbone 45^{o}	50	$Y= -0.005x^2 + 0.2562x$	25.62	3.28
27	Uni-pave	60	7	Herringbone 45^{o}	50	$Y= -0.0088x^2 + 0.3273x$	18.60	3.04
28	Uni-pave	100	3	Stretcher	50	$Y= -0.0003x^2 + 0.2577x$	42.95	5.53
29	Uni-pave	100	5	Stretcher	50	$Y= -0.0036x^2 + 0.3144x$	25.93	2.42
30	Uni-pave	100	7	Stretcher	50	$Y= -0.011x^2 + 0.4078x$	18.54	3.78
31	Uni-pave	100	3	Herringbone 90^{o}	50	$Y= -0.0019x^2 + 0.147x$	38.68	2.84
32	Uni-pave	100	5	Herringbone 90^{o}	50	$Y= -0.0036x^2 + 0.1867x$	25.93	2.42
33	Uni-pave	100	7	Herringbone 90^{o}	50	$Y= -0.0061x^2 + 0.2239x$	18.35	2.05
34	Uni-pave	100	3	Herringbone 45^{o}	50	$Y= -00004x^2 + 0.1128x$	34.10	2.95
35	Uni-pave	100	5	Herringbone 45^{o}	50	$Y= -0.0027x^2 + 0.152x$	28.15	2.14
36	Uni-pave	100	7	Herringbone 45^{o}	50	$Y= -0.0051x^2 + 0.1888x$	18.51	1.75

Appendix K

The results of horizontal creep on push-in test with load position 40 cm, 60 cm and 80 cm from edge restraint

No	Block Shape	Block thick. (mm)	Bedding sand thick.(mm)	Joint width (mm)	Slope (%)	Equation
1	Rectangular	60	30	3	0	$Y = -0.0009x^2 + 0.0868x$
2	Rectangular	60	50	3	0	$Y = -0.0011x^2 + 0.0994x$
3	Rectangular	60	70	3	0	$Y = -0.0013x^2 + 0.1212x$
4	Rectangular	60	30	5	0	$Y = -0.001x^2 + 0.09x$
5	Rectangular	60	50	5	0	$Y = -0.0012x^2 + 0.1093x$
6	Rectangular	60	70	5	0	$Y = -0.0014x^2 + 0.1282x$
7	Rectangular	60	30	7	0	$Y = -0.0011x^2 + 0.0964x$
8	Rectangular	60	50	7	0	$Y = -0.0012x^2 + 0.1147x$
9	Rectangular	60	70	7	0	$Y = -0.0014x^2 + 1318x$
10	Rectangular	100	30	3	0	$Y = -0.0006x^2 + 0.0595x$
11	Rectangular	100	50	3	0	$Y = -0.0006x^2 + 0.0627x$
12	Rectangular	100	70	3	0	$Y = -0.0007x^2 + 0.0667x$
13	Rectangular	100	30	5	0	$Y = -0.0006x^2 + 0.0556x$
14	Rectangular	100	50	5	0	$Y = -0.0006x^2 + 0.0618x$

Appendix K

15	Rectangular	100	70	5	0	$Y = -0.0007x^2 + 0.0694x$
16	Rectangular	100	30	7	0	$Y = -0.0006x^2 + 0.0563x$
17	Rectangular	100	50	7	0	$Y = -0.0006x^2 + 0.0646x$
18	Rectangular	100	70	7	0	$Y = -0.0007x^2 + 0.0706x$
19	Rectangular	60	30	3	4	$Y = -0.0009x^2 + 0.0816x + 0.0484$
20	Rectangular	60	50	3	4	$Y = -0.001.x^2 + 0.0948x + 0.0493$
21	Rectangular	60	70	3	4	$Y = -0.0012x^2 + 0.1161x + 0.0396$
22	Rectangular	60	30	5	4	$Y = -0.0009x^2 + 0.0859x + 0.0503$
23	Rectangular	60	50	5	4	$Y = -0.0011x^2 + 0.1046x + 0.0463$
24	Rectangular	60	70	5	4	$Y = -0.0013x^2 + 0.1234x + 0.0512$
25	Rectangular	60	30	7	4	$Y = -0.001x^2 + 0.0948x + 0.022$
26	Rectangular	60	50	7	4	$Y = -0.0012x^2 + 0.1116x + 0.0386$
27	Rectangular	60	70	7	4	$Y = -0.0013x^2 + 0.1279x + 0.0468$
28	Rectangular	100	30	3	8	$Y = -0.0005x^2 + 0.0509x - 0.0014$
29	Rectangular	100	50	3	8	$Y = -0.0006x^2 + 0.0576x - 0.0024$
30	Rectangular	100	70	3	8	$Y = -0.0007x^2 + 0.0681x - 0.0084$

Appendix K

31	Rectangular	100	30	5	8	$Y = -0.0005x^2 + 0.0533x - 0.0129$
32	Rectangular	100	50	5	8	$Y = -0.0006x^2 + 0.0593x - 0.0044$
33	Rectangular	100	70	5	8	$Y = -0.0007x^2 + 0.0705x - 0.0050$
34	Rectangular	100	30	7	8	$Y = -0.0005x^2 + 0.0545x - 0.0110$
35	Rectangular	100	50	7	8	$Y = -0.0006x^2 + 0653x - 0.0014$
36	Rectangular	100	70	7	8	$Y = -0.0006x^2 + 0.0709x + 0.0005$